LEVEL II

AGARD-CP-297

AGARD-CP-297

AD A101017

AGARD

ADVISORY GROUP FOR AEROSPACE RESEARCH & DEVELOPMENT

7 RUE ANCELLE 92200 NEUILLY SUR SEINE FRANCE

AGARD CONFERENCE PROCEEDINGS No. 297

Helicopter Fatigue Life Assessment

DTIC
ELECTE
JUL 7 1981
S D
A

This document has been approved for public release and sale; its distribution is unlimited.

DTIC FILE COPY

NORTH ATLANTIC TREATY ORGANIZATION

DISTRIBUTION AND AVAILABILITY
ON BACK COVER

81 7 07 031

(14) AGARD-CP-297

NORTH ATLANTIC TREATY ORGANIZATION

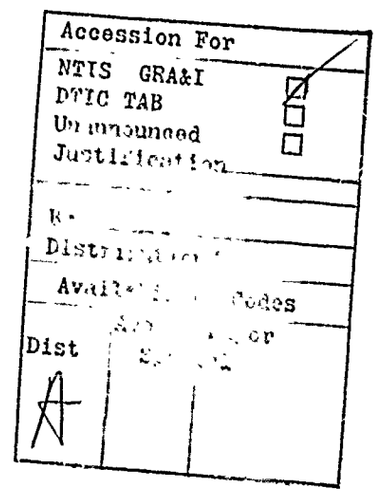
ADVISORY GROUP FOR AEROSPACE RESEARCH AND DEVELOPMENT

(ORGANISATION DU TRAITE DE L'ATLANTIQUE NORD)

(11) Mar 81 (12) 264

(9)
AGARD Conference Proceedings No.297
(6)

HELICOPTER FATIGUE LIFE ASSESSMENT.



This document has been approved for public release and sale; its distribution is unlimited.

Papers presented at the 51st Meeting of the AGARD Structures and Materials Panel held in Aix-en-Provence, France on 14–19 September 1980.

400042

THE MISSION OF AGARD

The mission of AGARD is to bring together the leading personalities of the NATO nations in the fields of science and technology relating to aerospace for the following purposes:

- Exchanging of scientific and technical information;
- Continuously stimulating advances in the aerospace sciences relevant to strengthening the common defence posture;
- Improving the co-operation among member nations in aerospace research and development;
- Providing scientific and technical advice and assistance to the North Atlantic Military Committee in the field of aerospace research and development;
- Rendering scientific and technical assistance, as requested, to other NATO bodies and to member nations in connection with research and development problems in the aerospace field;
- Providing assistance to member nations for the purpose of increasing their scientific and technical potential;
- Recommending effective ways for the member nations to use their research and development capabilities for the common benefit of the NATO community.

The highest authority within AGARD is the National Delegates Board consisting of officially appointed senior representatives from each member nation. The mission of AGARD is carried out through the Panels which are composed of experts appointed by the National Delegates, the Consultant and Exchange Programme and the Aerospace Applications Studies Programme. The results of AGARD work are reported to the member nations and the NATO Authorities through the AGARD series of publications of which this is one.

Participation in AGARD activities is by invitation only and is normally limited to citizens of the NATO nations.

The content of this publication has been reproduced
directly from material supplied by AGARD or the authors.

Published March 1981

Copyright © AGARD 1981
All Rights Reserved

ISBN 92-835-0289-2



Printed by Technical Editing and Reproduction Ltd
Harford House, 7–9 Charlotte St, London, W1P 1HD

PREFACE

Dans un passé récent et à plusiers reprises, la Commission Structures et Matériaux s'est intéressée aux problèmes de la fatigue pour les hélicoptères:

- Specialists Meeting on Helicopter Design Mission Load Spectra (Ottawa 1976, Agard Conférence Proceedings 206)

- Pilot papers on Helicopter Fatigue: A review of Current Requirements and Substantiation Procedures (Florence 1978, Agard Report 674).

Au terme des actions antérieures il avait été convenu de la nécessité d'une réunion de spécialistes en vue de compléter la mise en commun de l'expérience NATO dans le domaine de la justification des durées de vie en fatigue des hélicoptères, en insistant particulièrement sur la confrontation avec l'expérience en service, sur le développement de technologies nouvelles et sur l'apparition de concepts nouveaux.

Tel est l'objet de la présente publication qui rassemble un historique sur les rotors développés par l'Aérospatiale, les textes de 17 exposés présentés à Aix-en-Provence en septembre 1980, les comptes rendus des cinq sessions correspondantes et le compte rendu des débats de la table ronde finale.

Bien qu'on puisse regretter de n'avoir pu recueillir directement le point de vue de compagnies civiles exploitantes, il apparaît que le but proposé a été atteint de façon très satisfaisante: les exposés et les discussions ont mis en évidence l'importance du travail de réflexion de la part des services officiels et des industriels sur les concepts, les méthodologies, les techniques de justification des durées de vie en fatigue pour les hélicoptères.

Ce document constitue sans doute une base irremplaçable pour les spécialistes désireux de poursuivre cette réflexion en vue d'améliorer les procédures actuelles. Qu'il me soit permis, comme Président du Group de Travail correspondant, de remercier vivement tous ceux qui ont contribué à la préparation de ce document.

J.-M.FEHRENBACH
President, Groupe Travail sur la Fatigue
des Hélicoptères

PREFACE

In the recent past and on several occasions, the Structures and Materials Panel has been concerned with helicopter fatigue problems:

– Specialists' Meeting on Helicopter Design Mission Load Spectra (Ottawa 1976, AGARD CP-206)

– Pilot Papers on Helicopter Fatigue: a Review of Current Requirements and Substantiation Procedures (Florence 1978, AGARD Report 674).

When the previous actions were completed, it was agreed that a Specialists' Meeting should be held in order to complete the integration of NATO experience in the field of the substantiation of helicopter fatigue life, with particular emphasis on the comparison with operational experience, the development of new technologies and the advent of new concepts.

This is the subject of the present publication which provides a history of the rotors developed by "Aerospatiale" and includes the texts of 17 papers presented at Aix-en-Provence in September 1980, the summary records of the five corresponding sessions and the proceedings of the final round table.

Although it may be regretted that the points of view of the operating civilian firms could not be collected directly, it appears that the proposed objective has been very satisfactorily reached: the papers and discussions highlighted the importance of the consideration that has been given by official services and industrial firms to concepts, methodologies, and techniques for substantiating helicopter fatigue life.

The present document can unquestionably be regarded as an irreplaceable basis for the specialists wishing to continue their consideration of the problem in order to improve present procedures. In my capacity as Chairman of the Working Group, I wish to express my sincere thanks to those who contributed to the preparation of this document.

J.M.FEHRENBACH
Chairman, Working Group
on Helicopter Fatigue

CONTENTS

	Page
PREFACE	
by J.M.Fehrenbach (French)	iii
(English)	iv
	Reference
SESSION I – SURVEY OF CURRENT PROCEDURES	
STATE OF THE ART AND STATISTICAL ASPECTS OF HELICOPTER FATIGUE SUBSTANTIATION PROCEDURES	
by R.Noback	1
FATIGUE ASSESSMENT OF UK MILITARY AEROPLANES	
by J.I.M.Forsyth	2
SYNOPSIS OF SPECIALISTS' MEETING ON HELICOPTER FATIGUE METHODOLOGY	
by D.C.Borgman and D.P.Schrage	3
RAPPORTEUR'S REPORT, SESSION I	
by W.Schütz	R-1
SESSION II – NEW CONCEPTS/DAMAGE TOLERANCE	
APPLICATION OF DAMAGE TOLERANCE CONCEPTS FOR MBB HELICOPTERS	
by M.v.Tapavicza and F.Och	4
JUSTIFICATION EN FATIGUE DE PIECES EN MATERIAU COMPOSITE BENEFICIANT DU CONCEPT "FAIL SAFE"	
par G.Stiévenard	5
COMBAT DAMAGE ASSESSMENT	
by C.H.Carper, Jr	6
RAPPORTEUR'S REPORT, SESSION II	
by K.Brunsch	R-2
SESSION III – SURVEY OF SERVICE EXPERIENCE WITH REGARD TO EXISTING PROCEDURES	
AN EVALUATION OF FATIGUE PROCEDURES FOR UK MILITARY HELICOPTERS	
by R.Cansdale	7
HELICOPTER FATIGUE – A CIVIL VIEW	
by H.E. Le Sueur	8
HELICOPTER COMPONENT FATIGUE LIFE DETERMINATION	
by M.J.McGuigan	9
RAPPORTEUR'S REPORT, SESSION III	
by J.Darts	R-3
SESSION IV – TESTING TECHNIQUES AND METHODOLOGY	
ESSAI DE FATIGUE D'UNE STRUCTURE COMPLETE DE L'HELICOPTERE SA 341 "GAZELLE"	
par P.Pétard et J.P.Lambert	10
HELICOPTER GEARBOX TESTING	
by R.Zincone and J.H.Mancini	11

Reference

FATIGUE TESTING OF HELICOPTER GEARBOXES
by A.H.Baker 12

THE METHODOLOGY OF FATIGUE ANALYSIS AND TESTING – MAIN ROTOR BLADES AND HUB – HUGHES YAH-64 ADVANCED ATTACK HELICOPTER
by J.M.McDermott 13

FATIGUE TESTING OF COMPOSITE ROTOR BLADES
by F.Och 14

RAPPORTEUR'S REPORT, SESSION IV
by D.C.Borgman R-4

SESSION V – CONSTANT AMPLITUDE/SPECTRUM LOADING

DEVELOPMENT OF STANDARDIZED FATIGUE TEST LOAD HISTORIES FOR HELICOPTER ROTORS
1. Basic Considerations and Definition of HELIX and FELIX
by J.Darts and D.Schütz 15

2. Fatigue Test Program and Test Results
by D.Schütz, H.G.Köbler, W.Schütz and M.Hück 16

FATIGUE BEHAVIOUR OF HELICOPTER DYNAMIC COMPONENTS UNDER CONSTANT AMPLITUDE AND SPECTRUM LOADING
by G.Cavallini, A.Lanciotti, G.Aldinio and R.Rovellotti 17

RAPPORTEUR'S REPORT, SESSION V
by P.Alli R-5

SESSION VI – ROUND TABLE DISCUSSION

RAPPORTEUR'S REPORT, SESSION VI (French)
by G.Stiévenard (French) R-6a
(English) R-6b

STATE OF THE ART AND STATISTICAL ASPECTS OF HELICOPTER FATIGUE SUBSTANTIATION PROCEDURES

by
R.Noback
NATIONAL AEROSPACE LABORATORY NLR
P.O. Box 153
8300 AD EMMELOORD
Netherlands

SUMMARY

The recipe that is used to calculate safe fatigue life for helicopter components is described. Basic ingredients are flight loadspectrum, derived from measured flightloads and mission profile, a reduced S-N curve, based on statistically treated coupon and specimen test results, and a damage hypothesis. These ingredients are generally used, but many different ways of handling, especially statistically, exist and these may lead to a great variety of calculated safe fatigue lives. An example is used to illustrate the influence of various ways of handling on the end result. An attempt is made to bring together alternative statistical opinions.

1. INTRODUCTION

In almost any paper on helicopter fatigue (references 1-15) a diagram is used, implicitly or explicitly, that looks like figure 1. This might suggest that everything is clear and that indeed a well-established fatigue substantiation methodology for helicopter components exists. This is not exactly true. In an exercise, initiated by the American Helicopter Society (reference 8) seven manufacturers calculated the fatigue life (replacement time) of a pitch link. The results of constant amplitude tests on the pitch link were provided. Loads measured during flight tests were given and a mission profile was prescribed. Ground-Air-Ground cycles were not taken into account.

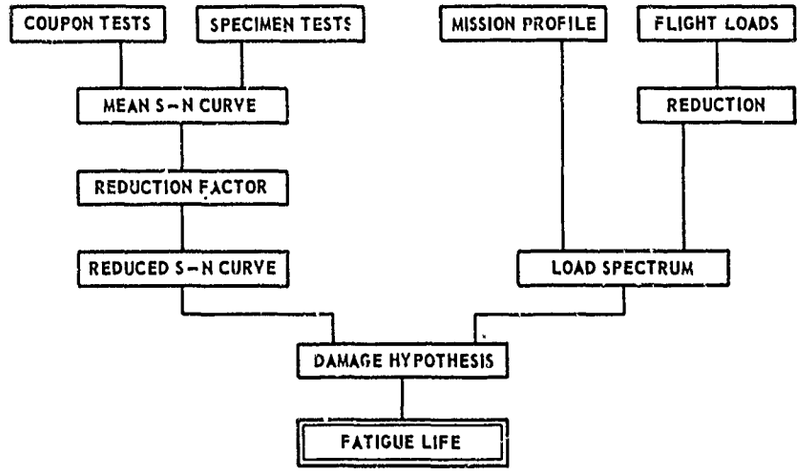


Fig. 1 Safe fatigue life calculation

Calculated replacement times ranged from 9 hours to 2594 hours, based on peak value flight loads, and from 58 hours to 27816 hours with flight load cycle counting.
The methods used were in accordance with the diagram given above.

Helicopter fatigue is characterized by a large number of load cycles with relatively small amplitude, alternated by (relatively large) Ground-Air-Ground (G.A.G.)-cycles. This is especially so for the dynamic parts with a total number of loadcycles in the order of 100 million. For these parts usually the safe life principle is applied. A certain life (in hours) is assigned to a component. Irrespective of its state it will be retired from service. The probability of catastrophic failure within the assigned time must be extremely remote. In fact the diagram is related to this design principle.
Fail safe/damage tolerance principles require inspection procedures. The airframe usually will be of a fail safe design with multiple load paths, crack stoppers, etc. Manoeuvre loads will be the main source of fatigue damage, although vibration, with a frequency at least equal to rotor r.p.m. times number of blades, might range from a nuisance to a fatigue problem.

The following will only deal with fatigue substantiation procedures for dynamic parts, that are based on the safe life principle.

Instead of the rather pretentious term "methodology" the word "recipe" will be used.

In the following first a description of recipe and ingredients will be given. Next special attention will be given to some aspects, especially statistical ones.

2. RECIPE AND INGREDIENTS

Fatigue life calculations for helicopter components are based on the Linear Cumulative Damage Hypothesis or (Palmgren-) Miner rule.

For the application of the Miner rule two sets of data for the section of interest of a component must be available, viz.

a. loadspectrum
b. S-N curves or Wöhlercurves

The loadspectrum gives the number of cycles of various load amplitudes and accompanying mean loads. Loads may be given as axial loads, bending moments, etc., combinations of these or stresses. The loadspectrum for the final fatigue life calculation is derived from the mission profile and measured flight loads.

The mission profile may be defined by the procuring agency, airworthiness authorities and/or manufacturer. It contains the percentages of time spent in various flight conditions. Manoeuvres may be given in numbers per hour or percentage of time.

Flight loads are measured for the flight conditions and manoeuvres of the mission profile. These loads are reduced to mean loads and number of cyclic loads and then combined with the mission profile to give the flight load spectrum.

It will be clear that during the design and development stage flight loads are not available. An estimate of the loadspectrum based on calculated flight loads will be used. This estimate also will be used to define testloads for the specimen fatigue tests.

An S-N curve gives the relation between cyclic load and number of cycles until failure for a certain mean load. The endurance limit is defined as the cyclic load level for which the number of cycles to failure approaches infinity. The S-N curve for the component is derived from specimen and component tests. These results show variability. In order that the probability of catastrophic failure is remote, measures have to be taken. A factor on life as used for fixed wing aircraft is impractical as insufficient knowledge is available on fatigue life distributions for small loadcycles/long fatigue lives. It is general practice to use a reduction on load, such that with reasonable confidence it can be stated that a large proportion of component S-N curves will lie above the reduced S-N curve. The reduced S-N curve is related to one mean load. The cyclic loads of the loadspectrum have to be reduced to the mean load of the S-N curve. Rather often a Goodman or Soderberg diagram is used for this purpose. This diagram gives the relation between endurance limit and mean load.

In the following some parts of the recipe will be discussed in more detail.

3. LOADSPECTRUM

The loadspectrum is based on an assumed mission profile and measured flight loads. Uncertainties in the two composing elements are of an entirely different nature. The mission profile is based on the expected future use of the helicopter. It can be defined, rather coarsely as in references 16 and 17 or very finely as proposed in reference 18. Often more than one type of future use is foreseen and accordingly more than one mission profile is defined. Calculated fatigue life is always related to the assumed mission profile and one could say that the mission profile by definition is neither conservative nor unconservative. It may turn out that the actual usage of the helicopter in a certain role differs significantly from the assumed mission profile. It is then possible to define a new mission profile and recalculate fatigue life.

For the loads the situation is quite different. Loads must be established for the various flight conditions of the mission profile.

In the first place it may be impossible to measure the load at the section of interest. Loads then have to be derived from loads measured at other sections.

The required number of straingauges may be too large to handle adequately. Some compromise than has to be made.

Thirdly the number of flight conditions, including weight, c.g. position, altitudes etc., can be so large that it is prohibitive from the point of view of cost and time involved to measure loads in all conditions. Some inter-or extra polation has to be done.

Flight loads show scatter, not only from one run to another, but also within a run. A distinction has to be made between steady flight conditions and manoeuvres.

During steady flight cyclic loads will show scatter that has a random nature. A probability density function can be established and this can be used in the fatigue life calculation (for example references 4 and 14). Others use "top of scatter" or add a certain percentage (reference 3).

During a manoeuvre cyclic load and mean loads will vary due to the manoeuvre. Various methods are available to count the cycles of a manoeuvre. One will find that the result of the cycle count will vary from run to run. This scatter can be dealt with in the same way as scatter in steady flight loads.

The simplest counting method is to assume that all cyclic loads have magnitude $(S_{max}-S_{min})/2$ with mean $(S_{max}+S_{min})/2$. S_{max} and S_{min} being the maximum and minimum loadlevel of the manoeuvre. This of course is a conservative counting method, sometimes referred to as uncycle count. Other counting methods are for example the range-mean count method and the range-pair-range count method (reference 27). The counting method has a large influence on the result of fatigue life calculations. In the excercise of the A.H.S., mentioned in the introduction the ratios of fatigue life, based on a cycle counting method, and that, based on peak value flight loads or uncycle count, ranged from 2 to 17.

Wolfe and Arden (reference 2) are of the opinion that "Initial usage of these measured data is usually very conservative. However, as the calculated fatigue lives become critical with respect to design requirements, the conservatism is whittled away sometimes at almost an alarming rate".

4. PALMGREN-MINER RULE AND MEAN LOAD REDUCTION

Once the loadspectrum is established the fatigue life of the component under this spectrum must be defined on the basis of fatigue testresults. This is never done by means of spectrum fatigue tests in which the actual unfactored load spectrum is applied. This would lead to extremely long testing times on a large number of test specimens. Normal practice is to calculate the fatigue life using a reduced S-N curve that has been derived from tests on coupons and specimens.

Total fatigue damage is assumed to be equal to the sum of the damages of the individual cycles. The damage of one cycle with amplitude S_i and mean S_m is equal to $1/N_i$, N_i being the number of cycles, with amplitude S_i and mean S_m, at which failure occurs. n_i cycles give the damage n_i/N_i and total damage is

$$D = \Sigma \frac{n_i}{N_i} \qquad (4.1)$$

It is now assumed that failure of the component occurs when D equals 1.

If the loadspectrum gives the number per hour n_i of k different load cycles with amplitude S_i, all at mean load S_m, then the fatigue life, according to the Palmgren-Miner rule, is

$$L = \frac{1}{\sum_k \frac{n_i}{N_i}} \text{ hours} \qquad (4.2)$$

However, usually mean loads of the loadspectrum are not all at the level S_m of the S-N curve, and the loadspectrum has to be reduced. Most commonly used is a reduction based on a diagram that gives the relation between mean load and endurance limit, derived from coupon tests, and referred to as (modified) Goodman diagram or Soderberg diagram.

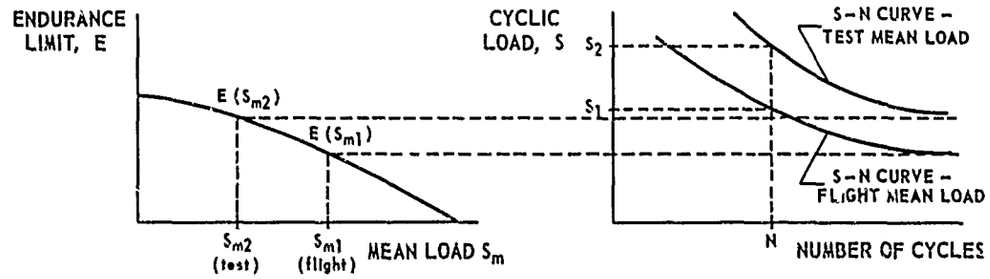


Fig. 2 Goodman diagram and S-N curves

It is assumed that one cyclic load S_1 at mean load S_{m1} gives the same damage as one cyclic load S_2 at mean S_{m2} S_2 being equal to

$$S_{red} = S_2 = \frac{E(S_{m2})}{E(S_{m1})} S_1 = \frac{E(S_{m2})}{E(S_{m1})} S_1 = \frac{E(S_{m2})}{E(S_{m1})} S_{flight} \qquad (4.3)$$

In reference 4 a correction method is given in which it is not a priori assumed that S is proportional to the endurance limit E.

Some manufacturers do not apply a correction if the test mean load is higher than the flight mean loads.

GAG cycles can be treated in the same way and many manufacturers do. Others feel that GAG cycles differ too much from flight loads and treat them separately. One method is to define the number of GAG cycles until failure (N_{gag}) on separate specimens. With n_{gag} G.A.G. cycles per hour in the loadspectrum and with a factor c on life, fatigue life becomes.

$$L = \frac{1}{\sum_k \frac{n_i}{N_i} + \frac{cn_{gag}}{N_{gag}}} \text{ hours} \qquad (4.4)$$

(reference 10 and 15 for example)

Another method is to carry out specimen fatigue tests in which GAG cycles are incorporated (reference 10 and 19 for example).

Still another method is to carry out flight simulation tests with flight loads that are the loads of the flightload spectrum multiplied with a factor larger than one and equal to the reciprocal of the reduction factor of the S-N curve. GAG cycles are applied with a factor on life. In such tests, the loadspectrum may be simplified and small load cycles are often omitted (see reference 9 and 19). Interpretation of test results, for example when the mission profile is redefined or when testresults differ significantly from expected results, may be difficult. One then has to rely on the Miner rule again although this then probably may be regarded as a relative Miner calculation.

Tests have shown that Miner's rule is not unconditionally valid. It is unable to account for interaction effects of subsequent loadcycles, which may be very important. This is especially so for Ground-Air-Ground cycles. Many examples are known where Miner's rule yielded unconservative life estimates. For this reason, in the application of Miner's rule the summation is not always carried out to unity. Quite often a service life or replacement time is prescribed, lower than calculated fatigue life (for example reference 5, 11, 19).

Nevertheless it can be stated that both rule-making agencies and manufacturers accept Miner's rule as a tool for fatigue life calculations.

5. REDUCED S-N CURVE

It is common practice to calculate safe fatigue life for a component using a reduced (or safe, or working) S-N curve. This S-N curve is based on coupon and specimen tests. Specimen tests are carried out on a limited number of components, for example six or less, in some cases higher numbers of specimen may be tested. These tests are usually constant amplitude tests. Sometimes cyclic load level is altered if no crack appears. Other types of tests are constant amplitude tests alternated with a number of GAG loads, programtests with blocks of flightloads with various amplitudes alternated with a number of GAG loads and flight-by flight simulation tests.

If only constant amplitude tests are carried out test results can be plotted and an S-N curve drawn through the data points. However, usually it is felt that insufficient specimen test data are available to draw an S-N curve and therefore a curve shape derived from coupon tests on the same type of material, with the same type of notches and fretting condition, is used.

Constant amplitude tests are carried out on a large number of coupons at various load levels until failure occurs. Number of cycles N until failure are plotted against loadlevel S. One method to present test results is by giving sets of S and N values of a curve drawn by eye through the test data points. More often results are presented as an equation with a number of constants. Two types of equation are used for this purpose

$$\text{I} \quad S = E + g\,(N) \tag{5.1}$$
$$\text{II} \quad S = E * f\,(N) \tag{5.2}$$

in which E is the endurance limit.
E can be defined as the S-value at a certain high value of N ($N = 10^7 - 10^8$ cycles) or at $N \to \infty$
The latter will be used here.

One example of the first type is the well known Weibull curve shape (reference 20)

$$S = E + \frac{b}{(N+B)^{\kappa}} \tag{5.3}$$

with constants b, κ and B

If this curve is drawn on semi-logarithmic paper it shows an inflexion at $N = B/\kappa$. At the high cycle end of the S-N curve, that is of interest for helicopter components, constant B usually is much smaller then N and the curve shape can be expressed as

$$S = E + \frac{b}{N^{\kappa}} = E\left\{1 + \frac{b/E}{N^{\kappa}}\right\} \tag{5.4}$$

An example of the second type is

$$S = E * f\,(N) = E\left(1 + \frac{A}{N^{\kappa}}\right) \tag{5.5}$$

with constants A and κ
This expression is often used for helicopter components to draw an S-N curve through specimen test data points. Usually it is assumed that the ratio $f(N) = S(N)/E$ of the specimen tests is equal to the same ratio of the coupon tests for a certain value of N.

Each test data point is then used to calculate an estimate for the endurance limit

$$E_i = S_i/f(N_i) \tag{5.6}$$

Arithmetic mean and standard deviation are

$$\bar{E} = \frac{\Sigma E_i}{n} \tag{5.7}$$

$$s = \sqrt{\frac{\Sigma(E_i - \mu)^2}{n-1}} \tag{5.8}$$

Logarithmic mean (median) and standard deviation are

$$\bar{E} = 10^a, \quad a = \frac{\Sigma \log E_i}{n} \tag{5.9}$$

$$\ell = \sqrt{\frac{\Sigma(\log E_i - a)^2}{n-1}} \tag{5.10}$$

The mean S-N curve for the specimen is now defined as

$$S(N) = \bar{E}\ f(N) \tag{5.11}$$

The number of cycles to failure N in the coupon tests will show scatter. As the aim of the fatigue calculation is to establish a safe fatigue life, it would be practical if variability in N could be used to establish a factor on life of the component. This, however, is not possible, as variability in N and even the probability distribution function often depends on the loadlevel. A distribution function of component fatigue life cannot be established, as it depends on the loadspectrum.

It is common practice to reduce the mean S-N curve in S-direction, such that the probability of a component having an S-N curve lower than this reduced S-N curve is small. The reduced S-N curve can be described by

$$S_{red}(N) = F.\bar{E}.\ f(N) \qquad (5.12)$$

and the reduced endurance limit is $\bar{E}_{red} = F\,\bar{E}$.

The steps needed for the construction of the reduced S-N curve will be illustrated with the excercise initiated by the A.H.S. The S-N curve shapes as used by the manufacturers for the fatigue life calculation of the hypothetical pitch link are presented in figure 3. These curves are given in references 9-15 or derived from mean or reduced S-N curves given in these references. These curve shapes are used to transform test data points into estimates of the endurance limit. The mean S-N curve goes through the mean endurance limit

$$S(N) = \bar{E}\ f(N)$$

Mean S-N curves are given in figure 4 and these seem to be in reasonable agreement.

In figure 5 reduced S-N curves are given and, as will be clear, little agreement exists. Finally, in figure 6 calculated safe fatigue lives are plotted as a function of the reduction factor F. This figure makes clear that the value of the reduction factor is of major importance. The effect of differences in S-N curve shape is small. This example is no proof that in all cases only the reduction factor is of prime importance, but it justifies further investigation of this factor.

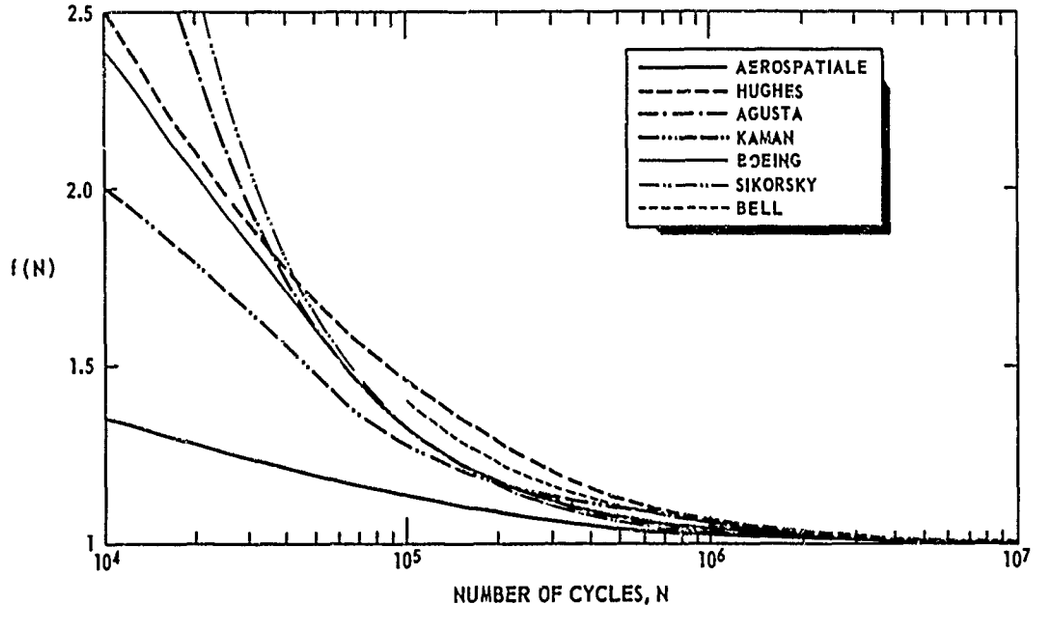


Fig. 3 S-N curve shapes hypothetical pitch link

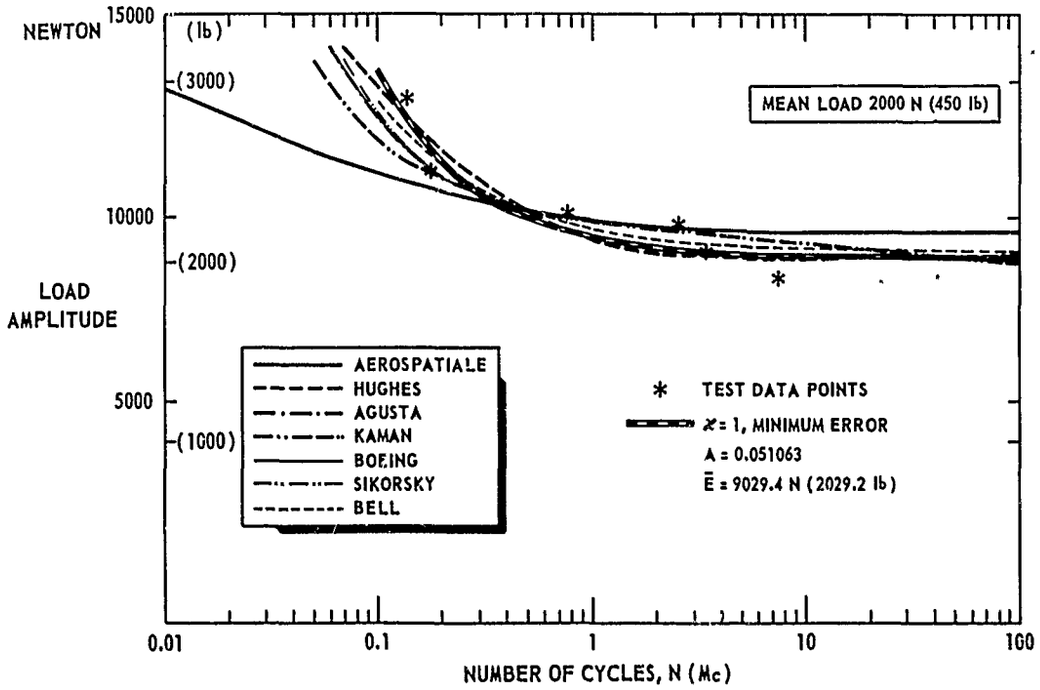


Fig. 4 Mean S-N curves hypothetical pitch link

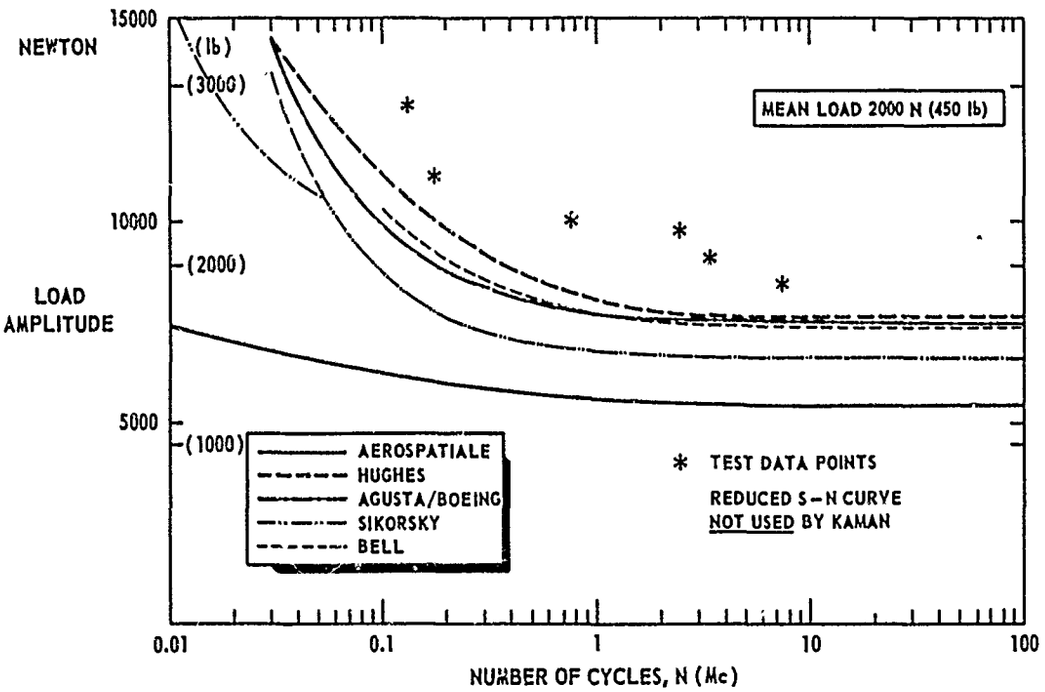


Fig. 5 Reduced S-N curves hypothetical pitch link

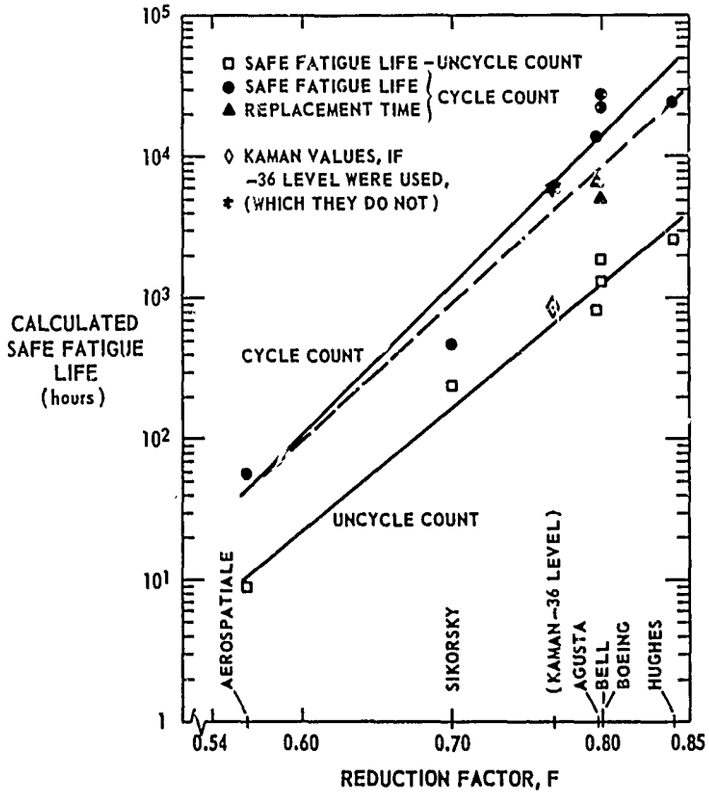


Fig. 6 Fatigue life as function of reduction factor

6. REDUCTION FACTOR

As already mentioned, the reduced S-N curve can be described by

$$S_{red}(N) = F\,\bar{E}\,f(N) \qquad (6.1)$$

with reduced endurance limit $E_{red} = F\,\bar{E}$.

The probability of a component having an S-N curve lower than the reduced S-N curve should be small. Various interpretations of this requirement lead to various values for F.

In most cases it is assumed that endurance limits E have a normal or a log-normal distribution function. The factor F then can be chosen such that with confidence β a proportion p of the endurance limits will be higher than $F.\bar{E}$. Suppose L has a log-normal distribution. The median and standard deviation as calculated with equations (5.9 and 5.10) only give an estimate of median and standard deviation of the population. The estimate of the mean is reasonably good if the standard deviation is small. For example, for 6 specimens it can be stated with 95 per cent confidence (in 95 per cent of the cases, the statement is true) that the median E_m of the population will be

$$\frac{\bar{E}}{g} < E_m < \bar{E}\,g \qquad g = 10^{1.049\,\ell} \qquad (6.2)$$

or

$$\frac{\bar{E}}{h} < E_m \qquad h = 10^{0.825\,\ell} \qquad (6.3)$$

For $\ell = 0.05$ $\quad g = 1.13$ $\quad$ and $\quad h = 1.10$

For $\ell = 0.10$ $\quad g = 1.27$ $\quad$ and $\quad h = 1.21$

The estimate of the standard deviation is worse. Under the same conditions the standard deviation Λ of the population is

$$0.62\,\ell < \Lambda < 2.45\,\ell \qquad (6.4)$$

$$\text{or } \Lambda < 2.09\,\ell \qquad (6.5)$$

With only a small number of specimens the measured standard deviation ℓ only gives a rough estimate of the standard deviation of the population. It is for this reason that a number of manufacturers assume that the standard deviation of the population of specimen tests is equal to the standard deviation Λ of the coupon tests.

If this assumption is correct, it can be stated with confidence β that a proportion p of all specimens will have an endurance limit greater then

$$10^{-\Lambda\left(U_p + \frac{U_\beta}{\sqrt{n}}\right)} \bar{E} = F.\bar{E} \tag{6.6}$$

with U_p and U_β defined with

$$\frac{1}{\sqrt{2\pi}} \int_{-\infty}^{U_p} \exp\left(-\frac{u^2}{2}\right) du = p \tag{6.7}$$

$$\frac{1}{\sqrt{2\pi}} \int_{-\infty}^{U_\beta} \exp\left(-\frac{u^2}{2}\right) du = \beta \tag{6.8}$$

and these can be found in tables of the normal distribution

For $\beta = 0.99$, $p = 0.95$, $n = 6$ and $\Lambda = 0.05$ it follows that

$$U_\beta = 2.326, \quad U_p = 1.645$$

and $F = 10^{-2.5946\ \Lambda} = 0.742$

Other manufacturers feel that the standard deviation of the population of specimens is not a priori equal to that of the coupon tests. The appropriate statistical quantity to be used in that case is the one-sided tolerance limit factor K (p, β, n) (reference 21). With confidence β, a proportion p of all specimens will have an endurance limit greater then

$$\bar{E}.\ 10^{-\ell K(p,\ \beta,\ n)} = \bar{E}.F \tag{6.9}$$

K (p, β, n) can be found in tables (reference 22 and 25) and can be approximated to (according to reference 22)

$$K(p,\ \beta,\ n) = \frac{U_p + \sqrt{U_p^2 - AB}}{A} \tag{6.10}$$

$$A = 1 - \frac{U_\beta^2}{2(n-1)} \tag{6.10a}$$

$$B = U_p^2 - \frac{U_\beta^2}{n} \tag{6.10b}$$

Another, rough, estimate for K(P, β, n) is obtained with

$$K(p,\ \beta,\ n) = \frac{c}{\sqrt{n}} + U_p \sqrt{\frac{n-1}{k}} \tag{6.11}$$

The first term gives the confidence interval of the mean. c can be found in a table for Student's t-distribution

$$\int_{-\infty}^{c} f(t)_{n-1}\, dt = \beta \tag{6.12}$$

The second term gives the confidence interval of the standard deviation. k can be found in a table for the χ^2 - distribution

$$\int_{0}^{k} f(\chi^2)_{n-1}\, d\chi^2 = 1-\beta \tag{6.13}$$

For n=6, $\beta = 0.99$ and $p = 0.95$ and thus

$$U_\beta = 2.326 \quad U_p = 1.645 \quad c = 3.37 \quad \text{and} \quad k = 0.55$$

the value for K(p, β, n) is

K (p, β, n) = 5.409 (from table A7 of reference 22)

K (p, β, n) ≃ 6.570 (equation 6.10)

K (p, β, n) ≃ 6.336 (equation 6.11)

For ℓ = 0.05, the values for F are 0.536, 0.469 and 0.482 respectively.

Although the one-sided tolerance limit is the appropriate statistical quantity to be used if the standard deviation of the population is not known, not many manufacturers actually use it. In reference 6 the use of this quantity, (Hald's formula, equation 6.10) is proposed. A very high value for p is used that on the other hand is drastically reduced as a truncated probability distribution is used. However, instead of the standard deviation of the specimens, that of the coupon tests is used. Besides that a fixed number of specimen tests is assumed and in fact constant (low) factors are used, only depending on the type of material. In reference 23 the rough estimate of K (p, β, n) according to equation (6.11) is used. (Instead of the one-sided confidence level, the two-sided level is erroneously used). However, very often manufacturers use the so-called three-sigma-level. That is, factor F is equal to

$$F = 10^{-3\ell} \tag{6.14}$$

To safeguard against a fortuitous low value of ℓ often a maximum limit for F is used.

$$F \leq F_{max} \tag{6.14a}$$

The recipe to establish the reduced S-N curve as described above is not universally used. Some alternatives are as follows.

Endurance limit E is assumed to have a <u>normal</u> distribution with mean $\bar{E}$ and standard deviation s (equation 5.8). The standard deviation of the coupon tests is σ. The E-value that, with confidence β, will be exceeded by a proportion p, is

- if the standard deviation σ of the coupon tests is assumed to be representative for the standard deviation of the specimen tests

$$E_{red} = \bar{E} - \sigma\left(U_p + \frac{U_\beta}{\sqrt{n}}\right) \tag{6.15}$$

$$\text{and } F = \frac{E_{red}}{\bar{E}} = 1 - \frac{\sigma(U_p + U_\beta/\sqrt{n})}{\bar{E}} \tag{6.16}$$

- if this assumption is not made

$$E_{red} = \bar{E} - sK(p, \beta, n) \tag{6.17}$$

$$\text{and } F = \frac{E_{red}}{\bar{E}} = 1 - \frac{sK(p, \beta, n)}{\bar{E}} \tag{6.18}$$

The quantities $\sigma/\bar{E}$ and $s/\bar{E}$ often are referred to as coefficient of variation. This expression should not be used as it easily leads to confusion (reference 15). It is <u>not</u> equal to the standard deviation of the log-normal distribution, in fact for small values of Λ,

$$\frac{\sigma}{\bar{E}} \simeq \Lambda \cdot \ln 10 \simeq 2.30\,\Lambda \tag{6.19}$$

Again, very often only a 3σ-reduction is applied.

In reference 3 and 15 the possibility that endurance limits have a Weibull distribution is put forward. This distribution function is equal to zero for $E < \gamma$. On all the samples analyzed it was found that the use of the three standard deviation level of strength came at or below the zero probability point estimated by the Weibull parameters (reference 3).

It should be noted that if a variable has a normal distribution and if a Weibull distribution is fitted to it (equal mean and equal first and second derivative of the distribution functions at the mean), the zero probability point (γ) is equal to the mean minus 2.83 σ. If the variable has a log-normal distribution approximately the same result is obtained (appendix A). A Weibull distribution function with zero probability point $\gamma > 0$ should be used only if on physical grounds such a value can be set or if statistically, in a very large number of tests, such a function with $P(E < \gamma) = 0$, can be established.

It is assumed that both loads and endurance limits have a certain probability density function. By means of Monte Carlo methods a large number of combinations of endurance limit and load environment is chosen and for each combination fatigue life is calculated. Safe fatigue life is chosen such that a large proportion (i.e. 99.95 per cent) of calculated fatigue lives exceeds this safe fatigue life (reference 14). In this method a reduction factor is not used. It seems to be debatable, however, that it can be assumed that a helicopter would meet a load environment that is systematically a certain amount lower or higher then the mean load environment. A more appropriate assumption seems to be that each individual helicopter meets the entire population of loads. This is proposed in reference 4.

7 DISCUSSION

The main problem that a helicopter fatigue analyst meets is that he actually never can test whether he is right or wrong. He has to establish a safe fatigue life such that the probability of a fatigue failure during the assigned life is extremely remote. An "allowable" failure rate of 10^{-7} per flight hour is sometimes quoted. If a component has a calculated safe life of 5000 hours, then several thousands of components would have to be tested with actual flight loads up to a multiple of 5000 hours to establish the lower "tail" of the distribution function of fatigue lives. Experience with helicopters only gives a rough indication about the occurrence of statistically predictable failures. Other causes of failure (corrosion, scratches, deviations from mission profile) darken the picture. This uncertainty is inherent to the safe life principle. For this reason, and other reasons as well, fail safe and damage tolerance principles are gaining impetus. It is to be expected, however, that the safe life principle will still be used at least in the near future and it therefore is worth while to look critically at the recipe. The aim of the calculations is to arrive at an assigned life of a component, during which the probability of fatigue failure is extremely remote and this means that in fact the lower "tail" of the distribution function of fatigue lives has to be established. To get a better insight, the problem hypothetically will be split up in two parts.

- What is the median fatigue life and what influences it.
- Given the median fatigue life, what is the safe fatigue life that with confidence β is exceeded by a proportion p of all components.

The first part could be regarded as the fatigue problem and all information on material and loads is needed. The second part is mainly a statistical problem. The first part of the problem will be considered first.

To start with, the mission profile must be defined and it should be realized that both median and safe fatigue life are related to a certain mission profile. This might be a mean profile or a worst case profile. However if the real mission profile differs systematically from the assumed mission profile, the assigned life has no relation to reality and a revision should be made.

Mission profile and measured loads together provide the loadsspectrum. In the most simple form loads are assumed to be equal to the maximum loads during the mission element (uncycle count). This of course is the most conservative counting method. Various cycle counting methods can be used, the optimum being the one that gives the best result with the Miner rule. This probably is the right place to ventilate the following. Never should conservatism in cycle-counting be used to compensate for unconservatism elsewhere. The remark about "conservatism being whittled away at an alarming rate", already cited, can be amplified with a remark from reference 24.

"Problems then arise when component strengths don't come up to expectations and the designer starts to manipulate his loads spectra to eleminate"conservatism"".

No part of the recipe should be unconservative, even when other parts of the recipe are evidently conservative.

It is questionable whether the Miner rule is valid, especially if a large number of flight load cycles is alternated with G.A.G. cycles. Nevertheless validity of this rule usually is assumed. In conjunction with the appropriate mean S-N curve, median fatigue life can then be calculated.

In many cases it may be difficult to decide on the appropriate S-N curve. It is almost common practice to derive the curve shape from coupon tests, with test conditions (fretting, notches, etc.) that give the best agreement with conditions of the specimen. However, as is pointed out, for example in references 13 and 15, often more than one failure mode for which different curve shapes should be used, are possible. Besides that,specimen test conditions hardly ever will be equal to those of the coupon test. And this raises the question whether it would not be preferable to use test data both from coupon- and specimen tests to define the curve shape.

In equation (5.5)

$$\frac{S}{E} = 1 + \frac{A}{N^{\kappa}}$$

the values for κ and A could be derived from coupon test and specimen tests respectively (reference 4). The value for A can be found on the basis of minimum error in E-values. For the test datapoints in figure 3, an S-N curve with $\kappa = 1$ has minimum error for $A = 0.051063$. The error is lower than for any of the other curves.

To summarize our discussions so far, it may be stated that, for a certain mission profile an estimate for the median fatigue life can be made. Confidence in the estimate increases with increasing sophistication of load analysis and testing methods and increasing number of specimen tests.

This hovever is insufficient to arrive at a statistically safe life. The term "statistically safe" is to be interpreted here and in the following as that value that with confidence β is exceeded by a (large) proportion p of the population.

The distribution function is needed for the definition of the statistically safe life. Unfortunately this function depends on loadlevel. This can easily be seen in the following figure, that is reproduced from reference 25.

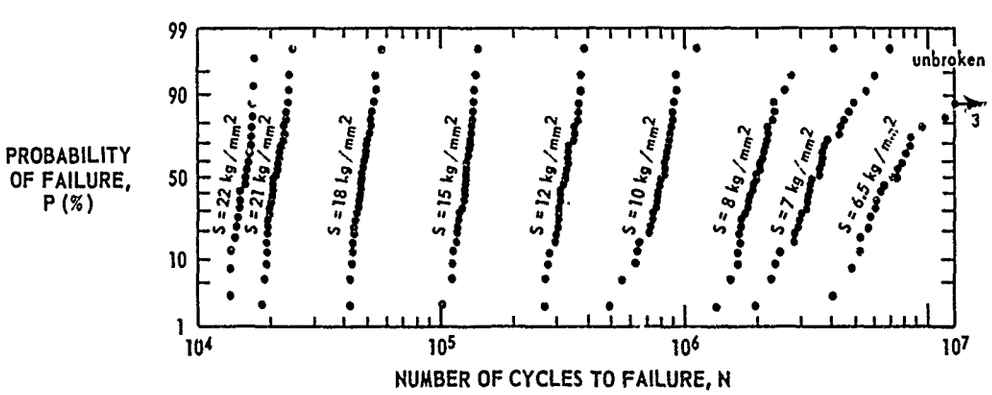


Fig. 7 Fatigue life distributions

For high values of stress S the distribution is approximately normal with a relatively low value of the standard deviation. For low values of S the distribution is not normal and the standard deviation is high. The data of figure 7 were analyzed in reference 26. A slightly different analysis is given in appendix B. All 252 test results are regarded as estimates for the endurance limit E. With the assumption that endurance limits have a log-normal distribution with median and standard deviation derived from the testdata, the distribution functions of fatigue lives as function of S can then be calculated. The result is given in figure 8.

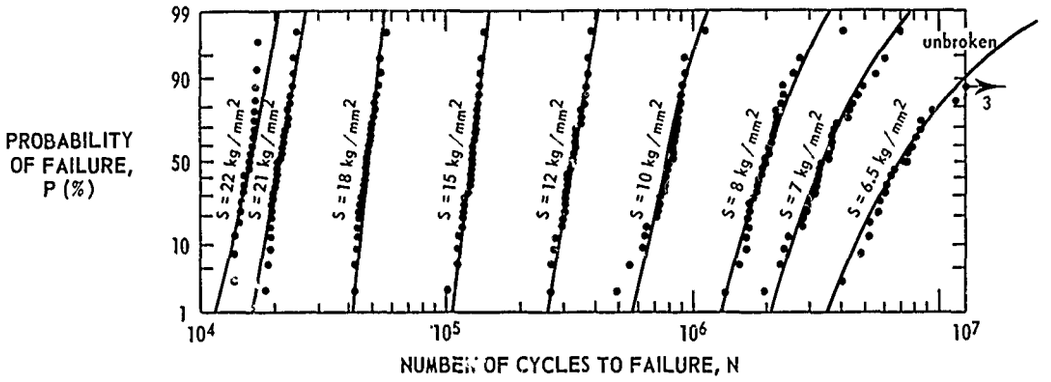


Fig. 8 Fatigue life distributions

The assumption seems to be a reasonable one, as fatigue life distributions are fairly well described. It follows from this analysis that, if a statistically safe reduced endurance limit is chosen, also the lives predicted by the S-N curve defined by the reduced endurance limit are statistically safe.

This of course is only one example, but it is thought to be representative. In the example it was assumed that all coupons have the same S-N curve shape, but different E-values. The curve shape was defined as the one giving minimum error in E-values.

The foregoing is not a proof that the reverse also is true but it seems reasonable to assume that if a specimen has a certain endurance limit E_i, that it has an S-N curve defined by

$$S = E_i + g(N)$$

or $$S = E_i * f(N)$$

depending on which type of function was used in the analysis.

If this is so, and in the recipe it is tacitly accepted, then only the statistically safe endurance limit has to be established. To do this the distribution function must be known. Usually however only a very limited number of specimen fatigue tests are carried out and one then has to rely on previous experience.

Usually it is assumed that endurance limits have a normal or log-normal distribution function. Results of coupon tests show that at least for not too large deviations from the mean these distributions give a fairly good description. For relatively low scatter the difference between the two functions is not large. Some arguments are in favor of the log-normal distribution. This distribution is limited to positive values and the use of a factor is more natural (Equations 6.6, 6.9, 6.16 and 6.18). In the following the log-normal distribution will be used.

As already mentioned in chapter 6 the Weibull distribution function should not be used, unless it can be proven that it is the right one(figure B3 shows that for the example given above, a Weibull distribution can not be used).

The first thing that should be done is to check whether endurance limits, obtained with the specimen test have a distribution function that is reasonably log-normal. For this purpose the log E-values can be plotted on normal probability paper. The problem is that, even when these values are from a perfectly log-normal population, the plot may deviate rather much from a straight line, when the number of tests is small (appendix C). Engineering judgment must be used if the plot shows a systematic deviation from a straight line.

Now it will be assumed that there is no reason to doubt the log-normality of the E-values. The median E and standard deviation $\hat{\lambda}$ can be calculated with equations (5.9) and (5.10). $\bar{E}$ and $\hat{\lambda}$ are estimates of the median E_m and standard deviation Λ of the population. As already shown in chapter 6 manufacturers do not agree whether factor F should be based on specimen or coupon test results. If a priori it is assumed that the standard deviation is known and is equal to that of the coupon tests, factor F is equal to (equation 6.6)

$$F = 10^{-\Lambda(U_p + U_\beta/\sqrt{n})}$$

If on the other hand this assumption is not made and if results of specimen tests are used, factor F is equal to (equation 6.9)

$$F = 10^{-\hat{\lambda}K(p,\beta,n)}$$

For $\beta = 0.99$, $p = 0.95$, $n = 6$ and $\hat{\lambda} = \Lambda = 0.05$, factor F is 0.742 and 0.536 respectively. As shown in figure 6 this difference in factor F may correspond with a factor of nearly 100 in calculated safe life. In the next chapter, an expression for F is proposed that combines the two views.

8 PROPOSAL FOR FACTOR F

It is assumed that scatter in test results depends on properties of the test items and on properties of the testing machine or apparatus. Both types of scatter are independent of each other. For the population of coupon tests the variance is

$$\Lambda^2_{\text{coup}} = \Lambda^2_{\text{coup. mat}} + \Lambda^2_{\text{mach.}} \tag{8.1}$$

$\Lambda_{\text{coup.mat}}$ is the standard deviation of the endurance limits of the coupons that depends on the type of material and the quality of fabrication of the coupons. Λ_{mach} is the standard deviation of scatter due to the testing machine. For the population of endurance limits of a certain specimen test the variance is

$$\Lambda^2_{\text{spec}} = \Lambda^2_{\text{spec. mat}} + \Lambda^2_{\text{app.}} \tag{8.2}$$

Λ_{app} is the standard deviation of scatter due to the apparatus used for the specimen test.
$\Lambda_{\text{spec.mat}}$ is the standard deviation of the endurance limits of the specimens, that depends on the type of material and the quality of fabrication of the specimens.

Two cases will be considered

A: It can not be assumed that scatter due to type of material and quality of fabrication of coupons and specimens are equal.

$$\Lambda_{\text{spec. mat}} \neq \Lambda_{\text{coup. mat}} \tag{8.3}$$

In this case the scatter in the specimen test results bears no relation to the scatter of the coupon test results. Both mean and standard deviation of the specimen test results are estimates for mean and standard deviation of the population. The appropriate statistical quantity to be used in this case to define the statistically safe endurance limit is the one-sided tolerance limit (equation 6.9).

B: It can be assumed that scatter due to type of material and quality of fabrication of coupons and specimens are equal.

$$\Lambda_{\text{spec. mat}} = \Lambda_{\text{coup. mat}} = \Lambda_{\text{mat}} \tag{8.4}$$

The estimate $\bar{E}$ for the median E_m of the specimens is based on the outcome of specimen tests and it has the standard deviation $\Lambda_{\text{spec}}/\sqrt{n}$. Scatter of the estimate $\bar{E}$ depends on scatter in material properties and on scatter due to the testing apparatus. However Λ_{spec} is not known. Only an estimate, viz. ℓ_{spec}, is available and Student's t-distribution has to be used to establish the lower confidence limit of the mean. With confidence β it can be stated that

$$E_m > \bar{E} \cdot 10^{-\frac{c}{\sqrt{n}}\ell_{\text{spec}}} = F_1 \bar{E} \tag{8.5}$$

c can be found in tables for Student's t-distribution, and is equal to 3.37 for n = 6 and β = 0.99.
For $\ell_{\text{spec}} = 0.05$, factor $F_1 = 0.8535$

Scatter in endurance limits of the components depends only on scatter in material properties, not on scatter due to testing apparatus. A proportion p of the population will have an endurance limit, that exceeds

$$E(p) = E_m \, 10^{-U_p \Lambda_{\text{mat}}} \tag{8.6}$$

The value Λ_{mat} is not known. From equations (8.1) and (8.4) it follows that

$$\Lambda_{\text{mat}} = \Lambda_{\text{coup mat}} = \sqrt{\Lambda^2_{\text{coup}} - \Lambda^2_{\text{mach}}} < \Lambda_{\text{coup}} \tag{8.7}$$

and this gives

$$E(p) = E_m \, 10^{-U_p \Lambda_{\text{mat}}} > E_m \, 10^{-U_p \Lambda_{\text{coup}}} = F_2 E_m \tag{8.8}$$

With the assumptions given above it can be stated with confidence β that a proportion at least equal to p of the specimens will have an endurance limit that exceeds

$$E_{\text{red}} = F_1 F_2 \bar{E} = F \bar{E} \tag{8.9}$$

with

$$\boxed{F = 10^{-\frac{c}{\sqrt{n}}\ell_{\text{spec}} - U_p \Lambda_{\text{coup}}}} \tag{8.10}$$

For β = 0.99, p = 0.95, n = 6 and $\ell_{\text{spec}} = \Lambda_{\text{coup}} = 0.05$, factor F is

$$F = F_1 F_2 = 10^{-0.0688} \cdot 10^{-0.08225} = 0.8535 \times 0.8275 = 0.706$$

In this expression for factor F scatter of the specimen tests is used to define the lower confidence limit of the median of specimen endurance limits. Scatter of coupon tests is used to ensure that a certain proportion will exceed the reduced endurance limit.

It will be clear that the choice of values for confidence β and proportion p needs some consideration.

The factor should be in accordance with those previously used for a well defined specimen test with a relatively large number of specimens and low scatter. Various combinations of β and p can be used. It is felt that confidence β should be at least equal to proportion p. The value for β is used to calculate the lower confidence limit of the median of the population. In 100 β per cent of the tests the median of the population will be higher then the lower confidence limit. However in 100 (1-β) per cent of the tests the median will be lower. This affects the entire fleet. If the estimate of the median is equal to the median of the population a proportion (1-p) will have an endurance limit lower then the reduced endurance limit.

For β = 0.99 and p = 0.95 curves for factor F are given in figure 9.

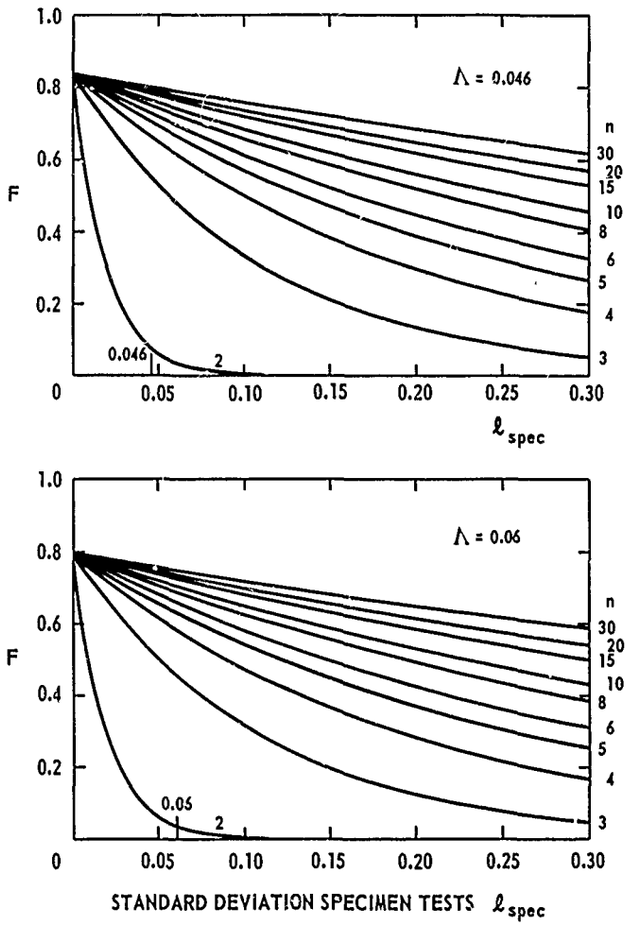


Fig. 9 Factor F for confidence β=0.99 and proportion p=0.95

9 CONCLUSIONS

1 There appears to be agreement between the majority of helicopter manufacturers with regard to the general procedures to determine the safe fatigue life of helicopter dynamic components.

2 The mean S-N curve is multiplied with a reduction factor to obtain the safe S-N curve. This reduction factor turns out to have a major effect on the calculated fatigue lives.

3 In this paper, an expression for the reduction factor is proposed, that takes into account the results of both specimen and coupon tests.

10 REFERENCES

1. Helicopter fatigue. A review of current requirements and substantiation procedures. Five papers presented at the 47th meeting of the Structures and Materials panel held in Florence, Italy on 25-29 September 1979. AGARD Report No. 674, February 1979.
2. R.A. Wolfe, R.W. Arden, U.S. Army helicopter fatigue requirements and substantiation procedures, pages 1-12 of reference 1.
3. A.D. Hall, Helicopter fatigue evalution (The U.K. Approach) pages 13-20 of reference 1.
4. F. Och, Fatigue life estimation methods for helicopter structural parts, pages 21-27 of reference 1.
5. P.Alli, Present fatigue analysis and design of helicopters - Requirements and qualification procedures, pages 29-46 of reference 1.
6. F. Liard, Fatigue des helicopteres - Methode d'evaluation des durées de vie (In French and English), pages 47-69 of reference 1.
7. Proceedings of the AHS (American Helicopter Society) Midwest Region Helicopter fatigue methodology specialists' meeting. March 25-27, 1980, St. Louis, Missouri.
8. R.W. Arden, Hypothetical fatigue life problem, paper no. 18 of reference 7.
9. G. Stievenard, Hypothetical fatigue life problem. Application of Aerospatiale method. Paper no. 19 of reference 7.
10. G. Aldinio, P. Alli, The Augusta solution of AHS' hypothetical fatigue life problem. Paper no. 20 of reference 7.
11. G.W. McCloud, A method of determining safe service life for helicopter components (Bell Helicopter). Paper no. 21 of reference 7.
12. G.H. Thompson, Boeing Vertol fatigue life methodology. Paper no. 22 of reference 7.
13. J.McDermott, Hughes Helicopters - fatigue life methodology. Paper no. 23 of reference 7.
14. C.P. Hardersen, Fatigue life prediction of helicopter pitch link using Kaman life calculation methods. Paper no. 24 of reference 7.
15. B. Altman, J. Pratt, The challenge of standardizing fatigue methodology (Sikorsky Aircraft). Paper no. 25 of reference 7.
16. Fatigue evaluation of rotorcraft structure.Advisory circular No. 20-95. Federal Aviation administration, 5/18/76.
17. Structural design requirements (helicopters). Aeronautical Requirements - 56. Naval Air Systems Command 1 July 1954.
18. J.P. Ryan et al, Helicopter fatigue load and life determination methods. U.S. Army Air Mobility Research and Development Laboratory - TR-75-27. Aug. 1975.
19. A.D. Hall, The fatigue substantiation of the Lynx helicopter. Aircraft Engineering, October 1975.
20. W. Weibull, Fatigue testing and analysis of results.Pergamon Press, London, 1961.
21. A. Wald, J. Wolfowitz, Tolerance limits for a normal distribution.Reprinted in Selected papers in statistics and probability by Abraham Wald. Mc Graw-Hill Book Company Inc, New York 1955.
22. Mary Gibbons Natrella, Experimental Statistics, National Bureau of Standards Handbook 91,issued August 1, 1963, reprinted October 1966 with corrections. United States Department of Commerce.
23. E. Jarosch, A. Stepan, Fatigue properties and test procedures of glass reinforced plastic rotorblades 25th Annual National Forum of the American Helicopter Society, Paper No. 370, May 1969.
24. F.H. Immen, Critique and summary of the specialists meeting on Helicopter design mission load spectra, Agard-CP-206, August 1976.
25. Statistical methods, ISO Standards Handbook 3. International Organization for Standardization, 1979.
26. T. Shimokawa, Y. Hamaguchi, Relationship between scatter of fatigue life and S-N curve of 2024-T4 Aircraft Structural Aluminum Alloy specimens with a sharp notch (K_t = 8.25) under a constant temperature and humidity condition. Report TR-412T, National Aerospace Laboratory, Chōfu, Tokyo, Japan, October 1977.
27. G.M. van Dijk, Statistical Load Data Processing. Proceedings, 6th ICAF Symposium, Miami, May 1971 (Also NLR MP 71007 U).
28. T. Shimokawa, A new plotting method to estimate the population parameters of the normal distribution. Report TR-464 T, National Aerospace Laboratory, Chōfu, Tokyo, Japan, November 1977.
29. S.S. Shapiro, M.B. Wilk, An analysis of variance test for normality (complete samples). Biometrika 52 (1965) p. 591-611.

APPENDIX A

NORMAL AND LOG-NORMAL DISTRIBUTION APPROXIMATED BY A WEIBULL DISTRIBUTION.

Suppose a variable X has a normal or log-normal distribution function and that this distribution will be approximated to by a Weibull distribution. Various criteria could be used. A reasonable criterium seems to be to equalize the first and second derivative at the median x_m.

In the following the logarithm with base 10 and base e will be indicated with "log" and "ln", respectively.

Distribution function F(x), median x_m for which F(x) = 0.5, the first and second derivatives for the three distribution functions are as follows:

Normal distribution function:

$$F(x)= \int_{-\infty}^{x} \frac{1}{\sqrt{2\pi}\,\sigma} \exp\left\{ - \frac{(t-\mu)^2}{2\sigma^2} \right\} dt \qquad (A1)$$

$$x_m = \mu$$

$$\frac{dF}{dx} = \frac{1}{\sqrt{2\pi}\,\sigma} \exp\left\{ - \frac{(x-\mu)^2}{2\sigma^2} \right\} \qquad \left\{ \frac{dF}{dx} \right\}_{x_m} = \frac{1}{\sqrt{2\pi}\,\sigma} \qquad (A2)$$

$$\frac{d^2F}{dx^2} = - \frac{1}{\sqrt{2\pi}} \frac{(x-\mu)}{\sigma^3} \exp\left\{ - \frac{(x-\mu)^2}{2\sigma^2} \right\} \qquad \left\{ \frac{d^2F}{dx^2} \right\}_{x_m} = 0 \qquad (A3)$$

Log-normal distribution function:

$$F(x) = \int_{0}^{x} \frac{1}{\sqrt{2\pi}\,\Lambda} \exp\left\{ - \frac{(\log t - A)^2}{2\,\Lambda^2} \right\} \frac{dt}{t \ln 10} \qquad (A4)$$

$$x_m = 10^A$$

$$\frac{dF}{dx} = \frac{1}{\sqrt{2\pi}\,\Lambda \ln 10} \exp\left\{ - \frac{(\log x - A)^2}{2\,\Lambda^2} \right\} \frac{1}{x} \qquad \left\{ \frac{dF}{dx} \right\}_{x_m} = \frac{1}{\sqrt{2\pi}\,\Lambda \ln 10\, x_m} \qquad (A5)$$

$$\frac{d^2F}{dx^2} = - \frac{1}{\sqrt{2\pi}\,\Lambda \ln 10} \exp\left\{ - \frac{(\log x - A)^2}{2\,\Lambda^2} \right\} \left\{ \frac{\log x - A}{\Lambda^2 \ln 10} + 1 \right\} \frac{1}{x^2} \qquad (A6)$$

$$\left\{ \frac{d^2F}{dx^2} \right\}_{x_m} = - \frac{1}{\sqrt{2\pi}\,\Lambda \ln 10\, x_m^2} \qquad (A6a)$$

Weibull distribution function:

$$F(x)= 1 - \exp\left\{ - \left(\frac{x-\gamma}{q}\right)^p \right\} \qquad F(x)=0 \text{ for } x < \gamma \qquad (A7)$$

$$x_m = q(-\ln 0{,}5)^{1/p} + \gamma$$

$$\frac{dF}{dx} = \frac{p}{q} \left(\frac{x-\gamma}{q}\right)^{p-1} \exp\left\{ - \left(\frac{x-\gamma}{q}\right)^p \right\} \qquad \left\{ \frac{dF}{dx} \right\}_{x_m} = \frac{p}{2q} (-\ln 0.5)^{\frac{p-1}{p}} \qquad (A8)$$

$$\frac{d^2F}{dx^2} = \frac{p}{q^2} \left(\frac{x-\gamma}{q}\right)^{p-2} \exp\left\{ - \left(\frac{x-\gamma}{q}\right)^p \right\} \left\{ p-1-p\left(\frac{x-\gamma}{q}\right)^p \right\} \qquad (A9)$$

$$\left\{ \frac{d^2F}{dx^2} \right\}_{x_m} = \frac{p}{2q^2} (-\ln 0.5)^{\frac{p-2}{p}} \{ p-1+p \ln 0.5 \} \qquad (A9a)$$

Equalization of median, first and second derivative gives:
for the normal distribution

$$p = \frac{1}{1+\ln 0.5} = 3.2589 \tag{A10}$$

$$q = \sqrt{\frac{\pi}{2}}\ \sigma \frac{(-\ln 0.5)^{\frac{p-1}{p}}}{1+\ln 0.5} = 3.1681\ \sigma \tag{A11}$$

$$\gamma = \mu - C\sigma \qquad C = -\sqrt{\frac{\pi}{2}}\ \frac{\ln 0.5}{1+\ln 0.5} = 2.8311 \tag{A12}$$

for the log-normal distribution

$$p = \frac{1}{1+\ln 0.5 - \sqrt{\frac{\pi}{2}}\ \ln 0.5\ \Lambda \ln 10} = \frac{3.2589}{1+C\,\Lambda \ln 10} \tag{A13}$$

$$q = x_m\, p\, \Lambda \ln 10 \sqrt{\frac{\pi}{2}}\ (-\ln 0.5)^{\frac{p-1}{p}} \tag{A14}$$

$$\gamma = \frac{x_m}{1+C\ \Lambda \ln 10} \sim x_m - C\, x_m\ \Lambda \ln 10 \tag{A15}$$

The value at which a Weibull distribution function, approximated to a normal distribution function, will be truncated, will always be at the mean minus 2.8311 σ. Approximately the same is true for a Weibull distribution, approximated to a log-normal distribution as the standard deviation is approximately equal to $x_m\ \Lambda \ln 10$. Weibull approximations for normal and log-normal distributions are given in figure A1.

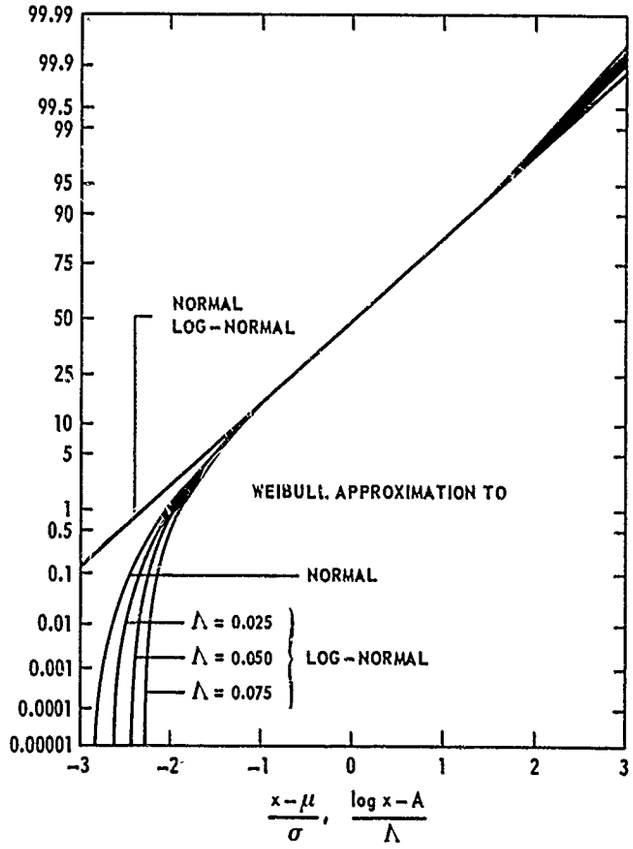


Fig. A1 Weibull approximation for normal and log-normal distributions

APPENDIX B

ANALYSIS OF 252 FATIGUE TEST RESULTS.

The results of fatigue tests on 252 notched aluminium alloy coupons are presented and analyzed in reference 26 The results are also presented in figure 7, which is reproduced from reference 26. A slightly different analysis is given in the following.

The tests were carried out at nine stresslevels S_j on n_j coupons. The number of cycles to failure is N_{ij}

From each testresult (S_j, N_{ij}) an estimate E_{ij} for the endurance limit is derived, using the Weibull S-N curve shape

$$S=E+\frac{A}{(N+B)^{K}} \tag{B1}$$

The constants A, B and K are chosen such that the variance of the logarithm of the E_{ij}-values is a minimum.

The variance

$$\ell^2=\frac{\sum_j\sum_i (Y_{ij}-m)^2}{n-1} \tag{B2}$$

$$\text{with } Y_{ij}=\log E_{ij} \tag{B2a}$$

$$E_{ij}=S_j-\frac{A}{(N_{ij}+B)^{K}} \tag{B2b}$$

$$m=\frac{\sum_j\sum_i Y_{ij}}{n} \tag{B2c}$$

$$\text{and } n=\sum_j n_j \tag{B2d}$$

is a minimum for

$$\begin{aligned} K &= 0.564 \\ A &= 3.4266 \\ B &= 0.050 \end{aligned} \tag{B3}$$

With these values the mean m_j and the standard deviation ℓ_j, pertaining to the various stress levels can be calculated

$$m_j=\frac{\sum_i Y_{ij}}{n_j} \tag{B4}$$

$$\ell_j^2=\frac{\sum_i (Y_{ij}-m_j)^2}{n_j-1} \tag{B5}$$

These values are given in table B1.

TABLE B 1

Statistical data

stress level S_j	number of coupons n_j	mean m_j	standard deviation ℓ_j	lower limit μ	upper limit μ	lower limit Λ	upper limit Λ
22	21	0.7826977	0.0118347	0.777	0.788	0.0091	0.0171
21	30	0.7610314	0.0160620	0.755	0.767	0.0128	0.0216
18	30	0.7217473	0.0233504	0.713	0.730	0.0186	0.0314
15	30	0.7681646	0.0227018	0.760	0.777	0.0181	0.0306
12	30	0.7786293	0.0225405	0.770	0.787	0.0180	0.0303
10	30	0.7907578	0.0250865	0.781	0.800	0.0200	0.0338
8	30	0.7552585	0.0183169	0.748	0.762	0.0146	0.0247
7	30	0.7243482	0.0216167	0.716	0.732	0.0172	0.0291
6.5	21	0.7297790	0.0168953	0.722	0.737	0.0129	0.0244
all levels	252	0.7569858	0.031827	0.753	0.761		
ℓ_{mat}	252		0.0202587			0.01865	0.02222

If the assumptions made so far are right, each of the mean values m_j can be regarded as an estimate of the mean μ. Assuming a normal distribution for Y_i it follows that

$$m_j - \frac{c\,\ell_j}{\sqrt{n_j}} \leq \mu \leq m_j + \frac{c\,\ell_j}{\sqrt{n_j}} \qquad \text{(B6)}$$

The value for c is determined by Student's t-distribution. For confidence $\beta = 0.95$ the values for c are

$$\begin{aligned} &\text{for } n_j = 21 \quad c = 2.09 \\ &\text{for } n_j = 30 \quad c = 2.04 \\ &\text{for } n_j = 252 \quad c = 1.96 \end{aligned} \qquad \text{(B7)}$$

Lower and upper limits for μ are given in table B1 and figure B1.

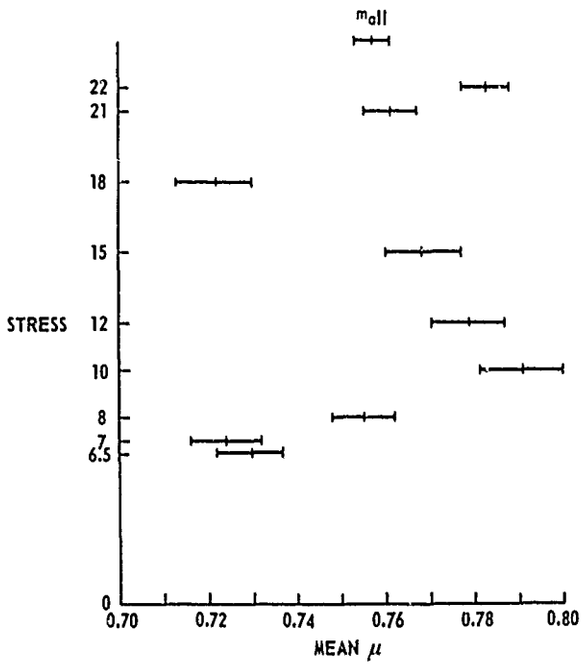


Fig. B1 Confidence intervals of means

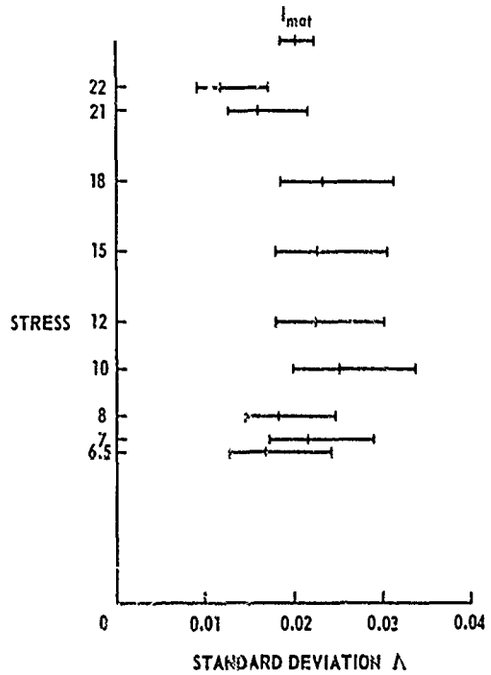


Fig. B2 Confidence intervals of standard deviations

The confidence intervals are not in agreement with each other. For example the interval based on all measurements is overlapped by only three confidence intervals. Therefore it is concluded that the means thus obtained are not estimates for the mean of the population. It is assumed now that for each stresslevel an error exists. This error could be due to an error in the assumed S-N curve shape or to a systematic error in the stress S_j. The best estimate for this error is

$$\delta_j = m_j - m \qquad \text{(B8)}$$

This will be used to find new estimates for the endurance limit.

$$Z_{ij} = Y_{ij} - \delta_j \qquad \text{(B9)}$$

or $$\tilde{E}_{ij} = c_j E_{ij} \qquad \text{(B10)}$$

$$\text{with } c_j = 10^{m - m_j} = \frac{E_m}{E_j} \qquad \text{(B11)}$$

The revised S-N curve shape becomes

$$S = \frac{\tilde{E}}{c_j} + \frac{A}{(N+B)^K} \qquad \text{(B12)}$$

The totel error $\Sigma\Sigma(Y_{ij} - m)^2$ will now be split up in two parts. One part is due to the error described above, the other part will be attributed to material properties.

$$\sum_j \sum_i (Yij - m)^2 = \sum_j \sum_i (Y_{ij} - m_j + m_j - m)^2$$

$$= \sum_j \sum_i (Y_{ij} - m_j)^2 + 2 \sum_j (m_j - m) \sum_i (Y_{ij} - m_j) + \sum_j n_j (m_j - m)^2$$

$$= \sum_j \ell_j^2 (n_j - 1) + \sum_j n_j (m_j - m)^2 \qquad \text{(B13)}$$

and it follows that

$$\ell^2 = \frac{\sum_j \sum_i (Y_{ij} - m)^2}{n-1} = \frac{\sum_j \ell_j^2 (n_j - 1)}{n-1} + \sum_j n_j \frac{(m_j - m)^2}{n-1} = \ell^2_{mat} + \ell^2_{mach}. \qquad \text{(B14)}$$

ℓ_{mat} is the variance due to material properties. ℓ_{mach} is the variance due to the testing machine and deviations of the assumed S-N curve shape.

The values ℓ_j can be regarded as an estimate for the standard deviation Λ of the population. Assuming a normal distribution for Y_i it follows that

$$\sqrt{\frac{n_j - 1}{c_2}}\, \ell_j < \Lambda < \sqrt{\frac{n_j - 1}{c_1}}\, \ell_j \qquad \text{(B15)}$$

The values for c_1 and c_2 are determined by the chi- square distribution. For confidence $\beta = 0.95$ the values c_1 and c_2 are

for $n_j = 21$ $\quad c_1 = 9.59 \quad c_2 = 34.17$
$n_j = 30 \quad c_1 = 16.0 \quad c_2 = 45.7$
$n_j = 252 \quad c_1 = 208.6 \quad c_2 = 296.3$

Lower and upper limits are given in table B1 and figure B2. All confidence intervals, except one, have an overlap and it is concluded that all values ℓ_j are an estimate for Λ, the best estimate being ℓ_{mat}

It is now assumed that the corrected endurance limits $\tilde{E}$ have a log-normal distribution. The median is $E_m = 5.7146 = 10^{\mu}$, with $\mu = m = 0.7569858$ and the standard deviation is $\Lambda = \ell_{mat} = 0.0202587$.
The distribution of $Z = \log \tilde{E}$ is given in figure B3.

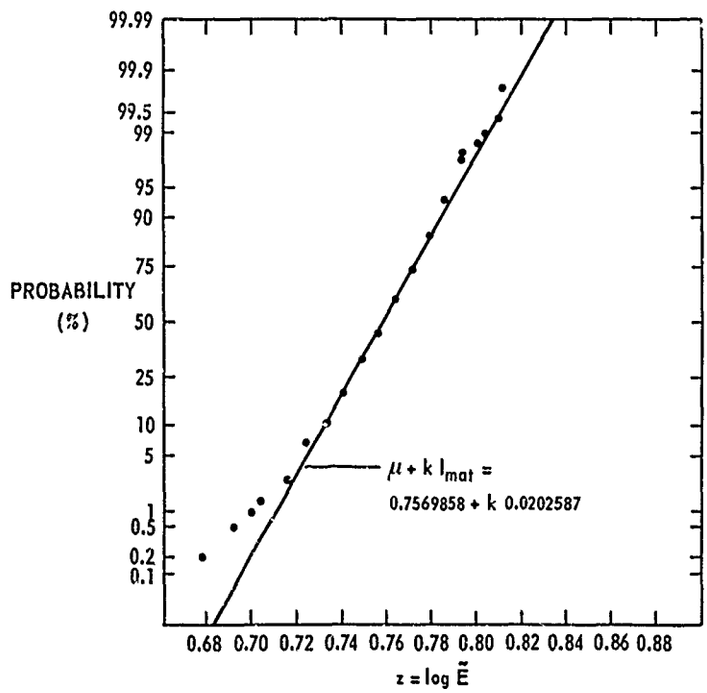


Fig. B3 Probability distribution of the corrected endurance limits

The proportion p of the population that will have an endurance limit higher then $E(p)=10^{\mu-k\Lambda}$ is defined by

$$\int_{-\infty}^{k} \frac{1}{\sqrt{2\pi}} e^{-\frac{t^2}{2}} dt. = p \qquad \text{(B16)}$$

and this can be found in tables of the normal distribution.

The fatigue life $N_j(p)$ that will be exceeded by a proportion p of the population can now be calculated with the revised S-N curve shape (equation B12)

$$N_j(p) = \left| \frac{A}{S_j - \frac{E(p)}{c_j}} \right|^{1/\kappa} - B \qquad \text{(B17)}$$

Probability distribution functions $N_j(p)$, with parameter S_j, are given in figure 8 and show good agreement with the measured probability distributions.

APPENDIX C

NORMALITY OF DISTRIBUTIONS.

Suppose a variable X has a normal distribution with mean $\mu = 0$ and standard deviation $\sigma = 1$.
A sample of size n is drawn from this population and plotted on normal probability paper (reference 25).
For the determination of the probability $P(x_i)$ several alternative methods exist (reference 28). The following expression will be used here.

$$P(x_i) = \frac{i-0.5}{n} \qquad (C1)$$

One expects this plot to be a straight line passing through $x = 0$, $P(x) = 0.50$ and with slope, indicating $\sigma = 1$.
Ten samples of size $n = 6$, drawn from a normal population ($\mu = 0$, $\sigma = 1$) are plotted in figure C1.

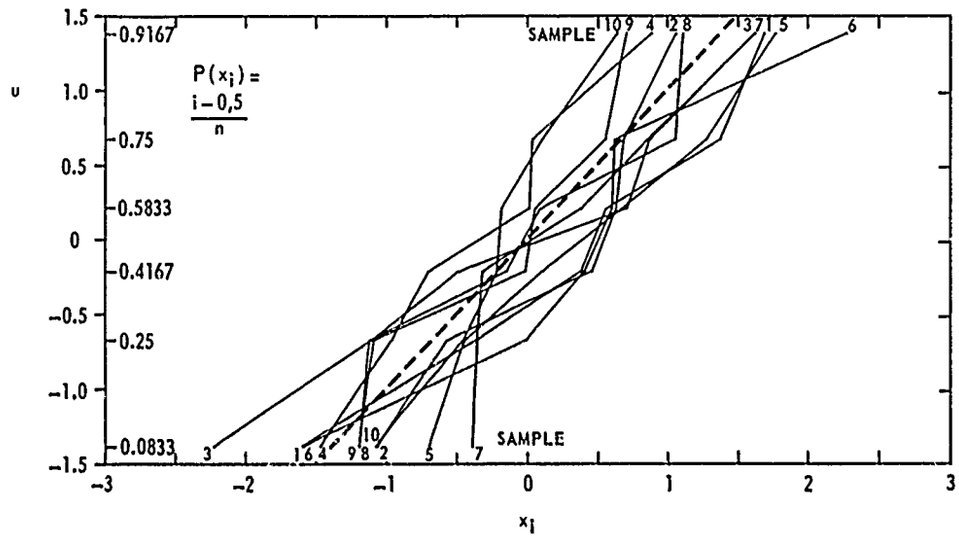


Fig. C1 Ten samples of size 6 from a normal population

This figure shows clearly that deviations from the theoretical straight line may be large.

Many methods exist to test the normality of a sample. A test that can be used for small samples is described in reference 29.

In the following a statistic v will be considered that gives an impression of the deviations to be expected.

A sample of size n of the variable X is normalized to

$$y_i = \frac{x_i - m}{s} \qquad (C2)$$

$$\text{with } m = \frac{\Sigma x_i}{n} \qquad (C3)$$

$$s = \sqrt{\frac{\Sigma(x_i - m)^2}{n-1}} \qquad (C4)$$

The normalized values of the ten samples of figure C1 are plotted in figure C2.

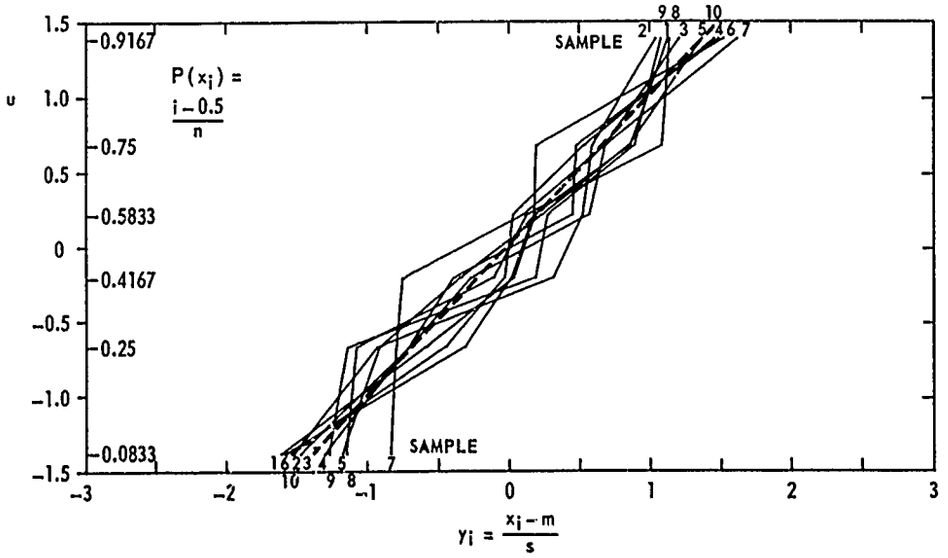


Fig. C2 Ten normalized samples of size 6 from a normal population

The statistic ν is defined as

$$\nu = \sqrt{\frac{\sum_{i=1}^{n} (y_i - u_i)^2}{n-1}} \qquad (C5)$$

In which the quantity u_i is defined with

$$\int_{-\infty}^{u_i} \frac{1}{\sqrt{2\pi}} \exp(-\frac{t^2}{2}) \, dt = \frac{i-0.5}{n} \qquad (C6)$$

For 1000 samples of size n from a population with normal distribution ($\mu = 0$, $\sigma = 1$) the statistic ν was calculated.
Values for ν exceeded by 5, 10, 50 and 90, per cent of the samples are given in figure C3.
The samples of figure C1 and C2 have values for ν between 0.17 and 0.36.

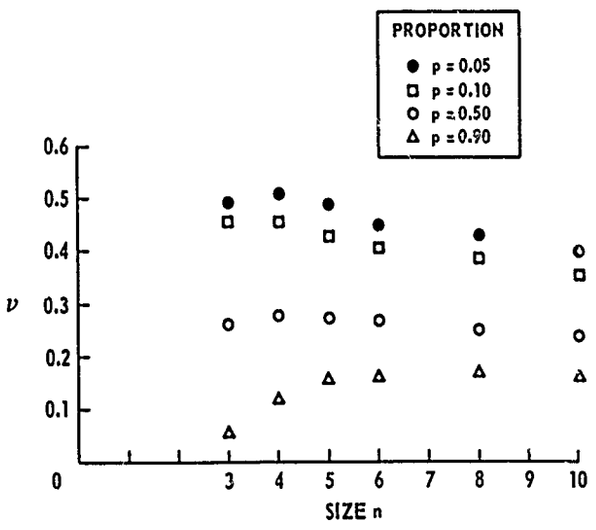


Fig. C3 Values of ν exceeded by a proportion p of the samples

FATIGUE ASSESSMENT OF UK MILITARY AEROPLANES

by

J I M Forsyth

Airworthiness Division, Structures Department
Royal Aircraft Establishment
Farnborough, Hants GU14 6TD
England

SUMMARY

This paper outlines the approach to the fatigue assessment procedures used in the United Kingdom to derive the life of military aeroplanes. It describes these procedures at all stages from the initial specification of the mission profile to the monitoring of Service use. It also indicates the present thinking on fatigue assessment procedures for fibre reinforced plastic and damage tolerant structures as well as the latest work on loads measurement and in-service monitoring.

1 INTRODUCTION

The requirements for the design of structures of United Kingdom Military aeroplanes against fatigue are contained in Aviation Publication No 970 (AvP 970). This document consists of a number of mandatory chapters together with associated advisory leaflets. The leaflets relating to fatigue are currently in need of revision. In this circumstance the design procedures and practices adopted recently have been agreed project by project, Structures Department advising the Project Directors in the light of the latest available knowledge.

This paper deals with the procedures that are in use now for ensuring an acceptable fatigue performance. They provide for compliance with the mandatory design requirements and for the subsequent monitoring of Service usage.

The fatigue assessment procedures can be considered under three general headings:-

(1) Estimation of the load spectra and hence the stress spectra for the various parts of the aeroplane structure.

(2) Assessment of the fatigue performance of these parts when subjected to the estimated spectra.

(3) Monitoring the fatigue usage of these parts when subjected to the actual service load spectra and environmental conditions.

Together they form a continuous sequence through all the stages of the design, development, production and in-service use of a project.

This paper describes the sequence in detail, and concludes by indicating the latest thinking on damage tolerant and composite structures, loads measurement and in-service fatigue monitoring.

This paper expresses the views of the author and does not necessarily represent the official view of the Royal Aircraft Establishment.

2 THE AEROPLANE SPECIFICATION

When a new type of aeroplane is proposed its specification includes a statement of the fatigue life that will be required in-service. Usually this is the life that will be expected, under a particular load spectrum agreed with the operators, from all aeroplanes of the type including those which, due to scatter in fatigue performance, prove to be the weakest members of the fleet. For the best assurance that the structure will be both safe and efficient it is essential for the designer to know as accurately as possible how the aeroplane will be used. This means that the role or roles in which the aeroplane will operate must be clearly and precisely defined. It is also essential that the definition of the roles must be sufficiently detailed to allow accurate load spectrum estimates to be made.

The details should include:-

(1) The types of role for which the aeroplane will be used.

(2) The length of time spent in each role.

(3) The operating weights, together with armament and fuel distribution, for each of the roles.

(4) The flight profiles for each role.

(5) The number of landings.

(6) The number of cabin pressurizations.

From this information average load spectra can be estimated, using both generalised design data and information from records taken on other existing aeroplanes in similar roles.

The specification must state whether the structure is to be designed to safe-life or damage-tolerance principles. In the latter case the specification needs to include the servicing intervals upon which the damage-tolerance inspection schedule can be based.

Inevitably in the course of service the weight of the aeroplane increases and changes of usage occur. Generally some allowance for these eventualities is made in the design but often the changes are more severe than the designer could anticipate.

3 FATIGUE CLEARANCE PHILOSOPHY

The general philosophy for lifing aeroplanes in the UK is that the weakest member of the fleet shall have a low probability of failure during the specified life. This is attained in practice by dividing either the calculated or the test life by a factor of safety, to obtain a service life within which there is a low statistical probability of failure. In service, checks are kept on the usage by means of a fatigue meter to determine the fatigue life consumed in any period of operation. This philosophy is vindicated by the acceptable standard of safety that has been achieved over a period of many years.

3.1 Factors

Analysis of structures tested under variable-amplitude loading has shown that, when the mean life demonstrated by test is reduced by a factor of $3\frac{1}{3}$, a probability of failure about $1/1000$ is achieved. This is the factor that has been adopted to be applied to the life of the major fatigue test specimen. When individual parts are tested a factor of 5 for one test, or a lower factor for more than one test, is required.

Analysis of many tests on structural features has shown that, as an alternative to the use of a factor on life, the same probability of failure in service may be achieved by using a different factor to reduce the stresses. The strength factors are 1.4 for steels and 1.6 for aluminium and light alloys when six specimens are tested; larger factors are required if fewer than six tests are done. These factors account for scatter in fatigue strength and uncertainties in the stress analysis.

To cover the uncertainties caused by differences in loading from aeroplane to aeroplane in a fleet and by the determination of fatigue life by calculation only, extra factors are used. To allow for differences in loading a factor of 1.5 on life or 1.2 on strength is used. (If loads are monitored in-service, or are naturally limited, then this factor is omitted.)

If the life is to be determined by calculation alone then the life is reduced by a further factor of at least 2. In the case where a strength factor is to be used to determine a calculated life, a total factor of 3 is used.

All factors are continually under review.

3.2 Usage Monitoring

All UK military aeroplanes are fitted with fatigue meters. These instruments count the number of exceedences of particular levels of normal acceleration, measured at the centre of gravity of the aeroplane. As they record only centre of gravity acceleration they are of no direct value in assessing the fatigue damage due to any asymmetric manoeuvres. However they do enable an estimate to be made of the aeroplanes' usage.

After every sortie a formula is used to estimate the total fatigue life that has been consumed by each aeroplane. There may be more than one formula for a particular aeroplane, to take care of different structural features. The counts of normal acceleration at the various 'g' levels are multiplied by coefficients derived from the results of the fatigue test and from the S-N curve for the part involved. Other coefficients and factors are used, with data from the sortie record, to take account of the ground-air cycle, the type of role, the all up mass, stores carried etc.

4 ESTIMATION OF LOAD SPECTRA

The loads that make up the load spectra for any particular type of aeroplane arise from several sources. These can be listed as:-

(1) Gust loads due to atmospheric disturbances.

(2) Manoeuvring loads in flight.

(3) Loads on the ground due to taxying, take off and landing.

(4) The ground-air cycle.

(5) Cabin and fuel tank pressurization.

(6) Other loads.

These sources will affect different types of aeroplanes in different ways. If the damage caused by loads from one source is a very small proportion of the total damage then this source would be ignored in the design calculations. For example gust loads on a large aeroplane with a relatively low wing loading can be as great as the manoeuvre loads and therefore will cause a significant amount of fatigue damage. On the

other hand the damage caused to a high speed, high-wing-loading type of aeroplane by gust loads is small compared to that caused by the manoeuvring loads, and for design purposes the effects of gust loading are often ignored.

For design purposes the load spectra are estimated from previous load measurements from similar types of aeroplanes used in a manner similar to that expected for the new design. As the design develops and instrumented prototypes fly then load measurements made on these aeroplanes allow the data to be refined.

Considering now the various load sources.

4.1 Gust Loads

These are derived from the flight profiles defined in the aeroplane specification. The numbers and magnitudes of gust loads are normally estimated in terms of the acceleration at the centre of gravity of the aircraft, using rigid body theory to derive the structural loads. In the case of large aeroplanes some allowance is made for structural flexibility. The fin is treated in a similar manner but an arbitrary factor of 3 is applied to the gust frequencies to cover all gust and manoeuvre cases, including the Dutch roll. The tailplane is designed on the balance loads with allowance for overswing loads during manoeuvres. The gust loads are highly significant on aeroplanes with a low wing loading where such loads contribute to a large proportion of the total wing fatigue damage.

4.2 Manoeuvre Loads

In general, manoeuvre loads on the wing and fuselage are derived from counting accelerometer records from comparable aeroplanes, which are analysed to obtain load spectra for each particular sortie type. As the counting accelerometer records only accelerations normal to the flight path, any asymmetric manoeuvres are not fully represented. Some account must be taken of such manoeuvres and generally rate-of-roll information is used to estimate the asymmetric loads. Tailplane loads have, in the past, been derived by considering the tail forces necessary to produce the various normal acceleration excursions at the centre of gravity of the aircraft. In general it has been found that such loads are about twice the balance loads.

Loads from this source contribute the major proportion of the fatigue damage to fighter, strike and advanced trainer aeroplanes.

4.3 The Ground-Air Cycle

The ground-air cycle is defined as the range through which the load on a part varies during a sortie. The ground-air cycle for a typical large aeroplane, expressed in terms of the normal acceleration at the centre of gravity, might extend from -0.3 g to +2.3 g. Account needs to be taken of the aeroplane configuration when the load range in a part is assessed. For example, take-off flap may induce higher loading in the rear spar area of large aeroplanes than at other times in the flight. Such loading is particularly likely at relatively low airspeed and high fuselage weight during a rolling pull-up turn. Ground-air cycles contribute the major portion of the fatigue damage in transport and strategic bomber aeroplanes.

4.4 Ground Loads

Loads produced during taxying and during the take-off and landing runs can be large enough to cause fatigue damage. Generally these loads are of significance only to the undercarriage and the attachment fittings but in large-span aeroplanes, especially those where the undercarriage is close to the fuselage, large amounts of fatigue damage may be caused to the upper surface of the wing. In such cases the inertia loads caused by engines and fuel in the wings can be particularly damaging to the centre-section top skin during take-off.

4.5 Other Loads

These are mainly associated with auxiliary parts such as flying controls, flaps, airbrakes etc. In these instances the local loading must be taken into account in the fatigue design. Another source is that of acoustic noise. This can produce fatigue-damaging loads by resonance at high frequencies. Unsupported panels are prone to this kind of damage.

4.6 Analysis

Once all the fatigue loads spectra have been estimated they are converted into stress spectra and a fatigue life is calculated for each part of the design. The stresses in fatigue-sensitive areas are calculated from the 'g' exceedences of the load spectra. As the design progresses and prototype aeroplanes fly with instrumentation the design may be modified in the light of the loads measured under actual flight conditions. It is important to know the utilization of the aircraft in some detail, because the normal acceleration at the centre of gravity must be associated with the aircraft mass and the flight conditions to obtain the correct stresses in the various parts.

5 ASSESSMENT OF FATIGUE LIFE

5.1 Initial Assessment

From the stress spectra and the S-N curves an initial assessment of the fatigue life of the aeroplane is made with the aid of Miner's Rule. The S-N data used by the designer are often obtained from test data on previous designs. If the design is a novel one and no relevant data exist then recourse is made to general information on the properties of materials. Then due allowance must be made for the various differences between the basic material and the component, eg stress concentrations, fretting etc. When calculation shows that a part will barely have sufficient safe life then fatigue tests are done as part of

the process of development to check the calculation. Such tests are preferably done under a realistic loading spectrum and may be done on a flight-by-flight basis.

5.2 Component Tests

Following the initial assessment of the fatigue life, critical areas of the structure will have been identified. Components or parts of the structure embracing these critical areas should be tested in order to gain confidence in the overall design.

5.3 Assignment of a Provisional Service Life

By the time that the first aeroplane enters service some development flying and component testing will have been done. It is unlikely that the major airframe fatigue test will have been completed. In order to safeguard the development and early service aeroplanes a provisional life for the airframe has to be assessed. This will be obtained by calculation based on the component fatigue tests so far obtained, using the best available S-N curves and an average load spectrum for the sortie or sorties expected to be flown. From these calculations a mean life will be obtained. Because of the lack of a major fatigue test to prove the validity of the fatigue calculation, allowance for this uncertainty is made by applying a factor of safety. This factor has to cover not only the uncertainties in the stressing and calculation of life, but also the scatter in the material properties as well as usage differences from aeroplane to aeroplane.

6 FULL SCALE FATIGUE TEST

There are many difficulties in making accurate assessments of the behaviour of structural components. The main causes of inaccuracies are the difficulties of identifying the critical features and determining the local load distributions within the components. For this reason it is now accepted that a fatigue test of a complete airframe is necessary to give confidence in the calculations and to show up any shortcomings in the assessment of the critical areas.

Normally the Test Specimen is an early production airframe to ensure that it is comparable with all the service aircraft. The test load spectrum is derived from a knowledge of the anticipated utilization of the aircraft and from load measurements made in development flying.

It is generally considered that all major loading actions should be represented in a fatigue test to obtain a reliable determination of both where and when the airframe is likely to suffer damage. The loads in the spectrum should be arranged in a realistic sequence so that the loading can be applied to the test specimen on a flight-by-flight basis. Within each 'flight' the gust and manoeuvre loads are applied in a random pattern unless there are known reasons why it is not appropriate to do so. On trainers, for example, it is acceptable to apply 10 to 12 set sequences of manoeuvre loads.

The test loads are normally the average loads expected to be experienced by all the aircraft in the fleet in their life-time. To cover manufacturing tolerances, variations in material properties and uncertainties in stressing, together with variations in usage, the test is continued for at least 5 times the specified life.

7 SERVICE LIFE

AvP 970 allows the designer the choice of designing the aeroplane to have either a safe-life or a fail-safe structure. The definition of fail-safe as given in AvP 970 is a structure which retains, after initiation of any fracture or crack, sufficient strength and stiffness to allow operation of the aeroplane with an acceptable standard of safety until the damage will be detected by inspection. To date no British Military aeroplanes, other than civil aeroplanes adopted for Military use, have been designed to have a fail-safe structure. However, in service many, if not all, aeroplanes are to a greater or lesser degree operated on a fail-safe basis. To understand how this system is operated it is best to consider first the manner in which the safe life of the structure is assessed.

During the test on the full-scale airframe various failures occur under the test load spectrum. These failures have to be related to the load spectra for the various service roles. To determine what service life shall be given to a particular area that has failed the following procedure is used:-

a. The S-N curve for the particular feature is adjusted, by multiplying the stresses by a factor, until the calculated life under the test load spectrum equals the test life to failure.

b. Using this adjusted S-N curve, the life in each of the various roles is calculated using Miner's Rule. The same curve is also used to determine the coefficients to be used in the fatigue meter formula.

c. The lives for each role are now factored to take account of scatter in fatigue performance. Generally for the airframe the number of load applications during the specified life is low enough to allow the use of a factor on life.

d. If the loads are not to be monitored in service then the further factor on life or on strength is required.

Those components with a safe life greater than the specified life will be treated on a safe-life basis. However, there are likely to be parts that will fail before the specified life of the aeroplane is consumed. Also there are likely to be failures in service which were unpredicted and not found during the full-scale fatigue test. Such failures will be assessed when they occur, to determine whether they can meet the fail-safe criterion or must be treated as safe-life items. This will entail fracture-mechanics calculations to estimate the growth of the largest crack that may remain undetected at the failure point under the stress spectrum associated with the failure area. Also crack propagation tests may well be done

on representative specimens, or may have been done on the full-scale fatigue test specimen, to assist in the determination of the inspection frequency. The operator will be consulted on these matters as he may prefer to replace components at regular intervals rather than inspect much more frequently.

At the end of the fatigue test the specimen is subjected to static-loading to determine its residual strength. Such a system has been found to work reasonably well and it is with this system of life assessment that the factor $3\frac{1}{3}$ is used.

8 FATIGUE MONITORING IN SERVICE

The monitoring procedure is described in paragraph 3.2. It enables the total life consumed and the rate of life consumption to be determined for each individual aeroplane. At appropriate stages lifed items can be changed and inspections for particular failures can be initiated.

Some areas, for example the tailplanes, are not covered by such monitoring. In these instances the life is normally assessed by counting the number of hours flown.

When an aeroplane which usually carries a fatigue meter is flown without one, the life is assumed to be consumed at 1.5 x the average rate of consumption prior to that flight.

The measurements of normal acceleration are made at the centre of gravity and hence do not record asymmetric manoeuvres adequately. Allowance for asymmetrical manoeuvres must thus be made without the aid of a direct monitoring system.

It can be seen that though the present method does give a large gain over unmonitored aeroplanes it leaves much to be desired in asymmetric flight. Also it does little to assist in the assessment of the true magnitude of the ground-air cycle. More advanced systems are needed to cover such requirements.

9 FUTURE DEVELOPMENT

This paper has dealt with the procedures for fatigue assessment of aeroplanes as presently practised in the UK. It has shown also certain deficiencies in various areas. The difficulties in the work of life assessment are well known and there is a continuing need for more knowledge in all the fields associated with this assessment. To conclude this paper it would seem appropriate to look into the near future to see what changes are likely to occur.

AvP 970, particularly the section on fatigue life assessment, is under active review. New requirements are in draft form covering the clearance of structures incorporating fibre reinforced plastic materials. Because these materials are sensitive to changes in their environment, particularly moisture, the major fatigue test may need to be more complex. The present indications are that composite structures have higher variability of fatigue life than metal structures. Because of this the major fatigue test is unlikely to give as great an assurance of performance for the composite parts as for the metal parts. It seems likely that the major fatigue test will be used to life the metal parts, and the composite parts will be cleared by element and component tests. Whether or not environmental conditions are applied to the major fatigue test will be a matter for debate. Clearly such measures would reduce the uncertainties of the test but any advantages will need to be weighed against the increased effort and cost. Such environmental conditions would however have to be applied to the element testing and possibly to the component testing.

New requirements are also being drafted for the design of damage-tolerant structures. Whilst these are broadly in agreement with the damage-tolerance concepts introduced in the US Mil Specs they differ from the US requirements in that they retain the requirement for the safe-life factor to be demonstrated. This is essential if unforeseen critical features are to be found with the usual degree of confidence. Inspectable areas where failures occur before completion of the full-scale fatigue test can be treated on a damage tolerance basis that has much in common with our present fail-safe approach. Uninspectable structure, however, does not have this option available and the life will be governed by the safe life shown by test.

It is envisaged that our design of future aeroplanes will be governed by both the 'composite' and the 'damage tolerance' requirements. For composites, compliance is likely to be demonstrated by a static strength test (covering early Service usage) followed by a major 'fatigue' test (possibly under environmental conditions). This major fatigue test may involve a factor on life together with a factor on loads to cover scatter in fatigue properties of composites. Following completion of the fatigue test, during which some parts may need to be repaired or replaced, the residual strength will be demonstrated.

In the field of loads measurement and analysis it is now generally accepted that the range-mean-pairs or rain-flow analysis is the optimum method. This background work is of great importance in the selection of future in-flight fatigue monitoring systems.

As mentioned earlier there are well recognised limitations to the present system of fatigue monitoring. Some method of assessing the fatigue loads on all the main units of the structure is needed.

One approach is to measure the loads and flight parameters under operational conditions on a few fully instrumented aeroplanes. These data are then analysed using statistical regression techniques to give load equations containing terms in all the flight parameters. Measurements of these parameters only on all aeroplanes then provides a means of load monitoring for fatigue life purposes.

Another method of monitoring entails the use of strain gauges on every major component on the aircraft. These gauges are located in carefully selected areas, well away from local stress concentrations. Records from these gauges then enable the loading to be found directly.

In both of these methods the signals would be fed into microprocessors in the flight data processing system. In this equipment the signal peaks and troughs are recognised and are converted into a range-mean-pairs matrix. Software development on microprocessors has achieved a capacity to handle a number of channels simultaneously and in real time. It is expected that there would be simultaneous monitoring of from 8 to 16 channels at 16 to 64 samples per second each from different areas located over the whole airframe.

From the range-mean-pairs analysis the fatigue damage at each sensitive location near the strain gauge installation can be assessed by using the S-N curve for the feature and Miner's Rule. There is a strong lobby to have this calculation done by the in-flight data processor and to give a read-out of the life consumed for each channel on each flight. This requires a different programme for each sensitive location. This is acceptable only where the fatigue tests are complete and the position of the S-N curve is established, as any large changes in the S-N curve position will invalidate all data and require re-programming of the load monitoring device. In the real world these criteria are unlikely to be satisfied.

Copyright ©
Controller HMSO London 1980

SYNOPSIS OF SPECIALISTS' MEETING ON HELICOPTER FATIGUE METHODOLOGY

Mr. Dean C. Borgman
Director of Advanced Systems
Dr. Daniel P. Schrage
Chief, Structures and Aeromechanics Division
Directorate for Development and Qualification
US Army AVRADCOM
4300 Goodfellow Boulevard
St. Louis, Missouri USA 63120

SUMMARY

This paper summarizes the principal results from the American Helicopter Society (AHS) Specialists' Meeting on Helicopter Fatigue Methodology held in St. Louis, MO, on March 25-27, 1980. The meeting was divided into six sessions. There were four general sessions representing the four essential elements of fatigue methodology--usage spectrum, flight loadings, component testing, and life calculations. In addition, an opening session included a keynote address and a review of the fundamentals, while a panel discussion on the last morning discussed the feasibility of standardization of helicopter fatigue methodology. A highlight of the meeting was the presentation of the manufacturers' fatigue methodology based on a calculated fatigue life of a hypothetical helicopter component.

The meeting served as an excellent forum for the exchange of information in a field of interrelated disciplines. While considerable participant feedback on the meeting has been obtained, this AGARD meeting presents a further assessment of the status of helicopter design.

INTRODUCTION

Helicopter fatigue methodology has been well defined in each helicopter company for many years, as commercial and military helicopter development couldn't have proceeded without it. However, the exchange of methodologies and fatigue information between companies has almost been nonexistent. There are several reasons for this situation. First, each company is liable for its own products so that a company proprietary exists. Second, since helicopter fatigue methodology encompasses several disciplines, there are usually only a few engineers in each company who understand its full application. Third, the variation in methods appears small and is not perceivable to all involved.

The large differences in fatigue lives caused by small variations in life determination methods were highlighted by the reference 1 study. The observations and conclusions drawn from the results of calculations of this study are summarized in Table 1. Further awareness came as a result of the US Army's UTTAS and AAH Development Programs. Each of these programs had two competing helicopter companies so that the US Army had the opportunity of assessing and comparing the fatigue methodologies of four companies. In recent years there have also been several composite blade development programs where fatigue methodologies could be reviewed. Reference 2 summarized these experiences of the US Army and called for a reexamination of the needs and objectives in determining fatigue lives. It also stated that the materials, equipment, tools and knowledge are available to develop a standardized method of establishing fatigue lives of dynamic components. The primary objective of the standardized method would be to eliminate excessive conservatism and consequently reduce the cost and weight of dynamic components without compromising safety.

With this background, the American Helicopter Society decided to proceed with the Specialists' Meeting on Helicopter Fatigue Methodology. The agenda for the meeting is presented in Table 2. The objective of the meeting was not only to bring together the fatigue specialists of industry and Government, but also to attract specialists of the various other disciplines interrelated with helicopter fatigue methodology. This included the helicopter operators, as they have the greatest understanding of how the helicopter will be operated once it is fielded. For this meeting, the US Army represented the helicopter operator. The US Army is fortunate in that it has just about every category of helicopter in its inventory, e.g., attack, cargo, scout, and utility. Since the usage spectrum is somewhat different for each of these categories, and is continually changing with new tactics, each representative from the US Army user community was asked to discuss the past, present, and future spectrums of each type helicopter. These presentations made up the first formal session of the meeting.

Session II was devoted to Helicopter Flight Loadings since these are the sources of the series of stresses that result in structural fatigue and form the complex helicopter dynamic environment. The sequence of the papers in this session was chronologically aligned with helicopter life calculations. The first paper dealt with helicopter rotor load predictions while the second and third papers dealt with the flight load survey and how data is acquired and interpreted. The final session paper discussed a flight condition recognition technique currently being evaluated on US Army operational helicopters to determine actual usage.

The third session dealt with component fatigue testing. Since rotor blades, controls, and drive system components have their own peculiarities with respect to fatigue testing, a paper was sought addressing each item. Additionally, with the large influx of composite materials into helicopter design, several papers were requested to discuss composite component testing.

Session IV was planned as the highlight of the Meeting. For this session, a means was sought which would allow each helicopter manufacturer the opportunity to apply its own methodology to a common fatigue problem. A hypothetical pitch link with given flight loads and component fatigue test results was chosen as a means of keeping the problem simple while simultaneously illustrating the differences in calculated lives due to various methodologies.

On the final morning of the meeting, a panel discussion on standardization of helicopter fatigue methodology was conducted. The purpose of this panel discussion was to summarize the meeting and determine if steps toward standardization were feasible and acceptable to the industry and government participants. The remainder of this paper will survey the results of each session and draw conclusions and recommendations.

OPENING SESSION

The Opening Session consisted of a keynote address and a review of the fundamentals of helicopter fatigue life determination. In the keynote address, the Speaker gave an excellent overview of the history of fatigue, its application to both fixed and rotary wing, and the technical management system called fatigue methodology. Having served as the Chief Structural Engineer at three different aircraft companies, he was able to draw on numerous individual experiences to highlight his presentation. The review of fundamentals presented by the second speaker in this session set the format for the meeting and helped to familiarize individual specialists with all aspects of fatigue life determination. A simple life calculation for a rotor blade root end section was used for illustrative purposes.

SESSION I--ARMY HELICOPTER MISSION SPECTRUMS (PAST, PRESENT, FUTURE)

Representatives from the US Army's Training and Doctrine Command (TRADOC) presented typical helicopter mission spectrums for four categories of helicopters. Past, present, and projected future missions were considered. The emphasis from the Attack Helicopter Presentation was that we must design our machines for the most stringent future profiles. It was also stressed that the user and designer must work together. The user must strive to describe realistic combat environments to the designer, and the designer must describe realistic and economical design points. The theme derived from the Cargo Helicopter Presentation was that the enemy threat has driven us to provide more maneuverable cargo systems which must be able to effectively work both day and night. A challenge was issued to the designers to develop logistical helicopters and cargo acquisition systems which reduce their vulnerability and simultaneously increase productivity.

In the presentation, "Evolution of the Aeroscout," a description was provided of how scout helicopter tactics were developed in Southeast Asia with the OH-6A. Quick stops, sideward and rearward flight, and rapid pedal turns occurred frequently but had not been encompassed in the manufacturer's design criteria.

During the Utility Helicopter Presentation, emphasis was again placed on designing for the most severe combat conditions. Future missions for the utility helicopter were described as, "quick, of short duration, very abrupt, and with high exposure to the very worst elements of combat."

There is no doubt that military helicopters in all mission categories must be designed to perform a variety of jobs, for long periods of time, under combat conditions. Therefore, the usage spectrum in modern military helicopter specifications is particularly severe. A logical question is whether fatigue lives based on these wide spectrums should apply in peacetime? If not, can fatigue lives be safely extended? An examination of this question was a primary purpose for this Meeting.

SESSION II--HELICOPTER FLIGHT LOADINGS

The prediction, measurement, and understanding of helicopter flight loadings have improved considerably in the last decade. Prior to this time, standardization of helicopter fatigue methodology could not have even been considered. During the presentation on Helicopter Rotor Load Predictions, emphasis was placed on the importance of including unsteady aerodynamics, rotor wake, and an accurate definition of rotor blade airfoil pitching moments in the simulation modeling. A previous empirical design approach was compared with the current analytical design approach to demonstrate the resultant improvements.

The importance of the Flight Load Survey was clearly defined in the second paper of this Session. Table 3 is a reproduction of Table A from this paper and illustrates it as the focal point for all other development testing. The benefits and importance of modernized data acquisition and reduction systems were expounded in this paper as well as the subsequent presentation on Flight Test Data Acquisition and Interpretation. In the latter presentation, it was stated that the computer age has opened the door to optimization of data handling. It was also emphasized that the point has now been reached

in flight test data analysis where the fatigue methodology should no longer be constrained by limitations in the handling of flight load survey data. With the advent of these new data systems, the statistical nature of flight loads can easily be accommodated. As a result, a rational approach similar to that which has already been applied to fatigue strength can be provided for flight loads in fatigue methodology.

The presentation on Force Determination demonstrated an innovative approach to assessing helicopter loads and response through the calibration and subsequent measurement of only fixed system parameters. This method has the advantage of providing a better understanding of helicopter flight loadings and how they interact throughout the airframe, as well as reducing the cost and unreliability of slip rings and rotating instrumentation.

The final presentation during Session II, Flight Condition Recognition (FCR), dealt with a cost effective method of tracking the accumulation of fatigue damage on critical helicopter dynamic components. The Structural Integrity Recording System (SIRS) is being developed by the US Army Aviation Research and Development Command to permit monitoring the usage spectrum of each helicopter. Success of this technique could do much to reduce cost in the acquisition and life cycle of fatigue critical components. Standardization and a better understanding of fatigue methodologies would do much toward implementation of a successful FCR technique.

SESSION III--COMPONENT FATIGUE TESTING

Component fatigue testing is an art in itself. Each helicopter company has developed its own techniques. As was mentioned in the Introduction, presentations in this Session were made on fatigue testing of a drive system component, control component, and rotor blade. Additionally, several papers were presented on the impact of fatigue testing of composites and how to detect and identify modes of failure. An overview of the Advanced Attack Helicopter (AAH) Fatigue Testing was also presented. Many excellent presentations were given during this Session, and the reader is encouraged to review each of the individual papers in this Session.

SESSION IV--FATIGUE LIFE PREDICTION

As stated in the Introduction, Session IV was planned as the highlight of the Meeting. It was also noted that the variations in helicopter fatigue methodologies between companies appear small and are not perceivable to all involved. To ask each manufacturer to present a general overview of his methodology would have masked the subtle differences which have a major impact on calculated lives. For these reasons, it was determined that the most effective way would be to request each manufacturer to calculate the fatigue life of a hypothetical helicopter component.

The component chosen was a main rotor pitch link which typifies one of the simpler helicopter fatigue problems. Further simplification was included in the problem and is summarized in Table 4. Interpretation of flight loads, S/N curve shape reductions from the mean, notch factor, stress ratio or Goodman corrections were left to the discretion of each participant. Statistical distribution of material allowables or flight loads were to be based on the participants' experience with similar materials and/or aircraft. It was hoped that the problem had not been oversimplified to the point of obviating the significant differences in calculated fatigue lives experienced previously.

Seven manufacturers made presentations with variations in calculated fatigue lives from 9 to 2594 hours based on peak loads and from 58 to 27,816 hours based on cycle-counted loads. Comparison of several parameters, as shown in Table 5, provides some insight into the large differences into calculated lives. The mean loads for the S/N curves varied between ± 2024 pounds to ± 2200 pounds which illustrates some differences in the S/N curve shapes utilized. The endurance limits established varied from ± 1225 pounds to ± 1722 pounds which illustrated a large variation in reduction factors due to the different statistical treatment of the component strength data. A good summary of life as a function of reduction factor is illustrated in Figure 1 from Reference 3. This plot clearly shows that fatigue lives are significantly impacted by the reduction factor desired or required. A final parameter that illustrates a large variation is the ratio of cycle counted life to peak load life. These ratios varied from 1.96 to 17.40 which emphasizes that cycle counting methods have a significant impact and that they vary considerably between manufacturers.

The American Helicopter Society is extremely grateful to the seven manufacturers who participated by calculating fatigue lives for the hypothetical component. There is no correct solution to the problem. The authors feel that all solutions are conservative, and it is the level of excessive conservatism that we are seeking to understand through open and frank discussion.

PANEL DISCUSSION ON STANDARDIZATION OF HELICOPTER FATIGUE METHODOLOGY

A standard as defined by the American College Dictionary is "anything taken by general consent as a basis of comparison; an approved model." The purpose of the panel discussion on standardization of helicopter fatigue methodology was to see if the "general consent" was present so that an "approved model" of helicopter fatigue methodology could be established. Members of the Panel represented most of the formal helicopter certification authorities in America, e.g., the Federal Aviation Administration (FAA), the US Navy, and the US Army. The manufacturers were represented formally by a panel member and informally by open discussion from the audience.

In the opening presentation, it was stated that the FAA has attempted to attain standardization by publication of the policy in its Federal Aviation Regulations (FARs) and Advisory Circulars (ACs). Unlike the specific guidelines given in Civil Aviation Manual (CAM) 6, Appendix A, the new FAA policy stresses the applicant meet minimum standards of airworthiness while encouraging higher standards. "These higher standards are dependent on the applicant's or his prospective customer's objectives."

In the past, the US Navy has provided much leadership in the area of helicopter fatigue. An attempt to establish a standard helicopter fatigue methodology for US Navy evaluation is presented in Reference 4. An interest to assist in future standardization was evident in their presentation. The US Army's view was a reiteration that standardization would be advantageous and should be sought in areas of "general consent."

The manufacturers' view was expressed, both in the formal presentation and from the manufacturers in the audience. While most thought that some form of standardization would be beneficial, there was much concern that standardization would restrict engineering judgment and provide unnecessary constraints. As the open discussion continued, a general consensus was reached that there are many areas of helicopter fatigue methodology that can be standardized and, in view of the large differences in calculated fatigue lives for the hypothetical component, that exchange of information among fatigue specialists is essential. One manufacturer's view of what could be successfully standardized is presented in Table 6.

There were several views expressed on how the standardization of helicopter fatigue methodology could be accomplished. One view is that a technical committee or working group of Government and industry fatigue specialists be formed under the auspices of AGARD. The working group would outline, by priority, the elements of helicopter fatigue methodology that should be standardized and would meet periodically to review and approve the work accomplished.

Another view expressed, and one which appears to be favored by industry, is that an independent council on helicopter fatigue be established with no particular affiliation. The American Aerospace Flutter and Dynamics Council was cited as an example of an existing independent working group made up of technical specialists. The Council meets periodically behind closed doors and exchanges technical information that is not documented formally for the public domain. Many specialists agreed with this approach in view of the liabilities associated with in-flight component fatigue failures and the reluctance to document individual problems publicly. It is suggested that Round Table Discussion during Session VI of this AGARD Meeting discuss the merits of fatigue methodology as well as means of implementation.

CONCLUSIONS AND RECOMMENDATIONS

The excellent presentations given, the open and frank discussion that accompanied them, and the positive feedback that has been received since the Meeting indicate that helicopter fatigue methodology was a worthwhile and interesting topic. The following are the significant conclusions drawn from the Meeting:

1. A statistical treatment of flight loads as well as fatigue strength is now possible and should be included in helicopter fatigue life calculations.

2. The uncertainties of usage spectrum can never be completely eliminated but can be improved by close coordination between the user, developer, and manufacturer during the design process.

3. Standardization of some areas of helicopter fatigue methodology are highly desirable and a means of implementation should be defined.

4. The exchange of helicopter fatigue information and experiences among fatigue specialists is highly desirable provided necessary proprietaries are observed.

While the emphasis in this paper has centered on US involvement in the standardization of helicopter fatigue methodology, its universal application was evident by the international participation at the AHS Specialists' Meeting. The AHS Meeting provided the opportunity to obtain an informal consolidated US position on standardization prior to this meeting. In view of the conclusions stated above, it is recommended that the AGARD Panel proceed with the development of a handbook on the fatigue design of helicopters.

REFERENCES

1. Alex, W. F., and Maloney, P. E., "Comparative Study of Fatigue Life Determination Methods," Kaman Aircraft Report Number R-770 prepared for the US Army Aviation Command, St. Louis, MO, under Contract DAAJ01-68-C-0889(31).

2. Wolfe, R. A., and Arden, R. W., "US Army Helicopter Fatigue Requirements and Substantiation Procedures," AGARD-R-674 Helicopter Fatigue.

3. Chappel, D. P., "Hypothetical Fatigue Life Problem," Letter to USAAVPADCOM (DRDAV-DS), 8 November 1979.

4. Woods, G. W., "Rotorcraft Dynamic Component Life Factors," Report Number NADC-ST-6901, 30 October 1969.

TABLE 1

CONCLUSIONS

The following observations and conclusions can be drawn from the results of calculations reported herein:

1. Using various treatments of the same basic data, fatigue lives have been calculated that range from a low of 745 hours to a life in excess of 1,000,000 hours.

2. CAM-6 Appendix A, the only definitive regulation on this subject, permits sufficient latitude that the highest of these lives would meet its requirements.

3. Flight spectrum variations involving as little as 1 1/2% of flight time can cause variations in calculated life as high as 46% (Case Vb.2).

4. A fatigue life determined by the "cyclic unit" method of CAM-6 was found to be 48 times as high as that which would be determined for the same components by an S-N, cumulative damage calculation. (Cases VIa and b) Operation to this higher life amounts to the assumption of a risk of failure that is 40 times as great as that associated with the S-N cumulative damage calculated life.

5. The sensitivity of calculated fatigue life to minute variations in critical values of the parameters indicates that any arbitrarily selected schedule or technique may produce a highly erroneous estimate of fatigue life.

TABLE 2

AHS SPECIALISTS' MEETING AGENDA

SESSION	PAPER NO.	TITLE	AUTHORS
Opening	Keynote Address	Fatigue Methodology--A Technical Management System for Helicopter Safety and Durability	L. Douglas
	1	Fundamentals of Helicopter Fatigue Life Determination	D. Schrage
I	2	Attack Helicopter Missions--Past, Present and Future	C. L. Shrader
	3	The Cargo Helicopter: A Logistical Vehicle	R. L. Stoessner R. C. Heehn
	4	Evolution of the Aeroscout	G. Fossum II
	5	Utility Helicopters	C. F. McGillicuddy, Jr.
II	6	Helicopter Loads Predictions	J. Yen and M. Glass
	7	Modern Techniques of Conducting a Flight Loads Survey Based on Experiences Gained on BLACK HAWK	B. Groth

AHS SPECIALISTS' MEETING AGENDA (CONT'D)

	8	Flight Test Data Acquisition and Interpretation	C. Hutchinson H. Steinmann
	9	Hub Force Determination and System Identification	N. Calopodas
	10	Flight Condition Recognition (FCR) Technique	D. Saylor
III	11	Advanced Attack Helicopter Fatigue Testing: Overviews	Deveaux
	12	NDE of Composite Rotor Blades During Fatigue Testing	R. Shufford W. Houghton J. R. Mitchell J. W. Sobczak
	13	Application of Fatigue Crack Propagation and Strain Survey Testing to the CH-46 Aft Rotor Drive Shaft	H. Faust
	14	Environmental Fatigue Behavior of Aramid Composites	M. Roylance R. Lewis
	15	Structural Testing of Composites with Known Defects	P. Maloney
	16	Fatigue Substantiation of Non-Linear Structures	B. Stocker
	17	Fatigue Test of the Typical Main Rotor Controls Component	J. Slack J. Cernosek
IV	18	Hypothetical Fatigue Life Problem	R. Arden
	19	Hypothetical Fatigue Life Problem Application of Aerospatiale Method	G. Stievenard
	20	The Agusta's Solution of AHS's Hypothetical Fatigue Life Problem	G. Aldinio P. Alli
	21	A Method of Determining Safe Service Life for Helicopter Components	G. McCloud
	22	Boeing Vertol Fatigue Life Methodology	G. Thompson
	23	Hughes Helicopters--Fatigue Life Methodology	J. McDermott
	24	Fatigue Life Prediction of Helicopter Pitch Link Using Kaman Life Calculation Methods	C. Hardersen
	25	The Challenge of Standardizing Fatigue Methodology	B. Altman J. Pratt
Panel Discussion	26	The FAA View--Standardization of Helicopter Fatigue Methodology	J. Major
	27	Helicopter Fatigue Methodology Standardization--The Navy's View	J. McGinn
	28	Helicopter Fatigue Methodology Standardization--The Army's View	R. Wolfe
	29	Helicopter Fatigue Methodology Standardization--A Manufacturer's View	J. Dress

TABLE 3

INTERACTIONS OF FLIGHT LOADS SURVEY WITH OTHER TEST REQUIREMENTS

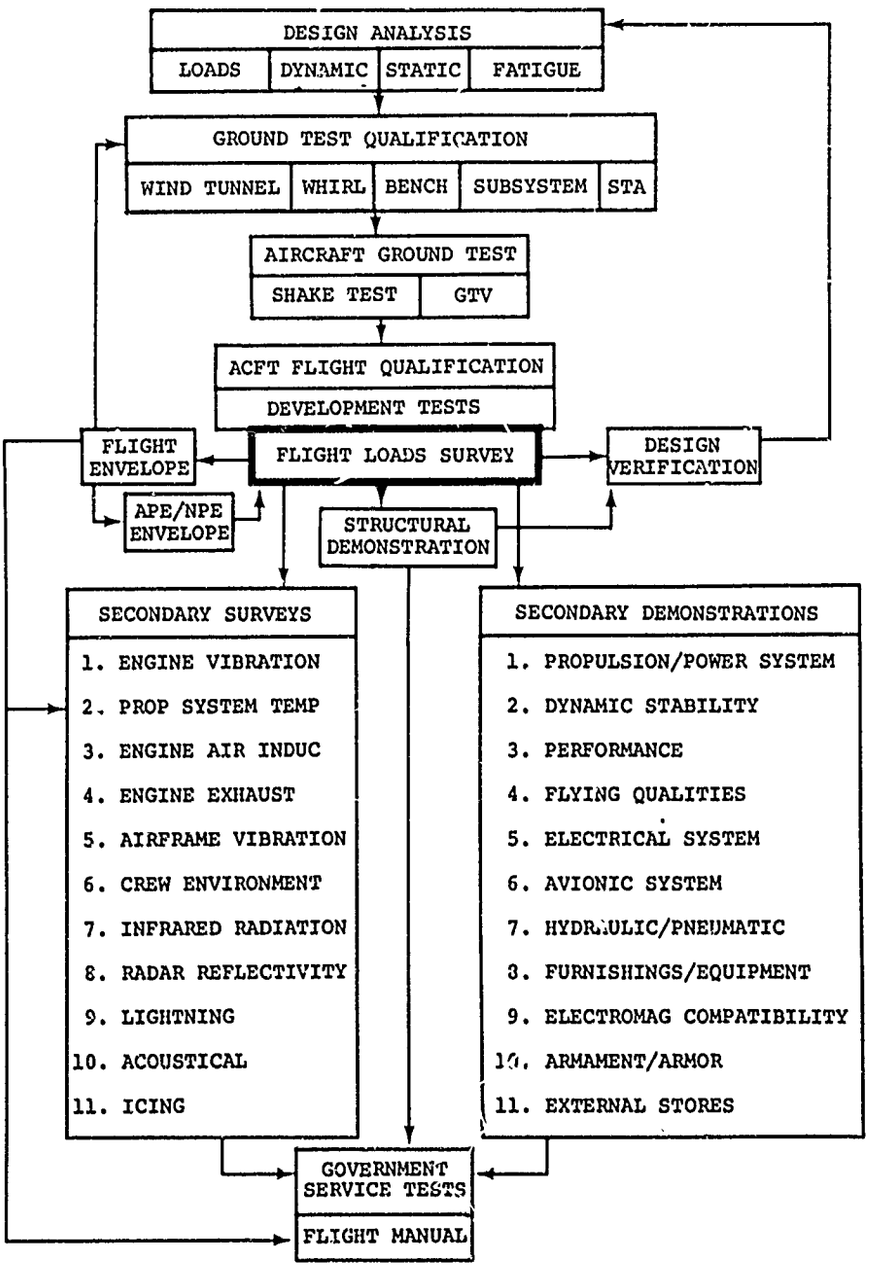


TABLE 4

HYPOTHETICAL FATIGUE COMPONENT

COMPONENT DESCRIPTION:	Main rotor pitch link, critical area is threaded section of the end fitting. Geometry, material, and heat treatment given. MIL-HDBK-5C referenced for material. MIL-S-8874A referenced for details of thread design.
FLIGHT SPECTRUM:	Given and simplified with no weight, cg, altitude or rotor RPM distribution.
FLIGHT LOADS:	Given and simplified with the assumption that each maneuver duration is equal to the total time shown in its flight load figure. Pitch link is only axially loaded.
COMPONENT STRENGTH:	Laboratory test results of six specimens were given. Simplifications were no runouts, all failures, and all failures occurred at the same location.

TABLE 5

RESULTS OF HYPOTHETICAL FATIGUE LIFE PROBLEM

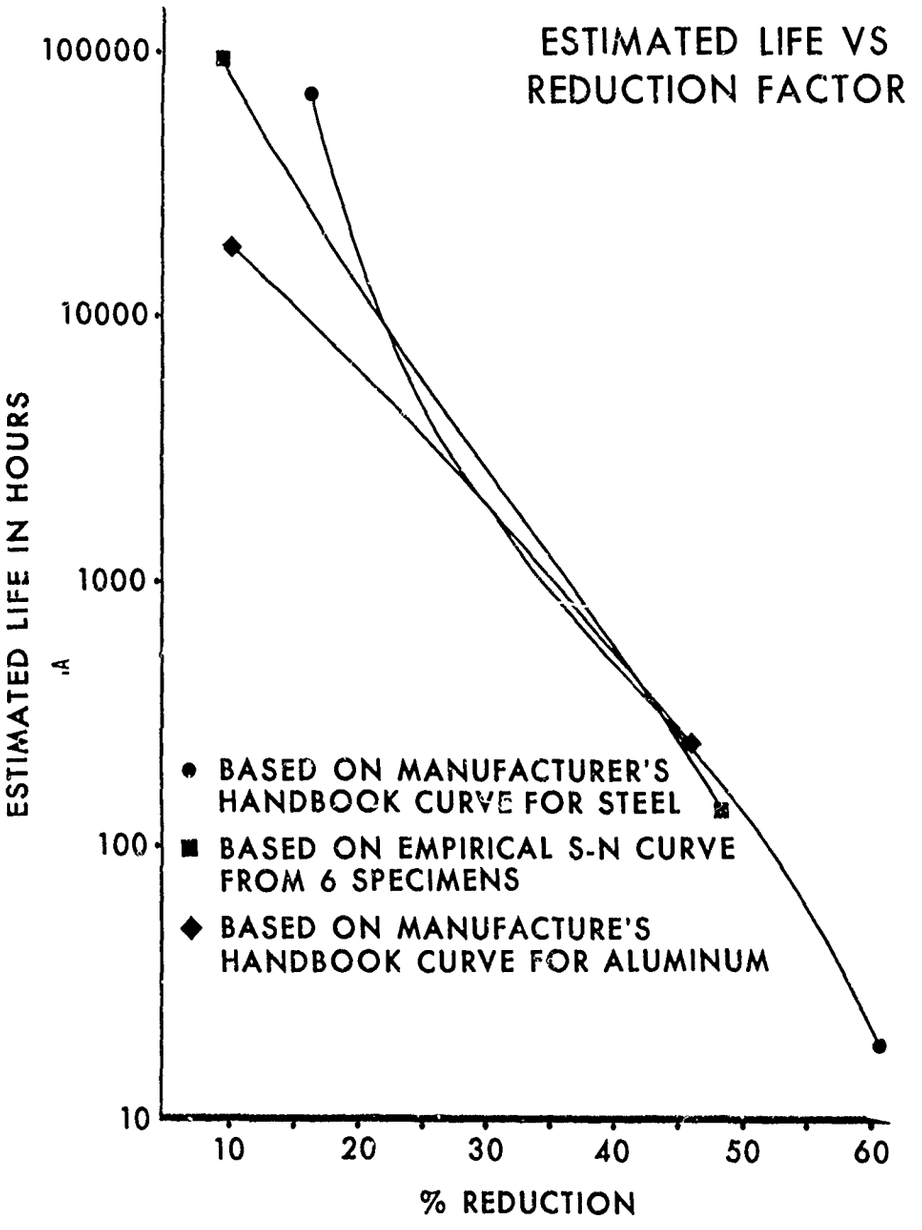
MANUFACTURER	MEAN LOAD S/N CURVE (LBS)	ENDURANCE LIMIT (LBS)	PEAK LOAD LIFE (HRS) (A)	CYCLE COUNTED LIFE (HRS) (B)	RATIO OF (B) TO (A)
A	±2176	±1225	9	58	6.44
B	±2200	±1673	804	13866	17.25
C	±2061	±1722	1831	27816	15.19
D	±2106	±1685	1294	22523	17.40
E	±2024	±1717	2594	24570	9.47
F	±2101	±1615	67	191	2.85
G	±2200	±1500	240	470	1.96

TABLE 6

AREAS OF FATIGUE METHODOLOGY THAT COULD BE STANDARDIZED

- Number of test specimens required
- S/N curve shapes for specific materials
- Reduction factors for working curves or ground rules for their establishment
- Ground rules for mission spectrum development, flight data selection and number of data points required
- Use or non-use of Goodman corrections
- Selection of test steady loads
- Requirements for treating non-linear stress
- Definition and application of GAG in fatigue substantiation
- Limitations and use of cycle counting
- Use of runout data
- Determination of primary frequency
- Identification of new risk areas as indicated by service problems and incorporation of new compensating factors in the methodology

FIGURE 1


ESTIMATED LIFE VS
REDUCTION FACTOR
ESTIMATED LIFE IN HOURS
100000
10000
1000
100
10
10
20
30
40
50
60
% REDUCTION
BASED ON MANUFACTURER'S HANDBOOK CURVE FOR STEEL
BASED ON EMPIRICAL S-N CURVE FROM 6 SPECIMENS
BASED ON MANUFACTURE'S HANDBOOK CURVE FOR ALUMINUM

Report on Session I

SURVEY OF CURRENT PROCEDURES

by

Dr-Ing. Walter Schütz
Industrieanlagen-Betriebsgesellschaft mbH
Einsteinstrabe 20, 8012 Ottobrunn, Germany

I have to report on Session I "Survey of Current Procedures". Three papers were presented by Noback, Cansdale and Schage.

Mr Noback gave a description of the methods used for predicting the fatigue life by the various manufacturers. In principle, they are all similar, that is. SN tests in the region of the fatigue limit are carried out, establishing a more or less well defined mean SN-curve. Using an assumed stress spectrum and an assumed coefficient of variation, an SN-curve for a high probability of survival is calculated. Using this as a basis, Miners rule is employed to calculate the life under the assumed or agreed-to load spectrum, the maximum loads of which are only slightly higher than the calculated fatigue limit at this high probability of survival due to the large number of cycles occurring. This is the principle used by all manufacturers, and one would expect the results to be similar, however, due to the many individual steps and the many assumptions necessary for this procedure, there are extreme differences between the actual lives predicted by the various manufacturers. the example presented at the American Helicopter Society meeting and mentioned by Messrs Noback, Dr Schage and some other speakers showed differences in life between 6 and 27,000 hours, that is a variation of about 1.3000. After this, to me, somewhat disturbing introduction, Mr Noback made several proposals on how to improve the present, obviously unsatisfactory situation regarding fatigue life prediction.

Mr Cansdale had been expressly asked by the Working Group to talk on the fatigue life prediction methods used for fixed wing aircraft.

Dr Schage presented a synopsis of the American Helicopter Society meeting on Helicopter Fatigue Methodology. Apart from the example already mentioned which showed the extreme differences in calculated fatigue lives, the topics at this meeting were

- mission spectra
- flight loadings
- component testing and, last but not least
- standardisation of helicopter fatigue methodology.

It was generally agreed that there was an urgent need for standardisation. One view was that a technical committee or working group of Government and industry fatigue specialists be formed under the auspices of AGARD.

My personal view of the situation as presented not only by the three speakers I have reported on but also by most other speakers and discussors is that now is the time to improve the unsatisfactory situation in helicopter fatigue life prediction.

One big step in the right direction is the introduction of damage tolerance requirements to safeguard against battle damage and for the occasional undetected manufacturing or service-induced flaw.

Another step, which fits quite well into the damage tolerance requirements is the necessity of spectrum testing.

APPLICATION OF DAMAGE TOLERANCE CONCEPTS FOR MBB HELICOPTERS

by

M.v.Tapavicza and F.Och

Messerschmitt-Bölkow-Blohm GmbH

Postfach 801140

8000 München 80, Germany

SUMMARY

The more and more pronounced tendency of modern helicopters towards higher efficiency and reliability requires materials and structural designs possessing high strength and good damage tolerance behaviour.

This paper outlines the damage tolerance methodology used at MBB for helicopters of the BO 105 family as well as for the BK 117. One example of each type of damage tolerant design, realised in or developed for MBB helicopters is discussed in detail and the design criteria for the other vital components are summarized.

It is shown that only a few vital components are designed according to the safe life philosophy.

1. INTRODUCTION

Current fatigue substantiation philosophy can roughly be represented by the following scheme:

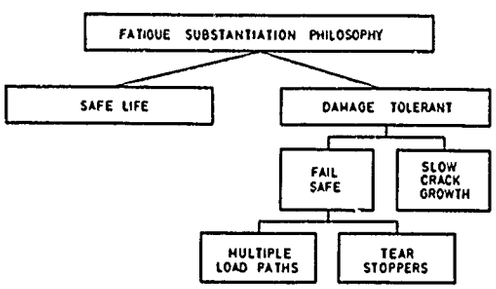


Fig. 1 Fatigue Substantiation Philosophy

Fatigue evaluation of rotorcraft structures has to establish that within the working life, the expectation of catastrophic failure from fatigue origins is extremely remote and, additionally, the incidence of non-catastrophic cracking is maintained at a sufficiently low level to enable economic utilisation of the rotorcraft structure to be attained [1].

These aims have to be achieved within the framework of a minimum weight and cost as well as a maximum performance concept. In depth knowledge of the fatigue properties of materials and components is necessary

- in design - to avoid unsuitable construction,
- in production - to consider the effect of manufacturing technology,
- in maintenance - to implement adequate inspection.

However, the reliable estimation and prediction of a part's lifetime are still greatly hampered by insufficient knowledge and data concerning the fatigue and fracture properties of materials. Furthermore, reliable mission spectra are difficult to set up, especially as operational requirements of light helicopters, such as MBB's BO 105, may vary within a broad field of operations [2]. When fatigue evaluation is based on safe-life considerations, these uncertainties are compensated for by very conservative assumptions with respect to flight loads and working S/N curves.

The more and more pronounced tendency of modern helicopters towards higher power and improved performance, towards better manoeuverability and qualification for extreme nap-of-the-earth flights, towards improved survivability and reliability and towards reduced maintenance and improved mission availability demands materials and structural design with high strength and good damage tolerant behaviour [3].

Guidance material and detailed requirements on damage tolerance can be found in [4] and [5], respectively.

2. DAMAGE TOLERANCE METHODOLOGY

During design, production and maintenance of modern helicopter structures, considerable effort is expended to ensure a crack-free fatigue life, without an absolute guarantee that fatigue cracking will not occur. The structure must therefore be designed so that should serious fatigue, corrosion, or accidental damage occur within the operational life, the remaining structure can withstand reasonable loads without failure or excessive structural deformation until the damage is detected.

Structures can be designed in two different ways to achieve this goal, namely with either redundant load paths or crack-arrest capability, known as "failsafe", or by ensuring that crack propagation will be slow, known as "slow crack growth" (see Fig. 1).

Fail Safe Evaluation

The fuselage, as the major part of the helicopter structure, is usually a semi - monocoque construction of stressed skin, stringers and frames, representing a highly redundant system, where the stiffening elements act as skin crack stoppers. This structure is generally stressed using static load cases. Full scale fatigue tests are carried out under manoeuvre load conditions, neglecting high frequency vibratory loading, in order to show crack-arrest capability and to provide guidance information for the maintenance manual.

Failsafe behaviour of components may be achieved by two or more load paths. Duplicate structures, where a failure occurring in one element of the member will be confined to that element, the remaining structure still possessing applicable load-carrying ability, or backup structures, where one member carries all the load, with a second member available to assume the load in case the primary member fails, are used. Damage detection can be achieved either visually or by a change in helicopter vibration level.

Tests are conducted on components to determine the location and modes of damage and to establish how many of the redundant elements may fail without questioning residual strength to withstand the design limit loads. The difference between the time at which the damage becomes detectable and the time at which the extent of damage reaches the value critical for residual strength, will be determined by these tests as a basis of an inspection programme.

Slow Crack Growth Evaluation

Fatigue always comprises three distinct stages:

- crack nucleation,
- crack propagation,
- rapid failure.

Crack initiation is of a statistical nature, as structures may go into service already containing cracklike manufacturing defects or just unavoidable notches, where at the notch root a crack must first be initiated [6]. A completely reliable method for the prediction of time to fatigue crack initiation therefore does not exist.

Crack propagation analysis, i.e. predicting the time available from damage detection to failure of the part, is best covered by fracture mechanics. Fracture mechanics is a discipline that relates the crack extension characteristics of a material to the part's geometry and the applied stress. The governing parameter in fracture mechanics is the stress intensity factor K which can be related to applied stress in the loading mode I, which is both the most developed and the one of greatest interest, by the following relationship

$$K_I = \beta \cdot \sigma \sqrt{\pi \cdot a} \quad , \qquad (1)$$

where σ is the gross applied stress, i.e. the stress if there were no crack, a is the half crack length and β is a nondimensional function of crack size and structural geometry. β can be derived from classical theory of elasticity and will be found in handbooks for many crack cases.

Fracture will occur when the stress intensity factor exceeds a critical value, e.g. K_{IC} for plane strain conditions, which can be considered a material property called fracture toughness and can be determined by experiment. Fracture toughness in combination with equation (1) leads to the conditions (crack size and applied stress) at which a part will fail.

To establish subcritical crack growth under fatigue loading we use the well known Forman equation

$$\frac{da}{dN} = \frac{C \cdot \Delta K^n}{(1-R) \cdot K_C - \Delta K} \qquad (2)$$

A computer programme, commonly agreed within the German aircraft industry, is used to calculate the constants C and n from the test data.

The accuracy of predictions is limited by the variability in properties and by the unknowns in load history, therefore adequate safety factors must be taken into account. Tests on full scale components are carried through with simulated damage, where actual fatigue cracks could not be produced.

For structures made of composite material, fracture mechanics is not applied, up to now, at MBB's helicopter division.

Combination of Safe Life and Slow Crack Growth Evaluation

In establishing replacement time for safe life components which exhibit slow crack growth capability we use a combination of the safe life and slow crack growth concepts by evaluating both the fatigue strength and the fatigue damage propagation rate. A replacement time and an inspection period must be assigned to these components. In the determination of the replacement time a working S/N curve derived from the experimental mean curve with a strength reduction factor is used. This factor depends on slow crack growth capability and the detectability of an impending failure and can produce a working S/N curve anywhere between the 99.9% probability line and the bottom of scatter line.

3. DAMAGE TOLERANT DESIGN

The BO 105 family, i.e. civil and military versions and the BK 117 show the concept of redundancy not only in two engines and two independent hydraulic systems, but also in the damage tolerant design of many components in the main and tail rotor as well as the drive system, leading to a more forgiving structure in respect to poor maintenance, environmental deterioration and operating abuses. The advantages to the customer are apparent in the form of greater safety and reliability, elimination of unnecessary component replacements, reduced maintenance and improved mission availability of the helicopter.

One example of each type of damage tolerant design, present in or developed for MBB helicopters is discussed in detail and the design criteria for the other vital components are summarized.

Quadruple Nut

The quadruple nut is an element of the main rotor system, Fig. 2, situated in the center of the rotor hub, used to balance the centrifugal forces of opposite rotor blades, Fig. 3.

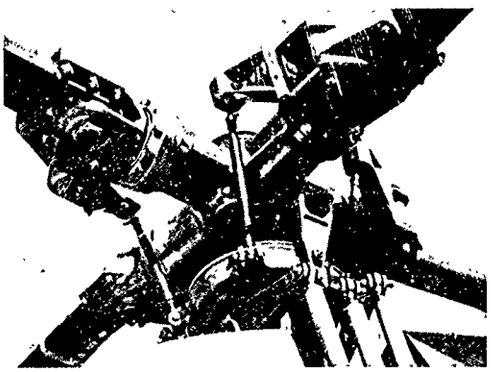


Fig. 2 BO 105 Main Rotor System

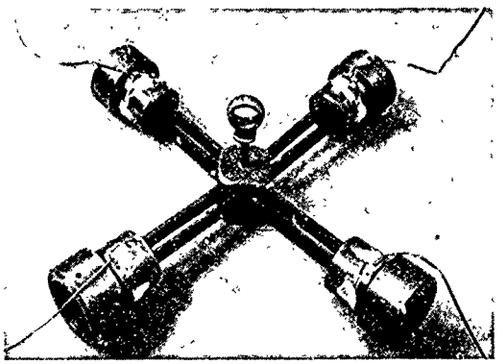


Fig. 3 Centrifugal Force Retention System

Hitherto, the quadruple nut has been a safe life component. A damage tolerant approach was also considered, where the design consisted of an additional wrapping of high strength steel wires, Fig. 4, forming a second load path, as backup structure, if the monolithic part failed.

Tests were conducted with loads equivalent to a rotor speed of 118%. After about 5000 start-stop cycles cracks could be detected with the naked eye, as shown in Fig. 4. Complete failure of the monolithic part was found after a total of about 13 500 cycles and the wire started to fail after an additional 16 000 cycles (Fig. 5).

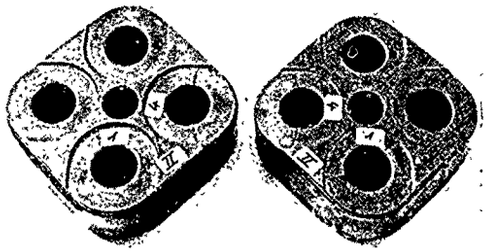


Fig. 4 Cracks in a Quadruple Nut

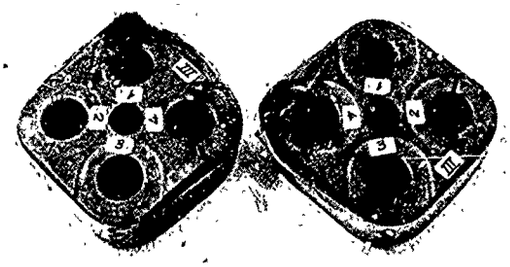


Fig. 5 Fatigue Tested Quadruple Nut

A failure of the primary part would be immediately indicated by the vibration resulting from the unbalance caused by the blade moving outboard until the wires, as the secondary load path, fully reacted the centrifugal force. In tests we measured a radial displacement of about 2 mm at 100% rotor speed.

Tail Rotor Drive Shaft Coupling

The tail rotor drive shaft couplings transmit the tail rotor torque and balance angular and longitudinal misalignments of the drive shaft. The coupling consists of 12 steel laminates packed between a pair of titanium adapters (Fig. 6), and represents an example of simultaneous multiple load paths.

Under normal environmental conditions these couplings together with the adjacent components provide sufficient static strength and an unlimited life time. To establish inspection periods under an adverse environment we conducted fatigue tests in a salt water atmosphere, Fig. 7, 8.

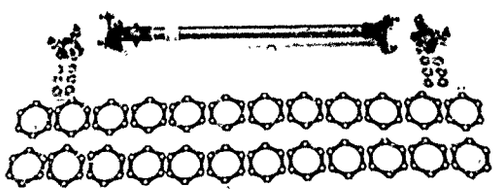


Fig. 6 Tail Rotor Drive Shaft with Disassembled Couplings

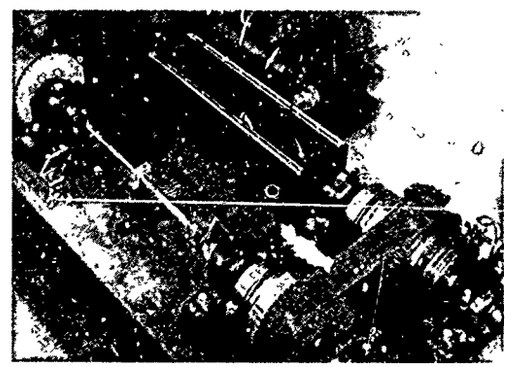


Fig. 7 Salt Water Corrosion Fatigue Test Set-Up

Both constant amplitude torque tests and flight-by-flight load history simulation show that the remaining structure possesses sufficient load carrying ability when 4 laminates out of 12 have failed. An inspection period of 1200 flight hours was found to be adequate even with a corrosive environment.

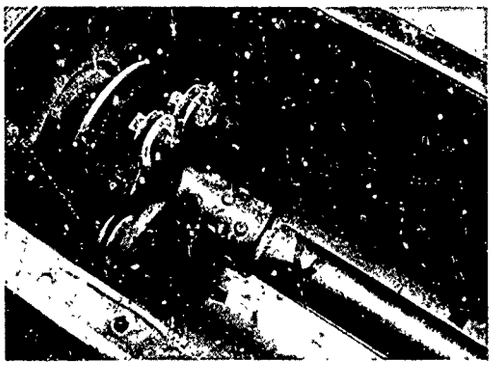


Fig. 8 Coupling Failed in Corrosion Fatigue Test

Main Rotor Shaft

The main rotor shaft or transmission output shaft is joined to the rotor hub with a multiple stud and bushing connection. Due to the hingeless rotor system of the BO 105 and BK 117 the shaft is highly loaded in bending with the critical section in the connecting flange.

The damage tolerance method used is that of slow crack growth, performed by a highly pure steel (Böhler Stern NMH) with a fracture toughness of $K_{IC} \sim 4500\ Nmm^{-3/2}$.

Tests to show the damage tolerance behaviour have been carried out with ballistically impacted and artificially notched specimens (see Figs. 9, 10, 11).

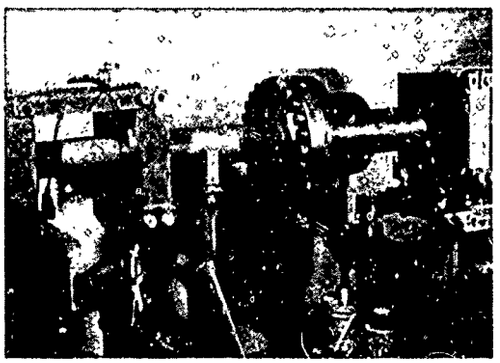


Fig. 9 Main Rotor Shaft Fatigue Testing Set-Up

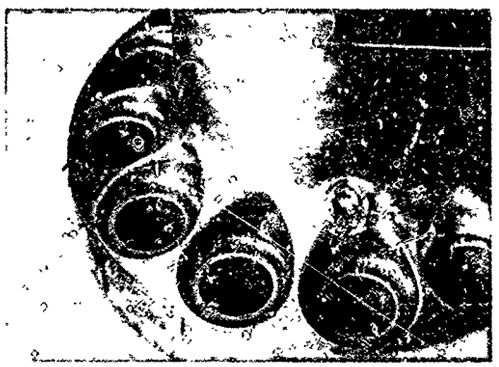


Fig. 10 Ballistically Impacted Main Rotor Shaft



Fig. 11 Artificially Damaged Main Rotor Shaft

Spectrum tests revealed a very low crack propagation rate. After more than 9 million cycles with elevated loads the crack of the artificially notched specimen had propagated as shown in Fig. 12, but the full loads could still be reacted.

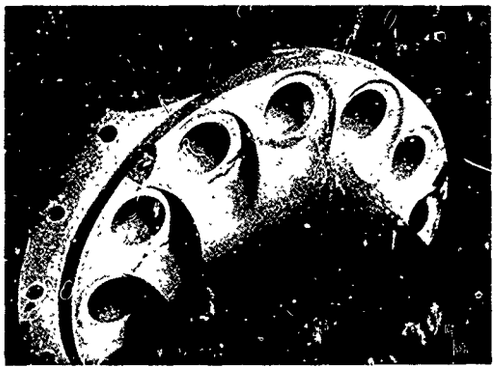


Fig. 12 Crack in an Artificially Notched Rotor Shaft

Main Rotor Blade

The main rotor blade, Fig. 13, is of glass fibre composite (GFC) with a PVC foam core. There is a titanium erosion protection strip on the aerofoil section and a lead balance weight. The root end of the blade is potted into a titanium attachment fitting.

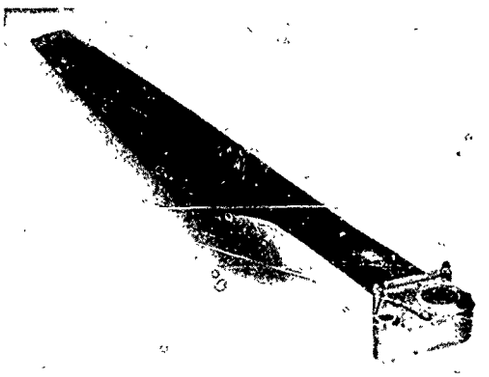


Fig. 13 BO 105 Main Rotor Blade

The spar, made of unidirectional GFC, reacts centrifugal load and bending. The skin, made of glass fabric with a fibre orientation of $\pm 45^0$, reacts torsion and chordwise bending.

As a single fibre failure does not influence the surrounding fibres, composites may be regarded as highly redundant systems. Cracks normally propagate parallel to the fibres. If there are layers with different fibre orientation, cracks will not propagate from one layer to the other. Thus composites show good crack-arrest capability and very low crack propagation rates.

Damage tolerant behaviour of the main rotor blade was demonstrated on artificially notched blade skin areas (Fig. 14) and ballistically impacted blade sections (Fig. 15).

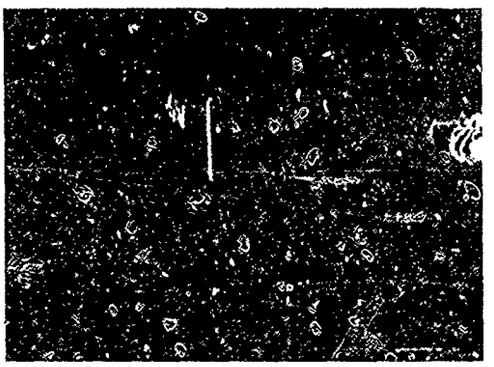


Fig. 14 Artificially Notched Blade Skin

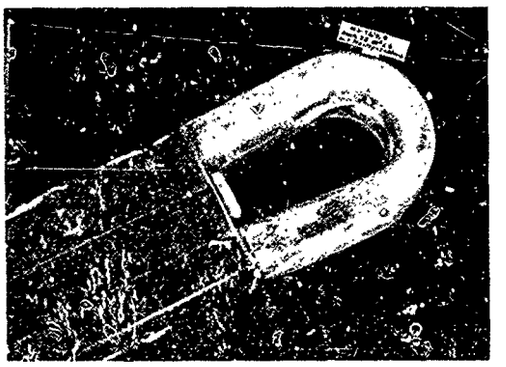


Fig. 15 Ballistically Impacted Blade Root End

The blade skin area was loaded to ± 0.4% strain and showed, up to about 60 million cycles, only a minor enlargement of the delamination, seen in Fig.14,and did not change further with more than 100 million cycles.

The ballistically impacted blade root end was loaded by simulated flight loads for more than 7 million cycles without any damage propagation [7]. Fig. 16 shows the cross-section of this damaged part.

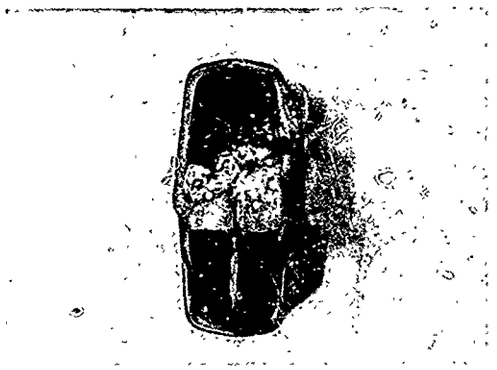


Fig. 16 Cross-Section of Ballistically Impacted Blade Root

Another blade was ballistically impacted in the aerofoil section near the leading edge (Fig. 17). Subsequent bending fatigue testing with 2 million cycles at an alternating surface strain of ± 0.06% showed no damage propagation.

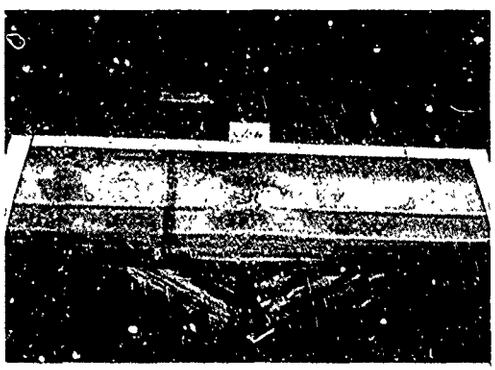


Fig. 17 Ballistically Impacted Aerofoil Section



Fig. 18 Cross-Setion of Ballistically Impacted Aerofoil Section

4. CONCLUSION

Although a conventional safe life design approach is normally considered sufficiently safe and reliable, the damage tolerant approach is already widely used. Additionally, damage tolerant solutions are continuously sought for MBB helicopters. Most of the vital components may already be safely operated "on condition", i.e. without definite replacement times.

The following damage tolerant parts are used in the BO 105 family:

- Fail safe design
  - main rotor blade assembly
  - connection between hub and rotor shaft
  - attachment of tailboom to fuselage
  - airframe
  - tail rotor drive shaft coupling (Thomas type)

· Slow crack growth design

- main rotor hub
- inner sleeve
- upper control assembly
- tail rotor control
- tail rotor shaft
- engine mount system

The traditional safe life concept or a combination of safe life and slow crack growth is used where the attainment of damage tolerance is impractical or where additional conservatism was required for want of experience. The following parts are certified for the BO 105 with replacement times less than 10 000 flight hours:

- main rotor shaft
- main gearbox support struts
- main rotor blade retention system
- tail rotor blade assembly
- tail rotor blade retention system
- tail rotor inner sleeve
- drive shafts (Bendix type)

5. REFERENCES

[1] FAR Part 27, Airworthiness Standards: Normal Category Rotorcraft, Federal Aviation Administration

[2] Och, F. Fatigue Life Estimation Methods for Helicopter Structural Parts, AGARD Report No. 674, Florence, 25.-29.9.1978

[3] Reichert, G. The Impact of Helicopter Mission Spectra on Fatigue, AGARD-CP-206, Ottawa, 4.-9.4.1976

[4] Advisory Circular, AC 25.571-1, Federal Aviation Administration, Washington, D.C., 9/28/78

[5] Airplane Damage Tolerance Requirements, MIL-A-83444, 7/2/1974

[6] Schütz, W. Fatigue Crack Growth, AGARD Lecture Series No. 97, München, 9.-10.10.1978

[7] Brunsch, K. Wackerle, P.M. Ballistic and Impact Resistance of Composite Rotorblades, Second European Rotorcraft and Powered Lift Aircraft Forum, Bückeburg, 20.-22.9.1976

JUSTIFICATION EN FATIGUE DE PIECES EN MATERIAU COMPOSITE BENEFICIANT DU CONCEPT "FAIL SAFE"

par

G.Stiévenard
Aerospatiale
Division Hélicoptères
B.P.13, 13722 Marignane
France

0. PREAMBULE

L'hélicoptère, par sa conception, présente de nombreuses sources d'excitation vibratoire et de ce fait un nombre très important de pièces travaillant en fatigue. Le souci permanent du constructeur est de réaliser des pièces répondant à des critères de sécurité très sévères tout en conservant un caractère compétitif du point de vue masse et prix de revient. Un réglement de fatigue établi conjointement entre la SNIAS et les Services Officiels Français impose que la probabilité individuelle de rupture en fatigue d'une pièce d'hélicoptère ne dépasse par 10^{-6} pour la durée de vie affichée.

Le développement durant ces quinze dernières années, de matériaux composites permetà l'Aérospatiale de concevoir de nouveaux rotors satisfaisant au mieux le compromis précedemment évoqué.

Ces matériaux présentent un bon comportement en fatigue associé à un caractère fail-safe évident (début de délaminage facile à déceler et vitesse de propagation lente).

Ces propriétés ont permis de faire évoluer les méthodes de justification sans pour autant augmenter le risque de rupture en vol.

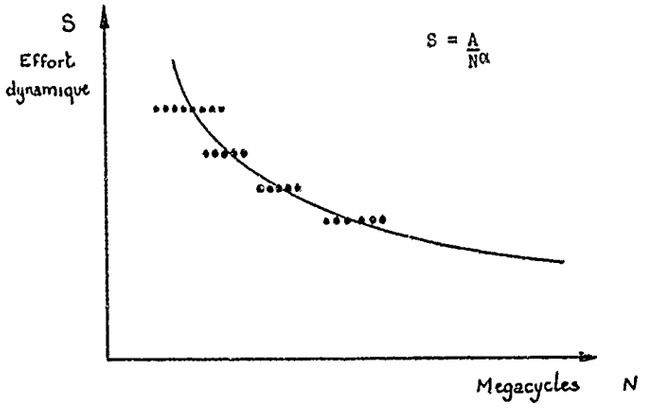
Si nous appelons par R1 la probabilité d'avoir une crique sur une pièce de vol et par R2 celle de voir cette crique se propager entre deux visites périodiques, le risque global de rupture est le produit R1 x R2 et c'est ce produit qui ne doit pas dépasser 10^{-6}.

Le but du présent exposé est d'expliquer la méthode utilisée par la SNIAS afin de calculer ces deux risques R1 et R2

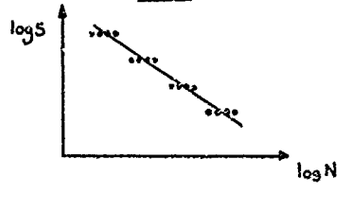
Cette méthode est basée sur une étude complète des caractéristiques de fatigue et des vitesses de propagation de criques dans le matériau utilisé.

1. CALCUL DU RISQUE R1 (risque d'avoir une crique en utilisation)

Le premier stade de l'étude consiste à déterminer l'équation de la courbe S/N du matériau servant à fabriquer la pièce d'hélicoptère. Ces équations sont en général de la forme (fig : 1)



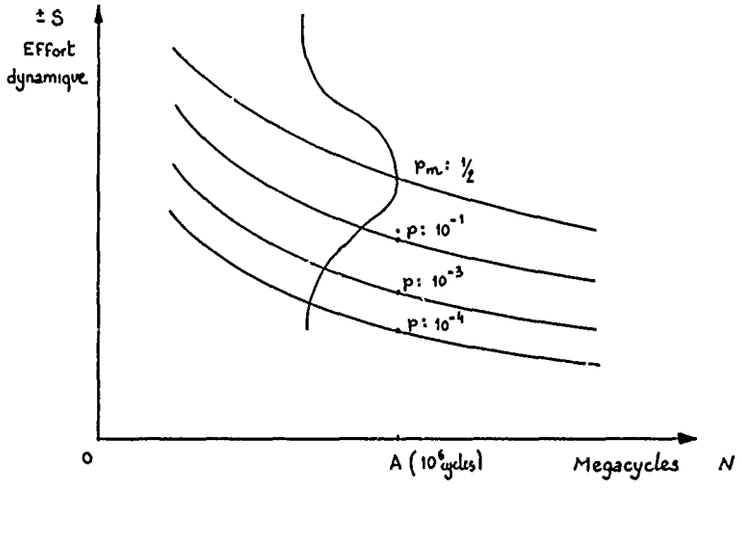
A partir d'essais sur éprouvettes effectués en assez grand nombre, il est possible de calculer pour un matériau les coefficients A et α qui lui sont propres. La méthode utilisée est une régression linéaire sur log N en fonction de lot S (fig 2)



$$\log N = \frac{\log A}{\alpha} - \frac{\log S}{\alpha}$$

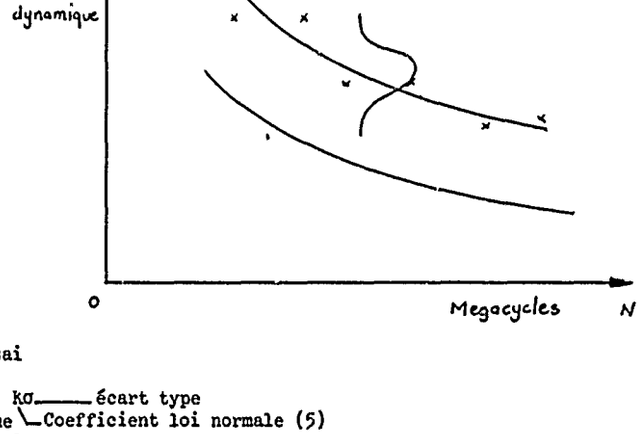
La deuxième hypothèse de calcul consiste à admettre qu'il existe des courbes S/N affines de la courbe moyenne de même équation au A près que nous admettons suivre une loi de probabilité logarithmo-normale.

Ces courbes sont donc des courbes à isoprobabilité de crique (fig : 3)



Cette hypothèse qui peut paraître arbitraire à priori est assez bien vérifiée par l'expérience et les tests statistiques.

L'expérimentation que nous venons de décrire serait trop onéreuse si elle était réalisée en totalité sur pièces appareils, aussi l'équation de la courbe S/N est elle déterminée sur éprouvettes et considérée comme reconductible pour les pièces que nous n'essayons qu'en quelques exemplaires (6 pts mini) fig:4



Formulation des calculs

(1) $S = \frac{Ai}{N_i^{\alpha}}$

(2) $|\log A|_m = \frac{\Sigma \log A_i}{n}$

n → nombre de points d'essai

(3) $\log A_r = |\log A|_m - K\sigma$

A_r : risque considéré ; $|\log A|_m$: limite de fatigue moyenne à 10^6 cycles ; σ : écart type ; K : Coefficient loi normale (5)

(4) $\sigma = \sqrt{\frac{\Sigma \left[(\log A)_m - \log A_i \right]^2}{n-1}}$

(5) $K = \frac{kr + kq\sqrt{\frac{1}{n}\left[1 - \frac{kq^2}{2(n-1)} + \frac{kr^2}{2(n-1)}\right]}}{1 - \frac{kq^2}{2(n-1)}}$

kr = marge correspondant au risque r dans la loi normale simple.
kq = marge correspondant au risque q dans la loi normale simple.
q = coefficient de confiance.
Connaissant les 6 résultats d'essai, il nous est donc possible de calculer Am et les Ar correspondant à différents risques r.

L'utilisation de l'hélicoptère est connue, soit par enregistrement des paramètres de vol durant plusieurs centaines d'heures, soit par informations émanant des utilisateurs. Nous disposons donc d'un spectre donnant pour chaque configuration de vol le pourcentage de temps lui correspondant. Pour chacune de ces configurations nous enregistrons à l'aide de jauges extensométriques les efforts de vol.

Ces efforts associés à leur pourcentage servent à calculer la durée de vie en appliquant la règle de MINER (voir fig 6).

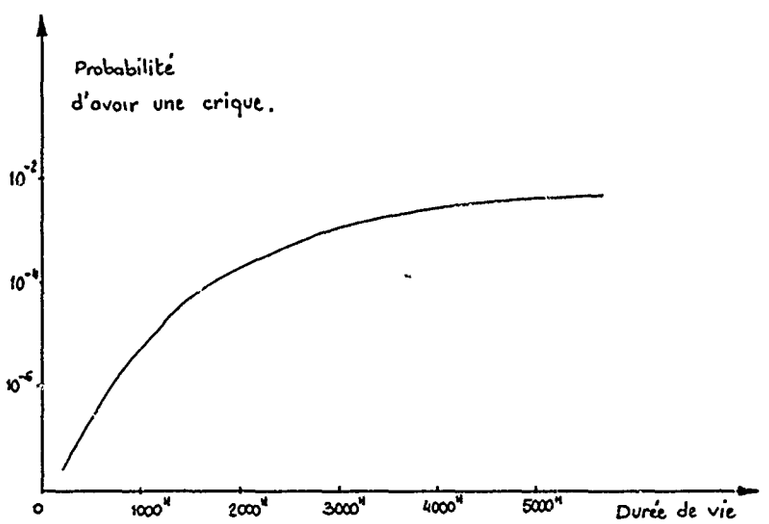
Ce type de calcul est conduit pour différents risques, ce qui nous donne la courbe de la figure 7.

Tableau 1 figure 6

CONFIGURATIONS	% Pourcentage d'utilisation	Effort de vol	Limite de fatigue au risque r	Nombre de cycles admissible $N = (\frac{A}{\Delta})^{k}$	Nb d'h de vol N × t par Mc (t: temps pour 1 mégacycle)	$\%/Nbh$
1. Stationnaire	p_1	$\pm F_1$	A_r	N_1	Nbh_1	p_1/Nbh_1
2. Vi transition	p_2	$\pm F_2$	"	N_2	Nbh_2	p_2/Nbh_2
.						
.						
.						
.						
.						
.						
.						
.						
i-2 Palier	p_{i-2}	$\pm F_{i-2}$	"	N_{i-2}	Nbh_{i-2}	p_{i-2}/Nbh_{i-2}
i-1 Approche	p_{i-2}	$\pm F_{i-1}$	"	N_{i-1}	Nbh_{i-1}	p_{i-1}/Nbh_{i-1}
i Atterrissage	p_i	$\pm F_i$	"	N_i	Nbh_i	p_i/Nbh_i
						$\Sigma p_i/Nbh_i$

durée de vie : $\dfrac{100}{\Sigma p_i/Nbh_i}$

Figure 7



2. CALCUL DU RISQUE R2
(Risque d'avoir une rupture catastrophique entre deux contrôles périodiques).

Les essais réalisés sur pièces afin de calculer le risque R1 sont stoppés dès l'apparition du premier signe de détérioration pour être repris aux charges de vol à l'aide d'un bloc programme respectant :

- le pourcentage d'utilisation de chaque configuration.
- l'ordre chronologique de ces configurations (afin de reproduire d'éventuels effets retard de la propagation dus aux changements de niveaux de contraintes)

(Voir spectre de charges tableau II fig : 8)

Tableau II
Spectre de charges programmées

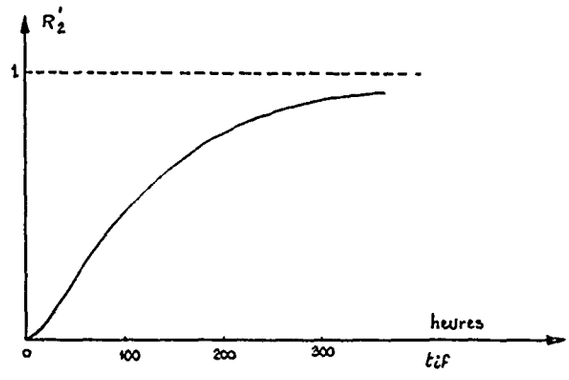
	Battement Statique	Battement Dynamique	Trainée Statique	Trainée Dynamique	Nombre de cycles
	— 235	0			
Stationnaire	84	± 79	145,5	± 118	320
Départ en translation	84	± 168	100	± 170	175
Croisière vitesse mini.	83,5	± 69,5	29	± 75	224
Virage	105	± 149,5	172	± 410,5	64
Croisière vitesse économique	83,5	± 28	100	± 138	465
Virage	105	± 149,5	172	± 410,5	64
Croisière vitesse économique	83,5	± 28	100	± 138	465
Virage	105	± 149,5	172	± 410,5	64
Croisière vitesse max.	83,5	± 31,5	258	± 168	384
Virage	105	± 149,5	172	± 410,5	64
Croisière vitesse max.	90	± 31,5	258	± 168	384
VNE	74	± 49	201	± 173,5	61
Virage VNE	96	± 35	158	± 176	4
Croisière vitesse max.	90	± 31,5	258	± 168	384
Croisière vitesse économique	83,5	± 28	100	± 138	465
Virage	105	± 149,5	172	± 410,5	64
Croisière vitesse mini.	83,5	± 69,5	100	± 138	224
Virage	105	± 149,5	172	± 410,5	64
Ralentissement	84	± 168	100	± 170	176
Autotrotation	61	± 109	277	± 140	64
Stationnaire	84	± 79	145,5	± 118	320
Approche flan	74	± 126	132,5	± 201,5	320
Arrêt rotor	— 235	0	0	0	

Ces essais sont poursuivis jusqu'à rupture avec mesure et enregistrement des longueurs de crique et de la rigidité des pièces.

Si nous appelons par t_{if} le temps mis pour passer du temps t_i correspondant à l'apparition de la première dégradation bénigne au temps t_f correspondant à la rupture catastrophique, il est possible d'ajuster une loi de probabilité à cette variable aléatoire t_{if} trouvée en essai.

Il semble à priori que ce soit la loi logarithmo-normale la mieux adaptée au phénomène.

Connaissant la loi de probabilité, la valeur moyenne t_{ifm} et l'écart type, il est possible de calculer un temps de vol admissible en fonction du risque (voir fig : 9)



La courbe ainsi tracée correspond au risque de rupture en considérant que la première dégradation décelable survient aussitôt après le début du vol. Il convient donc maintenant d'évaluer la courbe du risque R2 en admettant que cette première dégradation survienne à un instant quelconque du vol.

Soit x heures de vol entre deux inspections

Deux possibilités se présentent

(a) Il n'y a pas apparition de détérioration entre deux contrôles considérés (ce cas ne nous intéresse pas, puisqu'il reporte au cas b), au cours des contrôles suivants :

(b) Il y a apparition de détérioration entre deux contrôles. Seul ce cas nous intéresse ; donc nous poserons que la probabilité d'apparition de détérioration est égale à 1.
Soit t_1 l'instant où apparaît la première dégradation décelable (t compté à partir de zéro dernier contrôle) ;
Soit t_2 le temps de propagation, qui entraîne une détérioration catastrophique de la pièce.
Il convient de remarquer que t_1 et t_2 sont deux variables aléatoires indépendantes.

$$\text{Probabilité} \left\{ x < t_1 < x + dx \right\} = \frac{dx}{x}$$

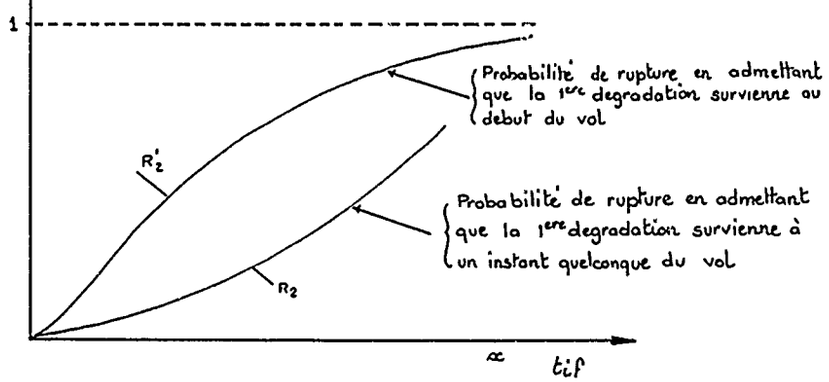
d'après la courbe précédente

$$\text{Probabilité} \left\{ t_2 < X - x \right\} = R\,(X - x)$$

$$\text{d'où } dP = \frac{dx}{X} \cdot R\,(X - x)$$

$$P(x) = \frac{1}{X} \cdot \int_0^X R\,(X - x) \cdot dx = R_2$$

C'est la valeur moyenne de 0 à X de la fonction R'_2 explicitée précédemment (voir fig : 10).



3. CALCUL DU RISQUE R (ou risque d'avoir une rupture en vol)

Comme nous l'avons déjà mentionné ce risque s'obtient en faisant le produit R1.R2 dont nous venons d'expliquer la méthode de calcul.

R1 et R2 se présentent donc sous forme de deux courbes. Le constructeur a donc plusieurs choix possibles, soit afficher une durée de vie élevée assortie d'inspections périodiques fréquentes de la pièce, soit au contraire une durée de vie faible avec inspections très espacées.

Mieux encore, ces courbes permettent de moduler les périodicités d'inspection en fonction du temps de vol de la pièce.

DUREE DE VIE	PERIODICITE D'INSPECTIONS	R1	R2	R TOTAL
1 000 h	100 h	10^{-4}	10^{-2}	10^{-6}
2 000 h	50 h	10^{-3}	10^{-3}	10^{-6}
5 000 h	10 h	10^{-2}	10^{-4}	10^{-6}

Fig. 11

COMBAT DAMAGE ASSESSMENT

by
Clarence H. Carper, Jr.
Chief, Safety and Survivability Technical Area
Applied Technology Laboratory
US Army Research and Technology Laboratories (AVRADCOM)
Fort Eustis, Virginia 23604

ABSTRACT

The effectiveness of the helicopter as an item of combat equipment for the United States Army has steadily and sharply increased since its baptism in Korea, where it helped to significantly reduce the fatality rate of the wounded by performing the medical evacuation mission. In Vietnam the helicopter's inherent and diverse capabilities were further exploited to include tactical missions such as scout, attack, troop insertion/withdrawal, resupply and command, control, and communication. The success of the helicopter in Vietnam was fundamental in helping to shape tactical doctrine for military aviation throughout the world. Today, the helicopter is a vital and integral part of the stable of equipment required by the modern US Army to satisfactorily fulfill its combat and combat support missions. As such, the helicopter must possess many capabilities and features, not the least of which is an inherent toughness that will allow it to take ballistic hits, complete the assigned mission, and then return its occupants for a safe landing in a friendly area.

This paper focuses on ballistic damage, with primary attention given to the airframe structure, and on ballistic vulnerability reduction issues for US Army helicopters. A synopsis is provided of the air defense threat systems and nature of combat damage received by Army helicopters in South Vietnam versus the threat and nature of ballistic damage anticipated in today's environment. New materials, structural concepts, and other vulnerability reduction measures presently being employed on Army helicopters and promising concepts currently under development are addressed. The paper is concluded with an overview of the combat threats anticipated for the helicopter in the near future.

INTRODUCTION

Since Korea, the combat helicopter has faced an ever-increasing hostile air defense system considering the quantity of weapons, their increased caliber and lethality, and their improved capability for detecting, acquiring, tracking and placing accurate fire on the helicopter. It is highly improbable that the helicopter will ever again face the limited air defense threat or enjoy the relative air superiority that was encountered in Vietnam. Relative safety from ballistic damage in South Vietnam could be obtained by one of two basic tactics: high-speed terrain flying, or cruise at 914 meters or more above ground level. In this relatively unsophisticated threat environment, however, thousands of helicopters were lost over an 8 to 10 year period, with approximately half of the losses being attributed to ballistic damage.

In today's more sophisticated threat environment the helicopter that exposes itself for more than a few seconds in a combat encounter will most likely receive ballistic damage. As such, the helicopter must be made to be more difficult to be detected and tracked by enemy threat acquisition systems, and it must be made to be more damage tolerant. Figure 1 shows how the helicopter's combat survivability probability varies as a function of the threat system when considering protective measures provided by tactics, signature reduction and electronic countermeasures (ECM), and ballistic hardening. In general, the Vietnam era would be represented by the left-hand half of the figure while the right-hand half is more representative of today's battlefield environment. As would be expected, overall probability of survival decreases as weapon size and sophistication increase.

Tactics

Operational tactics will play a vital part in whether or not the helicopter survives on the modern battlefield. US Army pilots, in particular those who fly the scout and attack helicopter missions, are receiving intensive training in nap-of-the-earth (NOE) flight. NOE flight is low and slow and provides stealth by masking the helicopter behind available terrain and vegetation. While this tactic enhances combat survivability by degrading the effectiveness of the threat detection/acquisition systems, it unfortunately reduces other survivability aspects by reducing margins of safety for the helicopter. For example, NOE operation eliminates the safety margin that is normally associated with altitude when malfunctions occur with the propulsion system. This gives rise to increased emphasis on the crash survivable aspects of the helicopter, to include the primary structure. Further, NOE operation is resulting in an increased number of both natural and man-made obstacle strikes for the helicopter. The most frequently occurring problem involves tree strikes with the main and tail rotor blades. This results mostly in additional maintenance and downtime, although the helicopter occasionally suffers catastrophic damage with fatalities. The more serious obstacle strike problem relative to helicopter loss and crew/passenger fatality results from wire strikes. Approximately one of every six US Army aviators killed in helicopter crashes over the past 10 years of peacetime operation has been the result of wire strikes. The overall obstacle strike problem is expected to worsen when complicated by performing NOE operations while in combat in

unfamiliar terrain. Further work is required in developing helicopter wire strike avoidance/protection systems and in improving the obstacle strike tolerance of the helicopter structure and other components in general.

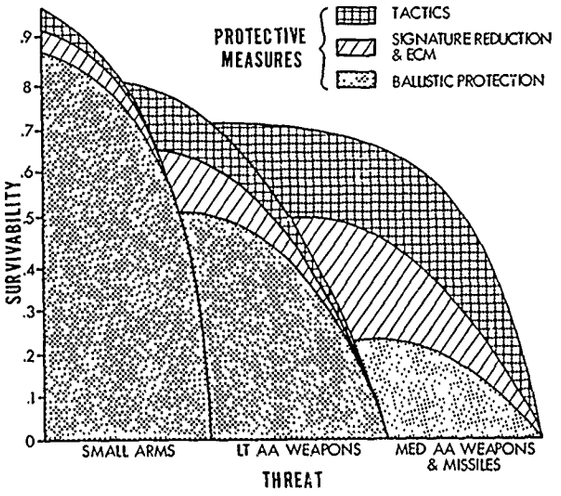


Figure 1. Protective Measures Versus Ground Fired AA Threats.

Signature Reduction

All weapon systems use one or more of the helicopter's signatures, or observables, for detection, acquisition, and fire control. These include the acoustical, visual, infrared, and radar signatures. The external noise generated by the helicopter is very distinctive and easily recognized, and, depending on conditions, can extend several kilometers from the helicopter. The primary noise sources are the main and directional control rotors. Significant work has gone into reducing the noise generated by the rotors. but it still remains a problem in current technology helicopters. The exposure time, and thus the probability of ballistic damage to the helicopter, can be reduced if the aural detection range can be reduced to less than the maximum range of the principal threat weapons, which is on the order of 1000 to 4000 meters.

Reduction of the visual signature of the helicopter is highly important considering the quantity of threat weapons which utilize it for fire control purposes. Primary offenders are sun glint off the canopy, rotor sun reflections resulting in rotor flicker and helicopter/background contrast. Very little can be done to reduce the visual detection cues of the helicopter within a range of approximately 1.5 kilometers. Beyond that range, however, detection can be reduced through such measures as shaping, applying coatings and glint reduction fairings/covers, and using open structural concepts. In addition to aural and visual detection considerations, the infrared (IR) and radar signatures of the helicopter are key elements to the success of several enemy weapon systems of today in acquiring and placing accurate fire on the helicopter. It is imperative that these two signatures be reduced to the maximum extent practical if the helicopter is to survive and carry out its combat mission. The helicopter is a complex IR radiator having emissions from a number of sources from within and on its outer surfaces. These are generated by heated surfaces (hot metal radiation), engine exhaust gasses (plume radiation), and solar reflections. Of this multitude of IR sources, the viewable hot engine parts and engine exhaust plume are the major concerns in countering IR seeker weapons. Although some success has been achieved in reducing IR signatures, additional work is required to reduce the weight and cost of the suppressor devices.

NOE flight in conjunction with a low radar cross section (RCS) of the helicopter will perhaps be the most effective and practical method of degrading the threat weapons that use radar reflectivity as the means of detection and tracking. The radar cross section, or echo area, is primarily a function of surface material, external shape, physical size of the helicopter and characteristics of the illuminating radar system. Although no low RCS helicopter per se is in production today, concepts have been applied to some helicopters to reduce their reflectivity through the selective use of absorbing materials and shielding. Ever-increasing research is being conducted, however, to define radar detectability and to investigate methods and concepts for RCS reduction. Potentially significant reductions in helicopter RCS are possible through fuselage shaping and the incorporation of radar absorbing/scattering materials. If low RCS is to be effectively incorporated, it must be considered in the initial design phases of a new helicopter system since the fuselage shape/skin material characteristics will most likely be a significant departure from those generally known today. The rapidly expanding use of advanced composite materials (nonmetals) for primary structure will provide the structural designers and manufacturing engineers with considerably more flexibility in developing and producing a low RCS helicopter fuselage.

Ballistic Protection

The Army helicopter in combat today would be faced with a wide variety of ballistic threat weapons, ranging from the infantryman's rifle through relatively large caliber artillery and missile systems. Further, a serious air-to-air threat would be posed by the presence of armed enemy attack helicopters. Regardless of how good a job is done considering the operational tactics used and the passive (discussed above) and active detection/suppression countermeasures concepts employed, the helicopter will continue to receive hits and suffer ballistic damage in significant proportions. Therefore, the Army, who is still the primary developer of the helicopter, must continue to identify and specify the ballistic threat requirements. It then becomes incumbent on the designer to continue to strive to minimize the effects of the ballistic projectiles by incorporating specialized vulnerability reduction (VR) concepts, damage tolerant materials, and structural configurations and techniques to reduce the severity of damage and battle damage

repair times and complexities. Further, it is imperative that this be achieved at acceptable cost and weight factors, especially when retrofitting or product improving existing helicopter systems is a consideration.

The remainder of this paper addresses the different ballistic threats to the helicopter, defines typical ballistically caused damage, and highlights some of the approaches being used and under investigation for reducing the ballistic vulnerability of the helicopter. Focus is placed as much as possible on the helicopter structure, to help provide the structural engineer/designer with a better understanding of the type, nature, and severity of problems he faces in dealing with the damage producing potential of the various ballistic threat projectiles.

SOUTH VIETNAM (RVN) EXPERIENCE

Although the helicopter faced a variety of threat weapons in South Vietnam, ballistic damage was primarily caused by the 7.62mm and 12.7mm small arms bullet fired from automatic and semiautomatic weapons. These two small caliber weapons are not generally classified as air defense weapons, yet the 7.62mm threat was responsible for approximately 85% of all ballistic damage suffered by US helicopters in RVN. General characteristics of the 7.62mm and 12.7mm projectiles are shown in Table 1. Table 2 lists the other threat systems and devices that also caused damage to the helicopters. In a general sense, the combat in RVN for the helicopter fell in the low intensity category. An example of an exception to this, however, is discussed later in this section of the paper. Some helicopters were lost to single 7.62mm hits while others survived a virtual barrage of multiple hits, including direct hits by rocket propelled grenades (RPG). In approximately 90% of the incidents the crew knew the helicopter had been hit, and approximately 60% of the time they saw the enemy firing the weapon that caused the ballistic damage.

TABLE 1. PRIMARY THREAT PROJECTILES--RVN

PARAMETER / THREAT	PROJECTILE LENGTH (MM)	PROJECTILE WEIGHT (GRAINS)	SERVICE MUZZLE VELOCITY (M/S)	TACTICAL RANGE (METERS)
7.62mm	36.8	155	884	400
12.7mm	64.5	745	854	1000

TABLE 2. ADDITIONAL THREAT SYSTEMS/DEVICES--RVN

THREAT
AA Weapons - 23mm, 37mm
Rocket Propelled Grenade - 80mm
Mortar - 82mm
Rockets - 122mm
Artillery - 152mm
SAM - SA-7
Land Mines - (Landing Zones)
Booby Traps - (Landing Zones)
Satchel Charges - (Sapper Action)

Some brief summary statistics are presented for the OH-6 observation/scout helicopter to help provide a better understanding of the nature and severity of the low intensity combat generally experienced in RVN. The OH-6 is a relatively small helicopter having a gross weight of approximately 1225 kg. It was introduced to Vietnam in 1967. Between 1967 and 1971 an average of 436 armed and unarmed OH-6 helicopters operated in RVN. They flew a total of 2.5 million sorties in 1.1 million flight hours, averaging 2.0 flight hours per day. During this period they experienced 3,174 incidents involving enemy ground fire, with 532 helicopters being lost. Table 3 breaks out the threat for 499 (approximately 94%) of these losses. As is evident, the 7.62mm and 12.7mm threat accounts for 80% of the total losses (71% and 9% respectively). Although not broken out, the total incidents include forced landings and mission aborts as adverse reactions, and continue to fly reactions in addition to the losses shown. Table 4 shows the percentages relative to the direction from which the ballistic hit was received and the general location of the hit on the helicopter. Over half of all the incidents for the OH-6 involved only a single hit, and over three-fourths involved no more than four hits per incident. It was rare to have 10 or more hits for a single incident. The average number of hits per incident was approximately 2.5 and the average number of incidents per helicopter lost was approximately 6, which results in a helicopter loss approximately every 15 hits. Also, over three-fourths of the incidents occurred at altitudes of less than 30.5 meters AGL (10.7 meters median) and less than 75 knots airspeed (50 knots median).

TABLE 3. OH-6 BALLISTIC DATA (1967-1971)

	7.62mm	12.7mm	HE	OTHER	UNK	TOTALS
Incident	2535	156	126	6	115	2938
Hits	6781	314	234	16	157	7502
Losses	354	46	38	2	59	499
Incident/Losses	7.2	3.4	3.3	X	X	5.9
Hits/Incidents	2.7	2.0	1.9	X	X	2.6

These latter points should be explored a little further since a part of the overall vulnerability/survivability of the helicopter is mission dependent. For a helicopter like the OH-6, over 90% of its mission involved combat surveillance and reconnaissance operations, i.e., scouting/in-route low-level flying and some target attacking for the armed versions. In general terms, this means relatively low and slow flight in a combat area by a helicopter with defensive fire power ranging from very little to none. Although the above hit percentages for the OH-6 are considered to be generally representative for RVN, they would vary somewhat, depending on the helicopter type and its mission. For example, the armed AH-1 helicopter in the attack role would have a smaller percentage of hits from

the front quadrant and a greater percentage in the aft fuselage/tail sections since the enemy would be less willing to commit to a frontal assault.

TABLE 4. DIRECTION AND LOCATION OF HIT--OH-6

HIT DIRECTION--%		HIT LOCATION--%	
Front Quadrant	29	Cockpit	31
Right Quadrant	28	Cabin	24
Left Quadrant	26	Engine/Equipment	18
Rear Quadrant	17	Main Rotor	14
	100	Tail Section (Incl Tail Rotor)	13
			100

During one 60-day period in the early 70's, the Army was involved in an intensive airmobile operation in an area that had been long established and well developed by the enemy, an area that was heavily defended. The combat damage sustained by the Army helicopters during this period is considered to be representative of a mid-intensity conflict and is summarized here solely for comparative purposes relative to the low intensity data discussed above. During this 60-day period the U.S. experienced 644 damage incidents to 451 different helicopters and lost 90 helicopters to enemy fire, including 2 Marine CH-53's. Table 5 summarizes the 88 Army helicopter losses versus the different threat systems for this period. In this mid-intensity environment the hit per loss ratio for the OH-6 was nearly 6 (over 7 for all 88 helicopters) as compared to a ratio of 15 for the OH-6 in RVN in general. This attests to the increased effectiveness of the larger caliber weapons against the helicopter.

TABLE 5. MID-INTENSITY LOSSES--RVN

ARMY HELICOPTERS	NUMBER OF HELICOPTERS LOST						TOTAL LOST
	7.62mm	12.7mm	RPG	HE	MORTAR	OTHER	
OH-6 22 Damaged 34 Hits	1	3	1	1			6
AH-1 101 Damaged 152 Hits	7	6			3	2	18
UH-1 285 Damaged 410 Hits	20	19	3	2	10	7	61
CH-47 30 Damaged 33 Hits	2				1		3
TOTAL LOST	30	28	4	3	14	9	88

The helicopters that were introduced early into RVN had very little inherent ballistic hardness/protection. As the combat intensity increased and as additional types of helicopters were employed, some protection was provided. For the most part, however, the ballistic hardness was parasitic in nature and was limited to partially protecting the crew and selected components and subsystems. This was accomplished by providing personnel body armor and by adding armor plates to shield such critical components as flight control tubes and actuators, engine compressor and fuel control, and transmission pump and oil cooler.

Vulnerability analyses of all US Army helicopters have identified the major vulnerability contributors for various types/sizes of ballistic threats. The 10 major contributors to the vulnerable area (A_V) of current helicopters versus the 7.62mm and 12.7mm threats are ranked in Table 6, which shows both attrition and forced landing kills. A_V is defined as helicopter presented area (A_P) times the probability of kill (P_K) given that a hit has occurred. Also, attrition kill is generally defined as one wherein the helicopter falls out of manned control immediately after being ballistically damaged. As can be seen, the main rotor flight control components account for the top 4 and for 6 of the total 10 contributors for the attrition kill A_V of the helicopter. This results from the A_V being approximately equal to the A_P since the P_K is very high given a hit. For the OH-6 helicopter, the 10 contributors listed for attrition kill represent approximately 70% of the total helicopter A_V for the 7.62mm projectile and 60% of the total A_V for the 12.7mm projectile. Considering the 10 forced landing contributors, the percentages are approximately 90 and 60 respectively.

TABLE 6. MAJOR CONTRIBUTORS TO VULNERABLE AREA (7.62MM AND 12.7MM API)

ATTRITION KILL	RANK	FORCED LANDING KILL
Main Rotor Flight Control Rod Ends	1	Main Transmission - Lube
Main Rotor Flight Control Rods	2	Tail Rotor Drive Shaft
Main Rotor Flight Control Actuators	3	Engine Lube
Main Rotor Flight Control Swashplate	4	Engine Combustion Chamber
Fuel Cells - Fuel Fire	5	Tail Rotor Flight Control Rods
Main Rotor Flight Control Pitch Horn	6	Tail Rotor Flight Control Rod Ends
Engine - Fuel Fire	7	Fuel Lines - Leak
Main Rotor Flight Control Bellcranks	8	Oil Cooler/Bypass Valve
Main Transmission - Gears and Bearings	9	Engine Compressor
Main Rotor Drive - Mast	10	Tail Rotor Control Rod Ends

It should be noted that even for these relatively small caliber threats, the fuel system ranks second behind the flight control system in helicopter attrition kill as associated with in-flight fuel fires caused by incendiary type projectiles.

Also, it should be noted that the tail rotor system shows up only in the forced landing kill column. This results from the approach taken in assessing the kill wherein the helicopter was credited with sufficient altitude and forward speed to permit it to execute a safe autorotative landing following loss of directional control. In considering today's requirement for NOE operation, the tail rotor system would also show up as a contributor in the attrition kill column as the helicopter would most likely not have sufficient altitude or forward speed to recover or effect an autorotative landing if directional control were lost while in NOE flight. This is representative of the "flexibilities" associated with performing vulnerability analyses, since many assumptions, estimations (especially P_K's), etc., must be made in accomplishing an analysis.

Finally, the trends shown in this section of the paper are considered to be generally applicable for all of the US Army helicopters that were in combat in RVN. As such, it should be noted that the airframe structure was not a significant contributor to the ballistic vulnerability of the helicopter when considering the primary threats faced (7.62mm and 12.7mm). This would probably have changed had the U.S. remained longer in Vietnam, since the quantity and size of the enemy antiaircraft (AA) weapons and the quantity of the surface-to-air missiles (SAM) were on the increase.

TODAY'S SCENARIO

The objectives of Army aviation are:

- To augment the Army's capability to conduct prompt and sustained land combat.
- To provide the ground commander with mobility, fire power, and staying power to win the first battle.
- To help the ground forces win while outnumbered.

Nonnuclear combat today would find US forces greatly outnumbered in terms of infantry, tanks, and artillery. The seriousness of the situation would be further compounded by the presence of fast, heavily armed enemy attack helicopters on the battlefield. Under such adverse combat conditions, the Army helicopter must play a significant part if the United States is to win. In today's combat, the helicopter will face an awesome array of air defense threat systems relative to what was encountered in Vietnam. A partial listing of the key threat systems is presented in Table 7. The threat would also include the mass deployed 7.62mm and 12.7mm weapons as well as a variety of other missiles, mortars, rockets, and artillery. As such, the helicopter must show marked increases in mobility and fire power over its RVN counterpart, and it must possess inherent features that will give it sustainability for extended periods of combat. Combat sustainability of the helicopter is considered extremely vital and will be a function of issues such as tactics, operational environment, threat system characteristics, and inherent helicopter features, including the ability to accomplish rapid repair of combat damage to prevent the helicopter from effectively being attrited by maintenance backlog. The key to this paper, however, is the sustainability that must be obtained through inherent ballistic toughness of the helicopter.

TABLE 7. KEY THREAT SYSTEMS--TODAY'S ENVIRONMENT

THREAT	SIZE	RANGE	GUIDANCE
ZSU-23-4	23mm	2500-3000 m	Optical and Radar
M53/59	30mm	3500-4000 m	Optical and Radar
S-60	57mm	6000 m	Optical and Radar
SA-6,7,8,9	1-60 kg Warhead	1-20 km	IR and Radar

The relatively small caliber high explosive (HE) and high explosive incendiary-tracer (HEI-T) projectiles (23-30-57mm) are of particular importance to the helicopter designer considering both their damage mechanism and the fact that they are pushing the limits as far as being able to "harden" the airframe and subsystems to withstand their destructiveness. Survival of the helicopter against threats beyond these will largely depend on countermeasures to avoid being hit. The major contributors to the total A_V for the typical current inventory Army helicopter against these three HEI-T threats are presented in Figure 2. The 30mm HEI-T would fit somewhere between the two bars shown. The estimates were made for the current helicopter fleet, excluding the UH-60 BLACK HAWK which is now in production and the YAH-64 attack helicopter which is approaching a production decision. Even though these two helicopters were designed for improved ballistic tolerance (12.7mm), the relative percentages shown would probably not change significantly if they were included in the estimates. Average A_V values are shown. Also, absolute values of A_V are very dependent on helicopter gross weight (size) as component criticality (P_K) generally increases

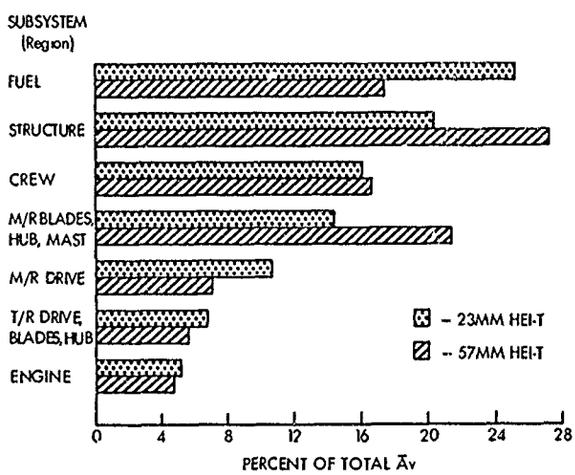


Figure 2. Subsystem Contribution to HE Vulnerable Area (Percent) (Average of Current Fleet Helicopters).

rapidly as sizes get smaller considering the HE projectiles. As can be seen in the figure, the helicopter structure (primarily tail boom) is the major contributor to the total A_V, followed closely by the fuel system, main rotor system, and crew. With exception of the crew, each of these will be addressed in more detail later in this section.

Explosive Projectile Characteristics

Considerable work has been accomplished toward defining AA explosive projectile characteristics and kill mechanisms and developing methods for reducing the helicopter's vulnerability to these explosive threats. Typical of these threats would be the 23mm HEI-T projectile. The primary threat weapon utilizing the 23mm round is the Soviet ZSU-23-4 quad-barreled automatic AA system, which is capable of firing approximately 60 rounds per second. Summary characteristics of the projectile portion of the round are provided in Table 8.

TABLE 8. 23MM HEI-T PROJECTILE CHARACTERISTICS

PARAMETER / THREAT	PROJECTILE LENGTH (MM)	PROJECTILE WEIGHT (GRAINS)	SERVICE MUZZLE VELOCITY (M/S)	TACTICAL RANGE (METERS)
23mm HEI-T	109	2986	976	2500

The HE projectiles normally have a delay contact fuse that is armed by centrifugal force and is activated when the nose of the projectile strikes the target. They then travel for a finite time within the target before exploding. Some of the earlier projectiles used a super quick fuse which caused explosion immediately upon contact of the projectile with the outer surface of the target, but they are not generally considered to be the primary threat to helicopters and only the delay fused projectile will be discussed further. The delay fuse HE projectile produces damage from any or all of the following mechanisms:

- Penetration of the target by the intact projectile (i.e., before detonation occurs).
- Fragment damage to the target produced when the projectile detonates.
- Blast loading of the target from the overpressure produced in the detonation process.
- Initiation of fires from (1) heat produced by detonation, (2) fragments striking certain materials, and (3) the incendiary mix contained in the explosive pellets.

The nature of the damage experienced by the helicopter is dependent on the projectile velocity, the depth of penetration before explosion, the medium in which the explosion takes place, and the nature of the target failure mode. For the structure, for example, the blast pressure and fragments are the most lethal mechanisms, whereas the blast pressure and incendiary are the most lethal for the fuel cell.

Figure 3 depicts the general sequence of events that occur during the detonation of a high explosive projectile. Figure 4 and Table 9 show typical fragment spray zones and characteristics for the projectiles. Objects within 1 to 3 case diameters distance would be subject to the blast wave followed immediately by fragment impact. Beyond 3 to 6 case

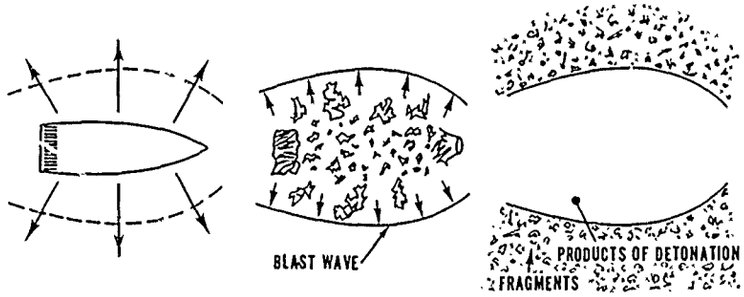


Figure 3. Sequence of Events During Deconation of a HE Projectile.

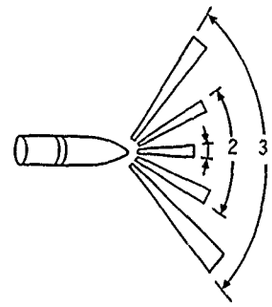


Figure 4. Fragment Spray Zones--Typical HE Projectile.

TABLE 9. TYPICAL NUMBER, AVERAGE WEIGHT AND VELOCITY OF HE PROJECTILE FRAGMENTS.

ZONE	NO. FRAGMENTS	WT GRAIN		VELOCITY M/S	
		AVG	MAX	AVG	MAX
1	5	9	40	732	976
2	175	7	100	884	1189
3	600	3	30	1006	1098

diameters, damage would first occur by fragment impact followed closely by the overpressure and the other products of detonation. This later mechanism is the predominate one when considering vulnerability of the helicopter structure.

Representative pressure levels associated with the HE detonation in the air medium are shown in Figure 5. This is a combination of peak pressure associated with the blast shock front (approximately 1 millisecond duration) and the static pressure generated by the overall detonation energy release. The peak pressure is of such short duration that the structure may not have time to respond to it. The greater hazard to the structure may come from the longer duration static overpressure, especially in areas where the structure has been weakened by the fragments in advance of the overpressure.

One aspect of fuel cell vulnerability is the explosion of the HEI-T projectile within the combustible vaporous mixture above the liquid fuel level in the tank. Figure 6 presents typical blast/combustion response pressures for this situation as determined through testing. Worst case peak pressures measured were in the neighborhood of 4.6×10^3 kilopascals (KPa) for 5 to 10 milliseconds (msec) duration. This is addressed in more detail later in the paper.

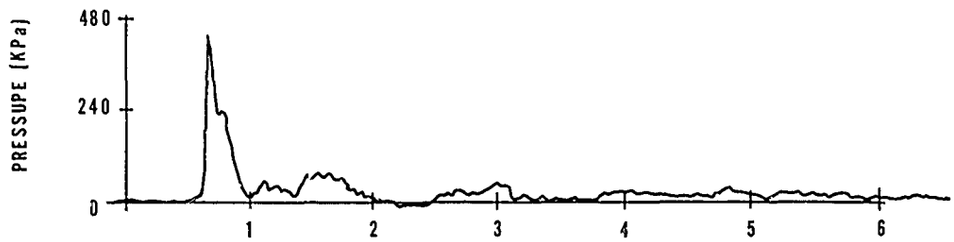


Figure 5. Typical Blast Pressure--Air Medium.

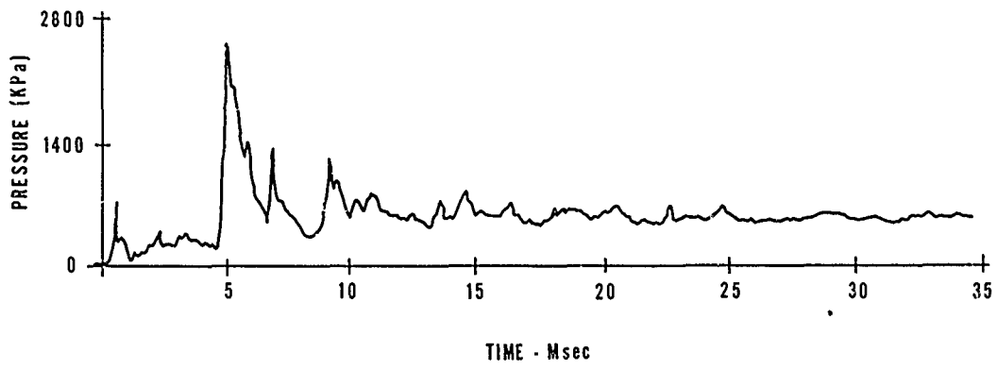


Figure 6. Typical Combustion Response--4% Volume Propane Medium.

Fuselage Vulnerability

With the exception of the tail boom of a single main rotor helicopter, the airframe structure has relatively low vulnerability to the explosive projectile. This holds true even for the conventional metal skin, stringer,frame, semi-monocoque structure of the helicopters which were used in RVN and which did not have ballistic hardening as a part of their basic design requirements. The cabin/cargo section of the helicopter is usually fairly large in volume, is structurally redundant in nature, and is designed primarily against stiffness requirements. As such, when the projectile penetrates the skin and detonates, assuming it does not function in or near a highly vulnerable component or subsystem, the damage caused to the structural members although serious in nature is not usually catastrophic to the helicopter. The damage could possibly result in changes in the helicopter system's dynamic response characteristics, but the residual (after damage) strength of the airframe will probably be adequate for continued flight, especially if the in-flight loads are reduced, i.e., the pilot throttles back and conducts slow speed, level cruise flight.

The tail boom, on the other hand, is a highly vulnerable area of the fuselage to the explosive projectile. In today's conventional helicopter (i.e., main rotor/tail rotor concept) the tail boom is in essence an inclosed metal structure of semi-monocoque design. Detonation of an HEI-T projectile within this structure, as represented in Figure 7, induces several potentially catastrophic events, including: massive removal of structure caused by the heavier fragments in the inner (1 and 2) cones; penetration of the structure

by the hundreds of smaller fragments in the outer (3) cone; and excessive "breathing" of the structure in response to the high blast overpressure. Also present is the incendiary fire, but without a medium to sustain the fire it does not pose a significant hazard in the tail boom. Figure 8 shows the exit hole in a typical medium sized helicopter tail boom that had been impacted in test with a delay fuse explosive projectile. Less evident than this large ballistic hole, but perhaps equally as catastrophic to the helicopter, is the damage related to the breathing of the structure. Additional massive failure (tearing) of the tail boom structure can occur when subjected to the overpressure/breathing in the weakened area along the line of holes caused by the fragments in the larger spray cone. Further, the magnitude of the breathing can be such as to cause excessive misalignment of the tail rotor drive shaft resulting in failure of the shaft, coupling or hanger bearing and subsequent loss of helicopter directional control.

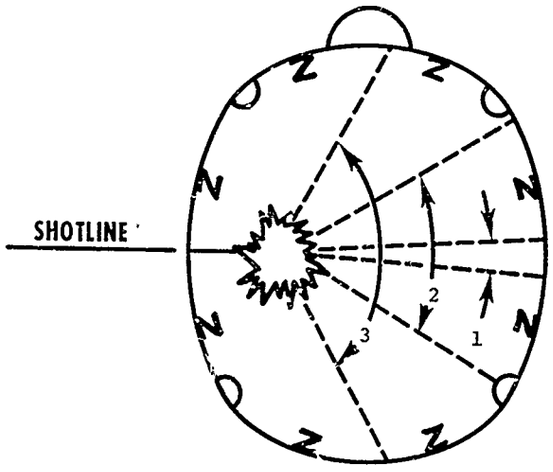


Figure 7. Typical HE Projectile Detonation Within a Tail Boom.

The tail boom, however, is an area of the fuselage structure where much is being done to improve the overall survivability of the helicopter against this type of explosive ballistic damage. To a limited extent this also includes the conventional metal booms through the application of relatively inexpensive "quick fix" hardening concepts. These include the selective addition of straps and plates longitudinally along the boom and circumferential straps at the frames to serve as doublers for added strength and to act as crack stoppers; the addition of high strength rivets between existing skin attachment rivets for increased strength; and the installation of reticulated foam within the boom to help suppress the blast overpressures, thus reducing the blast loading on the structure. Although these concepts have demonstrated some success in reducing the vulnerability of the tail boom to the explosive projectile, they are considered only temporary measures which do not properly address the fundamental issues of the problem. To satisfactorily do this will require the development and application of more efficient materials to achieve the necessary toughness and structural redundancy at acceptable weights, and the development and application of advanced structural concepts to help minimize the effects of the blast pressures.

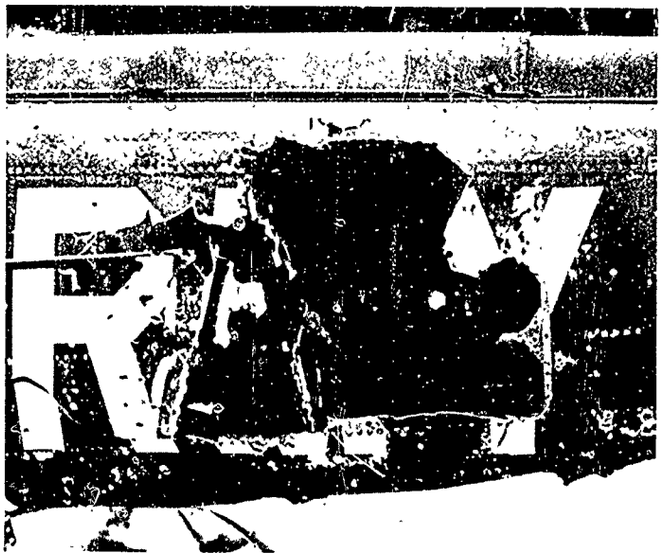


Figure 8. Exit Side of a HE Damaged Tail Boom.

In this light, the utilization of fibrous composite materials offers the greatest opportunity to resolve the tail boom ballistic vulnerability problem, as well as generally revolutionalize the overall helicopter design process. Composite materials such as fiberglass, Kevlar, and graphite are presently being widely used for helicopter rotor blades and airframe secondary structure and are being developed and tested for mechanical flight controls, rotor hubs, airframe primary structure and landing gears. The unique properties inherent to the composite materials are generally well known and will not be addressed in this paper. However, the potential payoffs for using them in the helicopter include:

- Greater structural efficiency through the higher specific strength and stiffness of the material systems.
- Greater design flexibility through the ability to easily dynamically tailor the structure and utilize complex shapes.
- Improved safety through inherent slow crack propagation and greater ballistic tolerance.

- Lower acquisition cost through the use of more automated fabrication processes/ techniques, fewer mechanical fasteners, and less material scrappage.

- Lower ownership cost through longer fatigue life, inherent damage tolerance, and easier field repair.

The helicopter industry is only on the threshold of exploiting the full potential of the application of these composite materials.

Several programs have been conducted within the US Army R&D community relative to composite booms. One program recently completed involved the laboratory test and flight demonstration of a composite replacement tail boom on the AH-1G Cobra helicopter. The composite boom was a monocoque sandwich structure having graphite inner and outer skins with a Nomex honeycomb core and a wall thickness of approximately 1.5 cm. The boom was fabricated by the wet filament winding process with a one-step cure cycle. Primary design objectives for the boom were reduced manufacturing costs and reduced weight. Both goals were generally met although the weight was not optimized as the composite boom was fabricated resin rich. Being designed primarily for stiffness, the composite boom demonstrated (through accelerated testing) a fatigue life in excess of seven times greater than its metal counterpart. Although ballistic tolerance was not a design consideration for this composite boom, the residual flight test boom was subjected to two 23mm explosive projectiles, the first impacting the large diameter end and the second the small diameter end. Being a closed structure, the detonation overpressure literally "ripped" the boom open along the line of holes created by the spray of fragments, resulting in catastrophic damage of the small diameter end. Figure 9 shows the ballistically damaged composite boom.



Figure 9. Ballistically Damaged AH-1 Composite Tail Boom.

Concurrent with this program was an investigation of the ballistic tolerance of a variety of simulated tail boom sections manufactured from different composite materials and using various structural configurations, including shell structure, sandwich structure with various honeycomb cores, and sandwich structure with a sinewave core. Although the composite materials demonstrated improved damage toughness, the fate of these closed structure specimens was generally the same as that experienced by the AH-1G composite tail boom. It was evident from these tests that the high pressures from the explosive projectile detonating within the relatively small internal volumes of the tail boom must be neutralized through some type of venting process, as designing the structure to contain the blast forces would result in unacceptable weight penalties.

This led to the investigation of composite tail boom specimens using an open weave, or "spacewound" structural concept. The spacewound structure allows rapid venting of the blast pressure as well as provides redundant load paths. Figure 10 describes the spacewound principle. In all, 16 composite specimens were fabricated against operational tail boom specifications and structurally and ballistically tested. The specimens included a variety of composite materials, fiber coverage ratios (FCR), helix angles, diameters and lengths; some were skinned (nonstructural skin) and some unskinned. The fiberglass and Kevlar specimens with 50% FCR showed lowest damage coefficients to the 23mm HEI-T projectile. Peak internal pressures measured were in the neighborhood of only 300 KPa. The test sequence for one of the final Kevlar specimens is outlined to show the severity of the testing and the success obtained against this explosive projectile.

Preballistic Structural Test:

- Cantilever mounted with vertical shear load of 952 kg (limit load) at free end. Repeated after 180° rotation.

- Static torsional moment applied twice in each direction to 13,556 n-m (limit load) in 2,259 n-m increments.

- Fatigue cycled at $\pm$ 6,778 n-m (50% limit torque) for 15,000 cycles.

- Static torsion test repeated.

Ballistic Test:

- Ballistically tested with a 23mm HEI-T projectile while statically loaded to represent 125 knots flight load condition.

Post Ballistic Test:

- Cantilever mounted and loaded to 635 kg (66% of limit) in 159 kg increments.
- Static torsional test to 6,778 n-m (50% of limit) in each direction.
- Fatigue cycled at 1,130 ± 3,389 n-m for 5,000 cycles (simulated maneuver load at 150 knots).
- Static torsion test repeated.

Second Ballistic Test:

- Impacted with a second 23mm HEI-T projectile (within 20.3 cm of first impact point) while under 125 knots static flight loads.

Post Second Ballistic Test:

- Static torsion test to ± 6,778 n-m each direction.
- Fatigue cycled at 1,130 ± 3,389 n-m for 1,500 cycles.
- Static torsion test to ± 6,778 n-m each direction.

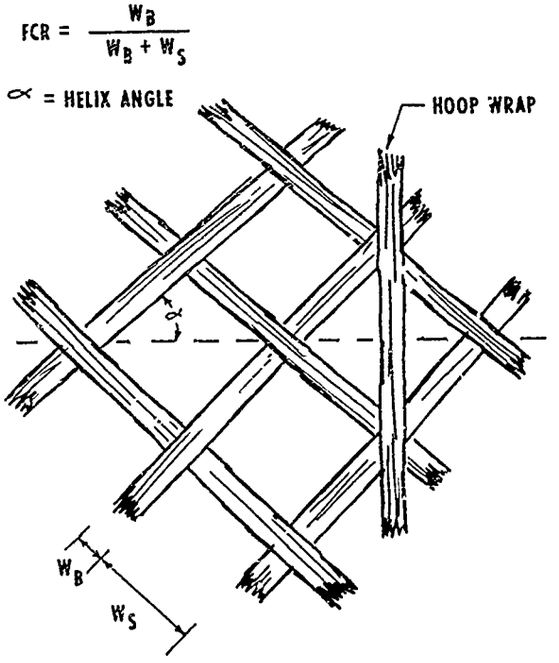


Figure 10. Spacewound Structural Concept.

The above specimen was still capable of carrying load although the maximum tip deflection measured had nearly doubled over that of the undamaged specimen. Figure 11 shows the specimen on the test fixture following the second ballistic impact. Note that the skin has mostly been blown away. The spacewound structural concept has proven to be effective in providing ballistic survivability to the helicopter tail boom against the explosive projectile.

Other "open" composite structural concepts are being investigated to develop a lighter weight, lower cost, more ballistically tolerant tail boom. Two of the more promising ones include the truss and tetracore structural concepts. Both of the concepts use the wet filament winding, single-step cure fabrication processes. In the truss program a variety of configurations were analyzed concerning primarily the number of longerons used (four through eight) and the capability of the diagonals to take both tension/compression loads or tension loads only.



Figure 11. Kevlar 50% FCR Specimen After Second Ballistic Impact.

The six longeron, tension/compression diagonals graphite concept was determined optimum for meeting the design requirements at minimum weight. The ballistic survivability requirements called for the loss of a compression side longeron joint and one opposite side diagonal member. Three specimens were fabricated which represented a relatively small sized helicopter, i.e., a .368 meter diameter boom, and were ballistically tested against the 23mm explosive projectile. The specimens were unskinned and had approximately 50% open area. Figure 12 shows one of the test specimens. The target impact point for all three specimens was the frame/longeron/diagonal member joint. Two of the specimens were statically loaded to loads representative of high-speed level flight conditions, ballistically impacted, and continued to carry the flight loads for 30 minutes after impact with negligible measured deflections. The third specimen was statically loaded to 150% of high-speed level flight load conditions and failed upon impact. Damage on the exit side of this specimen was far more extensive than anticipated. In general,

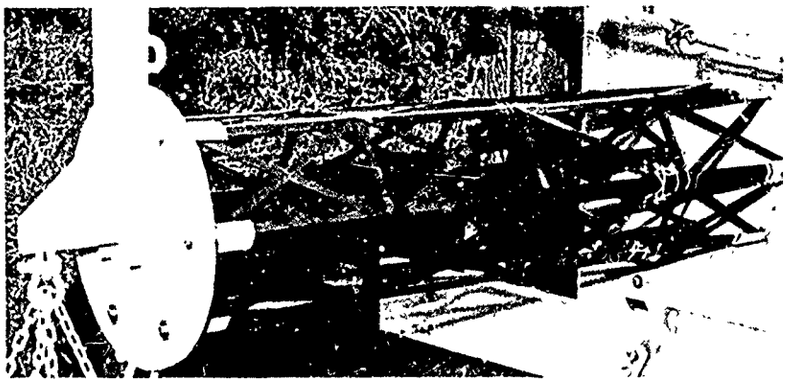


Figure 12. Truss Tail Boom in Ballistic Test Fixture.

the composite truss structural concept demonstrates a vary high potential for improving the ballistic survivability of the tail boom, as the projectile blast pressures are vented and do not play a part in the damage mechanism. Also, if the truss tail boom is left unskinned, the probability is introduced that the threat projectile will pass through the boom without being activated, or that it will strike a member on the exit side and detonate outside of the boom.

Tetracore is still another variation of a highly efficient open structure concept that can be readily fabricated from composites. In principle, it is a series of alternately inverted tetrahedron shaped cells continuously joined together. Work is in progress to more completely define the structural properties of tetracore, and to fabricate a demonstrator tail boom out of tetracore for an existing medium-sized helicopter. Structural and ballistic testing of the boom are planned. A trial winding of the tetracore tail boom is shown in Figure 13.

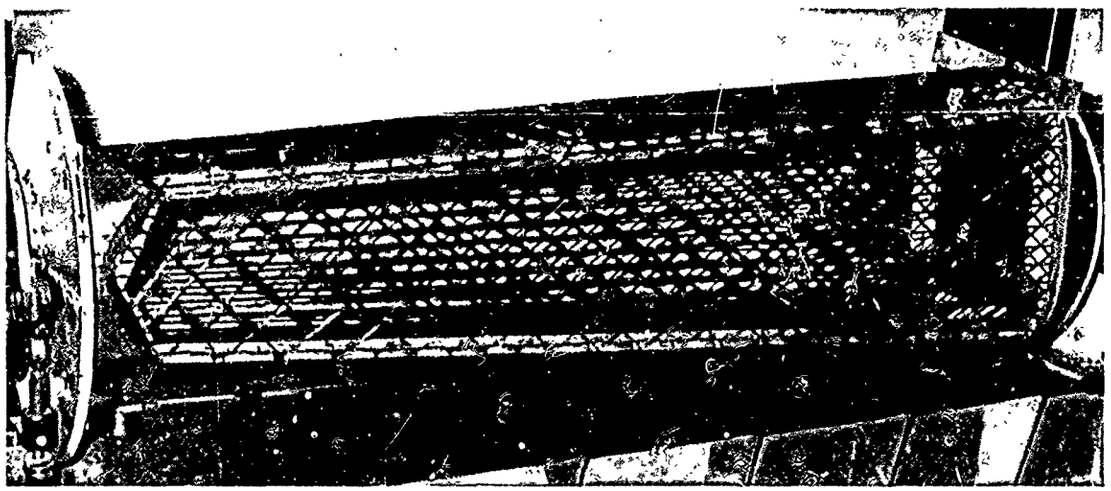


Figure 13. Tetracore Tail Boom Specimen.

Fuel System Vulnerability

Testing and analysis has shown that the fuel tank is the single most vulnerable helicopter component to the 23mm HEI-T projectile. For HEI-T projectiles larger than 23mm the helicopter structure becomes most vulnerable but only by a small margin over the fuel system (refer to Figure 2). The schematic shown in Figure 14 indicates the impact points for the threat projectile that are of primary concern for precipitating different types of catastrophic failures of the fuel tank and causing related in-flight fuel fires. The combined kinetic energy and blast overpressure associated with a projectile impacting the outer wall and detonating within the liquid fuel can cause hydraulic ram pressures high enough to rupture the fuel tank. This can result in massive fuel loss and possible fire if the leaking fuel contacts a secondary ignition source. Damage can also occur to the structure adjacent to the tank due to the rapid expansion in tank volume. Hydraulic ram pressures in the neighborhood of 2.07×10^4 KPa have been measured in tests against the 23mm HEI-T projectile. The detonation of an HEI-T projectile within the ullage area above the liquid fuel level in the tank can generate combustion overpressures of sufficient magnitude to also rupture the tank. In this case the spilling fuel would most likely be ignited by the incendiary products in the projectile. Finally, detonation of an HEI-T projectile outside of and adjacent to the tank wall, and below the liquid fuel level, either in the dry bay areas or near the outer skin, will most likely result in fragment/blast damage to the tank wall with the spilling fuel being ignited by the incendiary products.

Significant research work has been accomplished over the past few years toward reducing ballistically caused in-flight fuel fires through the investigation of concepts and methods of reducing the vulnerability of the fuel system to the explosive/incendiary projectile. Considering hydraulic ram, the high ductility of current self-sealing, crashworthy

helicopter fuel tanks offers a degree of protection against the ram effects. Additional protection can be readily obtained by the designer through such measures as inclosing the fuel cell within a rigid structure and providing smooth, elastic surfaces for the cell to react against and and to spread out the load. Other specific add-on protective measures have been investigated and found to be effective in helping to defeat hydraulic ram, including installing reticulated flexible foam inside the tank to slow down the shock front and absorb pressure; providing elastic energy absorbing buffers to prevent failure/permanent deformation of the adjacent structure; and providing shielding material, e.g., ballistic nylon or Kevlar, to slow the projectile down before impacting the fuel cell as the hydraulic ram pressure is proportional to the square of the velocity of the projectile.

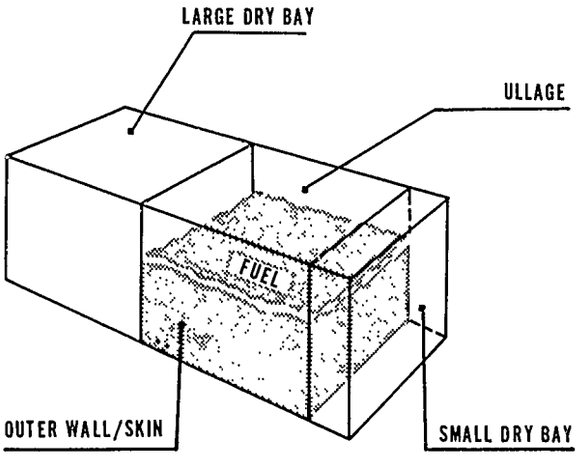


Figure 14. Fuel Tank Damage Producing Impact Points.

In considering the remaining areas of concern identified above for the fuel system, several highly promising vulnerability reduction approaches/concepts are evolving, i.e., lightweight foams, powder-filled panels, ullage inerting systems, and active detection/suppression systems. Rigid foams are presently used selectively around the fuel cells of both the UH-60 BLACK HAWK and YAH-64 attack helicopters, and flexible foams are being evaluated for use inside the YAH-64 tank. In considering the foams used internal to the tank to reduce hydraulic ram and ullage fire dangers, Figure 15 shows the effectiveness in reducing peak combustion overpressures of several newer foam concepts under investigation as compared to reticulated polyurethane foam. Testing was conducted in a rigid test tank of 1.13 cubic meters volume using "worst case" propane/air combustible mixtures and the 23mm HEI-T projectile as the initiator. The weight of the foam in the tank is shown on top of the bar. Explosafe is a metal void filler material made by slitting, expanding, and stacking thin aluminum sheets. Its primary advantage over nonmetallic foams is the ability to tolerate high ambient temperatures (over 150° C) that are present, for example, in high performance fighter or transport applications. Promel is made from sheathed nylon fibers that have been woven into a mesh-type structure and heated to create a miniature weld at each fiber contact point. Its primary advantage is low weight. Figure 6 shows that all of the internal foams appreciably reduce peak combustion overpressures when compared to the unprotected tank. This protection comes, however, with increased weight to the helicopter and in the case of internal foams some fuel denial made up of displaced fuel and absorbed/retained fuel.

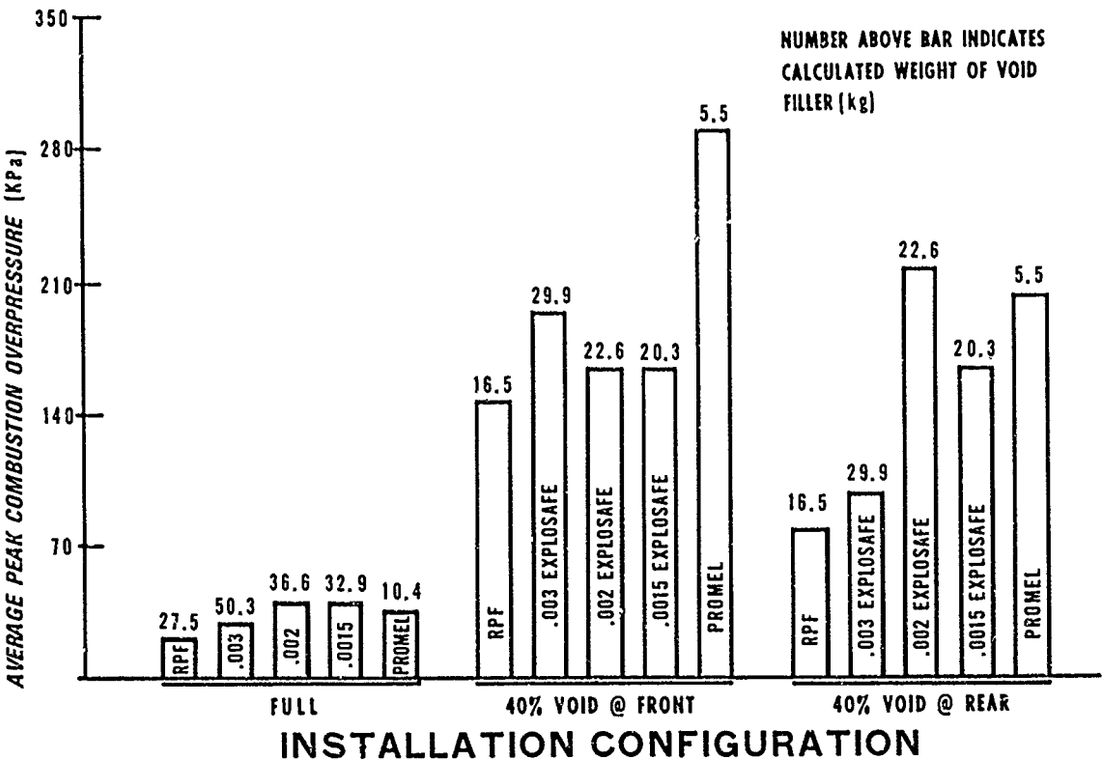


Figure 15. Comparison of Various Void Filler Materials in Reducing Peak Combustion Overpressure.

The powder panel concept is one wherein the fire extinguishing agent is contained integral to the panel (within the honeycomb) and is released by the kinetic energy, detonation, and/or fragments of the projectile. The concept is applicable for use as separate add-on panels or as an integral part of an existing structural panel/skin (i.e., primary structure) of the helicopter and is proving to be highly effective in preventing fires when used against the explosive projectiles in the outer wall/skin and small dry bay areas. Numerous ballistic tests have investigated both metallic and nonmetallic panel specimens, various panel thicknesses, and various types and quantities of extinguishing agents. Work is also in progress toward obtaining long-term environmental/operational effects on the powder panels, extinguishing agent corrosion hazards, and details concerning manufacturing processes and test and inspection procedures. Powder densities as low as 14.4 Pascals within the honeycomb panel have proven successful in preventing ballistic related fuel fires. Figure 16 shows a typical nonmetallic specimen following HE ballistic impact.



Figure 16. Ballistically Damaged Kevlar Powder Panel Test Specimen.

For ullage explosion to occur in the fuel tank, a flammable fuel/air vapor must be present and there must be an ignition source. Given a hit by an explosive incendiary projectile into a combustible mixture in the ullage area, the severity of the ullage explosion is dependent on the ullage volume and the specific fuel/air vapor ratio present. The severity of the explosion related damage is then dependent on the fuel cell strength, the proximity of the cell to critical structure, and whether or not the tank is ruptured. If the tank is ruptured and fuel spillage occurs, the probability of related catastrophic in-flight fuel-fed fire approaches unity. Considering the effects caused by the blast and combustion overpressure of ullage explosion, much of the discussion concerning hydraulic ram pressure generally applies. In addition to using internal foams, the concept of inerting the combustible vapors in the ullage is highly effective in preventing explosions and fire. Testing has shown that if the oxygen level in the ullage is kept below 10% by volume, combustion cannot occur. One of the leading approaches for accomplishing this is through inerting the ullage with nitrogen gasses. Nitrogen can be readily generated onboard the helicopter by taking engine bleed air and passing it through an air separator module (i.e., molecular sieve or permeable membrane) which dumps the oxygen enriched air overboard and passes the oxygen depleted (nitrogen enriched) air through the fuel tank ullage area. Such a nitrogen inerting system would weigh approximately 6 kg for a helicopter similar to the AH-1 Cobra. The danger of having an ullage explosion, however, may be significantly reduced if JP-8 fuel replaces JP-4 fuel, as anticipated in the next few years, due solely to the lower volatility of JP-8.

Active detection/suppression systems are also proving successful in providing protection against ballistically caused fuel system fires primarily in the large dry bay areas adjacent to the tanks. Two concepts initially developed in the U.K. are being tested in the U.S. for potential application in Army helicopters. One concept uses transducers located within the tank to sense pressure change resulting from ballistic impact and activates appropriate high rate Halon 1301 extinguishers. A second concept uses optical detectors which respond to U.V. radiation during incendiary or HE projectile impact on the fuel tank and provides a signal to discharge extinguishers which contain a powdered agent. Ballistic testing of this latter concept in an actual helicopter dry bay wherein fuel was leaking from the wound in the cell demonstrated that fire suppression is completed within 200 msec after detonation of the projectile utilizing an extinguishant concentration of approximately 150 gm/m^3. No attempt was made to establish the lower limit of concentration. Such a system would weight approximately 4.5 kg for a helicopter similar to the AH-1 Cobra.

Effort is presently underway by the Army to accomplish detail design and development of a fuel fire protection system to reduce the vulnerability of its helicopters to the explosive/incendiary projectile. The system will employ select pieces of the individual concepts discussed above, i.e., powder-filled panels/structure, U.V. active detection/suppression and nitrogen inerting. The system will be designed for subsequent demonstration on the AH-1 Cobra; however, the major components of the system will be generic so as to be applicable to all Army helicopters.

Rotor System Vulnerability

In discussing rotor system vulnerability, focus will be placed on the primary components of the main rotor, i.e., blades, hub, and control rods/linkages. The rotor system is a much more complex structure than the fuselage, being subjected to a considerably wider variety of conditions within which it must operate. Combat damage to a rotor blade, for example, can easily prove catastrophic to the helicopter due to the effects on the in-flight dynamic response of the total helicopter system even though the blade has sufficient residual strength to carry flight loads after the damage. As such, the design of a ballistic tolerant rotor system must involve a "total systems" approach even beyond that necessary for the fuselage.

The rotor system was not a major contributor to the overall helicopter A_V against the small arms (7.62mm and 12.7mm) threat encountered in RVN, even though the P_K for the main rotor controls was extremely high when impacted with a projectile. In fact, the main rotor blades on the Army helicopters in RVN were capable of receiving multiple small caliber hits without catastrophic effects even though ballistic tolerance was not specifically a part of their design. Considering today's threat, however, the main and tail rotor systems combined comprise a significant portion of the total of A_V of the helicopter against the 23-57mm high explosive projectiles, including both attrition and forced landing kills.

Within the rotor system the main rotor blade has by far received the greatest attention to date. Numerous reports and papers have addressed the many R&D efforts directed toward improving the blade's ballistic qualities while also improving other design and performance features. It is well established that the prevention of the separation of a part of the rotor blade at a spanwise station is fundamental to the ballistic survivability of the blade/helicopter system. The loss of individual pieces of the blade such as box sections, especially from inboard stations, may not necessarily be catastrophic, but the separation of virtually any spanwise section of the blade generally will be. Such spanwise losses usually result in large unbalanced forces which in turn cause high vibrations and/or asymmetrical lift, either or both of which usually result in an uncontrollable helicopter. Further, the rotor blade must be able to withstand major structural damage in high strain locations and still have sufficient stiffness and fatigue life to permit the helicopter to make a safe landing. Key parameters then in the design of a ballistically survivable rotor blade are the spar chord length, structural configuration, and materials used. In general terms, it is imperative to spread the structure out and provide redundant load paths and to use materials that possess low notch sensitivity and high fracture toughness characteristics. Numerous programs over the past few years have investigated various advanced structural concepts and materials toward the development of rotor blade designs that are tolerant to the high explosive projectiles. A consistent result from these programs is that rotor blades constructed from composite materials show significant improvement in HE ballistic survivability over equivalent sized metal blades.

Rotor blade ballistic survivability has received increased emphasis within the US Army as evidenced by the capabilities of the blades shown in Table 10. In assessing the

TABLE 10. HELICOPTER MAIN ROTOR BLADE BALLISTIC SURVIVABILITY COMPARISON

HELICOPTER	NO. BLADES	BLADE CHORD (M)	BLADE CONSTRUCTION	RELATIVE 23MM HEI VULNERABILITY (ATTR+F.I. KILLS)	
UH-60A	4	.528	TITANIUM D. SPAR, NOMEX HONEYCOMB CORE, FIBERGLASS SKIN GRAPHITE TRAILING EDGE	9.0	
YAH-64 AAH	4	.533	MULTI-TUBULAR STAINLESS STEEL/ FIBERGLASS SPAR, NOMEX HONEYCOMB CORE, FIBERGLASS SKIN STAINLESS STEEL TRAILING EDGE	10.0	
CH-47D	6	.813	FIBERGLASS D. SPAR/ TI NOSE CAP, NOMEX HONEYCOMB CORE, FIBERGLASS SKIN GRAPHITE TRAILING EDGE	9.5	
AH-1S	2	.762	MULTI-TUBULAR FIBERGLASS SPAR, NOMEX HONEYCOMB CORE, FIBERGLASS SKIN KEVLAR TRAILING EDGE	8.0	
UH-1H	2	.533	ALUMINUM D. SPAR/ HONEYCOMB CORE/SKIN/ TRAILING EDGE	6.5	
OH-58C	2	.330	ALUMINUM D. SPAR/ HONEYCOMB CORE/SKIN/ TRAILING EDGE	5.5	

relative vulnerability numbers shown, 10 is considered best, i.e., least vulnerable. Although the BLACK HAWK and attack helicopters' rotor blades were designed against the small API threat, they both have proven through testing to be tolerant to the small high explosive projectile. Typical of such testing would be that shown in Table 11 for the AAH blade where a 1.83 meter specimen was ballistically impacted and subsequently tested. No discernible crack growth was observed during the first 76 minutes (21,900 cycles) of representative flight loads. The specimen continued to carry the test loads after approximately 5 hours of testing although the damage had grown significantly. The objective of the test was to demonstrate the capability of flight for 30 minutes (8,670 cycles) subsequent to the ballistic damage. This objective was appreciably exceeded. Although the BLACK HAWK main rotor blade utilizes a welded titanium "D" spar concept, it has also proven tolerant to the small high explosive projectile. Basic design philosophy for this spar includes additional material to safely operate at very high stress allowables, and a wider spar planform, i.e., almost 50% of the chord length.

TABLE 11. YAH-64 MAIN ROTOR BLADE SECTION TEST

- BALLISTIC TEST
  - HE Projectile Impact in Spar at Midspan
  - 19,000 kg Tensile Load (Combined Loads in Hover due to CF and Flap, Chord and Torsion Moments)
- FATIGUE TEST
  - 5.1 Hours Total (89,350 cycles)
    - 9,615 kg CF
    - ± 678 n-m Flap Moment
    - 2,180 ± 428 n-m Chord Moment
    - 112 n-m Torsion Moment

Although significant progress has been made in reducing the vulnerability of the rotor blades, continued work is necessary, particularly relative to improving the survivability of the small chord blades to the HE projectile.

The main rotor hub, although not generally designed for ballistic tolerance, proved to be relatively invulnerable against the small arms (7.62mm and 12.7mm) threat in RVN. It is believed that this results from the hub being one of the most compact, strongest components on the helicopter. Although very little testing has been accomplished to verify it, these existing hubs would probably also demonstrate relatively low vulnerability to the high explosive projectiles. The more modern BLACK HAWK helicopter hub, which is titanium, was designed against the small API threat, but has shown through testing to be tolerant to the small HE projectiles as well. The hub area is again one wherein composite materials offer a good opportunity to improve ballistic survivability while at the same time obtaining significant reduction in hub weight and cost. In pursuing this opportunity, the Army conducted a research program wherein a graphite hub was investigated as a replacement component for the existing titanium hub on the CH-54 Heavy Lift Helicopter. A one-half scale model graphite hub was fabricated and structurally tested which demonstrated, among other desirable features, the capability for a 25% weight savings and a 75% cost savings over the existing metal hub. Although not experimentally verified, analysis showed the composite hub to be highly tolerant to the HE threat. Figure 17 shows the three-plate composite hub concept investigated.

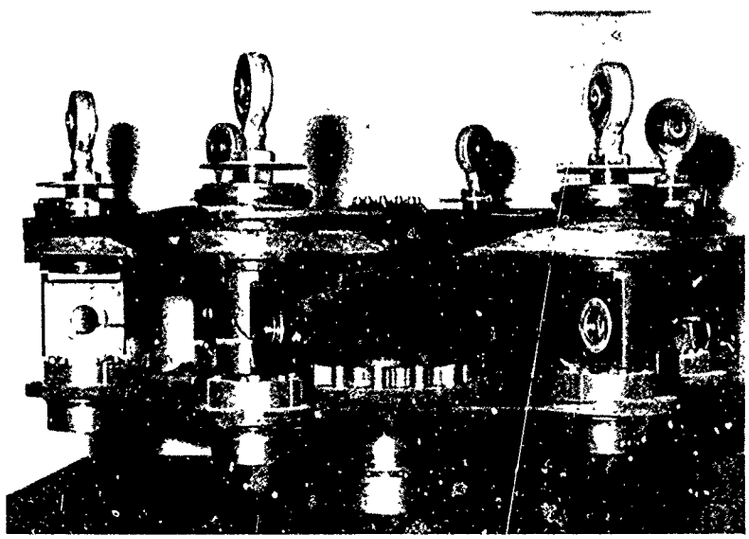


Figure 17. Composite Plate Hub, Assembly.

As mentioned earlier in the paper the flight controls on RVN era helicopters are highly vulnerable to essentially all ballistic threats. Their vulnerable area is generally the same as their presented area since the probability of kill approaches unity given a hit on one of the control components. Fortunately their total presented area accounts for only a small percentage of the overall helicopter presented area. Considerable effort has been expended in investigating, testing, and developing ballistic tolerant flight control components, once again with the focus on composite materials application. Lightweight, low cost, highly survivable designs for mechanical components such as connecting links, bellcranks, idler arms, etc., are readily available for incorporation into existing helicopters. Due to size effects, however, the very low gross weight helicopters may still require some parasitic armor to protect parts of their control systems. Typical composite ballistic tolerant flight control components investigated are shown in Figure 18. Flight control system survivability for future helicopter systems should be capable of even further improvements with the continued development of the advanced fly-by-wire/

fly-by-light concepts. These advanced control concepts will permit the designer to more efficiently accomplish the wide separation of components and system redundancy which are keys to ballistic survivability of the flight control system.

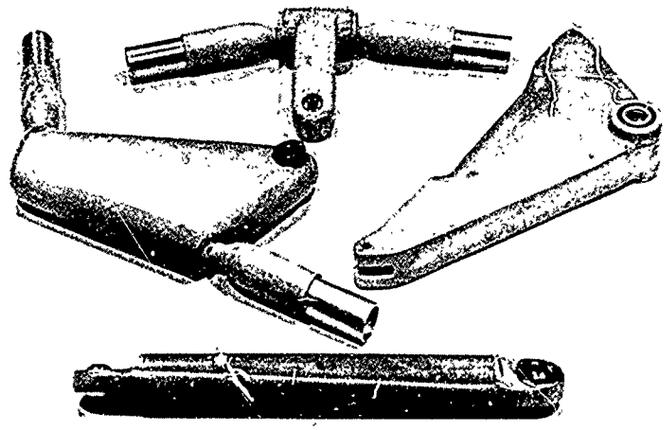


Figure 18. Composite Ballistic Tolerant Flight Control Components.

Higher Caliber AA Threat

For purposes of comparison, Table 12 provides the general characteristics of the 30mm HEI-T projectile versus the 23mm HEI-T projectile. As can be seen, the 30mm projectile has over three times the high explosive weight and over two times the body weight of the 23mm. The kill mechanisms would be generally the same for both projectiles, except for a larger radius of damage for the 30mm. Analyses indicate that the vulnerable area for a typical helicopter would be between three and four times greater for the 30mm versus the 23mm, in the attrition kill category. Notwithstanding this, the prognosis for reducing the vulnerability of the helicopter against the more formidable 30mm HEI-T threat is very good. Testing is presently ongoing to better define the explosive characteristics and damage producing potential of the 30mm HEI-T projectile, and to evaluate means of reducing the vulnerability of the helicopter against this threat.

TABLE 12. 30MM VERSUS 23MM HEI-T CHARACTERISTICS

PROJECTILE	FUSE WEIGHT (GRAINS)	BODY METAL WEIGHT (GRAINS)	HE FILLER WEIGHT (GRAINS)	TOTAL PROJECTILE WEIGHT (GRAINS)	SERVICE MUZZLE VELOCITY (M/S)
30mm	1185	4462	662	6431	765
23mm	569	2123	215	2954	930

FUTURE THREATS

Broad scaled combat in the near future would be very intense and would subject the helicopter to additional threats beyond those already discussed in this paper. Foremost among these additional threats would be laser and nuclear weapons and chemical and biological warfare. Reduction of the vulnerability of the helicopter to these threats is presenting new and difficult challenges to the designer, especially since considerable effort still remains in defining and understanding the enemy threats and in determining their lethality and kill mechanism for the various helicopter systems.

The laser threat is generally broken out into two categories: low energy lasers (LEL) and high energy lasers (HEL). The LEL's, such as those associated with target detection, range finding and illumination, are considered a current battlefield threat for the helicopter, primarily concerning the crew's eyes and the helicopter's sensors and optics subsystems. They do not normally pose a threat to the helicopter structure. Although probably still a few years away from becoming a viable tactical weapon on the battlefield, the HEL's do possess sufficient energy to do catastrophic damage to the helicopter structure and other subsystems which are exposed to the laser beam for only a few seconds. The nature of the damage done to the structure is dependent both on the fluence level on the target and the characteristics of the beam, e.g., high fluence concentration on a small spot; high fluence knife-edge like cut by quickly moving the beam in a line over the structure; or a low fluence, large spot beam which flood loads the structure. Unless a critical component within the fuselage is damaged, the high fluence burn through of a small hole in the helicopter structure may be no more serious than a hole made by a ballistic projectile. Properly designed, the structure should be capable of taking many such holes, especially if constructed of composite materials. At the other end of the spectrum, however, catastrophic structural damage may easily result from area heating highly stressed structure with relatively low fluence levels. In this case, composites would be cause for added concern in predicting the structural/dynamic response since they have lower temperature limits and lesser homogeneous characteristics than do the metal.

A number of techniques and materials are being investigated and evaluated toward reducing the vulnerability of the helicopter to the laser threats. For the LEL, protective films and coatings are being developed for the sensors and optics subsystems and eye shields for the crew, all of which generally reflect the laser incident energy away. Also, the soft structures of the helicopter, i.e., transparencies, are being investigated toward providing mechanisms, preferably field replaceable, to absorb the incident energy, probably turning opaque in the process but protecting the eyes of the personnel onboard. Helicopter-mounted smoke/aerosol dispensing systems are proving effective in providing protection against both the low and high energy lasers by attenuating the incident energy through absorption and scattering within the cloud dispensed between the helicopter and the laser threat system during a combat encounter. Protecting the helicopter per se against the HEL direct attack will probably require a two-phased effort. The first and easiest step will be to provide shields or barriers constructed of laser resistant materials to cover critical components, subsystems or structure. These barriers will perform in the same general context as the parasitic armor plates presently used on helicopters to protect against ballistic projectiles except that they will use reflective, absorption, or ablative mechanisms to defeat the incident laser energy. The second step will be to integrally harden the component or helicopter structure against the direct laser threat. Although this is potentially a more efficient method of protecting the helicopter against laser threat weapons, it is by far the greatest challenge to the designer and will require a much greater period of time for accomplishment.

The nuclear threat, considering both tactical and strategic weapons, has been prevalent for years but very little has been accomplished directly toward hardening the helicopter against this threat. In elementary terms, the primary by-products of a nuclear explosion include the flash, thermal radiation, nuclear radiation, blast overpressure, and an electromagnetic pulse (EMP). The first three (flash, thermal, and nuclear radiation) are considered a threat primarily to the crew, whereas the final two (overpressure and EMP) are a more direct threat to the helicopter system per se. The EMP resulting from a nuclear explosion, both near surface and exoatmospheric, or from a nonnuclear EMP generating weapon poses a potentially serious threat to the electrical and electronic subsystems of the helicopter. The threat becomes especially serious considering mission completion for the modern helicopter since it possesses considerably larger quantities of sophisticated communication, navigation, and weapons fire control equipment over the helicopters of the 60's. This is an area where much work remains concerning defining the EMP threat and the countermeasures required for each specific helicopter system.

The greatest amount of damage to the helicopter in a potentially survivable nuclear encounter will probably result from the blast overpressure associated with a near surface explosion. Several simulated explosion tests have been conducted over the past few years wherein the helicopter was included as a specimen to assess its vulnerability to the nuclear blast threat. In one of these tests a UH-1B helicopter was in hover flight when the simulated nuclear explosion occurred, being flown remotely by a ground-located pilot. The blast simulated a weapon of approximately 1 kiloton in size, and the helicopter was hovered approximately 792 meters from ground zero so as to be subjected to a 12.41 KPa overpressure shock. The intent was to cause severe, but not catastrophic, damage to the helicopter. The helicopter had onboard instrumentation for obtaining data on main and tail rotor blade flap bending, vehicle rigid body motion, fin and tail boom lateral bending, and blast induced strain in the tail boom structure. Although there were some inconsistencies in the data obtained and poor correlation with predictions for some parameters, the test of the helicopter was highly successful. The ground-based pilot continued to fly the helicopter during and following passage of the overpressure shock wave, which lasted approximately 340 msec, and subsequently brought it to a successful landing. Referring to Figure 19, highest main rotor flap bending moment occurred at an inboard station on the blade, having a peak value of approximately 4,858 n-m. The spike peaked approximately at 120 msec and was approximately 20 msec duration. Average peak-to-peak value at this location prior to the blast was 1,920 n-m. Referring to Figure 20, the highest peak-to-peak value recorded for tail boom lateral bending moment was approximately 36,149 n-m, with the spike peaking at approximately 95 msec and lasting approximately 150 msec. Average peak-to-peak value recorded prior to the blast was 6,213 n-m for the boom. Tail boom lateral bending moment allowable in the UH-1B is 40,668 n-m. The helicopter experienced, on the side facing the blast, considerable wrinkling of the skin panels, some local yielding of stringers and loss of the soft, transparent structure.

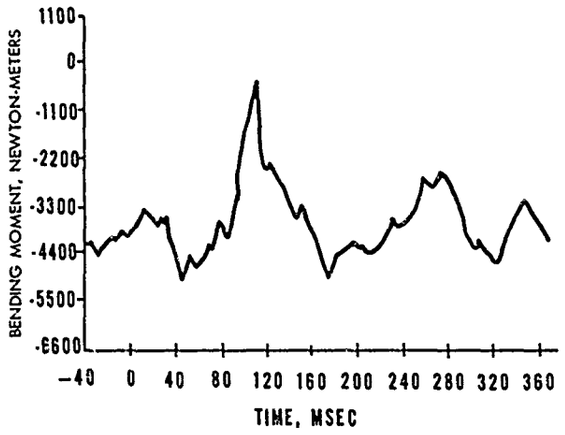


Figure 19. Main Rotor Blade Flapwise Bending Moment (STA 35).

Airmobile operations under NOE flight conditions will make the helicopter particularly vulnerable to the chemical and biological agents used at low levels against ground troops. Of these two, chemical warfare poses the greatest immediate threat and, in fact, must be looked upon as a "conventional" weapon for the modern battlefield.

Since the biological agents use living organisms or toxic by-products of living organisms, they are very difficult to handle and do not normally produce immediate casualties. As such, they are not considered a major near-term threat. On the other hand, the chemical agents are much easier to handle and to dispense and normally produce immediate results. Primary agents used for these gasses would include phosgene, chlorine, mustard, lewisite, hydrocyanic acid and cyanogen chloride. Countermeasures for chemical and biological warfare will involve the development of both personnel protection devices and hardening concepts for the helicopter, the latter of which has not been addressed in helicopter design to any great extent to date. Hardening of the helicopter against these threats will without question be extremely difficult to accomplish. Two primary concerns exist: to prevent/minimize infiltration of the agents into the cockpit/cabin areas and into the external access compartments, both while the helicopter is parked and in-flight; and decontamination of the helicopter once contaminated. The decontamination concern alone can have major impact on the design of the helicopter as the materials used in its construction must be totally compatible with the decontaminating agents/processes utilized.

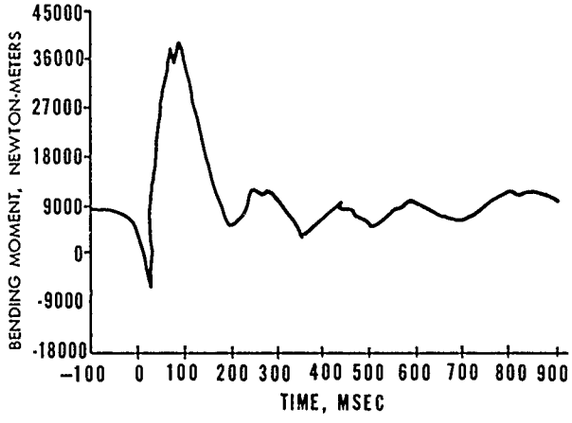


Figure 20. Tail Boom Lateral Bending Moment (STA 112).

The above discussion on future threats is very superficial in nature. Each threat addressed is within itself a subject for further intense analysis and reporting. It is hoped, however, that the information provided properly scopes the immensity of the challenge faced by the designer in effecting countermeasures within the helicopter system to reduce its vulnerability to these types of threats. It should also be evident that such countermeasures must be considered early in the design phase and, for maximum effectiveness, must be integral to the overall design of the helicopter as a total system.

SUMMARY

- The helicopter is a combat proven machine that has become an integral part of the inventory of US Army equipment that is required to satisfactorily fulfill the combat and combat support roles.

- The lethality and sophistication of today's threat has significantly increased over that of the Vietnam era and the prognosis for near future threats is further cause for concern.

- Survival of the helicopter on the modern battlefield will depend on several key factors, including: signature reduction and electronic countermeasures; tactics; and hardening of the helicopter against the various threat systems.

- The helicopter will continue to be ballistically and otherwise damaged in combat. As such, it must have combat sustainability. It must have the ability to continue to fly at guaranteed flight load levels following damage from specific threats. The design should be such that the combat induced failure of a single element or subelement should not result in catastrophic failure. Further, the combat damage must be readily repairable, to the maximum extent possible at unit maintenance levels.

- Efficient and economic measures for improving helicopter combat survivability must continue to be developed and applied. This will result in increased mission effectiveness and the preservation of resources, to include men, material, and equipment.

- Design criteria and needs must be periodically adjusted as necessary to reflect the changing threats.

- The structural designers must be kept abreast of these threats and understand their various effects/kill mechanism for each specific helicopter/component.

- For maximum effectivenss the designer must consider survivability issues in the same light as other design considerations, e.g., weight, load factors, and fatigue life, during the initial design phases of the helicopter.

- It is considered imperative to the long term esprit de corps of the crew that they have confidence that the equipment they fly has been specifically designed to better help them survive in combat considering reduced vulnerability against hostile air defense systems.

REFERENCES

1. Lindenmuth, J.R., and Malick, D., "An Analysis of Combat Data for OH-6 Aircraft," AMSAA TR No. 87, March 1974.

2. Smith, H.C., "Combat Data Analysis of the AH-1G (67-68)," AMSAA TM 28, March 1969.

3. "Airmobile Operations in Support of Operation LAMSON 719, 8 February - 6 April 1971," DDC Report.

4. Zabel, P.H., "Reduction of Army Helicopter Fuel Tank Vulnerability to 23mm HEI-T Projectile," USAAMRDL TR 75-32, August 1975.

5. Pedriani, C., and Hogan, T., "A Study of the Blast and Combustion Overpressure Characteristics of the 23mm HEI-T," to be published.

6. Good, D., "Spacewound Composite Structure," Presented at the 34th Annual National Forum of the American Helicopter Society, Washington DC, May 1978.

7. Symonds, M., "Design Tolerant Design of the YAH-64 Main Rotor Blade," Presented at the AHS/NASA Ames Conference on Helicopter Structures Technology, November 1977.

8. Zartarian, G.; Cole, E.; and Lee, W., "Correlation Study of the UH-1B Helicopter Blast Test Results from the DICE THROW Event," USABRL Contract No. 352, October 1977.

9. Bernier, R., "Some Trends of the Terminal Ballistic Performance of Russian 23mm Projectiles (API and HEI-T)," BRL Memorandum Report No. 638, December 1952.

10. "Fragmentation Characteristics of Small Projectiles, CII, 30mm-T-306E10 (MOX 26)," Project THOR Technical Report No. 28, June 1956.

Report on Session II

NEW CONCEPTS/DAMAGE TOLERANCE

by

K.Brunsch
MBB GmbH/D-u V D-132
Postfach 80 11 40
8000 Munchen 80, FRG

In this Session three papers were given:

1. "Application of Damage Tolerance Concepts for MBB Helicopters" by M.v.Tapavicza and F.Och.
2. "Justification en Fatigue de Pièces en Matériau Composite Bénéficiant du Concept "Fail-Safe" by G.Stiévenard.
3. "Compact Damage Assessment" by C.H.Carper.

The first paper gave a survey of the damage tolerance methodology used by MBB for the BO-105 and MBB's share of the BK-117. For introduction, fracture mechanics are described briefly and the well known Forman equation $\frac{da}{dN} = \frac{C.\Delta K^n}{(1-R).K_C - \Delta K}$ is presented. General reference is made to the determination of the service life of "safelife components with slow crack growth" capability. Service life time and inspection intervals are calculated depending on damage detectability, fatigue strength of the components and crack growth rate.

Components, developed to damage tolerance are presented:

- Quadruple nut – a part of the main rotor centrifugal force retention system to link the tension-torsion straps to the hub. The primary load path is solid steel; the secondary path is a wrap around of high strength steel wire. Failure of the primary path results in a noticeable unbalance of the rotor. The service life is unlimited and inspection is not required.
- Tail rotor drive shaft coupling – laminated steel, 12 sheets. Salt atmosphere reduces fatigue life but results in partial failure only – infinite life, 1200 hrs inspection.
- Main rotor shaft-to-hub joint – multiple stud and bushing. Damage tolerance due to material used – steel with fracture toughness of $K_{IC} = 4500\ Nmm^{-3/2}$.
- Glass fibre composite main rotor blade – well known damage tolerance of composite material.

Mr Stiévenard's paper very clearly described the determination of the service life of components with damage tolerance, i.e. of composites. This methodology was successfully applied to the Starflex rotor hub.

At Aerospatiale the basis for the work presented is:

The joint Aerospatiale-French authorities request failure probability for any individual part below or equal to 10^{-6} during service life, requiring:

- knowledge of material fatigue properties
- knowledge of representative load spectrum
- knowledge of probability of onset of crack in component
- knowledge of component crack propagation rate if the load spectrum is applied.

Having evaluated the probability of onset of crack and the probability of crack propagation to ultimate failure, it is very easily possible to combine these two to an overall failure probability. By that, the service life can be determined depending on inspection intervals, as shown in the concluding table. Service life of a component ranges from 1000 hrs at a 100 hr inspection interval to 5000 hrs at a 10 hr inspection period.

Mr Carper's paper starts with an impressive graph on combat field survivability of helicopters as it was in past (Vietnam), is today and will be in future.

Measures to improve survivability are indicated -- reduction of visual, radar and IR-signature, reduction of noise, ECM and tactics such as nap-of-the-earth flight but also it is stated that the helicopter will receive ballistic hits. The need for specialized vulnerability reduction concepts is pinpointed.

Vietnam experiences are presented for low intensity and mid-intensity battle fields. From 1967 to 1971, OH-6 helicopters flew 1.1 million flight hours, experienced 3,774 incidents and 532 losses by energy ground fire.

In a mid-intensity battle field, 90 helicopters of different sizes were lost within 60 days, most of them by 7.62 mm fire. Information is given on major contributors to vulnerability with 6 components of the main rotor control system among the 10 first ranking components.

Finally, some designs of tail rotor boom with reduced ballistic vulnerability were shown. All of them were "advanced technology" framework design like, e.g. "isogrid" filament winding technology. The papers were very clear and produced little discussion only. The need to adequately instruct users of composite primary structures on crazing, delaminations and cracks was pointed out in discussion.

AN EVALUATION OF FATIGUE PROCEDURES FOR UK MILITARY HELICOPTERS

by

R Cansdale

Airworthiness Division, Structures Department
Royal Aircraft Establishment
Farnborough, Hants GU14 6TD
England

SUMMARY

Current UK procedures for the fatigue substantiation of military helicopters are reviewed in the light of practical experience of testing and of service usage.

The problems of demonstrating both "safe lives" and "damage tolerance" are examined. Mention is also made of the philosophy and problems of clearing composite components.

1 INTRODUCTION

The formal UK requirements concerning fatigue strength of military helicopters are set out in MOD Aviation Publication 970, Volume 3. However in many areas these are known to be deficient and the recent practice has been for more stringent clearance procedures to be stated in the Specification against which new helicopters are procured. These procedures, applying to the Westland Lynx, were very ably described by Mr A D Hall in his paper given two years ago at the 47th meeting of this panel.

It is these procedures, rather than the word of AvP 970, which I have tried to evaluate in this paper. Additionally I have looked at some of the problems associated with the use of composites. It is perhaps worth noting that amendments to AvP 970 at present being debated may differ both from the old AvP 970 requirements and from the procedures used for the Lynx, so that some of the problems discussed here will have already been taken into account.

This paper expresses the views of the author and does not necessarily represent the official view of the Royal Aircraft Establishment.

2 GENERAL

The first question to answer in an evaluation of fatigue clearance procedures is how successful are they in safeguarding the airworthiness of the fleet – how many helicopters are lost or damaged due to fatigue failures?

Looking back over the last twenty years the British Services have had about two dozen major helicopter accidents due to fatigue failures, in which the aircraft suffered Category 3 damage* or worse. Unfortunately from the point of view of this paper, none of these accidents occurred to aircraft which were designed to current procedures. Nevertheless, I believe that there are some valuable lessons to be learnt from them.

I do not propose to dwell on the cause of each accident, but it is instructive to see where the failures occurred (Fig 1). There are two Category 3 accidents, three Category 4 and twenty Category 5; However six of the Category 5s involved ditching and it is possible that the aircraft would have been repairable had the failures happened over land.

It is clear from the table that it is very rare for an airframe failure to cause an accident. Although one Category 5 is listed under the airframe heading this is only a tentative identification because the aircraft was not recovered from the sea. The rest of the accidents were due to failure of parts which would normally be classified as "vital" or "primary". It is tempting therefore to dismiss airframe fatigue as being unimportant, but a review of accidents gives only one side of the picture.

In addition to the failures which cause accidents, there are many lesser failures whose cost is more difficult to quantify. Even when failures do not occur there is a cost to the Services in terms of loss of operational capability due to the time spent on inspection and repair. If it were possible to allocate these costs to various components, the picture would be rather different to Table 1 and airframe fatigue would play a more significant part.

In writing this review of our fatigue procedures I have found it convenient to consider the subject in broadly two parts, the first concerned with vital parts, which are basically the dynamic components and a few airframe parts, and the second with the rest of the airframe.

---

* Category 3: Damage which is repairable on site but beyond unit technical resources.

Category 4: Damage which is not repairable on site.

Category 5: Damaged beyond repair.

3 VITAL PARTS

3.1 At the moment the parts of the helicopter which are classified as "vital", that is to say whose failure would immediately hazard the safety of the aircraft, are treated on a "safe-life" basis (the only exception being some rotor blade spars protected by the BIM (Blade Inspection Method) systems). By safe-life we mean a life during which the probability of failure is at an acceptably low level. To demonstrate this we use factors on test which mean that failure of a component will occur only if its strength is about three standard deviations below the mean value for the population. What probability of failure this implies depends on the distribution of strength which is assumed - about 1 in 1000 if it is normal or approaching zero if it is a Weibull distribution, as seems more likely. Whatever the number, it appears to be a broadly acceptable level.

In general it is not practicable to test large numbers of each component to establish the variability of strength and since there is a large amount of data on metallic materials the factors are based on past experience of variability. For newer materials such as composites we have yet to build up this bank of data and the clearance procedures are more involved; I will return to this in Section 5.

For the low frequency loads such as those imposed by landings, rotor starts, etc, the factors are applied on a life basis as is usually the case for fixed wing aircraft. However for loads induced by the rotor at high frequency it is necessary to factor the magnitude of the loads to give a margin of safety at the flat end of the S-N curve.

3.2 Looking first at the Design Phase (Fig 2), the only real problem about the operational requirements is that they always seem to change as the project progresses; this of course is inevitable in an interactive military scenario. All that can be done to guard against it is to design with something in hand and try to preserve this against the inevitable weight saving exercises. On the Ministry side we can try to ensure that the requirements are reasonable and necessary and not just specified as an automatic improvement on the previous aircraft.

The fact that the airworthiness requirements of Avp 970 are due for revision has already been acknowledged. One of their shortcomings was simply that the factors called for to cover variation in fatigue strength were too small. Nevertheless we still have helicopters giving satisfactory service which, for example, have gearboxes designed with a stress factor of 1.1 rather than the 1.3 currently used for 4 test specimens. This however should not be taken as justification for the 1.1 factor but more as a demonstration of the perspicacity of the designer who made the gearbox capable of tolerating the odd gear tooth failure without disaster.

Of the factors used for the Lynx, all I can say is that they appear to be adequate insofar as the few fatigue failures which have been found in service have been due to causes other than those which would be expected to produce failures on test - such as inclusions occurring very rarely in the material. Whether this is because the factors are just right to allow for the strength variability, and all the other assumptions are correct, or whether the factors are larger than needed for material variability and are also covering our ignorance of other matters is harder to say. I suspect that the latter is true to some degree.

One of the problems in writing the Aircraft Specification is the definition of the aircraft's usage. In the past we have tended to use the American AR56 and CAM 6 documents as a basis for the spectrum of forward speed etc. This has led to a somewhat anomalous situation in at least one case, possibly due to differences in terminology in defining speeds. The spectrum in this case included 30% at V_{NO} (normal operating speed), 3% at V_{NE} (never exceed speed) and 0.5% at 1.1 V_{NE}. Clearly to obtain a reasonable fatigue life for dynamic components it is necessary for the loads to be virtually non-damaging at V_{NO}. The loads tend to increase rapidly with speed so that the life is very dependent on the time spent at V_{NE} and 1.1 V_{NE}. The maximum speed now defined in the aircraft's CA Release corresponds to V_{NO} so we have the odd situation that the fatigue life is largely governed by flying which in theory should not be done.

In fact this spectrum has now been modified to what is believed to be a more realistic usage. However fatigue lives are always likely to be sensitive to the amount of time assumed in the more damaging parts of the flight regime. Hopefully in future our estimates of usage will derive more realism from the monitoring programmes currently being undertaken.

Fatigue strength data can be a problem, particularly at the very long lives, 10^8 or 10^9 cycles, needed for many helicopter components. There is also a growing awareness that constant amplitude test data is not always a reliable guide in the selection of items such as fasteners where the beneficial effects of compressive stress introduced by interference fits can be much reduced by occasional high loads.

3.3 Turning next to the Development and Production Phases (Fig 3), it is worth noting the importance of designing even the prototype aircraft with production in mind. Obviously the fewer differences there are between the two standards the more relevant the development testing will be to the final substantiation.

It is necessary to be aware of the assumptions made in the derivation of the spectra of loads for the various components. The intended role will have been specified together, probably, with a speed spectrum and the number of landings per hour. The designer then has to decide what the role will entail in the way of manoeuvres, and which of these is likely to be critical from the fatigue point of view. Test flying is then done to measure loads. Inherent in this procedure are the assumptions that the critical flight regimes can be identified and that the test pilots can reproduce the sort of flying that will be done in service.

On fixed wing aircraft there have been occasions when these assumptions have been shown to be false; for example on one type the Service pilots found that they could improve the roll rate by using the rudder. This unanticipated use of the control resulted in fatigue cracks in virtually every aircraft in the fleet.

However on helicopters the severity of the fatigue environment, even in level flight, may reduce the significance of the finer detail of the manoeuvre spectrum. Nevertheless the possibility of error in this link in the chain of fatigue substantiation must not be forgotten.

Fatigue testing of helicopters is a complex process and the various components present different problems so I shall discuss them separately. In general though there has been a move away from constant amplitude testing towards the use of better mixed loading, usually in the form of block programmes. Although this makes for more complicated testing we believe that it produces more realistic results.

3.3.1 Main Rotor Blades

Although any future design is almost certain to have composite blades, our experience to date has been mostly with stainless steel or light alloy blades. Most of the fatigue testing has been done using a single mechanical exciter to provide combined flap and lag loading. Because of the difficulty in simulating the centrifugal field loading on a blade and the fact that there is often more than one critical area, it is not usually possible to substantiate the whole blade by single tests on the complete blade. This problem may get worse if the full potential of composites is realized in tailoring the strength and stiffness of blades to the local loads; this will increase the number of critical areas to be cleared.

3.3.2 Rotor Hubs

The main rotor hub is subject in service to a very complex pattern of loading, particularly if it is of a non-articulated design such as the Lynx. On-off centrifugal loads, on-off torque and the oscillatory flap, lag and torque loads all have different influences on different parts of the hub, and it is very difficult to simulate accurately the whole loading pattern on test. Because some areas are likely to be overtested compared to others it may not be possible to obtain a fatigue life for the hub directly from the test duration. Instead it may be necessary to use the test to establish an endurance limit for the failure site and then to use this in conjunction with flight stress measurements to calculate the life. This method has its own problems, one of which is that the exact failure location is unknown until the hub breaks and, unless fortune has been unusually kind, this will not be where strain gauge measurements were taken either on test or in flight. It may be possible to deduce the local stress if the failure is in one of the simpler areas to analyse. However it is often in an area of stress concentration with a rapidly changing stress field in which case further strain gauge or photoelastic work may be necessary to determine accurately the local loading.

This problem may become somewhat easier in future if we turn to designs where separate elements are used to carry the different loads, such as Aerospatiale's "Starflex" hub or other split-load-path designs. It might then be possible to do individual and simpler tests on the various components.

3.3.3 Gearboxes

Our standard method of testing gearboxes is to run them under a programme of various power levels to provide a well mixed loading. The levels are subject to a factor of 1.4 for a single test and 1.3 for four tests. These factors originated in the British Civil Airworthiness Requirements and there seems little doubt that they provide a very good guarantee of in-service life. The size of the factors does mean however that there could be a risk of the mode of failure on test being different from that in service. It is therefore important to check that the meshing patterns of the test gears are of similar character to those in service and that excessive distortion of the casing is not taking place. The use of special lubricants may be necessary to ensure that the higher contact pressures do not cause unrepresentative failures due to scuffing etc.

The outer casings of the gearboxes are tested under loading from the rotor and control systems as well as from the gears using the usual structural safe life factors; this does not seem to produce too many problems.

On some of our more modern gearboxes we are in a situation where most flight power levels are non-damaging and the life is governed by the time assumed in the spectrum at contingency powers. If this time could be logged the gearboxes could be lifed on condition. Gearboxes are an interesting mixture of safe life and damage tolerance because although we demonstrate safe lives for the gears, shafts and casing, some items such as bearings and shims, are not amenable to this treatment. They have to be protected by the fault detection systems, eg, chip detectors and magnetic plugs. These will also provide early warnings of some gear failures.

3.3.4 Airframe Vital Parts

We are talking here chiefly of the main gearbox attachments and the adjacent structure. Attempts have been made to test these parts by using a complete airframe as the specimen and loading it via a dummy gearbox and rotor head. Although this has the merit of providing the correct back-up stiffness, it has given a good deal of trouble. The major difficulty lies in obtaining a distribution of high frequency loading which is even approximately correct. Even if all but loads at blade passing frequency are ignored, the pattern of shears, bending moments and torques produced by the rotor is very complex and very hard to reproduce.

The fact that these high frequency loads must be factored also tends to produce unrepresentative failures elsewhere in the structure, due to panel buckling etc, which although not very significant from a fatigue point of view, do hold up the test.

For these reasons it has been found more satisfactory to do separate tests on the individual attachment points using several hydraulic jacks on each to obtain the correct stress distribution.

4 AIRFRAME NON-VITAL PARTS

Although there are many parts in this category whose failure would be highly undesirable, the rather less severe loading environment and perhaps greater degree of redundancy prevent them from being classed as vital. As was noted earlier, failures in the airframe cause few crashes. Nevertheless airframe fatigue can cause a great many headaches, starting with the Aircraft Specification.

Because even non-catastrophic cracks cost time and money to repair it is not unreasonable for the customer to write in some requirement relating to airframe fatigue performance. If, as has happened in the past, this requirement is written in terms of a safe life for the airframe, then strictly a test using the vital part factors is called for to demonstrate compliance. This is not too difficult to do if only low frequency loading is considered, since a life factor can be used as in fixed-wing practice. However on helicopters there are often many areas where the high frequency rotor induced loading cannot be ignored. At the very least it imposes a fretting environment on the structure which must be simulated on test to get the right conditions for crack initiation. However if the loads are sufficiently high to be themselves damaging, then they have to be reproduced on test and at factored levels.

Our experience has shown up two fundamental difficulties here. Firstly, if both high and low frequency loads are to be applied on the test in a well mixed spectrum, a system will be needed to apply and react the low frequency loads in addition to the system used for the high frequency. Thus the airframe is constrained in a very different manner to that which it experiences in flight and hence its vibration mode shapes are changed and its response to test loading may be quite different. To ensure that the whole structure is adequately tested, load levels may have to be raised so that many parts will be overtested.

The other problem is that even if a realistic stress distribution is obtained, the fact that the high frequency loads must include a stress factor of about 2 tends to produce unrealistic behaviour such as panel buckling. In practice these two things mean that the test is plagued by a succession of failures, most of which are unrepresentative and unlikely to occur in service.

It would seem that the only circumstance in which a true "safe life" will be able to be demonstrated for a helicopter airframe will be if the Specification calls for vibration levels sufficiently low as to give non-damaging high frequency stresses even when factored. In view of the other obvious benefits which a low vibration environment confers this would seem to be the right solution, but of course it will probably have to be paid for in terms of weight for vibration control measures.

If specification of a "safe life" for the entire airframe leads to all these difficulties, the alternative is to recognise that some cracking can be allowed to happen without immediately hazarding the aircraft, and to call up a damage tolerance requirement.

Fatigue requirements for damage tolerant design are under intensive discussion in the UK at the moment so it is difficult to say what effect these will have on testing in future.

The American damage tolerance requirements for fixed wing aircraft require propagation times to failure to be calculated for defined sizes of cracks which are assumed to be present as flaws in the aircraft structure as built; inspection times can then be defined. It is a little difficult to see how this type of requirement will be applied to a helicopter airframe since it does not appear at present to be within the state of the art to predict the high frequency stress distribution with sufficient accuracy.

It seems likely that, at least in the near future, our airframes will be built to a compromise between the full Mil-Spec type damage tolerance requirement and the old method of designing for a safe life under the low frequency levels; the aim probably will be to design for a safe life under the low frequency loads plus an assumed high frequency stress distribution whilst at the same time trying to build in the obvious damage tolerance virtues of redundancy and inspectability.

We shall in future have to examine very carefully what it is that we are hoping to achieve by doing a major airframe fatigue test. It has been suggested that ideally we should do two, one fairly simple one at an early stage in the development programme to highlight weaknesses which could then be corrected for production, and one later on a full production standard structure to demonstrate compliance with the Specification. In practice however it is doubtful whether an early test would produce sufficiently reliable results soon enough to affect the production design, and the airworthiness of the aircraft could probably be better safeguarded by doing individual fatigue tests of the critical areas. Provided therefore that the Specification can be worded in such a way as to protect the customer's interests without requiring demonstration of compliance by test, I think it is rather unlikely that we shall again attempt a complete airframe fatigue test, at least until the high frequency stresses are reduced to non-damaging levels.

5 COMPOSITES

Although many of our present helicopter designs in UK have composite components, in the main these have been in non-fatigue critical areas or parts where a large ad-hoc superfactor to cover uncertainty could be accepted without compromising the design. However we are now embarking on the design of rotor components in reinforced plastic materials and clearance procedures have had to be agreed for these programmes.

The main problems are the lack of background knowledge of strength variability in the various failure modes and of the long term effects of environment on the properties. The latter is the more difficult to provide rapid answers to and we may have to have some form of progressive clearance procedure which might not be completed until after the aircraft enters service. Those who have experience of making composite blades may well ask why we do not just take note of their experience and sidestep the problem; the answer is that certain features of our designs are significantly different from what has been done before and could have a different susceptibility to things like moisture ingress. These factors have to

be checked out since one of the basic tenets of our composites programme is that these components shall be shown to have a standard of airworthiness at least equal to metal parts already in service.

We have a number of composite demonstrator programmes running at the moment and the strategy here has been initially to avoid the environmental issue by aiming only for a limited clearance, say 50 hours flying. Fig 4 shows an outline of a typical clearance programme. We start by using a hopefully conservative estimate of variability to obtain factors which are used in the design phase. The component is then built and tested to find out where and how it fails. Structural elements representing these failure modes are then tested in larger numbers to determine the variability. Tests on actual components, if necessary after redesign, are again carried out to obtain the mean strength and confirm that failure modes have not changed if there has been any redesign. Initial lives can then be calculated from this knowledge of mean strength and variability using calculated loads. Provided that the lives are satisfactory, ground running and initial flight trials to measure loads can take place. The lives can then be recalculated, using at least for the moment, Miner's hypothesis.

We would expect a production clearance to follow a similar pattern but perhaps with a somewhat different emphasis on the various parts, reflecting the confidence gained from earlier programmes and the need to cover environmental effects.

6 SAFE-LIFE OR DAMAGE-TOLERANCE?

Those parts of our helicopters whose structural integrity is essential to the safety of the aircraft are lifed almost entirely on safe life principles. As we have seen, these involve a long chain of assumption and actions. There must undoubtedly be weaknesses in some of the links at times, but on the whole a measure of conservatism at all stages maintains the overall integrity of the process.

Occasionally however some defect introduced in manufacture or service, or some flight regime whose damaging characteristics have not been recognised, will cause a catastrophic failure against which the safe life philosophy is no protection.

An additional objection to the safe life system is its sheer wastefulness: by definition the vast majority of life-expired components are thrown away when perfectly sound in order to guard against the rare weak one. For these reasons I would strongly support the view, expressed in Mr Hall's paper two years ago, that we should try to apply damage tolerant design principles to vital parts.

This means that the parts will have to be designed so that even if a crack is initiated early by a defect, it will not propagate to failure before it is detected. This approach obviously throws more emphasis on inspection. In spite of the various drawbacks of the safe life system, the fit-and-forget-until-time-expired concept has obvious attractions for Services who are short of manpower. They will certainly not thank us for increasing the amount of inspection effort required.

All the same the wisdom of not relying entirely on safe life was clearly demonstrated to us a few years ago when one of our in-service types suffered a series of early fatigue cracks due to corrosion in the main rotor blade spars. Fortunately the blades were fitted with BIM. But for this we should undoubtedly have lost at least one aircraft. Furthermore, we should have been forced to ground the whole fleet for inspection, causing our Services considerable operational embarrassment. As it was the aircraft kept flying, although it was necessary to do a rapid check to see that the inspection period for the BIM was still adequate. Even this would have been unnecessary if a cockpit-indicating system had been installed.

This example highlights another snag with safe life and advantage for damage tolerance - what happens when things go wrong? If the failure is due to something such as corrosion which invalidates the safe life clearance and which may apply to all aircraft of a type, they must all be inspected. If there is no adequate degree of damage tolerance or system such as BIM, the aircraft may have to be grounded and a massive amount of work is suddenly generated.

In the end it all comes down to a question of cost effectiveness. For this reason I suspect that we may find the civil market leading the way in developing additional devices on the lines of BIM. Health monitoring systems for engines and gearboxes are commonplace, and as individuals we ourselves have a system which guards our personal structural integrity, called pain. Pain of course not only tells us when a failure has occurred but when the loads are approaching damaging levels, so it combines the functions of a BIM system with those of a cruise guide indicator and a 'g' meter. However mechanical analogues to pain cannot be allowed to increase the work of the already overloaded crew, but the use of on-board computer-based systems, perhaps coupled to speech synthesisers, could avoid a proliferation of warning lights and buzzers in the cockpit.

Wide scale use of active monitoring systems for structure is probably a long term possibility. In the short term composites and elastomeric bearings seem to offer the prospect of relatively slow and benign failure modes which should enable some rotor system components to be lifed on condition without increasing the amount of inspection much beyond what is normally done as routine husbandry. In addition some of the uncertainties about aircraft usage may be removed by the use of on-board computer facilities to record aircraft usage by monitoring either flight parameters or perhaps loads directly; fatigue meters are of course already widely used on fixed wing aircraft.

7 CONCLUSION

The fatigue substantiation methods currently in use in the UK appear to be succeeding in maintaining an adequate level of airworthiness in our military helicopters, mainly by means of the safe life philosophy. Nevertheless there are recognised areas of weakness in the system and in many respects it is wasteful. These factors are moving us towards damage tolerant designs and on-condition lifing.

REFERENCES

No	Author	Title, etc
1	A D Hall	Helicopter Fatigue Evaluation "(The UK Approach)" AGARD Report No 674 - September 1978.

Copyrigh
Controller HMSO 1980

HELICOPTER FATIGUE – A CIVIL VIEW

by

H.E.Le Sueur
Civil Aviation Authority
Airworthiness Division
Brabazon House
Redhill, Surrey RH1 1SQ
UK

1. INTRODUCTION

Until now being fully aware of the sensitivity of the helicopters to fatigue, and the inability to provide alternate load paths, the helicopter structural engineer has been forced to adopt a safe fatigue life approach in determining the airworthiness of the helicopter structure. This has been unsatisfactory as a few statistics will show.

2. IMMEDIATE HISTORY

Using the well known methods specified in Appendix A to CAR 6 (now AC20-95 Ref 1) estimates of Safe Fatigue Lives have been obtained for such items as Main Rotor Blades.

Applying these Approved Safe Fatigue Lives in service has led to the following statistics for a twin engined helicopter type :

YEARS IN SERVICE	18
TOTAL NUMBER OF HOURS	915,000
NUMBER OF ACCIDENTS	42
NUMBER OF FATAL ACCIDENTS	12
NUMBER OF FATALITIES	133

OF THESE 12 FATAL ACCIDENTS

5 WERE DUE TO ROTOR FAILURE

2 WERE DUE TO TRANSMISSION FAILURE.

In United Kingdom Civil Operations we have accumulated 500,000 hours of twin engined helicopter flying resulting in 18 accidents with one fatality over a period of fifteen years.

So the average accident rate is >3 per 100,000 hours and the fatal accident rate approx 4 per 300,000 hours for Civil Twin Engined Helicopters.

We have reason to believe that the accident rates for military helicopters are of the same order, if not worse.

The important thing is that in the civil field these figures are not to be tolerated and steps must be taken to improve them.

What methods are available to reduce those accident rates which are due to structural failures.

3. METHODS IMMEDIATELY AVAILABLE

3.1 Reduction in Speed

It has generally been agreed that a scrap life on a rotor blade of less than one thousand hours is uneconomic, in fact a life of ten thousand hours would be more acceptable. Let us assume a life of ten thousand hours. This means that only 0.01% of the fatigue damage can be sustained in any one flight. In other words the majority of the flight is non-contributory to fatigue damage and the damage only occurs during the rare excursion to the extremes of the flight envelope in terms of manoeuvre, airspeed both lateral and forward. It would therefore appear that the flight envelope should be restricted in terms of forward speed. In the UK we restrict the forward speed such that the never exceed speed V_{NE} should not be exceeded in the event of a slight upset i.e. if the maximum level speed of the helicopter V_H is higher or equal to V_{NE} then a normal maximum operating speed V_{NO} should be imposed which is 10% or 10 kts less than V_{NE} (Ref 2). This we believe has been a major contribution to helicopter safety.

3.2 Landing Pull Ups

When the helicopter comes into land it is essential to ensure that the rotor carries its own weight until the helicopter is firmly on the ground i.e. there is no significant reduction in rotor speed likely to cause the blades to bang on the stops. The occurrence of such incidents requires monitoring. In the past it has been assumed that the fear of the Main Rotor striking the tailcone would prevent such an occurrence subject to proper training. However, there is evidence to suggest that such an incident led to a fatal accident some five hundred hours later.

3.3 Maintenance and Overhaul

In the maintenance of helicopters it is essential that the Rotor Heads be properly serviced to ensure that dampers have adequate fluids and that the blades are properly tracked. When overhauling components and reclaiming parts it is essential that techniques such as shot peening and debrittlement after plating are properly carried out.

3.4 Extensive Testing

The S-N curve for steel has in the past been considered to have a knee between a million and ten million cycles i.e. it was considered that if a component made of steel was tested to more than 10^7 cycles it would be free from fatigue. However, in the event, after a large number of gearboxes of an early design had accumulated many hours it was found that the planetary gears were failing due to fatigue and that such a failure resulted in a fatal accident. This demonstrates the necessity for fatigue testing. The use of life factors is inadequate when considering stress reversals of the order of 10 million cycles or more so there is a necessity for factoring the torque applied to the gearbox. For British Civil Helicopters we require a stress factor of 1.4 for a single test (Ref 3).

4. DEVICES

4.1 Early Warning Indicators

In examining the methods of calculating safe fatigue lives it becomes clear that the approved methods leave a lot to be desired. When considering the stress cycle involved for a rotor it is apparent that the major part of the cycle is start up - shut down and unless this part is below the fatigue limit for the material then there is bound to be some fatigue damage every flight or start up. If the blade has a calculated safe fatigue life of say 10,000 hours then during its life it has been subjected to 10^4 or more such cycles and will no doubt suffer some fatigue damage over and above any due to those stresses measured in flight if the above proviso is not applied.

Again the accepted method of calculating safe fatigue lives is based on :

a) Fatigue testing of new components.

b) Strain gauge analysis of prototype aircraft operated within a specified flight envelope.

c) A predetermined flight schedule that bears little relation to what occurs in practice.

This programme does not allow for :

I Deterioration in service due to corrosion and mishandling.

II Undiscovered mistakes in quality control such as inclusions, anodic burns etc.

III The occurrence of lightning strikes.

IV Inadvertent exceedance of the flight envelope due to weather conditions, inaccurate calibration of instruments etc.

V Increase in vibratory stresses due to imbalance of rotors, erosion of blades etc.

VI Any change in operational requirements.

It requires a lot of faith to expect the factors of the approved methods to cover all the above variables. So what have we available EARLY WARNING INDICATORS.

It took a number of accidents to convince the manufacturers, operators and airworthiness authorities that some form of early warning was necessary and that simply reducing the safe life everytime there was an accident was not a satisfactory solution.

Several methods have been tried

a) Blowing up the blade spar.

b) Evacuating the blade spar.

c) Electroconductant Paint, films etc.

Each of these methods have had some measure of success but the record is not one hundred per cent and improvements have been found necessary.

4.2 Adequate Warning

In providing an early warning indicator it is necessary to have adequate warning. In determining a SAFE FATIGUE LIFE it was assumed that failure occurred at crack initiation i.e. the component was no longer airworthy. With an EARLY WARNING system it is necessary to go beyond this point and allow some crack propagation and we are now in the realm of fracture mechanics. It is to be noted that once a crack has formed the stresses at the edge of the crack are well above the fatigue limit of the material for the crack to propagate. It is necessary to do crack propagation tests to determine the time from crack indication to ultimate failure. We therefore have two periods (1) the time from crack initation to crack indication, and (2) the time from indication to ultimate failure. It is essential that the latter time is sufficiently long for adequate steps to be taken to avoid a catastrophe. As we are dealing with stresses much higher than the fatigue limit a scatter factor of the order of 5 in terms of time as used in fixed wing theory should suffice. Unfortunately this measure did not avoid an accident and it was necessary to tighten the procedures.

4.3 Cockpit Warning

When considering the normal vibratory stress against speed of the helicopter it is of the shape shown in Figure 1, i.e. the stresses increase with increase of speed at normal cruising speeds so if it is possible to warn the pilot of an impending crack he can back off speed, decrease cyclic stress and have a comparatively longer time to make a safe landing.

5. OTHER COMPONENTS

5.1 Tail Rotors

In assessing the fatigue characteristics of tail rotors the maximum load is likely to occur near the ground in the hover. Surges of power to react rudder loads are required and unstable airflow through the tail rotor may occur.

There are too many accidents due to tail rotor failure and it is difficult to find a satisfactory solution. At the moment the requirements establish a design standard but the adequacy of that design standard can only be proved in service. The use of materials with low crack propagation rates and vibration monitoring may provide a partial solution but the present situation is not exactly happy.

5.2 Main Rotor Heads

Several accidents have occurred due to the fatigue failure of part of the main rotor head. It has not always been clear what caused the failure but some indications are

1) Inadequate shot peening during salvaging at overhaul.
2) Incipient damage due to pounding on the stops leading to crack propagation.
3) Corrosion fatigue in areas not visible for normal inspection.

There is no obvious method of preventing the above accidents except to learn by experience and after the accident be more vigilant to prevent a recurrence.

5.3 Landing Gears

Several cases of fatigue have occurred on landing gears both wheeled and skid. Usually the situation has been contained because of adequate inspection and the fact that a helicopter normally lands with zero forward speed and any undercarriage malfunction can be noted before catastrophe occurs. This did not however prevent a fatal accident on the PANAM roof in NEW YORK.

6. THE FUTURE

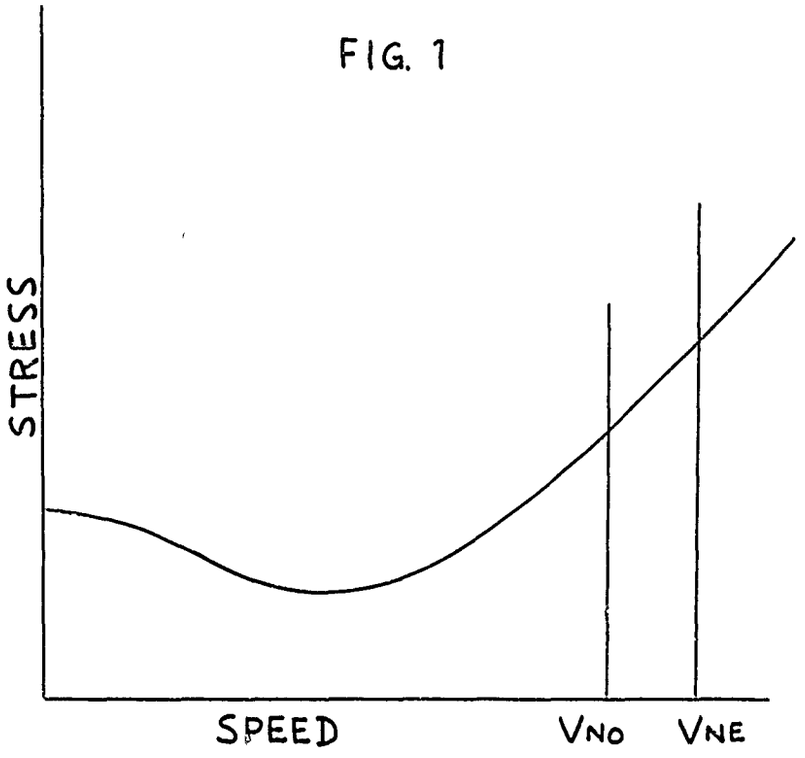
The majority of catastrophic accidents to helicopters involving structure have been due to fatigue of some kind and in comparing the civil helicopter with the civil jet aeroplane the accident rate for helicopters appears to be worse by a factor of at least two. Again a higher proportion of helicopter accidents are due to structural failure. This being the case there is need for improvement.

There would appear to be some benefit to be obtained by the introduction of damage tolerant materials, the incorporation of multi-load paths and the use of vibration monitoring but there is still a long way to go before we will be able to say we have learned to live with fatigue.

REFERENCES

1. FAA A.C. No 20-95 FATIGUE EVALUATION OF ROTORCRAFT STRUCTURES.
2. B.C.A.R. Section G Chapter G8-2 Para 2.3 NORMAL OPERATING LIMIT SPEED.
3. B.C.A.R. Section G Appendix to Chapter G3-4 FATIGUE TESTING OF GEARBOXES.

FIG. 1



HELICOPTER COMPONENT FATIGUE LIFE DETERMINATION

by
M. J. McGuigan
Manager of Structures Technology
Bell Helicopter Textron
P. O. Box 482
Fort Worth, Texas 76101 USA

SUMMARY

The fatigue evaluation program for helicopter components is reviewed and some of the uncertainties that can be encountered in each stage of the program are discussed in some detail. These include the fatigue test and the flight loads measurement phases. Also considered is the frequency of occurrence spectrum and the effects of changes in operational usage as well as possible solutions to the problem of the resulting changes in load spectrums. Variables in the final fatigue life calculations are discussed and some different approaches to setting component retirement time are discussed. In view of the existing uncertainties involved in the "safe life" determination process the "fail safe" approach is considered and some examples are discussed of damage tolerance testing for both metal and composite main rotor blades.

INTRODUCTION

The helicopter component fatigue life determination process is a complicated and many-faceted procedure. Many of the elements that go into this process are very difficult for the manufacturer to accurately define, and there are some over which he has little control. Realizing this, the manufacturer must apply certain conservatisms into each step of the total process. In some cases "state of the art" improvements and advances in other technologies have occurred which can be used to eliminate some of the uncertainties involved. The fatigue life determination process is described step by step, and it is shown how some recent advances can be used, in some instances, to improve the situation.

In order to determine the fatigue life of helicopter components, three basic factors must be known as shown in Table 1. The first factor is the fatigue strength of the component, the second is the loads or stresses to be expected in normal flight, and the third is the frequency of occurrence of these loads or stresses. To obtain the information necessary to adequately define these factors for the many fatigue critical components in a new model helicopter an extensive fatigue evaluation program must be undertaken. A detailed look at this program is appropriate.

Fatigue Strength

The information to define the first factor, fatigue strength, is usually obtained by constant level fatigue test of several specimens of the actual component in order to describe the S-N curve for that component.

A major reason for choosing constant level tests over spectrum loading tests points up one of the principal differences in the fatigue problem between fixed wing and rotary wing aircraft. That is, the rate of accumulation of loading cycles and, therefore, the total number of cycles to which components are subjected in a given amount of flight time is much greater for the helicopter. The helicopter is subjected to significant oscillatory loading at some multiple of the rotor speed even in steady one "g" level flight. A typical helicopter main rotor may accumulate one million load cycles in about fifty hours of flight at one load cycle per revolution. The tail rotor may be subjected to one million cycles in only ten hours.

The advantages of spectrum type tests are well known and some are listed in Table 2. While these advantages are significant, the disadvantages must also be considered and some of these are shown in Table 3. The primary disadvantage is that a very large number of load cycles are required to be applied in this type of test. As an example, to substantiate a fatigue life of 5,000 hours for a main rotor component by spectrum fatigue test of only one specimen, using a scatter factor of four, would require the application of four hundred million load cycles. For a tail rotor component two billion cycles would be required. Since tests of several specimens are required, this type of testing is beyond the realm of practicality. The only way to make it practical is to truncate the spectrum to obtain a reasonable number of load cycles. This procedure, however, carries the problem of showing incorrect effects from fretting which is one of the more significant items in the helicopter fatigue picture. Spectrum fatigue tests can, on the other hand, be a very useful tool in the conduct of crack propagation tests in which the flight time considered is reduced. The spectrum test then becomes practical.

An additional disadvantage is that the complete loading spectrum must be defined prior to starting the test. While the "state of the art" in analytically determining rotor loads has improved greatly in past years, the loads used for fatigue life determination are required to be measured in actual helicopter flight by all certifying agencies. This would therefore mean that the final flight loads survey program would have to be completed before any fatigue tests could be started.

The last disadvantage shown, that of assessing life changes with spectrum changes, is a particularly bothersome one for helicopters for which new methods of operation are continually being developed. This aspect will be discussed in more detail later.

In view of the foregoing, the fatigue strength of each component is usually obtained by constant level fatigue tests of several specimens of the actual component in order to describe an S-N or load versus cycles curve for that component. All facets of these tests are handled in a conservative manner in order to produce valid and yet conservative test results. The actual mating components, assembled as in the helicopter, are usually used to support and load the test specimen. Very large and complicated testing machines are custom built in order to obtain the proper loads and loading distributions on the large parts such as rotor blades and hubs. The load distributions are based on flight measured values. The steady test loads are maintained at a conservative level for the tests of all specimens. However every laboratory test is a compromise in some respects, and the exact simulation of oscillatory flight loads in a fatigue test machine is often difficult.

In actual flight, the ratio and phasing of inplane loads to flapwise loads will vary from one flight condition to another as will the steady load and the spanwise loading distribution. Also, multiple failure modes are frequently encountered in the tests making test results difficult to handle.

The data obtained from these tests is usually handled in some statistical manner to account for the scatter in fatigue strength as shown in Figure 1. In general, the methods of analyzing fatigue test data used by most helicopter companies are very similar, but there can be considerable differences in the detailed application. First, the typical small sample size makes statistical analysis for an individual part difficult. Therefore, most companies use additional information from more extensive small specimen tests, or their own data base from many past component fatigue tests, or both. Most all analysis uses an S-N curve shape equation and an assumed statistical distribution of stress at the endurance limit, i.e., normal, log normal, etc. Since neither of these are generally established or standardized, the variations in these factors can cause a considerable difference in the fatigue lives which are eventually determined. An effort has been initiated in the U.S.A. to achieve some degree of standardization (Reference 1).

Flight Loads

The information to define the second factor, the loads or stresses to be expected in normal flight, involves an extensive flight load survey wherein the flight imposed steady and oscillatory loading is measured in many level flight and maneuver conditions. The loads for these flight conditions are measured over a range of gross weights, rotor speeds, center of gravity positions, and altitudes as shown in Table 4. Since the flight loading must be measured on many fatigue critical components and the load distribution must be defined on some of these, many channels of information must be recorded. On a typical helicopter flight load survey 100 channels of data might be required. Since each level flight and maneuver condition must be repeated at several gross weight, center of gravity, rotor speed and altitude conditions, as many as 120,000 total data points must be obtained. This creates a rather large data handling problem. Magnetic tape recording and automatic data reduction and plotting systems must be used to obtain the necessary information in usable engineering units. Great care is taken in the automatic record reading systems to prevent the recording of erroneous data. Error detection safeguards are built in throughout the procedure.

Some knowledge of the uses or missions in which the helicopter is to be engaged in its lifetime is necessary in order to select the flight conditions to be investigated in this flight loads program. Even if this is accomplished there is some concern over the variation in loads from pilot to pilot and some from one aircraft to another since the helicopter is a finely tuned dynamic system. The individual pilot's technique and the severity of the maneuvers which he performs can affect the resulting loads; therefore maneuvers of different severity are frequently flown to investigate this effect. Also, the effects of normal atmospheric turbulence on the oscillatory rotor loads is another complicating factor. Therefore, some manner of accounting for the scatter in loads is employed by most manufacturers. When enough data is available an "upper edge of data scatter" approach can be used. Or a system can be employed wherein, for a given maneuver, the highest load recorded for any gross weight or altitude, as an example, may be used in the subsequent analysis.

Frequency of Occurrence Spectrum

Information on the third factor, the frequency of occurrence of these loads or stresses, is somewhat more difficult to define. This involves a description of the usage or mission profile for the new model helicopter in order to be able to assign a percent of the total flight time to each of the flight conditions investigated in the flight load survey. This information is not something that the manufacturer can completely define by any type of testing at his facility during the qualification or certification program. A conservative approach to this problem is attempted in order to create a loading spectrum as severe as any that the helicopter can be expected to encounter in actual service. To this end, extensive use is made of past experience with similar purpose helicopters. All available data from previous flight recorder programs of actual operations, as well as some operations analysis of particular missions are considered. However, in spite of this effort, new uses, environments, and methods of operation are continually being developed for the helicopter that cannot be foreseen during original qualification.

Concrete examples of these new uses that have arisen after helicopters have been in service for some time are a matter of record. In the case of military helicopters there is the nap-of-the-earth mission that has been in use for some time and the air-to-air combat mission which is now being seriously considered for some helicopters. In the commercial helicopter usage, an example is the repetitive heavy lift operations with an external cargo sling wherein the frequency of occurrence of extreme power excursions has become very high. This has resulted in accelerated fatigue damage and reduced retirement times for some components that would not otherwise have incurred significant fatigue damage in service.

One possible answer to this difficulty may lie in the use of flight recorders to determine just how the helicopters are used in actual service. A number of attempts at this approach have been made in the past, but the recent application of microprocessors to these recorders may make this approach both more practical and economically feasible. Micro-processor recorders have been tried recently in both military and commercial usage with some encouraging results. One such application was initiated by the U. S. Army (Reference 2) to develop a recorder which incorporated "flight condition recognition" features which stores in a microcomputer memory unit the information necessary to describe the frequency of occurrence for various flight conditions to record and describe the mission profile for the helicopter. With a recorder on each aircraft, a ground data retrieval unit, and a supplemental software system to calculate actual fatigue damage incurred, it is planned to replace parts on an as required individual basis rather than a blanket retirement time for the fleet. This system is now being implemented on several AH-1 Attack Helicopters and may be practical in a situation where one organization (U. S. Army) controls all helicopters and all spare parts in the fleet. Bell Helicopter Textron has acquired several similar flight recorders and thus far has sampled data from three aircraft of one commercial helicopter model used in off-shore drilling rig support in the Gulf of Mexico. The recorder, and data retrieval unit are shown in Figure 2. The flight recorder, including microprocessor mini computer, is small and weighs only 13 kilograms. This data is being used currently to aid in developing frequency of occurrence spectrums for new helicopters in process of certification that may be used in a similar role. The magnitude of this effort would, however, be considerable if each new use is to be sampled as it is developed by the commercial operator and component retirement times changed as dictated by the new spectrum. Any attempt at adjusting retirement times to be commensurate with a particular helicopter usage creates a whole new set of implementation problems in itself. So far the U. S. Federal Aviation Administration has not looked favorably on setting different retirement times for the same model, which are dependent upon the types of usage in which the helicopters are engaged. It is obvious that it would create additional problems of administration and enforcement for them considering how frequently aircraft are switched from one type of operation to another, and traded from one owner to another. One possible solution to this problem might be a procedure for factoring flight time based on the type of operation. In this system the retirement times would be established from a basic FAA approved frequency of occurrence spectrum. Then new and different types of operations could be assessed and a factor determined relative to the original basic spectrum and retirement times. Thus, in various operations each flight hour would be multiplied by a factor of 2, 3 or 0.5 as appropriate to determine the flight hours to be charged toward the basic retirement time.

In connection with the repetitive heavy lift problem, one difficulty is that operators who are not engaged in this type of operation must endure the same lower retirement times on some parts even though it is not necessary. One possible solution is to base retirement times on the number of sling loads carried rather than flight hours. Some precedent exists for this system since some parts of some fixed wing transport aircraft have retirement times based on number of landings rather than flight hours. The FAA still has problems with both of the possible solutions, but perhaps a workable arrangement can be implemented in the near future.

Fatigue Life Analysis

Once the information on the three basic factors is available, there remains the integration of all this data into the fatigue life calculation using The Cumulative Damage Theory (Miner's Method). Because of the differences in detailed application of each one of the many steps that go into the complete calculation, large differences in the calculated fatigue life can be obtained by fatigue analysts. This fact was illustrated at the American Helicopter Society Fatigue Methodology Conference in St. Louis, Missouri in March of 1980, Reference 1. For this conference, seven different helicopter companies calculated the fatigue life of a hypothetical part from the same set of information supplied by the U. S. Army. The results are summarized in Table 5 where it can be seen that considerable difference existed in the calculated lives. A large portion of this difference was caused by the amount of scatter reduction taken from the mean S-N curve to obtain the working S-N curve. Other factors which contributed to the difference were the shape of the S-N curve used, the statistical distribution of stress at the endurance limits, and the cycle-counting method used. In addition one company included a flight loads scatter factor based on its own model for statistical distribution of flight loads.

Since the hypothetical problem was contrived to make it useful for this purpose, many steps in the total process were not included. Some of the differences between the hypothetical problem and real situations are: the frequency of occurrence spectrum was oversimplified, there was no opportunity to consider scatter in flight loads, there were no fretting failures, non-failures, or different failure modes in the S-N data.

Each manufacturer handles each step in his own manner with differing degrees of conservatism in each. Therefore, it is possible that if the total process was handled by each company using its own methods, the final answers may not have been as different as in this hypothetical case.

Several companies use a recommended retirement time considerably less than the calculated life to account for some of the unknowns. Bell Helicopter Textron has established a policy in recent commercial helicopter certifications of setting the retirement time in both flight hours and calendar time. This policy has been instituted because aging, high time helicopters, if poorly maintained, present an increased risk of failure. The most recent commercial model certificated carries a maximum of 5000 hours or 10 years for all principal rotor and control system components above the boost actuators.

Damage Tolerance

Another approach to the fatigue problem that has been used in fixed wing aircraft for many years is the "failsafe" or damage tolerant approach. This procedure is very desirable, but is much more difficult to attain in helicopter dynamic components than in typical fixed wing structure. One reason is because of the flapping and feathering freedom that enable helicopters to fly and the necessary interface between rotating and non-rotating controls. Another reason is the rapid accumulation of loading cycles previously referred to and the consequent tie-in with the necessary inspection intervals and procedures to enable the "failsafe" approach to work properly. The U. S. Federal Aviation Regulations did not allow "failsafe" certification for helicopters until October 1968 (Reference 3) and the FAA policy material and guidelines outlining acceptable procedure for such certification were not published until May 18, 1976 (Reference 4).

One major helicopter component with which some success has been recently achieved using a "failsafe" approach is the main rotor blade. In the case of metal or principally metal blades the use of glass safety straps running spanwise inside the hollow spar (the main load carrying member) has achieved some degree of success. The installation of the glass strap is shown in Figure 3 where it can be seen that the unidirectional S-glass strap is bonded to the upper and lower sides of the hollow "D" spar and its presence is not necessary to carry the required design loads. The benefits of this strap are two-fold. First, the rate of fatigue crack propagation is greatly reduced, once a failure is initiated, giving normal inspection procedures the chance to find the crack before it becomes catastrophic. Secondly, the residual static strength of the blade with a crack present is greatly increased. The comparative crack propagation is shown in Figure 4 where the curve on the left is for the basic blade and the curve on the right is for the same blade but with the glass strap installed. It should be noted that the time shown is only that after the crack became externally visible, or about one inch in length. The crack was initiated by internally notching the D spar and a considerable portion of that spar was failed before the crack progressed into the externally visible blade skin. Two main rotor blade configurations which incorporate this feature are now certified and in production. The latest configuration as used in the Bell Model 222 blade is shown in Figure 5 and provides failsafe protection for the root retention system as well as the complete span of the blade. Neither of these blades are certified "failsafe" under the existing FAA procedures.

Another approach which perhaps holds even more promise is the all composite main rotor blade which can exhibit very favorable damage tolerant characteristics. One such blade used on the Bell Model 214B has received FAA certification and others are in the process of test and certification. The first blade to be certified has been in service for almost two years and is constructed principally of S-2 unidirectional filament wound fiberglass and therefore had to be certificated in accordance with the FAA's Advisory Circular on certification of composite aircraft structure (Reference 5). An extensive test program was required including environmental fatigue and static tests on coupons, structural elements and full scale structure (Reference 6) to develop environmental strength reduction factors for use in the analysis.

Fatigue tests were conducted on these composite blades in a manner similar to that used for previous metal blades and a retirement time is presently assigned. However, an example of their damage tolerance is illustrated by Figure 6. This blade specimen was fatigue tested at an elevated load level to provide a point on the S-N curve and then 5,000 start-stop cycles were applied. The complete afterbody was then sawed away leaving only the spar to react the loads. The spar was also inadvertently notched in the sawing operation. The notched spar was then tested for the equivalent of 125 hours of flight at a load level 1.35 times the maximum level flight loads at which time 500 additional start-stop cycles were applied with no further deterioration of the spar. This test demonstrated the damage tolerant characteristics of the composite blade with external damage present.

CONCLUSIONS

While there are uncertainties involved in each aspect of the helicopter component fatigue life determination process, some of which have been discussed herein, there are conservatisms deliberately built in to each step of the process. Those conservatisms tend to balance the uncertainties of a very difficult problem. In addition, progress is constantly being made in the assessment of each aspect. The aspect which is probably most difficult for the manufacturer to assess and over which he has little control is the variety of usage and new methods of operation that are continually evolving for this versatile aircraft. New developments in technology are making better assessment of this aspect appear more attainable. The use of composites in major components to achieve improved damage tolerance and corrosion resistance should improve the picture further in the future.

REFERENCES

1. PROCEEDINGS OF THE AMERICAN HELICOPTER SOCIETY, HELICOPTER FATIGUE METHODOLOGY SPECIALISTS' MEETING, St. Louis, Missouri, March 25-27, 1980.

2. Saylor, Duane M., FLIGHT CONDITION RECOGNITION, Applied Technology Laboratory, U. S. Army Research and Technology Laboratories (AVRADCOM), Ft. Eustis, Virginia. Presented at the American Helicopter Society, Helicopter Fatigue Methodology Specialists' Meeting, St. Louis, Missouri, March 25-27, 1980.

3. Department of Transportation, Federal Aviation Administration, CRITICAL ROTORCRAFT COMPONENTS, Federal Aviation Regulations, Part 29, Amendment 29-4, October 17, 1968.

4. Department of Transportation, Federal Aviation Administration, FATIGUE EVALUATION OF ROTORCRAFT STRUCTURE, Advisory Circular 20-95, May 18, 1976.

5. Department of Transportation, Federal Aviation Administration, COMPOSITE AIRCRAFT STRUCTURE, Advisory Circular 20-107, July 10, 1978.

6. Reddy, D. J., QUALIFICATION PROGRAM OF THE COMPOSITE MAIN ROTOR BLADE FOR THE MODEL 214B HELICOPTER, Journal of the American Helicopter Society, Vol. 25, No. 3, July 1980, pages 10-14.

TABLE 1

BASIC FACTORS

1. FATIGUE STRENGTH
2. FLIGHT LOADS
3. FREQUENCY OF OCCURRENCE

TABLE 2

ADVANTAGES OF SPECTRUM TESTING

- FATIGUE LIFE DIRECTLY FROM TEST RESULTS
- ELIMINATES USE OF CUMULATIVE DAMAGE THEORY
- INCLUDES HI-LO STRESS INTERACTION EFFECTS
- ELIMINATES S-N CURVE SHAPE UNCERTAINTIES AND EXTRAPOLATIONS

TABLE 3

DISADVANTAGES OF SPECTRUM TESTING

- VERY LARGE NUMBER OF LOAD CYCLES REQUIRED
  - ONE SPECIMEN, 5000 HRS., S.F. = 4
  - MAIN ROTOR: 400,000,000
  - TAIL ROTOR: 2,000,000,000
- COMPLETE SPECTRUM REQUIRED PRIOR TO TEST
- DIFFICULT TO ASSESS LIFE CHANGES WHEN SPECTRUM CHANGES

TABLE 4

FLIGHT LOADS SURVEY

- VARIABLES
  - GROSS WEIGHT
  - CENTER OF GRAVITY POSITIONS
  - ALTITUDE
  - ROTOR SPEED
- 100 DATA CHANNELS
- 120,000 DATA POINTS
- VARIATIONS IN LOADS
  - PILOT TECHNIQUE
  - AIRCRAFT

TABLE 5
FATIGUE LIFE SUMMARY

MANUFACTURER	FATIGUE LIFE - HRS.	
	WITHOUT CYCLE COUNT	WITH CYCLE COUNT
AEROSPATIALE	9	58
AGUSTA	804	13,866
BELL	1831	27,816 (5,000)*
BOEING VERTOL	1294	22,523
HUGHES	2594	24,570
KAMAN	67	191
SIKORSKY	240	470

* RECOMMENDED RETIREMENT TIME 5,000 HOURS OR TEN YEARS

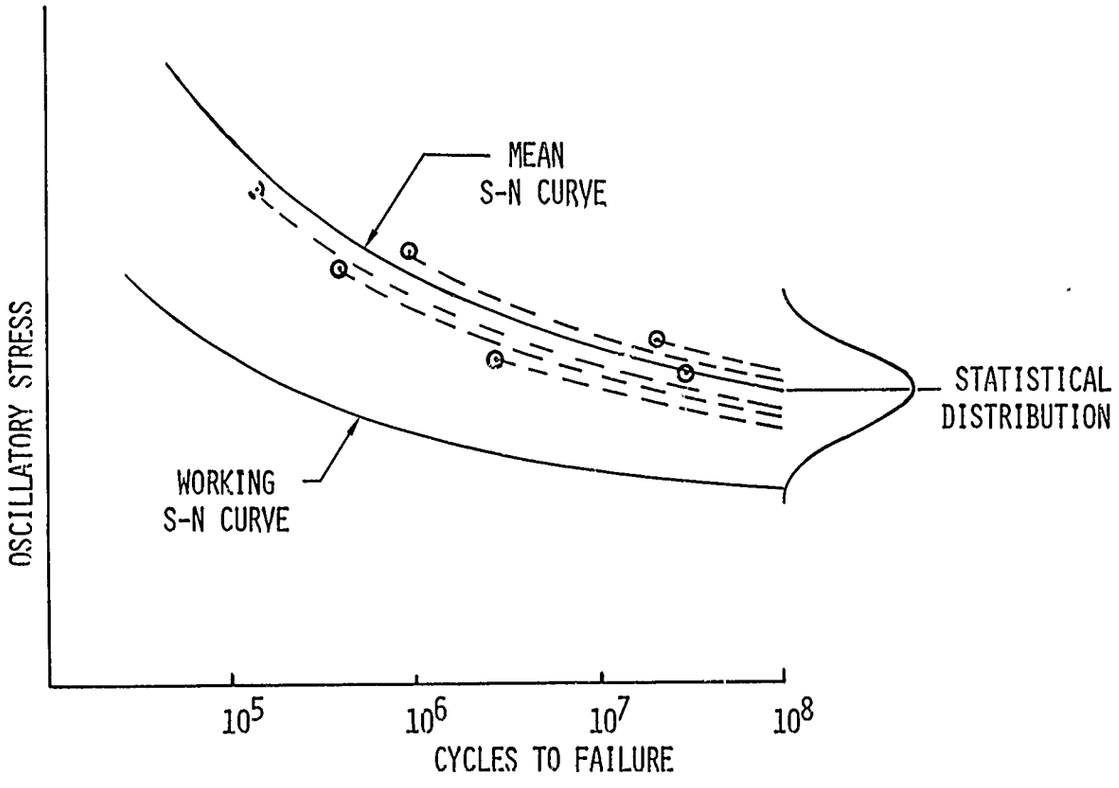


Fig.1 Analysis of fatigue test data

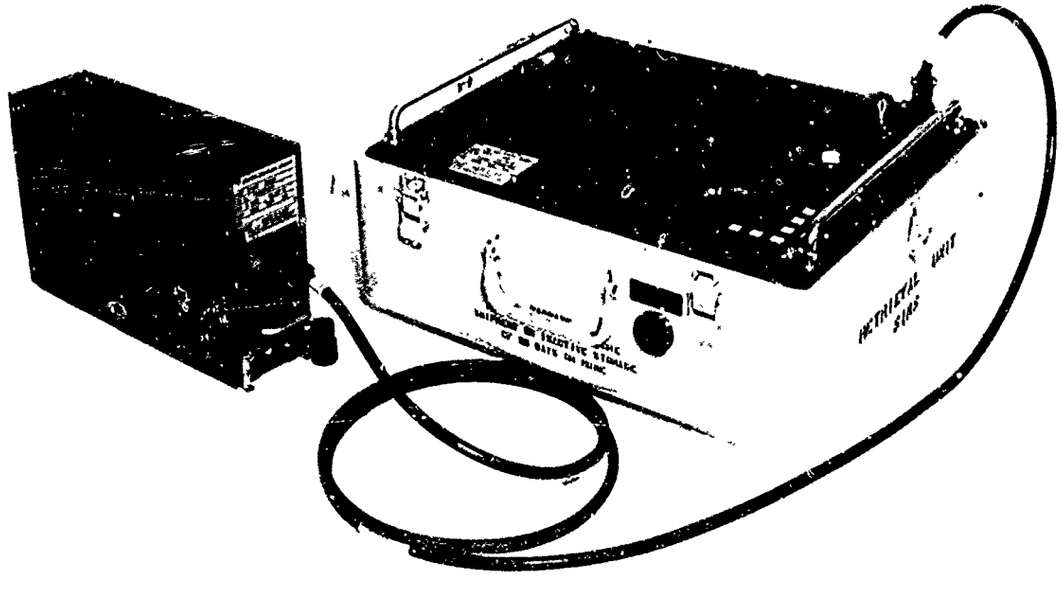


Fig.2 FCM system recorder and retrieval unit

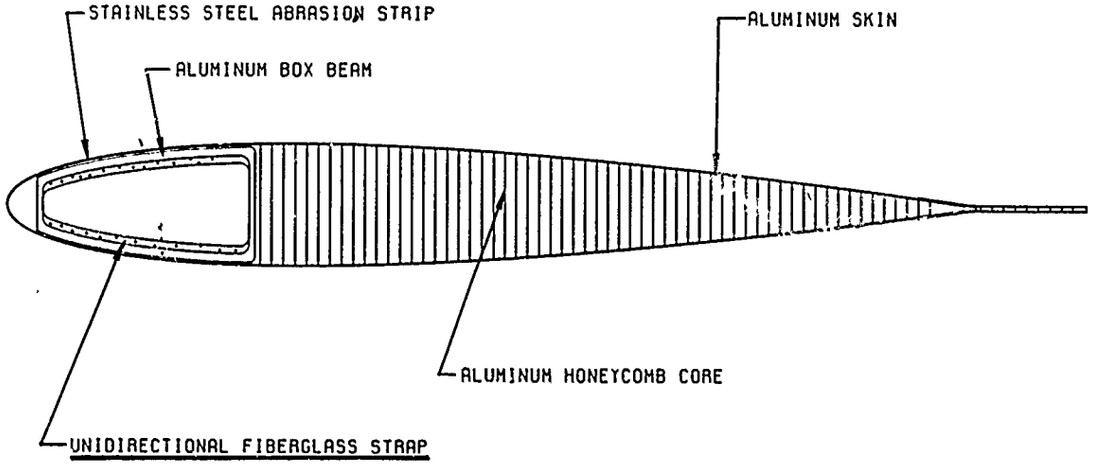


Fig.3 Installation of glass safety straps

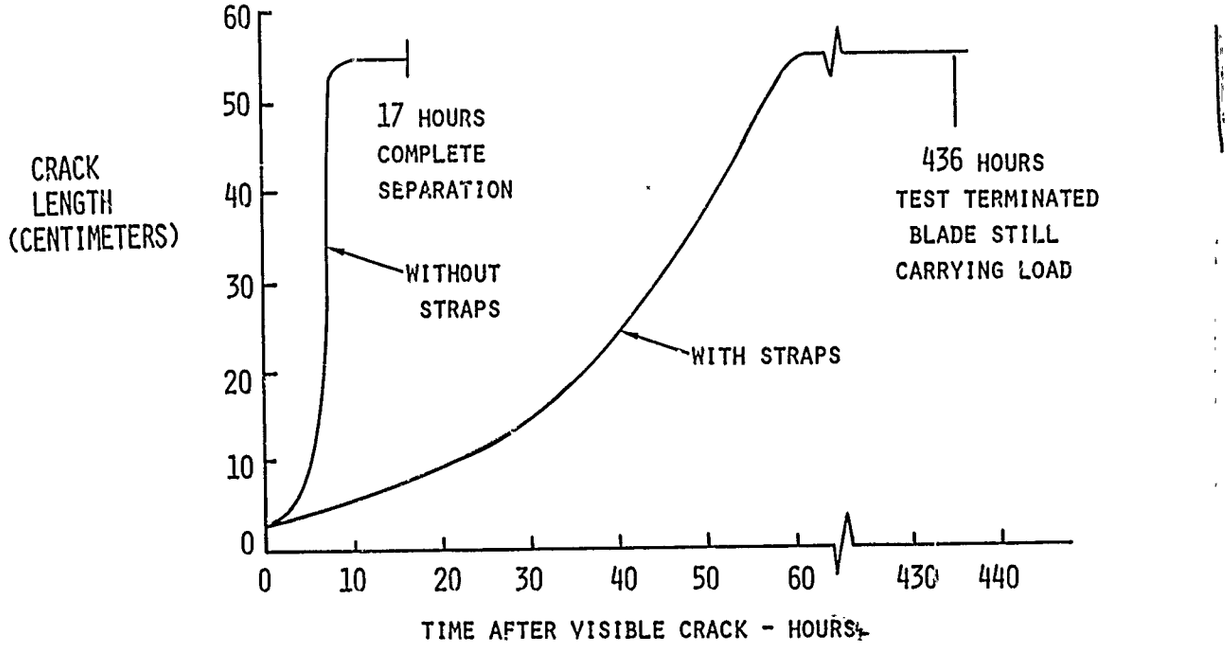


Fig.4 Comparative fatigue crack propagation

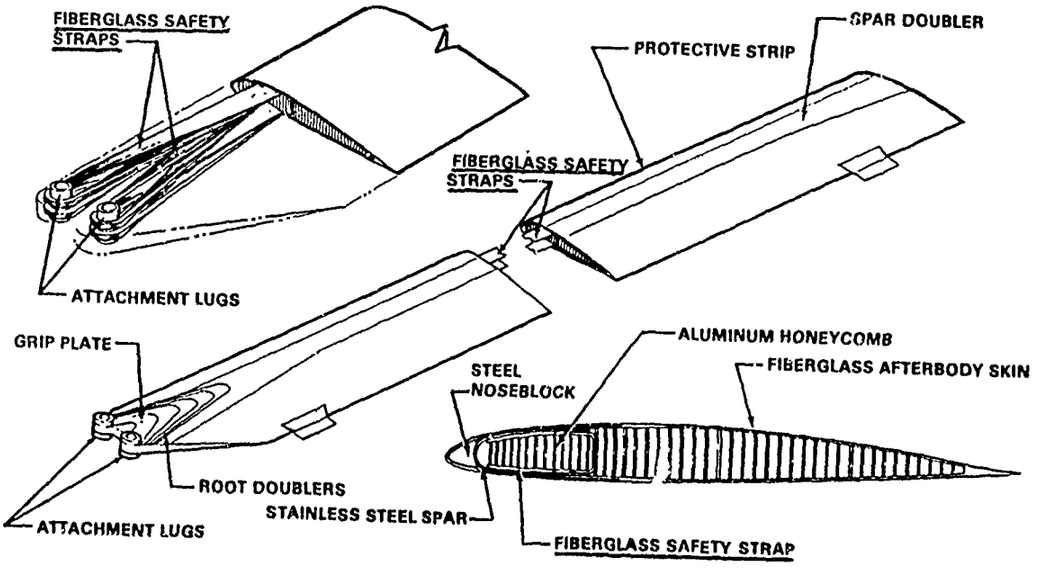


Fig.5 Model 222 glass strap configuration

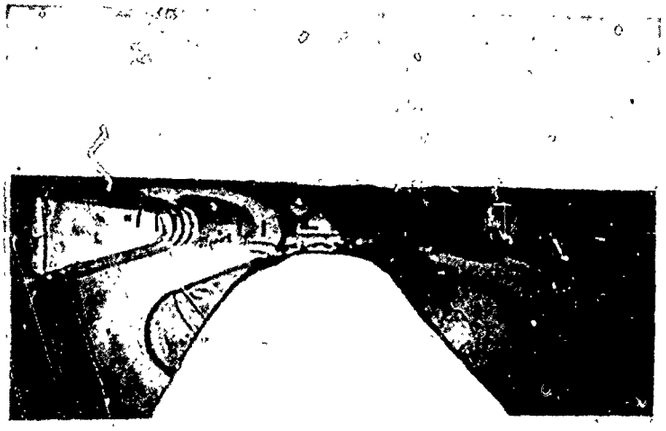


Fig.6 Fiberglass blade damage tolerance

Report on Session III

SURVEY OF SERVICE EXPERIENCE WITH REGARD TO EXISTING PROCEDURES

by

J.Darts
Royal Aircraft Establishment
Structures Department
Farnborough, Hants GU14 6TD, UK

A. Summary of paper by R.Cansdale – "An Evaluation of Fatigue Procedures for UK Military Helicopters"

This paper reviewed the current UK procedures for certification of military helicopters and gave the author's opinion of the way these procedures should develop in the future.

The present factors on stress and power levels used for testing and estimating the life of components were based on past experience. Factors for composites had not been derived because of the limited variability data available. The paper highlighted the problem of defining aircraft usage and that fatigue life was governed by flight conditions that theoretically were not flown.

A discussion of fatigue testing procedures concluded that testing techniques should simulate the loading environment in a more realistic manner. The paper recognised the difficulty of testing parts that experience a complex load environment often resulting in unrepresentative failure modes. The tailoring of composite structure to the loading environment may lead to there being more critical areas and therefore a need for more extensive tests. The paper indicated that certification of composite structure in the UK was at present using very conservative estimates of life.

For the future the paper considered that damage tolerant design could account for the effects of unknowns such as corrosion. The increase in manpower needed to perform inspections needed to be considered carefully when using this design approach. Finally the need for an on-board monitoring system to reduce the number of unknowns in the loading and usage environment was identified.

B. Summary of paper by H.E.Lesueur – "Helicopter Fatigue – A Civil View"

This review of certification procedures for civil helicopters indicated that a safe life approach towards fatigue was somewhat unsatisfactory. This conclusion had been reached from an assessment of civil accidents which gave an unacceptable accident rate of four fatal accidents per 300,000 hrs. The paper suggested accidents could be reduced by eliminating excursions to the extremes of the flight envelope and ensuring the rotor carried its own weight when landing. Proper servicing procedures and extensive fatigue test data were also aids to reducing accident rates.

The need for early warning indicators was identified as a result of the inability of safe life procedures to account for factors such as corrosion, flight envelope exceedance and changes in operational requirements. The paper concluded that future designs would benefit from the use of damage tolerant materials, multiple load paths and vibration monitors.

C. Summary of paper by M.J.McGuigan and M.E.Gloss – "Helicopter Component Fatigue Life Determination"

Fatigue strength of components, loads in flight and their frequency of occurrence were identified by this paper as important factors in determining helicopter fatigue life.

To determine fatigue strength of components conservative constant amplitude testing was preferred by the authors because spectrum tests were time consuming. Truncation of a spectrum to reduce testing time could result in an ineffective simulation of fretting. A standardised approach towards the methods of analysing fatigue life data was suggested. Results of an American Helicopter Society exercise had shown that detailed differences in the application of cumulative damage laws could lead to large differences in life.

The problem of defining the flight loads and their occurrence was discussed by the paper and the size of the loads data base required for an accurate assessment of usage estimated. As in previous papers the need for flight recorders and adoption of a damage tolerant design philosophy was suggested.

D. Discussion of the papers in Session III

Interest was expressed in the best way to perform a flight test programme and how piloting technique could be taken into account. The authors generally agreed that to achieve reliable results an extensive programme would be required hence the adoption of the conservative approach of using the highest load achieved in each flight condition. Evidence supplied from the floor agreed and disagreed with the conclusion that spectrum testing was unsuitable for testing helicopter components. Testing to large numbers of cycles had been achieved in other fields of fatigue design such as automobiles.

The discussion turned to a consideration of accidents and it was re-emphasised that premature failure of components was generally caused by flight envelope exceedance. Accident rates for both civil and military helicopters were discussed but evidence was supplied that 75% of helicopter accidents were caused by pilot error. Changes in helicopter tactics were leading to more accidents such as wire strike in NOE missions.

ESSAI DE FATIGUE D'UNE STRUCTURE COMPLETE DE L'HELICOPTERE SA 341 "GAZELLE"

- PREPARATION
- CONDUITE
- RESULTATS

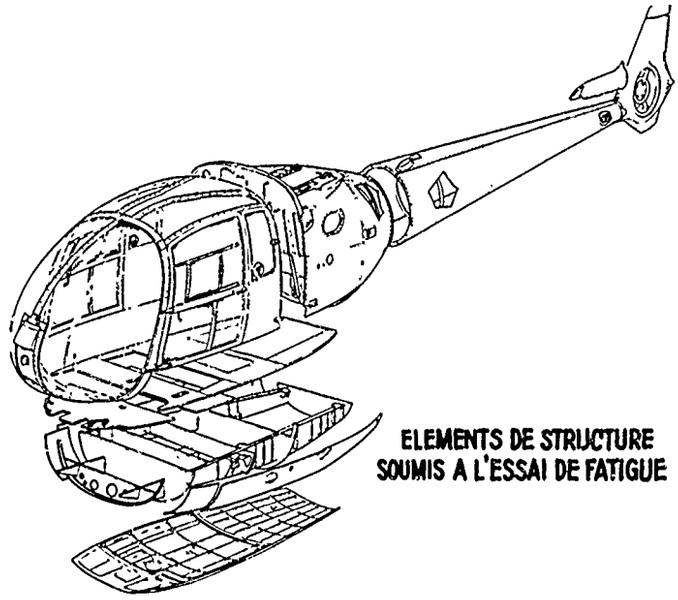
PAR :

Philippe PETARD
Ingénieur AEROSPATIALE
B.P N° 13
13 722 - MARIGNANE (France)

&

Jean-Pierre LAMBERT
Chef du Laboratoire d'Essais de Fatigue de Structure au C.E.A.T
23, Av. Henri Guillaumet
31 056 - TOULOUSE (France)

=-=-=-



ELEMENTS DE STRUCTURE
SOUMIS A L'ESSAI DE FATIGUE

FIGURE 1

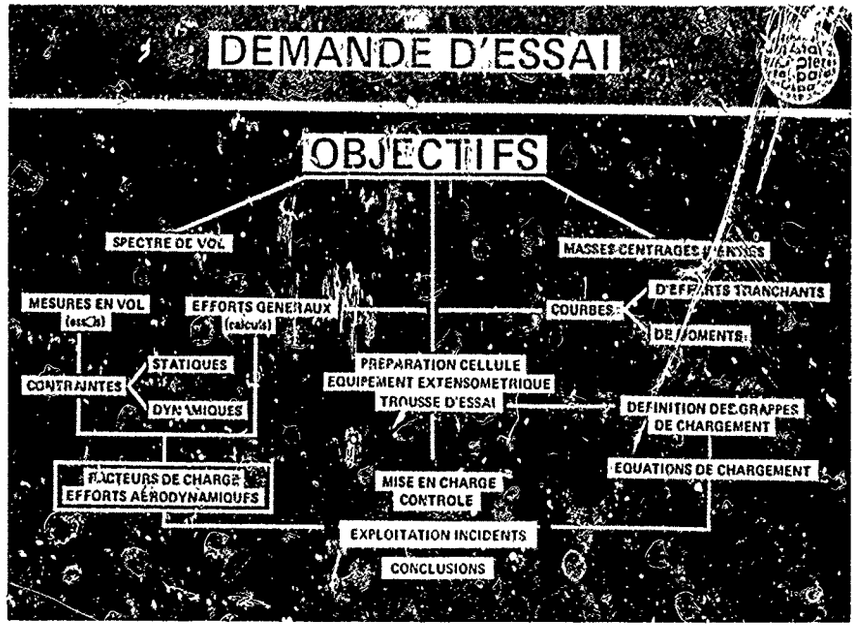


FIGURE 2

4 - PREPARATION DE L'ESSAI :

Le schéma de la figure 2 nous indique l'ensemble des opérations d'études de mesures et de préparation nécessaires pour aboutir à l'essai proprement dit et à son exploitation. Nous allons définir les points les plus caractéristiques de ce schéma.

4.1 - Spectre de vol :

Le spectre de vol définit l'ensemble des configurations rencontrées dans un vol type d'une heure. Certaines de ces configurations, combinées aux sollicitations dynamiques, peuvent avoir un effet endommageant sur la structure.

La répétition de ce spectre sera effectuée un nombre de fois suffisant pour couvrir la vie maximale d'un appareil compte tenu d'un coefficient de dispersion adopté.

Le spectre de vol servant de base à tous les calculs d'endommagement sur les pièces mécaniques de la Gazelle et qui a été utilisé pour l'essai de fatigue a été établi à partir des observations effectuées sur trois appareils militaires choisis pour trois genres différents de missions: tactique, de liaison et technique (école-radio). Les pourcentages de temps dans chaque configuration ont été établis statistiquement à partir des informations fournies par les trois appareils.

Ce spectre de vol couvre l'ensemble des utilisations civiles et militaires exception faite des utilisation agricoles et de débardage (travail à l'élingue).

4.2 - Collecte des informations intéressant les essais :

Les informations permettant de connaître les efforts de vol appliqués à l'hélicoptère sont extraites, d'une part des résultats d'essais en vol, d'autre part de calculs définissant les efforts aérodynamiques et les équilibres au centre du rotor principal.

La connaissance des efforts de vol en essai se fait essentiellement par l'intermédiaire d'équipements extensométriques étalonnés et d'accéléromètres.

Les postes extensométriques permettent de connaître directement les efforts ou moments appliqués aux points caractéristiques de la structure. Ils peuvent être reconduits sur la cellule d'essai pour vérifier l'équivalence des chargements.

Les niveaux vibratoires mesurés en vol dans les zones estimées les plus représentatives ont été reproduits sur la cellule d'essai avec une fidélité jugée satisfaisante.

Sur la Gazelle les postes de contrainte exploités ont été :

- les postes de moments en lacet et en tangage à l'encastrement de la poutre de queue
- les postes en traction sur chaque branche des "vés" (barres de fixation) de la boite de transmission principale (BTP)
- un poste de flexion en battement sur le tube longeron d'empennage
- un poste de flexion en tangage sur la poutre de barque
- un poste en traction sur une bielles de la platine souple sous la BTP.

Il faut préciser que tous ces postes de mesures ont essentiellement pour but de contrôler la mise en charge en essai et non de permettre l'analyse de contraintes dans des zones précises de la structure. Pour ces analyses ponctuelles des essais locaux sont plus appropriés.

4.3 - Mise en charge de la cellule d'essai :

La mise en charge a été effectuée sur une cellule lestée à une masse moyenne d'utilisation de 1550 kg au centrage moyen.

En plus des efforts aérodynamiques et de manoeuvres introduits par le rotor principal, le rotor arrière et l'empennage, la structure est soumise aux forces d'inertie dues aux accélérations linéaires et angulaires induites par les efforts de manoeuvre. L'application sur la structure des efforts d'inertie va nécessiter la mise en place d'un système de chargement qui doit tenir compte de la répartition des masses et de la position du centre de gravité de l'ensemble des masses constituant l'appareil. Le document de base pour cette opération est le document de masses et centrages qui détaille les masses de l'appareil en suffisamment de points pour tracer les courbes d'effort tranchant et de moment fléchissant sous charge statique (accélération linéaire unitaire vers le bas)sur toute la longueur de l'appareil (voir figure 3)



FIGURE 3

Pour les accélérations angulaires unitaires en lacet et en tangage on établira également les courbes d'effort tranchant et de moment (voir figures 4 et 5).

Les courbes unitaires de chargement massique et d'inertie étant établies, la phase préparatoire suivante consiste à définir le procédé de chargement en laboratoire qui reproduira le plus fidèlement possible les courbes définies précédemment.

Il est souhaitable d'avoir un minimum de points de chargement pour ne pas alourdir l'essai.

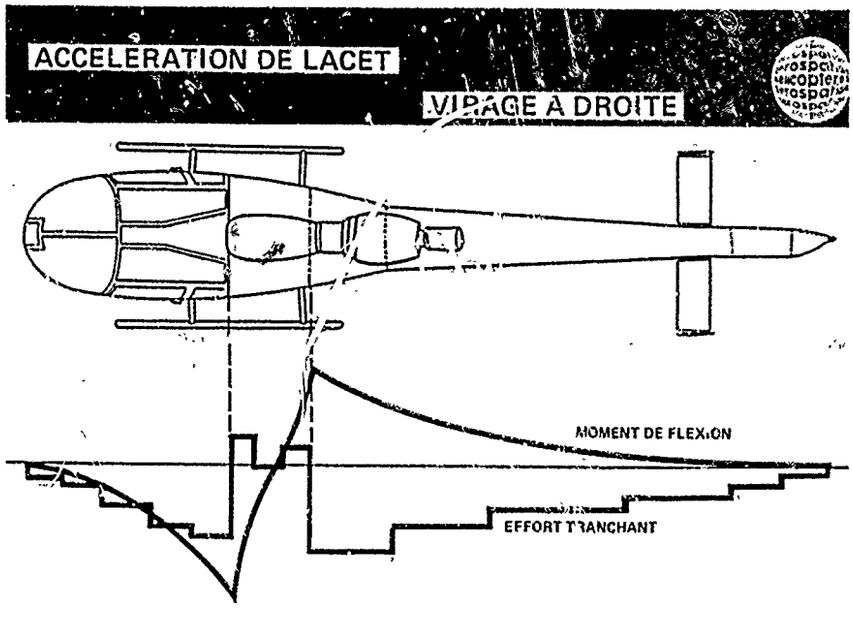


FIGURE 4

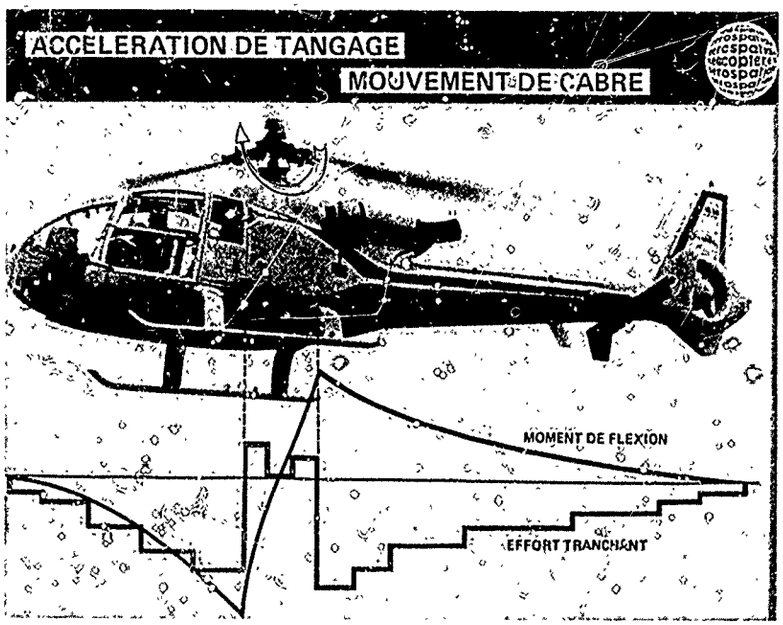


FIGURE 5

Sur la structure essayée le nombre de points de chargement était : (figure 6)

6 points pour les efforts massiques et d'inertie
3 points pour les efforts aérodynamiques
2 points pour les charges d'atterrisseur

Pour le rotor arrière et l'empennage, les efforts aérodynamiques seront mixés avec les efforts massiques et d'inertie.

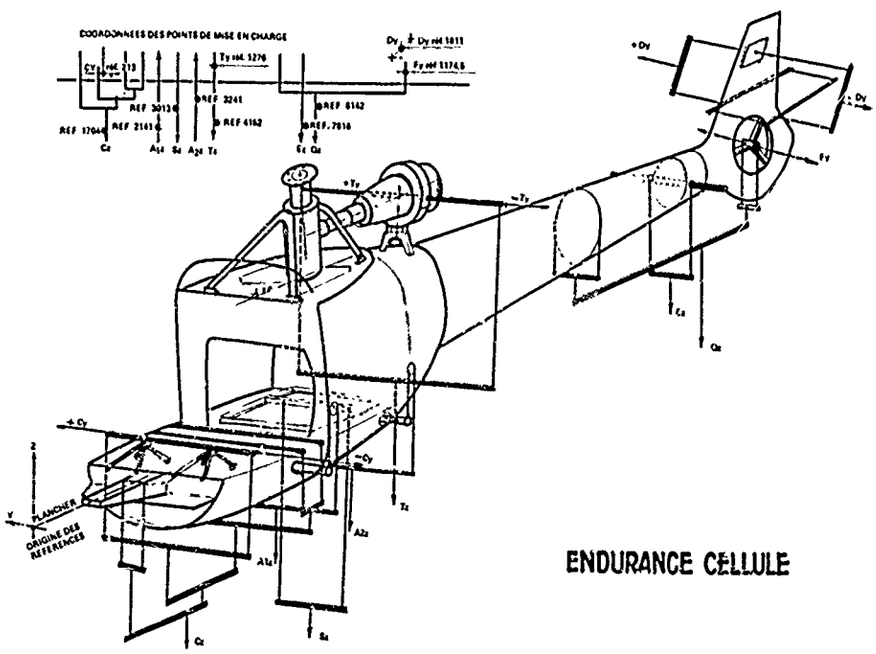


FIGURE 6

Après avoir défini les grappes de chargement on peut établir les équations de chargement d'essai sur chaque vérin qui sont de la forme :

a) Pour les chargements verticaux :

$$Fz = A\,\overline{nz} + B\,ny \quad (-Fz \text{ aérodynamique pour le chargement de l'empennage})$$

b) Pour les chargements latéraux :

$$Fy = C\,\widehat{nz} \quad (\pm Fy \text{ de manoeuvre ou d'équilibre pour le rotor arrière})$$

NOTA : $\overline{n}$ = étant le coefficient d'accélération linéaire
$\widehat{n}$ = étant le coefficient d'accélération angulaire

Pour la dérive, dans l'essai qui nous intéresse, seul l'effort aérodynamique a été appliqué.

Pour les charges appliquées sur les atterrisseurs, les efforts définis par l'analyse d'essais de chutes étaient donnés numériquement.

Les efforts aérodynamiques et de manoeuvre d'une part, les facteurs de charge d'autre part étant définis, on peut connaître les efforts sur chaque vérin et vérifier l'équilibre de l'appareil au centre du rotor principal en le comparant aux efforts théoriques définis par le Service Aérodynamique.

C'est d'après cette vérification des équilibres que les efforts ont été communiqués au laboratoire d'essai qui a lesté la cellule et mis en place les grappes de chargement.

5. PRESENTATION DE L'INSTALLATION D'ESSAI REALISEE AU CEAT

L'installation d'essai de fatigue de la cellule de l'hélicoptère SA 341 "Gazelle" a été conçue pour permettre la simulation des différentes sollicitations exposées précédemment, qui s'exercent sur la structure pendant le vol.

Un ensemble d'acquisition permet de vérifier la validité de l'essai en effectuant des mesures périodiquement. Ces mesures sont ensuite comparées à celles qui ont été effectuées sur les prototypes lors des campagnes d'essais en vol et qui ont permis d'établir le programme d'essai.

5.1. Description de la cellule essayée et de son bâti de chargement

La cellule est constituée par une structure de définition série qui ne comporte que l'ensemble des éléments travaillants. Les portes, les capots et les carénages ne sont pas montés. La majorité des organes mécaniques sont remplacés par des outillages qui permettent l'introduction des efforts et qui ont la même masse que la pièce réelle.

La cellule est lestée de façon à représenter les différentes masses emportées (pilotes, passagers, équipements, frêt, kérozène...). Elle est suspendue au bâti d'essai par l'intermédiaire d'un faux mât rotor (planches 1 et 2).

Afin de permettre l'excitation vibratoire de la cellule sans transmettre les vibrations à l'ensemble du bâti , un filtre a été réalisé, en utilisant des ressorts à compression d'élastomère, pour relier le faux mât rotor au bâti (planche 3).

5.2. Moyens de chargement

Le chargement de la structure est assuré par des vérins hydrauliques asservis soit en effort soit en déplacement (vérins de vibrations).

Les vérins de chargement sont, pour la plupart, fixés horizontalement sur le sol et appliquent les efforts au moyen de câbles et de poulies de renvoi (planche 1).

Les vérins de vibration sont suspendus à un bâti par une liaison très souple.

La tige est fixée sur les fausses pales du rotor et le corps est libre (montage sismique) ce qui permet d'introduire des efforts relativement importants avec des sections de vérin faibles (planche 4).

Les vérins de chargement (au nombre de 11) sont pilotés par des voies d'asservissement analogiques conçues et réalisées au CEAT.

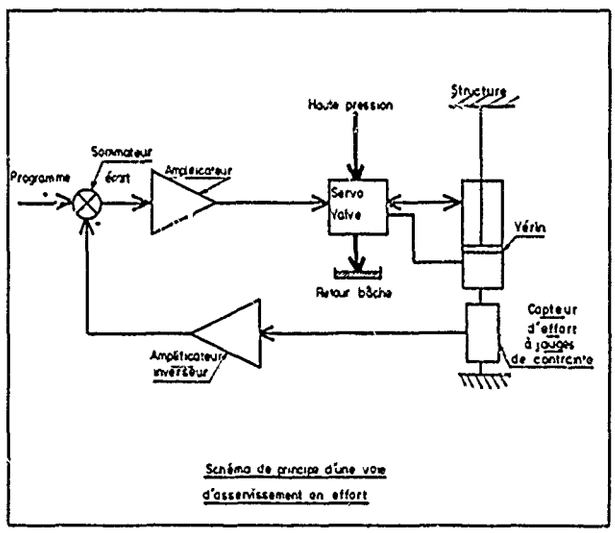


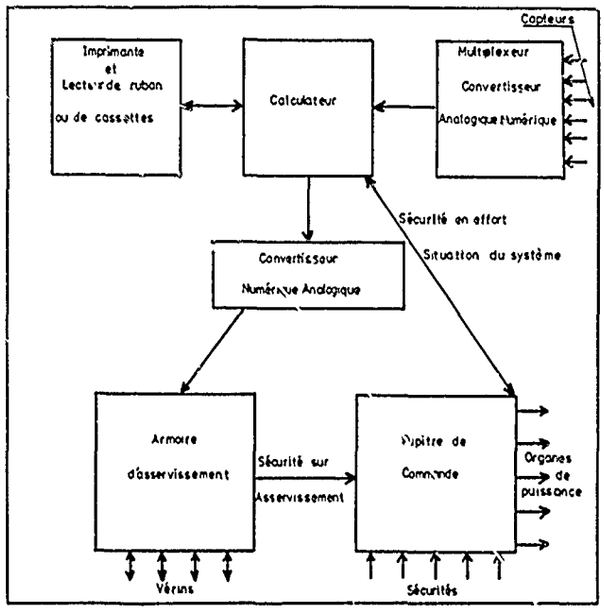
Schéma de principe d'une voie d'asservissement en effort

L'écart entre le programme et le signal du capteur d'effort à jauges de contraintes pilote, après amplification, une servo-valve débit qui régule la pression hydraulique dans les deux chambres du vérin.

Pour les vérins de vibration, c'est la position du corps du vérin qui est asservie. Le programme est une sinusoïde de fréquence 18,9 Hz et d'amplitude constante.

5.3. Système de commande

Le schéma ci-dessous montre les différents ensembles et leurs liaisons fonctionnelles.



Les voies d'asservissement reçoivent les programmes élaborés par un mini-ordinateur qui réalise aussi une fonction de surveillance du bon déroulement de l'essai.

Le pupitre de commande délivre la puissance électrique aux différents organes, regroupe les fonctions de sécurité, visualise l'état des différents systèmes et rassemble les commandes qui permettent d'intervenir sur le déroulement de l'essai.

5.3.1. Le mini-ordinateur et ses périphériques

Le mini-ordinateur et ses périphériques permettent d'assurer la conduite de deux essais de fatigue simultanément. La conception générale et la programmation ont été étudiées de telle façon que les deux installations soient totalement indépendantes.

Le calculateur est équipé d'une mémoire de 20 k mots de 16 bits.

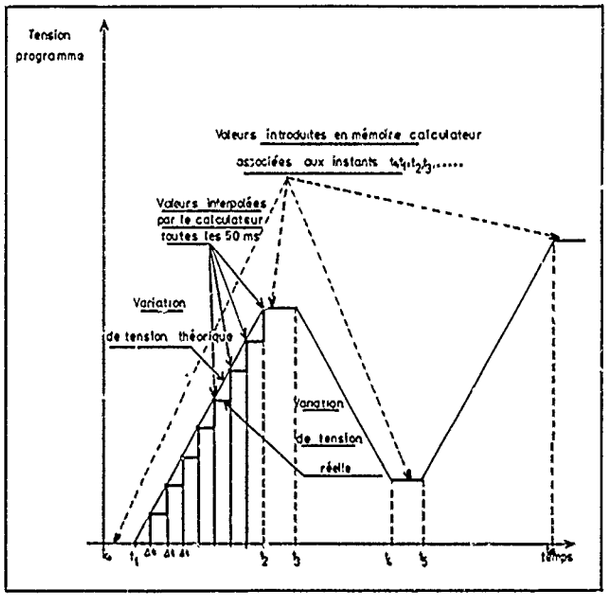
Sont associés à ce calculateur :

- un ensemble d'entrées - sorties numériques permettant les échanges avec le pupitre
- une télétype par essai
- un convertisseur numérique - analogique qui délivre les tensions programmes aux voies d'asservissement
- un convertisseur analogique - numérique et un multiplexeur capable d'acquérir 5000 mesures par seconde en bas et haut niveau
- un système de conditionnement de capteurs (efforts, pressions, contraintes).

Cet ensemble assure trois fonctions :

- la génération de programme
- la surveillance de l'essai
- le dialogue avec l'opérateur et les échanges avec le pupitre.

5.3.1.1. Génération de programme

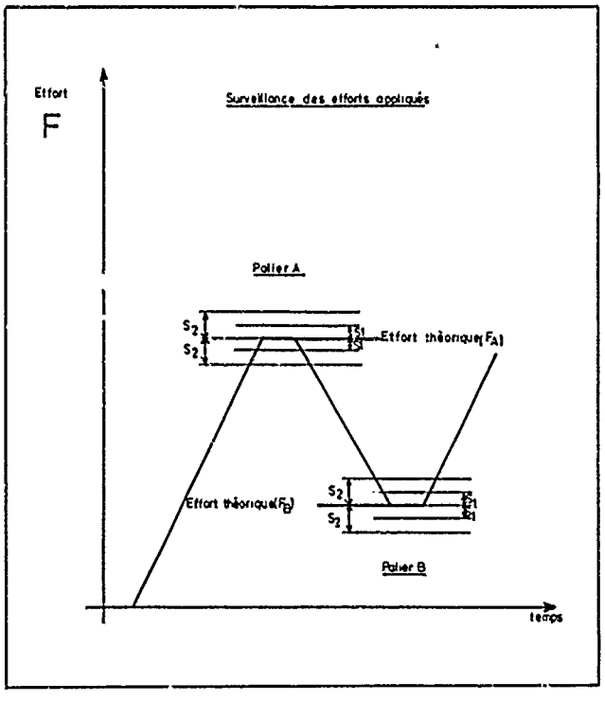


Le calculateur possède en mémoire la valeur des tensions programmes, pour toutes les voies, à chaque palier. Toutes les 50 millisecondes il effectue une interpolation et met à jour les valeurs envoyées sur les voies par les convertisseurs numériques analogiques.

La capacité mémoire permet la génération de plusieurs cycles dont la durée peut atteindre 30 minutes avec une trentaine de voies d'asservissement.

5.3.1.2. Surveillance de l'essai

A chaque palier de charge (et plusieurs fois par paliers lors de configurations stabilisées) le calculateur commande une acquisition de tous les capteurs et effectue une comparaison avec les valeurs théoriques qu'il a en mémoire (Les capteurs et leur chaîne de mesure sont indépendants de l'asservissement).



Pour chaque voie deux seuils, constants au cours du cycle, S1 (~ 5 % de l'effort maxi) et S2 (~ 10 % de l'effort maxi)sont entrés en mémoire.

- Si |Mesure - effort théorique| < S1 le fonctionnement est déclaré correct.

- Si S1 ≤ |Mesure - effort théorique| < S2 le calculateur édite un message sur l'imprimante.

- Si |Mesure - effort théorique| ≥ S2 le calculateur déclenche la séquence de sécurité qui comprend :

  . la coupure de la puissance hydraulique
  . le retour à zéro des tensions programmes
  . la sortie sur l'imprimante du type de défaut, du numéro de cycle, de l'instant, du numéro de la voie en défaut et de la valeur de toutes les mesures à l'instant du défaut.

5.3.1.3. Dialogue avec l'opérateur

Le dialogue se fait essentiellement par la télétype qui informe l'opérateur sur le déroulement de l'essai (numéro de cycle, cadence de fonctionnement, mesures effectuées ou défauts constatés) et fournit au calculateur les données nécessaires lors d'un démarrage.

5.4. Les sécurités

Si la sécurité apportée par la surveillance par calculateur de la bonne application des efforts est primordiale elle n'est cependant pas la seule à être utilisée.

Au niveau de la voie d'asservissement on mesure le courant de commande de la servo-valve et on le compare à un seuil, réglable pour chaque voie.

Ceci permet de se prémunir contre un départ de la voie en boucle ouverte dû, par exemple, à une rupture de la ligne de mesure du capteur d'asservissement.

Des sécurités électriques limitent le déplacement de la tige des vérins ce qui permet de déceler éventuellement un affaiblissement de la structure.

Des sécurités mécaniques limitent de manière absolue le déplacement de la tige des vérins au cas où aucune des autres sécurités ne fonctionnerait.

Sur toutes les lignes d'effort qui comportent des câbles on utilise des limiteurs d'efforts électromécaniques qui déclenchent la séquence de sécurité en cas de dépassement de l'effort maximum d'environ 10 %.

5.5. Avantages de cette installation

Cette installation conçue en 1972, différait radicalement de celles utilisées jusqu'alors au CEAT par la présence d'un mini-ordinateur. Celui-ci permet en particulier d'effectuer plusieurs types de cycles différents avec un enchainement quelconque, d'effectuer des cycles très longs sans difficulté et d'augmenter la vitesse d'application des charges.

Il permet surtout d'assurer une surveillance efficace des moyens de chargement en interrompant l'essai dès qu'un défaut est constaté.

6. DEROULEMENT DE L'ESSAI

L'essai de fatigue a débuté le 1er Juin 1974 et s'est terminé le 24 Mai 1978. Au cours de ces quatre années 8200 heures d'essai ont été effectuées qui ont permis de simuler 20 000 heures de vol.

6.1. Mise au point de l'installation

La mise au point a permis de reproduire en divers endroits de la structure des niveaux de contraintes vibratoires très proches de ceux qui avaient été mesurés lors des essais en vol.

Ceci a été obtenu en faisant varier l'amplitude et le déphasage des excitations vibratoires au niveau de la tête rotor. Une représentation correcte a été obtenue en utilisant une excitation verticale et une excitation horizontale déphasées de 140°.

6.2. Définition des cycles

4 cycles de vol qui comprennent chacun 30 configurations et 4 types d'atterrissages ont été définis par l'Aérospatiale. Les cycles de vol diffèrent entre eux par le sens des virages ou des dérapages et par le centrage. Les atterrissages sont soit durs, soit souples, avec un centrage avant ou arrière (planche 5).

Chaque cycle de vol représente 1/4 d'heure de vol. Les différents cycles de vol sont effectués en pourcentage égal, un atterrissage suit un vol de même centrage et un atterrissage sur quatre est dur.

6.3. Déroulement de l'essai de fatigue

On peut distinguer deux phases au cours de cet essai de fatigue.

6.3.1. Première tranche

Au cours de la première partie de l'essai, et pendant une durée de 2500 heures, les charges appliquées ont été égales aux charges rencontrées en vol et les configurations de vol stabilisé ont été représentées de façon à prendre en compte correctement l'influence des vibrations.

6.3.2. Deuxième tranche

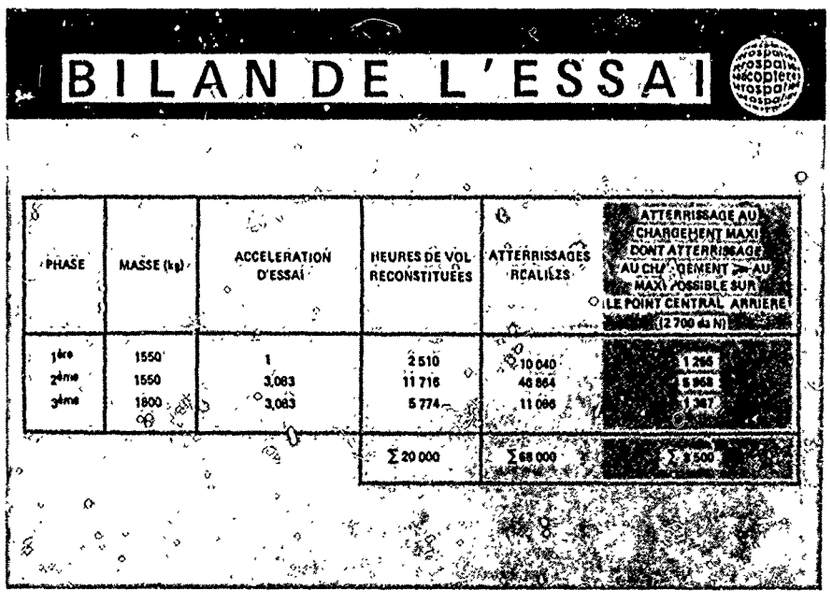
La première tranche d'essai ayant été jugée très représentative par rapport à des dommages survenus sur des appareils en service, il a été décidé de ne pas accélérer l'essai par augmentation des charges mais uniquement par suppression des configurations stabilisées ; le niveau des excitations vibratoires a été augmenté de façon à respecter la concordance des endommagements statiques et dynamiques dans le temps.

La suppression des configurations stabilisées a entraîné une accélération de l'essai dans un rapport 3,15.

A partir de 13910 heures de vol simulées et jusqu'à 20 000 heures les efforts appliqués ont été augmentés pour représenter une masse de 1800 kg au lieu de 1550 précédemment.

6.4. Bilan des atterrissages

L'ensemble de cet essai a reconstitué 20 000 heures de vol pendant lesquelles 68000 atterrissages ont été réalisés, 8500 atterrissages introduisant sur le point de fixation central de l'atterrisseur arrière des charges supérieures aux charges possibles. En effet, lorsque la charge centrale de la traverse arrière atteint 2700 daN cette traverse prend une flèche telle qu'elle vient en butée au niveau de son passage à travers les deux poutres latérales de la barque, déchargeant ainsi le point central. Cette flexibilité de la traverse arrière n'était pas représentée en essai.



BILAN DE L'ESSAI

PHASE	MASSE (kg)	ACCELERATION D'ESSAI	HEURES DE VOL RECONSTITUÉES	ATTERRISSAGES RÉALISÉS	ATTERRISSAGE AU CHARGEMENT MAXI DONT ATTERRISSAGE AU CHARGEMENT MAXI POSSIBLE SUR LE POINT CENTRAL ARRIÈRE (2 700 daN)
1ère	1550	1	2 510	10 040	1 266
2ème	1550	3,083	11 716	46 864	5 958
3ème	1800	3,083	5 774	11 096	1 367
			Σ 20 000	Σ 68 000	Σ 8 500

Figure 7

7. ENDOMMAGEMENTS

La carte des endommagements est représentée figure 8. Les endommagements apparus en cours d'essai sont classés en deux types principaux.

A : Les endommagements pouvant avoir une incidence sur le bon comportement en vol de la structure et sur sa résistance

B : Les endommagements mineurs, qualifiés ainsi car ils n'ont pas d'incidence importante sur la résistance de la structure.



Figure 8

A : Endommagements pouvant avoir une incidence sur le bon comportement en vol de la structure et sur sa résistance.

Trois catégories d'endommagements sont considérées.

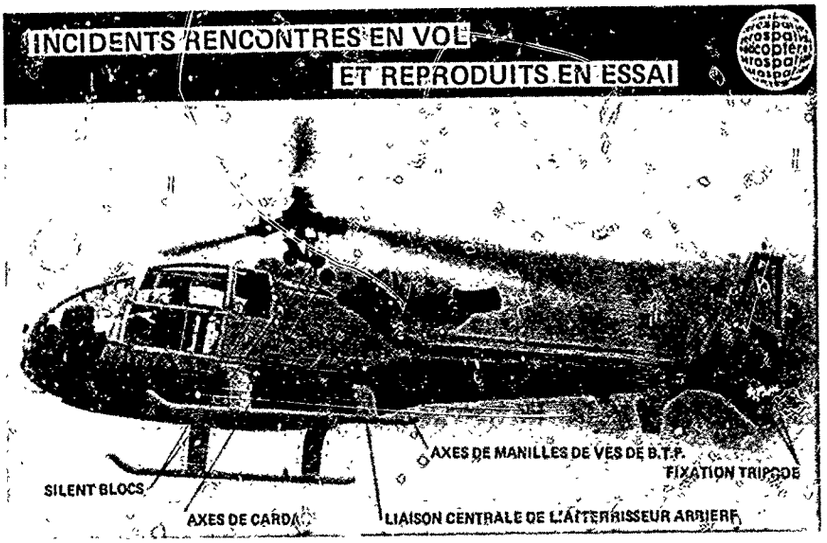
A1 : Les endommagements déjà rencontrés en exploitation et reproduits en essai.

A2 : Les endommagements apparus en exploitation après la fin de l'essai.

A3 : Les endommagements susceptibles d'apparaître sur la flotte des Gazelles.

A1 - Endommagements déjà rencontrés en exploitation et reproduits en essai (voir figure 9).

1 - Les silentblocs des vis de fixation de la boîte de transmission principale. Ce sont des éléments amortisseurs de vibrations qui se dégradent progressivement en conservant malgré tout leurs caractéristiques mécaniques. En exploitation ces absorbeurs de vibrations sont soumis à une procédure de remplacement suivant état.



En essai les endommagements sont apparus sensiblement au même nombre d'heures de fonctionnement : 700 à 1000 heures en essai pour 400 à 700 heures (7cas) en vol. On a pu conserver ces silentblocs bien au-delà de l'aspect demandant la mise au rebut sans qu'il y ait de répercussion sensible du comportement dynamique de l'ensemble de la structure.

2 - Axes de manilles des Vés de BTP.

Les axes ont été grippés au même nombre d'heures qu'en exploitation ≈ 600 heures. La possibilité de grippage ayant été mise en évidence et confirmée une surveillance a été mise en place pour ce point particulier.

3 - Axes du cardan de liaison de la turbine et de la boîte de transmission principale.

Ces axes ont montré des traces de cisaillement à des temps également proches de la réalité. Dans l'essai ces axes endommagés n'ont pas été remplacés pour connaître le degré de résistance après endommagement. On n'a jamais atteint la rupture.

En exploitation ces axes ont été l'objet d'une modification qui a permis de supprimer l'endommagement.

4 - Reprise centrale de la traverse arrière d'atterrisseur. La cellule essayée a montré comme sur les appareils en exploitation une zone fragile dans la partie centrale du cadre reprenant les efforts verticaux introduits pour l'atterrisseur. Un renforcement mis en place sur les appareils en exploitation a été testé sur la cellule en essai. On a pu réaliser avec ce renforcement 28400 atterrissages dont 3550 à un niveau supérieur au maxi possible sans endommagement.

5 - Dans la structure de la veine du fenestron, sous les pieds du tripode, des criques sont apparues à 14000 heures de vol simulé. C'est le seul point où l'endommagement n'est pas apparu à un nombre d'heures de vol correspondant à la réalité, l'absence de l'environnement dynamique du rotor arrière en étant la cause la plus probable. Sur les appareils en exploitation, une modification a été appliquée pour renforcer cette zone fragile. Cependant, l'endommagement constaté en essai n'a pas évolué de façon catastrophique entre 1400 et 2000 heures de vol simulées. Cette constatation montre l'aspect fail safe de cette partie de la structure.

A2 - Endommagements découverts en essai et constatés plus tard en exploitation. (voir figure 10).



Figure 10

1 - Cloison arrière du réservoir de carburant. Plusieurs criques ont été découvertes après 7135 heures de vol simulées. Leur développement sans renforcement ni arrêt de criques a été pratiquement nul. Cet endommagement est lié au chargement élevé introduit par la fixation de l'atterrisseur arrière sur la cloison.

Un cas en exploitation a été détecté après 2000 heures de vol.

2 - Fixations supérieures des montants de verrière sur la cloison arrière de la cabine.

Des criques sur les pieds de ces fixations se sont produites en essai à 600 et 4266 heures de vol équivalentes. Elles montrent que la verrière participe à la reprise du moment de flexion qui est théoriquement repris intégralement par les poutres de barque. Volontairement aucun renforcement n'a été appliqué jusqu'à la réalisation des 20000 heures.

Pour les appareils en exploitations une solution de réparation est appliquée dès la constatation de l'endommagement.

3 - Sur la cloison arrière de la cabine au niveau des fixations des pieds du Vé avant de la Boîte de Transmission principale les montants de la cloison sont criqués à 12685 et 19310 heures de vol équivalentes. Il n'y a pas eu de réparation en essai et les criques découvertes ne se sont pas développées.

Un cas d'endommagement similaire a été constaté sur un appareil après 1423 heures de vol. Une réparation a été appliquée qui pourra être reconduite le cas échéant sur d'autres appareils.

A3 - Endommagements jamais observés en exploitation mais susceptibles d'être détectés ultérieurement (voir figure 11).



Figure 11

Les incidents les plus probables sont :

1 - Encastrement du cadre incliné de la verrière sur la barque de l'appareil. Une crique a été constatée en essai à 6965 heures. Elle n'a pas eu d'évolution jusqu'à la fin de l'essai.

2 - Liaison entre la cloison arrière de la cabine et la barque de l'appareil.

Cette zone est très chargée et il semble que la crique constatée en essai se développe en même temps dans le gousset renfort et le revêtement de la barque.

Sur le côté droit un début de crique a été décelé à 1800 h.
Sur le côté gauche, la crique a été décelée à 5593 h.

On a laissé les criques se développer jusqu'à la rupture de chaque gousset. La vitesse la plus rapide de propagation était de 2 mm pour 100 heures. La périodicité des contrôles est suffisament serrée pour que l'endommagement soit décelé avant qu'il soit trop important. Le nouveau gousset qui a été placé sur le côté droit a subi 15000heures de vol sans être endommagé.

3 - Liaison du revêtement de la barque au cadre sous le siège pilote côtés droit et gauche.

Dans cette zone le revêtement a été cloqué puis s'est criqué en dépliage. Les criques ne se sont plus développées après avoir atteint le renfort de structure prévu à l'origine.

4 - Cornière de liaison du couloir des commandes de vol avec le plancher cabine.

Plusieurs criques se sont développées à partir de 1900 heures. Aucun arrêt de crique ni renforcement n'a été appliqué jusqu'à la fin de l'essai.

5 - Montant du cadre arrière de la cabine, sur le côté droit, au niveau de la jonction avec la barque.

Une cornière de ce montant s'est criquée au niveau d'un rivet à 9300 heures. L'endommagement paraissant inquiétant, un équipement extensométrique a été mis en place sur la nouvelle cornière mais les contraintes mesurées n'ont pas fait déceler un chargement anormalement élevé. La nouvelle cornière n'ayant pas été endommagée en 11000 heures de vol l'endommagement a été considéré comme un cas d'espèce et la fréquence de contrôle de cette zone est restée la même que celle de l'ensemble structure.

B - Endommagements mineurs

Ces endommagements ont un caractère aléatoire comparable à la dispersion de qualité dans une fabrication. Ils ne sont pas considérés représentatifs de l'ensemble de la flotte des Gazelles.

Les origines de ces endommagements sont multiples :

a) Mauvaise découpe d'un contour créant une concentration de contrainte dans une zone chargée modérément.

b) Arrêt insuffisament dégressif d'un raidisseur sur une âme relativement souple.

c) Mise en contrainte provoquée par le serrage de deux éléments rigides dont les faces d'appui ne sont pas parfaitement planes.

Tous ces endommagements sont apparus relativement rapidement au cours de l'essai (moins de 7000 heures) et ne se sont pas développés par la suite, les concentrations de contraintes ayant disparu.

Aucune action particulière n'a été entreprise pour surveiller ces points, les visites périodiques de la structure étant jugées suffisantes. Par contre, une action de sensibilisation sur ces incidents au niveau de la conception (dessin) et de la fabrication peut permettre de réduire de tels défauts sur les études et réalisations nouvelles.

A ce jour aucun de ces incidents mineurs n'a été enregistré sur toute la flotte des Gazelles.

CONCLUSION

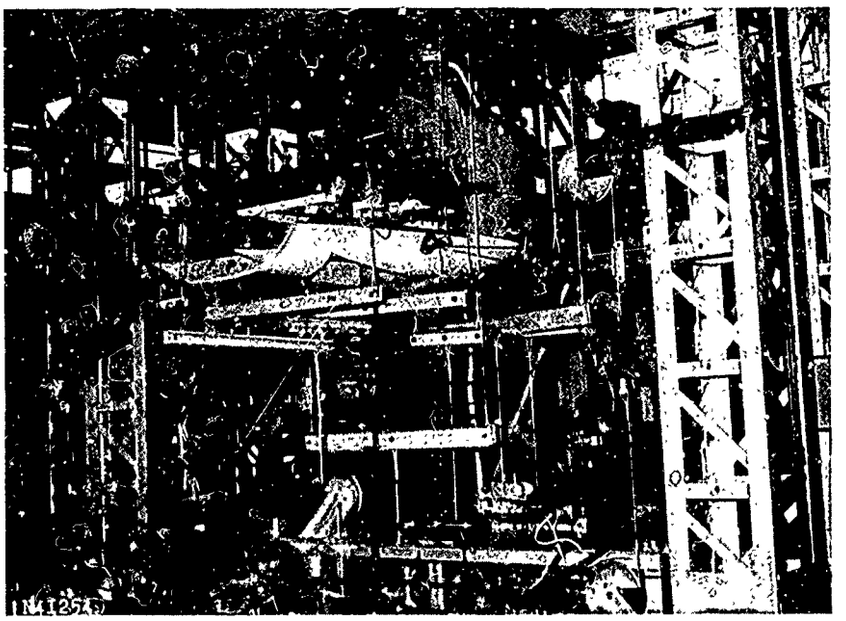
L'essai d'endurance a montré une bonne tenue générale de la structure de la Gazelle lorsqu'elle est soumise aux charges de vol et d'atterrissage définies par le spectre ALAT, spectre qui couvre l'ensemble des utilisations civiles et militaires à l'exception du travail à l'élingue. La souplesse et la précision des moyens d'essais ont permis d'obtenir des conditions très proches de la réalité.

L'essai a reproduit les incidents déjà rencontrés en exploitation, il a fait apparaître d'autres endommagements, susceptibles d'être rencontrés ultérieurement en service. Trois cas d'incidents sur appareils rencontrés précédemment en essai ont été enregistrés.

Les informations fournies dans l'essai ont aidé à la prise de décision sur les réparations à appliquer et à la définition des périodicités des contrôles.

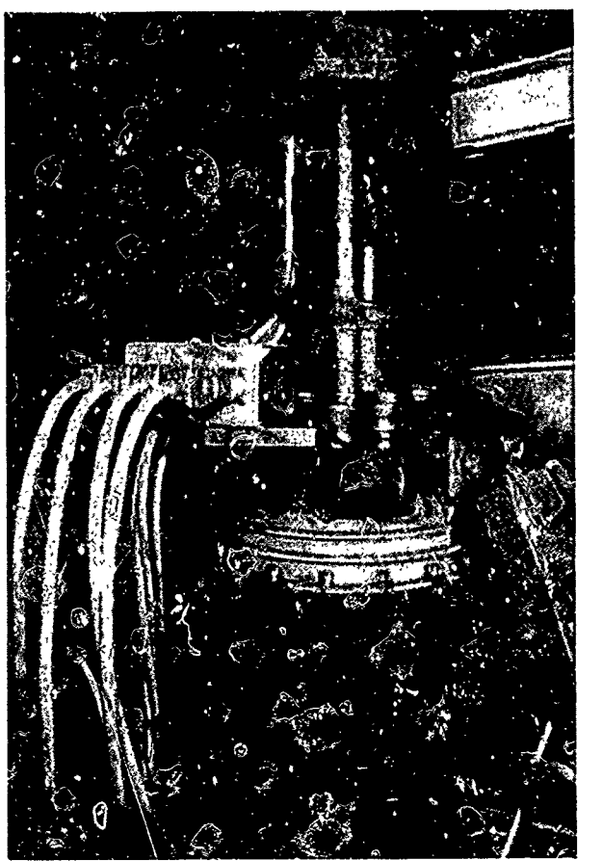
Aucun des endommagements mis en évidence n'a présenté un aspect catastrophique.

Il apparaît que, du fait des possibilités offertes par les moyens mis en oeuvre, ce type d'essai est parfaitement adopté pour les appareils de petit et de moyen tonnage, et apporte une grande quantité d'informations exploitables directement pour les appareils.



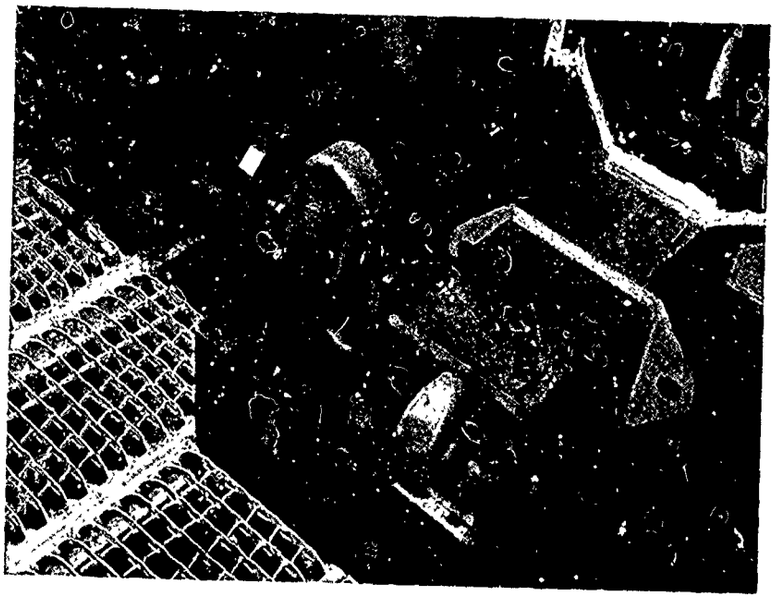
VUE D'ENSEMBLE DE L'INSTALLATION

PLANCHE 1



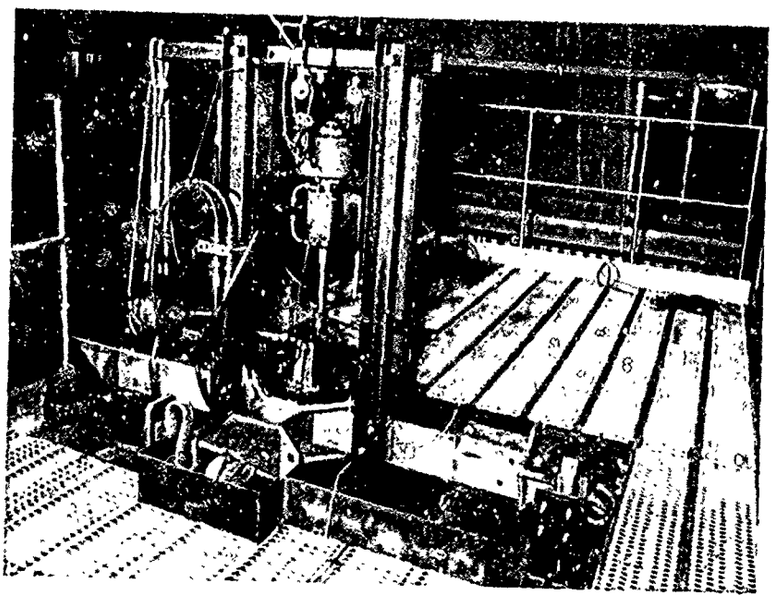
DETAIL DE LA FIXATION DE LA CELLULE
FAUX MAT ROTOR

PLANCHE 2



DETAIL DE LA SUSPENSION DE LA STRUCTURE
SUR LE BATI

PLANCHE 3

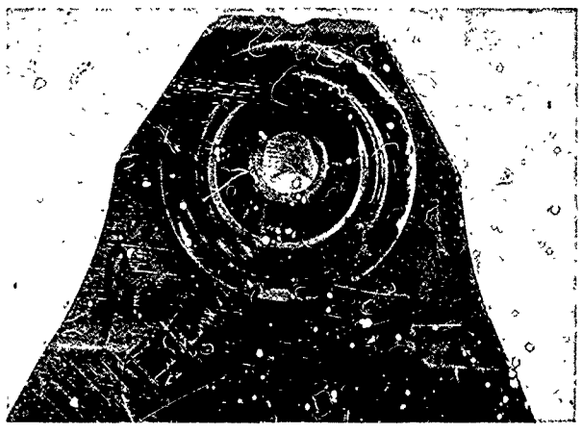


VERINS D'EXCITATION VIBRATOIRE

PLANCHE 4

SPECTRE DE VOL

	CYCLE configuration	centrage AR A ¼ heure Variante	temps	B ¼ heure Variante	temps	centrage AV C ¼ heure Variante	temps	D ¼ heure Variante	temps
1	Stationnaire HES		30		30		30		30
2	Montée à W maxi	Verticale	10	oblique	10	Verticale	10	oblique	10
3	Vol arrière Vi maxi		20		20		20		20
4	Départ vol avant/vol arrière		10		10		10		10
5	VI transition		30		30		30		30
6	Virage à Vi transition (1,5 g)		7		7		7		7
7	180 Km/h		95		95		95		95
8	virage à 180 Km/h (1,75g)		7		7		7		7
9	235 Km/h		110		110		110		110
10	Dérapage à 235 Km/h (J10)	à droite	9	à gauche	9	à droite	9	à gauche	9
11	Virage à 235 Km/h (1,75 g)		7		7		7		7
12	247 Km/h		100		100		100		100
13	Virage à 247 Km/h (1,5g)		7		7		7		7
14	Dérapage à 247 Km/h (J5)	à droite	9	à gauche	9	à droite	9	à gauche	9
15	VNE		55		55		55		55
16	Virage à 247 Km/h (1,75g)		7		7		7		7
17	Dérapage 247 Km/h (J5)	à gauche	9	à droite	9	à gauche	9	à droite	9
18	235 Km/h		110		110		110		110
19	Virage à 235 Km/h (2g)		7		7		7		7
20	Dérapage à 235 Km/h (J10)	à gauche	9	à droite	9	à gauche	9	à droite	9
21	180 Km/h		90		90		90		90
22	Virage à 180 Km/h (2g)		7		7		7		7
23	Dérage 180 Km/h (J10)	à gauche	9	à droite	9	à gauche	9	à droite	9
24	Vi transition		30		30		30		30
25	Virage à VI transition (1,5g)		7		7		7		7
26	Approche		30		30		30		30
27	Arrêt de virage stationnaire	à droite	7	à gauche	7	à droite	7	à gauche	7
28	Vol latéral	à droite	30	à gauche	30	à droite	30	à gauche	30
29	Flare		9		9		9		9
30	Stationnaire DES		30		30		30		30
31	Atterrissage		3		3		3		3



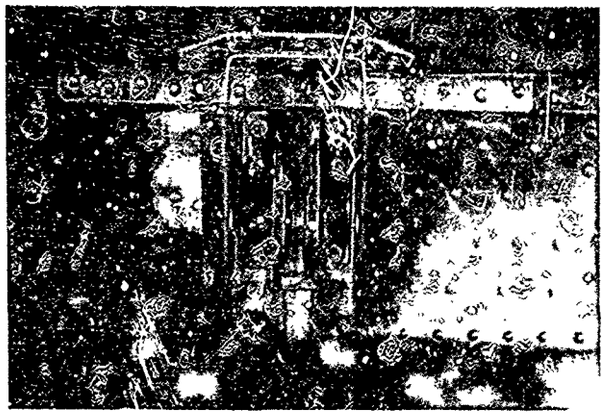
ENDOMMAGEMENT A1

SILENT BLOC DE VE DE BTP









REPRISE CENTRALE DE LA

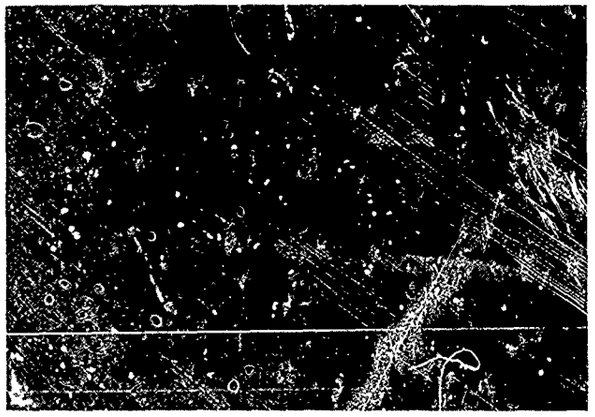
TRAVERSE ARRIERE D'ATTERRISSEUR

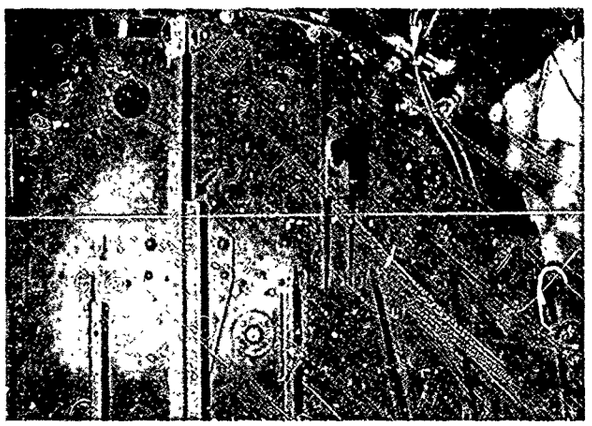
ENDOMMAGEMENT A1



VEINE FENESTRON

ENDOMMAGEMENT A1



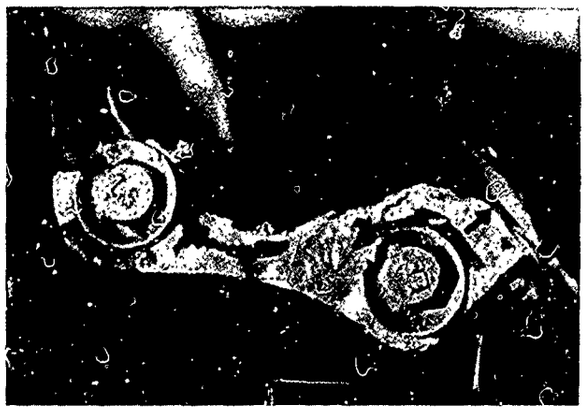




CLOISON ARRIERE CABINE

INCIDENT A2





FIXATION SUPERIEURE DES MONTANTS DE VERRIERE

INCIDENT A 2



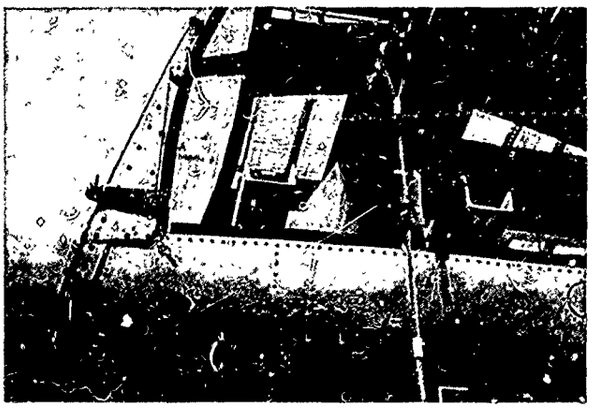
LIAISON ENTRE LA CLOISON ARRIERE

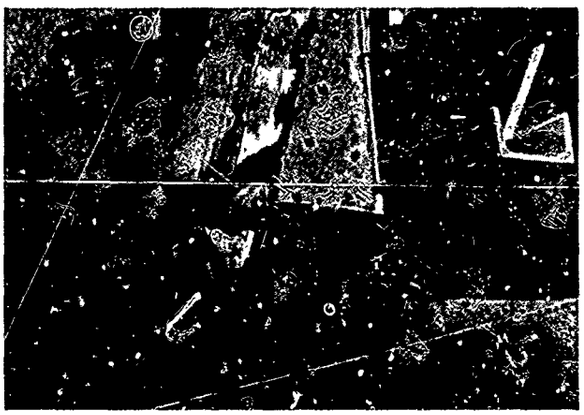
DE LA CABINE ET LA BARQUE

INCIDENT A 3



REPARATION.....



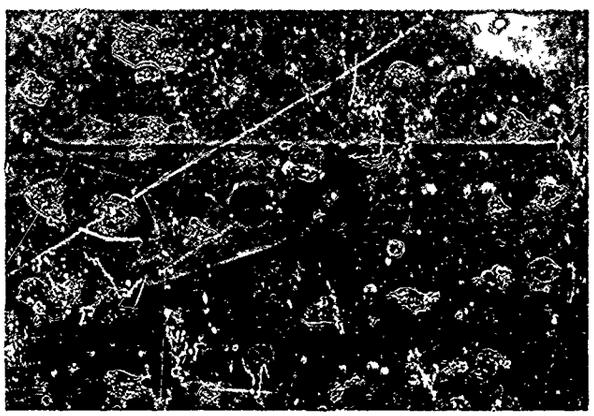


ENCASTREMENT DU CADRE INCLINE
DE VERRIERE

INCIDENT A 3

LIAISON ENTRE LE REVETEMENT
DE BARQUE ET LA POUTRE SOUS
SIEGE PILOTE

INCIDENT A 3



Helicopter Gearbox Testing

by

Robert Zincone
Vice President - Engineering
and
Joseph H. Mancini
Chief, Transmission Systems Design and Development

SIKORSKY AIRCRAFT
North Main Street
Stratford, Ct 06602, USA

SUMMARY

Helicopter gearboxes have benefited from improved materials and from new design concepts. However, in the design arena, exhaustive testing to verify that we achieve reliability, maintainability, and safety objectives remains the key to a successful product. Overstress testing and the methods used to design the gearboxes to meet these overstress test requirements are the key issues. A gearbox designed for mission reliability will most likely have an unacceptably high risk of not passing an accelerated test. This paper discusses the types of tests Sikorsky uses to qualify new gearboxes to provide reliability in the field. It also discusses the test approaches taken and the differences in acceptance criteria used by the various certifying agencies, the ramifications of overstress testing, and the reliability assessment used in the design of a modern helicopter gearbox.

INTRODUCTION

Each of the various certifying agencies for helicopters has its own unique test requirements and test criteria for helicopter transmission qualification. In the process of developing a helicopter transmission system, the manufacturer must incorporate these requisite test elements into his own overall test plan to satisfy both in-house and certifying agency needs. The ability to interpret the results of a variety of tests and to substantiate the safety and cost attributes of the transmission system becomes a difficult but essential task. These test requirements range in load severity from normal operating conditions to 140% overload. In many instances, the criteria for passing the qualification test is not clearly defined for such items as bearing spalls, gear scoring, scuffing, wear, fretting, and other transmission associated phenomena which are largely a matter of degree. No standardized acceptance or rejection criteria exists for these conditions in current specifications. Yet, one must pass the test successfully to get approval from the responsible approving agency to permit sale of the product. Without standardized acceptance or rejection criteria for these degraded conditions, the risk is imposed on the manufacturer that test results will be arbitrarily evaluated late in the test program. This risk is unnecessary because the mechanics of overstress testing are understood as they relate to post-test gearbox condition.

Almost all qualification testing can be classified as accelerated testing because either loads exceeding those experienced in service, or a spectrum of loads favoring high flight load conditions, are imposed during the test program. Accelerated testing at loads above those experienced in service offers a quick method for uncovering and resolving potential transmission failure modes early in a program. However, certain characteristics associated with accelerated testing must be understood in order to take full advantage of this test technique. Loads above design levels often create stresses that are not linear with load. Increased deflections from these overloads create load-shifts that generally accelerate stresses on critical gear and bearing contact surfaces. We can relate the effects of the overload to normal operating conditions once we understand the mechanism of failure associated with these overload conditions.

Consideration must also be given to the relationship between design, safety, and operational reliability requirements and the probability requirements associated with passing an overload test. Once these unique characteristics are fully appreciated and understood, overstress testing can be used as a highly useful tool for transmission system development. By considering the requirement to pass the qualification test as part of the design criteria, the probability of passing this test can be increased to acceptable risk levels. This increase in reliability can often be achieved with minor weight penalties. For example, on the Sikorsky S-76 Helicopter gearbox, we added only 8 pounds out of 639 pounds to achieve a 95% probability of passing the 140% British (CAA) qualification test, whereas the probability of passing the test prior to the addition of 8 pounds was 75%.

QUALIFICATION TESTING

The type of qualification testing required for a helicopter transmission depends upon which agency has cognizance over the certification for flight; and the manufacturer's concerns for safety, cost of operation, and cost of production.

The U. S. Army, U. S. Navy, FAA, CAA, and the helicopter industry all have different test requirements ranging from extreme overstress conditions to testing that only accelerates the mission spectrum slightly. Tiedown testing, illustrated in Figure 1, which is required for substantiation by the U. S. Army and the FAA, is the test that imposes the least severity on the transmission system. This is because the engines powering the tiedown helicopter are the engines used on the flight aircraft and they are not capable of generating more than their maximum output power. Since gears and shafts for the transmission system are designed for unlimited life at these conditions, this test is not a severe environment for them. However, the prorated bearing load in the FAA tiedown test is higher than the prorated load for the mission spectrum shown in Figure 2, resulting in a bearing life reduction factor greater than three for the Sikorsky S-76 Helicopter shown in Figure 3. Consequently, we must consider the effect of the test life reduction factor during the design phase to preclude premature bearing failure.

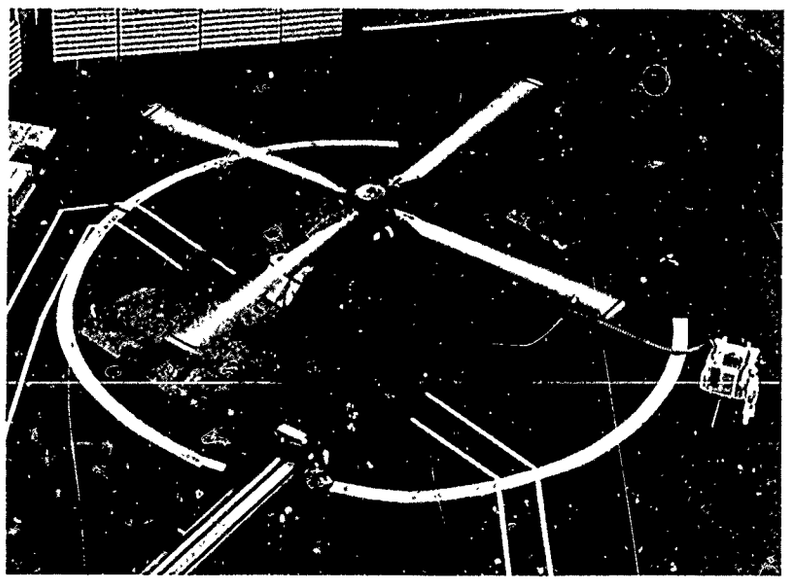


Figure 1. BLACK HAWK Tiedown Test

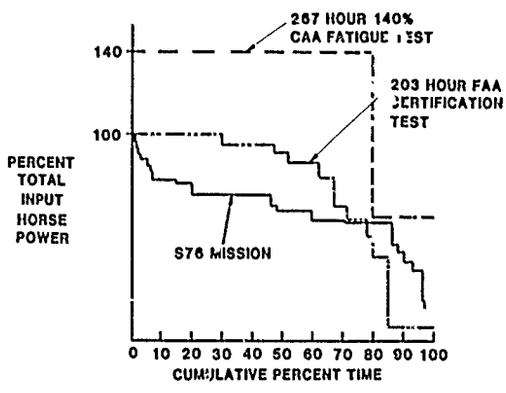


Figure 2. Horsepower Histogram for the S-76 Helicopter

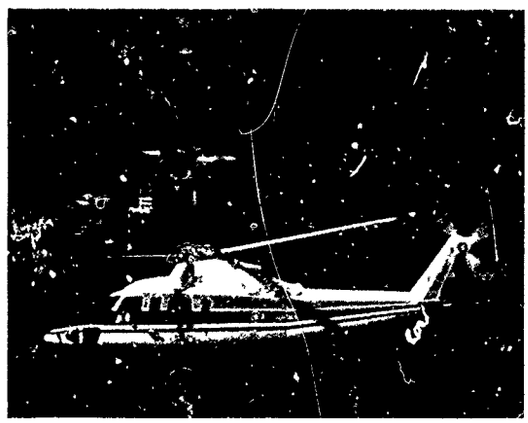


Figure 3. Spirit$_{TM}$

Figure 2 also shows that the CAA test requirement is 140% of input power for 10 million cycles. This test specifies the highest load conditions required by the various certifying agencies and is conducted for a total time equivalent to 10 million cycles on the slowest operating component. The CH-53E Super-Stallion Helicopter transmission was substantiated for Navy requirements set forth in Specification AS-3694, which calls for 120% of maximum input power for 15 hours of a 150 hour qualification test. Figure 4 shows the CH-53E test requirements versus mission requirements. Figure 5 shows the severe 200-hour overstress test conducted on the Army BLACK HAWK transmission system

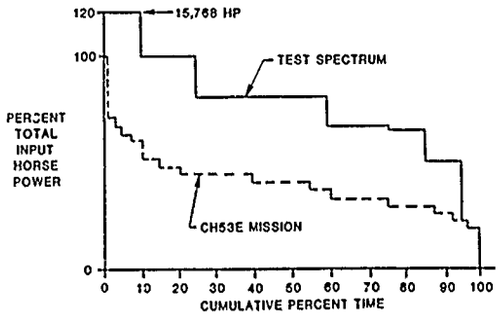


Figure 4. Horsepower Histogram for the CH-53E Helicopter

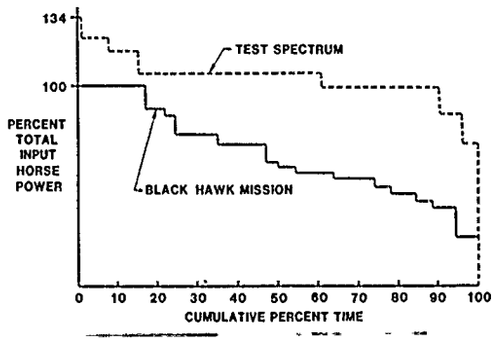


Figure 5. Horsepower Histogram for the BLACK HAWK Helicopter

The CAA, U.S. Army and U.S. Navy tests are all conducted in transmission regenerative or power-absorption test stands, which have the capability of applying the correct power-torque-speed relationships to duplicate and accelerate actual aircraft operating conditions. A typical transmission regenerative test stand is shown in Figure 6.

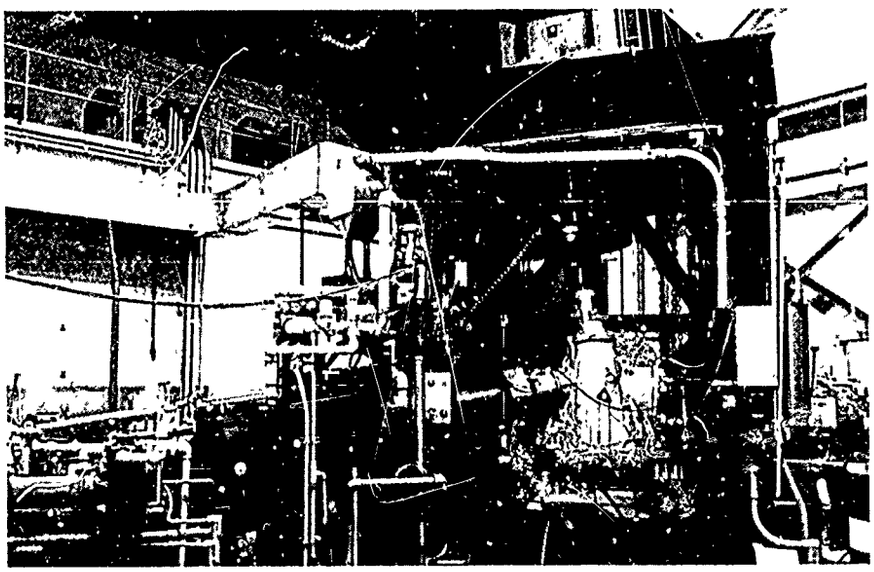


Figure 6. CH-53 Regenerative Transmission Test Stand

Sikorsky performs two basic types of tests to qualify helicopter gearboxes for production: bench tests and integrated systems tests. These are illustrated in Figure 7. Bench tests include component fatigue tests, no-load lubrication tests to confirm lubrication through full pitch and roll axes excursions, gear pattern development tests, overstress tests, and qualification tests. Systems tests include aircraft tiedown tests and flight tests. Systems tests monitor the performance of the transmission system as it interacts with the other aircraft systems. The most important aspect of the tiedown test is that it minimizes the risks associated with preproduction flight tests. Continued follow-up and evaluation of gearbox service history completes the feedback loop that relates design, test, and field performance.

QUALIFICATION REQUIREMENTS

Completion of a qualification test without apparent difficulty does not in itself qualify a gearbox. Careful disassembly, visual, dimensional, and non-destructive inspections (NDI) must also demonstrate successful results. A critical review then compares the results of the test and the inspections with the test criteria and with the loads the gearbox will experience in service.

Any severe degradation in gearbox condition is reason to withhold qualification, for example, a fatigue crack, heavy fretting of fatigue loaded components, or major wear of component mating surfaces. The intent of these inspections is to determine any non-detectable modes of failure that were generated during the tests. Cracked gear shafts, cracked teeth, or worn bearing rolling element retainers (cages) are examples of non-detectable failure modes. The criteria for bearing acceptance at the completion of testing depends upon the certifying agency. The U. S. Navy will not consider any gearbox qualified that spalls a bearing during the qualification test. Such a disqualifying spalled bearing is shown in Figure 8.

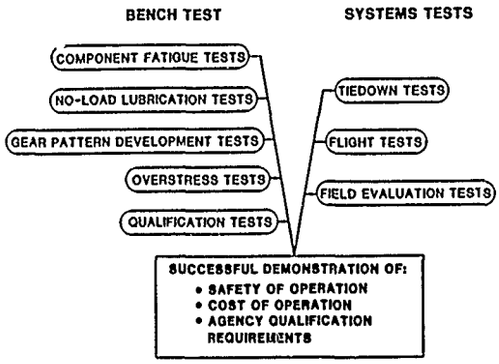


Figure 7. Helicopter Gearbox Tests

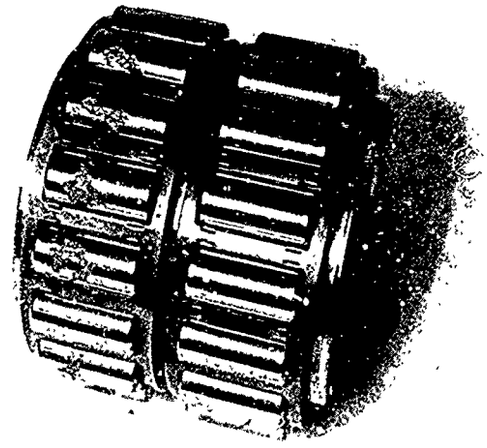


Figure 8. Typical Bearing Spalling Fatigue

The CAA, however, does not consider a spalled bearing as cause for rejection. This philosophy is based on the understanding that the condition of the bearing is monitored by chip detectors and does not represent a threat to flight safety. The same reasoning can be applied to the pitting and scoring of gear teeth, and if these conditions occur during qualification testing, the implication of unacceptably low durability in service must be evaluated. The test prorate power versus operational prorate power, maximum power compared with gearbox rated power, gearbox test temperature, lubricant used, and time between overhaul (TBO), are dominant considerations used to evaluate service durability. Table I illustrates some of the qualification test acceptance factors used by the various certifying agencies. The question marks indicate those conditions that may or may not be acceptable depending upon their relative severity at the end of the test.

Table 1. Qualification Test Acceptance Factors

	QUAL TEST ACCEPTANCE FACTORS					
	SPALLED BEARING	SCORED GEAR TEETH	BROKEN GEAR TEETH	FRETTING BETWEEN SURFACES		FRACTURES
				LIGHT	HEAVY	
FAA	?	?	NO	YES	NO	NO
CAA*	YES	YES	NO	YES	YES	NO
U.S. NAVY	NO	NO	NO	YES	NO	NO
U.S. ARMY	NO	?	NO	YES	NO	NO
[illegible]	?	?	NO	YES	NO	NO

*NOTE: CAA test is essentially a gear fatigue test and other parameters are of secondary importance.

GEARBOX STRUCTURAL INTEGRITY

Helicopters built by Sikorsky have compiled an impressive record with regard to the lack of major problems associated with their transmission systems. Figure 9 shows the increase in mean time between removals (MTBR) for main gearboxes from a helicopter where the gearbox malfunction caused damage to the aircraft.

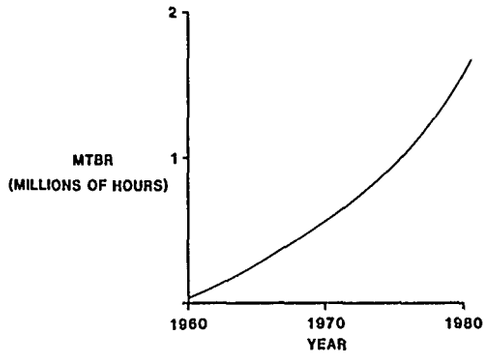


Figure 9. Mean Time Between Removal Associated with Forced Landings from Main Gearbox Causes

Improvements in analytical design methods, use of improved materials, application of advanced test techniques, and expanded field service follow-up contribute to the increase in this gearbox MTBR.

Gearbox structural reliability expected in service can be estimated with a high degree of confidence because the fatigue properties of primary gearbox components are understood. For example, if the component or system successfully completes its test at a stress level 40% above the normal usage level, a reliability associated with three standard deviations has been demonstrated for this one sample. This can be shown as follows:

$$\frac{\text{Test Load Level}}{\text{Usage Level}} = \frac{1}{1 - 3\nu}$$

where 3 represents the number of standard deviations from the sample mean associated with an acceptable survival probability and ν is the statistical coefficient of variation. This coefficient for aircraft steel components is usually between 9 and 10%. Substituting a value of 9.5% in the above equation gives

$$\frac{\text{Test Load Level}}{\text{Usage Level}} = \frac{1}{1 - 3\ (.095)} = 1.40$$

Thus, if we successfully conduct a test at 1.40 times the maximum expected service load, we demonstrate a structural reliability representative of three standard deviations. However, passing a highly accelerated test should not be construed as a demonstration of suitable long term wear out characteristics. We can only demonstrate this characteristic after a fleet of aircraft operate in the field for several thousand hours under mission conditions. A single accelerated test in a transmission test stand proves the structural integrity of the gearbox from the standpoint of flight safety but is not conclusive enough from a long term reliability standpoint. There are several reasons for this. First, the sample size is too small for the test components to be truly representative of future production quantities. Second, the extreme acceleration factors make it difficult to extrapolate data from the limited number of test hours to establish time dependent or wear associated failure modes. And third, the environment in a test stand does not duplicate the aircraft environment in all respects. This is especially true for vibrations induced into the gearboxes from the aircraft rotor head, ground-air-ground cycles, hot oil effects, and creep of castings.

An analytical method for estimating reliability is the distribution - interference technique. If the strength distribution of a component is known, or assumed, and the loads are expressed by a distribution which can be adequately described by a mean value and a standard deviation, the probability of passing a given test, or the reliability of a design with respect to a given usage spectrum can be determined using probabilistic analysis. Figure 10 shows the distributions of stress and strength for a typical component. It can be seen from Figure 10 that the probability of failure increases in overstress testing unless the strength of the component is correspondingly increased.

By subtracting the stress distribution from the strength distribution according to probabilistic theory, a third distribution results which represents the component or system structural margin. This is illustrated in Figure 11. The area under this distribution from zero to infinity represents the probability of passing a given test or the probability of surviving the given usage spectrum. Sikorsky's approach is to have a 95% probability of passing such tests.

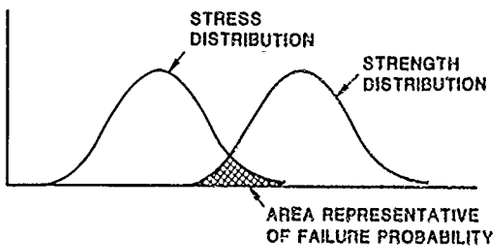


Figure 10. Component Stress and Strength Distributions

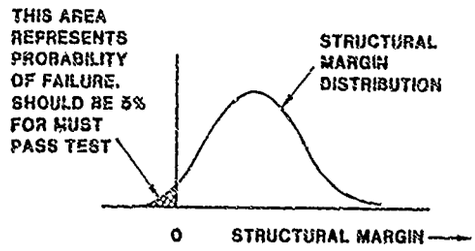


Figure 11. Margin of Safety Distribution

ACCELERATED TESTING

Accelerated testing at loads greater than those experienced in normal flight has long been used in the aerospace industry during aircraft development programs. The major advantage of accelerated testing is the reduced cost associated with the reduced test time required to substantiate the component being tested. At loads high enough to produce fractures, accelerated testing exposes the gearbox modes of failure and enables us to implement required corrective actions. This technique allows us to remove the weak links from the system and helps develop a higher-strength assembly in a relatively short period of time. Shafts and gears in a helicopter gearbox are classical examples of parts subjected to bending fatigue. Accelerated testing also substantiates these critical components for their classical fatigue modes of failure.

We use accelerated testing as a basic tool to gain confidence in a new helicopter transmission design during its early development stages. If the results of overstress and endurance testing are to be fully appreciated, it is necessary that quality controls make certain that production flight hardware is equal in quality and strength to the items tested. Consequently, any change in manufacturer or manufacturing processes during production that involves previously qualified parts requires requalification of the parts involved.

Accelerated tests can be run at a single high load level, or to a spectrum of loads that exceeds the normal usage spectrum. The relative severity of the test spectrum can be determined by reducing the spectrum to its prorated value. This prorate is a single value that is derived on the basis of equivalent life. The spectrum prorate can be calculated by:

$$P_R = \sum_i \left[P_i^a \; q_i \; (n_i/n) \right]^{\frac{1}{a}}$$

where P_i is the ith load, q_i is the percent usage at this load level, n_i is the rpm, a is the slope of the S-N curve, and n is a reference speed.

We find the prorated load for bearings by assuming that all loads are damaging to some degree. Gears and shafts, however, depend upon the specific endurance limit load of the component since loads below this value are assumed to be non-damaging. The load acceleration factor can be estimated by

$$\text{Load Acceleration} = \frac{\text{Test Prorate}}{\text{Mission Prorate}}$$

Another factor considered in component design and in the preparation of a fatigue test spectrum is the fluctuation of loads, or stresses, between the peak value and the minimum value that occur during the course of a flight. These stress cycles often occur at very low frequencies (as low as one cycle per flight) and are superimposed on the high frequency cycles. We commonly refer to these as GAG (ground-air-ground) cycles.

All parts of an aircraft that are repeatedly stressed and unstressed are subjected to GAG cycles, and must be analyzed accordingly. This is an important consideration in overall component reliability and one that was sometimes neglected in the past. For example, aircraft used in the logging business experience torque variations of plus or minus 40% in 5 minutes, occurring 12 times an hour, and low cycle fatigue is critical.

SPECIAL CONSIDERATIONS FOR ACCELERATED TESTING

Gear performance is affected by accelerated testing in more subtle ways than by their exposure to an increase in stress. High power transmission spur gears, for example, have the drive side tooth profile modified from a pure involute form to account for tooth deflections, and to provide smooth transition of load as the teeth enter mesh and leave mesh. This profile modification reduces tooth accelerations to a minimum, resulting in lower dynamic loads, lower stresses, and reduced vibration and noise. Since tooth profile relief is exact only for one load, overstress testing of these teeth will

reintroduce discontinuities in the load curve and result in increased stress, vibration, and noise.

Spur gears are sometimes ground with helix correction across the face of the tooth to allow for relative deflections between mating gears at the design load. This helix correction, like profile modification, is based on the design power and assures that load will be uniformly distributed across the face. Operation at loads in excess of the design loads can result in a maldistribution of load across the tooth face. Straight spur gears are very sensitive to end loading, and overstressing can lead to scoring, wear, and even tooth breakage. This situation is even more damaging on high contact ratio designs, which because of their inherent weaker individual tooth form, are more sensitive to overstressing than standard contact ratio gears.

Sikorsky uses experimental stress techniques as an integral part of the design/test philosophy to support our gearbox design effort. Figure 12 shows a section of a large high power spur gear with strain gages mounted on the tooth back-up rim. This test helped determine the distribution of the non-uniform load across the face width of the gear teeth, and helped provide the requisite lead correction to balance the load distribution.

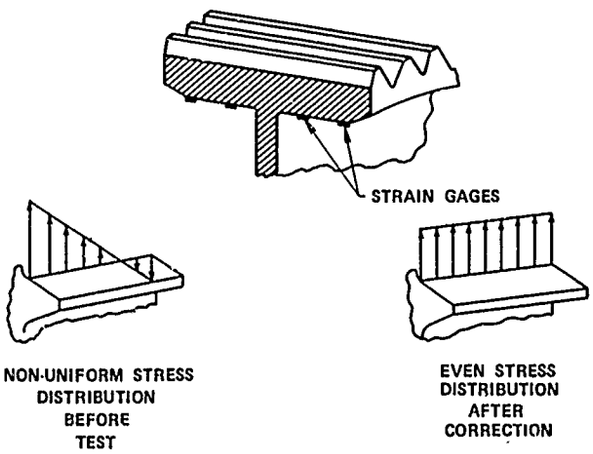


Figure 12. Experimental Stress Techniques Support Design

Spiral bevel gears are also sensitive to running for extended periods of time at loads in excess of design loads. Excessive tooth deflection and shaft misalignment caused by the higher loads drastically alter the tooth contact patterns of spiral bevel gears. Experience shows that most spiral bevel gear tooth failures can be traced to poor full-load contact patterns.

The British CAA recognizes the fact that overstress testing shifts gear patterns and allows the prospective qualifier to increase the profile modifications or lead corrections of the gear teeth to the point where the stress distribution is proportioned to the load distribution. This is an overstress test that qualifies the component for fatigue in normal operation. It does not predict the structural integrity of the part for momentary overloads. The British also permit other gearbox modifications to be used during overstress testing. such as the use of heavy weight oil, reinforcement of critical housing areas to reduce deflections and gear profile or helix modification. All of these reduce the non-linearity of stress with load to a more linear situation.

Another consequence of accelerated testing is the possibility of fretting between bolted connections on dynamic components. Figure 13, (Reference 1) shows how a stress/slip condition in a bolted connection can lay within various regions of operation depending on the vibratory stress and the relative motion between the parts. In region I, no failures occur. In region II, the surfaces of the bolted parts will be crazed with millions of microscopic cracks that will not propagate in service. Most of the bolted connections used in helicopter transmissions probably fall into these two regions. In region III, one of the microscopic cracks will eventually propagate to failure. It can be seen from this figure how a significant increase in load can shift the operating point from region II to region III of the curve by inducing higher stresses and by increasing relative motion.

Antifriction bearings are used on all shafts of the typical helicopter gearbox. Bearings are one of the few transmission components which are designed for a finite or predicted life. Design life is based on the industry accepted Lundberg-Palmgren theory for ball and roller bearings, which considers the Hertzian stresses at the rolling contacts and relates the magnitude and distribution of the stresses to a calculated life. In recent years, life adjustment factors have been used to account for improvements in bearing materials, elastohydrodynamic (EHD) lubrication, and the effect of misalignment or deflection.

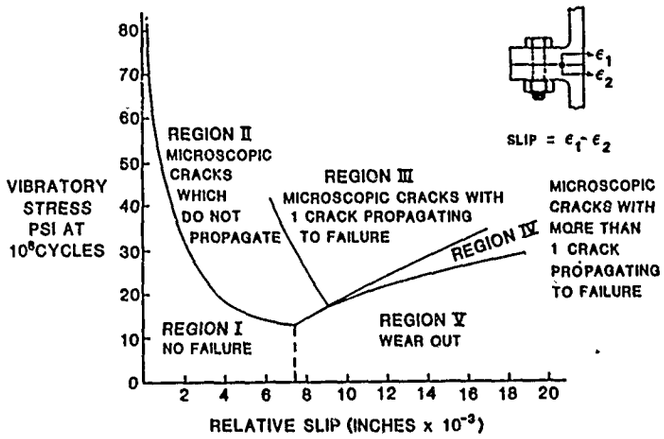


Figure 13. Stress versus Slip Fretting Curve

Figure 14 illustrates the life reduction factors that result from accelerated testing of a typical helicopter roller bearing considering the effects of load, misalignment, and lubrication film thickness. Examination of Figure 14 shows that load is the predominant influence on bearing life during accelerated testing. However, all factors contribute to bearing failures during overstress tests.

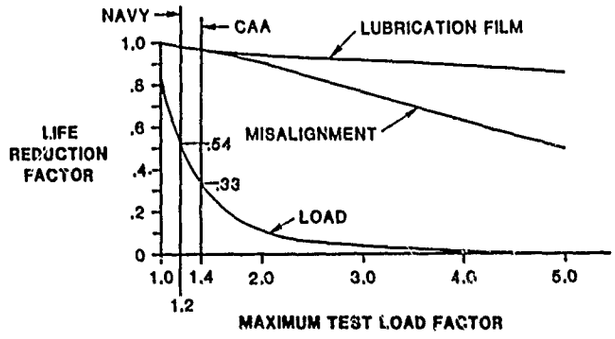


Figure 14. Bearing Life Reduction due to Accelerated Testing

With high test load factors, the reduction in life of a roller bearing due to edge loading at the roller end becomes significant and eventually exceeds the life reduction factor due to load. Designing the roller crown for the accelerated test conditions is not practical because the reliability of the bearing under normal conditions would be reduced. Another factor we must consider with accelerated testing is secondary damage caused by bearing creep that is defined as rotation of the bearing inner race with respect to the shaft. This damage is usually in the form of shaft wear or failure of retention devices. Designing for no bearing creep at accelerated test conditions would certainly result in a weight penalty.

Sikorsky designs for no creep at maximum continuous power using a combination of the two-ring press fit equation and an experimentally derived factor applied to the two-ring equation. Figure 15 shows the generalized relationship among power, assembly fit, and creep. No creep takes place below 100% power; creep is possible between 100% and 125% power, depending on the actual part dimensional tolerances; and creep probably takes place above 125% power. Less than 2% of aircraft mission time is spent above the possible creep level while 45% of the qualification test time is conducted above the possible creep level.

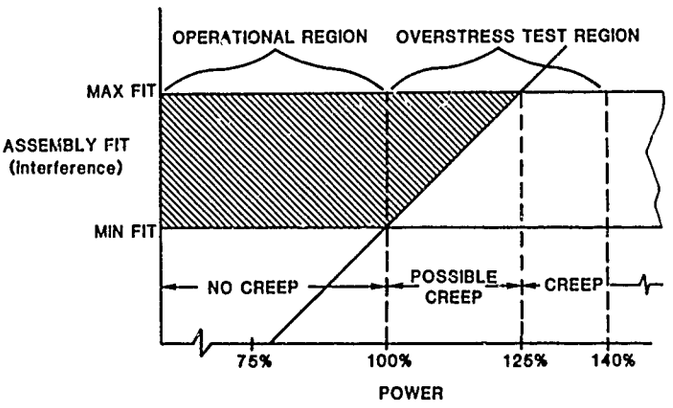


Figure 15. Relationship between Power and Bearing Race Creep

The reliability of a gearbox is directly related to the reliability of its gears and bearings. Therefore, accelerated testing will clearly influence the probability of passing a gearbox development test. Figure 16 illustrates the dramatic effects of acceleration factor on the relative reliability of gears and bearings. Figure 17 compares the probability of successfully passing an overstress test with the probability associated with test times at mission powers. When a gearbox is designed for a mission spectrum and is subsequently subjected to an overstress test, a substantial risk of not passing the test exists.

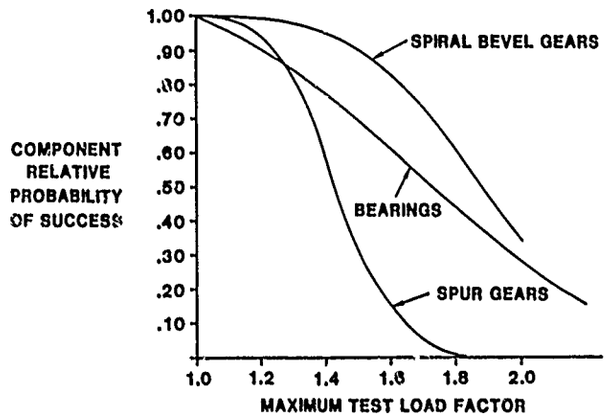


Figure 16. Maximum Test Load Factor versus Component Relative Reliability

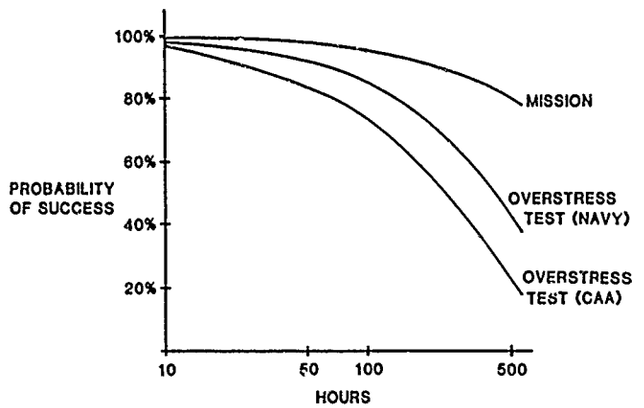


Figure 17. Probability of Success During Overstress Test

Regardless of all the ramifications of overstress testing, it still is the one most useful tool in transmission system development testing. It now remains to communicate to the procuring activities the aforementioned considerations and to evaluate test results accordingly. The Sikorsky S-76 gearbox achieved a 95% confidence level for passing the CAA 140% overstress test without a tooth fracture by adding only 8 pounds out of the total gearbox weight of 639 pounds. This small additional weight substantially reduced the gear tooth stresses during normal operation and added to the reliability of the gearbox.

For new designs, the test spectrums (whether overstress or at design level) must be considered a design condition and their effects on cost and weight must also be evaluated. The minimum acceptable probability of passing the overstress test must be determined, and this probability must then influence design.

CONCLUSIONS

1. Overstress testing is a highly useful tool in the development stages of a new helicopter transmission. Advantages are:

   - Determines potential failure modes
   - Substantiates fatigue strength
   - Provides confidence in the design
   - Accelerates redesign to eliminate "weak links" in the system

2. Tests at highly accelerated loads produce non-linear increases in stress, and action must be taken to counteract the effects of increased deflection.

   In gears:

   - Misalignments cause pattern shifts that concentrate gear tooth loads.
   - Tooth profile modifications are correct for one load condition. Higher loads create tip interference that leads to scoring and tooth breakage.
   - Lead modifications used to correct tooth misalignments are made for one load level. End loading results in concentrated stresses and leads to tooth fracture.

   In bearings:

   - Load is the predominant influence on bearing life during accelerated testing.
   - Roller crowns may not be sufficient to prevent roller end loading at overload conditions.
   - Accelerated load causes race "creep" on shafts when test loads are higher than the creep threshold
   - EHD films are reduced by overloads

3. The transmission designer must consider the overstress test spectrum as a design condition for must-pass tests.

4. The total stress versus torque versus rpm attributes of each element of the gearbox over the planned torque testing levels must be quantified and accounted for prior to the conduct of any overstress test.

5. Clear definitions of acceptance criteria must be negotiated with the certifying agency when accelerated testing is used as a qualification test.

6. The helicopter industry and the certifying agencies need to establish a helicopter gearbox test specification that includes standardized acceptance test criteria.

Reference (1) Nishioka, K, etal. "Fundamental Investigations of Fretting Fatigue", Bulletin of Japanese Society for Mechanical Engineers (JSME). Part I, Vol II, No 45, 1968, pp437-445.

FATIGUE TESTING OF HELICOPTER GEARBOXES

by
A.H. BAKER
Assistant Chief Development Engineer
Westland Helicopters Limited
Yeovil
Somerset
England
BA20 2YB

The fatigue testing of helicopter gearboxes as practised in U.K. at Westland Helicopters working to British Ministry of Defence regulations is time consuming and expensive. The testing covers not only the gears but the casings and shafts and other parts of the gearboxes. Testing with the required factors for fatigue scatter and extrapolation leads to difficulties with the tooth meshing and premature tooth surface damage requiring modified tooth profiles and high pressure lubricants. The principle test method has been on 'back to back' rigs but for the future open loop testing is planned to give greater flexibility and versatility. A comparison of service experience with test experience is of some value in assessing the merit of the test factors.

1. INTRODUCTION

The Transmission represents a very significant part of the cost and time of development of a helicopter. In the transmission the main rotor gearbox in particular is the key to a successful transmission development programme. It is often, and particularly for a new tooth form, a high risk programme since it is often difficult within the constraints of the casing to make changes should the strength be shown by test to be inadequate. It is thus most important that the testing is carried out early in the aircraft programme and that the method of test, the design of the test rig and the factors used are chosen in such a way that the service fatigue life is adequately and safely proven.

This paper is a review of the fatigue testing philosophy and test methods used by Westland Helicopters working to the requirements mostly of the Military Authorities as defined by MOD publications. Assessment for Civil Authorities has, at least in recent years, been based on a military certification programme, so only a brief reference is made to this. Since the experience of the past few years has been mostly of the Lynx gearboxes, these naturally form the main part of this paper, however valuable experience is gained from older aircraft and it is instructive to compare service experience on these with the test experience carried out at an earlier stage in our understanding of gearboxes.

In addition to fatigue testing, with which this paper is concerned, there is a whole field of work in assessing and substantiating a useful life of the gearbox from a purely functioning point of view. This is briefly touched on in this paper.

2. FATIGUE TESTING PHILOSOPHY

In the context of this paper, by testing philosophy is meant what parts of the gearbox are tested for strength, why are they tested, what are the testing loads to be applied, what is done if the gearbox is not strong enough, what is done in the event of a change of design or supplier.

The life objectives in current helicopters require fatigue lives of at least 7,000 hours. At first sight one thinks of testing gearboxes as testing to see how strong the gear train is, how strong the teeth are, at what loads will they fall off and what happens if they do. However, there is much more to a gearbox than the gear teeth and particularly for long life gearboxes it is important to consider the total structure to make sure it has been adequately tested, since the various parts of the box are significantly affected by different loading systems in the aircraft. The principal elements of the main rotor gearbox of the Lynx are shown in Figs. 1 and 2. This version shown is what is known as the 3 pinion gearbox where the loading from the two engine inputs is shared amongst three pinions in order to improve the load capability of the box. Looking at this gear layout one can see the principal elements of the loading system.

1. The main load path gear train (Fig. 1).
2. The hubs to which the gearwheels are attached (Figs. 2 & 4).
3. The accessory gears driving oil pumps, generators, hydraulic pumps, etc. (Fig. 1).
4. Miscellaneous assemblies such as freewheels (Fig. 1).
5. Casings (Fig. 2).

It is useful to look at each of these areas separately.

Main Load Path Gear Teeth

The loading on the gear teeth is clearly one of an oscillatory load from zero to the driving force once per revolution of the pinion or wheel. The usual way of representing this loading on a test is to apply torque to the gearbox in some way and to rotate this gearbox at its normal running speed until each tooth is subjected to a minimum of 5×10^6 cycles. Because of the widely varying conditions of flight it is usually required to apply a programmed torque/cycle system to allow for the short bursts of power at the top engine ratings, to cover the engine out cases (where the helicopter is powered by more than one engine) and to include the transient droop cases of low speed and high torque during engine failure, and

finally the autorotation case when the loading path inside the box can be significantly different. Fig. 3 shows the loading system of the Lynx production 3 pinion gearbox in main drive and autorotation. It can be seen from this that the lift is taken in quite a different route and it is important to consider features like this and to test accordingly.

Gear Wheel Hubs

The hubs to which the gear wheels are attached, for example the hub on the Lynx gearbox holding the main conformal ring gear (Fig. 4), are loaded in quite a different way from the gear teeth. The gear teeth have a load zero to maximum once per revolution, whereas the hub has an output torque which is proportional to the power demands and an input which is cyclic on the gear teeth but with a load diffused over a wider area. It is also subject in the case of the output shaft, to rotor moments and lifts. It is necessary to consider the hub with respect not only to the cyclic nature of the tooth loading but to the full power lift and moment spectrum which one applies to a rotor system.

Accessory Gears

Some accessory gears become important parts in that gear failure can lead to say hydraulic pump loss, and so must be considered in the substantiation of the gearbox.

Miscellaneous Assemblies

Some components are not tested adequately in the normal gearbox running test. For instance, in the case of the Lynx gearbox (Fig. 1) the load is shared between the three pinions by making use of the torsionally flexible input shafts known as quills. These quills are subjected to high torsional strains but not significantly high cyclic torque. They are therefore sensitive to the ground to air cyclic loading and need to be treated separately. Freewheel assemblies in the main load path form complicated mechanical assemblies which are subject to bending due to misalignment and are occasionally the source of fatigue failures on test.

Casings

The casing of a gearbox, particularly a main rotor gearbox, usually forms part of the structure of the aircraft, carrying the main rotor moment, lift and torque into the airframe. To reduce weight it is commonly manufactured as a lightweight complex casting, often magnesium, and is difficult to analyse theoretically although finite element analyses are nowadays of considerable assistance. It is important therefore to consider the strength testing, both static and fatigue, of the casings of the gearboxes. It is in any case a requirement of the British MOD publications to subject Class 1 castings to static tests, although fatigue testing is not a specified test for castings but is implied under a general requirement for Class 1 components.

Re-substantiation

It is sometimes necessary, having completed the total substantiation of the gearbox, to require substantiation of materials from a new source. It may be that the gears are made from a different material or are obtained from a different supplier. In this event, the current practice is to re-substantiate those gears which are renewed which, in the case of the main load path gears, means testing once again up to four sets of gears, and in the case of castings, to test more castings. It can thus be seen that a decision to resource materials for whatever reason, while perhaps not being a great risk, is expensive and time consuming and careful consideration has to be given to the need.

3. TEST FACTORS

Before describing the method of fatigue testing the various components of the gearboxes it is necessar to consider the factors which have to be applied under U.K. regulations.

For Military applications factors are defined in the Ministry of Defence document AvP 970. However, these have now been superseded and the practice has been to work to a Westland internal document which has been agreed with the appropriate military technical authorities at RAE Farnborough. For Civil applications the required factors are defined in British Civil Air Regulations. Since the basic requirement of BCAR is similar to the WHL rules, the WHL document with its more detailed statement is used.

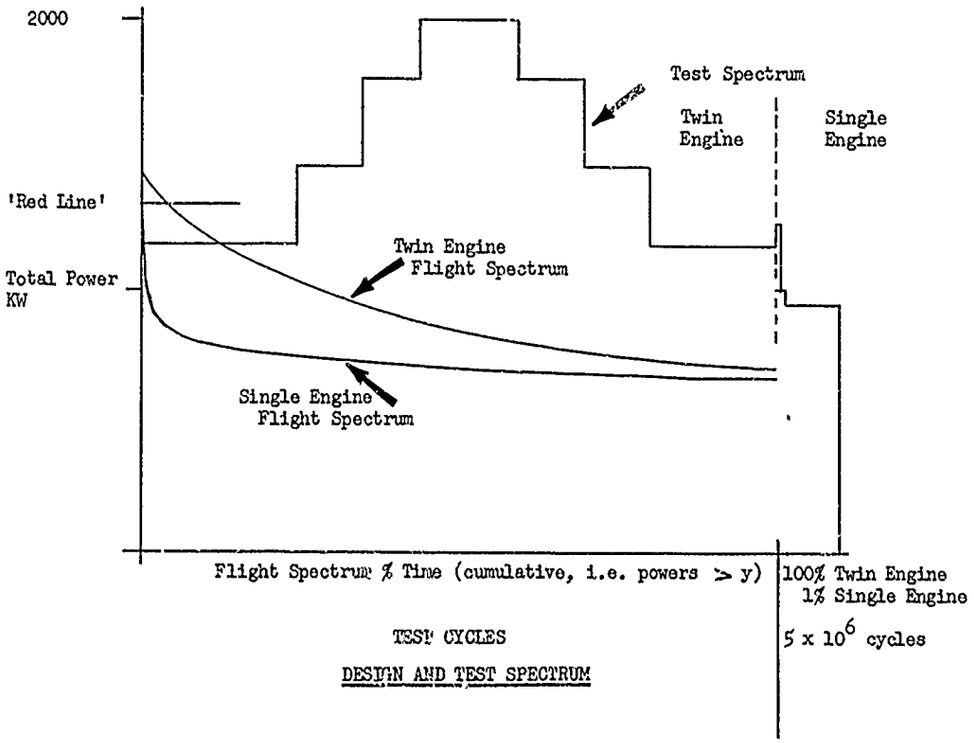
Main Gear Train

Looking first at the main gear train, the factors are:-

a)	Scatter factor	1.4 for 1 specimen 1.3 for 4 specimens
b)	Flight variability factor	1.0 for main gearbox 1.2 for tail gearboxes
c)	Extrapolation factor	1.2 from 10^6 cycles 1.1 from 5×10^6 cycles

At first sight the advantage of testing 4 specimens rather than 1 seems fairly modest, nevertheless a certain amount of prudence usually demands that four specimens are tested. Taking an average extrapolation factor, bearing in mind that a programmed load test is usually carried out and the total test time has to be a realistic one, the overall factor, for the purposes of this paper, is around 1.5. This has an important bearing on the test as the gears and lubricant are not designed for such high loads. For transient cases, such as the engine failure case, when the torque may increase by 2.4 for several seconds, it

becomes more practical to apply a life factor for scatter rather than a load factor. There is of course no need to apply an extrapolation factor and the test is conducted at the predicted in flight torque with a life factor of around 6. Similar reasoning can be applied to other high torque low occurrence conditions such as the 5 minute rating in order to reduce the factor on load. A typical design and test spectrum for the rotor gearbox might therefore be as follows:- (This relates to a typical twin engined helicopter).



DESIGN AND TEST SPECTRUM

The test spectrum is broken down on test into 20 programmes. Although the relationship between test powers and flight powers is not immediately obvious it can be seen that the factor on the 'Red Line' power (maximum continuous power) is just over 1.5 (2000/1300).

To date it has not been the practice at Westland to apply rotor moments to the main rotor gearbox in the gear test. Although service experience has not revealed any deficiencies as a result of this policy, it is likely that future tests will have unfactored moments, as well as lift, applied.

Hubs

The factors for hubs are the same as other components in the rotor system. For 4 specimens they are:-

Titanium	1.7 scatter factor 1.1 extrapolation factor from 5×10^6 cycles
Steel	1.7 scatter factor

Casings

Casings, which are usually castings, are generally designed so that high frequency loads are non-damaging. The casing test is, in the main therefore, a test under manoeuvring loads, which generally represent a small number of cycles. The factors are therefore applied to the life and are, for one specimen, 6. In addition, it is a requirement under AvP 970 rules to apply a casting factor of 1.3 to the proof and ultimate loads for a static test. Although the casing is designed such that vibrating loads are non damaging, it may happen that some of the ancillary loads can be damaging. In the case of the Lynx for instance, the main rotor servos which are subjected to rotor frequency loads, are attached directly to the casing (Fig. 5), and it has been necessary to assess the fatigue life of these attachments. The factor in this case is 2.0 plus some extrapolation factor.

4. METHOD OF TESTING

Main Load Path Gears

The major part of fatigue life assessment of gearboxes is centred on the testing of a complete gearbox rotating under factored torques.

The practice at Westland has been up to now to build special purpose rigs for each gearbox. They have all been of the same basic principle of a conventional closed mechanical loop. This is shown for the Lynx main rotor gearbox in schematic form in Fig. 6, and a photograph of the rig for the uprated 3 pinion gearbox in Fig. 7. It consists in essence of a rig in which the output shaft is connected to the input shaft

by a train of gears. A torque is then locked into this mechanical circuit after the rig has been brought up to speed and the rig rotated at normal aircraft speeds. Torque can be varied during running by rotating the outer ring of an epicyclic box in the circuit thereby increasing or reducing the torque. Torque is measured by means of strain gauge torquemeters which are capable of measuring not only the steady torque but also the vibratory torque in the rig. Vibratory torque is difficult to reduce to zero and an average level during normal running is 10%. Lift is applied to the output shaft by a hydraulic jack operating through a thrust bearing. Although the original rig was designed to apply a moment, this was subsequently not used. Instrumentation is a continuous measurement of oil temperatures and pressures, and visual monitoring of torque, although a trace record of torque is made periodically. The rig is run under continuous visual control. This method of testing is quite conventional and it is not intended to describe the rig in any more detail.

The major problem in the testing as carried out at Westland is that of testing with the high factors. The first effect of this is that the meshing of gears, in particular spiral bevels, changes considerably when the factored load is applied as compared with unfactored torque. This means that not only is the load on the tooth factored but the bending moment on the tooth is generally increased by a substantial amount leading to stresses at the likely point of failure in the root of the tooth which are excessively high. The procedure adopted to overcome this is based on the assumption that if the meshing pattern is the same then the stress distribution throughout the gears is the same, and all parts of the gear tooth will be equally affected. Fig. 8a shows a reproduction of a meshing pattern for a spiral bevel gear under 100% torque. The next figure shows the same tooth under torque factored by 1.5 which is a typical fatigue factor. Corrections are first attempted, in the case of spiral bevels, by altering the relative position of pinion and gear. If, as in Fig. 8c, this is still not completely effective then the gears may have to be reground to a modified profile. The last diagram in Fig. 8 shows the final corrected mesh and profile with a meshing pattern similar to that developed for the satisfactory running of the production box. The test is then conducted on this set of gears whose profile has been modified from the production standard and whose meshing position is different but whose meshing pattern as seen on the teeth is the same. One essential feature of this is that the meshing pattern becomes the standard which has to be met throughout production build, as it is this pattern which has the defined fatigue life. The conformal gears as used on the Lynx cannot be re-meshed by re-positioning and any changes have to be made by regrinding. This is a tedious and time consuming business but nevertheless is the only solution and has been carried out on a number of occasions.

Having achieved the desired meshing standard there still remains the problem of carrying out the tests with these higher loads. Scuffing and plucking of the teeth are much more likely and this may lead to premature failure. The usual option open is to improve the lubrication by either increasing the flow or the cooling or by using the most suitable lubricant available even though this may not be the oil used on the aircraft. This usually means using an EP oil such as OEP 220 or OEP 215. Having re-meshed the gears, reground them and used the best available lubricant, it is still necessary to conduct the tests in such a way that the gears stand a good chance of surviving without surface damage or with damage that can be contained or rectified. Experience has shown that running the test to a programmed load of ascending and descending powers (which is fundamentally to minimize the unknowns of cumulative damage) with around 30 mins. at maximum powers is more likely to lead to a successful outcome.

When conducting the test a judgement has to be made as to how often the box is looked at during the test. Magnetic plugs, temperature, vibration are all checked or measured during the test and give some guide as to what damage may be happening. There is a strong temptation to carry on with the test if all appears to be going well. However, experience has introduced some caution into the judgement and in a 100 hour test the gears are inspected perhaps four times. Inspection would consist of removing the gearbox from the rig, removing as little of the covers as possible and visually inspecting the gears. If no damage has occurred, then the cover is replaced and the gearbox put back on the rig. At the same time the bearings which are also a source of trouble at the high factors are looked at in any suspect areas and some re-working of these may be necessary. If working of the gears is necessary then further dismantling has to be done. All of this procedure takes a surprisingly long time and the average time for carrying out a nominal 120 hour fatigue test (which is the time for a Lynx main gearbox) is, with normal rig and test gearbox serviceability and availability, 5 to 6 months. It can be seen therefore that the total programme on four successful boxes can take 18 months to 2 years. Clearly the opportunity to assess strength of modifications or alternative materials is strictly limited.

Tail and Intermediate Gearboxes

The transmission to the tail rotor is commonly through an intermediate box along the tailboom and into a right angled gearbox driving the tail rotor. Westland experience in the gearboxes has been entirely on spiral bevel gears. They are tested in a conventional back to back rig as an assembly either using a second pair of aircraft boxes driven backwards to close the loop or using a specially designed gearbox for the purpose. Torque is wound into the system by rotation of the ring gear of an epicyclic and is measured by means of strain gauges with a rotary transformer coupling which has proved to be highly accurate but whose reliability has been a problem. Slip ring assemblies have been used but these have required a fair degree of maintenance. Instrumentation on the rig is fairly basic, oil temperature and some bearing temperatures if a specific problem arises. Torsional oscillations in these rigs have not been a problem and are generally less than 5%. Tail Rotor Thrust is applied but no tail rotor moment. A picture of the Lynx tail transmission rig is shown in Fig. 9.

There have been some failures of intermediate gearboxes on test and they were solved by careful choice of meshing standards which were rigorously controlled in production build acceptance tests, and by a web thickness increase. A more difficult problem for the tail transmission is derivation of an accurate spectrum of loading. Until realistic spectra from service experience in real conditions are obtained, the loading has to be derived from measurements made on development aircraft during high powered level flight and high torque manoeuvres. The factors around 1.8 (arrived at in a similar manner to the main gearbox) are applied except that a flight variability factor of 1.2 is included.

This high loading for sustained periods of running again leads to surface damage, premature bearing wear and high temperatures. The temperatures are controlled by choosing the optimum quantity of oil in the box and by external air cooling which has always proved adequate. Bearing wear and gear surface damage is controlled, as far as one is able, by choice of the best lubricant and by operating a spectrum of loading to avoid continuous running at the full torque, but the damage caused is a considerable delaying factor in the programme.

Hubs

The hubs have a dual function of supporting the main gear train to transmit the torque to the rotor and also to carry the rotor lift and moments into the airframe. The testing methods cover both of these load systems. The connection to the main gear train is tested adequately in the rotating gear test. The rotor moment conditions require a separate test and this is done by building a separate test rig in which the rotating moments are applied either by rotating the components with a steady load as was done for the Scout, or by phased dynamic loads on a stationary component for the Sea King and Lynx. The addition of lift and torque results in another substantial rig.

Castings

A diagram of the Lynx casting, including the servo jack attachments is shown in Fig. 5, and a photograph of the test on the Lynx main gearbox casting is shown on Fig. 11. As can be seen it results in a fairly complex arrangement of loads and reactions. The test requirements for a class 1 complex casting under MOD regulations is to test one casting statically and according to the WHL document, a number of castings in a fatigue test, the number of castings being related to the factor for the test. It is common to test four castings. The specimen consists primarily of a casting or assembly of castings (there are five castings in the Lynx main gearbox assembly) into which are assembled gears, bearings, etc., accumulated from other tests, sufficient to carry the torque. The loading system for both the static and fatigue tests is similar. In the case of the Lynx this consists of applying simulated engine torques and reactions to the input assembly and reacting the torque at the main rotor hub and tail rotor torque interfaces. Lift and pitch and roll moments are applied through hydraulic jacks to the gearbox hub and hence into the casting.

The dynamic loads from the aircraft hydraulic actuators, which are bolted to the casting, are applied, but as a separate test. The casting is assembled to a structure representing the aircraft structure in order to get the right stiffness at the attachment points. For static tests the loads are simply increased in a suitable sequence for two or three different loading cases. The fatigue case is one representing manoeuvre cases since except in the case of the hydraulic actuators, the rotor frequency loads are usually judged to be non damaging. A life factor is preferred to a load factor for the fatigue case and the test for a 7000 hours life lasts for around 200,000 cycles.

A typical test of a main rotor gearbox casing for the Lynx is as follows:-

	LIFT	PITCH MOMENT	ROLL LOAD	ENGINE TORQUE	TAIL TORQUE	MAIN ROTOR TORQUE
LEVEL 1	0	0	0	0	0	0
LEVEL 2	+27,000	-200,000	-143,000	18,000	4,000	300,000
LEVEL 3	+11,000	+ 57,000	+ 57,000	13,000	4,000	200,000
LEVEL 4	-11,000	0	0	13,000	4,000	200,000
LEVEL 5	0	0	0	0	0	0

This cycle to be repeated 210,000 times.

Autorotation case is not necessary in the fatigue test as the number of cycles is small.

The test on the servo jack attachments is done as a separate test.

As an aid to the understanding of the stress distribution in the casting stress measurements using brittle lacquer or photoelastic coatings are made.

Four specimens are tested in fatigue and one of these is tested in the static case. Testing of the tail transmission gearbox castings is not usually done since the regulations permit clearance by calculation in the case of fairly simple castings or castings whose construction or design is similar to previous experience.

Miscellaneous Gearbox Parts

Sometimes a careful analysis of the total internal loading system in a gearbox shows that some components are not adequately covered by the rotating back to back type tests. As already mentioned a typical example of this is the quill shaft in the Lynx three pinion gearbox, where the load is distributed evenly between the three pinions by means of flexible quills as shown in Fig. 1. These, by their nature, are highly stressed parts with stresses proportional to power demands and which are not of a cyclic nature. It is therefore necessary to conduct a separate test on these parts to apply a spectrum of loading representing the power demands in the aircraft. Components such as these are tested either in standard fatigue test machines or in special purpose rigs.

5. CRITERION OF GEAR FAILURE

It is quite likely that fatigue testing at high factored powers will lead to surface breakdown. This in turn can lead to a fatigue crack which may cause a substantial loss of metal and substantial secondary damage. The usual criterion of failure adopted by Westland is whether the gear train will continue to carry the full load without the risk of substantial secondary damage such as could be caused by large pieces of tooth breaking off and causing a failure of the load path. With this as the criterion it is considered legitimate to repair any surface damage such as plucking or scuffing by stoning the gears and continuing the test since it can be considered that this surface damage is caused largely by lubricant failures at the higher than normal bearing pressures and will not occur during normal service experience. Fig. 10 shows types of gear tooth damage which occur and a tooth subsequently stoned. A tooth which is classified as a failure is also shown.

6. ALTERNATIVE TEST METHODS

Since fatigue testing of gears is expensive, and in the case of re-sourcing of gears can be an inhibiting factor, attempts have been made to find alternative, cheaper ways of proving the strength of gears. The most attractive possibility is to test the gear wheel in a standard testing machine loaded with a piece of metal simulating a pinion, which has the obvious advantages of simplicity and a large number of possible specimens from one wheel. One feels this ought to have some value, particularly in the case of comparative tests of gear material but so far it has not found acceptance. A more sophisticated method was tried for the Lynx gearbox partly as an attempt to overcome some of the bearing wear and tooth wear problems of the full speed rig but also as a possible cheaper alternative method of testing. A diagram of this rig is shown in Fig. 12. It consists in principle of testing a single input only of the twin gearbox and driving the output into a standard aircraft box but using the twin inputs thus halving the loads on this slave gearbox. This has some advantage in the late stages of a development programme when suitable boxes are more readily available. To reduce wear this particular test was conducted at a speed 1/6 of the normal running speed of the box. A fatigue test was conducted satisfactorily on this single input with no wear problems or rig breakdowns but it is difficult to establish credibility for a system of testing which is different from the aircraft conditions. A similar fate, but in the design stage, befell another attempt to oscillate the gears over at least one tooth of the slowest gear in a quasi static test and using the casting rig, which would have resulted in considerable rig and test cost savings. It seems that the traditional conservatism of the mechanical engineer, born out of hard experience, means that such simplified tests, while perhaps adding to knowledge of SN curves for gear materials, would never contribute directly to the basic substantiation of a gear train.

7. FUTURE TESTING

The experience at Westland has largely been on back to back or closed loop type testing. This method, while giving some saving in power, does result in a number of constraints on the test rig design.

Firstly, the rig has to be designed specifically for each gearbox type. At the end of the fatigue and development programme the rig becomes of no value to any future project although sometimes some rigs are retained for production clearance purposes. Secondly, the design is inflexible so that any changes in aircraft configuration is extremely difficult to accommodate since the angle and positions of the slave gearboxes need to be fixed. This means that the rig design cannot proceed until the aircraft layout is frozen. Thirdly, the rig is a very complex mechanical system and is often more complicated than the gearbox that is being developed and fatigue tested. This leads to a low reliability and slow test rate.

In order to overcome these constraints, Westland are building, under MOD contract, a rig on the open loop principle, which while being designed for a specific project, is also capable of being used for a wide range of other gearboxes. Although this paper is not the place to describe the rig in great detail it is worth discussing the main features.

A photograph of a model of the rig is shown in Fig. 13. The basic principle is that three rafts with electric motors of 2600 KW each represent an engine. These drive into the test gearbox and the power is reacted by standard water dynamometers at the main and tail rotor. The power units together with their reduction and speed increasing boxes are on rafts which can be moved about the test cell to accommodate different aircraft design configurations or to test different parts of the transmission. All the components chosen, the motors, gearboxes, dynamometers, torque measurements, servo control, programming are standard commercial items and it is hoped by this means to have a rig which is much more reliable than has been the previous experience and also one which can be readily adapted for other projects when its primary task has been completed.

The rig of course uses a lot of power. It in fact represents about 60% of the total factory supply and the effect of this is that the rig can only run under high power at night. This in turn has lead to the concept of running the rig entirely automatically with a system of safety devices and supervisory instrumentation. The capability of the water dynamometer system to very rapidly reduce power as distinct from the wound-in torque system, adds confidence to the capability of safe running. Considerable thought has been given to re-circulating the energy by hydraulic or electric systems or to using the waste heat, but the intermittent usage characteristics of development testing and, over a year, the relatively small number of hours of running, means that any such system is unlikely to prove economic. It is hoped to run the rig in 1981.

8. SERVICE EXPERIENCE

The testing requirements and factors for gearboxes, as for most components, are arrived at by taking account of a knowledge of scatter of strength, Goodman diagrams, Miner's rule, S-N curves and engineering judgement based on experience gained in service. It is useful to review the experience gained on Westland gears and compare it with test experience.

Table 1 shows the in-service experience on three military helicopters. It is necessary to make one or two comments on this table before attempting to draw any conclusions. It is of course a simplified version of the overall picture. In the case of the Scout, a modified main gear was tested to an additional factor of 1.1 and has been introduced with no service failures but with so far limited experience so that the old gear is of more interest from a statistical point of view. The Scout work was done some years ago when knowledge of the behaviour of gearboxes and helicopters was less well known. The factor used was what is now regarded as a low one of 1.1 and the test was a simple one of testing for the 1 hour power rating times 1.1 for 5×10^6 cycles. No attempt was made to programme the loads and no loads were applied to represent any higher engine ratings.

The helicopter is single engined so there is no question of transients due to engine failure. Subsequent service experience revealed a tendency to overtorque up to 15% beyond the 5 minute rating. No other service failures have been found in any gears in any of these helicopters on military service.

Clearly the factor of 1.1 is no longer acceptable, at least for main gears, although the Scout experience compares not unreasonably with modern understanding of strengths. Whether the resultant factor of 1.8 now applied is the right one is difficult to judge from the limited experience but it is certainly a substantial margin over 1.1. It is interesting to note that in the Scout main gearbox the broken tooth generally remained in the bottom of the gearbox. It is perhaps useful to continue the test of all gearboxes until failure to establish the mode of failure and its likely outcome as an aid to arriving at a safe life. Unfortunately the cost and time of testing and potential rig damage tend to inhibit this practice from being followed.

The situation on the tail transmission is somewhat different. No failures of gear in these aircraft has occurred with test factors varying from 1.1 to 1.8 even though life calculations show only modest margins over the declared life. As described earlier a more difficult problem is an accurate prediction of the in service usage.

9. GENERAL GEARBOX DEVELOPMENT

The main objective of this paper has been to describe the methods of fatigue testing. There is however a whole field of development of gearboxes as distinct from fatigue testing and it is worthwhile outlining what the programme has been on the Lynx. The development of a satisfactory gearbox and extension of the Time Between Overhauls (TBO) was carried out in 5 phases.

1. Rig Testing on the back to back fatigue rigs.
2. Rig Testing on the rotor rig.
3. Development aircraft flying, including the formal Type Test.
4. Service aircraft Intensive Flying Trials Unit (IFTU).
5. Normal service experience.

The only formal requirement in the development programme is the Type Test, which for a twin engined helicopter represents 150 hours flying and 200 hours ground running. The total development hours are much more than this.

The rig testing using the same rigs as for fatigue testing, was extended to over 4000 hours for general experience and to develop and test improvements.

For the Lynx, a Rotor Rig was constructed (Fig. 14). This is essentially an airframe bolted to the ground and capable of accepting and driving the total transmission using aircraft engines. It is an excellent vehicle for assessing quickly with no flight safety problems, any development in the transmission but is limited in the amount of control power which can be used although this is of little consequence in transmission development. Over 1600 hours were run on this rig.

Development flying covers a whole range of activities during the course of which the transmission hours are built up. Some flying is specifically done for transmission development but this is a fairly small proportion. The total development flying for all purposes and on all Lynx variants with a common transmission was 6000 hours on 13 aircraft.

From this extensive development flying, a suitable life of 300 hours was allowed for the service flying on the IFTU, during the course of which almost 6000 hours were flown by 13 production aircraft of the Army and Naval variants. The timescale of this programme is shown below on Table 2.

The result of this extensive programme is a TBO of 600 hours with a potential to rapidly increase beyond this depending on the rate of service flying. As can be seen the total programme takes a long time but the value of a high TBO quickly, is quite an obvious advantage on expensive transmission components.

10. CONCLUSIONS

This paper is a review of the methods of fatigue testing of gearboxes as carried out at Westland Helicopters. It is clear that the testing has to include not only the gears but other components of the total gearbox. The fatigue testing is expensive and time consuming. It would be useful if there were an acceptable method of testing, or at least comparative testing, of gears in a much simpler form so that for instance material changes or small changes could be more economically assessed. The test rigs themselves are expensive to design and make and it is hoped that a universal rig now in manufacture, while perhaps being initially rather more costly than a purpose built rig, will lead to considerable savings in the future.

Gear case testing is also necessary, although it is difficult to deal adequately with in flight high frequency loadings if these become damaging in some manoeuvres. Development of a satisfactory overhaul life is a subject in its own right but it is clear from the outlines given that it occupies much time on

rigs and aircraft. The question of factors is dealt with and it would be of considerable value if a survey of service experience relative to test experience of helicopter and engine reduction gearboxes on a number of aircraft were carried out. This would be of value in arriving at a safe minimum factor for gearbox testing which should lead to safer aircraft and improve the reputation of helicopter transmissions.

TABLE 1 TEST AND SERVICE EXPERIENCE

COMPONENT	TEST CASE	NO. OF SPECIMENS	TEST RESULT	SERVICE EXPERIENCE
SCOUT/WASP - 500,000 HOURS SERVICE EXPERIENCE				
Main Gearbox	1.1 x max. continuous for 5×10^6 cycles	4	Crownwheel tooth failed	36 crownwheel failures
Tail Gearbox)	1.32 x max. measured on	4	No failure	No failures
Intermediate Gearbox)	development aircraft	4	3 failures, old standard) No failure, new standard)	No failures
LYNX - 55,000 HOURS SERVICE EXPERIENCE				
Main Gearbox	1.3 x 1.15 Extrapolation	4	No failures	No failures
Tail Gearbox)	1.3 x 1.2 x 1.15 = 1.8	4	No failures	No failures
Intermediate Gearbox)				
SEA KING (WHL MANUFACTURED COMPONENTS) - 300,000 HOURS SERVICE EXPERIENCE				
Main Gearbox	1.3 x max. continuous power	4	1 failed crownwheel low case depth	No failures

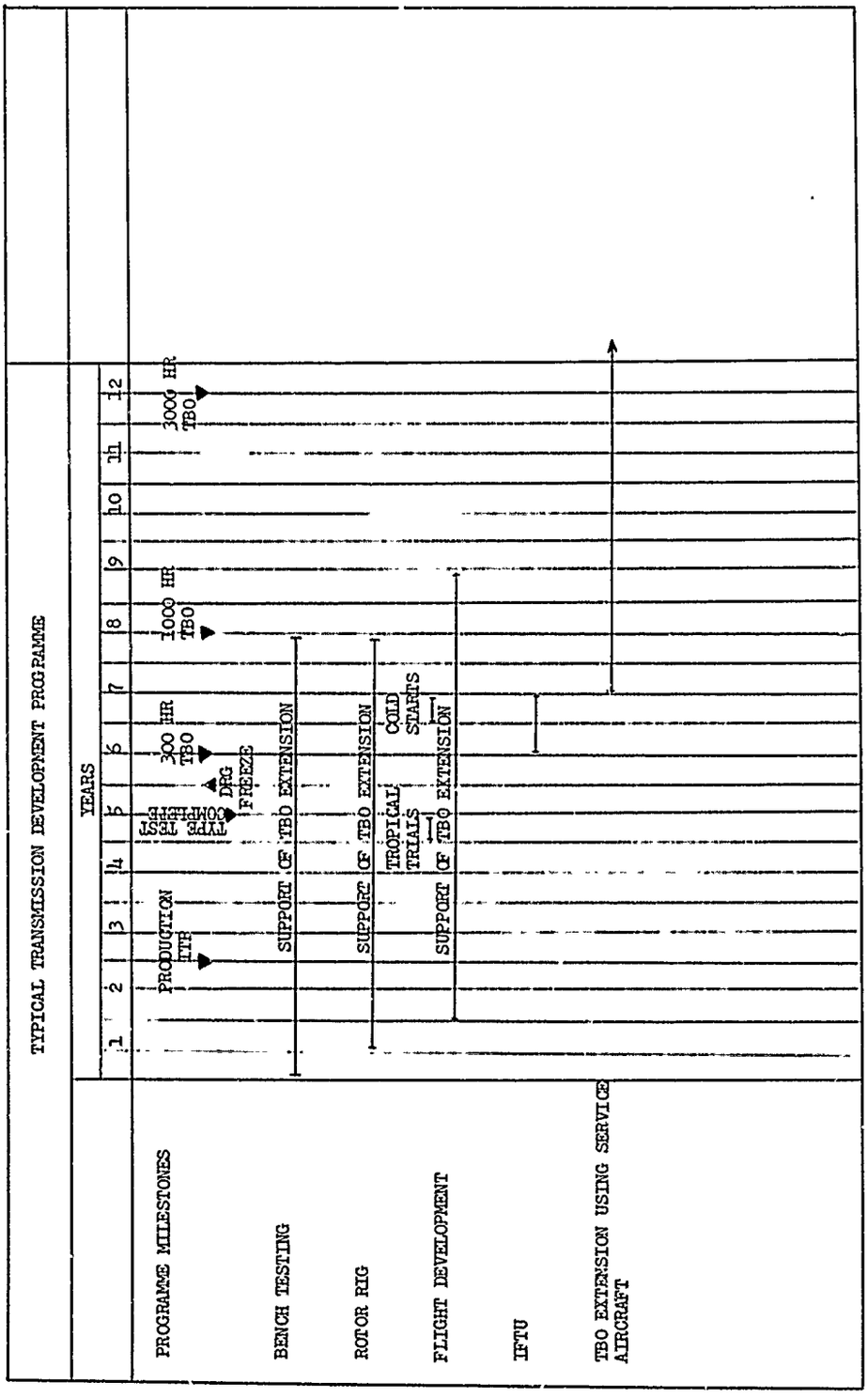


TABLE 2 TYPICAL TRANSMISSION DEVELOPMENT PROGRAMME

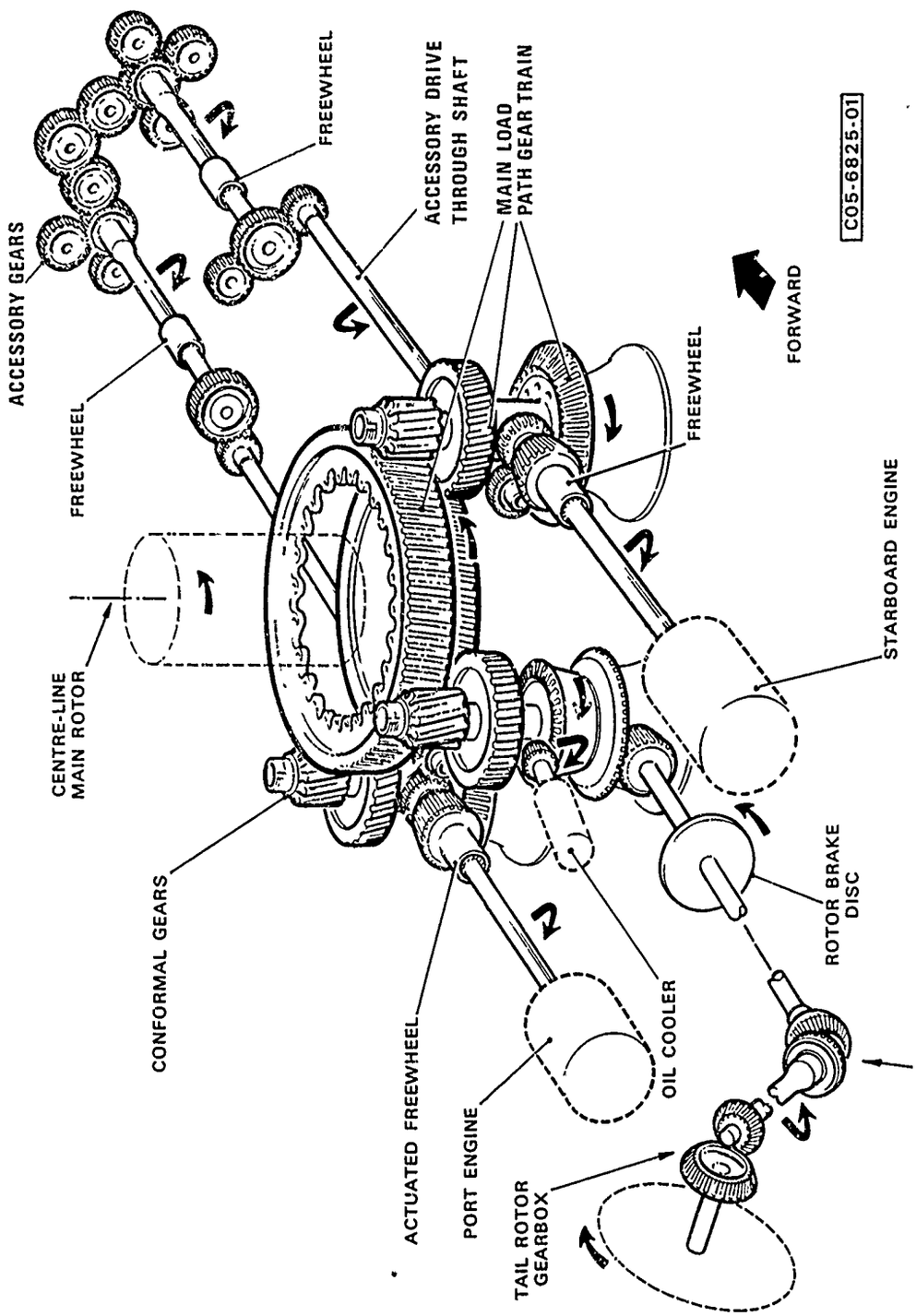


Fig.1 Lynx main rotor gearbox (3 pinion)

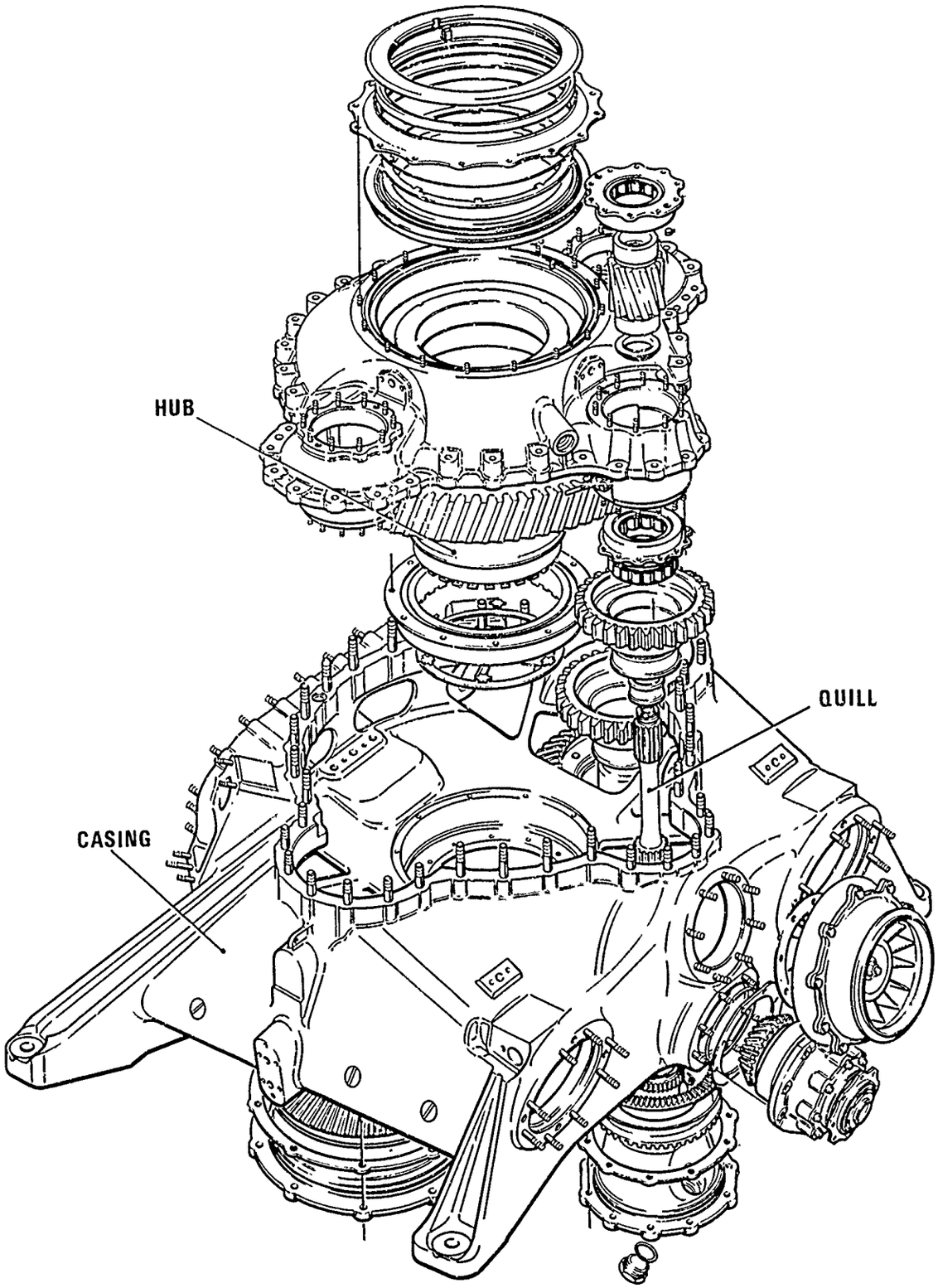
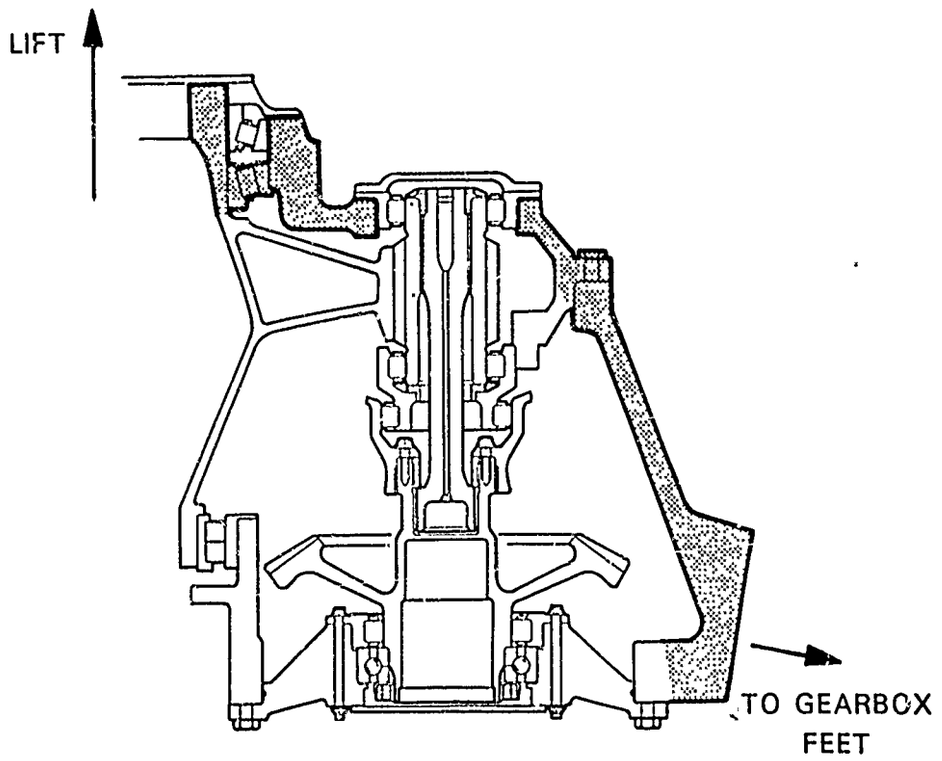
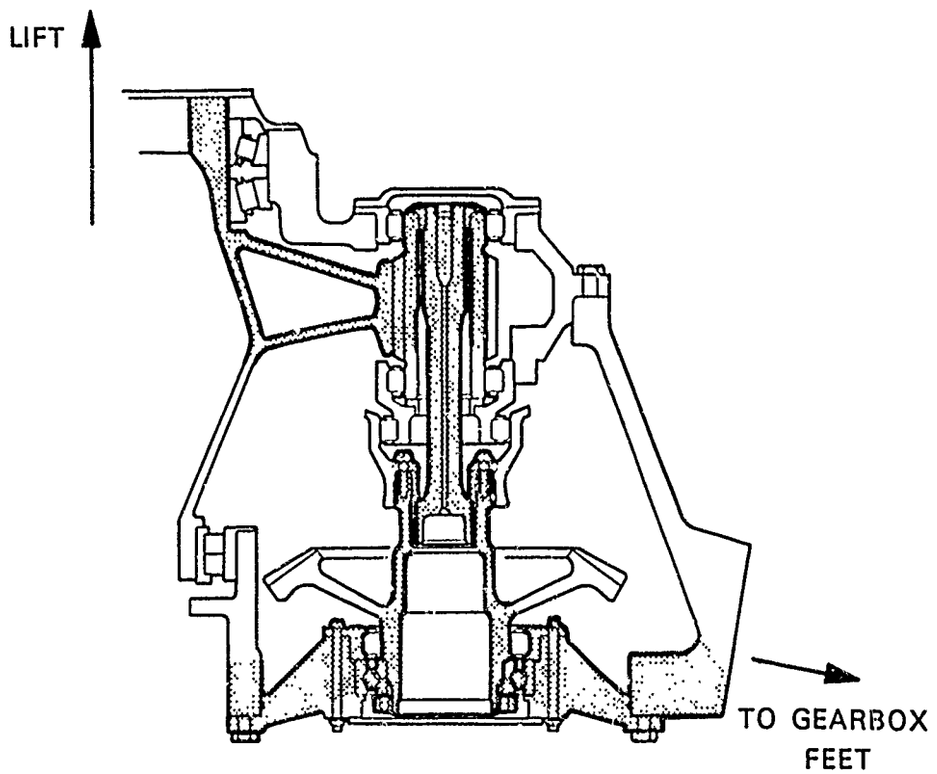


Fig.2 Lynx main gearbox exploded view



(a) AUTOROTATION



(b) POWERED FLIGHT

Fig.3 Lift load path in Lynx 3 pinion gearbox

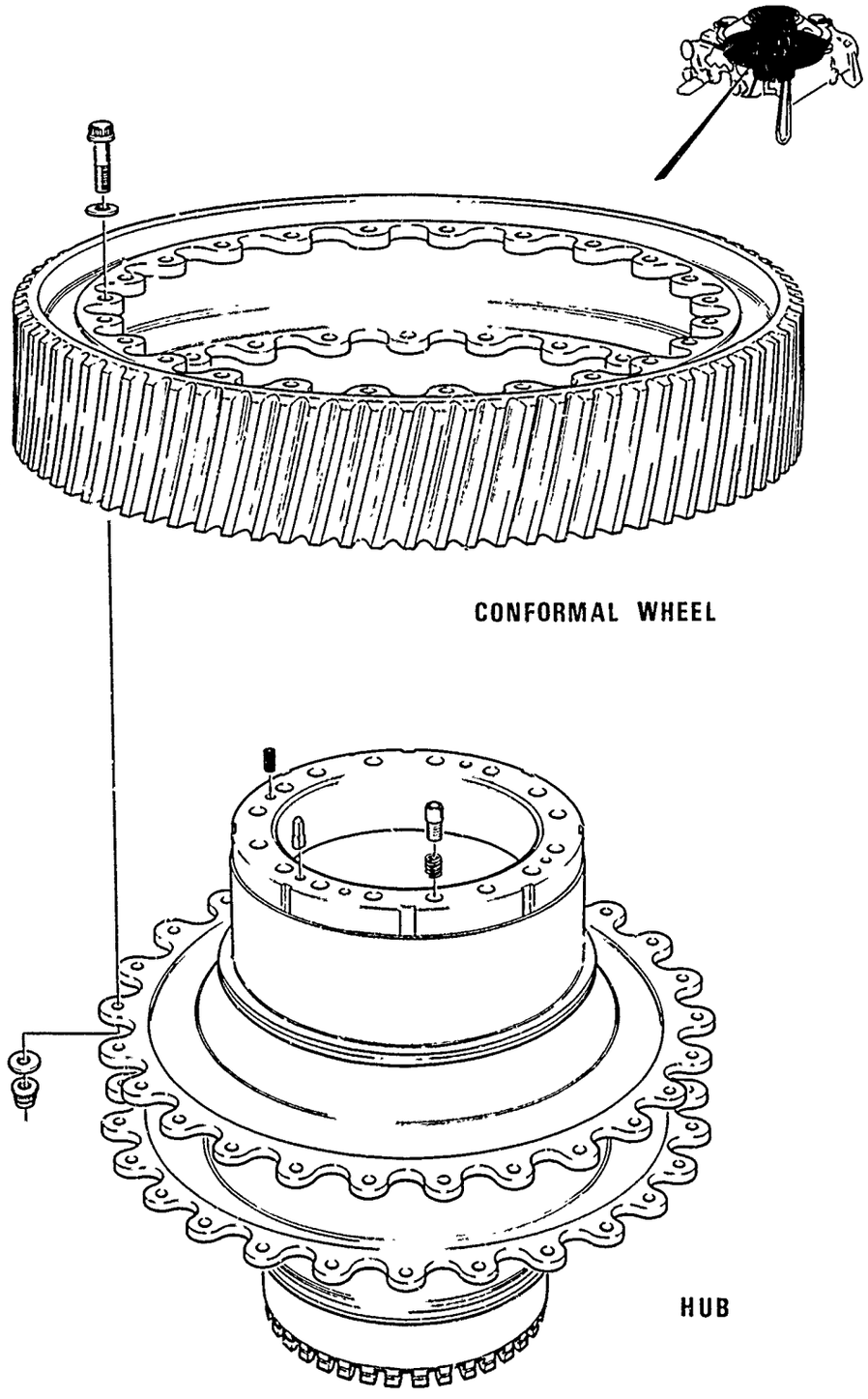


Fig.4 Lynx hub and gear assembly

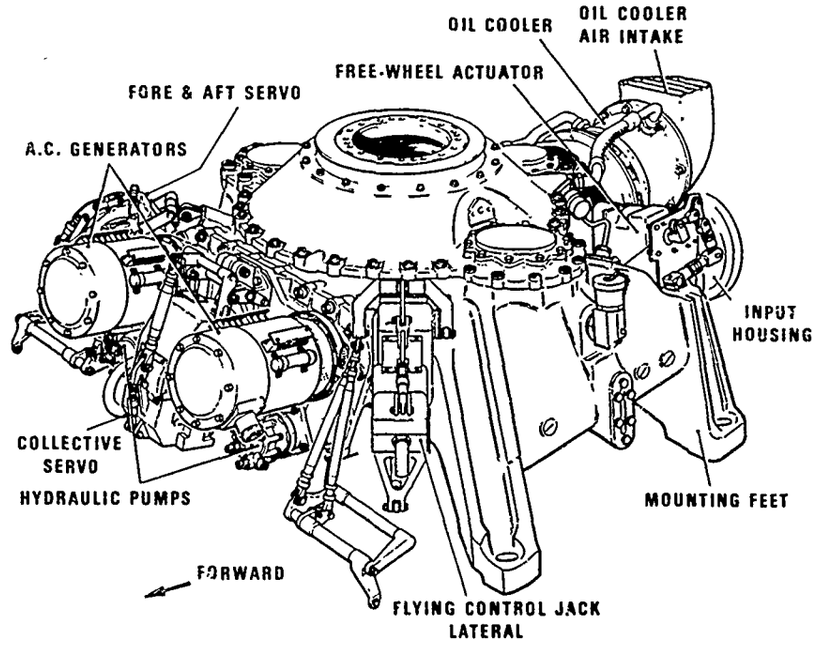


Fig.5 Lynx main gear case

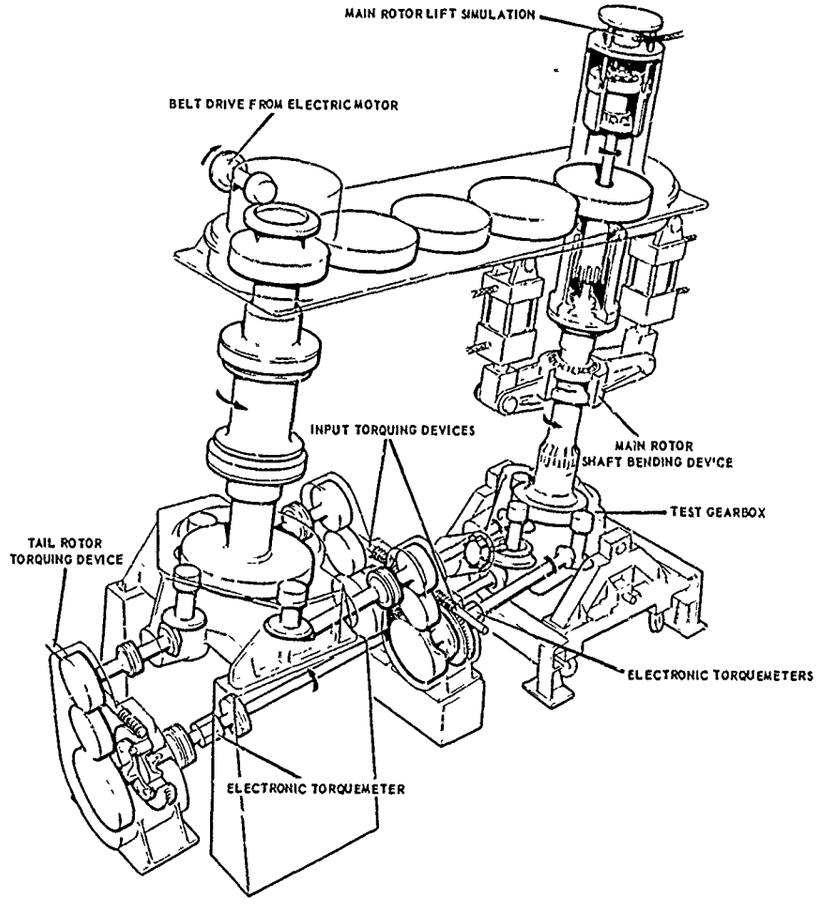


Fig.6 Diagrammatic of gearbox test rig

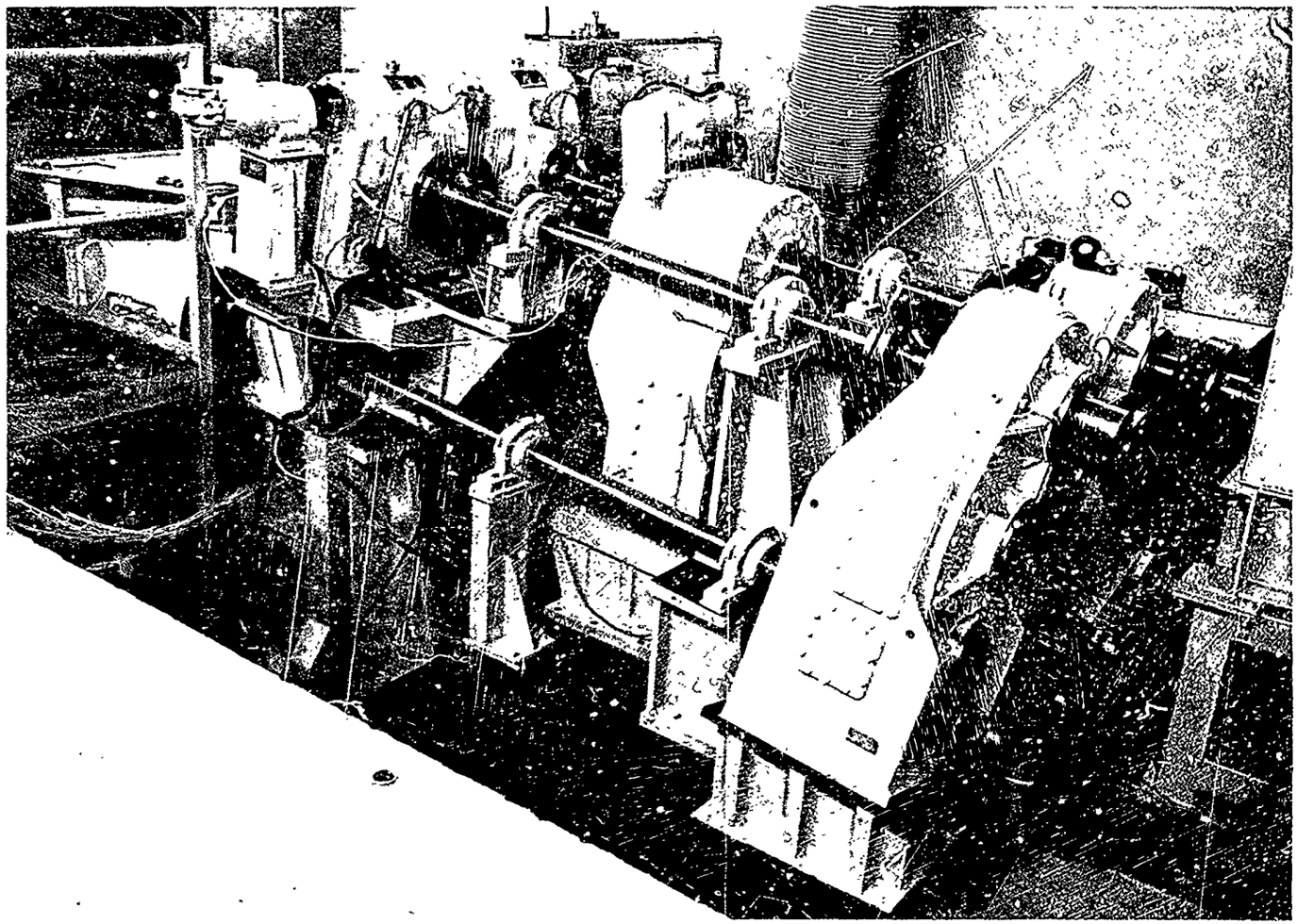
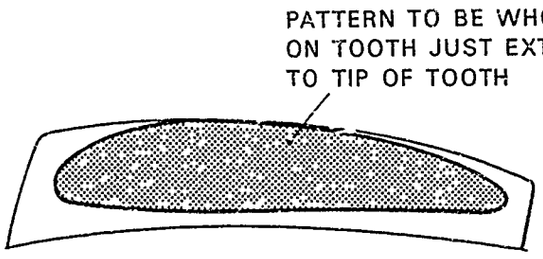
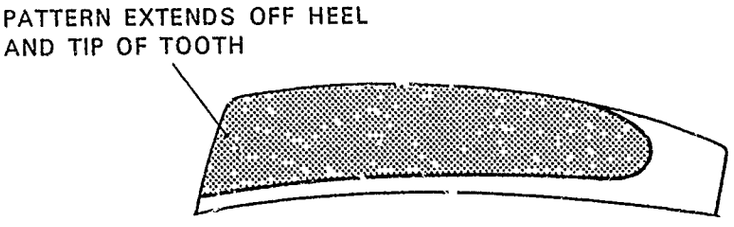


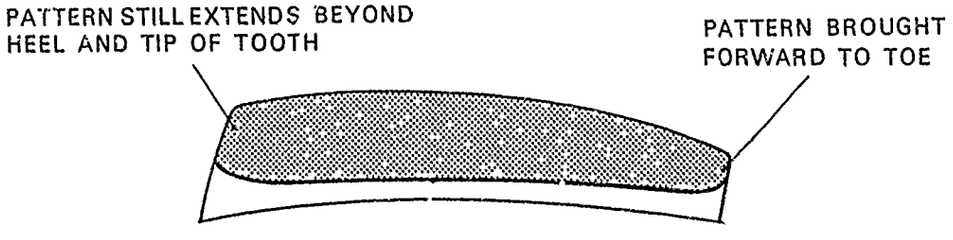
Fig.7 Lynx 3 pinion main gearbox test rig



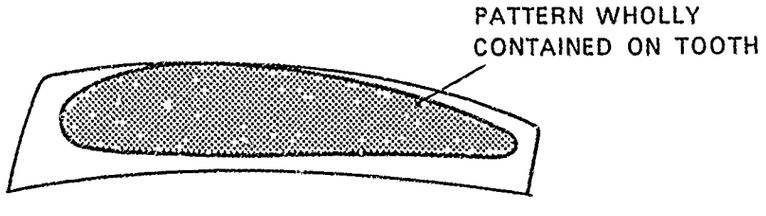
MESHING PATTERN AT 100% POWER



PATTERN ACHIEVED AT 150% POWER



PATTERN ACHIEVED AT 150% POWER AFTER
MESHING ADJUSTMENT



PATTERN AT 150% POWER AFTER REGRINDING PINION

Fig.8 Meshing patterns under factored load

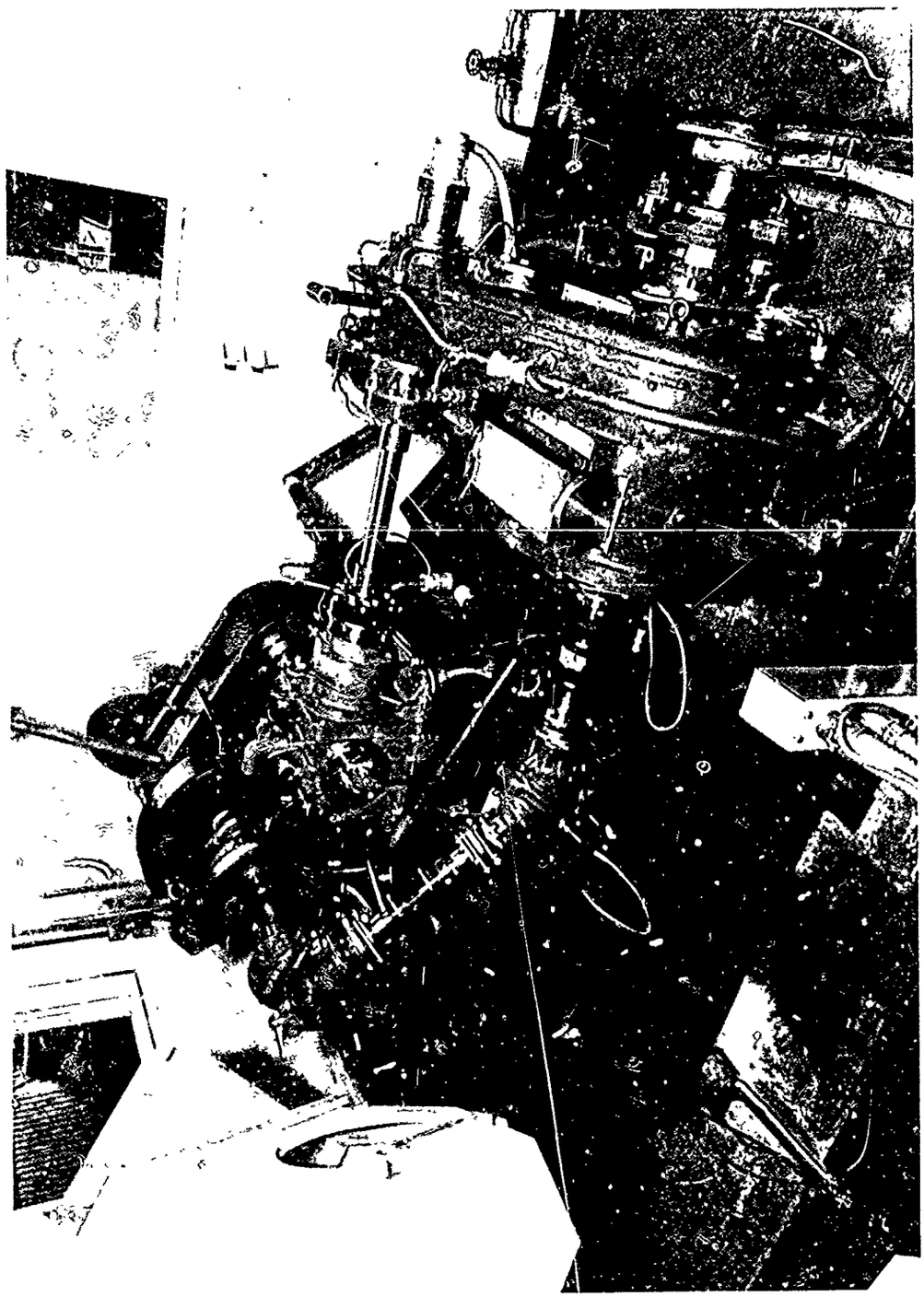


Fig.9 Lynx tail and intermediate transmission rig



Fig.10(a) Plucked teeth



Fig.10(b) Plucked teeth

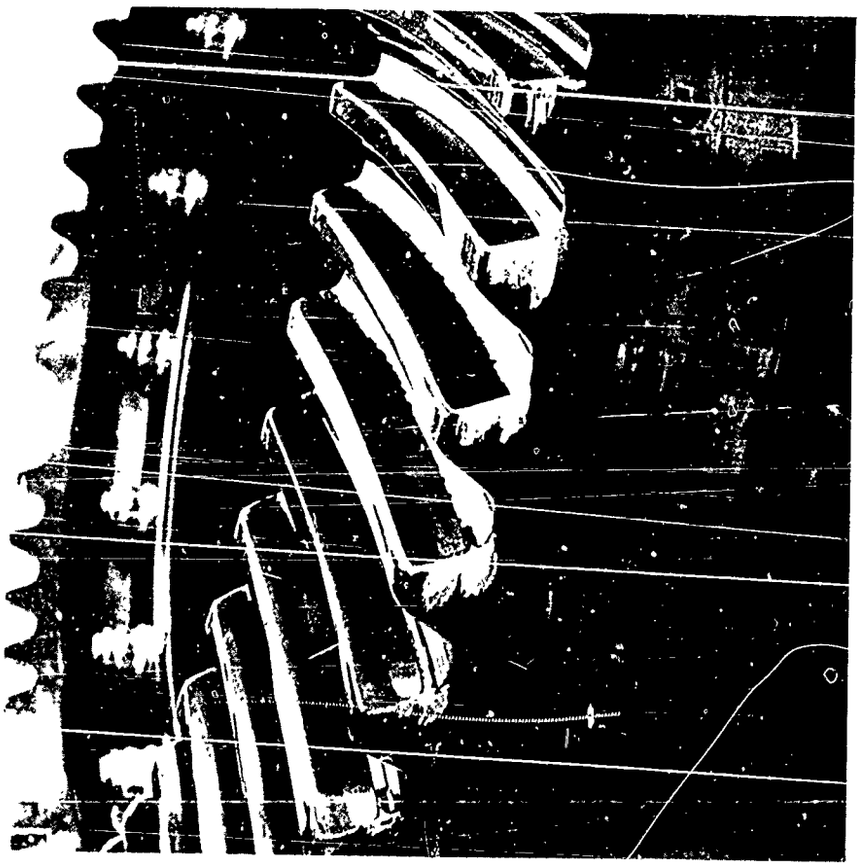


Fig.10(d) Scuffed tooth



Fig.10(c) Stoned tooth



Fig.10(e) Failure

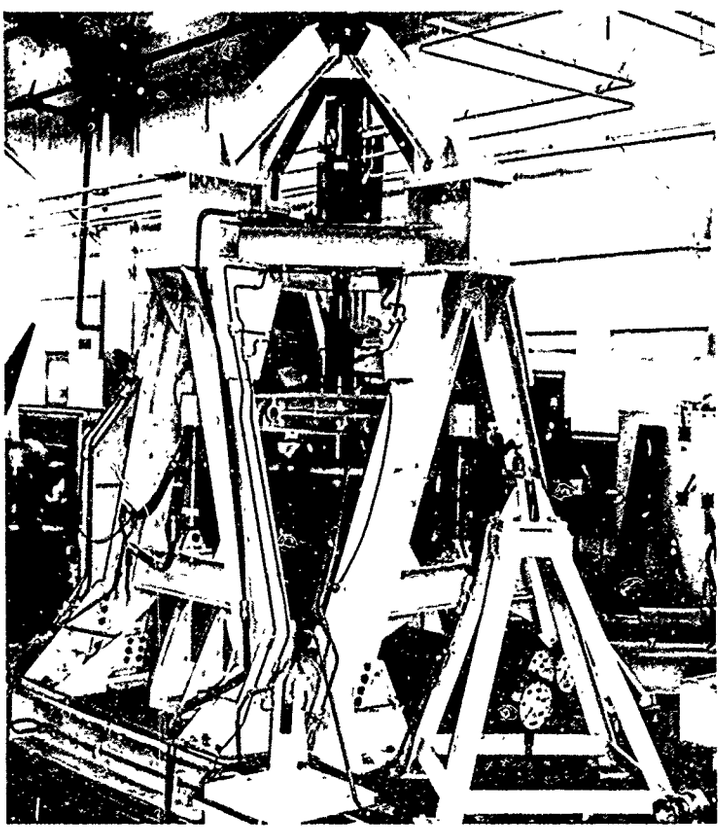


Fig.11 Lynx main gearbox casting rig

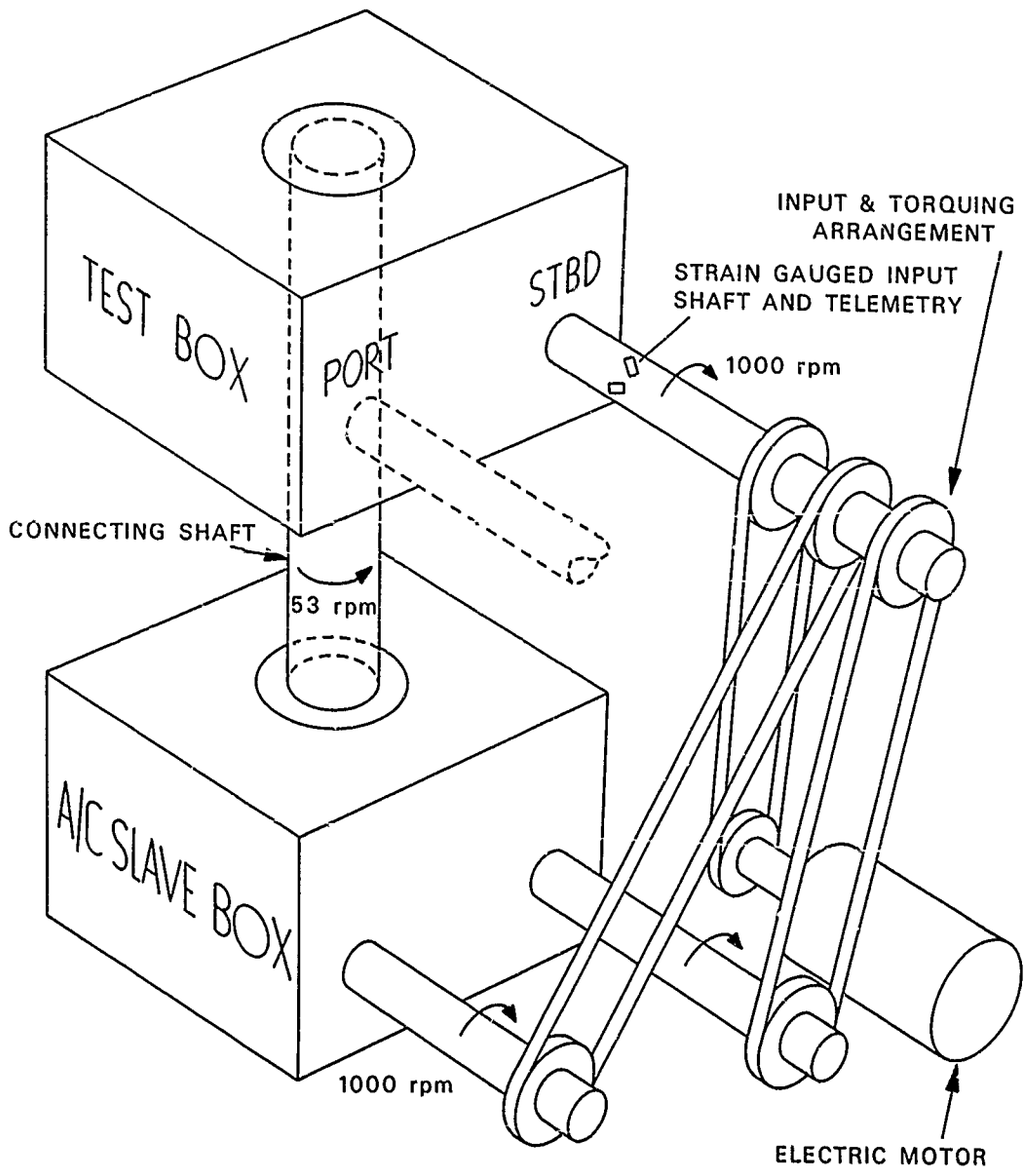


Fig.12 Lynx slow speed gearbox rig

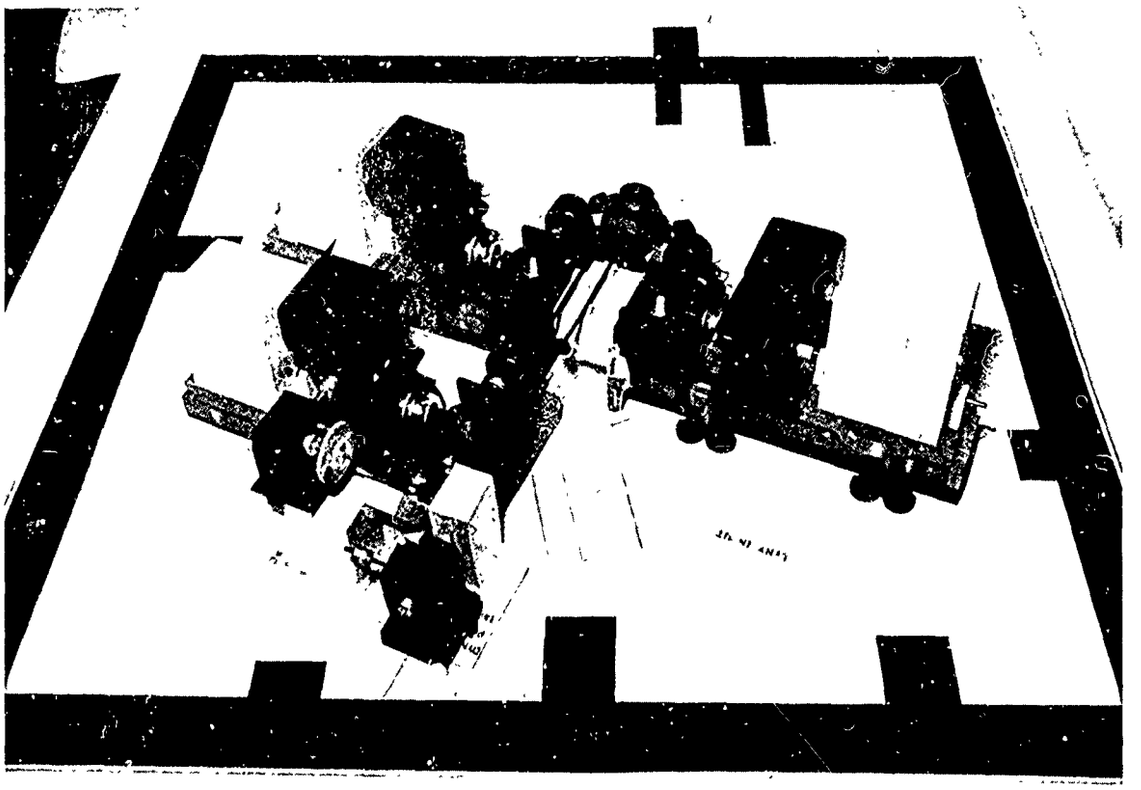


Fig.13(a) Model of open loop rig – View of rig showing motor rafts

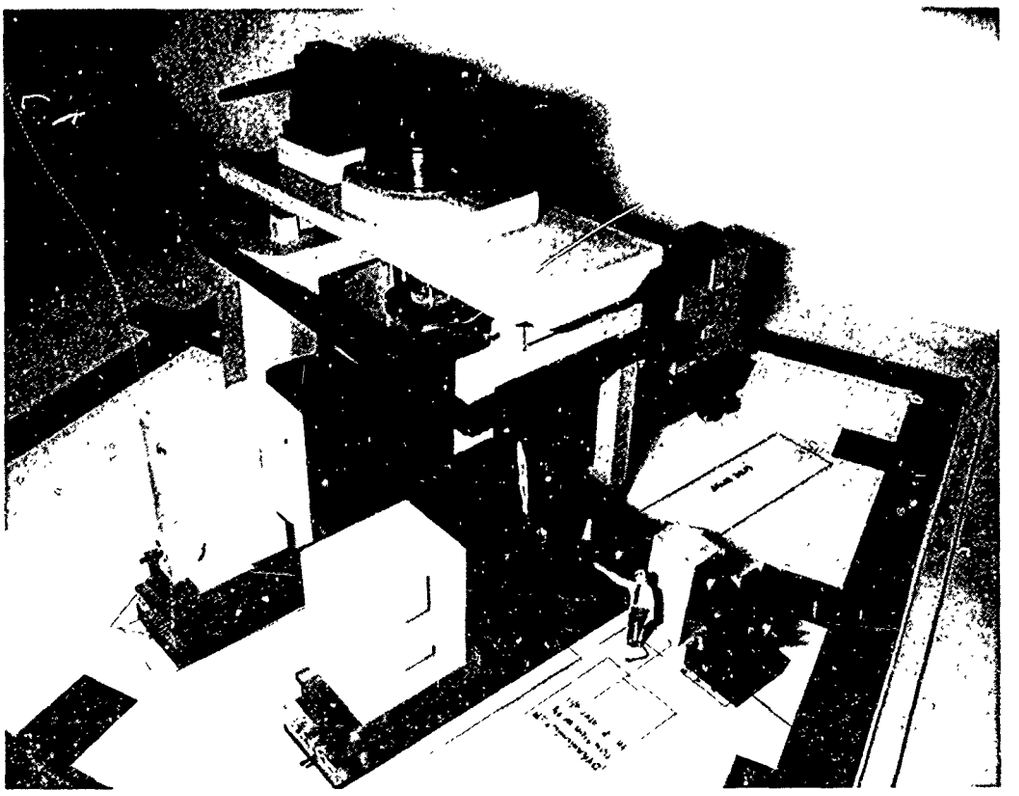


Fig.13(b) Model of open loop rig – View of rig showing main dynamometer in position

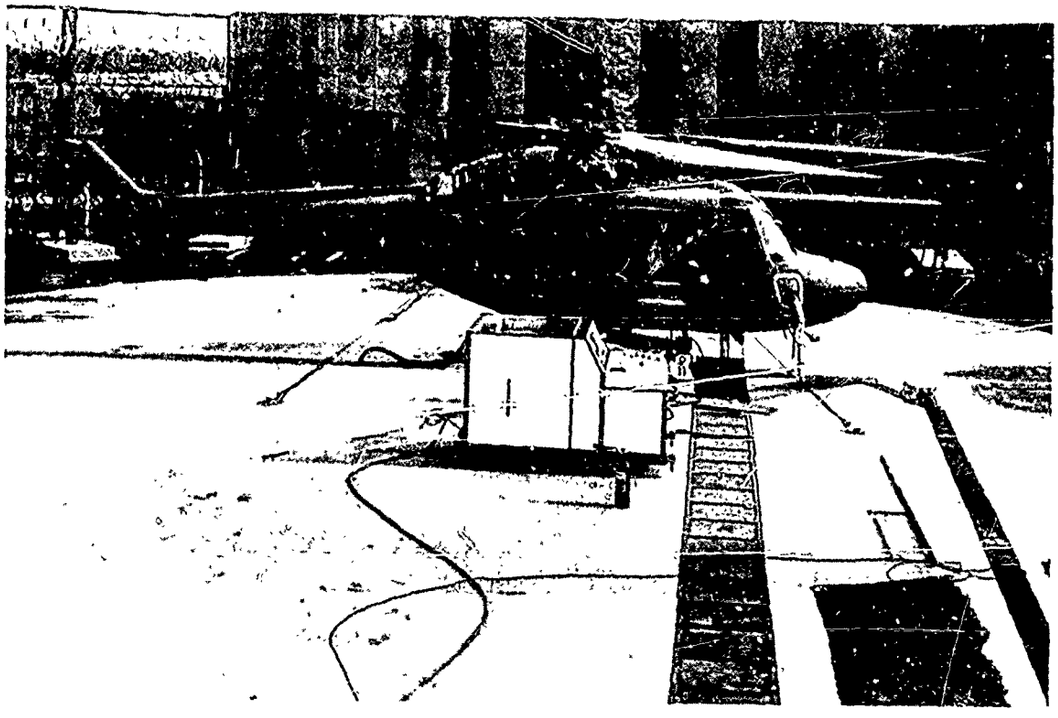


Fig.14 Rotor rig

THE METHODOLOGY OF FATIGUE ANALYSIS AND TESTING – MAIN ROTOR BLADES AND HUB – HUGHES YAH-64 ADVANCED ATTACK HELICOPTER

By
John M. McDermott, Manager
Structural Analysis Section
Hughes Helicopters
Centinela Avenue at Teale Street
Culver City, California 90230
U.S.A.

ABSTRACT

The paper outlines the fatigue methodology applied to the structural analysis and testing of the Main Rotor Blade, Blade Retention System, and Main Rotor Hub of the Hughes YAH-64 Advanced Attack Helicopter. The basic structural concepts are described, including provision of fail-safe redundant load paths, and damage tolerance. A description of the materials used for the various structural elements is given, and the factors affecting their choice are discussed. The strap retention system, which incorporates both flapping and feathering motion, is described with emphasis on its fail-safety.

The approach to fatigue testing of the main rotor elements is described. The rationale for testing various components in separate combinations, and also in a full-scale hub-retention fixture, incorporating four arms with simulated blade flapping and feathering motions, is discussed. Fatigue test results are presented, including failure modes and the ability of many components with large amounts of fatigue damage to sustain full loads. The methodology of transforming the results of fatigue testing into working S-N curves to be used for life verification is also outlined.

A description is given of the fatigue testing of parts with ballistic damage and also of the crack propagation testing of parts with a fatigue crack already developed. The analysis of failed parts to determine failure modes, origins of crack inception and possible improvements to extend fatigue life is discussed.

A general review of the fail-safety of the design which is inherent in fulfilling the requirements of ballistic survivability concludes the paper.

INTRODUCTION

The Hughes YAH-64 Advanced Attack Helicopter (shown in Figure 1) is currently in the final stages of development prior to a production contract being issued at the end of 1981. The requirements call for a highly damage-tolerant main rotor, with a high degree of survivability to battle damage. This was achieved by design methods as outlined in this paper, and verification was achieved by the test methods described. The rotor system on the YAH-64 is 4-bladed, fully articulated, with elastomeric lead-lag dampers providing restraint and in-plane damping. The rotor is mounted on a static mast with a rotating drive shaft inside. The system is similar in concept to that used on the Hughes OH-6 and 500 series helicopters, which have had a highly successful service usage.

DESCRIPTION OF MAIN ROTOR HUB

The main rotor hub general arrangement is shown in Figure 2. The hub body is made from an aluminum forging, machined to provide four sets of arms for mounting each blade. The driving torque for the main rotor is transmitted through the drive shaft to the splines in the drive plate and through the attachments on the top of the hub. The hub is mounted on a static mast by means of two tapered angular contact roller bearings, which transmit the thrust and hub moments to the helicopter. This is shown in Figure 3.

The main elements of each arm are:

i) The Lead-Lag Link which provides the articulation for the in-plane motion of the blade. The lead-lag joint is made up of teflon lined bearings with a pin connecting to the strap retention system. The attachment to each blade is shown in Figure 4.

The dampers are connected to the pitch housing at the inboard end, and the lead-lag motion of the blade is transmitted to them through the lugs of the lead-lag link. The Hub Assembly is approximately 2 meters in diameter (6.50 ft).



Figure 1. Advanced Attack Helicopter.

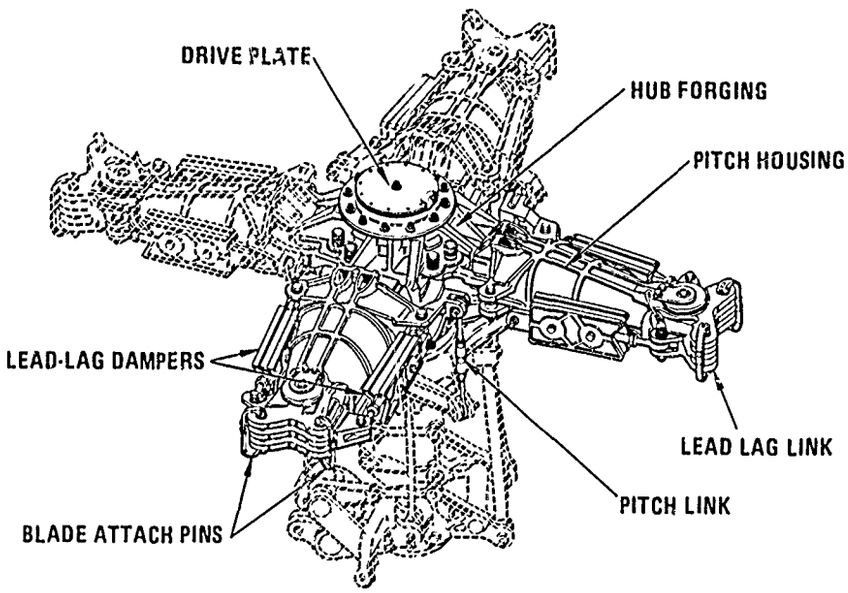


Figure 2. Main rotor hub assembly.

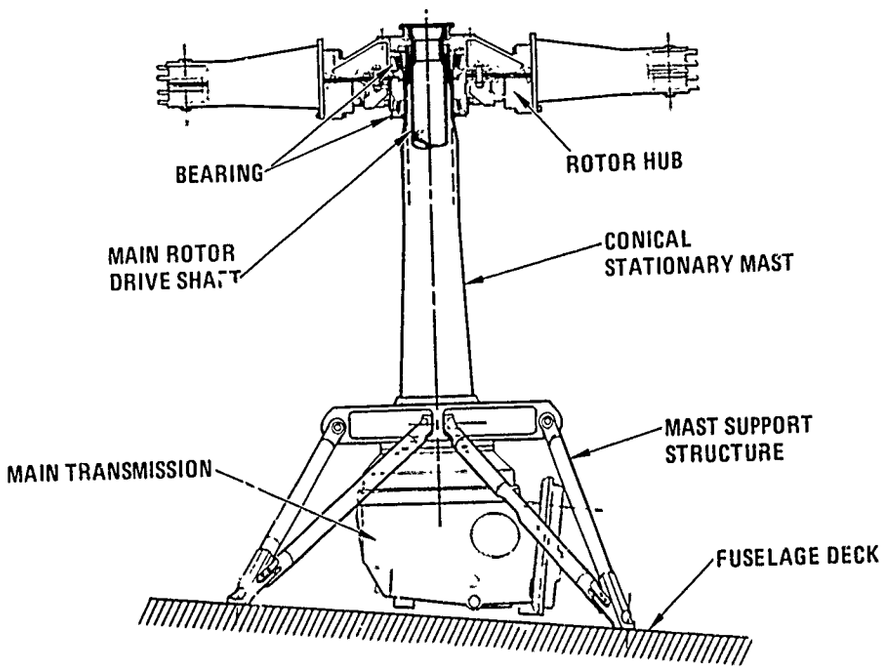


Figure 3. Static mast - rotor support.

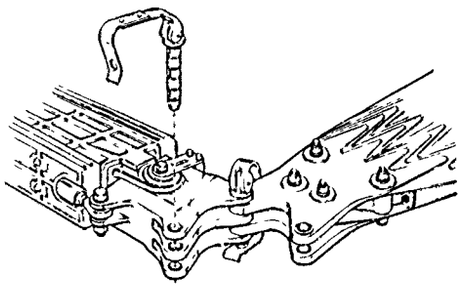


Figure 4. Main rotor blade root attachment.

ii) The Pitch Housing, which does not provide any centrigugal restraint, is free to flap and feather about the feathering bearing. The Pitch Housing is connected to the pitch link which controls the collective and cyclic angles of the rotor. The feathering bearing is housed on the inboard end of the pitch housing.

iii) The Strap Retention System provides the centrifugal restraint for each blade and is shown in Figure 5. This system, which is similar to that used on the Hughes 500 series helicopter, consists of a pack of 22 laminates each 0.36 MM (0.014 inches) thick made of AM355 stainless steel. The strap packs are free to flap and to twist, and provide a highly damage-tolerant retention system. Full loads can be carried with over 10 straps completely failed.

DESCRIPTION OF MAIN ROTOR BLADE

The main rotor of the YAH-64 Advanced Attack Helicopter is 14.63 meters diameter (48 ft). The four blades are mounted to the hub by means of the lead-lag link described above. The general arrangement of the root end is as shown in Figure 6. The blade attaches to the lead-lag link lugs by means of two pins of an expanding bushing type of design, shown in Figure 4, such that the pin expands in diameter upon installation in order to fill the holes of the blade attachment.

The cross section of the blade is as shown in Figure 7. The blade basic section is cambered and is of constant section throughout the span, except for the swept tip section. The material is rolled stainless steel sheet of AM355 CRT reinforced by uniaxial fiberglass forming the main box beam of the section

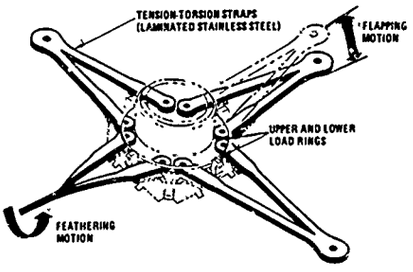


Figure 5. YAH-64 Main rotor blade retention.

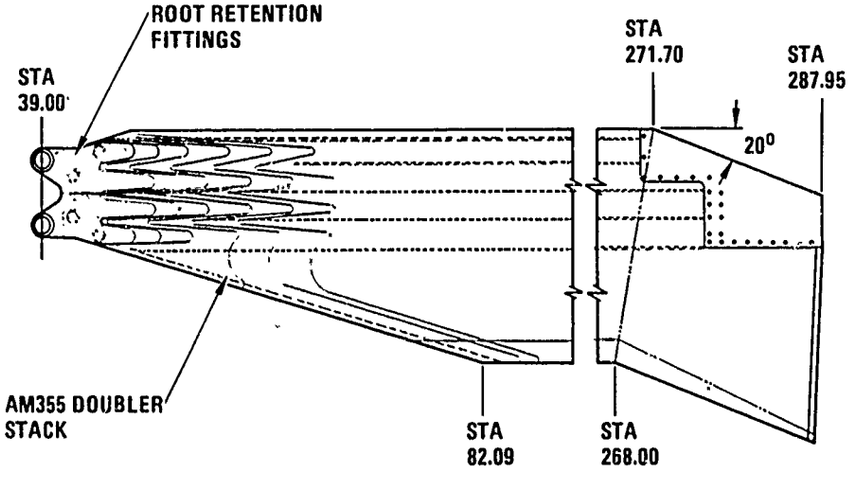


Figure 6. Planform of blade.

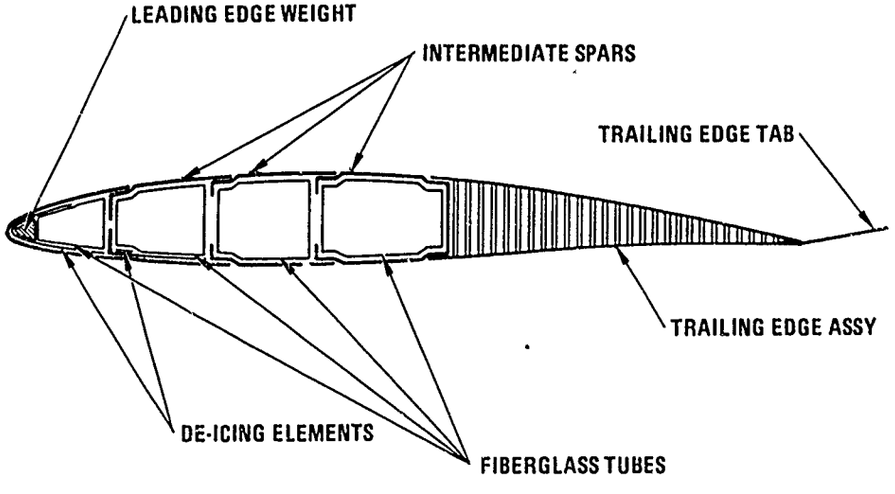


Figure 7. Blade cross section.

which comprises 50 percent of the total chord. The trailing portion of the blade is made of fiberglass and Nomex honeycomb, with a trailing edge tab of AM355 CRT stainless steel. The box beam consists of four torsion boxes bonded together and is highly redundant. The transition from this box beam to the root end section is achieved by means of a stack of doublers as shown in planform in Figure 6. The outboard portion of the blade is swept back at an angle of 20 degrees to minimize the compressibility effects on the advancing blade. This tip section is also thinner than the basic section of the blade. The general arrangement of the swept tip is shown in Figure 8.

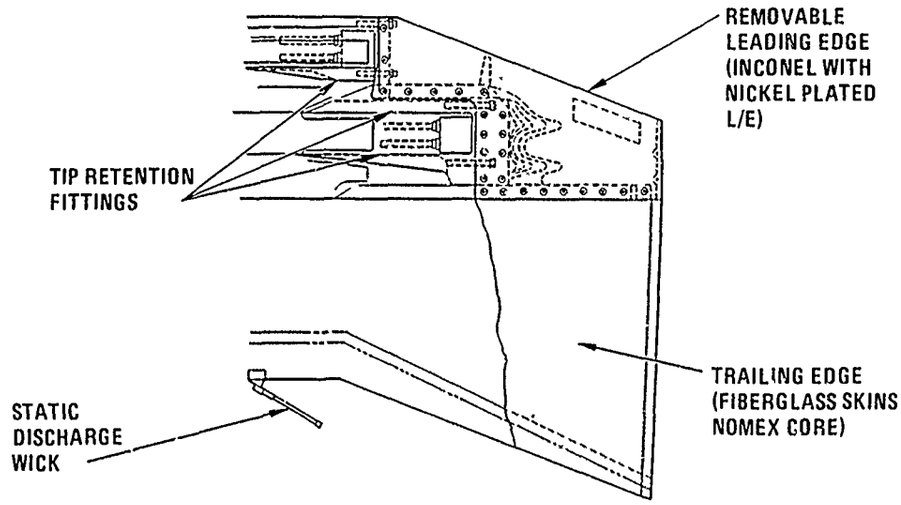


Figure 8. Swept-tip of blade.

DESIGN APPROACH

During the initial design of the main rotor, the approach used to establish the required fatigue strength was the concept generally referred to as Weighted Fatigue Approach. Using this method, a loading condition for each component is defined and the component is then designed to have an infinite life for those loads. In actual fact, each component is subjected to a spectrum of loads in service, and the relationship between these load occurrences and the S-N curves determines the fatigue life of the part. During the course of the design, it would be too cumbersome to apply this spectrum of loads to each design iteration, and so instead, a particular loading condition is chosen, and a factor applied to the loads for that condition. Generally a high speed level flight condition was taken as the basis for these loads, and a weighting factor of 1.5 to 2.0 was applied to the alternating fatigue load, depending on the material involved. The parts were then sized so that the resulting stresses did not exceed the endurance limit, with the effects of steady load and stress concentration factor included. By this means each part was required to have a specified endurance limit load - that is, a load which could be applied for an infinite number of cycles. More recently the approach taken at Hughes Helicopters has been to define for each part not only an endurance limit capability, but also, and in addition, a high load condition which could be sustained continuously at the peak values on the part for one hour before a fatigue failure would be encountered. This is referred to as the One Hour Load, and results in a more controlled definition of the fatigue strength than the Weighted Fatigue Load described above.

In addition to the fatigue strength, there exists the requirement for maximum static strength. This is achieved by the conventional use of Limit Loads which are the maximum loads which could be sustained without permanent deformation, and Ultimate Loads which are Limit Loads with a 1.5 Safety Factor applied. This defines the maximum static strength required from the component. A further strength requirement is for the Ground-Air-Ground fatigue capability. Each component, in addition to the fatigue spectrum of flight loads, is subjected to a large once per flight variation of load from the maximum positive peak to the maximum negative peak. For example, on rotor components the centrifugal force is varied once per each flight from zero to a maximum, with an additional maximum peak load from the worst maneuver superimposed. This is referred to as the Ground-Air-Ground Loading and is a high load/low cycle condition imposed in addition to the low load/high cycle fatigue requirements.

A further requirement on the Advanced Attack Helicopter is the ability to sustain relatively severe battle damage, and yet be able to fly a limited spectrum safely for a short period of time. This represents a safe completion of mission and return to base. This requires the design to have a large amount of residual strength subsequent to sustaining a high degree of battle damage. In some cases, the complete

loss of a particular load path was assumed, and yet the component had to retain structural integrity on a limited basis. This naturally led to a fail-safe design, with the consequence that large amounts of fatigue damage can be tolerated before failure occurs. Some examples of this are as follows:

Fail-Safety

- The strap retention system can tolerate up to 10 of the 22 straps completely failed.
- A complete loss of any lead lag damper assembly can be tolerated without failure.
- Any one attachment lug on the lead-lag link can be completely failed, and the remaining lugs will carry the loads.
- Any complete spar of the blade box beam can be completely cracked through and the loads can be safely carried by the remainder.
- The blade trailing edge member can be completely failed and the chordwise bending loads can be safely taken by the box beam.

In summary then, the design requirements led to a rotor system which was highly damage-tolerant and fail-safe.

FATIGUE TESTING

The verification of the fatigue life of the main rotor was established by means of a series of fatigue tests on full scale components. As is usual with helicopter components, S-N type testing was used rather than spectrum testing. The difficulty of predicting the dynamic loads prior to flight testing makes the use of spectrum testing inappropriate and difficult to apply. Therefore, constant amplitude testing was used to establish an S-N curve for use in calculating the fatigue life of a part. Since full scale tests are rather complex, only a limited number of specimens were tested, the nominal number being six to be tested at completion, on the Advanced Attack Helicopter.

The objective of the fatigue tests was to determine for each component, or group of components, a number of failure points and, where possible, run outs. A mean curve was then drawn through these test results, and a reduced curve determined by appropriate statistical methods was derived from this. The reduced curve is used to determine the fatigue life in conjunction with the results of the flight loads survey and the spectrum of frequency of occurrence. Additional supplemental fatigue test data was acquired by means of small scale design support tests and coupon data. The description of such tests is beyond the scope of this paper and attention will be confined to the major fatigue tests conducted on full scale specimens. These tests were as follows:

Main Rotor Hub

- Full Scale 4 Arm Fatigue Test
- Single Arm Fatigue Test

Main Rotor Blade

- Root End Fatigue Test
- Intermediate Section Fatigue Test
- Swept Tip Fatigue Test

Each of these tests will be described in some detail, concerning the techniques of testing, specimen design, load applications and results obtained.

MAIN ROTOR HUB FATIGUE TESTS

The main rotor hub fatigue test setup is as shown in Figures 9 and 10. This consists essentially of a complete hub assembly mounted into a large fatigue test fixture. The blade loads are applied by means of dummy blades attached to the lead-lag links, the centrifugal force being applied through straps. The dampers are omitted from the hub assembly and in their place are a pair of actuators which apply the damper loads. Figure 9 shows how the loads are applied to this specimen. Attention is directed to the skewing of a rotational axis of the fixture, which induces a wobble by means of which the flapping motion of the blades is simulated. This test consists of a combination of loads and motions representing the loading which the main rotor hub experiences in flight. As always when a large number of components are tested in a combination, a series of failure modes are encountered. In the test described above failures occurred in lead-lag links, in pitch housings and in individual strap laminates. No failure of the basic hub structure, either the aluminum forging or the centrifugal carry through plates has been experienced to date. Several more specimens are scheduled to be tested, at higher load levels and at higher flapping and coning angles.

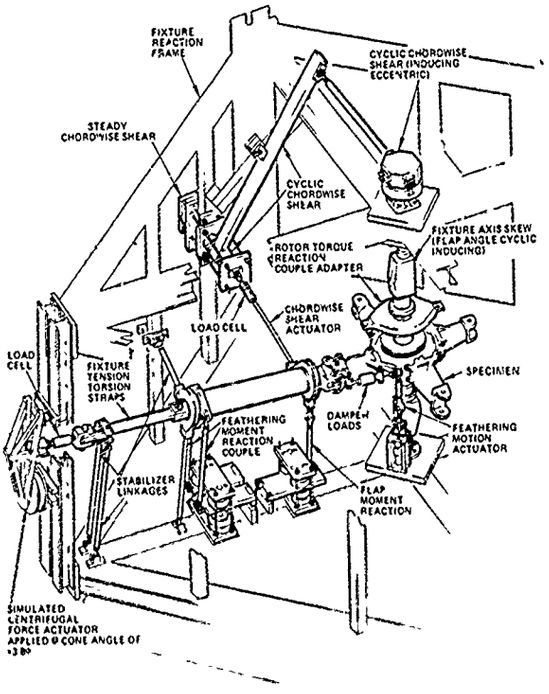


Figure 9. Main rotor hub fatigue test.

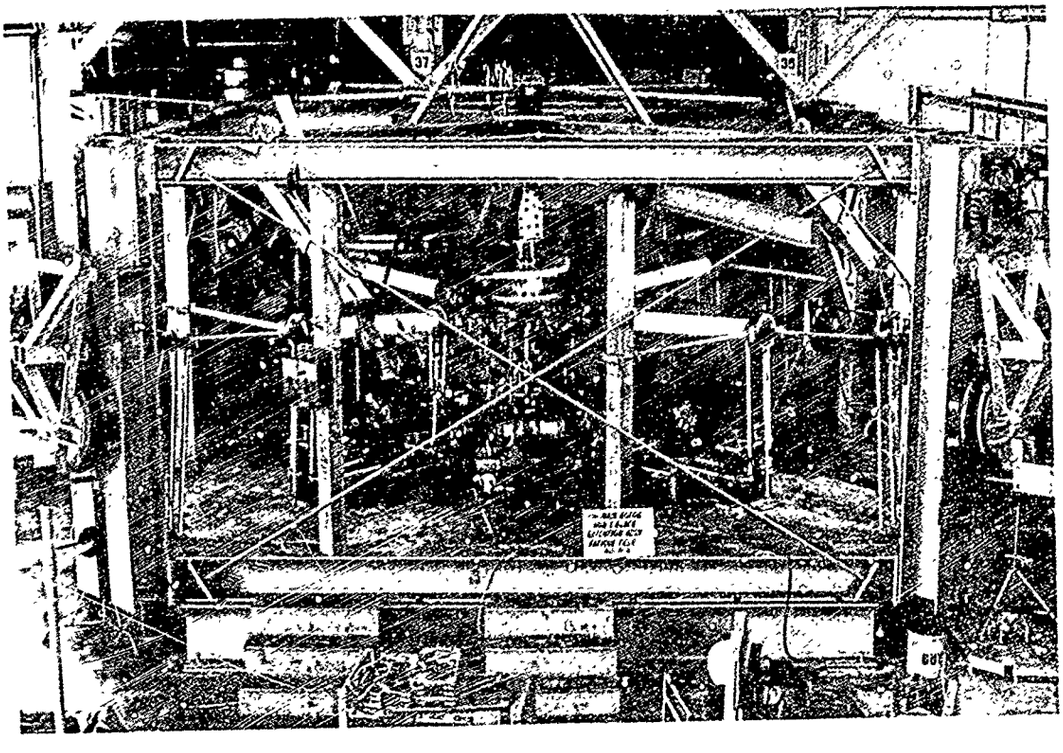


Figure 10. Main rotor hub fatigue test.

In addition to the testing just described, a further set up was used in which a single arm fatigue test was conducted. This is shown in Figure 11. This was designed to obtain accelerated data on the single arm components:

a. Strap Pack Assembly

b. Damper Assembly Attachments

c. Pitch Housing

d. Lead-Lag Link

This test does not provide flapping motion, but instead applies the alternating loads and centrifugal forces applied by the root end of the blade. It achieves more rapid results than the main hub set up, due to its simplicity, and has been very important in determining failure modes of the damper components and pitch housing. These have led to significantly better understanding of the fatigue problems associated with these components and have resulted in several important improvements. During the course of this testing, no failures of the strap packs have been encountered. This is attributable to the fact that this particular test does not apply motions to the strap packs other than the small amounts due to structural deflections, and therefore does not challenge the straps in fatigue. Figure 12 shows a fatigue failure of the pitch housing. The diagonal nature of the crack indicates a torsional mode of failure, due to pitch link loads reaction to the torsional moments from the blade. Figure 13 shows another fatigue failure of the pitch housing. This time the failure is more indicative of the interaction of local stresses feeding in the damper lug loads and general bending and torsion of the major section.

MAIN ROTOR BLADE FATIGUE TESTING

There were three large scale component fatigue tests conducted on the main rotor blade, these being respectively:

a. Main Rotor Blade Root End Fatigue Test

b. Main Rotor Blade Intermediate Section Fatigue Test

c. Main Rotor Blade Swept Tip Fatigue Test

The first of these, the blade root-end fatigue test, was conducted on a double-ended fatigue specimen as shown in Figure 14. The test set up is as shown in Figures 15 and 16. Basically, the double-ended specimen is pulled at each end to simulate centrifugal force and then loaded in the center with an actuator to produce the flapping and chordwise loads across the blade root-end. The centrifugal force loading devices and the chordwise centerline spring system were pneumatically operated air cell devices operating

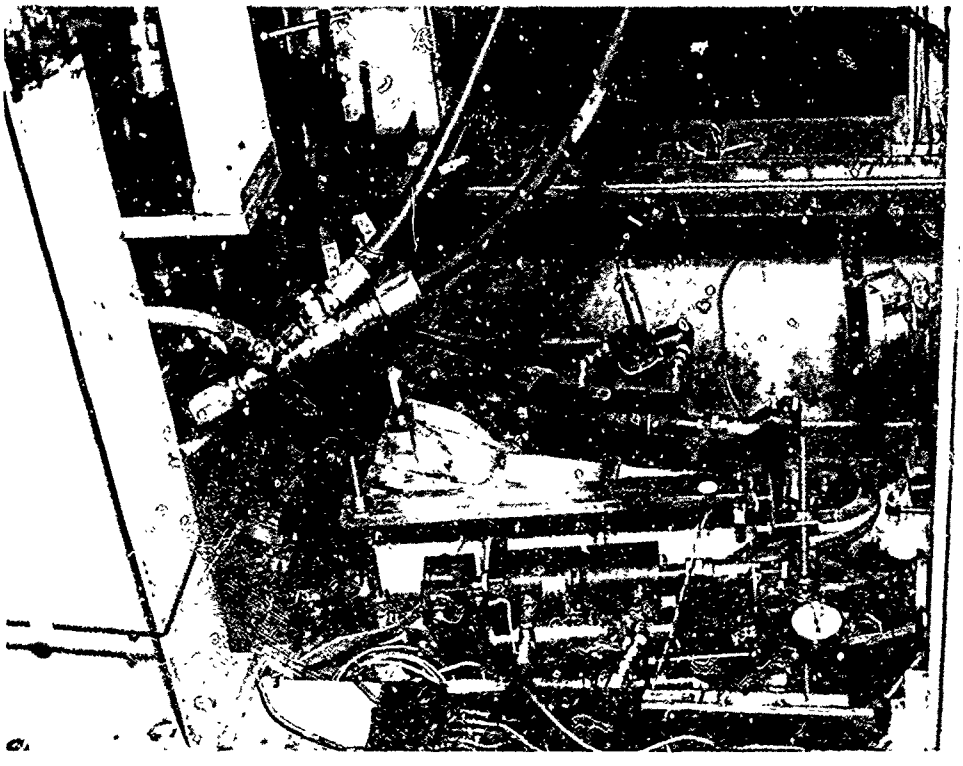


Figure 11. One arm fatigue test.

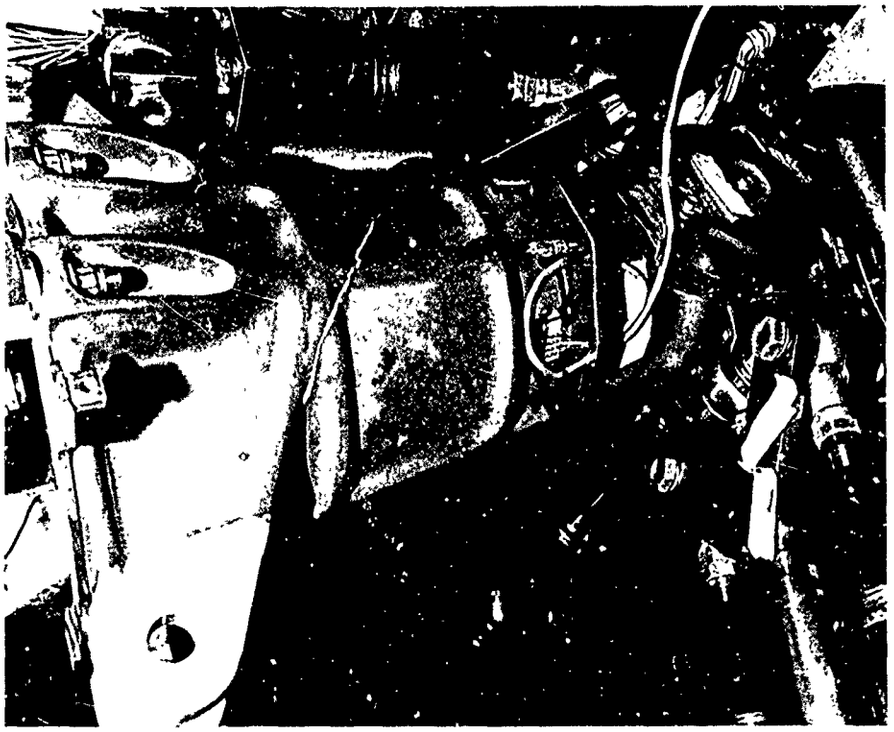


Figure 12. Pitch housing fatigue test.

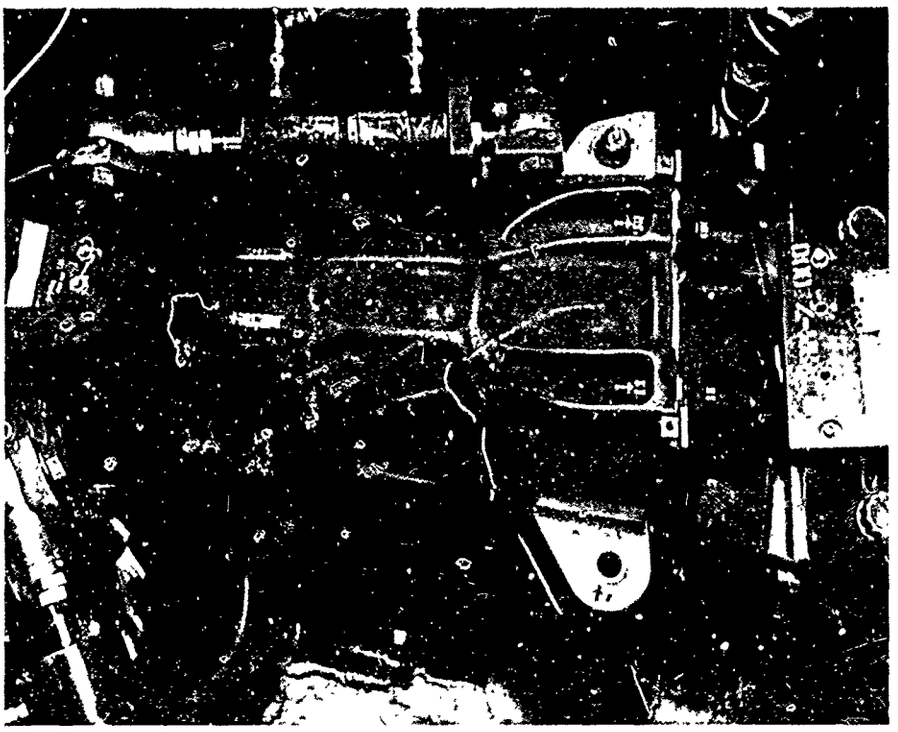


Figure 13. Pitch housing fatigue test.

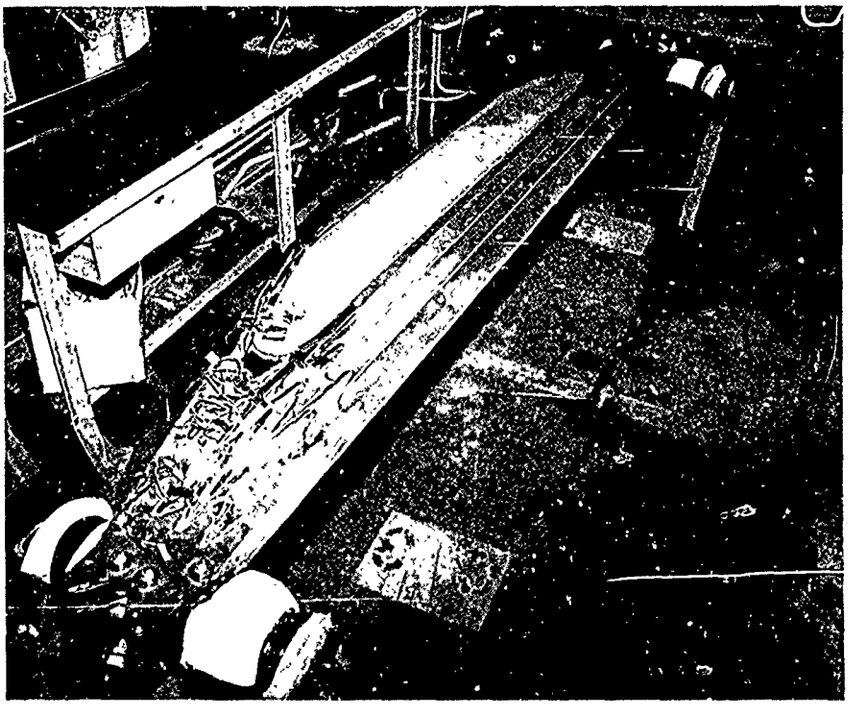


Figure 14. Main rotor blade root end test specimen.

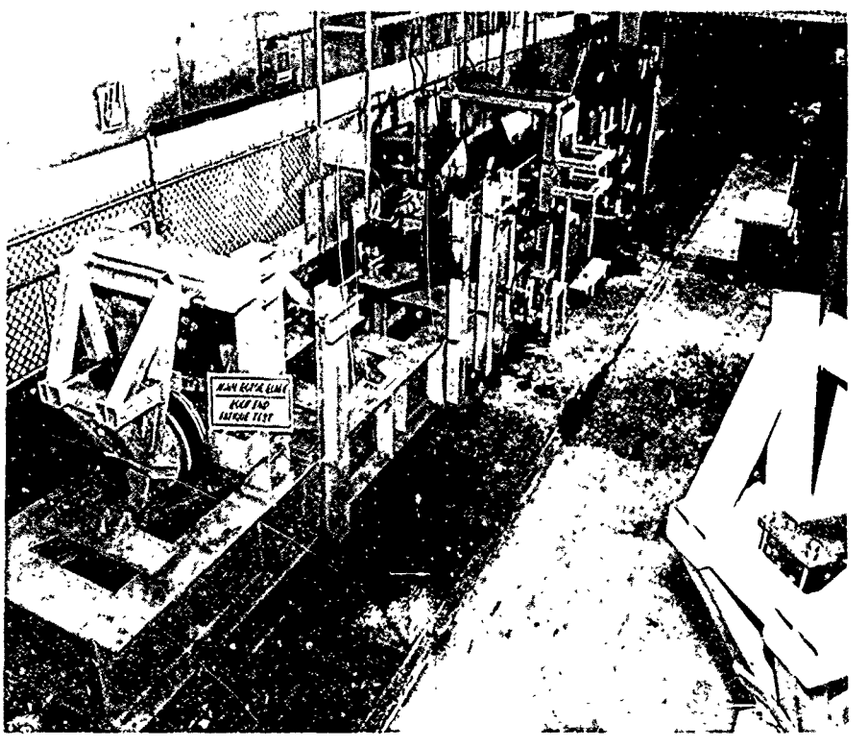


Figure 15. Main rotor blade root end fatigue test.

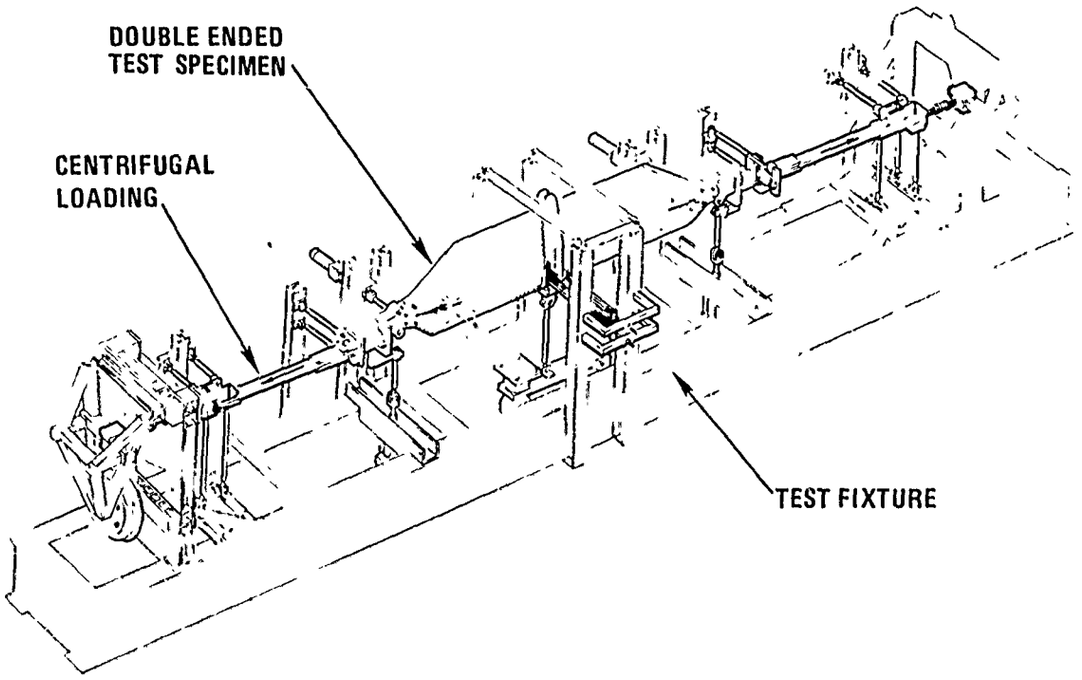


Figure 16. Test setup, main rotor blade root end fatigue test.

by means of manual air regulators. Flapwise and chordwise motion actuators had linear feedback, closed loop servo control systems that were operated by a sinuscidal signal input from a signal generator. An electrical counter operated by the signal generator was used for counting load cycles. The centrifugal force load cells and the torsion reaction links were tubular load carrying members instrumented with axial strain gage bridges. Each of the fatigue test specimens was instrumented with strain-gage bending bridges and calibrated by subjecting it to known moments in the axis system of the particular blade station being calibrated. The strain-gage bending bridge locations on the test specimens were identical to the locations on the flight test blades so that a direct comparison of loads could be made for the final analysis. The output of centrifugal force load cells, torsion links, and the specimen bending bridges were recorded by direct-writing pen recorders and visually monitored during the test. The load distribution was similar to that measured in flight. In the testing to date, no failures of the root-end joint have been encountered. However, several minor failures such as doubler delamination and cracking of a transition area have resulted in some design improvements. Testing is currently being continued to establish a higher S-N curve for this component.

The second fatigue test consists of a specimen simulating the blade constant section outside the doubler reinforcement area. This specimen is shown in the test set up in Figure 17. This test again, simulates the effect of centrifugal force by a straight pull, and the chordwise and flapwise moments are applied by means of a pair of actuators in the middle of the specimen. The two centrifugal force loading devices (one at each end of the fixture) used a total of eight air cells (springs) which were interconnected to one manually operated pressure regulator. The other load measuring elements were torque reaction links with instrumented and calibrated thin wall tubular sections. The two hydraulic actuators controlled by MTS Systems closed loop, displacement feedback, servo systems operated from a signal generator circuit. An electric counter activated by the electrical circuit was used to record loading cycles. Each specimen had calibrated strain gage bending bridges at the specimen centerline. Crack detection wires were placed on each specimen at appropriate critical locations. The output of the centrifugal force cells, the torsion reaction links, and specimen bending bridges were recorded by direct-writing pen recorders. Testing to date resulted in no failures due to basic fatigue loading and a satisfactory S-N curve was obtained which indicated that this part has an infinite life.

The swept tip fatigue test is shown in Figure 18 and the specimen is illustrated in Figure 19. The test specimen was a complete section of the main rotor blade swept tip, beginning at blade Station 239.95 and extending to the blade tip (Station 287.95). To assure valid load simulation and stress distribution, an adjustable whiffletree system was used to distribute the load in the required proportion to both balance weight supports and to the swept tip blade structure. The load was applied by a horizontally mounted, closed loop electrohydraulic actuator with load feedback. An electronic oscillator was used to drive the actuator valve sinusoidally between zero and peak tensile loads. Loads were monitored throughout the test by load cells located at each tip weight loading bar and at the actuator. Failsafe crack detection wire and limit switches were used for test fixture shutoff in the event of specimen failure. Initial load conditions for each specimen were maintained until failure, or until three million cycles were achieved.

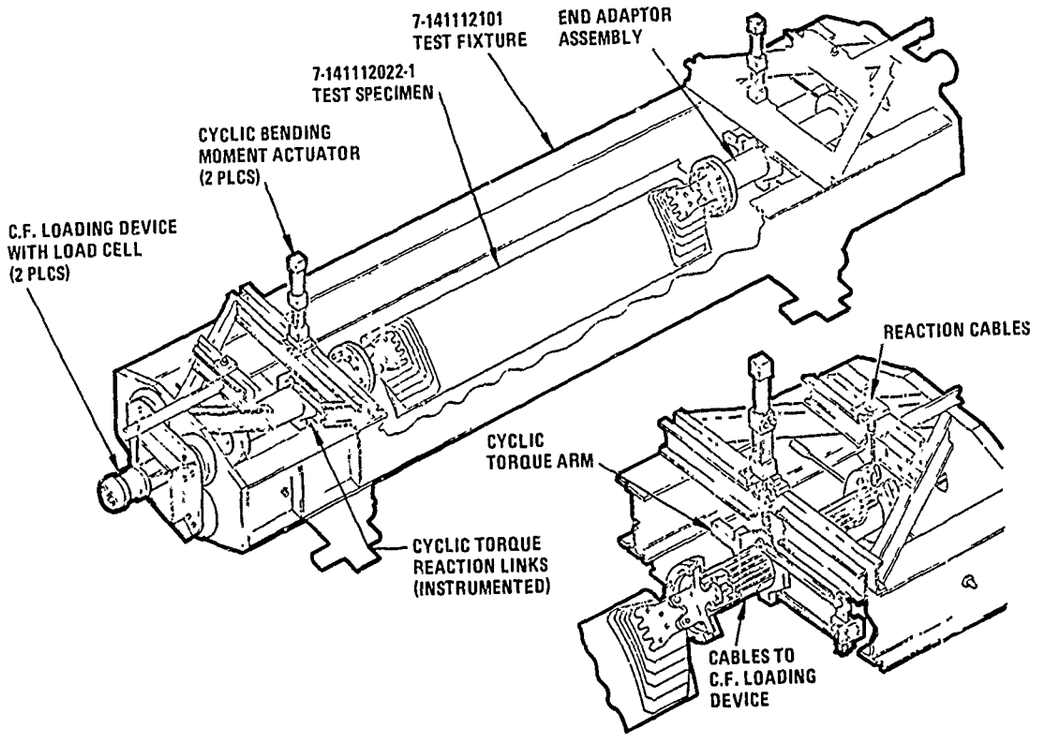


Figure 17. Typical test setup, main rotor blade intermediate section fatigue test.

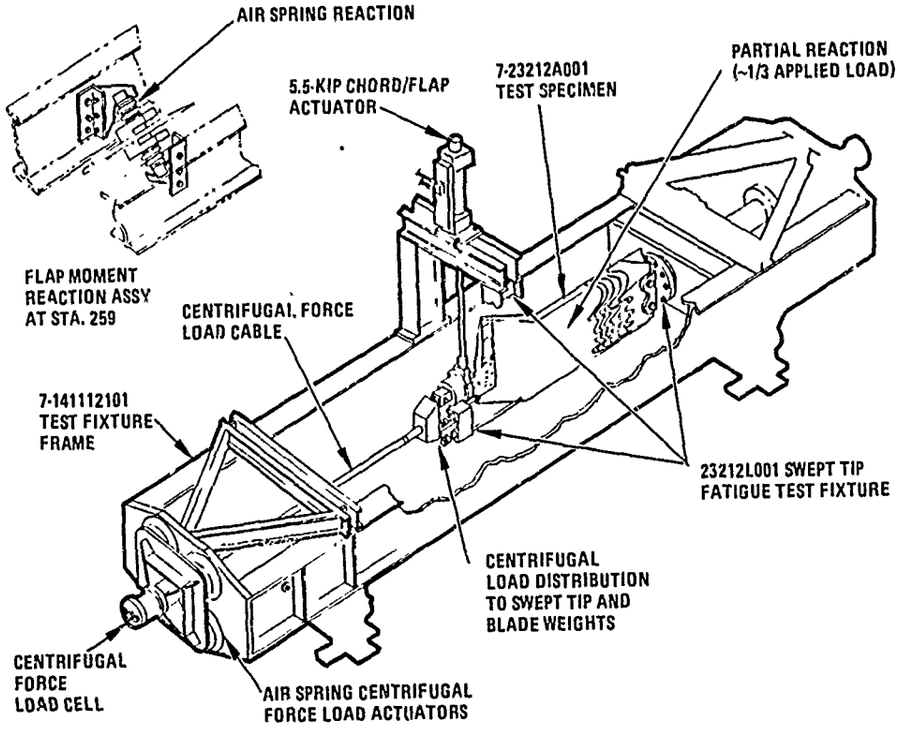


Figure 18. Fatigue test setup, blade swept tip section.

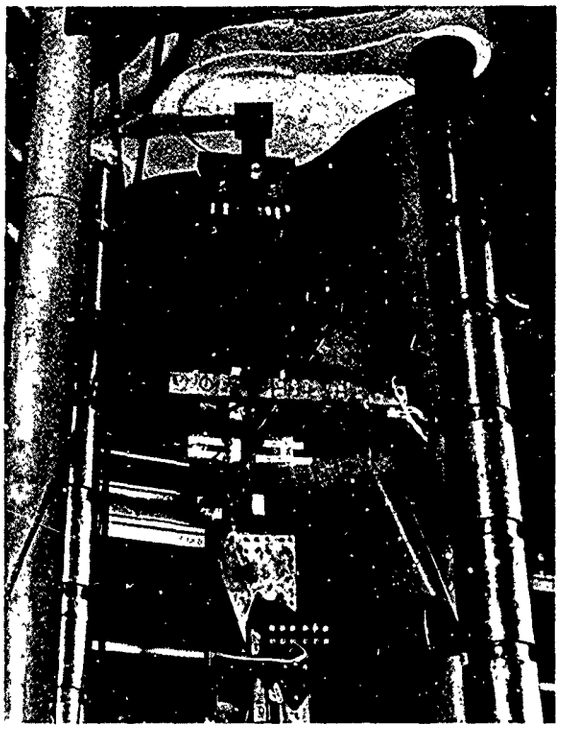


Figure 19. Swept tip specimen.

If three million cycles were obtained, the test was continued with increased cyclic loads to generate valid S-N fatigue data. Loads on subsequent specimens were based on previous specimen performance to ascertain blade tip fatigue strength. Testing was continued after the initial failure mode was encountered in order to ascertain crack propagation characteristics. There are several materials in this particular component - the basic stainless steel of the blade, an Inconel outer cover, and titanium fittings. Fatigue failures occurred in the cover and the fittings, but not in the basic blade section. S-N curves based on the material curve shapes were obtained for these components.

FURTHER TESTING

In each case, the inception of a detectable fatigue crack was defined as a failure point and used as such for the derivation of an S-N curve. However, in nearly all instances, the specimen continued to carry load, due to the nature of the highly damage tolerant design. Therefore, in order to obtain crack propagation data, testing was in many instances continued, with the loads set at the levels which would be encountered in normal flight at cruise speed. In this way, valuable data was obtained as to the margin of safety in fatigue for safe operation with a part already cracked. This is illustrated in Figure 20 on the blade root-end where a fatigue crack in the forward portion of the blade root-end was monitored through the application of many cycles. The blade leading edge has since been modified to improve this area.

Also, during the fatigue testing of the main rotor hub there were instances of lug failures in the lead-lag links. However, due to the fail-safe design of this component, the loads could still be carried through the joint and testing was continued. The results obtained indicate the high success of the fail-safe design. A further example of the fail-safe damage tolerant design was the fatigue testing of a ballistically damaged blade section. This is shown in Figure 21 which shows a blade which had been fired upon by a high-explosive round. As can be seen, a large amount of damage has been sustained, but the remaining section carried fatigue loads equal to 5 hours of flying. This fatigue test is shown in Figure 22 where the specimen is subjected to centrifugal loading with the bending moments superimposed. No discernible crack growth was observed for approximately 22,000 cycles which is equivalent to over 1 hour of flight, and crack growth was small up to 25,000 cycles. In the end, the equivalent of over 5 hours of flight (approximately 90,000 cycles) was applied, at which point the test was discontinued. However, even then, the specimen continued to carry the full application of load (Reference 1).

Mention was made in the early part of this paper of the strap retention system of the rotor. During the testing of the main rotor hub assembly, several laminate failures occurred in the strap packs. In order to obtain accelerated results, a subsidiary fatigue test was devised as shown in Figures 23 and 24. This test applies centrifugal load and chordwise bending and then superimposes the motion of the straps due to flapping and feathering. Testing was conducted at several combinations of loads and motions, and information was obtained regarding initial laminate failures. Subsequently, the testing continued in order to obtain data on the rate of propagation of laminate failures and the residual strength of the str.t

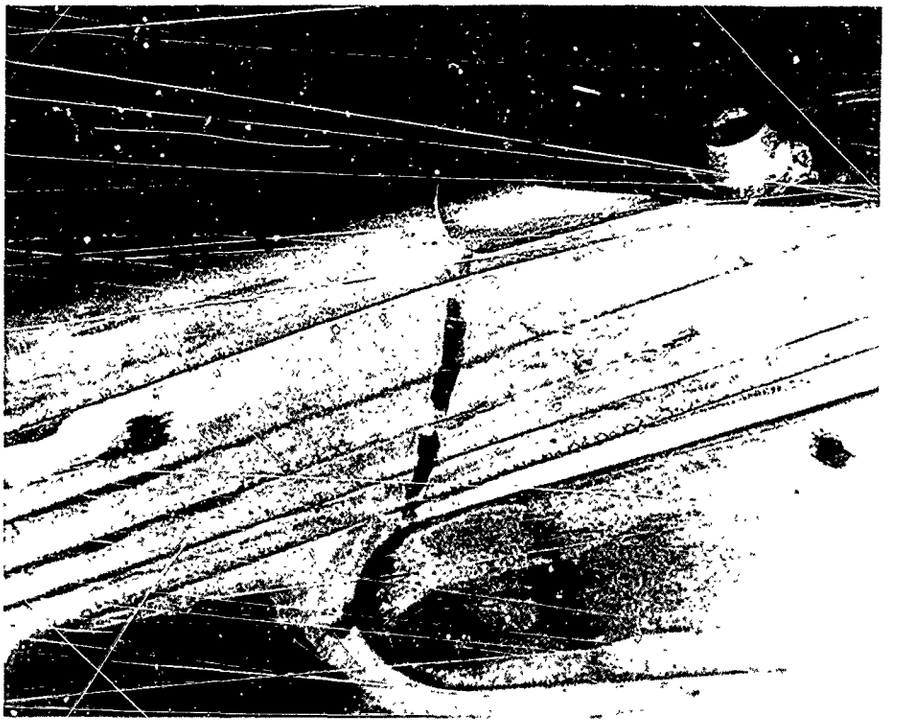


Figure 20. Root end fatigue test specimen failure.

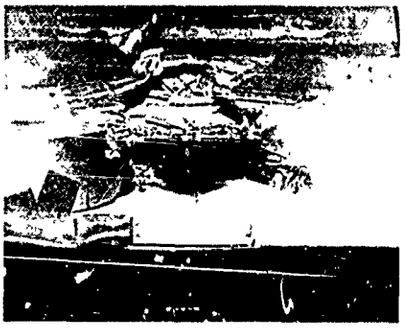


Figure 21. Exit damage prior to fatigue test.

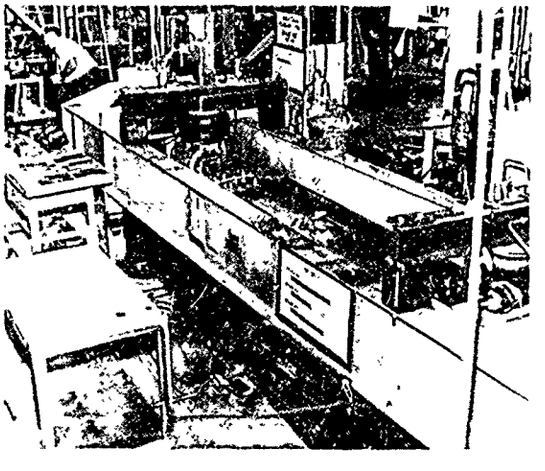


Figure 22. Blade specimen installed in fatigue test rig.

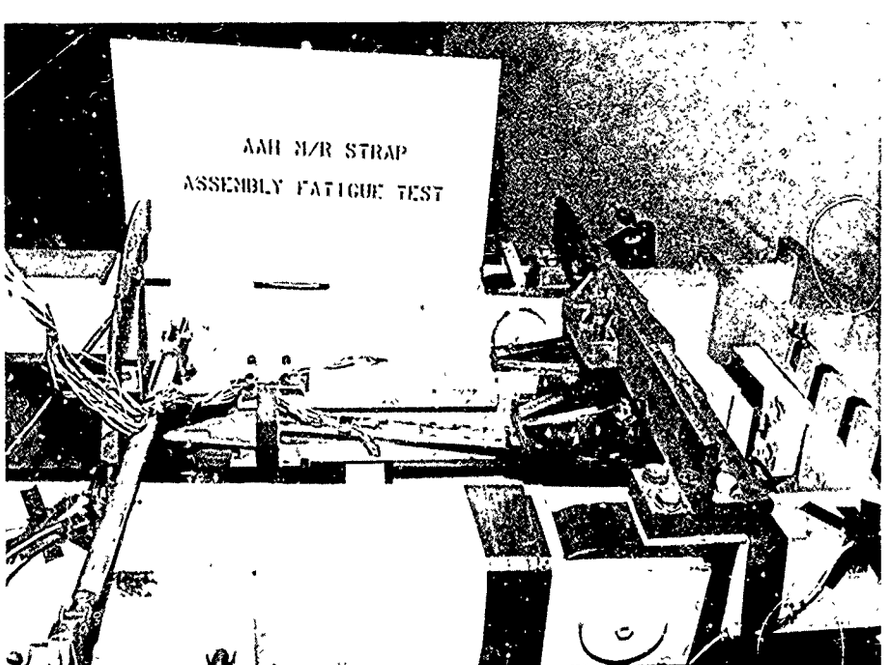


Figure 23. Strap fatigue test.

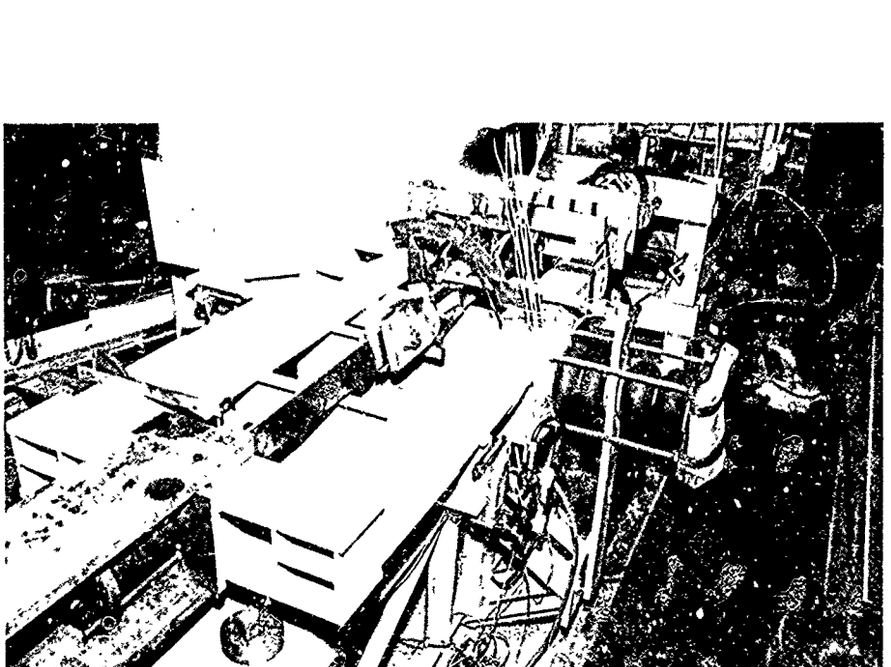


Figure 24. Strap fatigue test.

packs. During this testing, results were obtained which showed that the strap pack can sustain loads and motion equivalent to normal rotor speed condition with more than ten laminates failed out of a total of twenty-two. At that point, the elongation of the straps was such that the centrifugal unbalance of the blade on that arm would have given indication of the failure, so the test was discontinued.

Mention was made of the GAG (Ground-Air-Ground) cycles which is a once-per-flight excursion of loads to a peak value and then removal of load, or even slight reversal. In the case of the main rotor, the main loads imposed by such a condition are centrifugal to a peak value representing 104 percent normal rpm. During the testing of the main rotor hub, the fixture described earlier (Figure 9) was used to apply a series of GAG cycles.

Once every 12 seconds, the load was varied from zero to a full centrifugal force equal to that obtained at 104 percent rpm. Then a cycle of loads was obtained by rotating the hub at a wobble angle giving the equivalent of a maneuver. This was sustained for a total of 39,000 cycles representing 13,000 hours, successfully demonstrating the capability of the retention system for the GAG cycle. Similar testing was also conducted on the blade root-end specimen and on the swept tip section.

CONCLUSION

1. The fatigue testing of the main rotor on the YAH-64 Advanced Attack Helicopter was carried out on several full scale tests.

2. Testing was S-N type, constant amplitude loading, to obtain allowable fatigue curves. Figure 25 shows a typical S-N curve.

3. GAG (Ground-Air-Ground) testing was also demonstrated on the main rotor blade retention system, the blade root-end, and the swept tip.

4. Damage tolerance information was obtained by continuation of fatigue tests after first detection of crack initiation.

5. A specimen of the main rotor blade after having been damaged ballistically was fatigue tested, demonstrating over five hours of normal operating life.

The success of this fatigue testing to date, indicates that the main rotor blades and hub of the Advanced Attack Helicopter have satisfactory fatigue strength for all conditions of the operating spectrum. It also demonstrates that the design is highly damage tolerant, has many fail-safe features, and is highly survivable.

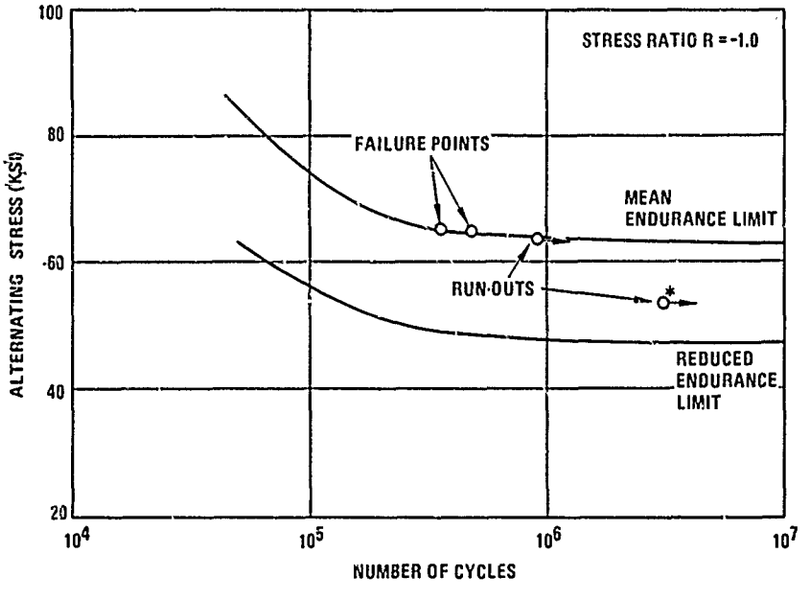


Figure 25. Typical S-N curve.

ACKNOWLEDGEMENTS

The author gratefully acknowledges the assistance of Mr. Mal Symonds, Chief of Rotor Stress Analysis and Mr. George Deveaux, Manager of Structural Testing, of Hughes Helicopters, in the preparation of this paper.

REFERENCES

1. Malcolm F. Symonds, "The Damage Tolerant Design of the YAH-64 Main Rotor Blade." Presented at the AHS/NASA Ames Conference on Helicopter Structures Technology, November 16-18, 1977.

FATIGUE TESTING OF COMPOSITE ROTOR BLADES

by

F.Och

Messerschmitt-Bölkow-Blohm GmbH

Postfach 801140

8000 München 80, Germany

SUMMARY

MBB's fatigue testing methodology for composite rotor blades, established and proved during the last 20 years, is based on nonlinear regression analysis.

An equation, proposed by WEIBULL, with four material-dependent parameters is used to derive mean and working S/N curves between static strength and endurance limit. To calculate a scatter factor, the fatigue failure load for a given number of cycles is chosen as statistical variable.

The fatigue testing programme is comprised of testing coupons, cut out of production blades, to establish basic S/N curve shapes both for fibre and matrix failure. Coupon testing includes temperature/humidity preconditioning effects and the effect of test temperature as well as service usage on the fatigue strength of unidirectional glass fibre composite.

Full scale fatigue tests are conducted with root end and aerofoil sections. These tests include effects of ballistic impact damage and long term environmental effects incurred during service usage in different climatic zones.

It was found by the tests that the S/N curve shapes and scatter factors determined from coupon data could be applied to the full scale specimens. A reduction in interlaminar shear fatigue strength was found with coupons, after artificial environmental exposure. With coupons, cut out of used blades, no degradation could be found, as it is with full scale specimens.

Composite rotor blades show excellent damage tolerance characteristics, where damage will be indicated by changes in the eigenfrequencies, due to decreasing stiffnesses, long before the structural integrity will be questioned.

LIST OF SYMBOLS

A	ratio of stress amplitude to mean stress
N	cycles to failure
R	ratio of minimum stress to maximum stress
a,b	material-dependent parameters
j_p	reduction factor
n	number of test specimens
s	oscillatory stress
s_N	fatigue failure stress for a given number of cycles
s_u	static strength
s_∞	endurance limit
s^*,x	material-dependent parameters
y,z	material-dependent parameters
α,β	material-dependent parameters
c	scatter factor

1. INTRODUCTION

Our activities in fibre composites for primary structures began in the middle 1950s. The high elasticity of glass fibre composites and their high specific static and fatigue strength in combination with the ability of composite materials to "tailor" the mechanical properties became evident. These advantages, as well as the flexibility to achieve the desired geometry and the ease of fabrication led to the successful development of the hingeless rotor "SYSTEM BÖLKOW", of which the glass fibre rotor blades are an essential design feature. This rotor system can be regarded as a quasi-articulated rotor, the flapping and lagging hinges of which, are replaced by elastic deformations of the composite blades [1].

Up to now, more than 500 BO 105 helicopters, equipped with such a rotor system, have been delivered to customers and next year the BK 117 with the same rotor system will follow.



Fig.1 BO 105 Production Version



Fig.2 BK 117 Prototype

The operations of the BO 105 helicopters in civilian as well as in military missions, have accumulated over 1 000 000 main rotor blade and 500 000 tail rotor blade hours in the past ten years, with the fleet-leaders approaching 10 000 flight hours on main rotor blades.

As the BO 105 was the first production helicopter with composite rotor blades, fatigue testing techniques and methodologies had to be established and proved for certification purposes.

The successful application of composites requires a detailed knowledge of the influence of the fabrication technology and service environment on the material system. At MBB fatigue testing of composite rotor blades therefore started with coupon testing to provide an adequate design data base. Mechanical properties of composites generally depend on

- fibre and matrix properties
- fibre content and orientation
- curing temperature and time
- moisture absorption
- testing temperature
- environmental effects .

In order to take care of any influence on mechanical properties induced by the manufacturing process, the coupon specimens were cut out of production blades and the blades' fatigue strength assessment was performed on full scale components [2].

2. BLADE DESCRIPTION

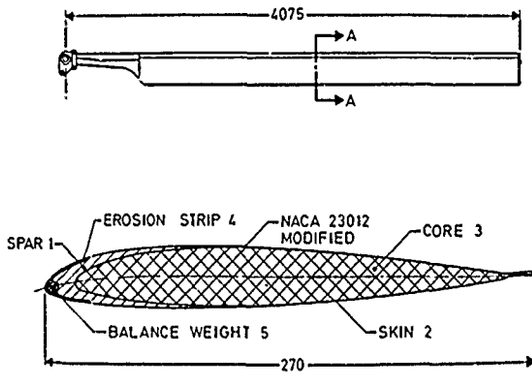


Fig.3 BO 105 Main Rotor Blade

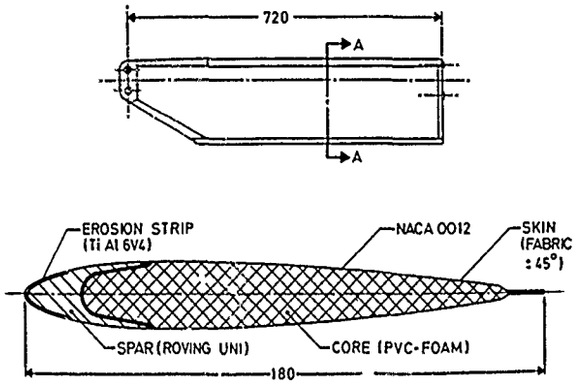


Fig.4 BO 105 Tail Rotor Blade

As main and tail rotor blades are similar in design, manufacture and constituent materials, we restrict ourselves to the main rotor blade.

The aerofoil section has a 270 mm chord modified NACA 23012 airfoil. To match the first inplane natural frequency, the root end area has a reduced chord ("swan neck"). The BO 105 blade consists of the following structural parts, having various functions:

- spar, made of unidirectional E-glass, contributes to flapwise (77%), chordwise (40%), and torsional (32%) stiffness and reacts centrifugal forces as well as bending and twisting moments;
- skin, made of ± 45^0 orientated E-glass fabric, contributes to chordwise (52%), torsional (44%) and flapwise (14%) stiffness and reacts twisting and bending moments;
- core, made of modified PVC foam, contributes to torsional stiffness (12%) and prevents skin buckling when bending and twisting moments are applied;
- erosion strip, made of TiAl6V4, contributes to torsional (12%), flapwise (9%) and chordwise (8%) stiffness, joins the upper and lower skins and provides the necessary leading edge protection;
- balance weight, made of lead, to position the centre of gravity near the quarter chord line.



Fig.5a Rotor Blade Production Process (Skin Lay-Up)





Fig.5b Rotor Blade Production Process (Roving Tape Lay-Up)

The production process starts with hand lay-up and impregnation of the skin in an upper and lower female aluminium mould. Roving tapes of slightly more than twice the blade length are impregnated by special equipment. These tapes are then placed in the moulds onto the skin in such a way that the glass fibres run from the blade tip to the root end area, around the attachment bushing, and back to the blade tip. The tapes are pressed together and against the skin with simple tools, removing any entrapped air, and producing a reasonably homogenous spar which has practically no voids. The inside profile of the spar is adjusted and checked by templates guided by milled grooves in the mould face. The foam core and the balance weight are then inserted into the lower mould. The upper mould is placed upon the lower mould, the two halves are pressed together and heated up to curing temperature which is 105 ± 3°C for 8 hours. There is only one curing cycle necessary for the structural elements of the blade, i.e. spar and skin. The blade is finished by bonding the erosion strip, the tip cover as well as the torsion caps in the root end area and potting it into the clamshell type titanium root end fitting.

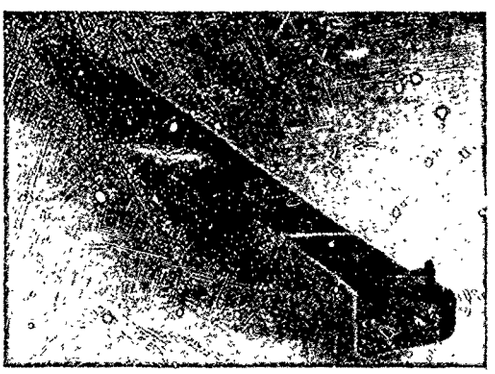


Fig.6 GFC Main Rotor Blade

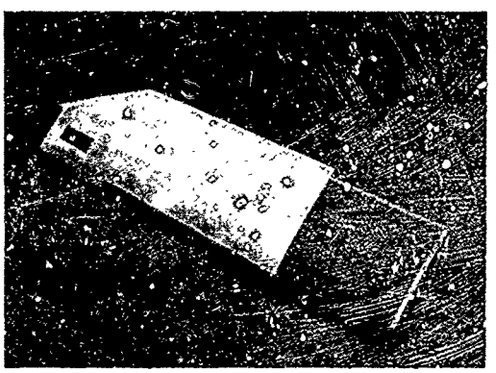


Fig.7 GFC Tail Rotor Blade

3. LOADING SITUATION

It is obvious that when a blade rotates, it is subjected to centrifugal forces cyclically applied with each start-stop cycle.

For hingeless rotors i.e. without flapping hinges it is possible to transfer high moments from the blades to the hub and the fuselage, producing high moment loading at the blade root area. This moment loading can be reduced by coning the hub arms and thus producing an unloading moment from the centrifugal forces. Normally the precone angle will be chosen for zero moment at design rotor thrust. Other thrust conditions will result in corresponding moments and it should be pointed out that these moments, primarily resulting from cyclic control inputs, are the basis of improvements in handling qualities of hingeless rotor systems. Trim conditions which need a rotor produced moment to overcome for instance c.g.-travel or slope landing conditions, require an alternating first harmo-

nic moment in the rotating system for the hingeless rotor.

Higher harmonic blade loads and moments at the blade root result from unsteady aerodynamic flow conditions in forward flight. For a dynamically well-tuned hingeless rotor these higher harmonic moments are relatively low compared with the first harmonic moments needed for trim or flight manoeuvres.

The highest loaded section of the blades of a hingeless rotor is therefore the blade root attachment area. To correspond closely to actual flight conditions, the following loading has to be considered:

- centrifugal forces;
- flapwise bending moments;
- chordwise bending moments;
- torsional moments .

4. FATIGUE STRENGTH PHILOSOPHY

Life prediction methods which have been established and proved successful at MBB's helicopter division consist of three basic steps: (1) the estimation of the magnitude and frequency of occurrence of the loads that will be encountered during the operational life of the structure; (2) the estimation of the components fatigue strengths, taking into account scatter, size and shape effects, surface finish and environmental influences; and (3) the combination of the interactive effects of these loads and strengths by means of the "Linear Cumulative Damage Hypothesis" (Miner's rule) [3].

As fatigue tests should be conducted over a range of oscillatory stresses or loads at steady stresses or loads representative of those occurring in flight [4], the following questions arise: (1) which S/N curve shape shall be applied to these data; (2) how can the influence of steady stresses be taken into account; (3) how to determine the scatter in fatigue strength to arrive at a working S/N curve.

The simplest method to evaluate a mean curve is to draw an averaged curve by eye. A more exact method, however, is to formulate an analytical expression for S/N curves and to evaluate the free parameters by regression analysis. At MBB's helicopter division the following formula, proposed by WEIBULL, is used:

$$s = s_\infty + (s_u - s_\infty)/e^{\alpha(\log N)^\beta}. \qquad (1)$$

This formula allows the establishment of mean and working S/N curves between static strength $s_u(N = 1)$ and endurance limit $s_\infty(N \to \infty)$.

For modern helicopters the minimum required fatigue life for all dynamic components is at least 5000 hours, leading to minimum load cycles of 10^4 even for such components which are loaded by start-stop cycles only. In this case, a simplified formula can be drawn from equations (1) by setting $\beta = 1$ which leaves:

$$s = s_\infty + (s^* - s_\infty)/N^x . \qquad (2)$$

x may be chosen as 1/2, 1/3 and 1/6 for steel, light alloys and fibre composites, respectively.

The influence of steady stresses may be taken into account when replacing s^* and s_∞ in equation (2) by the following expressions:

$$s^*(A) = s^*/(1 + b/A^z) \qquad (3)$$

$$s_\infty(A) = s_\infty/(1 + a/A^y), \qquad (4)$$

where the material-dependent parameters a, b, y and z must also be evaluated by regression analysis.

To establish a working S/N curve, statistical methods have to be applied, as fatigue strength is of a statistical nature. In order to determine scatter, a statistical variable, a function of s or N, must be selected. As the number of cycles N yields infinite scatter in the region of the endurance limit, it is not appropriate and we have chosen the fatigue strength for a given number of cycles s_N as statistical variable. Normally we use $N \to \infty$ i.e. s_∞ or $N = 1$ i.e. s_u or s^* respectively. The validity of normal distribution of $\log s_N$ is verified and the fatigue strength therefore can be characterized by its median and standard deviation.

In arriving at a working S/N curve, we usually use a survival probability of 99.9% and a confidence level of 95% which yields the following reduction factor:

$$j_p = e^{3.090 + 1.645/\sqrt{n}} \qquad (5)$$

5. FATIGUE TESTING PROGRAMME

The fatigue testing programme is comprised of testing coupons, cut out of production blades to take care of any influences of the manufacturing process, and full scale sections of the blade .

Fibre composites may fail either by a fibre failure or by a failure of the matrix or the interface of fibre and matrix. Two different types of coupon specimens are therefore fatigue tested to establish basic S/N curve shapes both for fibre and matrix failure. The specimens of unidirectional E-glass are cut out of the blade spar from various stations and differ mainly in the length to height ratio, relating to bending and shear fatigue strength respectively. Coupon testing includes temperature/humidity preconditioning effects, both unloaded and loaded, and the effect of test temperature as well as service usage.

Full scale fatigue tests are conducted with the following sections of the blade:

- root end section;
- transition root end/aerofoil section;
- aerofoil section.

These tests include effects of ballistic impact damage and long term environmental effects incurred during service usage in different climatic zones.

As the full scale components never fail catastrophically, which is typical of composite materials, in some cases the testing is continued after initial damage to establish crack propagation rates and to demonstrate damage tolerance characteristics.

Bending Fatigue Tests

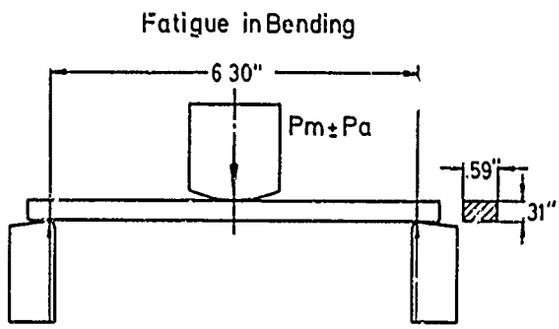


Fig.8 Bending Fatigue Test Set-Up

Three point bending of relatively slender specimens (Fig. 8) leads to high stresses in the glass fibres on the upper and lower surface, thus producing fibre failure. Damage starts on the surface with the highest tension loading by delamination and fibre cracking and propagates into the specimen causing a decrease in the bending stiffness. Crack propagation rate depends on the stresses applied, but is very low compared with metals. In this way we conducted tests with different stress ratios ($-1 \leq R \leq 0.5$).

The data points and the regression curve for a stress ratio of R = 0.2 are presented in Fig. 9. Results of specimens (marked with triangle) which were cut out of a rotorblade, in service for 2600 flight hours in the Gulf of Mexico region, are well within scatter. The results of all bending fatigue tests carried through up to now on E-Glass with 55% fibre content are presented as a Haigh diagram in Fig. 10.

We have also fatigue tested notched long beam bending specimens with different notch shapes and found no stress concentration effects. The results fit reasonably into unnotched data, when the strength is referred to net section. Cracks started at the notches and propagated parallel to the fibres, thus not effecting the net section.

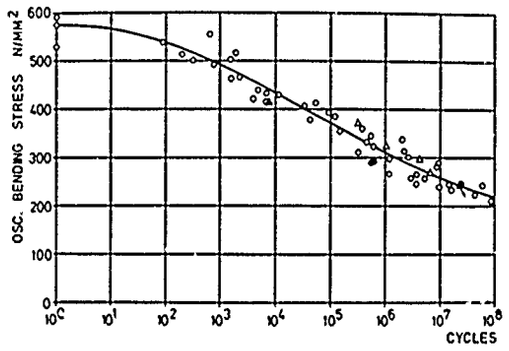


Fig.9 Bending Fatigue S/N Curve

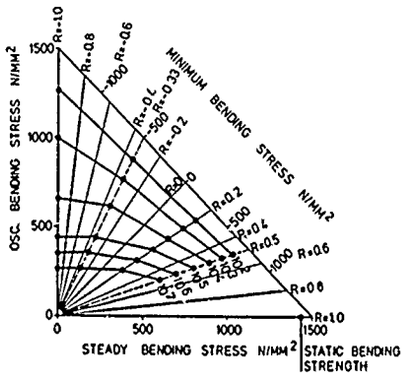


Fig.10 Bending Fatigue Haigh Diagram

Shear Fatigue Tests

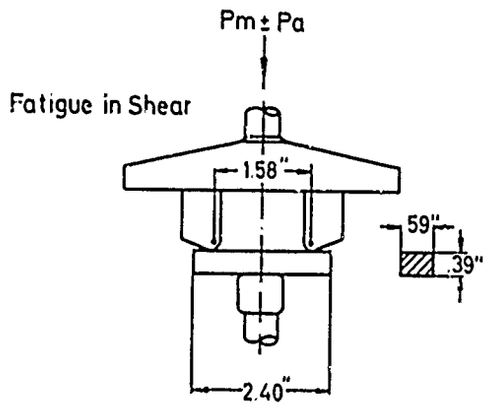


Fig.11 Shear Fatigue Test Set-Up

Three point bending of shorter specimens (Fig. 11) leads to high interlaminar shear stresses in the neutral plane of the specimen which produces matrix or interface failure. Shear crack propagation was observed to be as fast as with metals. Tests were conducted with different stress ratios ($-1 \leq R \leq 0.5$). The data points and the regression curve for a stress ratio of R = 0.11 are presented in Fig. 12. Results of specimens (marked with triangle) which were cut out of a rotorblade, in service in the Gulf of Mexico region for 2600 flight hours, are well within scatter. The results of all shear fatigue tests, carried through up to now, are presented as a Haigh diagram in Fig. 13.

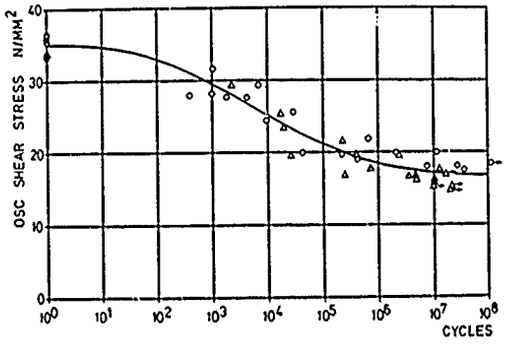


Fig.12 Shear Fatigue S/N Curve

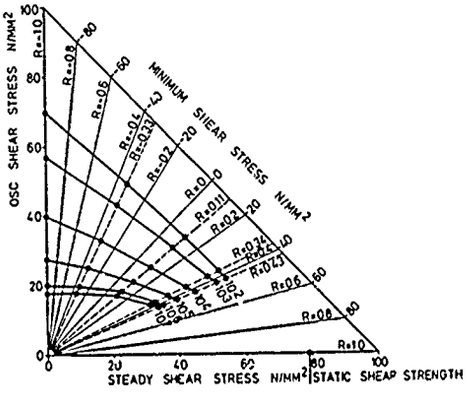


Fig.13 Shear Fatigue Haigh Diagram

As environmental exposure is expected to mainly influence the matrix and the interface of fibre and matrix, short beam bending tests were conducted to evaluate both temperature and humidity preconditioning effects, unloaded and loaded, on the shear fatigue strength. The specimens were exposed to the following three variations of simulated weathering:

Climatic Condition No. 1:

x hours at 90°C and 70% relative humidity
(x = 10 resp. 100 resp. 1000)

Climatic Condition No. 2:

1 cycle = 168 hours
= 4 · (15 hours at ultraviolet radiation +
+ 9 hours water submersion) + 72 hours at 70°C

Climatic Condition No. 3:

1 cycle = 168 hours
= 4 · (10 hours at 72°C and 92% relative humidity +
+ 14 hours at -40°C) + 10 hours at 72°C and 92%
relative humidity + 62 hours at 23°C and 50%
relative humidity .

Fig. 14 summarizes the endurance limits (values at 10^8 cycles and R = 0.11) of each preconditioned data set plotted versus number of cycles or hours of climatic exposure. The difference of the three climatic conditions is insignificant within the exposed cycles and after about 5000 hours of exposure, there was an average 12% reduction in endurance limit.

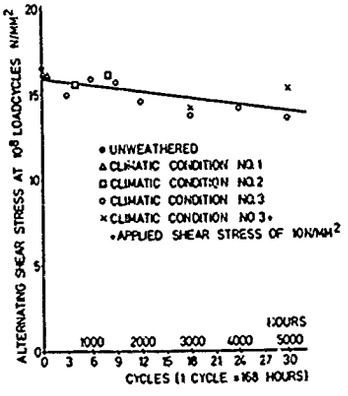


Fig.14 Weathering Effects on the Shear Fatigue Strength

Short beam bending tests were also conducted at -40°C, 30°C and 70°C respectively to evaluate the effect of test temperature on static and fatigue shear strength. From the data of Fig. 15, it is observed that test temperature effects both static and fatigue strength by the same amount, i.e. about 25% higher shear strength at -40°C and about 25% lower shear strength at +70°C in comparison with room temperature.

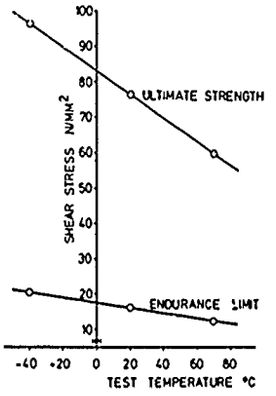


Fig.15 Test Temperature Effects on Shear Strength

For both bending and shear fatigue strength a scatter factor in stress direction of the magnitude of $\epsilon \approx 1.06$ is found. This value is about the same as that typically encountered in fatigue test data for the competing materials.

Root End Section Fatigue Tests

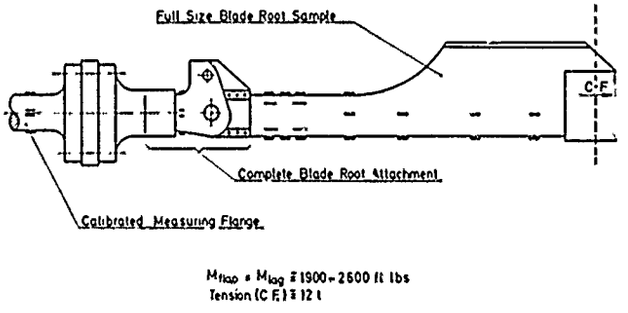


Fig.16 Blade Root Specimen

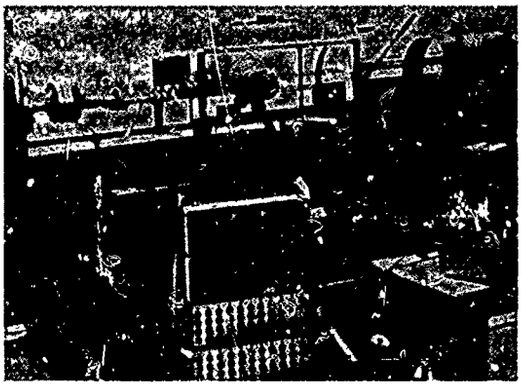


Fig.17 Test Bench for Blade Root Testing

As with a hingeless rotor system the root end section is the highest loaded part of the rotor blade, we concentrate our activities on this item. The specimen consists of blade section inboard of aerofoil section, titanium attachment fitting, main and lead lag bolts as well as titanium inner sleeve.

The purpose of the test is to evaluate the fatigue strength of the blade root end section and the blade to hub attachment joints. The outboard end of the specimen is built up with loading doublers and load application attachments, where flapwise, chordwise and torsional loadings are applied through excenters. An axial steady load which simulates centrifugal force is also applied to the specimen.

Failure occurs in the composite material within the attachment fitting (Fig. 18) after the stiffness of the blade has dropped significantly at relatively high stress levels. The reason for the failure may be a hot spot due to high stresses and fretting between the blade loop and the fitting.

Fig. 19 shows the root end section data and the mean S/N curve. As we have tested up to now more than 30 specimens, the full scale data can be used to establish the scatter factor.

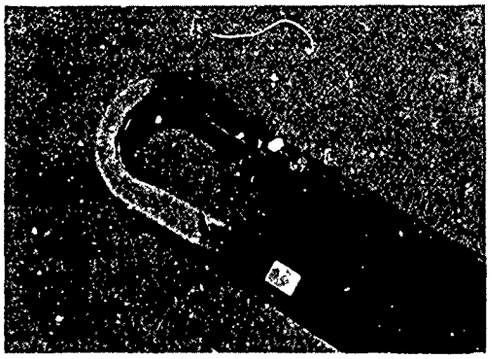


Fig.18 Failure of the Root End Specimen

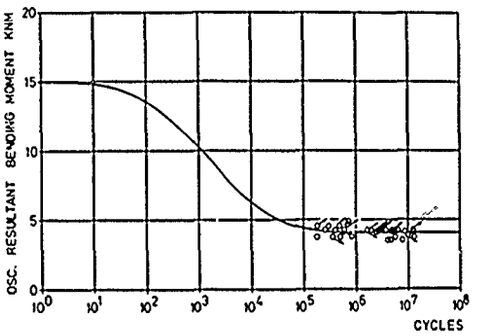


Fig.19 Root End Section S/N Curve

One specimen was subjected to more than 70 000 start-stop cycles without failure. Another specimen was tested at 70^0 C and no difference to testing with room temperature could be found. One specimen was tested unter artificial weathering conditions (-40^0 C to 50^0 C and 90% to 95% relative humidity) without failure.

Resistance to ballistic impact was shown by testing a specimen penetrated by armour piercing ammunition .30 APM 2 [5]. After more than 7 million cycles at highest flight loads the damage had not propagated at all.

To evaluate the long term effects of the environment on structural integrity, MBB has started a project, sponsored by the German Ministry of Defence, to inspect and test high time service main rotor blades. Up to now two blades, one with 2600 flight hours flown in the U.S.A. over the southern coastal region of Louisiana and the Gulf of Mexico and the other with 3700 flight hours flown in U.K. over the North Scottish coastal region and the North Sea were tested.

The physical property tests showed no differences between new and used blades which were attributable to composite material. All stiffnesses and frequencies were within the same range of scatter. Both blades, however, showed indications of delaminations in the torsion caps near the root end fitting. To demonstrate damage tolerance characteristics, testing was performed with flight loads.

After 400 000 cycles of the 2600 hours blade the delaminated torsion caps showed indications of cracks and therefore were removed for inspection of the spar, but no damage could be found. The test was stopped at this stage for reasons other than the components fatigue strength.

After about 1 million cycles, the second blade (with 3700 flight hours) also showed cracks in the torsion caps, but testing was continued with very low crack propagation in the caps up to more than 15 million cycles without any decrease in stiffness. Thereafter the load was increased by nearly 50% and the crack propagation accelerated. The test was stopped after 2.5 million cycles of elevated loading with a crack length in the caps of more than 200 mm and a stiffness reduction, both flapwise and torsional, of more than 10%.

Transition Section Fatigue Tests

The specimens, consisting of root end section and part of aerofoil section, are loaded chordwise in three point bending, with the highest bending moments occuring at the transition from "swan neck" to aerofoil section. The outboard end of the specimen is built up with loading doublers and load application attachments, where chordwise oscillatory loads and axial steady loads, to simulate centrifugal force, are applied.

Failure occurs in the composite material at the beginning of the aerofoil section (Fig. 20). The loads applied to the specimen, representing elevated levels of flight load distribution, initiated delaminations after about 1 million cycles. The test was stopped after more than 30 million cycles with a crack length larger than 100 mm. As this test has shown that a very low crack propagation rate even with extreme high loading may be expected, only two specimens were tested.

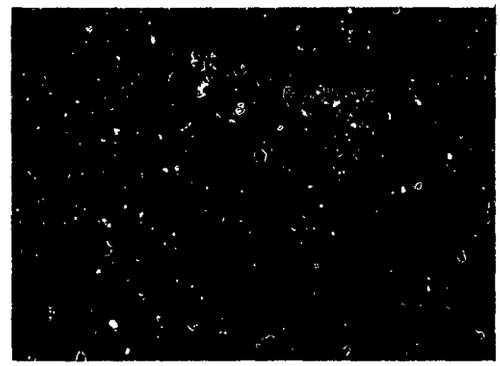


Fig.20 Failure of the Transition Section

Aerofoil Section Bending Fatigue Tests

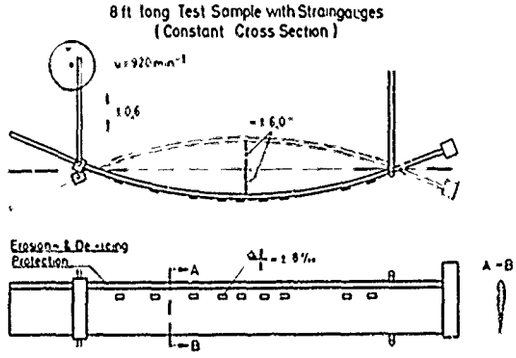


Fig.21 Aerofoil Section Bending Specimen

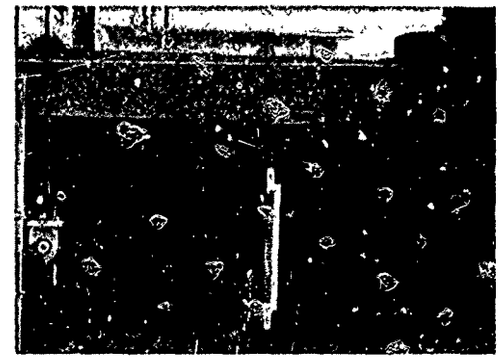


Fig.22 Resonance Test Bench

The blade's aerofoil section, where centrifugal forces are low and flapwise bending predominates, is tested on the blade resonance test bench in flapwise bending. In this machine the first free-free mode is excited by an excenter at a point near a node, whereas the blade is supported at another node of its flapwise bending mode. The amplitude is controled by the stroke and the speed of the excenter.

The tests are conducted to establish the fatigue strength under alternating strain of the basic blade as well as of the erosion strip, the deicing mat and the bonding of these to the blade.

Failure in the composite material occurs when the alternating strain exceeds 0.6% which is equivalent to a stress of 250 N/mm^2. This is in good agreement with the results of bending fatigue tests on coupons as shown in Fig. 10.

Combat damage resistance of the blade is shown by testing an aerofoil section which has been penetrated by armour piercing ammunition. Damage propagation can be seen with an applied alternating strain of at least 0.5% [5].

The aerofoil section of a blade with 2600 flight hours (see Root End Section Fatigue Tests) shows no failure after more than 14 million cycles at 0.6% alternating strain.

Fig. 23 shows the aerofoil section bending fatigue data and the mean S/N curve with a shape based on coupon bending fatigue tests.

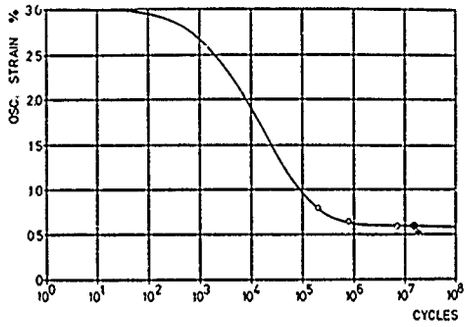


Fig.23 Aerofoil Section Bending S/N Curve

Aerofoil Section Torsion Fatigue Tests

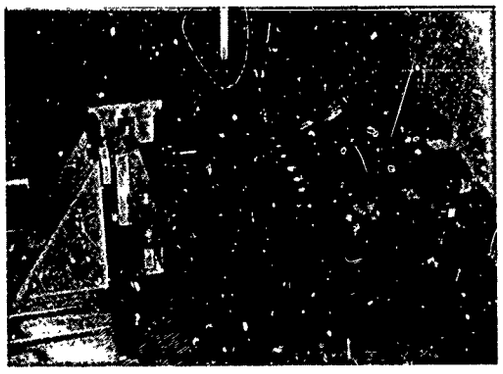


Fig.24 Torsion Test Set-Up

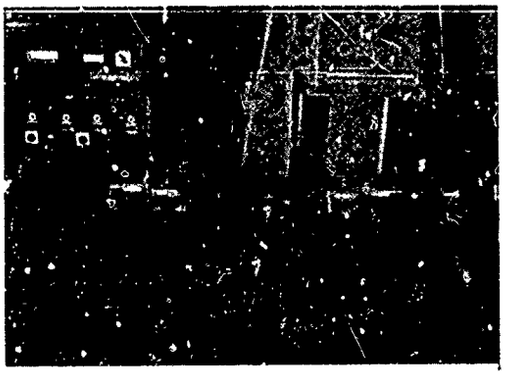


Fig.25 Tension-Torsion Test Set-Up

As the ends of the aerofoil section specimens are not very highly loaded during bending tests, these parts will be cut off thereafter and tested for torsion fatigue. We apply alternating torsional load on specimens of 600 mm length (Fig. 24) and additional axial steady loads on specimens of 900 mm length (Fig. 25).

Failure occurs either by cracks in the blade skin (Fig. 26) or by separation between skin and foam (Fig. 27) or by delamination of the trailing edge. In all cases damage propagation is very slow and failure is indicated by a decreasing torsional stiffness.



Fig.26 Crack in the Blade Skin



Fig.27 Buckling of the Blade Skin

The aerofoil section torsion fatigue data and the mean S/N curve are shown in Fig. 28

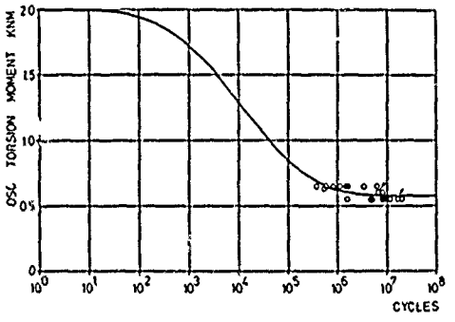


Fig.28 Aerofoil Section Torsion S/N Curve

6. CONCLUDING REMARKS

From more than 20 years experience at MBB with composite rotor blades, through testing some thousand specimens cut out of blades and more than hundred full scale specimens, the following conclusions can be drawn:

- S/N curve shape between a few cycles and the infinite may be represented by a single equation;
- influence of steady stresses may be taken into account in this formula;
- material-dependent parameters must be evaluated by non linear regression analysis;
- log S_N shall be selected as statistical variable;
- scatter factors of composite materials are not dissimilar to those for metals;
- coupons shall be cut out of production blades to take care of any influence of the manufacturing process;
- two different types of coupons are necessary, as fibre composites may fail either in or between the fibres;

- coupon data shows a 12% reduction in interlaminar shear fatigue strength due to 5000 hours artificial environmental exposure;
- test temperature effects both static and fatigue interlaminar shear strength by the same amount, i.e. 25% higher at -40^0C and 25% lower at $+70^0$C compared with room temperature strength;
- S/N curve shapes and scatter factors determined from coupon data can be applied to the full scale specimens;
- full scale subcomponent testing is a practical way of showing compliance with the strength requirements;
- composite main rotor blades following almost 4000 hours of flight time show no degradation in their properties;
- fatigue failure modes in the full scale tests are of gradual nature, even when ballistically impacted;
- changing eigenfrequencies, due to decreasing stiffnesses, will indicate damage long before the structural integrity will be questioned.

7. REFERENCES

[1] Reichert, G. Weiland, E. — Long Term Experience with a Hingeless/Composite Rotor, AGARD Flight Mechanics Panel Symposium on Rotorcraft Design, Ames, 16.-19.5.1977

[2] Jarosch, E. Stepan, A. — Fatigue Properties and Test Procedures of Glass Reinforced Plastic Rotorblades, AHS 25th Annual National Forum, Paper No. 370, Washington, D.C., 14.-16.5.1969

[3] Och, F. — Fatigue Life Estimation Methods for Helicopter Structural Parts, AGARD Report No. 674, Florenz, 25.-29.9.1978

[4] — Fatigue Evaluation of Rotorcraft Structure, FAA Advisory Circular No. 20-95, 18.5.1976

[5] Brunsch, K. Wackerle, P.M. — Ballistic and Impact Resistance of Composite Rotorblades, Second European Rotorcraft and Powered Lift Aircraft Forum, Bückeburg, 20.-22.9.1976

Report on Session IV

TESTING TECHNIQUES AND METHODOLOGY

by

Dean C.Borgman
Director of Advanced Systems
US Army Aviation R&D Command
AVRADCOM
St Louis, MO 63120, USA

This session on Helicopter Fatigue Testing Techniques and Methodology included five papers. The papers covered the spectrum of testing, from discussion of test techniques for a complete aircraft, down to major assemblies such as transmissions and rotor hubs, down to major components such as the main rotor blade.

The first paper of the session was presented by Messrs. Petard and Lambert and was entitled, "Fatigue Testing of the Complete Structure of the Aerospatiale SA 341 Gazelle". The paper was very interesting and discussed three major topics. First the loading distribution and the techniques for simulating the loading distribution were described, secondly, the test facilities and testing techniques utilized were discussed, and thirdly, the results of the tests were described. The testing simulated in excess of 20,000 flight hours over a four-year period. Included in this simulation were 68,000 take-off and landing cycles. The failures which were identified as a result of the testing were categorized into four types. The first of these were of minor consequence and were primarily cosmetic in nature. The three remaining types of failures were progressively more serious and related to safety of flight. Of these, the most serious appeared to be the development of cracks in bulkhead areas where the canopy was supported. The authors reported good correlation between the testing which was accomplished and experience which has been gained from field service. From the questions which were asked by the audience during the discussion period, there was evidence of considerable interest in the motivation for the test. In addition, questions were raised as to the cost effectiveness of this type testing.

The second paper of the session was presented by Mr Zincone and was entitled, "Helicopter Gearbox Testing". This extremely informative and interesting paper discussed the advantages of over-stress testing in the development of new helicopter transmissions. The author pointed out that testing at accelerated loadings generally produces non-linear increases in stresses and, therefore, precautions must be taken to accurately account for the increased deflections which can result from this condition. Also, over-stress testing requirements place design conditions on the helicopter transmission which must be accounted for by the helicopter designer. Finally, and perhaps most importantly, Mr Zincone pointed out the differences which exist in the acceptance criteria laid down by various certifying agencies. He recommends the establishment of a standardized acceptance criteria as part of a helicopter gearbox test specification. This specification would be developed jointly by the industry and the certifying agencies.

The third paper of the session presented by Mr Baker was entitled, "Fatigue Testing of Helicopter Gearboxes". Mr Baker provided a comprehensive review of the fatigue testing philosophy and techniques utilized at Westland Helicopters. He stressed the significant costs which are associated with fatigue testing, both in terms of time as well as materials and labor. This paper also recommended further standardization of test methods and factors utilized in fatigue testing. This paper generated a discussion on testing requirements for main gearboxes, during which time the advantages and disadvantages of main gearbox fatigue testing were discussed.

The fourth paper of the session authored and presented by Mr McDermott was entitled, "The Methodology Applied to Fatigue Analysis and Testing of the Main Rotor Blade and Hub of the YAH-64 Advanced Attack Helicopter". The presentation included an excellent description of the helicopter system and a complete review was provided of the full-scale fatigue testing of the YAH-64 main rotor. The testing that has been completed to date has been done at constant amplitude loadings. S-N allowable curves have now been generated. Some components have also been G-A-G tested, and damage tolerance information is being collected. A significant result from the damage tolerance testing that has been completed is the demonstration of over five hours of operating life on the main rotor blade after it has sustained significant ballistic damage.

The last paper of the session authored and presented by Mr Och was entitled, "Fatigue Testing of Composite Rotor Blades". This was a very thorough paper, based on the MBB's experience of more than 20 years of composite rotor blades. Mr Och pointed out that the S-N curve shape may be represented by a single equation, with the material-dependent parameters being evaluated by a non-linear regression analysis. MBB has concluded that S-N curve shapes

and scatter factors which are determined from coupon data can be applied directly to full scale composite specimens. In the discussion period which followed, Mr Och indicated that MBB's most recent data indicates a 6% scatter factor. All of MBB's experience confirms the soft failure mode of composites. The failure modes which have been identified are all gradual, even in the presence of ballistic damage. The affect of decreased stiffness on frequency which results from material failure is a good indicator of damage long before the structural integrity of the component becomes a problem.

In summary, Session IV was an unusually good collection of presentations and provided a significant contribution to the overall success of this Specialists' Meeting.

DEVELOPMENT OF STANDARDISED FATIGUE TEST LOAD HISTORIES FOR HELICOPTER ROTORS - BASIC CONSIDERATIONS AND DEFINITION OF HELIX AND FELIX

J. Darts
Royal Aircraft Establishment, Farnborough, Hampshire, England

D. Schütz
Fraunhofer-Institut für Betriebsfestigkeit, LBF,
Darmstadt-Kranichstein, West Germany

SUMMARY

The loading environment experienced by helicopter rotor components is generally around the constant amplitude fatigue limit. Realistic assessment of the fatigue performance of helicopter materials and design details by flight simulation loading therefore results in long testing times which are expensive on electrohydraulic machines. The adoption of a standard loading history for such assessments should reduce the amount of testing required and greatly increase the technical value of individual test results. This is because with an agreed standard a wealth of relevant data accumulates quickly, which may negate the need for some tests and gives extensive comparative data for others. Large evaluation programmes can therefore be more readily shared between different organisations and countries because the results of the programme will be comparable with the organisations' own standard data and the standard data previously accumulated. This paper describes the development of two standard load histories for the fatigue evaluation of helicopter rotor materials and design details.

The work presented in the paper is the result of collaboration between LBF, IABG and MBB of West Germany, NLR of The Netherlands and RAE of the UK.

1 INTRODUCTION

The loading environment for a helicopter is the result of the combined action of turbulence, manoeuvres performed by the helicopter and the rotating machinery which gives the helicopter its unique performance. A large number of stress cycles are induced in the helicopter by this environment and fatigue is a major consideration in its design. This Report concentrates on one aspect of the well documented[1,2] fatigue substantiation procedures of helicopters.

Fatigue evaluation unrelated to specific projects, that is fatigue testing of materials, material that has undergone different manufacturing processes and design details of components, is an essential part of the design and development of a helicopter. For fatigue evaluation it is normal practice that the testing is carried out with constant amplitude loading but in the rare case where variable amplitude loading is used the spectrum of loads is very simplified[3]. There is however extensive evidence[4,5] of the inherent inaccuracies in using constant amplitude loading for evaluation purposes and of the need to assess the accuracy of the life estimation method by flight simulation loading. Flight simulation loading can be, however, an unpopular evaluation tool because its application requires expensive electrohydraulic fatigue machines. Also these machines give testing times at least twice that of conventional methods.

The problem of expense that results from using flight simulation loading for the fatigue evaluation of fixed-wing aircraft materials, etc, has in recent years been mitigated by the development of standard loading sequences. Adoption of standard sequences reduces the amount of testing required in some cases and greatly increases the technical value of individual test results. This is because a wealth of relevant data accumulates quickly which negates the need for some tests and gives extensive relevant comparative data for others. Large evaluation programmes can therefore be more readily shared between different organisations and countries because the results of the programme will be comparable with the organisations' own standard data and the standard data previously accumulated. This co-operation in fatigue test evaluation programmes promotes collaboration in other research areas.

A detailed discussion of the theory of standard load sequences follows in section 2 but the success of this approach to evaluation programmes can be judged by the number of countries that have used or intend using the standard loading for a fighter aircraft, FALSTAFF[6]; Australia, Canada, France, West Germany, Holland, Israel, Italy, Sweden, Switzerland, UK and US.

This Report describes part of a collaborative study between West Germany, Holland and the UK in which standard loading sequences for the fatigue evaluation of helicopter rotor materials, etc, are being defined. Details of the contributing organisations and individuals are given in Appendix A. The ultimate aim of the study is to assess the suitability and economics of using standard flight simulation loading instead of constant amplitude loading for the fatigue evaluation of helicopter rotor materials, etc. This Report describes two phases of the study. Firstly the analysis of usage and loading data at the fatigue critical rotor section of four helicopters to assess the similarity of spectra. The helicopters considered in the study were Sea King and CH-53, articulated rotor helicopters, and Lynx and BO-105, semi-rigid rotor helicopters. Secondly the definition of standard spectra and the methods of generating the loading pattern to give

a realistic representation of helicopter usage. In both phases the articulated and semi-rigid rotors are discussed separately as it was considered that a standard spectrum was required for each of the rotor types. The definition of the standard loading sequence for an articulated rotor is complete but that for the semi-rigid rotor still requires further work.

A second report[7] describes the practical use of these loading sequences and some initial fatigue test results.

Past experience has shown that the assignment of a simple name to a standard loading history promotes discussion and avoids confusion between the different standards. The transport aircraft loading standard is called TWIST[8] (Transport WIng STandard loading) and the fighter aircraft loading standard is called FALSTAFF[6] (Fighter Aircraft Loading STAndard For Fatigue evaluation). For the helicopter standard loadings the origin of the word helicopter (helix-spiral, pteron-wing from Greek) has provided suitable names for the standards, *viz*:

Helix - loading standard for 'hinged' or articulated rotors
Felix - loading standard for 'fixed' or semi-rigid rotors.

The second of the names proves to be particularly appropriate as an early pioneer in helicopter development was Felix Tournachon. The lower case lettering is because the names Helix and Felix are not acronyms.

2 DEFINITION OF STANDARD LOAD HISTORY

The loading pattern experienced by a helicopter, fighter or transport aircraft varies tremendously because of different aircraft capabilities and usage. There is, however, a degree of commonality between the loading experienced by similar aircraft types. For example the bending load histories near the wing roots of fighter aircraft will differ widely in severity but the spectrum of loads will have a similar shape. The spectrum is generally asymmetric (larger positive loads than negative) and the spectrum of positive loads has a convex shape. In contrast the spectrum of wing root bending moments for a transport aircraft is symmetric and the spectrum of positive loads is concave. In both cases examination of flight records of loads reveals that flights are divided by recognisable ground-to-air transitions and different severities of flight are apparent. A loading sequence that, say, represents the characteristics of a transport aircraft spectrum can be said to be a typical service loading history.

A standard load sequence is a well defined load history that is considered representative of typical service loading in a specific type of structure. It is a tool for comparing the fatigue life of A with B where, for example, A and B are materials, design details or tests with and without corrosive environment. A standard load sequence is not intended for the fatigue testing components for a specific aircraft because a loading sequence that reflects that aircraft usage would be more appropriate.

From the above discussion it can be seen that the standard load sequences for helicopter rotors need to reflect the general pattern of aircraft usage. There should also be similarity in loading spectra for any group of aircraft covered by one standard.

3 DESCRIPTION OF HELICOPTERS IN THE STUDY

The four helicopters discussed in this Report are as follows.

(a) Westland Helicopters Ltd - Sea King

A twin-engined aircraft having a maximum take-off weight of 9530 kg used mainly for anti-submarine warfare operations. The rotor is articulated, 18.9 m in diameter, and has five blades. The rotor head materials are titanium and steel and the blade spars are aluminium.

(b) Sikorsky - CH-53D/G

A heavy transport, twin-engined aircraft with a maximum take-off weight of 19050 kg. The rotor construction is similar to the Sea King but there are six blades and the rotor diameter is 22 m.

(c) MBB-BO-105

A twin-engined, multi-purpose aircraft with a maximum take-off weight of 2400 kg. The semi-rigid rotor, 9.8 m in diameter, has four blades. The rotor head material is titanium and the blade material is glass reinforced plastic.

(d) Westland Helicopters Ltd - Lynx

A twin-engined, multi-purpose aircraft with a maximum take-off weight of 4760 kg. The semi-rigid rotor, 12.8 m in diameter, has four blades. The rotor head material is titanium and the blade spars are stainless steel.

The four helicopters above have two fundamentally different rotor designs. The Sea King and CH 53 have an articulated or 'hinged' rotor whose characteristics locate the maximum flapwise bending moment in a rotor at about half rotor radius. The Lynx and BO-105 have a semi-rigid or 'hingeless' rotor whose characteristics locate the maximum

bending moment inboard of, or at the blade root. In the discussion of loading data in the sections that follow the data for the two rotor designs are considered separately and are referred to as articulated and semi-rigid rotors.

4 ASSESSMENT OF HELICOPTER USAGE AND LOADING PATTERNS

4.1 Introduction

To define a standard load sequence aircraft usage and loading patterns should be assessed and loading spectra similarity demonstrated (see section 2). In the following sections helicopter sortie patterns and flight length variations are discussed to determine typical aircraft usage. In this Report flight is a term used to describe the period between take-off and landing while a sortie describes a type of flight fulfilling a particular role. Loading patterns are considered by the assessment of the type of manoeuvres and time spent therein to perform a sortie. For the articulated rotor helicopters data on manoeuvre mixes were available for three characteristic sorties while for the semi-rigid rotor helicopters there was only an average usage mix of manoeuvres. Loading in the critical rotor section induced by the helicopter manoeuvres is considered, concluding with a comparison between Sea King and CH-53 transport spectra and BO-105 and Lynx average usage spectra.

4.2 Mix of sorties

The helicopter is a utility aircraft that can be used in a variety of roles. One helicopter may perform one role in preference to others, for example a helicopter may be allocated to search and rescue operations, but will on occasions fly training and transport sorties.

In section 4.4 it will be seen that the different sorties have different loading spectra and therefore any loading sequence must take account of the variety of sorties performed by a helicopter. In 1974 a survey[9] of UK Service use of helicopters was conducted and sortie types recorded. The aircraft types in the survey included Sea King, Gazelle, Scout, Wasp, Wessex, Whirlwind and Puma, totalling 500 individual aircraft and 75000 flying hours. The results of the survey were considered suitable for this study because other surveys of helicopter usage have generally been limited to one theatre of operation[10].

An objective of this study was that the loading sequence should reflect the general pattern of usage of helicopters and therefore the sortie mix was taken to be the average of all the aircraft sortie patterns in the survey. In the survey a wide variety of sortie codes was recorded but to represent all of these sorties in the loading standard would have been a difficult task. Examination of the survey revealed that the majority of sorties could however be categorised under the general headings of Training, Transport, Anti-Submarine Warfare (ASW) and Search and Rescue (SAR). An examination of the manoeuvres performed by a helicopter would also result in these four sortie categories being evident. Table 1 lists the percentage time spent in each of these four sorties for all the helicopters in the survey in comparison with the sortie mix for just Sea King. This comparison reveals the above-average use of Sea King in an ASW role.

The sortie mix for all aircraft in Table 1 was selected for the loading standards for both the articulated and rigid rotor aircraft. The major reason for choosing this sortie mix was that the loading standards needed to reflect the general usage of helicopters in order to represent all the significant loading patterns experienced by the rotor (see section 2). Adoption of, say, the Sea King sortie mix would have resulted in a standard that was only applicable to a helicopter used mainly in ASW operations. Despite the survey data being only of UK origin it was found to be a good representation of what was known about Dutch and German helicopter usage.

4.3 Flight time for a sortie

The major alternating loads on a helicopter rotor blade are a result of varying loading conditions as the blade rotates and changes in lift induced by pilot control movements. The number of load cycles accumulated by the blade is therefore related to the flying time. (This is unlike the case of a transport fixed-wing aircraft where the majority of loading cycles occur during the climb and descent phase of flight. The number of cycles accumulated is therefore dependent on the number of flights.) The flight times and mix of sorties determine the minimum number of flights the standard loading has to simulate in order to represent the most infrequent flight duration. The survey of UK helicopter usage discussed in section 4.2 also gave the flight durations for each sortie.

In order to represent adequately the variability of usage of helicopters, more than one flight duration per sortie was necessary as had been used in other aircraft standard loadings[6,8]. Only detailed information on Sea King flight durations was readily available from the survey and it was considered that representation of flight length variation was more important than the differences that might exist between Sea King and all-aircraft flight durations. The Sea King flight durations were categorised into intervals of 15 min to compress the data. The results of this analysis are illustrated in Fig 1 for Training and Transport and Fig 2 for ASW and SAR sorties.

To sensibly represent the distribution of flight durations, illustrated in Figs 1 and 2, in the loading standards a further compression of the data was needed. Three flight lengths for each sortie were chosen by considering the data in Figs 1 and 2, the

maximum length of the loading sequence and the occurrence of the most infrequent sortie and flight length (see Appendix B). In the generation of both Helix and Felix flight durations of 0.75, 2.25 and 3.75 h were chosen for each of the four sorties.

4.4 Mix of manoeuvres in a sortie

To perform a defined sortie a helicopter will need to fly certain patterns of manoeuvres. For example a helicopter in an ASW role involving sonar dunks will go through a transition from cruising speed to hover, deploy and retrieve the sonar buoy, accelerate and manoeuvre to a new search area. By recording this information the average time spent in a manoeuvre during a sortie can be estimated. The time spent in some manoeuvres will depend on the flight duration while others may occur only once or twice per flight. With a knowledge of the manoeuvres performed and the loading on the aircraft during these manoeuvres a spectrum of loads can be compiled for the sortie. The recording of frequency and duration of manoeuvres during operational sorties is an area of current study[9,11,12] but from experience mixes of manoeuvres have been defined for use in design and certification of aircraft. Loading spectra synthesised from design mix of manoeuvres have in most cases compared favourably with measured operational spectra[13,14].

The design mix of manoeuvres for Sea King in the Transport, ASW and SAR roles are listed in Table 2 in terms of percentage time spent in 24 manoeuvres. The definition of the Training role in these terms is difficult because this role can vary from say half an hour of handling exercises to a two-hour route following sortie. The inclusion of the Training sortie in the loading standards is discussed in section 6.4. Table 2 demonstrates the dependence of the severity of loading on the sortie performed. For example a Sea King performing an ASW sortie spends about one-third of its time hovering while in the Transport role over three-quarters of the flight time is occupied by forward flight at 103 kn. Hover is a manoeuvre that generates relatively minor loads whereas the loading in forward flight at 103 kn is significant (see Table 6, section 6.2).

At the time of the study a design mix of manoeuvres was not available for the CH-53.

The design mix of manoeuvres for the Lynx and BO-105 are similar and are in turn similar to published design spectra[15]. Unlike the Sea King manoeuvre mix, that for Lynx, listed in Table 3, is for an average sortie. The 43 flight conditions defining this average sortie are listed in terms of percentage time spent in a manoeuvre and occurrences per hour for infrequent flight conditions.

The Sea King mix of manoeuvres was used to develop the Sea King spectrum for comparison with the overall loading spectrum of CH-53 (section 4.7) while the Lynx mix of manoeuvres was used to develop the BO-105 spectrum for comparison with the overall loading spectrum of Lynx (section 4.10).

4.5 Sea King blade loads

During the Sea King main rotor flight test stress histories for a number of locations on the rotor were recorded to aid the fatigue substantiation. The area of the rotor of interest to the current study was at about half rotor radius, where in an articulated rotor system the maximum flapwise bending moment occurs, on the lower surface of the blade which is generally under tensile load.

Stress histories were available for the lower rear corner of the blade spar at 55.9% rotor radius for most of the manoeuvres describing a Sea King sortie (see Table 2). These stress histories were analysed with a range-mean pairs counting method by Westland Helicopters Ltd (WHL) to form for each manoeuvre a mean-alternating stress matrix. An example of a stress matrix is illustrated in Fig 3 for normal approach to hover, one of the manoeuvres that produces the severest loading. The mean stresses include a contribution due to centrifugal force. As a range-mean pairs counting method was used to analyse the stress histories, the counts recorded in the matrix are whole stress cycles. For each matrix the flight time analysed varied but was generally around 5 s. Examination of two matrices for the same manoeuvre did indicate a considerable variation in the number and magnitude of stress cycles in the matrix and therefore for each manoeuvre the matrix considered most damaging was used in the study.

At the time the Sea King transport spectrum was constructed for comparison with the CH-53 transport spectrum stress matrices were not available for take-off, forward flight at 20 kn, 30 kn and 40 kn, recovery from rearwards flight, descent, spot turns and landing. Examination of the peak loading in flight suggested that take-off, forward flight at 20 kn and 40 kn, and landing could be simulated by sideways flight to starboard, forward flight at 30 kn by forward flight at 113 kn, recovery from rearwards flight by recovery from sideways flight to starboard, descent by forward flight at 103 kn, spot turns by rearwards flight. In the final stages of defining the standard loading matrices were available for all the manoeuvres except descent which, based on recent WHL experience, could be simulated by 60 kn forward flight. This latest data confirmed the validity of the assumptions made earlier in the comparison of the two spectra.

4.6 CH-53 blade loads

To determine fatigue load spectra for German Air Force usage of CH-53 helicopters, in-flight measurements of strain were recorded for a number of simulated sorties. The strains were measured at the lower rear corner of the blade spar at about half rotor radius, a position compatible with the Sea King measurements. Out of a total of

26 flights flown nine flight records were analysed using a range pairs counting method. Five of these nine flights were Transport sorties and the remainder Training sorties. Only overall loading spectra could be determined from the flight records because the transition from one manoeuvre to another could not be accurately determined, making an analysis on a manoeuvre-by-manoeuvre basis difficult. The spectra for the five Transport and four Training sorties are illustrated in Figs 4 and 5 respectively. For ease of presentation the mean stress of the cycles has been ignored. In addition to the individual flight spectra, mean spectra for transport and training are illustrated.

4.7 Comparison of CH-53 and Sea King spectra

Spectra for both CH-53 and Sea King performing a transport role were compared to assess the similarity of spectra from two different articulated rotor aircraft. The CH-53 data had been collected in the form of an overall spectrum describing the transport role (see section 4.6) but the spectrum for the Sea King in the transport role had to be synthesised from the loads in individual manoeuvres combined in the appropriate ratio for a transport role.

The initial step in the synthesis of the Sea King transport spectrum was to reduce the number of counting intervals for the stress amplitudes so, for example, counts of cycles between stress amplitudes of 17.2 MPa to 18.95 MPa and 18.95 MPa to 20.7 MPa were all counted in the interval of 17.2 MPa to 20.7 MPa (see Fig 3). Then assuming that

n = number of cycles counted between stress amplitudes σ_{a1} and σ_{a2} at a mean stress of σ_m in matrix analysis time of t hours;

p = proportion of time a manoeuvre occupies in the transport role;

k = number of manoeuvres in transport role;

N = number of cycles per hour between σ_{a1} and σ_{a2} at a mean stress of σ_m in the transport role; then

$$N = \sum_{i=1}^{i=k} \frac{p_i n_i}{t_i} .$$

The result of this analysis is presented in Fig 6 in the form of a mean-alternating stress matrix. Development of this spectrum includes the assumptions discussed in section 4.5 on the loads in manoeuvres for which data were unavailable. The large number of cycles in the lowest stress amplitude counting interval in Fig 6 were a result of loads accumulating at frequencies higher than fundamental. Counts in the other intervals indicate that the higher stress amplitudes accumulate at less than or about the fundamental frequency of one rotor revolution. Aside from the counts in the lowest counting interval the majority of the cycles occur at mean stresses between 75.8 MPa and 82.7 MPa and it was therefore considered reasonable that for this comparative exercise all the stress cycles in the Sea King spectrum could be taken to be at one mean stress.

The CH-53 and Sea King spectra are presented in Fig 7 in which variations of mean stress have been ignored to ease comparison. Fig 7 reveals that both spectra have the characteristic shape reported in the literature[16] for helicopter spectra and despite the different data sources, aircraft weights, usage, number of rotor blades and the fact that the Sea King spectrum was synthesised the spectra compare favourably even in the high stress region, particularly important to blade fatigue life. The severity of the two spectra can be judged by comparing them with the constant amplitude fatigue limit of a titanium alloy indicated in Fig 7.

The favourable comparison of the CH-53 and Sea King spectra for the transport role led to the conclusion that a standard loading sequence for an articulated rotor could be defined and that data from both Sea King and CH-53 could be used in its synthesis.

4.8 BO-105 blade loads

An instrumented BO-105 was flown to the pattern of manoeuvres that describe the design mix of manoeuvres discussed in section 5. Strains were measured on the lower surface of the blade root, the most highly stressed region, for each of these manoeuvres. The flight record of a single flight was analysed by the rainflow counting technique (generally equivalent to range-mean pairs counting) to form mean-alternating strain spectra for each manoeuvre. The counts of cycles in each mean-alternating strain interval were factored to account for the duration of the manoeuvre in the design mix of manoeuvres. Summation of the individual spectra for the manoeuvres would then result in a spectrum for the design mix of manoeuvres. An example of a mean-alternating strain diagram for a longitudinal control reversal in autorotation, the most severe manoeuvre in the spectrum, is illustrated in Fig 8.

4.9 Lynx rotor loading

Mean and vibratory flap bending moments at the root of the inner flexible element of the Lynx main rotor hub, 3.4% rotor radius, had been estimated for the fatigue substantiation programme. At this location, the critical rotor section for the Lynx, the loading caused by lag is not significant. These flap bending moments were estimated so

as to describe the average sortie (see Table 3) rather than the loading caused by individual manoeuvres. The flap bending moments were converted to mean and alternating strains for the lower surface of the inner flexible element and the resulting spectrum is presented in Fig 9. The contribution of the centrifugal load is included in the mean strain. For completeness cycles which accumulate once per flight and are therefore not dependent on flight time have also been included in Fig 9. The cycle counting method was again range-mean pairs and the cycles recorded in Fig 9 are therefore whole strain cycles.

4.10 Comparison of BO-105 and Lynx spectra

The spectra for BO-105 and Lynx were compared to assess the similarity of spectra for two different semi-rigid rotor helicopters.

Summation of the mean-alternating strain matrices of the individual manoeuvres for BO-105 results in a spectrum for the same mix of manoeuvres used to define the Lynx spectrum. The results of this analysis are illustrated in Fig 10. Comparison of Fig 9, the Lynx spectrum, with Fig 10 reveals some similarity. The majority of cycles in both spectra occur at tensile mean strains, a result of the contribution of the centrifugal load. In the Lynx spectrum, however, many cycles have compressive mean strains and while most of the large amplitude cycles occur about similar mean strains in the BO-105 spectrum in the Lynx spectrum the mean strain varies significantly. One reason for this is the inclusion of the once per flight cycles in the Lynx spectrum.

To further the assessment of spectra similarity the data presented in Figs 9 and 10 has been replotted in terms of alternating strain *versus* number of cycles in Fig 11. Mean strains of the cycles have been ignored, as they were for the CH-53 and Sea King spectra comparison, and the once per flight cycles have been omitted from Fig 11. Examination of Fig 11 reveals that the characteristic S-shape, observed for the CH-53 and Sea King spectra, is for both spectra not so evident, the cumulative number of cycles increasing more smoothly with reducing strain amplitude. The Lynx spectrum differs in severity from the BO-105 spectrum because of the different materials used in rotor construction. At the critical section for the BO-105, the blade root, the material is glass reinforced plastic while at the critical section for Lynx, the inner flexible element, the material is titanium. Division of the strain amplitudes of the Lynx spectrum by a simple factor of 2.1 makes the spectra for both aircraft more comparable as can be seen from Fig 11. While the spectra compare favourably in the strain amplitude region of 500 to 900 με there is little correspondence between the spectra in higher strain regions of particular importance to fatigue damage.

A certain amount of disparity of this type between the two spectra was expected because the Lynx spectrum is a calculated design spectrum while that for the BO-105 is a flight test spectrum from one sample flight. It is unfortunate that the spectra disagree at the end of the spectra which is of major importance to fatigue damage. Development of the loading standard for the semi-rigid rotor, Felix, is continuing with a detailed examination of the loading data for both helicopters and therefore a complete definition of Felix in this Report has not been possible.

5 DISCUSSION OF THE METHOD OF GENERATING THE LOADING STANDARDS

Previous sections in this Report have discussed data that can define the loading seen by a helicopter rotor but little consideration has been given to how this data can be formed into a loading history. The objective of this section is to discuss the reasoning behind the choice of the generating method.

In defining a standard load history factors other than the available data have to be considered. The most important consideration is that the standard must represent in a reasonable manner the typical usage of the aircraft taking into account the limitations that exist in the data from which the standard is defined. Secondly it must be possible to include the standard in computer programs that control fatigue testing machines. Many mini-computers used for controlling fatigue tests do not have a large available storage capacity and the storage requirements of the standard must therefore be minimised. It is interesting to note, however, that the development and use of computers in fatigue test control has been accelerated by the development of standard loadings. Finally the definition of the standard should not be oriented towards one computer or system type although past experience has shown that a FORTRAN program definition of a standard gains the widest acceptability. With the above factors in mind the method of generation can be considered.

Two major alternative methods of generating the standards were considered. The first method generates the loading from mean-alternating load matrices for sorties, using random draw techniques, thereby losing the separate identity of manoeuvres. This is similar in concept to the well documented[17] methods of generating TWIST and FALSTAFF loadings. The second method defines sorties by fixed logical sequences of manoeuvres thereby retaining the identity of manoeuvres and some sense to the order of load application during flight. This latter method of generation was used for helicopter loading sequences by Crichlow *et al*[1] in 1972. For either generation method an average sortie could be formed to simulate the four sorties defined in section 4.2 or they could be simulated on an individual basis and single or a number of flight lengths for each sortie simulated. The sequence of sorties could be defined by a random draw algorithm or a predetermined sequence.

The method chosen to generate the loading standards was that using logical sequences of manoeuvres to define each sortie, three flight lengths for each sortie and pre-determined sequences of loads in a manoeuvre and sequence of sorties because of the following considerations.

(a) The reason for choosing to define sorties by logical sequences of manoeuvres was that this method would simulate more accurately the complex load interactions that influence fatigue life. A criticism of the loading standard for fighter fixed-wing aircraft is that all logical sequence of in-flight loading has been lost.

(b) Variation of the flight lengths of a sortie was chosen because of the need to represent accurately the position in the loading sequence of the transition from the ground condition to level flight. This transition combined with the peak loading in flight form the once per flight load cycles which can cause major amounts of fatigue damage. The decision to simulate three flight lengths is a result of considering the most infrequent flight length for the sorties and is discussed in Appendix B.

(c) Simulation of four separate sorties was chosen in preference to one average sortie because of the importance attached to realistic modelling of the complex load interactions that affect fatigue life. The loading varies significantly from sortie to sortie as discussed in section 4.4.

(d) Pre-determined sequences of loads in a manoeuvre and sequence of sorties were chosen in preference to random draw algorithms because in the opinion of the authors the implementation of random draw algorithms in a computer program controlling fatigue machines creates unnecessary problems. It is interesting that although FALSTAFF is defined by random draw algorithms, in many laboratories FALSTAFF loading is stored in the computer as the individual loading cycles that make the FALSTAFF sequence.

(e) Finally this generation method results in a loading sequence of no greater length than that produced by the random draw technique which has no logical sequence of manoeuvres. This is because the length of sequence is determined by the need to simulate the most infrequent sortie length. It does, however, require more detailed information to describe the sorties but this has not led to excessive computer storage requirements as will be seen in section 7.2.

The general plan for generating the loading standards discussed above is used in the next section to turn the data described in section 4 into the loading standard for articulated rotors, Helix. The loading standard for semi-rigid rotors, Felix, is similar in that the same sortie sequence and flight durations will be used and similar sequences of manoeuvres for each sortie will be defined. The load matrices and sequence of loads for each manoeuvre will be different to that of Helix but more work is required to define these parts of Felix as discussed in section 4.10.

6 DEFINITION OF THE LOADING STANDARDS HELIX AND FELIX

6.1 Sequence of sorties

An analysis of the length of sortie sequence required to represent the most infrequent flight duration using the mix of sorties for all aircraft, discussed in section 4.2 and flight durations of Sea King, discussed in section 4.3 is presented in Appendix B. The results of this analysis indicate that the sequence of sorties should be 140 flights long with a mixture of flight durations of 0.75, 2.25 and 3.75 h for each sortie. The sequence in which the 140 flights are applied in Helix and Felix, created by a once and for all random draw, is listed in Table 4. A summary of the results of the analysis in Appendix B is given in Table 5 which lists the number of flights of each duration for each of the four sorties that are required to achieve the correct mission mix. The 140 flights simulate 190.5 h of flight; 63.75 h in the Training role, 92.25 h of Transport, 18 h of ASW and 16.5 h of SAR.

6.2 Loads in Helix manoeuvres

The generation technique requires the definition of loading patterns for individual manoeuvres. The comparison of overall loading spectra of CH-53 and Sea King had demonstrated not only similarity between the spectra but that the spectra could be synthesised from manoeuvres. Loading patterns for individual manoeuvres were only available for Sea King but it was considered reasonable to base Helix or Sea King data because of the success of the above comparison.

Representation of all the loads in the Sea King spectrum would be difficult because of the numbers of small amplitude loads. In an attempt to obtain a compromise between a representative simulation of the loading and short testing times, stress amplitudes below 20.7 MPa have been omitted (see Fig 7). Examination of the mean-alternating stress matrices for individual manoeuvres suggested that a single mean stress for each manoeuvre was adequate as the majority of the large amplitude cycles occurred at similar mean stresses (see Fig 3). An average mean stress for each manoeuvre was estimated and counts of cycles in the same stress amplitude counting interval were summed. The counting interval for the stress amplitudes were doubled to the same values used in the comparison of the CH-53 and Sea King spectra (see section 4.7). The cycles recorded for a manoeuvre were then taken to be equal in amplitude to the mid point of the upper and lower bounds of the counting interval, *eg* a count in the interval 48.3 MPa to 51.7 MPa became a stress cycle of 50.0 MPa in amplitude.

The results of the above analysis are listed in Table 6 which defines what are termed the standard load matrices for Helix manoeuvres. For each manoeuvre the mean stress, number of cycles at each stress amplitude and the matrix analysis time are listed. The number of cycles in each manoeuvre has been reduced by dividing by the highest common factor and the matrix analysis time adjusted likewise. The 20.7 MPa omission level has resulted in no loading being attributed to hover. Hover could be represented by periods of steady load, dwell periods, but current practice for loading sequences for fixed-wing aircraft is to omit dwell periods although their omission has been found to be both detrimental and beneficial to fatigue life[12]. The conclusion was reached that dwell periods associated with hover would be omitted in Helix because of the already lengthy testing time for helicopter components but the influence of dwells in loading close to the constant amplitude fatigue limit should be investigated. For completeness hover has still been included in the flight descriptions.

6.3 Sequence of loads in a Helix manoeuvre

To aid presentation of the sequence of loads in a manoeuvre and their inclusion in a computer program the mean and alternating stress amplitudes in Table 6 have been non-dimensionalised in Table 7.

A sequence of loads has been defined for each manoeuvre in a once and for all random selection because an examination of helicopter flight load traces revealed the peak loading to be random. The sequence of loads in the Helix manoeuvres is listed in Table 8. In each matrix in the Table the first element is always the non-dimensionalised equivalent of the mean stress. For example in manoeuvre one, take-off, the first element contains 31, which from Table 7 translates to a mean stress of 53.4 MPa. The second and third elements contain the numbers 13 and 15 respectively, which means that the stress sequence equivalent to +13, -13, +15, -15 is applied about the mean stress. In all manoeuvres the whole cycles are always applied as positive then negative going loads. The flying time simulated by the sequences of loads in Table 8 is the matrix flight time (see Table 6) of each manoeuvre. To simulate flight time in a manoeuvre in excess of the matrix flight time the sequences of loads in Table 8 are repeated.

6.4 Sequence of manoeuvres in a sortie

Describing a sortie by a logical sequence of manoeuvres is a technique that has been used previously[1]. The lack of operational statistics describing the sequences of manoeuvres in a sortie resulted in the sequence being compiled by common-sense consideration of the flight profile and the objective of the sortie. In the simplest case the above approach says for example that the helicopter cannot perform a bank turn without first having taken off. The above approach has been used to develop the sequences of manoeuvres in the four sorties of Helix and Felix. The sequences of manoeuvres that define the 3.75 h Training, Transport, ASW and SAR sorties are listed in Tables 9, 10, 11 and 12 respectively. In these Tables the position of the manoeuvres in the flight is numbered, the name and number of the manoeuvre, time occupied by the manoeuvre and number of applications of the standard load sequence for the manoeuvre are listed. Although hover does not generate any significant loading, see previous section, it had to be included in the flight description to achieve the correct mix of manoeuvres in 3.75 h. During the formulation of the ASW sortie it was found that, to represent accurately the mix of manoeuvres while simulating a reasonable number of sonar dunk operations, a sequence of nearly 500 manoeuvres was required. To simplify the description of the ASW sortie the portion of the flight where a sonar buoy is deployed has been standardised to 16 manoeuvres and referenced by manoeuvre number 25, the combined manoeuvre. The order of application, time in the manoeuvres and matrix applications for the individual manoeuvres that simulate this combined manoeuvre are listed in Table 13. The time spent in hover varies for each sonar dunk.

Tables 9 to 13 have been compiled by considering the general pattern of flying that the sequence of manoeuvres must represent in each sortie as follows.

(a) Training

This was the most difficult sortie to describe because of the wide-ranging operations that are flown. The assumption was made, however, that this sortie should simulate the essential aspects of flight needed to perform the other sorties. In addition a pure training exercise in which the helicopter is performing manoeuvres to demonstrate the handling characteristics was simulated.

(b) Transport

This sortie represents take-off and low-speed manoeuvres away from the terminal area, flight at cruising speed while manoeuvring to take into account terrain and air-traffic-control restrictions and finally low-speed manoeuvres and landing in the terminal area.

(c) ASW

In this sortie, apart from the requirement to move to and from the base area, the helicopter repeatedly decelerates to allow deployment of a sonar buoy and accelerates to move to a new search area.

(d) SAR

The essential part of this sortie is the flying of low-speed manoeuvres to execute a rescue.

To define the 0.75 h and 2.25 h flights it was considered reasonable to firstly define the 3.75 h flights and then to take fractions of these flights for the other durations because the percentage times spent in a manoeuvre (section 4.4, Table 2) are only applicable for flight durations between 3 h to 4 h. The adoption of this technique resulted in only one sequence of manoeuvres being defined for each sortie and the common-sense result that, for example, landing and take-off phases of flight were independent of total sortie time. Consider the altitude-time profile that might be generated by the sequence of manoeuvres that define a 3.75 h transport flight as illustrated in Fig 12a. In the sequence of manoeuvres, Tables 9 to 12, what are termed flight markers are included; a 0.75 h and 2.25 h flight marker and a landing sequence marker. An example of their position in the 3.75 h flight is indicated in Fig 12a. To simulate a 2.25 h flight all the manoeuvres from take-off to the 2.25 h flight marker are applied followed by all the manoeuvres between the landing sequence marker and the end of the flight. The resulting altitude-time profile is illustrated in Fig 12b and the result of simulating a 0.75 h flight in Fig 12c. The process described above was used for Training, Transport and ASW sorties but additional markers were required in the SAR sortie because of the search and rescue operation performed at about mid-sortie. Fig 13a illustrates an altitude-time profile that might be generated by the sequence of manoeuvres that define the 3.75 h SAR sortie. For each of the intermediate flight durations there are now two flight markers and a SAR marker as well as a landing sequence marker. To simulate a 2.25 h flight all the manoeuvres, from take-off to the first 2.25 h marker, are applied, then all the manoeuvres between the SAR marker and the second 2.25 h marker and finally all the manoeuvres between the landing sequence marker and the end of flight. The resulting altitude-time profile is illustrated in Fig 13b and the result of simulating a 0.75 h flight in Fig 13c. The markers described above are positioned in the sequence of manoeuvres for each sortie such that not only is the required flight time simulated exactly but continuity of flight is maintained. As discussed in Appendix C for programming convenience the 0.75 h and 2.25 h flight markers are given position numbers and called manoeuvre types -1 and -2 respectively while the landing sequence markers and SAR marker are not given position or identification numbers.

The loading in each of the manoeuvres has only been defined for the flying times listed in Table 6 and therefore the time spent in a manoeuvre in the sorties must be an integer number of times the standard flying time in Table 6. The total time in a manoeuvre for a sortie had to be slightly modified to allow an exact number of manoeuvre load sequences to be applied. The results of these modifications are in Table 14 where the exact time in a manoeuvre for a 3.75 h sortie is listed along with the times that are exactly divisible by the standard flying time. No times are given for training because this sortie has been defined without an initial estimate of the manoeuvre mix.

6.5 Ground load

The final item of information that completes the definition of Helix is the stress induced in the blade by the action of its own weight when the helicopter is on the ground and the rotor stationary. At the lower rear corner of the blade near at about half rotor radius this has been measured as -27 MPa or in non-dimensional Helix units as a stress level of -16. To simulate the ground condition after the final manoeuvre in each flight the stress is lowered to a level of -16.

6.6 Example of Helix load-time history

Illustrated in Fig 14 is the load-time history for the start of the Training sortie in Helix. The manoeuvres that create the loading are indicated in the Figure with the relevant part of the load-time history.

7 DISCUSSION

7.1 Limitations in the data base used in the formulation of the loading standards

It is considered that the best use of the available data has been made in defining the loading standard for articulated rotors, Helix and in progressing towards the definition of the loading standard for rigid rotors, Felix. The limited availability of recorded operational data on Service usage of helicopters has, however, led to some assumptions being made, and noted in the previous sections, regarding the usage and loading conditions experienced by the helicopters in this study. Much of the data was based on design assumptions and limited flight trials which, in particular, has led to difficulties that have resulted in Felix not being fully defined. The operational data that has been used in the study such as sortie mixes and flight durations are descriptions of past usage which may not reflect the pattern of usage in the future. The rapid changes that occur in helicopter usage[19] may render some of the assumptions in the loading standards invalid. The development of any loading spectrum requires an assessment of which infrequently-occurring events should be included. Extensive research[20] has been conducted on fixed-wing aircraft to decide, for example, the magnitude of the load that the aircraft may encounter only ten times in its service life. At the present time this type of research for helicopters is limited and research into infrequently-occurring events is necessary to assess the validity of the loading standards.

7.2 Inclusion of the loading standards in a computer program controlling a fatigue machine

Although only the loading sequence for Helix has been fully defined the generation method for Felix will be essentially the same. The description of the sorties by manoeuvres has been supplied in full to allow an assessment of the basis of the generation method but for a computer program it is only necessary to store the sequence of sorties, Table 4, the sequence of loads in each manoeuvre, Table 8, and finally the manoeuvre type and number of times the manoeuvre load sequence is repeated for each of the four sorties, Tables 9 to 12.

A FORTRAN program to generate Helix and Felix is under development and some guidelines for the program are discussed in Appendix C but Helix has been incorporated in an RAE utility computer program[21] that controls three independent fatigue machines. The utility program generates constant amplitude, flight-by-flight block, TWIST and FALSTAFF loading and can apply fixed sequences of peaks and troughs either stored in the computer or held on magnetic tape. Helix therefore had to be incorporated into the current structure of the program but storage of the data and generation algorithm required only 1K of 12-bit words.

7.3 Future work

The work reported here is not completed and the collaborative programme to define the standard load sequences is continuing. There are a number of areas requiring further research before the final loading standards are agreed between the contributing organisations and before their usefulness can be fully assessed.

The following items are examples of the research required.

(a) The loading data for Lynx and BO-105 have to be assessed further for compatability and applicability before defining Felix.

(b) Inclusion of the semi-rigid rotor loading pattern into the Helix generation method has to be implemented without greatly increasing the data storage requirements.

(c) A standard FORTRAN computer program to generate the loading sequences needs to be defined.

(d) The loading standards have to be compared with conventional methods of evaluation testing to assess the suitability of using flight simulation loading for the fatigue evaluation of helicopter components. As part of this study the influence of infrequently occurring events on fatigue life should be assessed and an attempt made to reduce the number of cycles included in the standards that are below the constant amplitude fatigue limit as has been done for TWIST[22] to create MINITWIST.

It is intended that at the completion of the study that a joint LBF, IABG, MBB, NLR and RAE report will be issued describing the whole project.

8 CONCLUSIONS

(a) A favourable comparison between two articulated rotor helicopter spectra has enabled the definition of Helix, a standard loading sequence for the fatigue evaluation of articulated rotor components.

(b) Spectra for two semi-rigid rotor helicopters were compared and found to differ substantially in the high strain region which is of major importance to fatigue damage. Research is continuing on the definition of Felix, a standard loading sequence for semi-rigid rotors.

(c) The algorithm that generates Helix is easily programmed and in combination with data storage requirements occupies a small amount of core store in a mini-computer.

Table 1

PERCENTAGE TIME IN TRAINING, TRANSPORT, ASW AND SAR SORTIES FOR UK SERVICE USAGE

Sortie	Percentage time in sortie	
	All aircraft	Sea King
Training	33.0	22.3
Transport	48.5	25.3
ASW	9.0	49.1
SAR	9.5	3.3

Table 2

MIX OF MANOEUVRES IN SEA KING TRANSPORT, ASW AND SAR SORTIES

Number	Manoeuvre description	Percentage time per hour		
		Transport	ASW	SAR
1	Take-off	0.34	0.12	0.27
2	Forward flight 20 kn	0.40	2.79	0.23
3	Forward flight 30 kn	0.40	2.79	0.23
4	Forward flight 40 kn	0.40	2.79	0.23
5	Forward flight 60 kn	8.49	5.99	25.92
6	Forward flight V_{NO} 103 kn	81.79	35.90	64.82
7	Maximum power climb 70 kn	0.57	1.20	0.44
8	Shallow approach to hover	0.17	-	-
9	Normal approach to hover	-	1.40	0.08
10	Hover	2.83	33.01	4.85
11	Bank turn port 30° V_{NO}	0.79	5.51	0.45
12	Bank turn starboard 30° V_{NO}	0.79	5.51	0.45
13	Sideways flight to port 30 kn	0.28	0.20	0.22
14	Recovery from 13	0.11	0.08	0.09
15	Sideways flight to starboard 30 kn	0.28	0.20	0.22
16	Recovery from 15	0.11	0.08	0.09
17	Rearwards flight 20 kn	0.28	0.20	0.22
18	Recovery from 17	0.11	0.08	0.09
19	Spot turn port	0.28	0.20	0.22
20	Spot turn starboard	0.28	0.20	0.22
21	Autorotation	0.57	0.40	-
22	Recovery from 21	0.05	0.03	-
23	Descent	0.34	1.20	0.53
24	Landing	0.34	0.12	0.13

Table 3

LYNX DESIGN MISSION MIX

Number	Flight description	Percentage flight time	Number per hour
1	Rapid increase in rpm and engage clutch		5
2	Take-off		5
3	Steady hovering	20	
4	Spot turns		10
5	Low speed flight control reversals - longitudinal		2.5
6	Low speed flight control reversals - lateral		2.5
7	Low speed flight control reversals - yaw		2.5
8	Low speed flight control reversals - collective		2.5
9	Rearwards flight	0.5	
10	Sideways flight port	0.5	
11	Sideways flight starboard	0.5	
12	Forward flight 0.2 V_{NE}	10	
13	Forward flight 0.4 V_{NE}	5.4	
14	Forward flight 0.6 V_{NE}	6.3	
15	Forward flight 0.8 V_{NE}	11.7	
16	Forward flight 0.9 V_{NE} (V_{NO})	18	
17	Forward flight 1.0 V_{NE}	2.7	
18	Forward flight 1.1 V_{NE}	1.0	
19	Cruise turn 0.4 V_{NE}	0.6	
20	Cruise turn 0.6 V_{NE}	0.7	
21	Cruise turn 0.8 V_{NE}	1.3	
22	Cruise turn 0.9 V_{NE}	2.0	
23	Cruise turn 1.0 V_{NE}	0.3	
24	Transition from hover		7
25	Maximum power climb 70 kn	4	
26	High-speed flight control reversals - longitudinal		2.7
27	High-speed flight control reversals - lateral		2.7
28	High-speed flight control reversals - yaw		2.7
29	High-speed flight control reversals - collective		2.5
30	Descent		7
31	Transition to hover		7
32	Flare		7
33	Entry into autorotation		0.4
34	Recovery from autorotation		0.4
35	Steady flight autorotation	2.5	
36	Control reversals in autorotation - longitudinal	0.1	
37	Control reversals in autorotation - lateral	0.1	
38	Control reversals in autorotation - yaw	0.1	
39	Collective pull up in autorotation		0.4
40	Right turn in autorotation	0.2	
41	Left turn in autorotation	0.2	
42	Single engine flight	3.0	
43	Landings		5

Table 4

SEQUENCE OF SORTIES FOR 140 FLIGHT SEQUENCES OF HELIX AND FELIX

21, 11, 43, 11, 21, 12, 22, 11, 11, 21, 21, 21, 23, 42, 23, 21, 12, 11, 21, 22, 11,
42, 22, 21, 32, 21, 11, 22, 32, 22, 11, 31, 21, 22, 11, 11, 42, 42, 21, 21, 33, 12,
31, 22, 22, 11, 11, 11, 11, 11, 21, 21, 11, 41, 11, 12, 22, 22, 22, 11, 21, 11, 21,
11, 21, 21, 21, 21, 11, 11, 22, 21, 21, 21, 11, 21, 11, 12, 12, 21, 11, 11, 22, 11,
41, 21, 11, 11, 11, 23, 11, 21, 11, 21, 11, 21, 11, 22, 32, 23, 11, 12, 22, 22, 23,
12, 21, 11, 22, 11, 11, 41, 33, 22, 32, 21, 11, 21, 21, 22, 21, 21, 12, 21, 11, 21,
21, 13, 11, 11, 12, 11, 11, 11, 41, 11, 22, 11, 41, 12.

Key:
Training - 10
Transport - 20
ASW - 30
SAR - 40

Shortest flight duration - 1 (0.75 hour)
Middle flight duration - 2 (2.25 hours)
Longest flight duration - 3 (3.75 hours)

therefore 23 is a transport flight of the longest duration

Table 5

NUMBER OF FLIGHTS OF EACH SORTIE FOR THE THREE FLIGHT DURATIONS IN HELIX AND FELIX

Flight duration (h)	Number of flights			
	Training	Transport	ASW	SAR
0.75	47	38	2	5
2.25	11	20	4	4
3.75	1	5	2	1

Table 6

LOAD MATRICES FOR HELIX

Alternating stress MPa				22.4	25.9	29.3	32.8	36.2	39.6	43.1	46.5	50.0
No.	Manoeuvre	Flight time s	Mean stress MPa	Number of cycles								
1	Take-off	6	53.4	1	1	-	-	-	-	-	-	-
2	Forward flight 20 kn	4	88.9	12	1	-	-	-	-	-	-	-
3	Forward flight 30 kn	6	87.4	-	-	12	1	1	-	-	-	-
4	Forward flight 40 kn	4	74.1	-	4	9	1	-	-	-	-	-
5	Forward flight 60 kn	4	77.8	-	11	2	-	-	-	-	-	-
6	Forward flight 103 kn	5	82.3	1	1	4	10	2	-	-	-	-
7	Max. power climb 70 kn	3	84.5	1	-	-	-	-	-	-	-	-
8	Shallow approach to hover	5	73.0	9	3	5	4	2	8	2	2	-
9	Normal approach to hover	4	75.8	5	6	2	2	2	3	5	-	1
10	Hover	-	-	-	-	-	-	-	-	-	-	-
11	Bank turn port 30° V_{NO}	6	87.6	-	-	1	5	15	1	-	-	-
12	Bank turn starboard V_{NO}	5	84.7	-	-	1	7	9	1	-	-	-
13	Sideways flight port 30 kn	4	68.4	2	1	-	-	-	-	-	-	-
14	Recovery from 13	5	63.9	7	4	5	5	4	1	2	-	-
15	Sideways flight starboard	3.5	75.3	1	2	3	2	1	-	-	-	-
16	Recovery from 15	5	65.0	7	4	2	3	-	2	4	-	1
17	Rearwards flight 20 kn	2.5	87.9	1	-	-	-	-	-	-	-	-
18	Recovery from 17	6	78.0	3	1	-	2	7	10	1	-	-
19	Spot turn port	18	82.9	13	17	8	2	-	-	-	-	-
20	Spot turn starboard	18	86.8	3	-	-	-	-	-	-	-	-
21	Autorotation	5	74.5	17	2							
22	Recovery from 21	5	77.8	-	-	2	2	8	4	1	-	-
23	Descent	5	77.8	-	11	2	-	-	-	-	-	-
24	Landing	6	91.4	-	1	3	1	-	-	-	-	-

Table 7

NON-DIMENSIONALISATION OF HELIX LOADS

The original loading data for Helix was expressed in units of lb in^{-2}. The stress interval for the amplitudes was exactly 0.5×10^3 lb in^{-2}. To non-dimensionalise Helix 1 unit has been made equivalent to 0.25×10^3 lb in^{-2}. The alternating and mean stresses are expressed below in terms of MPa, the units used throughout this document.

Conversion tables

1 Alternating stress

Stress MPa	Units
22.4	13
25.9	15
29.3	17
32.8	19
36.2	21
39.6	23
43.1	25
46.5	27
50.0	29

2 Mean stress

Stress MPa	Units	Nearest whole unit
53.4	31.0	31
63.9	37.1	37
65.0	37.7	38
68.4	39.7	40
73.0	42.4	42
74.1	42.9	43
74.5	43.2	
75.3	43.7	44
75.8	43.9	
77.8	45.1	45
78.0	45.3	
82.3	47.8	48
82.9	48.1	
84.5	49.0	49
84.7	49.1	
86.8	50.4	50
87.4	50.7	51
87.6	50.8	
87.9	51.0	
88.9	51.6	52
91.4	53.0	53

Table 8

SEQUENCE OF LOADS IN EACH FUNDAMENTAL MANOEUVRE MATRIX FOR HELIX

NB First element in matrix is the manoeuvre mean stress

1 Take off

31	13	15

2 Forward flight 20 kn

52	13	13	15	13	13	13	13	13	13	13	13	13	13

3 Forward flight 30 kn

51	17	17	17	21	19	17	17	17	17	17	17	17	17	17

4 Forward flight 40 kn

43	17	17	17	15	15	15	17	17	19	15	17	17	17	17

5 Forward flight 60 kn

45	15	17	15	15	15	15	15	15	15	17	15	15	15

Table 8 (continued)

6 Forward flight 103 kn

48	19	19	19	19	19	17	15	19	19	19	19	17	21	17	17
19	13	21													

7 Maximum power climb 70 kn

49	13

8 Shallow approach to hover

42	23	13	23	27	15	13	19	13	27	13	15	23	13	23	15
25	21	17	13	23	13	25	13	23	23	19	21	17	19	13	19
17	17	23	17												

9 Normal approach to hover

44	13	21	13	15	19	25	15	19	25	21	13	17	15	25	25
29	17	13	23	23	23	13	15	25	15	15					

10 Hover

There are no significant loads in the hover manoeuvre

11 Bank turn port 30° V_{NO}

51	21	21	21	19	21	21	21	21	21	23	21	19	21	21	19
21	21	21	19	19	21	17									

12 Bank turn starboard 30° V_{NO}

49	17	23	21	21	19	19	21	21	19	21	21	21	19	19	21
19	21	19													

13 Sideways flight port

40	13	15	13

14 Recovery from sideways flight to port

37	15	19	19	25	17	13	17	19	15	23	15	13	25	13	13
17	19	21	13	19	21	13	17	13	17	21	21	15			

15 Sideways flight to starboard

44	17	13	15	17	17	19	19	21	15

16 Recovery from sideways flight to starboard

38	25	13	25	23	13	19	29	25	25	15	13	17	13	17	15
13	19	13	19	15	15	23	13								

17 Rearwards flight 20 kn

51	18

18 Recovery from rearwards flight

45	23	21	23	21	21	19	23	21	21	25	13	13	23	23	15
21	23	21	23	23	23	13	23	19							

Table 8 (concluded)

19 Spot turn port

48	13	15	15	15	13	19	15	17	15	15	19	15	17	17	13
13	15	13	15	13	15	15	17	13	13	17	13	15	17	15	15
17	13	13	15	13	13	15	17	15							

20 Spot turn starboard

50	13	13	13

21 Autorotation

42	13	13	13	13	13	13	13	13	13	13	15	13	13	13	13
13	13	13	15												

22 Recovery from autorotation

45	21	21	17	21	17	23	25	21	21	19	23	21	21	23	23
21	19														

23 Descent

45	17	15	15	15	15	15	15	15	15	15	15	15	17

24 Landing

53	19	17	17	17	15

Table 9

SEQUENCE OF MANOEUVRES IN A TRAINING SORTIE

Position number	Manoeuvre	Manoeuvre number	Time in manoeuvre (s)	Matrix applications
1	Take-off	1	36	6
2	Forward flight 20 kn	2	12	3
3	Forward flight 30 kn	3	12	2
4	Forward flight 40 kn	4	12	3
5	Forward flight 30 kn	3	18	3
6	Forward flight 20 kn	2	20	5
7	Normal approach to hover	8	12	3
8	Hover	10	62	0
9	Spot turn port	19	18	1
10	Hover	10	45	0
11	Sideways to starboard	15	14	4
12	Recovery from sideways to starboard	16	10	2
13	Sideways to port	13	16	4
14	Recovery from sideways to port	14	10	2
15	Spot turn starboard	20	18	1
16	Hover	10	25	0
17	Forward flight 20 kn	2	12	3
18	Forward flight 30 kn	3	12	2
19	Forward flight 40 kn	4	12	3
20	Forward flight 60 kn	5	32	8
21	Maximum power climb 70 kn	7	21	7
22	Forward flight 103 kn	6	210	42
23	Bank turn port	11	12	2
24	Bank turn starboard	12	10	2
25	Forward flight 103 kn	6	115	23
26	Bank turn port	11	12	2
27	Forward flight 103 kn	6	350	70
28	Bank turn starboard	12	10	2
29	Forward flight 103 kn	6	260	52
30	Bank turn starboard	12	10	2
31	Forward flight 103 kn	6	175	35
32	Bank turn port	11	12	2

Table 9 (continued)

Position number	Manoeuvre	Manoeuvre number	Time in manoeuvre (s)	Matrix applications
33	Forward flight 103 kn	6	315	63
34	Bank turn starboard	12	10	2
35	Forward flight 103 kn	6	105	21
36	Bank turn port	11	12	2
37	Forward flight 103 kn	6	25	5
38	Bank turn starboard	12	10	2
39	Forward flight 103 kn	6	415	83
40	Bank turn port	11	12	2
41	Forward flight 103 kn	6	40	8
42	0.75 hour flight marker	-1	-	-
43	Bank turn starboard	12	10	2
44	Forward flight 103 kn	6	195	39
45	Descent	23	25	5
46	Forward flight 60 kn	5	32	8
47	Forward flight 40 kn	4	24	6
48	Forward flight 30 kn	3	24	4
49	Forward flight 20 kn	2	24	6
50	Normal approach to hover	9	12	3
51	Hover	10	55	0
52	Forward flight 20 kn	2	12	3
53	Forward flight 30 kn	3	12	2
54	Forward flight 40 kn	4	36	9
55	Forward flight 30 kn	3	24	4
56	Forward flight 20 kn	2	12	3
57	Normal approach to hover	9	12	3
58	Hover	10	45	0
59	Forward flight 20 kn	2	12	3
60	Forward flight 30 kn	3	12	2
61	Forward flight 40 kn	4	40	10
62	Forward flight 30 kn	3	24	4
63	Forward flight 20 kn	2	12	3
64	Normal approach to hover	9	12	3
65	Hover	10	450	0
66	Spot turn port	19	18	1
67	Forward flight 20 kn	2	12	3
68	Forward flight 30 kn	3	12	2
69	Forward flight 40 kn	4	12	3
70	Forward flight 60 kn	5	40	10
71	Maximum power climb 70 kn	7	18	6
72	Forward flight 103 kn	6	35	7
73	Bank turn starboard	12	10	2
74	Forward flight 103 kn	6	65	13
75	Bank turn starboard	12	10	2
76	Forward flight 103 kn	6	215	43
77	Bank turn port	11	12	2
78	Descent	23	25	5
79	Forward flight 60 kn	5	40	10
80	Forward flight 40 kn	4	16	4
81	Forward flight 30 kn	3	18	3
82	Forward flight 20 kn	2	12	3
83	Normal approach to hover	9	12	3
84	Hover	10	159	0
85	Forward flight 20 kn	2	36	9
86	Normal approach to hover	9	12	3
87	Hover	10	530	0
88	Spot turn starboard	20	18	1
89	Rearwards flight	17	10	4
90	Recovery from rearwards flight	18	6	1
91	Forward flight 20 kn	2	12	3
92	Forward flight 30 kn	3	12	2
93	Forward flight 40 kn	4	12	3
94	Forward flight 60 kn	5	48	12
95	Maximum power climb 70 kn	7	18	6
96	Forward flight 103 kn	6	35	7
97	Bank turn starboard	12	10	2
98	Forward flight 103 kn	6	45	9
99	Bank turn starboard	12	10	2
100	Forward flight 103 kn	6	75	15
101	Bank turn port	11	12	2
102	Forward flight 103 kn	6	225	45
103	Bank turn starboard	12	10	2
104	Forward flight 103 kn	6	15	3
105	Bank turn port	11	12	2
106	Forward flight 103 kn	6	475	95
107	Bank turn port	11	12	2
108	Forward flight 103 kn	6	335	67

Table 9 (continued)

Position number	Manoeuvre	Manoeuvre number	Time in manoeuvre (s)	Matrix applications
109	Bank turn starboard	12	10	2
110	Forward flight 103 kn	6	95	19
111	Bank turn port	11	12	2
112	Forward flight 103 kn	6	15	3
113	Bank turn port	11	12	2
114	Forward flight 103 kn	6	530	106
115	Bank turn starboard	12	10	2
116	Forward flight 103 kn	6	265	53
117	Bank turn starboard	12	10	2
118	Forward flight 103 kn	6	115	23
119	Bank turn port	11	12	2
120	Forward flight 103 kn	6	85	17
121	Bank turn port	11	12	2
122	Forward flight 103 kn	6	315	63
123	Bank turn starboard	12	10	2
124	Forward flight 103 kn	6	50	10
125	2.25 hour flight marker	-2	-	0
126	Bank turn starboard	12	10	2
127	Forward flight 103 kn	6	415	83
128	Bank turn port	11	12	2
129	Forward flight 103 kn	6	25	5
130	Bank turn port	11	12	2
131	Forward flight 103 kn	6	15	3
132	Bank turn port	11	12	2
133	Forward flight 103 kn	6	20	4
134	Bank turn starboard	12	10	2
135	Forward flight 103 kn	6	35	7
136	Bank turn port	11	12	2
137	Forward flight 103 kn	6	15	3
138	Bank turn starboard	12	10	2
139	Forward flight 103 kn	6	45	9
140	Bank turn starboard	12	10	2
141	Forward flight 103 kn	6	15	3
142	Bank turn port	11	12	2
143	Forward flight 103 kn	6	490	98
144	Autorotation	21	60	12
145	Recovery from autorotation	22	5	1
146	Forward flight 60 kn	5	164	41
147	Forward flight 40 kn	4	24	6
148	Forward flight 30 kn	3	24	4
149	Forward flight 20 kn	2	12	3
150	Shallow approach to hover	8	10	2
151	Hover	10	116	0
152	Forward flight 20 kn	2	88	22
153	Normal approach to hover	9	12	3
154	Hover	10	560	0
155	Sideways to port	13	8	2
156	Recovery from sideways to port	14	10	2
157	Rearwards flight	17	15	6
158	Recovery from rearwards flight	18	12	2
159	Spot turn port	19	18	1
160	Spot turn starboard	20	18	1
161	Hover	10	320	0
162	Sideways to starboard	15	14	4
163	Recovery from sideways to starboard	16	5	1
164	Spot turn port	19	18	1
165	Rearwards flight	17	15	6
166	Recovery from rearwards flight	18	12	2
167	Hover	10	215	0
168	Forward flight 20 kn	2	12	3
169	Forward flight 30 kn	3	12	2
170	Forward flight 40 kn	4	12	3
171	Forward flight 60 kn	5	48	12
172	Maximum power climb 70 kn	7	12	4
173	Forward flight 103 kn	6	20	4
174	Bank turn starboard	12	10	2
175	Forward flight 103 kn	6	15	3
176	Bank turn port	11	12	2
177	Forward flight 103 kn	6	25	5
178	Bank turn port	11	12	2
179	Forward flight 103 kn	6	295	59
180	Bank turn port	11	12	2
181	Forward flight 103 kn	6	465	93
182	Bank turn starboard	12	10	2
183	Forward flight 103 kn	6	155	31
184	Bank turn port	11	12	2

Table 9 (concluded)

Position Number	Manoeuvre	Manoeuvre number	Time in manoeuvre (s)	Matrix applications
185	Forward flight 103 kn	6	380	76
186	Bank turn port	11	12	2
187	Forward flight 103 kn	6	15	3
188	Bank turn starboard	12	10	2
189	Forward flight 103 kn	6	10	2
190	Bank turn starboard	12	10	2
191	Forward flight 103 kn	6	55	11
192	Bank turn port	11	12	2
193	Forward flight 103 kn	6	180	36
194	Bank turn starboard	12	10	2
195	Forward flight 103 kn	6	305	61
196	Bank turn port	11	12	2
197	Forward flight 103 kn	6	320	64
	Landing sequence marker	-	-	-
198	Descent	22	20	4
199	Forward flight 60 kn	5	24	6
200	Forward flight 40 kn	4	16	4
201	Forward flight 30 kn	3	12	2
202	Forward flight 20 kn	2	16	4
203	Normal approach to hover	9	12	3
204	Hover	10	15	0
205	Spot turn port	19	18	1
206	Landing	24	18	3

Table 10

SEQUENCE OF MANOEUVRES IN TRANSPORT SORTIE

Position number	Manoeuvre	Manoeuvre number	Time in manoeuvre (s)	Matrix applications
1	Take-off	1	36	6
2	Forward flight 20 kn	2	12	3
3	Forward flight 30 kn	3	12	2
4	Forward flight 40 kn	4	12	3
5	Forward flight 60 kn	5	156	39
6	Maximum power climb 70 kn	7	60	20
7	Forward flight 103 kn	6	980	196
8	Bank turn starboard	12	5	1
9	Forward flight 103 kn	6	170	34
10	Bank turn starboard	12	5	1
11	Forward flight 103 kn	6	130	26
12	0.75 hour flight marker	-1	-	-
13	Bank turn port	11	6	1
14	Forward flight 103 kn	6	495	99
15	Bank turn port	11	6	1
16	Forward flight 103 kn	6	580	116
17	Bank turn starboard	12	5	1
18	Forward flight 103 kn	6	660	132
19	Bank turn port	11	6	1
20	Forward flight 103 kn	6	165	33
21	Bank turn starboard	12	5	1
22	Forward flight 103 kn	6	295	59
23	Bank turn starboard	12	5	1
24	Forward flight 103 kn	6	110	22
25	Bank turn starboard	12	5	1
26	Forward flight 103 kn	6	260	52
27	Bank turn port	11	6	1
28	Forward flight 103 kn	6	60	12
29	Bank turn starboard	12	5	1
30	Forward flight 103 kn	6	320	64
31	Bank turn starboard	12	5	1
32	Forward flight 103 kn	6	60	12
33	Bank turn port	11	6	1
34	Forward flight 103 kn	6	370	74
35	Bank turn port	11	6	1
36	Forward flight 103 kn	6	390	78
37	Bank turn port	11	6	1
38	Forward flight 103 kn	6	75	15
39	Bank turn port	11	6	1
40	Forward flight 103 kn	6	50	10

Table 10 (continued

Position number	Manoeuvre	Manoeuvre number	Time in manoeuvre (s)	Matrix applications
41	Bank turn port	11	6	1
42	Forward flight 103 kn	6	705	141
43	Bank turn starboard	12	5	1
44	Forward flight 103 kn	6	155	31
45	Bank turn port	11	6	1
46	Forward flight 103 kn	6	175	35
47	Bank turn starboard	12	5	1
48	Forward flight 103 kn	6	375	75
49	2.25 hour flight marker	-2	-	-
50	Bank turn starboard	12	5	1
51	Forward flight 103 kn	6	360	72
52	Bank turn port	11	6	1
53	Forward flight 103 kn	6	245	49
54	Bank turn starboard	12	5	1
55	Forward flight 103 kn	6	390	78
56	Bank turn starboard	12	5	1
57	Forward flight 103 kn	6	380	76
58	Bank turn starboard	12	5	1
59	Forward flight 103 kn	6	305	61
60	Bank turn starboard	12	5	1
61	Forward flight 103 kn	6	195	39
62	Bank turn starboard	12	5	1
63	Forward flight 103 kn	6	260	52
64	Bank turn port	11	6	1
65	Forward flight 103 kn	6	250	50
66	Bank turn port	11	6	1
67	Forward flight 103 kn	6	105	21
68	Bank turn starboard	12	5	1
69	Forward flight 103 kn	6	175	35
70	Bank turn starboard	12	5	1
71	Forward flight 103 kn	6	25	5
72	Bank turn port	11	6	1
73	Forward flight 103 kn	6	215	43
74	Bank turn starboard	12	5	1
75	Forward flight 103 kn	6	160	32
76	Bank turn port	11	6	1
77	Forward flight 103 kn	6	370	74
78	Bank turn starboard	12	5	1
79	Forward flight 103 kn	6	425	85
80	Bank turn port	11	6	1
81	Forward flight 103 kn	6	25	5
82	Bank turn port	11	6	1
83	Forward flight 103 kn	6	360	72
84	Bank turn starboard	12	5	1
85	Forward flight 103 kn	6	125	25
86	Bank turn port	11	6	1
87	Forward flight 103 kn	6	110	22
88	Bank turn starboard	12	5	1
89	Forward flight 103 kn	6	100	20
90	Autorotation	21	60	12
91	Recovery from autorotation	22	5	1
92	Descent	23	20	4
93	Forward flight 60 kn	5	152	38
94	Forward flight 40 kn	4	12	3
95	Forward flight 30 kn	3	12	2
96	Forward flight 20 kn	2	12	3
97	Shallow approach to hover	8	15	3
98	Hover	10	272	0
99	Forward flight 20 kn	2	12	3
100	Forward flight 30 kn	3	12	2
101	Forward flight 40 kn	4	12	3
102	Forward flight 60 kn	5	116	29
	Landing sequence marker	-	-	-
103	Descent	23	15	3
104	Forward flight 60 kn	5	732	183
105	Forward flight 40 kn	4	20	5
106	Forward flight 30 kn	3	18	3
107	Forward flight 20 kn	2	16	4
108	Shallow approach to hover	8	10	2
109	Hover	10	113.5	-
110	Sideways to port	13	32	8
111	Recovery from sideways to port	14	10	2
112	Spot turn to port	19	18	1
113	Rearwards flight	17	30	12
114	Recovery from rearwards flight	18	12	2
115	Sideways to starboard	15	31.5	9

Table 10 (concluded)

Position number	Manoeuvre	Manoeuvre number	Time in manoeuvre (s)	Matrix applications
116	Recovery from sideways to starboard	16	10	2
117	Spot turn to starboard	20	18	1
118	Landing	24	36	6

Table 11

SEQUENCE OF MANOEUVRES IN ASW SORTIE

Position number	Manoeuvre	Manoeuvre number	Time in manoeuvre (s)	Matrix applications
	Initial transit			
1	Take-off	1	18	2
2	Forward flight 20 kn	2	12	3
3	Forward flight 30 kn	3	12	2
4	Forward flight 40 kn	4	12	3
5	Forward flight 60 kn	5	24	6
6	Maximum power climb 70 kn	7	12	4
7	Forward flight 103 kn	6	50	10
8	Bank turn starboard	12	10	2
9	Forward flight 103 kn	6	10	2
10	Bank turn port	11	12	2
11	Forward flight 103 kn	6	35	7
12	Bank turn port	11	12	2
13	Forward flight 103 kn	6	40	8
14	Bank turn starboard	12	10	2
15	Forward flight 103 kn	6	60	12
16	Bank turn port	11	12	2
17	Forward flight 103 kn	6	40	8
18	Bank turn starboard	12	10	2
19	Forward flight 103 kn	6	65	13
20	Bank turn starboard	12	10	2
21	Forward flight 103 kn	6	20	4
22	Bank turn port	11	12	2
23	Forward flight 103 kn	6	40	8
24	Bank turn starboard	12	10	2
25	Forward flight 103 kn	6	45	9
26	Bank turn starboard	12	10	2
27	Forward flight 103 kn	6	40	8
28	Bank turn starboard	12	10	2
29	Forward flight 103 kn	6	35	7
	First sonar dunk			
30	First combined manoeuvre (hover time 243 s)	25	452	1
	Second sonar dunk			
31	Second combined manoeuvre (hover time 162 s)	25	371	1
	Third sonar dunk			
32	Third combined manoeuvre (hover time 101 s)	25	310	1
33	Forward flight 103 kn	6	65	13
34	Bank turn starboard	12	10	2
35	Forward flight 103 kn	6	70	14
36	Bank turn starboard	12	10	2
37	0.75 hour flight marker	-1	-	-
	Fourth sonar dunk			
38	Fourth combined manoeuvre (hover time 296 s)	25	505	1
39	Forward flight 103 kn	6	10	2
40	Bank turn port	11	12	2
41	Forward flight 103 kn	6	60	12
42	Bank turn starboard	12	10	2
43	Forward flight 103 kn	6	65	13
44	Bank turn starboard	12	10	2
45	Forward flight 103 kn	6	45	9
46	Bank turn starboard	12	10	2
47	Forward flight 103 kn	6	45	9
48	Bank turn port	11	12	2
49	Forward flight 103 kn	6	40	8
50	Bank turn port	11	12	2

Table 11 (continued)

Position number	Manoeuvre	Manoeuvre number	Time in manoeuvre (s)	Matrix applications
	Fifth sonar dunk			
51	Fifth combined manoeuvre (hover time 474 s)	25	683	1
52	Forward flight 103 kn	6	45	9
53	Bank turn port	11	12	2
54	Forward flight 103 kn	6	20	4
55	Bank turn port	11	12	2
56	Forward flight 103 kn	6	30	6
57	Bank turn port	11	12	2
58	Forward flight 103 kn	6	25	5
59	Bank turn starboard	12	10	2
	Sixth sonar dunk			
60	Sixth combined manoeuvre (hover time 373 s)	25	582	1
61	Forward flight 103 kn	6	55	11
62	Bank turn port	11	12	2
63	Forward flight 103 kn	6	40	8
64	Bank turn starboard	12	10	2
65	Forward flight 103 kn	6	25	5
66	Bank turn starboard	12	10	2
67	Forward flight 103 kn	6	55	11
68	Bank turn starboard	12	10	2
	Seventh sonar dunk			
69	Seventh combined manoeuvre (hover time 330 s)	25	539	1
70	Forward flight 103 kn	6	45	9
71	Bank turn port	11	12	2
72	Forward flight 103 kn	6	35	7
73	Bank turn port	11	12	2
74	Forward flight 103 kn	6	35	7
75	Bank turn port	11	12	2
76	Forward flight 103 kn	6	70	14
77	Bank turn port	11	12	2
78	Forward flight 103 kn	6	65	13
79	Bank turn starboard	12	10	2
	Eighth sonar dunk			
80	Eighth combined manoeuvre (hover time 419 s)	25	628	1
81	Forward flight 103 kn	6	35	7
82	Bank turn port	11	12	2
83	Forward flight 103 kn	6	35	7
84	Bank turn port	11	12	2
85	Forward flight 103 kn	6	45	9
86	Bank turn starboard	12	10	2
87	Forward flight 103 kn	6	30	6
88	Bank turn starboard	12	10	2
89	Forward flight 103 kn	6	30	6
90	Bank turn port	11	12	2
91	Forward flight 103 kn	6	50	10
92	Bank turn starboard	12	10	2
93	Forward flight 103 kn	6	15	3
94	Bank turn port	11	12	2
95	Forward flight 103 kn	6	60	12
96	Bank turn port	11	12	2
	Ninth sonar dunk			
97	Ninth combined manoeuvre (hover time 390 s)	25	599	1
98	Forward flight 103 kn	6	10	2
99	Bank turn port	11	12	2
100	Forward flight 103 kn	6	10	2
101	Bank turn starboard	12	10	2
102	Forward flight 103 kn	6	75	15
103	Bank turn port	11	12	2
104	Forward flight 103 kn	6	35	7
105	Bank turn starboard	12	10	2
106	Forward flight 103 kn	6	30	6
107	Bank turn starboard	12	10	2
108	Forward flight 103 kn	6	5	1
109	Bank turn starboard	12	10	2
110	Forward flight 103 kn	6	45	9
111	Bank turn starboard	12	10	2
112	Forward flight 103 kn	6	25	5
113	Bank turn port	11	12	2
114	Forward flight 103 kn	6	20	4
115	Bank turn port	11	12	2
116	Forward flight 103 kn	6	40	8

Table 11 (continued)

Position number	Manoeuvre	Manoeuvre number	Time in manoeuvre (s)	Matrix applications
117	Bank turn starboard	12	10	2
118	Forward flight 103 kn	6	10	2
119	Bank turn port	11	12	2
120	Forward flight 103 kn	6	10	2
121	Bank turn starboard	12	10	2
122	2,25 hour flight marker	-	-	-
	Tenth sonar dunk			
123	Tenth combined manoeuvre (hover time 190 s)	25	399	1
124	Forward flight 103 kn	6	70	14
125	Bank turn port	11	12	2
126	Forward flight 103 kn	6	30	6
127	Bank turn starboard	12	10	2
128	Forward flight 103 kn	6	50	10
129	Bank turn starboard	12	10	2
130	Forward flight 103 kn	6	25	5
131	Bank turn port	11	12	2
	Eleventh sonar dunk			
132	Eleventh combined manoeuvre (hover time 290 s)	25	499	1
133	Forward flight 103 kn	6	40	8
134	Bank turn port	12	10	2
135	Forward flight 103 kn	6	45	9
136	Bank turn port	11	12	2
137	Forward flight 103 kn	6	30	6
138	Bank turn starboard	12	10	2
139	Forward flight 103 kn	6	35	7
140	Bank turn port	11	12	2
141	Forward flight 103 kn	6	80	16
142	Bank turn starboard	12	10	2
143	Forward flight 103 kn	6	75	15
144	Bank turn port	11	12	2
145	Forward flight 103 kn	6	30	6
146	Bank turn port	11	12	2
	Twelfth sonar dunk			
147	Twelfth combined manoeuvre (hover time 207 s)	25	416	1
148	Forward flight 103 kn	6	25	5
149	Bank turn port	11	12	2
150	Forward flight 103 kn	6	35	7
151	Bank turn port	11	12	2
152	Forward flight 103 kn	6	65	13
153	Bank turn starboard	12	10	2
154	Forward flight 103 kn	6	45	9
155	Bank turn starboard	12	10	2
156	Forward flight 103 kn	6	30	6
157	Bank turn port	11	12	2
	Thirteenth sonar dunk			
158	Thirteenth combined manoeuvre (hover time 374 s)	25	583	1
159	Forward flight 103 kn	6	55	11
160	Bank turn starboard	12	10	2
161	Forward flight 103 kn	6	15	3
162	Bank turn starboard	12	10	2
163	Forward flight 103 kn	6	20	4
164	Bank turn port	11	12	2
165	Forward flight 103 kn	6	5	1
166	Bank turn port	11	12	2
167	Forward flight 103 kn	6	25	5
168	Bank turn starboard	12	10	2
169	Forward flight 103 kn	6	25	5
170	Bank turn port	11	12	2
171	Forward flight 103 kn	6	35	7
172	Bank turn port	11	12	2
173	Forward flight 103 kn	6	50	10
174	Bank turn starboard	12	10	2
175	Forward flight 103 kn	6	40	8
176	Bank turn port	11	12	2
	Fourteenth sonar dunk			
177	Fourteenth combined manoeuvre (hover time 290 s)	25	499	1
178	Forward flight 103 kn	6	5	1
179	Bank turn port	11	6	1
180	Forward flight 103 kn	6	25	5
181	Bank turn starboard	12	10	2
182	Forward flight 103 kn	6	80	16

Table 11 (concluded)

Position number	Manoeuvre	Manoeuvre number	Time in manoeuvre (s)	Matrix applications
183	Bank turn port	11	12	2
184	Forward flight 103 kn	6	60	12
185	Bank turn port	11	12	2
186	Forward flight 103 kn	6	15	3
187	Bank turn starboard	12	10	2
188	Forward flight 103 kn	6	50	10
189	Bank turn port	11	12	2
190	Forward flight 103 kn	6	40	8
191	Bank turn starboard	12	10	2
192	Forward flight 103 kn	6	50	10
193	Bank turn port	11	12	2
194	Forward flight 103 kn	6	30	6
195	Bank turn port	11	12	2
196	Forward flight 103 kn	6	110	22
197	Bank turn port	11	12	2
198	Forward flight 103 kn	6	30	6
199	Bank turn port	11	12	2
200	Forward flight 103 kn	6	20	4
201	Bank turn port	11	12	2
202	Forward flight 103 kn	6	40	8
203	Bank turn port	11	12	2
204	Forward flight 103 kn	6	20	4
205	Bank turn starboard	12	10	2
206	Forward flight 103 kn	6	30	6
207	Bank turn port	11	12	2
208	Forward flight 103 kn	6	35	7
209	Bank turn port	11	12	2
210	Forward flight 103 kn	6	15	3
211	Bank turn starboard	12	10	2
212	Forward flight 103 kn	6	35	7
213	Bank turn port	11	12	2
214	Forward flight 103 kn	6	40	8
215	Bank turn port	11	12	2
216	Forward flight 103 kn	6	60	12
217	Bank turn starboard	12	10	2
218	Forward flight 103 kn	6	30	6
219	Bank turn starboard	12	10	2
220	Forward flight 103 kn	6	30	6
221	Bank turn port	11	12	2
222	Forward flight 103 kn	6	55	11
223	Bank turn starboard	12	10	2
224	Forward flight 103 kn	6	100	20
225	Bank turn port	11	12	2
226	Forward flight 103 kn	6	20	4
227	Bank turn port	11	12	2
228	Forward flight 103 kn	6	75	15
229	Bank turn starboard	12	10	2
230	Forward flight 103 kn	6	25	5
231	Bank turn port	11	12	2
232	Forward flight 103 kn	6	55	11
233	Bank turn port	11	12	2
234	Forward flight 103 kn	6	65	13
235	Bank turn port	11	12	2
236	Forward flight 103 kn	6	20	4
237	Bank turn port	11	12	2
238	Forward flight 103 kn	6	60	12
239	Bank turn port	11	12	2
240	Autorotation	21	60	12
241	Recovery from autorotation	22	5	1
	Landing sequence marker	-	-	-
242	Descent	23	40	8
243	Forward flight 60 kn	5	108	27
244	Forward flight 40 kn	4	28	7
245	Forward flight 30 kn	3	30	5
246	Forward flight 20 kn	2	28	7
247	Normal approach to hover	9	20	5
248	Hover	10	293.5	0
249	Sideways to port	13	32	8
250	Recovery from sideways to port	14	10	2
251	Spot turn port	19	18	1
252	Rearwards flight	17	30	12
253	Recovery from rearwards flight	18	12	2
254	Sideways to starboard	15	31.5	9
255	Recovery from sideways to starboard	16	10	2
256	Spot turn starboard	20	18	1
257	Landing	24	18	3

Table 12

SEQUENCE OF MANOEUVRES IN SAR SORTIE

Position number	Manoeuvre	Manoeuvre number	Time in manoeuvre (s)	Matrix applications
1	Take-off	1	36	6
2	Forward flight 20 kn	2	8	2
3	Forward flight 30 kn	3	6	1
4	Forward flight 40 kn	4	8	2
5	Forward flight 60 kn	5	32	8
6	Maximum power climb 70 kn	7	30	10
7	Forward flight 103 kn	6	315	63
8	Bank turn port	11	6	1
9	Forward flight 103 kn	6	195	39
10	First 0.75 hour flight marker	-1	-	-
11	Bank turn starboard	12	5	1
12	Forward flight 103 kn	6	550	110
13	Bank turn port	11	6	1
14	Forward flight 103 kn	6	320	64
15	Bank turn starboard	12	5	1
16	Forward flight 103 kn	6	155	31
17	Bank turn starboard	12	5	1
18	Forward flight 103 kn	6	115	23
19	Bank turn starboard	12	5	1
20	Forward flight 103 kn	6	255	51
21	Bank turn starboard	12	5	1
22	Forward flight 103 kn	6	300	60
23	Bank turn port	11	6	1
24	Forward flight 103 kn	6	375	75
25	Bank turn starboard	12	5	1
26	Forward flight 103 kn	6	605	121
27	Bank turn starboard	12	5	1
28	Forward flight 103 kn	6	260	52
29	Bank turn port	11	6	1
30	First 2.25 hour flight marker	-2	-	-
31	Forward flight 103 kn	6	310	62
32	Bank turn starboard	12	5	1
33	Forward flight 103 kn	6	640	128
34	Bank turn starboard	12	5	1
35	Forward flight 103 kn	6	250	50
36	Descent	23	20	4
37	Forward flight 60 kn	5	2000	500
	SAR marker	-	-	-
38	Descent	23	20	4
39	Forward flight 60 kn	5	580	145
40	Forward flight 40 kn	4	8	2
41	Forward flight 30 kn	3	6	1
42	Forward flight 20 kn	2	8	2
43	Normal approach to hover	9	8	2
44	Hover	10	600	0
45	Sideways to port	13	32	8
46	Recovery from sideways to port	14	10	2
47	Rearwards flight	17	30	12
48	Recovery from rearwards	18	12	2
49	Spot turn starboard	20	18	1
50	Forward flight 20 kn	2	8	2
51	Forward flight 30 kn	3	6	1
52	Forward flight 40 kn	4	8	2
53	Forward flight 60 kn	5	64	16
54	Maximum power climb 70 kn	7	30	10
55	Bank turn port	11	6	1
56	Forward flight 103 kn	6	390	78
57	Second 0.75 hour flight marker	-1	-	-
58	Bank turn port	11	6	1
59	Forward flight 103 kn	6	680	136
60	Bank turn port	11	6	1
61	Forward flight 103 kn	6	230	46
62	Bank turn starboard	12	5	1
63	Forward flight 103 kn	6	355	71
64	Bank turn starboard	12	5	1
65	Forward flight 103 kn	6	830	166
66	Bank turn starboard	12	5	1
67	Forward flight 103 kn	6	290	58
68	Second 2.25 hour flight marker	-2	-	-
69	Bank turn port	11	6	1
70	Forward flight 103 kn	6	525	105
71	Bank turn port	11	6	1
72	Forward flight 103 kn	6	415	83
73	Bank turn port	11	6	1

Table 12 (concluded)

Position number	Manoeuvre	Manoeuvre number	Time in manoeuvre (s)	Matrix applications
74	Forward flight 103 kn	6	405	81
75	Descent	23	15	3
76	Forward flight 60 kn	5	792	198
	Landing sequence marker	-	-	-
77	Descent	23	20	4
78	Forward flight 60 kn	5	32	8
79	Forward flight 40 kn	4	8	2
80	Forward flight 30 kn	3	12	2
81	Forward flight 20 kn	2	8	2
82	Normal approach to hover	9	4	1
83	Hover	10	58.5	0
84	Sideways to starboard	15	31.5	9
85	Recovery from sideways to starboard	16	10	2
86	Spot turn port	19	18	1
87	Landing	24	18	3

Table 13

SEQUENCE OF MANOEUVRES IN COMBINED MANOEUVRE IN ASW SORTIE

Position number	Manoeuvre	Manoeuvre number	Time in manoeuvre (s)	Matrix applications
1	Descent	23	10	2
2	Forward flight 60 kn	5	24	6
3	Forward flight 40 kn	4	12	3
4	Forward flight 30 kn	3	12	2
5	Forward flight 20 kn	2	12	3
6	Normal approach to hover	9	12	3
7	Hover	10	variable	none
8	Forward flight 20 kn	2	12	3
9	Forward flight 30 kn	3	12	2
10	Forward flight 40 kn	4	12	3
11	Forward flight 60 kn	5	24	6
12	Maximum power climb	7	12	4
13	Forward flight 103 kn	6	20	4
14	Bank turn starboard	12	10	2
15	Forward flight 103 kn	6	15	3
16	Bank turn starboard	12	10	2

Table 14

DURATION OF MANOEUVRES IN SORTIES TAKING INTO ACCOUNT INDIVIDUAL MANOEUVRE LOAD SEQUENCE FLIGHT TIMES

No.	Load sequence flight time (s)	Time in manoeuvre for 3.75 hour sortie (s)							
		Training		Transport		ASW		SAR	
		Accurate	Divisible by flight time	Accurate	Divisible by flight time	Accurate	Divisible by flight time	Accurate	Divisible by flight time
1	6			36	36	18	18	36	36
2	4			54	52	375	376	31	32
3	6			54	54	375	378	31	30
4	4			54	56	375	376	31	32
5	4			1155	1156	804	804	3499	3500
6	5			11140	11160	4824	4845	8748	8765
7	3			60	60	180	180	60	60
8	5			23	25	-	-	-	-
9	4			-	-	188	188	11	12
10	-			385	385.5	4432	4432.5	655	658.5
11	6			108	108	740	738	61	60
12	5			108	110	740	740	61	60
13	4			30	32	30	32	30	32
14	5			12	10	12	10	12	10
15	3.5			30	31.5	30	31.5	30	31.5
16	5			12	10	12	10	12	10
17	2.5			30	30	30	30	30	30
18	6			12	12	12	12	12	12
19	18			30	18	30	18	30	18
20	18			30	18	30	18	30	18
21	5			60	60	60	60	-	-
22	5			5	5	5	5	-	-
23	5			36	35	180	180	72	75
24	6			36	36	18	18	18	18

Table 15

SEA KING FLIGHT DURATIONS DISTRIBUTIONS WITH COUNTING INTERVALS OF 15 min, 1 h AND 1.5 h

Initial counting interval (min)	Number of flights in each counting interval											
	Training			Transport			ASW			SAR		
	1*	2**	3†	1	2	3	1	2	3	1	2	3
0- 15	106	777	1168	87	592	869	24	218	524	5	47	80
15- 30	213			141			48			12		
30- 45	167			155			63			10		
45- 60	291			209			83			20		
60- 75	226	535		137	468		93	744		13	73	
75- 90	165			140			213			20		
90-105	68			83			152			17		
105-120	76			108			286			23		
120-135	39	125	269	76	278	469	156	505	943	5	25	63
135-150	38			79			128			5		
150-165	15			47			75			8		
165-180	33			76			146			7		
180-195	8	24	25	48	109	120	80	366	422	5	15	18
195-210	11			25			98			3		
210-225	3			19			62			3		
225-240	2			17			126			4		
240-255	-	3	2	5	14	6	44	63	13	1	3	2
255-270	1			6			12			2		
270-285	2			2			4			1		
285-300	-			1			3			0		
300-315	-			1	3		4	6		1	1	
315-330	-			1			2			-		
330-345	-			0			-			-		
345-360	-			1			-			-		
Total for each sortie	1464			1464			1902			165		

* Counting interval of 15 min ** Counting interval of 1 h
† Counting interval of 1.5 h

Table 16

ESTIMATION OF FLIGHT SEQUENCE LENGTH FOR LOADING STANDARD

t_i (h)	Training		Transport		ASW		SAR	
	$NFPH_{im}$	NF_{im}	$NFPH_{im}$	NF_{im}	$NFPH_{im}$	NF_{im}	$NFPH_{im}$	NF_{im}
	Case 1: 6 time intervals of 1 h							
0.5	0.1602	1232	0.1333	1025	0.0048	37	0.0167	128
1.5	0.1103	848	0.1054	811	0.0164	126	0.0259	199
2.5	0.0258	198	0.0626	482	0.0111	854	0.0089	68
3.5	0.0049	38	0.0246	189	0.0081	62	0.0053	41
4.5	0.0006	5	0.0032	25	0.0014	11	0.0011	8
5.5	-		0.0007	5	0.00013	1	0.0004	3
	NF_s = 6395							
	Case 2: 5 time intervals of 1 h							
0.5	0.1615	147	0.1343	122	0.0043	4	0.0171	16
1.5	0.1112	101	0.1062	96	0.0248	23	0.0265	24
2.5	0.0260	24	0.0631	57	0.0112	10	0.0091	8
3.5	0.0050	5	0.0247	22	0.0081	7	0.0054	5
4.5	0.0006	1	0.0032	3	0.0014	1	0.0011	1
	NF_s = 677							
	Case 3: 3 time intervals of 1.5 h							
0.75	0.2447	47	0.1954	38	0.0115	2	0.0278	5
2.25	0.0564	11	0.1055	20	0.0207	4	0.0226	4
3.75	0.0052	1	0.0270	5	0.0093	2	0.0063	1
	NF_s = 140							

Table 17

DESCRIPTION OF THE VARIABLES USED IN THE HELIX GENERATION ALGORITHM FLOW CHARTS

Variable	Description
I	Incremental counter for sortie sequence
IASWTYPE	Sequence of manoeuvres in the standard ASW sonar dunk operation (Table 13)
ISARJ	Counter to indicate search and rescue portion of SAR sortie
ISEQUENCE	Sequence of 140 sorties that define Helix (see Table 4)
ISORTIE	The sortie to be simulated
K,L	Dummy variables
LSM	Sequence of loads in each manoeuvre (see Table 8)
MANNO	The manoeuvre to be simulated
MASW	Number of applications of LSM required for each manoeuvre in the manoeuvre sequence IASWTYPE (see Table 13)
MTYPE	Sequence of manoeuvres in each of the four sorties (see Tables 9 to 12)
N	Incremental counter for manoeuvre sequence in a sortie
NASW	Incremental counter for standard ASW sonar dunk manoeuvre sequence
NEWN	Manoeuvre sequence number in each sortie that starts the landing sequence and the manoeuvre sequence number that starts the search and rescue routine in the SAR sortie
NOMA	Number of applications of LSM required for each manoeuvre in the manoeuvre sequence for each sortie, MTYPE (see Tables 9 to 12)
NMS	Number of manoeuvres in each of the four sorties

REFERENCES

No.	Author	Title, etc
1	W.J. Crichlow C.J. Buzzetti J. Fairchild	The fatigue and fail-safe program for the certification of the Lockheed model 286 rigid rotor helicopter. In *Aircraft Fatigue - Design, Operation and Economic Aspects*, Proceedings 5th Symposium, Melbourne, edited by J.Y. Mann and I.S. Milligan, pp 171-219, Pergamon Press, Australia (1972)
2	E. Jarosch A. Stepan	Fatigue properties and test procedures of glass reinforced plastic rotor blades. *Journal of American Helicopter Society*, Vol 15, No.1, pp 33-41, January 1970
3	J.C. Ekvall L. Young	Converting fatigue loading spectra for flight-by-flight testing of aircraft and helicopter components. *Journal of Testing and Evaluation*, Vol 4, No.4, pp 231-247, July 1976
4	W.T. Kirkby	A review of the work in the United Kingdom on the fatigue of aircraft structures during the period May 1977 to April 1979. RAE Technical Report 79106 (1979)
5	D. Schütz	Zur Verwerdung von bemessungsunterlagen aus versuchen mit btriebsähnlichen lastfolgen zur lebensdauerabsihätzung. LBF-FB-109 (1976) [Available as "Application to life prediction of design data derived from fatigue tests with service-like load sequences", translated by B. Garland and F.E. Kiddle; RAE Library Translation 1939 (1977)]
6	-	FALSTAFF - description of a Fighter Aircraft Loading STAndard For Fatigue evaluation. Common research work of F+W, LBF, NLR, IABG. Published 1976
7	D. Schütz H.G. Köbler W. Schütz M. Hück	Development of standardised fatigue test load histories for helicopter rotors - fatigue test programme and test results. Paper to be presented at AGARD 51st SMP meeting, September 1980
8	J.B. de Jonge D. Schütz H. Lowak J. Schijve	A standardised load sequence for flight simulation tests on transport aircraft wing structures. LBF Report No.FB-106 (1972) NLR Report No.TR 73029U (1973)
9	A.D. Hall	Helicopter design mission load spectra. In Helicopter design mission load spectra AGARD-CP-206, pp 3-1 to 3-5 (1976)
10	J.D. Porterfield P.F. Maloney	Correlation and evaluation of CH 47A flight spectra data from combat operations in Vietnam. USA AVLABS-TR-69-77 (1970)
11	P.B. Hovell D.A. Webber	Operational flight data from a helicopter in the training role. RAE Technical Report 78014 (1978)
12	T.L. Cox F.J. Giessler	Acquisition of operational data during NOE missions. USARTL-TR-78-3 (1978)
13	T.L. Cox R.B. Johnson S.W. Russell	Dynamic loads and structural criteria. USAAMRDL-TR-75-9 (1975)
14	R. Boocock L.L. Erle J.F. Needham G.D. Roeck H.G. Smith	OH-6A design and operational flight loads study. USAAMRDL-TR-73-21 (1974)
15	J.E. Dougherty H.C. Spicer	Helicopter fatigue substantiation procedures for civil aircraft. In *Symposium on Fatigue Tests of Aircraft Structures - Low Cycle, Full-scale and Helicopters*, ASTM STP 338 (1963)
16	R. Prinz	Die Ermittlung der Lebensdauer von Hubschrauberbauteilen. DLR Mitt 69-26 (1969) [Available as "Determination of the life of helicopter structural members", translated by A.D. Norris and A.M. Stagg; RAE Library Translation 1520 (1972)]

REFERENCES (concluded)

No.	Author	Title, etc
17	J.H. Argyris W. Aicher H.J. Ertelt	Analyse und Synthese von Betriebsbelastungen. ISD Report 193 (1978) [Available as "Analysis and synthesis of operational loads", translated by B. Garland and J. Darts; RAE Library Translation 2008 (1979)]
18	F.E. Kiddle J. Darts	The effects on fatigue life of omitting small loads, large loads and load dwells from a loading spectrum. RAE Technical Report 77153 (1977)
19	S.I. Sikorsky	The helicopter - today and tomorrow. *The Aeronautical Journal*, Vol74, pp 105-110, February 1970
20	J. Schijve	Cumulative damage problems in aircraft structures and materials. NLR-MP 69005 (1969)
21	W. Watt	A time-sharing computer program to drive up to three independent fatigue testing machines. RAE Technical Report 79054 (1979)
22	H. Lowak J.B. de Jonge J. Franz D. Schütz	MINITWIST - a shortened version of TWIST. NLR MP 79018U (1979) LBF Report No.TB-146 (1979)

Copyright ©, Controller HMSO, London

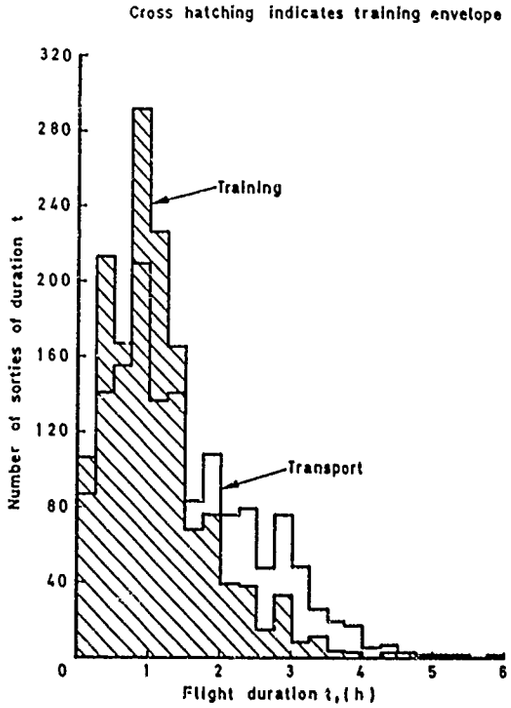


Fig 1 Variation of flight duration for Sea King Training and Transport sorties

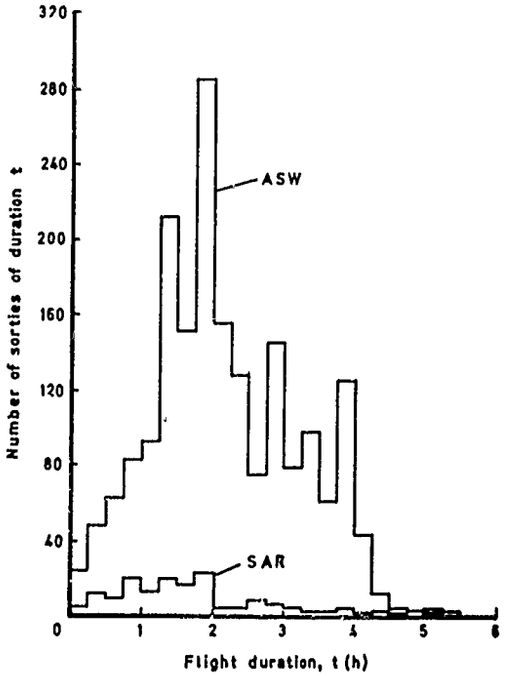


Fig 2 Variation of flight duration for Sea King ASW and SAR sorties

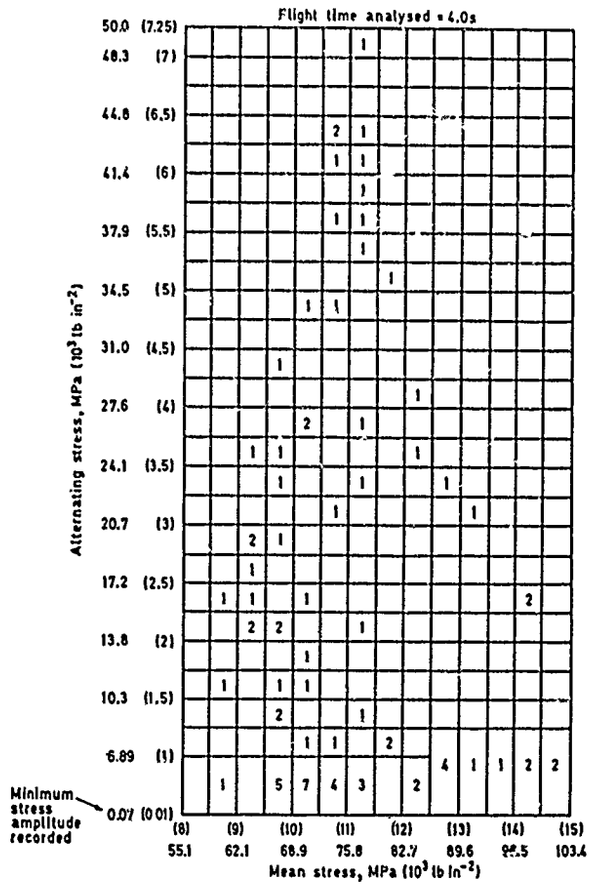


Fig 3 Stress spectrum at the bottom rear corner of Sea King blade spar at half rotor radius for a normal approach to hover

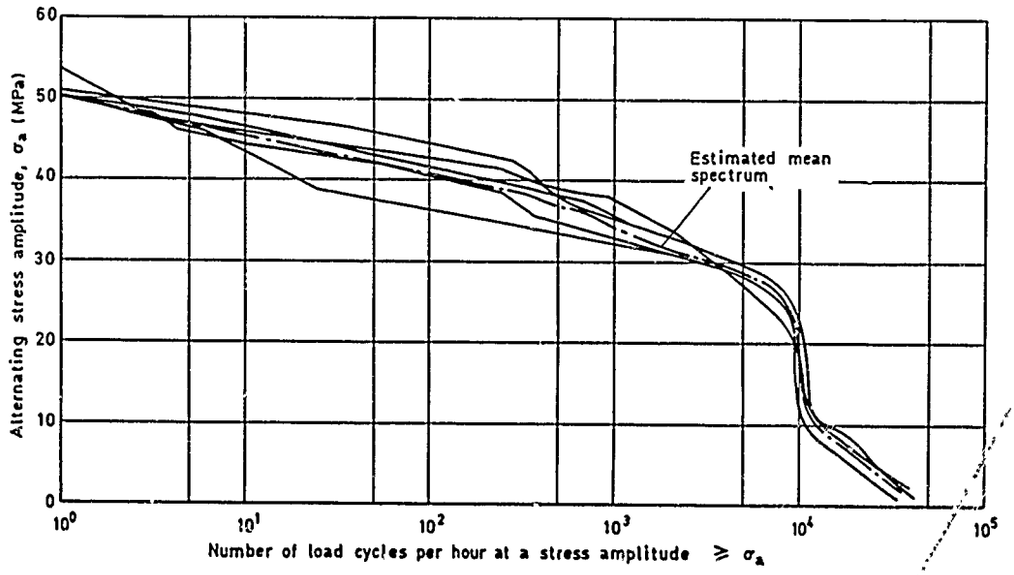


Fig 4 Stress spectra for five CH 53 Transport flights

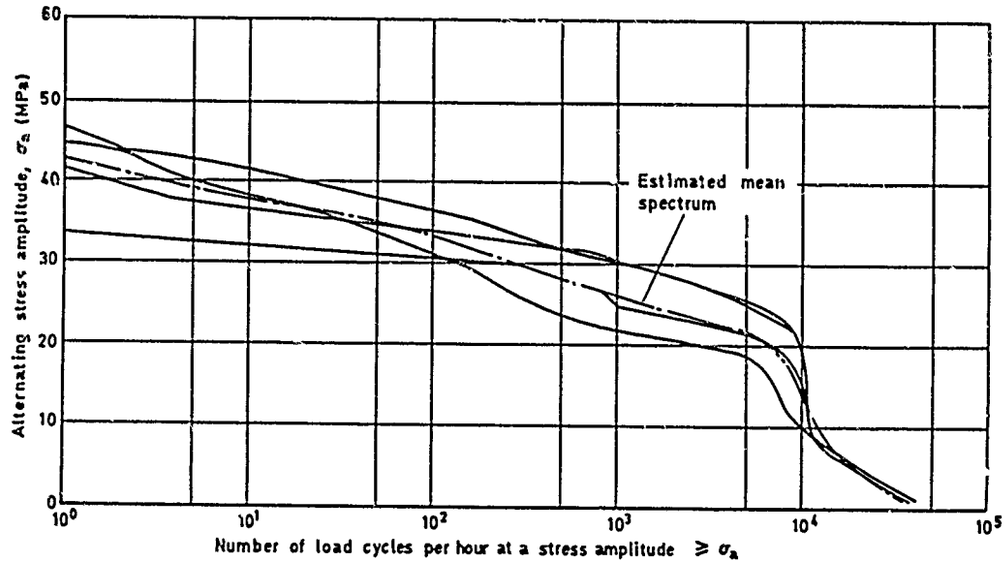
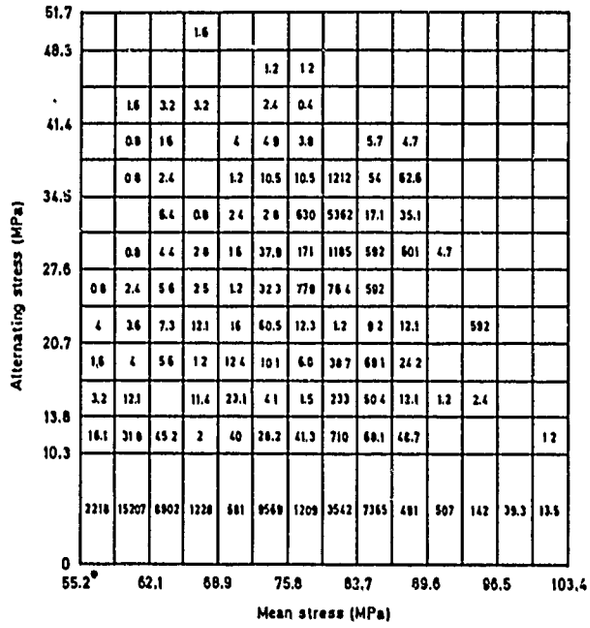


Fig 5 Stress spectra for four CH 53 Training flights

Numbers in boxes are the number of cycles per hour



* Non - integral numbers caused by conversion of lb in^{-2} to MPa

Fig 6 Synthesised stress spectrum for Sea King blade at half rotor radius for the transport role

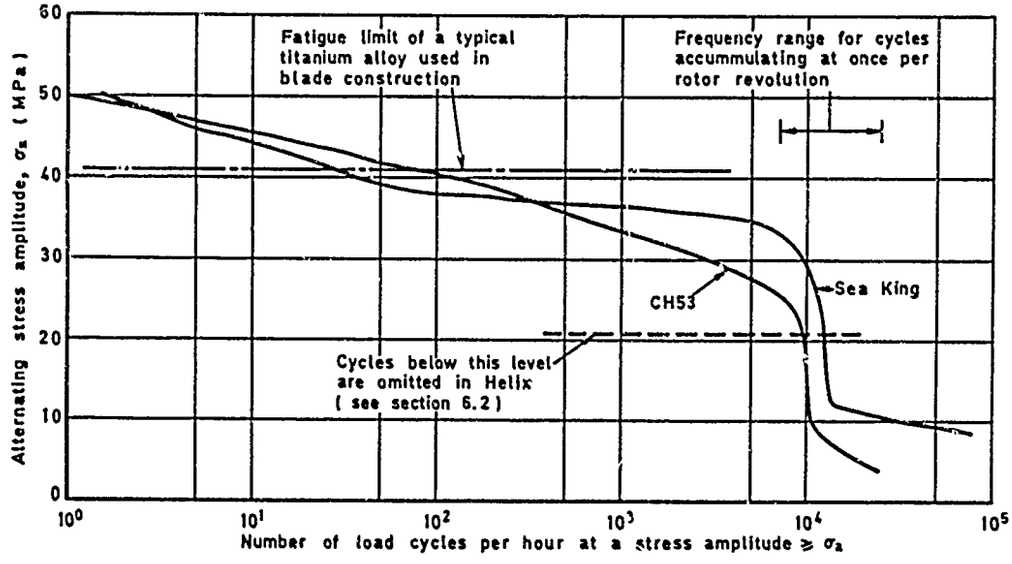


Fig 7 Comparison of stress spectra at half rotor radius for CH 53 and Sea King Transport sorties

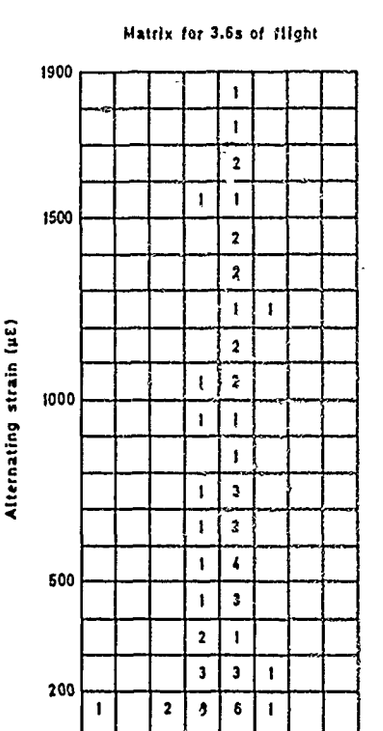


Fig 8 Strain spectrum for the lower surface of BO-105 blade root for a longitudinal control reversal in autorotation

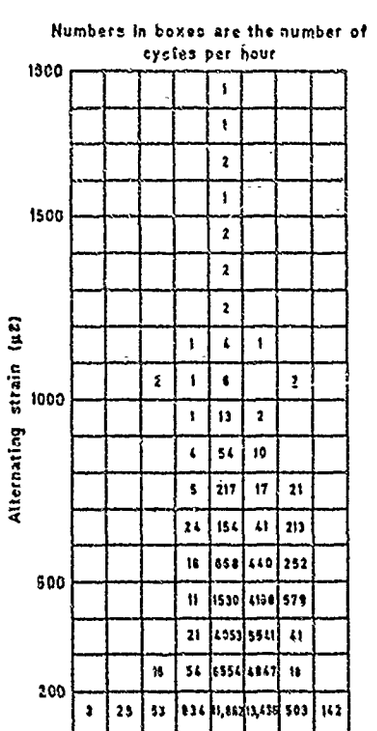


Fig 10 Strain spectrum for lower surface of BO-105 blade root

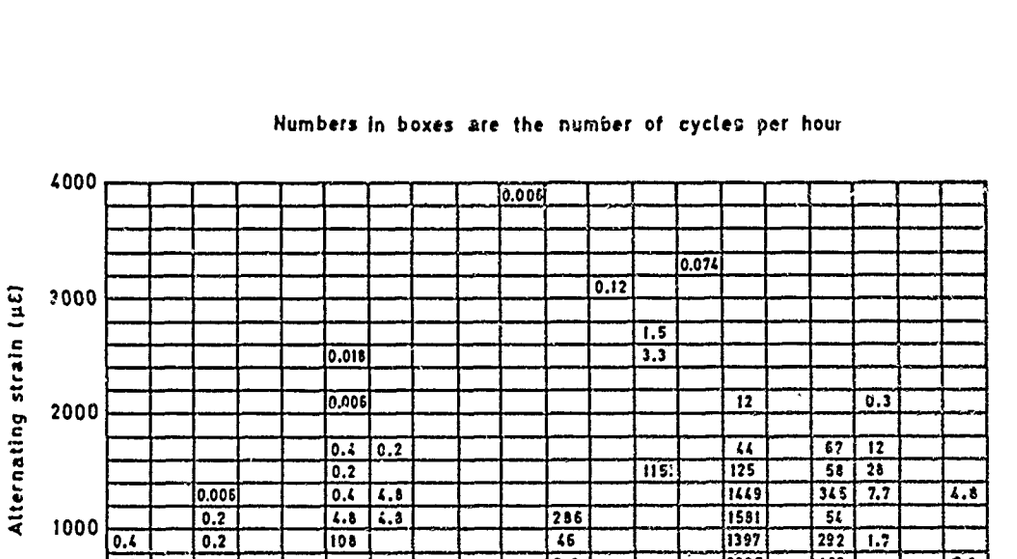


Fig 9 Synthesised Lynx strain spectrum for lower surface of inner flexible element at 3.4% rotor radius

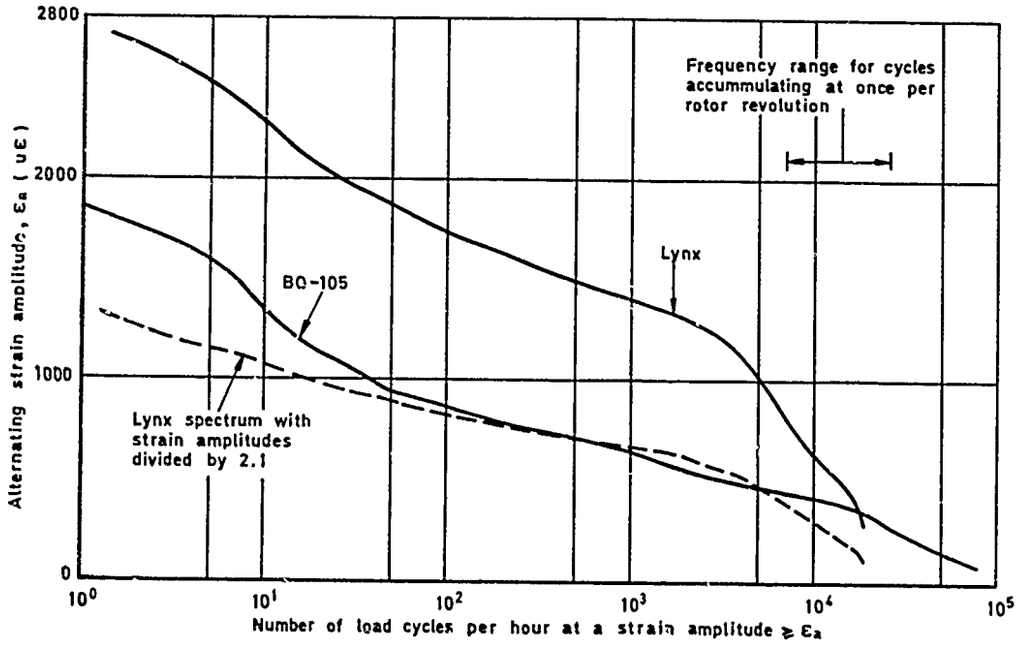
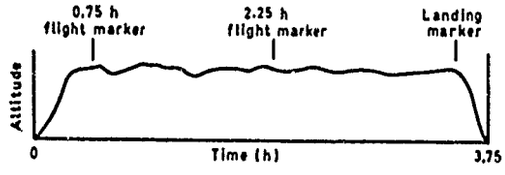
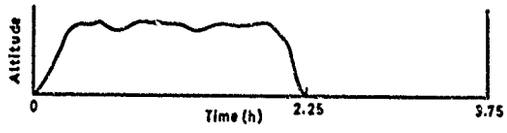


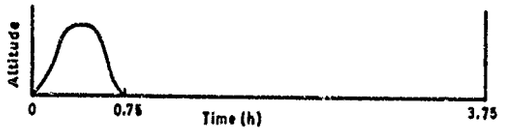
Fig 11 Comparison of strain spectra for BO-105 and Lynx design sortie



a Altitude profile for 3.75h transport flight

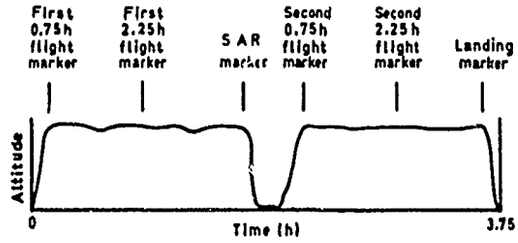


b Altitude profile for 2.25h transport flight

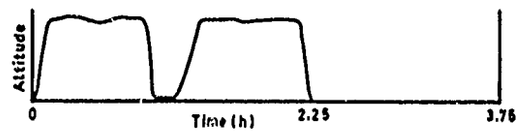


c Altitude profile for 0.75h transport flight

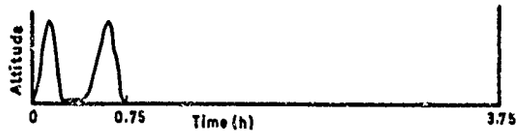
Fig 12 Example of the construction of the 0.75 h and 2.25 h Transport flights



a Altitude profile for 3.75h SAR flight

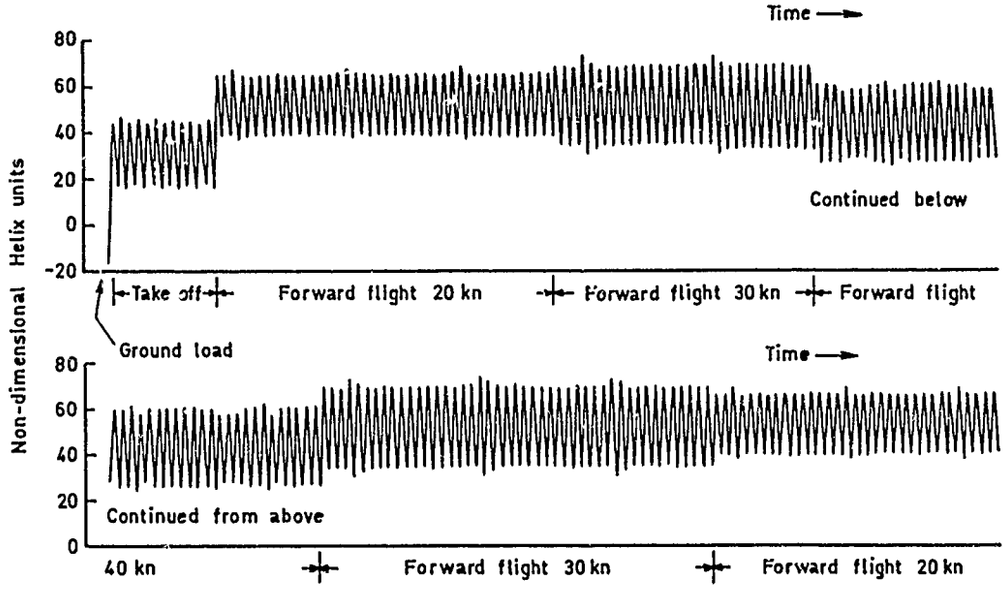


b Altitude profile for 2.25h SAR flight



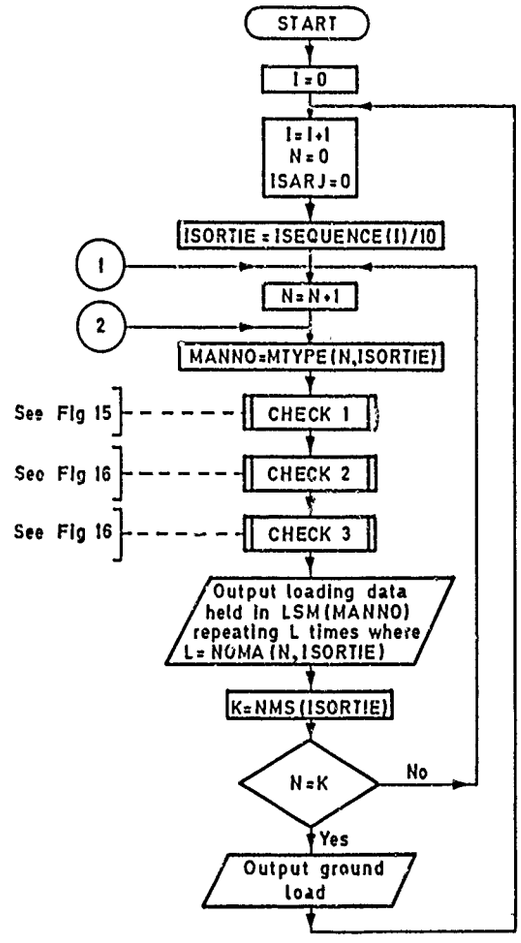
c Altitude profile for 0.75h SAR flight

Fig 13 Example of the construction of the 0.75 h and 2.25 h SAR flights



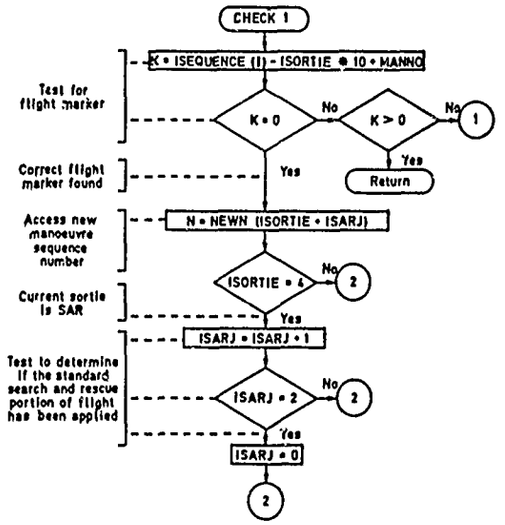
The representation above is schematic, fatigue test load histories are normally formed from half cosine cycles

Fig 14 Example of the load time history for the first phase of a training flight in Helix



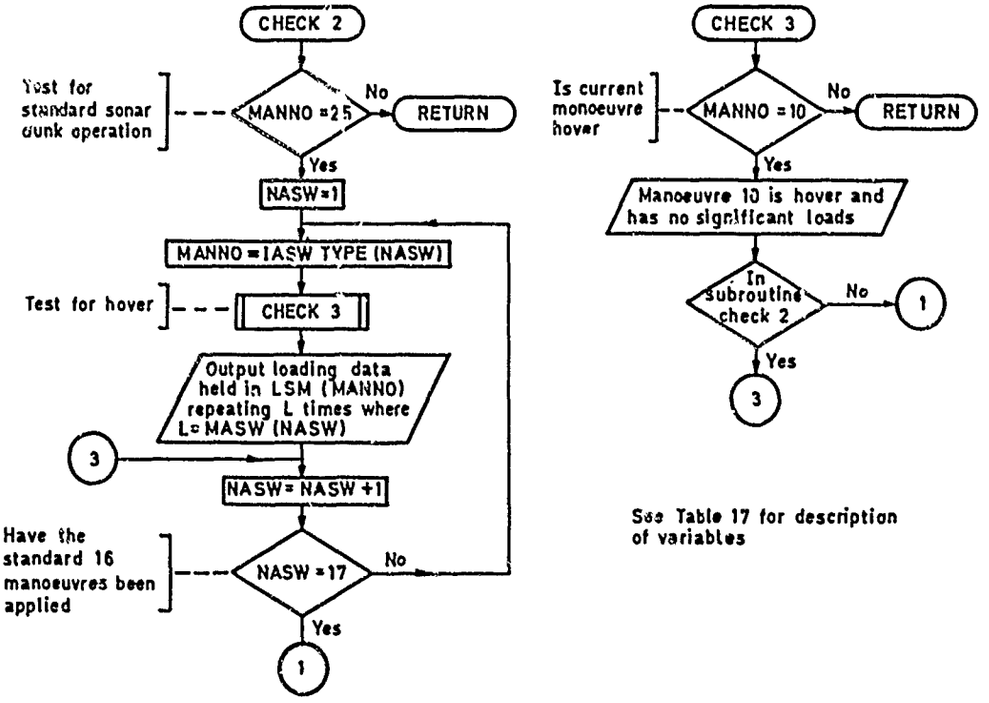
See Table 17 for description of variables

Fig 15 Generation algorithm for Helix



See Table 17 for description of variables

Fig 16 Subroutine that identifies the flight markers and skips manoeuvres to form the 0.75 h and 2.25 h flight durations in Helix



See Table 17 for description of variables

Fig 17 Subroutines to test for the standard sonar dunk operation and the hover manoeuvre

Appendix A

CONTRIBUTING ORGANISATIONS, INDIVIDUALS AND ACKNOWLEDGMENTS

A.1 Organisations

The following organisations have made major contributions to this collaborative project.

A.1.1 LBF: Fraunhofer-Institut für Betriebsfestigkeit
LBF
Bartningstrasse 47
D-6100 Darmstadt-Kranichstein
West Germany

A.1.2 IABG: Industrienlagen-Betriebsgesellschaft mbH
Einsteinstrasse 20
8012 Ottobrun bei München
West Germany

A.1.3 MBB: Messerschmidt-Bölkow-Blohm GmbH
Post fach 801140
8000 München 80
West Germany

A.1.4 NLR: Nationaal Lucht-en Ruimlevaartlaboratorium
Voorsterweg 31
Post Emmeloord
NOP
The Netherlands

A.1.5 RAE: Procurement Executive
Ministry of Defence
Royal Aircraft Establishment
Farnborough
Hampshire GU14 6TD
UK

A.2 Individuals

The following individuals have made major contributions to this collaborative project and can answer any queries regarding the basis and implementation of the loading standards.

B de Jonge	NLR
J Darts	RAE
F Daske	MBB
M Hück	IABG
H G Köbler	LBF
F Och	MBB
Dr D Schutz	LBF
Dr W Schutz	IABG
Dr V Tapavicza	MBB

A.3 Acknowledgments

The continuing support of Westland Helicopters Ltd to this project, particularly Mr A.D. Hall and Mr D. Boocock, is gratefully acknowledged.

Appendix B

ASSESSMENT OF SUITABLE FLIGHT DURATIONS AND SORTIE SEQUENCE LENGTHS

B.1 General considerations

The collection of the Sea King flight durations has been discussed in section 4.3 and the data presented in graphical form in Figs 1 and 2. For the analysis presented here it is more convenient to have the data in tabular form, Table 15. In this Table for each sortie the number of flights recorded in the initial duration counting interval of 15 min is listed along with the results of using counting intervals of 1 h and 1.5 h. To represent flight durations differing only by 15 min would prove a difficult task and an initial estimate suggested that flight durations differing by 1 h or 1.5 h would be more suitable. The criterion that assesses the suitability of these flight durations is that the most infrequently occurring sortie must occur at least once in the sequence of sorties of the standard. In addition the length of the sequence of sorties should be of the order of 200 sorties long. Details of the analysis follow.

B.2 Symbols and data for the analysis

k — number of counting intervals for the flight length data

m — sortie number
m = 1 for Training
m = 2 for Transport
m = 3 for ASW
m = 4 for SAR

n_{im} — number of flights of duration t_i for sortie m recorded in Table 15

NF_{im} — number of flights of duration t_i for sortie m in the loading standard

NF_s — total number of flights in the loading standard

$NFPH_{im}$ — number of flights per hour of duration t_i for sortie m in the data

$NFPH_{crit}$ — number of flights per hour of duration t_{crit} in the data

$p(t_{im})$ — proportion of flights of duration t_i for mission m for the data in Table 15

$p(T_m)$ — fraction of one hour spent in sortie (all-aircraft sortie mix in Table 1, section 3)

t_i — mean time of counting interval i for the data in Table 15

$\bar{t}_m$ — average flight duration of sortie m in the loading standard

t_{crit} — duration of the most infrequent flight in the loading standard.

B.3 Analysis

The proportion of flights of duration t_i for mission m for the data in Table 15 is:

$$p(t_{im}) = \frac{n_{im}}{\sum_{i=1}^{i=k} n_{im}} .$$

The average flight duration of sortie m in the loading standard is then:

$$\bar{t}_m = \sum_{i=1}^{i=k} p(t_{im}) t_{im} .$$

Using the sortie mix for all aircraft the number of flights per hour of duration t_i for sortie m is therefore:

$$NFPH_{im} = \frac{p(t_{im}) p(T_m)}{\bar{t}_m} .$$

The criterion has been set that the most infrequent flight must occur once in the loading standard, therefore

$$NF_{im} \geq 1$$

and it follows that

$$NF_{im} = \text{nearest integer value of } \frac{NFPH_{im}}{NFPH_{crit}} ,$$

and that the length of the loading standard will be:

$$NF_S = \sum_{m=1}^{m=4} \sum_{i=1}^{i=k} NF_{im}$$

with the final constraint that:

$$NF_S \triangleq 200 .$$

B.4 Results of analysis

Three cases were studied using the analysis described above and values of $NFPH_{im}$, NF_{im} and NF_S are listed in Table 16 for each case. In the first case to be studied six counting intervals of 1 h were considered, resulting in flight durations of 0.5 to 5.5 h in hourly increments. It can be seen from the data in Table 16 that the critical sortie is a 5.5 h duration ASW mission and for this to occur at least once the sequence of sorties would have to be 6395 flights long. In the second analysis only five counting intervals of an hour were considered, counts recorded between 5 and 6 h being disregarded. Details of the analysis are again presented in Table 16 which indicates that the 4.5 h duration flights for Training, ASW and SAR are the critical sorties that determine the 677 flights of the sortie sequence. In the final analysis presented in Table 16 the counting interval was increased to 1.5 h and again counts in the longest flight duration region were disregarded. The 3.75 h flights for Training and SAR determine the length of the sortie sequence which at 140 flights was an acceptable length.

Appendix C

GUIDELINES TO WRITING A GENERATING ALGORITHM FOR HELIX

C.1 Outline

A flow chart of the general generation algorithm for Helix is illustrated in Fig 15 and flow charts for the three subroutines in Fig 15 are given in Figs 16 and 17. A description of each of the variables used in the flow charts is given in Table 17 along with a reference to the tables in this Report that list the appropriate data. A description of this data is given in section 6. The notation and arithmetic logic used in the Appendix is that used in FORTRAN.

The algorithm to generate Helix, increments through the sequence of sorties and for each sortie increments through the sequence of manoeuvres that define the sortie. For each manoeuvre accessed the appropriate load sequence is applied the required number of times. Three subroutines, CHECK1, CHECK2 and CHECK3, respectively decide when to skip manoeuvres in the sequence to achieve the required flight length, when to apply the standardised sonar dunk operation in the ASW sortie and when the manoeuvre to be applied is hover which has no loading sequence.

The most important aspects of the algorithm are described in the sections that follow.

C.2 Calculation of sortie number and flight length

The sortie number and flight length are derived from the sequence of sorties, ISEQUENCE, as follows.

ISORTIE = ISEQUENCE(I)/10 using integer arithmetic

eg

ISORTIE = 23/10 = 2

ie the sortie to be applied is type 2 which is transport (see Table 4).

The flight length = ISEQUENCE(I) - (10 × ISORTIE)

eg

flight length = 23 - (10 × 2) = 3

ie flight length 3 is required which is 3.75 hours duration (see Table 4).

C.3 Skipping of manoeuvres to achieve the required flight length

If a 3.75 h flight duration is required then all the manoeuvres in MTYPE for the sortie are applied. To simulate the 0.75 h and 2.25 h flight durations some manoeuvres in MTYPE are skipped by the identification of the flight markers (see section 6). The 0.75 h and 2.25 h flight markers are stored in MTYPE as manoeuvre numbers -1 and -2 respectively for each of the four sorties. The addition of the manoeuvre type number, MANNO, to the flight length number indicates whether manoeuvres must be skipped. When Eq.(C-1) is zero the flight marker for the correct flight length has been reached in MTYPE.

$$K = ISEQUENCE(I) - (ISORTIE \times 10) + MANNO \qquad (C\text{-}1)$$

For the Training, Transport and ASW sorties the next manoeuvre is that following the landing sequence marker. For the SAR sortie two jumps in the manoeuvre sequence are performed to achieve the 0.75 h or 2.25 h flight durations. On first encountering a 0.75 h or 2.25 h flight marker, with K equal to zero, the next manoeuvre is that following the SAR marker. On the second encounter of a 0.75 h or 2.25 h flight marker, with K equal to zero, the next manoeuvre is that following the landing sequence marker. The counter ISARJ is set to one on the first encounter of a flight marker and to zero on the second encounter in the SAR sortie thereby indicating the search and rescue portion of the SAR sortie. The manoeuvre sequence numbers for the manouvres that follow the landing sequence markers and SAR marker are stored in the one-dimensional matrix NEWN which has five elements. The first three elements are the manoeuvre sequence numbers of the first manoeuvre after the landing sequence marker for Training, Transport and ASW sorties. The fourth element is the manoeuvre sequence number of the manoeuvre that follows the SAR marker and the fifth element is the manoeuvre sequence number of the manoeuvre that follows the loading sequence marker in the SAR sortie. Therefore if K is zero in Eq.(C-1) then the next manoeuvre to be applied is at sequence number N, where

$$N = NEWN(ISORTIE + ISARJ) \quad .$$

If ISORTIE equals 1, 2 or 3 then ISARJ equals zero and the first three elements of NEWN are accessed according to the value of ISORTIE. If ISORTIE equals 4 and K in Eq.(C-1) is zero for the first time then ISARJ is zero so that the fourth element of NEWN is accessed. ISARJ is then set to one. The second time K is zero the fifth element of NEWN is accessed.

FATIGUE TEST PROGRAM AND TEST RESULTS

by D. Schütz, H.-G. Köblar; Fraunhofer-Institut für Betriebsfestigkeit, Darmstadt (LBF) and
W. Schütz, M. Hück; Industrieanlagen-Betriebsgesellschaft, München (IABG)

1. Foreword

In order to prevent any readers disappointment at the end of this paper it must be stated at once, that the following chapters had to be essentially restricted against the earlier concept in the initial phase of planning the contributions to this meeting.

The theoretical development of the HELIX/FELIX - standards is indeed nearly finished now, but caused by some delay during the development of these standards unfortunately fatigue tests could not at all be carried out up to now. Therefore only a general scope of the test program considered and some spotlights in this context can be given at present. Because the authors are not intended to fulfill the allotted time by more or less sophisticated digressions instead of presenting test results, this report will be briefer than scheduled in the meeting program.

2. Introduction

In a previous study the concept of a standardized load sequence based on service experience of helicopter rotors has been estimated as feasible and useful. When such a standard is available as shortly will be, its presumed advantages according to an improved realism against the conventional methods have to be substantiated by suitable fatigue tests. Fig. 1 describes schematically how the two conventional methods of life estimation in helicopter design that are based on constant amplitude tests and on blockprogram tests respectively are compared with a life estimation based on HELIX and FELIX.
For that purpose the HELIX and FELIX spectra are used:

- for the constant amplitude method as the basis for the linear damage calculation (Miner's rule) and
- for the block-program method as the basis for deriving the blocked test program.

The HELIX/FELIX tests will give a basis of fatigue lifes which are at least from the viewpoint of the load program very realistic.

3. Details of the test program considered

Material selection and test specimens have to be oriented on current helicopter rotor design on the one hand, on the other hand test results obtained should be comparable with results of other investigations on fatigue performance of structural materials. Fig. 2 shows the three specimen types provided for the fatigue test program considered in relative scale, each type used already for numerous fatigue test programs in the past.

The stress concentration factor $K_t = 2.5$ of the notched Titanium and Aluminium specimens with a centre hole of 8 mm diameter has been considered as representative for structural components. The final rolling direction of these sheet specimens coincides with the direction of the axial loading.

The glass fibre reinforced plastic (GFRP) specimens are smaller in size because this material tends to heat up under vibratory loading if the mainly stressed area is too voluminous. The stress concentration factor of the GFRP-specimens is chosen to be $K_t = 1.0$ with respect to helicopter rotor components manufactured of such materials which are also unnotched.

The GFRP-Specimens provided for axial loading include either unidirectional or multidirectional laminates. The GFRP-specimens for 3-point-bending tests generally contain unidirectionally oriented glass fibres only.

A survey of the test program considered in this context is shown in Fig. 3. The cross symbols in the single fields of this table indicate which parameter combinations, i.e. material, specimen type, type of loading and type of test, will be investigated. Dashes mean that tests will not be run. In all cases constant amplitude tests will be performed as a basis for subsequent life calculations and shall verify or complete resp. already existing S-N curves. It is the intention to investigate the differences in fatigue life predictions based on the application of the standard load sequences also with predictions based on results of block program tests for some selected cases. Therefore also block program tests with the HELIX and FELIX spectra will be carried out.
Finally, with respect to e.g. shortening of the testing time, the effect of omitting low stress amplitudes but also of truncating high stress amplitudes on the fatigue life shall be checked by socalled development tests.
The test program will be carried out as a joint venture of RAE, NLR, IABG and LBF.

4. Relationship of measured and standardized load sequences

With the intention to give a visual impression of load sequences experienced by a helicopter rotor blade lower side in the region of maximum bending moments a short cutout of a strain-time history relevant to a semirigid rotor is shown in Fig.4. Although this strain trace does not represent a continuous record of an original flight, but is artificially built up by a synthesis of several manoeuvres measured under stabilized flight conditions each, some typical attributes used for considering the loading standards can be recognized as follows:

- The mean strain is significantly different from zero and can be assumed to be nearly constant over relative wide discrete ranges.
- The amplitude of the vibratory strain does not vary too much within most of the single manoeuvres with lower loads.
- During manoeuvres with more severe loading the amplitude of the vibratory strain varies much more.
- In some cases the strain-time history dips into the compression region.

Among others the above mentioned characteristics have been realized in the standards. Fig. 5 shows a short cutout of a standardized manoeuvre sequence. Regarding this figure it should be emphasized that the manoeuvre durations indicated in seconds relate to the original flight times to be simulated by the standardized loading in which low intermediate vibratory stresses are already omitted. The stress cycle sequence shown in this graph represents for example a flight time of 1 minute, but it will be reproduced during about 2.4 seconds in fatigue test, if a test frequency of 40 Hz is applied. In the following the prove is undertaken that the simplification of the original stress-time history by collecting samples of stress cycles with approximately the same amplitude into blocks is permissible.
Fig.6 shows results of an other investigation concerning the influence of load cycle mixture on the fatigue life. Each symbol represents an average value of ten bending tests with a stress ratio of $\bar{R} = 0$ valid for the maximum stress amplitude of the spectrum.
The amplitude distribution of the spectrum is a straight line in the usual log-linear scale. It has been taken from long time measurements on motor car rear axles.
Service duplication tests on notched cylindrical specimens with $K_t = 2.15$ manufactured of steel equivalent to SAE 5140 and an aluminium alloy equivalent to 2024 respectively delivered the fatigue life curves established by circular symbols. Conventional block program tests based on the same load spectrum with a total number of mean crossings of $H_0 = 3 \cdot 10^5$ per period delivered the fatigue life curves assigned by open quadratic symbols. Evidentially the life is unrealistic long in the block program test. After diminishing the cycle-block size by a factor of one hundred the test results symbolized by half coloured squares were obtained which coincide favourably with the results of the service duplication tests.

From this data the conclusion can be drawn that random load sequences are allowed to be replaced by cycle blocks if only the block size is short enough in comparison with the number of cycles to failure. There is no doubt that blocking of single manoeuvres in a flight is admissible when considering the fact that one period of the HELIX/FELIX standards include 140 single flights each of which composed of many different manoeuvres. Another example in this context is given in Fig. 7. It is shown that blocking the random sequence of gust cycles in one flight in an ascending-descending order

has no significant effect on the fatigue life.

5. Concluding remarks

5.1 Further applications of HELIX/FELIX

When the present investigation will be finished by the end of next year, only initial work will have been done leaving still many questions open, e.g. see Fig. 8. In this context the estimation of fatigue strength of helicopter rotor parts is mainly important. The fatigue life data obtained by application of the standardized load sequences can be directly used for life estimation of a structural component only in cases when the service and standard load spectra are very similar. If there are service load spectra significantly different from the spectra of the loading standards the test results are to be converted by e.g. relative Miner's rule. The range of validity of Miner's rule can be deduced e.g. by converting the test results from HELIX into FELIX and vice versa.

Comparative testing of different design solutions under standardized loading will give more accuracy and confidence to support the decision for either one solution or the other than constant amplitude testing can provide (e.g. what if SN-curves intersect?). All test results collected within this program and the following programs yield data for the design of helicopter main rotor parts in form of fatigue life curves. Beyond getting reliable data for supportable vibratory stresses versus fatigue life the knowledge of realistic scatter factors will grow. On this basis well founded allowable stresses can be deduced.

A lot of other points where the loading standard can be useful or does be extremely important respectively can be named, e.g.:

- investigation on damage tolerance concepts
- investigation of usedup life time of components used already in service
- investigation of the influence of corrosion.

More than in all other cases cited above the application of damage tolerance concepts demands the prove of the assumptions under realistic load conditions.

Besides, fatigue testing can be advanced: The influence of cutting off the standard spectra at low and high stress amplitudes (omission of low and truncation of high stress amplitudes) can be studied with the loading standards and may lead to more insight into the phenomenon of damage accumulation. Investigations of the influence of increased test frequencies may lead to a shortening of testing time in connection with cut-off load spectra.

5.2 Testing time and costs

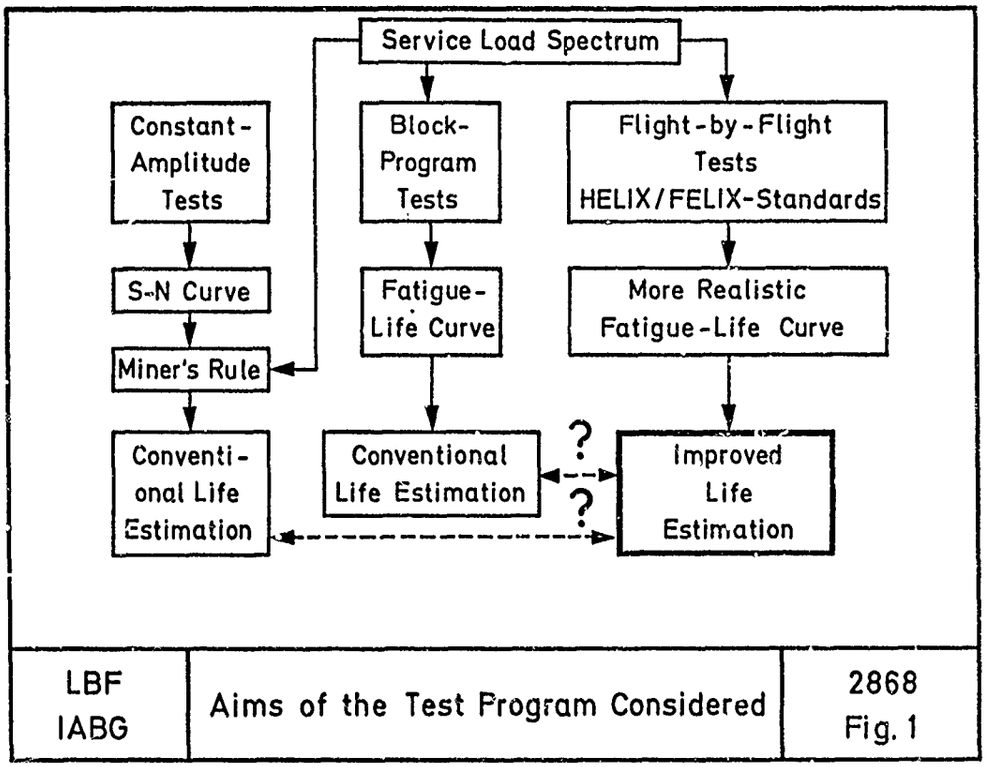
One of the arguments brought forward against the usually socalled spectrum testing is that it is too expensive and takes too long testing times particularly for the rotating components of helicopters. Therefore it is worthwhile to compare costs and testing times for constant amplitude tests with those of HELIX/FELIX. To define the area of the fatigue limit of an SN-curve with sufficient confidence one has to carry out about 30 to 40 tests up to 10^7 load cycles and more. If one can use Amsler vibrophores the testing frequency is about 100 Hz (fiber reinforced plastic components about 35 Hz only because of heating up). If an average fatigue life of $5 \cdot 10^6$ cycles to failure is assumed the testing time amounts to about 500 hours (fiber reinforced plastic components about 1500 hours). HELIX/FELIX consist of about 10^7 load cycles for 1000 flights. If the assumed testing frequency of the neccessary servohydraulic equipment is about 35 Hz one can test up to about 15 specimens or components between 500 and 1000 flights within the same 500 hours (about 40 fiber reinforced plastic parts within 1500 hours respectively). Therefore it may well be not more time - consuming and even not much more costly using the loading standards instead of constant amplitude testing, but the reliability of results will be much better.

5.3 Information for the users of HELIX/FELIX

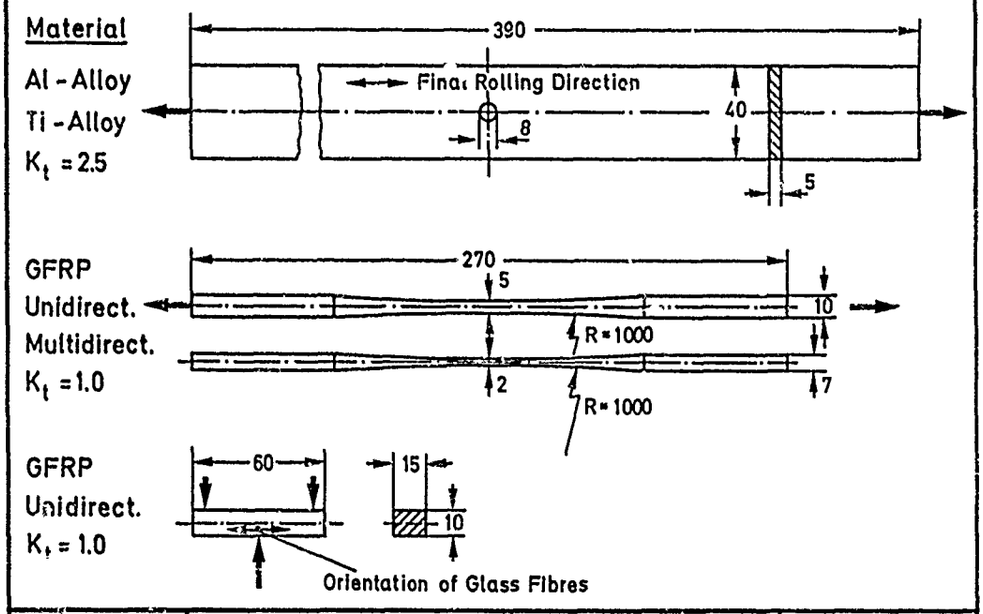
A report describing the generation of both standards is beeing prepared and will be available by the beginning of 1981. This report contains all the informations for the generation of the standards. The standards will also be available on

punched cards (FORTRAN IV) which may be requested at the participating institutes.

The standard load sequences HELIX/FELIX may be used to investigate the open questions connected with statistical and damage behaviour in spectrum testing near the fatigue limit in order to improve the life prediction methods used up to now.



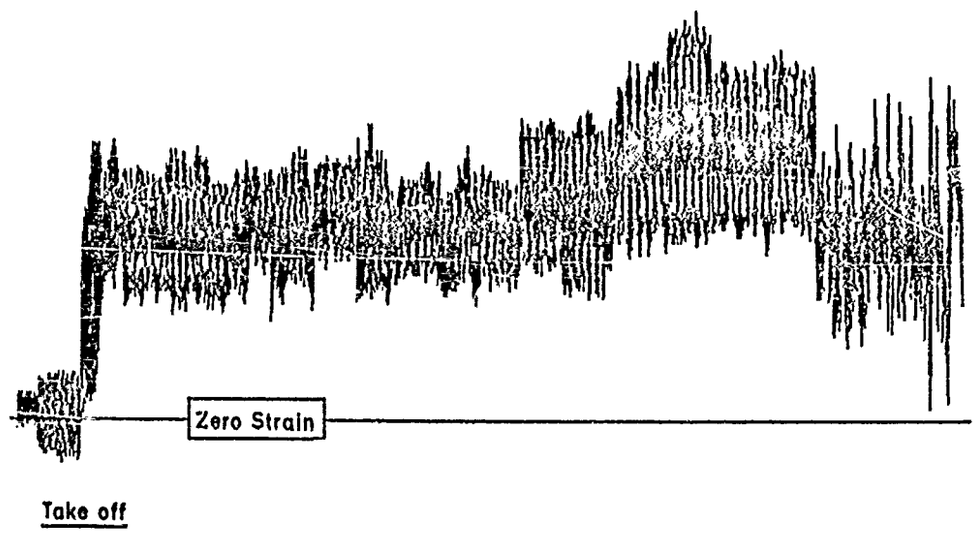
LBF IABG	Aims of the Test Program Considered	2868 Fig. 1



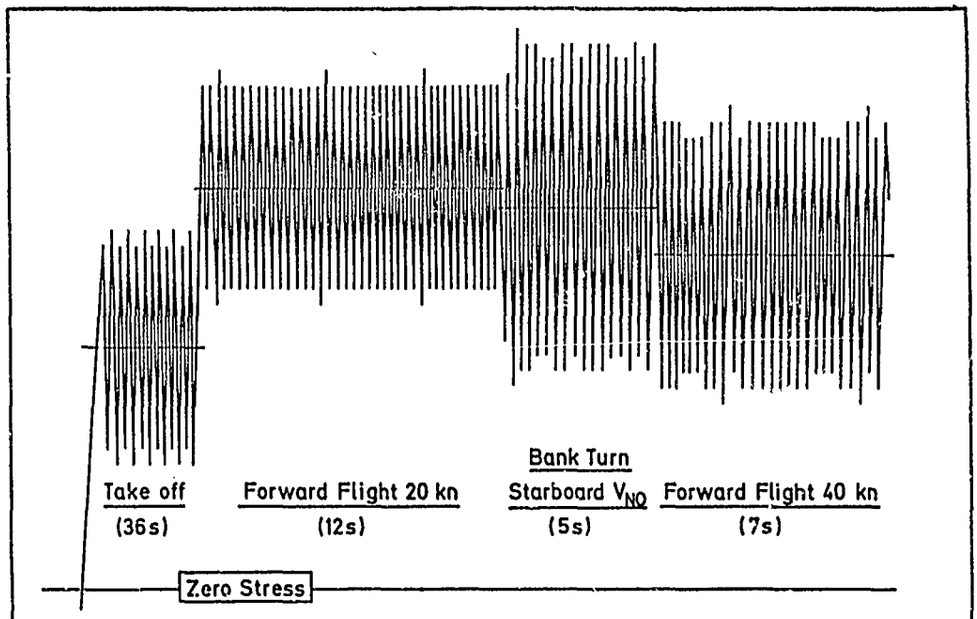
LBF IABG	Test Specimens	2869 Fig. 2

Type of Test \ Loading	Material: Titanium Equivalent to 4911	Material: Aluminium Equivalent to 2024	Material: Unidirectional GFRP		Material: Multidirect. GFRP
	Axial	Axial	3-Point Bending	Axial	Axial
Constant Amplitude	X	X	X	X	X
Block Program According to HELIX	—	X	X	—	—
Block Program According to FELIX	X	—	—	X	X
HELIX-Standard	—	X	X	—	—
FELIX-Standard	X	X	X	X	X
Additionally: "Development Tests"					

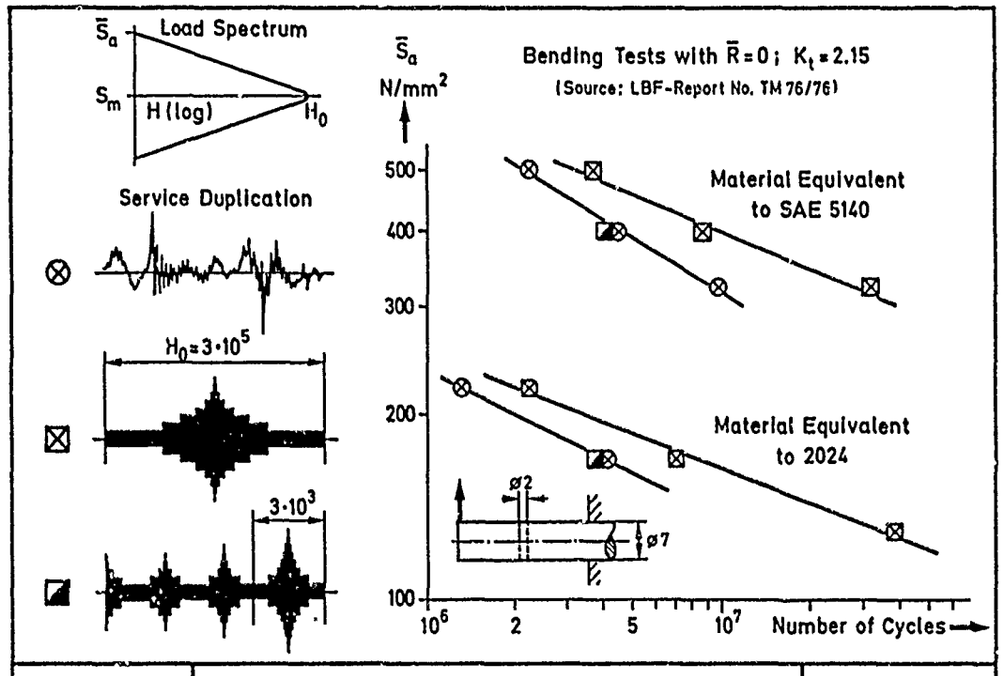
LBF IABG	Test Program	2870 Fig. 3



LBF IABG	Strain Measurements on a Semirigid Rotor Blade (Synthetical Manoeuvre Sequence)	2871 Fig. 4



LBF IABG	Cutout of a Standardized Manoeuvre Sequance Representing 1 Minute Flight Time	2872 Fig. 5



LBF IABG	Influence of Cycle-Block Size on Fatigue Life in Block Program Tests	2873 Fig. 6

Load Sequence	Remarks	Crack Propagation Life (Flights)	
		2024-T3	7075-T6
	Random Sequence of Full Cycles	11781	5062
 Source: J. Schijve, AGARD Rep. No. 157 (1972)	Blocked Sequence of Gust Cycles	11365	5061
LBF IABG	Effect of Load Cycle Sequence in One Flight		2874 Fig. 7

● Estimation of Fatigue Strength – Life Prediction Based on HELIX/FELIX Fatigue Data (Relative Miner's Rule) – Collection of Fatigue Performance Data for Structural Materials and Components. – Derivation of Realistic Scatter Factors. ● Investigation on Damage Tolerance Concepts ● Advancement of Fatigue Testing – Influence of Omitting Low Stress Amplitudes – Influence of Test Frequency – Influence of Truncating High Stress Amplitudes	LBF IABG Examples for Applications of HELIX / FELIX 2875 Fig. 8

FATIGUE BEHAVIOUR OF HELICOPTER DYNAMIC COMPONENTS UNDER CONSTANT AMPLITUDE AND SPECTRUM LOADING

by

G.Cavallini,A.Lanciotti
Institute of Aeronautics,University of Pisa
Via Diotisalvi,2-Pisa-Italy

and

G.Aldinio,R.Rovellotti
Costruzioni Aeronautiche G.Agusta
Gallarate-Italy

SUMMARY

This paper gives a certain number of results obtained in a research on helicopter fatigue. The main objective of this research was a comparison of various approaches to design for fatigue in helicopter components and, subsequently, an evaluation of improvement in this area.

Current methodologies used in helicopter industries are considered, as well as nominal stress approach, and advanced methods, namely methods based on local stress-strain approaches. Fatigue tests -constant amplitude and variable amplitude loading- have been carried out on a typical dynamic component, the tail rotor mast of A 109A helicopter.

Spectrum loading tests have been performed using a sequence directly deduced from flight load survey.

Such experimental data, and theoretical data from of all the methods considered, are then compared.Useful indications concerning fatigue evaluation methodologies are given.

1. FOREWORD

The way to deal with the fatigue problem in helicopter industries is generally a safe-life approach which assures safety by a rather high reduction factor of estimated life; this is due to the very complex nature of the problem for this machine. The mission spectrum and the load spectrum can be established with rough approximation and the actual usage -and,therefore, the fatigue loading- often differs from one user to another and is different from the one predicted.

The other aspects of the problem, namely the fatigue allowable and the life evaluation performed by simplified methods, also present equally considerable uncertainties.

In the past this approach has been successful, but in recent years the required performance and payload capabilities for new projects have increased,Furthermore the service life of components is required to last longer for economic reasons. In these conditions, such an approach is no longer useful because its application produces heavy structures if the required safety level must be maintained as is certainly necessary in order to avoid catastrophic failures.

And, on the other hand, the weight penalty so produced is in contrast with the required increase in performance and service life.

It is possible to get out of this dead-end in two ways: one is to maintain a safe-life approach while substantially improving knowledge of the fatigue problem thereby reducing the excessive degree of conservation, or alternatively, by applying a damage-tolerance approach which has already proved to be very successful as far as the fixed-wing in the same situation is concerned.

This second method is certainly suitable for the helicopter fuselage structure, but at present there are real difficulties as to its application to dynamic components and the first method seems to be the better one. This, moreover, is a fundamental step towards the right application of damage-tolerant methodology.

So Agusta and the Institute of Aeronautics have been developing cooperative research in the field of the safe-life design of dynamic components. The following topics have been investigated: fatigue strength representation, counting methods of load cycles, fatigue life estimation methods.

The research has been carried out according to the following rationale: -to review the present possibilities in these fields, to pick out the most effective methods in the case of helicopter fatigue, to try out these methods with the fatigue test data for helicopter dynamic components subjected to realistic load sequences.

The final goal is a significant improvement in fatigue life assessment methodologies.

2.1. FATIGUE STRENGTH REPRESENTATION

The relationship used so far between the nominal stress and the number of cycles at failure (the S-N curve) is a basic step in fatigue analysis which raises uncertainties and rightly so.

For the critical components,specific tests are performed on a few specimens and three kinds of S-N relationship can be obtained.

The first kind (F1 curve) is obtained as a mean curve among the family of curves, each passing through a failure point,[1]. The curves are assumed in the three parameters Weibull form. Two parameters are fixed depending only on the alloy kind (steel,aluminum alloy, magnesium alloy, titanium alloy) and the third is the endurance limit to be deduced by the fit with the experimental points. The second kind (F2 curve) is obtained in the same way of the previous, but the two fixed parameters are depending on specific alloy (2024,7075,4130,.....), treatment, notch or not notch, type of loading.

The third (BF curve) is always a three parameter Weibull form curve,but the three parameters are now obtained from a best-fit with all the experimental data.

Basically,the following questions have to be answered:- if the fatigue test data of the components is correctly represented in this Weibull form- what the most effective representation is among the curves considered and what the most correct definition of the reduction factor must be to obtain the operative S-N curve from the mean S-N curve.

To this end, the S-N curves have been compared with the experimental results of large sets of fatigue tests carried out by Agusta and others,|2|.

It is observed (Fig. 1a,b,c,d,) that F1 curve do not fit very well the experimental results in quite all the range while F2 curve agrees with the BF curve from 10^5 cycles and then can be considered an effective tool in fatigue data analysis.In the low cycle range, the fatigue data should be represented more correctly by a four parameters Weibull form curve, as otherwise the fatigue strength is overestimated. But this N range is not used in helicopter construction, so the error makes no difference. So it should be adequate the use of the F2 curve for drawing S-N curves of full scale component fatigue tests. In this case the number of tests is indeed so reduced that a more appropriate best-fit analysis is impossible.

The definition of the S-N curve in the high cycle range is a complicated question. The S-N curve from constant amplitude tests usually presents a characteristic value, the fatigue limit. Formerly |3| the stress cycles below this limit were not regarded as damaging. Recently, experiments have clearly demonstrated that these stress cycles can be damaging if stress cycles above the fatigue limit are present. These give rise to a microcrack which grows because of the small amplitude cycles below the fatigue limit.

So the use of the fatigue limit in the evaluation of fatigue damage for variable amplitude loading can lead to an unconservative life estimate. The fatigue limit maintains its significance only when the entire stress spectrum is below this value.

But this is to be found in the case of structures which are oversized from the fatigue point of view and which therefore are not critical in this respect.

The dangerous error due to use of the S-N curve with a fatigue limit is overcome in helicopter construction where it is current practice to extend the S-N curve of the finite life range at high cycles and to establish the fatigue limit at very high cycles; this is the procedure applied for the F2 curve definition,|1|.A more correct and conservative procedure, recently proposed, seems, however, to be to eliminate the fatigue limit idea and to use a S-N curve obtained by extrapolating the S-N curve of the finite life range at high cycles.

Finally, a remark must be made on the use of the F2 curve. The definition of parameter values for the selection of the right F2 curve is sometimes difficult and presents some degree of uncertainty. The F2 curves have been defined by Agusta after detailed analysis of the available data and a comparison with its own component fatigue data, but very different results can be obtained with data from other sources. So, a more general procedure by helicopter people and a standard approach to the problem of drawing S-N curves are surely to be hoped for.

The definition of the reduction factor is a even more complicated question.

The first point is where to apply the factor, directly to the S-N curve to be used in estimating fatigue life or to fatigue life evaluated by the mean S-N curve. The second point is the procedure of reduction factor definition. While it is certainly true that the solution generally adopted in helicopter construction is open to criticism and is often too conservative, we must, nevertheless, have adequate information on the fatigue behaviour of helicopter components under typical spectra before a different solution can be found.

2.2. COUNTING METHODS

A substantiation stage follows the preliminary design stage in the assessment of the fatigue behaviour of the critical components; constant amplitude tests are performed and from flight load survey more accurate data on load history can be obtained to be used in subsequent fatigue analysis.

The problem arises of defining the load cycles from the irregular load history; this is not a simple question as the solution must take the nature of fatigue phenomena into account, namely it must pick out and count the events which really produce the damage.

The principal counting methods (Tab.I) have been examined from this point of view while also bearing in mind the results from these produced in fatigue analysis |4|. Each method has been implemented by a computer program.

Detailed analysis of the features and fundamentals of the methods allows us to point out that:

- certain methods -namely, level crossing, peak, mean crossing peak, range restricted peak, range, range pair exceedance- cannot take the mean value of the damage event into account, but the mean stress effect is well known to be an important factor in phenomena. For these methods, it is suggested that an average mean stress for the full history or for the segments of this should be considered; the procedure,however, is not clearly defined and in some cases can lead to considerable errors;
- the peak method and mean crossing peak method are easily shown to be unconservative in some cases since they neglect the small but damaging stress amplitudes which are superimposed on large cycles,and so range and range mean methods can also be unconservative,|5|;
- rain-flow and range-pair-range methods alone can take into account sequence effects which experimental data shows to be significant in fatigue analysis;
- rain-flow and range-pair-range methods seem to work correctly in cycle counting,without

the basic errors of other methods; moreover, the first seems to be a better representation of the origin of the damage event.

The analysis has been completed by comparing the various methods on the basis of results provided in fatigue life prediction. To this end, all counting methods have been used with the simplest life prediction method, that is, Miner's rule, applied to the fatigue data from constant amplitude tests expressed by S-N curves.

Tab.I shows two sets of data. The first concerns the application of the FALSTAFF spectrum to an aluminum alloy notched component, the fatigue data of which is obtained from ESDU data sheets E.02.01 in the figure of the S-N curves for various values of S_m. The second set of data refers to a typical load history of a component of a ground vehicle; component fatigue data is reported in [6] for the case in which $S_m=0$ and the Heywood correction is used for the other values of the mean stress. For this case experimental data for typical spectrum loading is also available.

The data from the rain-flow counting method is most conservative and in close agreement with experimental data.

The range-pair-range method also provides similar data.

The other methods forecast longer lives because they do not allow for mean stress effect and small amplitude damage.

The conclusions of this analysis of counting methods point out that rain-flow is certainly the more effective and reliable method. This demands a little more computer time in comparison with other methods, but this makes little difference when considered in relation to the entire fatigue analysis process.

So the rain-flow counting method has been introduced in all the fatigue-life prediction methods used described in the following.

2.3. FATIGUE-LIFE ESTIMATION METHODS

A general critical review of fatigue-life estimation methods under variable amplitude loading has been carried out [7]. The following methods have been considered: the nominal stress approach, the local stress-strain approach, the E.S.D.U. method, the Impellizzeri method, Miner's rule as a transfer function method, the Haibach method, the typical methods for fixed wing aircraft concerning the use of the Fatigue Quality Index or such like.

Considering the specific field and the state of knowledge, the nominal stress approach, the local stress-strain approach and the Haibach method seemed the most effective tools and their application is discussed in the following pages.

All the other methods contain certain aspects which make them unusable or less suitable in comparison with the ones mentioned above.

Miner's rule as a transfer function, for instance, may become a useful method in the future, but at present the lack of an adequate amount of experimental data in variable amplitude loading prevents it from being reliably applied.

2.3.1. NOMINAL STRESS APPROACH

This type of method is based on the acquisition of fatigue data for the critical components; the fatigue data concerns constant amplitude tests with a steady stress level equal to the forecast mean stress level in flight. The results are expressed as S-N curves.

Two ways are used in the utilization of S-N curves for fatigue-strength evaluation under flight load spectrum. In the first, the nominal stress history is subdivided into segments and each segment is reduced to an equivalent number of constant amplitude stress cycles[1]. Then Miner's rule is applied using the S-N curve and the Soderberg correction on mean stress if the relevant value of the flight stress segment is different from that of the fatigue test. In the second, the rain-flow counting procedure is applied to nominal stress history, and then Miner's rule is used as in the previous case.

The first, the method using an equivalent number of c.a. cycles, has been employed until now at Agusta, but the second is certainly based more on fatigue phenomena complying with the use of rain-flow, which allows us to take the important sequence effect due to the memory property of material into account.

This latter approach can produce a significant improvement in fatigue analysis. The principal shortcoming is the use of the nominal value in the correction for the mean stress effect and so inaccuracy may be expected where this value may substantially disagree with effective mean stress, for instance in components with a large stress concentration factor and in stress histories with a considerable change in level in subsequent cycles.

It must be emphasized that the method is also applied in many fields employing general S-N curves obtained from tests on standard notched specimens and sometimes on smooth specimens. The suitable S-N curve for the specific component is carried out by making use of the stress concentration parameter K_t, or the notch parameter K_f. The basic difficulty is the evaluation of K_t or K_f and at Agusta this procedure is applied only in the design phase for the components which are not critical from the fatigue point of view; in all other cases fatigue tests on the specific component are performed.

2.3.2. THE LOCAL STRESS-STRAIN APPROACH

The basic concept of the local stress-strain approach is the assumption that notched and unnotched structures behave in the same way when subjected to the same local stress-strain history.

Therefore this approach starts with the computation of the local stress and strain history at the notch as a solution of two equations, the cyclic σ-ε relationship and the Neuber rule. In this step, a special procedure must be used to bring in the memory effect of the material; sometimes cyclic dependent phenomena, such as stress relaxation, are also introduced.

Afterwards, the damage event, generally the closed hysteresis loop, is computed from

the stress-strain history and the damage is evaluated by Miner's rule applied to the ε-N curve obtained from constant amplitude strain controlled fatigue tests on standard smooth specimens.

On this general basis, different procedures are developed by Wetzel, Landgraf, Soci et alii, with the principal aim of saving computing time: consequently, sometimes considerable simplifying hypotheses and approximations are introduced. All these procedures have been tested and comparison between them shows that the computer time saving is not such as to justify the approximations, [7].

So it is considered better to use a "right" procedure in which the stress and strain history is obtained by the numerical solution of the cyclic σ-ε relationship and the Neuber rule, taking the memory effect into account too and by applying the rain-flow counting method to identify the damage events, that is the closed loop hysteresis cycles; then the damage is evaluated by the Morrow parameter as proposed by Landgraf. Many questions still remain to be solved (i.e. the use of K_t or K_f in the Neuber rule, the introduction of a residual stress relaxation law, the definition of the damage parameter ,...), but the local stress-strain approach is very much worth using and further researchs because of its wider application -particularly in the design phase- and its predictable meaningful improvement.

2.3.3. THE HAIBACH METHOD

In the Haibach method, [8], the peculiarities of the nominal stress approach and the local stress-strain approach are to be found together.

The stress and strain history from load history, the damage events and the relevant values of the damage parameter are deduced in the same way as in the latter approach.

The damage is then evaluated by utilizing the S-N curve of the fatigue strength of critical components expressed by nominal stress.

At the loading conditions of constant amplitude tests the local stress-strain approach is applied, thereby obtaining a "transformed" curve which connects the value of the damage parameter with the life of critical components. Lastly, the damage due to variable amplitude loading is calculated by Miner's rule and by this "transformed" curve.

The following considerations can be made on the Haibach method :- like the local stress-strain approach, this method allows us to take into account the sequence effects and the effect of residual stress at the notch; the final result of the method is certainly less sensitive to the value of K_t or K_f, the evaluation of which is a very complicated problem in the local stress-strain approach; and the use of the S-N curve allows us to take the particular features of the critical component into account as far as fatigue phenomena are concerned.

Thanks to the features mentioned above, the Haibach method may be considered to be very useful for the assessment of the fatigue behaviour of the dynamic component.

3. FATIGUE TESTS

The main purpose of the research is to assess fatigue life evaluation methods by a comparison with fatigue test results for typical helicopter dynamic components under a realistic spectrum load.

As a first component, the tail rotor mast of a A 109A helicopter was selected (Fig.2).

The specimens to be tested have been obtained with the same working schedule as for the helicopter component. Only certain processings have been left out, as not being relevant to the fatigue behaviour of the critical area.

In order to carry out the research, standard fatigue tests had to be performed on component material, as well as constant amplitude fatigue tests and variable amplitude fatigue tests on components.

3.1. STANDARD TESTS ON COMPONENT MATERIAL

The properties of 9310 steel needed for the application of the local stress-strain method have been determined according to the recommended ASTM standard procedure, [9]. A Instron servo-hydraulic testing machine and extensometer have been used.

The cyclic curve σ-ε has been calculated from the standard smooth specimens with the companion method, by carrying out the stable hysteresis loop cycles (Fig.3a). Fig.3b shows the cyclic curve σ-ε and its relationship in the usual form; the monotonic σ-ε curve is also reported.

The same equipment and the same type of specimens have been used to obtain the ε-N strain-life curve in a strain-controlled fatigue test. No overstrain was applied during the tests. Fatigue failure has been considered to be the appearance of visible small-size crack, such as 2 mm large. Fig.4 shows the experimental data together with the ε-N relationship. Because of the breakdown of the test equipment, it was not possible to obtain a lot of experimental data such as is needed for a very accurate representation of fatigue strength.

3.2. FATIGUE TESTS OF THE COMPONENT

3.2.1. LOADING APPARATUS

The component has been loaded in a simplified way compared to its operative conditions on helicopters. Namely, the component was not rotating and a load was applied at the tip, as shown in Fig.5.

So the torque load has been left out, but its value in operative conditions is negligible as far as the fatigue behaviour of the tail rotor mast is concerned. The system of loading and restraint conditions is shown in Fig.5.

A steel bush has been applied to the component, connected with the first support to avoid fretting phenomena; such a bush is not applied on the mast of the helicopter.

The loading system is given in Fig.6. The component supports and the actuator were connected to a very stiff rig. The supports held the component in a different way from that shown in Fig.5, but the difference has been regarded as insignificant.

The load was provided by a 7 KN hydraulic actuator servocontrolled by the output of a load cell placed at the actuator stem tip.

This equipment was built by Agusta. The actuator was connected to the rig and the component by thin blades which allowed us to achieve the loading conditions previously calculated to be necessary (see Fig.5).

A function generator and a PDP 11/34 process computer -for constant amplitude tests and for variable amplitude tests, respectively- supplied the input signal to drive the actuator.

The correct working of the apparatus, namely the loading condition, was checked by specific tests, where stress and strain were measured on several stations of a dummy component and on thin blades and were compared with the expected values.

3.2.2. CONSTANT AMPLITUDE TESTS

Constant amplitude tests with an alternate load (R=-1) have been carried out to determine the relationship between fatigue life and nominal stresses. Fatigue life has been taken to correspond to the appearance of a small crack as in strain controlled smooth specimen fatigue tests. Nominal stress has been evaluated in the critical section of the component, shown in Fig.5.

The tests in the low and medium cycle range showed the crack started in the critical section as forecast. As far as tests in the high cycle range are concerned, the components broke under the steel bush because of a clear phenomenon of fretting. But no crack appeared in the critical section which was carefully examined with a 50 magnification glass. So the stress values relevant to these tests have been assumed to be an estimate of the fatigue limit for the critical section which was the focal point for comparison between the theoretical and experimental data.

In the subsequent tests the defect was eliminated by changing the type of bush, but other tests in the high cycle range could not be carried out because of the lack of specimens.

The experimental data and S-N relationship are reported in Fig.7.

3.2.3. VARIABLE AMPLITUDE TESTS

3.2.3.1. SPECTRUM LOADING

The load history utilized to carry out the loading spectrum for fatigue tests has been recorded during flight load survey of A 109A helicopter as the output of a strain-gauge bridge put on the tail rotor mast.

This load history is a typical sequence in civil transport mission. This is relevant to a medium range flight of 2400 sec. with a take off weight of 24 KN . The flight comprises take off and climb with normal manoeuvres, level flight at ≈1500 m. and manoeuvres, descent, approach and landing. The details of conditions and their length and occurrence are shown in Tab.II.

The fatigue test spectrum load has been calculated from the original load history by filtering the very low amplitude load cycles and by scaling up the load history so obtained. The first operation was necessary to avoid tests of prohibitive length: but the maximum level of load cycles omitted has been defined so that the test loading spectrum also has load cycles of an amplitude lower than the fatigue limit of the component calculated from the constant amplitude tests (see Fig.7). Indeed an important item of the research is to check the damaging effect of the load cycles at an amplitude below the fatigue limit. Fig.8 shows the cumulative diagram of the amplitude of load cycles (irrespective of the mean value) obtained by the rain-flow counting method for the original load history and the filtered load history.

The levels of the stress amplitudes of the filtered load history are not at all such as to cause the failure of the component, which has been designed with a high degree of safety for use on helicopters.

As the aim of the research is the comparison between the experimental fatigue life of the component and the relevant assessment of the theoretical methods, it was necessary to duly scale up the time history in order to give rise to component failure. The maximum level of nominal stress in the scaled up time history has been truncated to S_{MAX}= 638 N/mm^2 to avoid excessively high stress levels which are not realistic. The final distribution of nominal stress cycle amplitudes (irrespective of the mean value) obtained by the rain-flow counting method is shown in Fig.9 where the fatigue limit shown in the constant amplitude tests is also to be found.

3.2.3.2. FATIGUE TESTS UNDER SPECTRUM LOADING

The time history of the typical flight, established as described above, has been recorded on the memory of a PDP 11/34 process computer as a sequence of peaks and valleys. The process computer produced a continuous sinusoidal-type signal between the subsequent values of the peaks and valleys in order to drive the actuator. The frequency of the signal was approximately 7 c.p.s. selected as the maximum value allowed by the performance of

the fatigue machine.

Before each test and sometimes during the test, the output of the actuator load cell has been recorded with the computer and compared with the expected values. Comparison of the peak, valley, rise and fall values has always shown deviations which are not higher than 2%. Obviously, mechanical and electric limiters set at the maximum and minimum of the loading spectrum were applied during the test.

Four components have been tested with the same spectrum. The results expressed as number of flights at the appearance of a small visible crack are reported in Tab.III.The crack occurred in the critical section in all the tests.Surprisingly,the scatter of the result, is rather wide.

4. COMPARISON BETWEEN PREDICTED AND EXPERIMENTAL FATIGUE LIFE

The experimental data and the relevant data from the prediction methods are given in Tab.III.

The nominal stress method has been used with the Goodman correction for the mean stress effect (S_m=0 for S_m<0) and three different S-N curves have been utilized namely, the F2 curve and the two B curves shown in Fig.7. The F2 curve is the S-N relationship used as a rule at Agusta and has been obtained as already described in 2.1. The B curve is the best-fit straight line S-log N of the experimental data relevant to specimens with finite life.

The two different B curves come from either taking the estimated fatigue limit into account, or extending the curve of finite life range to S=0.

The Haibach method has also been applied using the above specified S-N curves.

The local stress-strain method has been used with the cyclic σ-ε curve in Fig.3b and the ε-N strain amplitude fatigue life in Fig.4, for several values of the stress concentration factor in the critical section. The estimated fatigue life versus the K_t value is given in Fig.10. Generally, two values of K_t are meaningful, namely the geometrical stress concentration factor -K_t- and the fatigue stress concentration factor -K_f-, which is deduced from the ratio between the fatigue strengths of the smooth specimen and the notched component.In this case about the same value is obtained for these two factors. A value of K_t=1.28 has been deduced in an approximate way from published literature relevant to axial loading. A similar value of K_f can roughly be determined by comparing the S-N data in Fig.4 and Fig.7, but an accurate assessment of this parameter is rather questionable because the value is strongly dependent on the value of N considered in the evaluation.

The value of K_t=1.28 has been also used in the Haibach method; other calculations with different values of K_t have demonstrated the method to be insensitive to K_t variations around this value.

Some significant observations can be made.

The nominal stress method and the Haibach method lead to very unconservative results when applied with the B curve which takes the fatigue limit into account. This result clearly demonstrates that the amplitudes below the fatigue limit are damaging if stress amplitudes above this value are also present in the spectrum. The curve without fatigue limit yields also unconservative fatigue life estimations. This is probably due to an inaccurate determination of the S-N curve in the knee zone.In fact, conservative estimates can be obtained by the use of a S-N curve obtained in the same way as the B curve, but considering only the four experimental data relevant to specimens with lower fatigue life. This latter S-N curve seems to be a better representation of fatigue strength in the finite life range, but it must be pointed out that this curve is not so strictly defined as the B curve, which is the best-fit of all data availables in the finite life range.

The experimental data and prediction fatigue life results agree quite well if the F2 curve is used. Indeed, as is shown in Fig.7, this curve gives the higher damage for most of load cycles the spectrum.

Anyway, the strong influence of the basic ingredient, that is the S-N curve of the component, on the results is remarkable; from this, an accurate definition of the S-N curve is the most important step in the application of this method.

The results of the nominal stress method and the Haibach method, are rather similar. This was foreseeable, as the component is low notched and the spectrum does not contain very large variations in subsequent peaks (or valleys); therefore, the difference between nominal mean stress and local mean stress is not very great.

A very conservative estimate of fatigue life is obtained by the local stress-strain method. In this case, too, the influence of input data of the method on the final results is noteworthy, as can be seen from fig.10. A fatigue life prediction in agreement with experimental data and results of the other methods is obtained by using a slightly different evaluation of K_t, i.e. K_t = 1.2 moreover, this value can be considered a quite well-founded estimate of the value of the fatigue stress concentration factor.

5. CONCLUSIONS

Research aimed at a considerable improvement of fatigue life assessment of the dynamic components of helicopters has been carried out. This is a fundamental goal for an effective design of such structures.

Generally components which are critical from the fatigue point of view are checked: by carrying out constant amplitude fatigue tests on a few specimens of the components -by assessing the fatigue load spectrum in the operative life from flight load survey- by evaluating the fatigue life of the component.

The fundamental tools relevant to the steps of the aforesaid procedure, namely fatigue strength representation from fatigue tests, counting methods to be applied to recorded load histories, fatigue life prediction methods - have been examined.

It has been noted that the methodology employed at Agusta adequately represents fatigue strength in the range of number of cycles of concern in the dynamic components fatigue loading. The S-N curve obtained takes alloy type, the presence of a notch and loading mode into account.

A rather conservative estimate of fatigue strength in the high-cycle range is given.

A different approach, namely the use of a S-N relationship in the finite life range extended to S=0, has been proposed and employed successfully in other applications for fatigue life assessment, under variable amplitude loading. In the present case, a correct application of the approach is unlikely because of the reduced number of fatigue tests of the component which is generally possible to carry out.An open problem is the evaluation of the reduction factor to be applied to the S-N curve used for fatigue life evaluation or, alternatively, of the safety factor on the life estimate. A well sound solution of the complex problem is attainable by analysing the results of the application of different procedures to experimental data relevant to typical dynamic components tested under a loading spectrum representative of operative conditions.The available data of this type, in the field of helicopter constructions, is still scarce and a considerable amount of research in this direction is certainly needed.

As far as counting methods are concerned, and as was already well-known, the rain-flow method proved to be the most effective in the counting of load cycles and fatigue events.

On this subject, the real problem is the significance of the flight load survey, but this point is farther the aims of this paper.

Several methods have been proposed for fatigue life assessment under variable amplitude loading. The nominal stress-strain method and the Haibach method seem to be the most suitable for helicopter construction applications.

The results of these methods have been compared with the fatigue test data of the tail rotor mast of the A 109A helicopter, subjected to a realistic spectrum, directly deduced from flight load survey.

This single result does not allow to draw final conclusions, but some useful indications can be obtained.

The first plain indication is the damaging effect of the stresses below the fatigue limit, estimated from constant amplitude tests, if stresses above this limit are present in the load spectrum, as it is typical for helicopter dynamic components. So, very unconservativc life estimates are obtained by using a S-N curve which takes the fatigue limit into account. On the contrary, there is a statisfying agreement between experimental data and fatigue life predictions from the nominal stress method and the Haibach method by using a S-N curve of finite life range extended to S=0 or the S-N relationship utilized at Agusta, which gives a conservative evaluation of fatigue strength in the high-cycle range. A conservative life estimate is obtained from the local stress-strain method employing the geometric stress concentration factor. Anyway, the results of the methods were found to be very sensitive to input data, i.e. S-N curve and stress concentration factor.

Therefore, the main problem, is not the selection of the most effective method for fatigue life evaluation, even if the Haibach method seems to be the most logical approach, at least on the basis of the case examined.

As it was already pointed out,it seems worthwile to gather further data from fatigue tests under load spectra representative of helicopter operational conditions of the components involved. Following this line,it is likely to get significant improvements of the fatigue life assessment procedures and therefore to obtain more reliable and more effective fatigue design of helicopter dynamic components.

REFERENCES

1. Alli,P.-Present Fatigue Analysis and Design of Helicopters Requirements and Qualification Procedures,in"Helicopter Fatigue"AGARD R-674,1979.
2. Aldinio,G. et al.-Analisi teorica delle curve S-N e conseguenze pratiche. Relazione n.100-45-02,Costruzioni Aeronautiche Agusta,1979.
3. Dowling,N.E. et al.-Notched Member Fatigue Life Predictions by the Local Strain Approach, in "Fatigue Under Complex Loading:Analyses and Experiments",SAE-Advances in Engineering, Vol.6,1977.
4. Lanciotti,A.Facchin,A.-Un'analisi comparativa fra i metodi di conteggio dei carichi. To be published in "L'Aerotecnica-Missili e Spazio".
5. Dowling,N.E.-Fatigue Failure Predictions for Complicated Stress-Strain Histories. J. of Materials, JMLSA,Vol.7,n.1,1972.
6. Tucker,L.Bussa,S.-The SAE Cumulative Fatigue Damage Test Program,in "Fatigue Under Complex Loading: Analyses and Experiments", SAE-Advances in Engineering,Vol.6,1977.
7. Cavallini,G.-Esame critico e messa a punto di metodi di analisi a fatica in presenza di sollecitazioni ad ampiezza variabile. Relazione n. 100-45-19, Contratto di Ricerca n.1AN/79 tra la Costruzioni Aeronautiche Agusta e l'Istituto di Aeronautica dell'Università degli Studi di Pisa,1979.
8. Haibach,E.-The Influence of Cyclic Material Properties on Fatigue Life Prediction by Amplitude Transformation-Int.J.Fatigue,January 1979.
9. Wagner,V.-et al. Prove per la determinazione delle curve σ-ε e ε-N dell'acciaio 9310-Relazione n.100-46-03,Costruzioni Aeronautiche Agusta,1980.

LIST OF SIMBOLS

F	Number of flights
K_f	Fatigue stress concentration factor
K_t	Geometrical stress concentration factor
N	Number of cycles
R	Ratio between minimum and maximum of load cycle
S	Nominal stress
S_m	Mean value of nominal stress in the load cycle
ε	Local strain
ε_a	Amplitude of local strain
σ	Local stress
ΔS	Variation of nominal stress in the load cycle

COUNTING METHOD	LIFE	LIFE
Level crossing	1.498	3228
Peak	1.469	3006
Mean crossing peak	2.078	5476
Range restricted peak	1.792	3399
Range	1.584	1871
Range-pair-exceedence	1.380	5587
Range-pair-range	1.298	1858
Rain-flow	1.000	1594
Experimental data	-	1533

Tab. I - Comparison between fatigue life predictions with several counting methods.

CONDITION NUMBER	CONDITION TYPE	LENGTH (sec.)	NUMBER OF OCCURRENCE
1	Vertical take off	17.07	1
2	Hovering OGE	7.48	4
3	Lateral control reversal (stationary flight)	6.67	1
4	Left-hand rotation	3.87	1
5	Acceleration to climb air-speed (60 KTS)	16.67	1
6	Max continuous power climb at Vy climb air-speed-twin engines	144.3	47
7	Acceleration from climb air-speed to 155 KTS	30.27	1
8	Forward level flight at 160 KTS	721.5	235
9	Rudder control reversal at 155 KTS	4.67	1
10	Right turn at 155 KTS	6.14	2
11	Forward level flight at 185 KTS	240.	78
12	Cyclic pull-up at 155 KTS	8.67	1
13	Forward level flight at 160 KTS	1025.4	334
14	Rudder control reversal at 155 KTS	4.67	1
15	Left turn at 155 KTS	4.34	2
16	Deceleration from 155 KTS at 60 KTS	27.47	1
17	Descent flight 2 engines 500 ft/min	89.	29
18	Approaching and normal landing 2 engines	41.07	1
	TOTAL FLIGHT LENGTH	2399.36	

Tab. II - Detail of a typical flight for the tail rotor mast of a A 109A helicopter.

	F,NUMBER OF FLIGTHS		
EXPERIMENTAL DATA	155.0 207.3 210.4 261.9	MEAN VALUE	207.2
NOMINAL STRESS METHOD (S-N curve used: B curve with fatigue limit)			378.2
NOMINAL STRESS METHOD (S-N curve used: B curve without fatigue limit)			246.8
NOMINAL STRESS METHOD (S-N curve used: F2 curve)			217.2
LOCAL STRESS-STRAIN METHOD (K_t=1.28)			148.0
HAIBACH METHOD (S-N curve used: B curve with fatigue limit)			407.7
HAIBACH METHOD (S-N curve used: B curve without fatigue limit)			259.9
HAIBACH METHOD (S-N curve used: F2 curve)			245.8

Tab. III - Experimental data and fatigue life predictions.

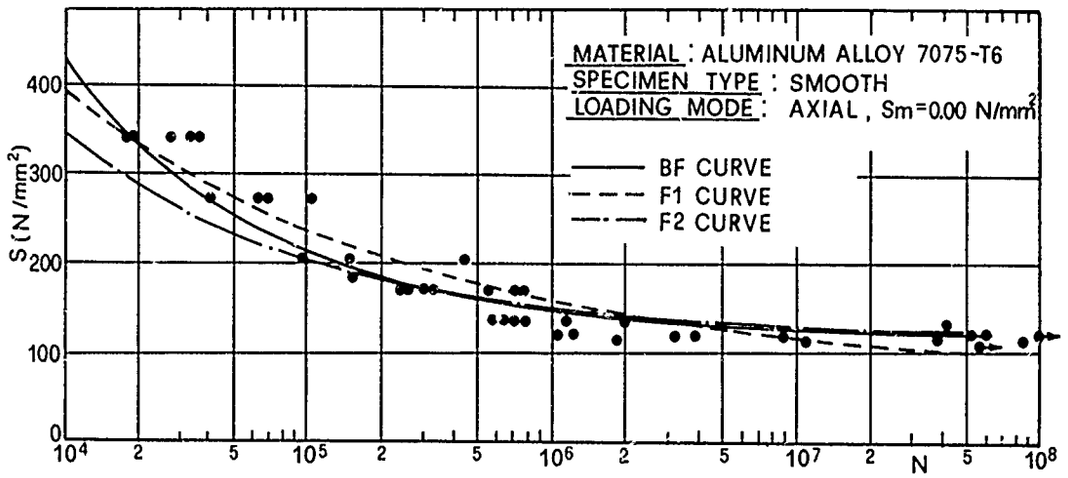


Fig.1a - Comparison between representations of fatigue strength. Material:aluminum alloy 7075-T6

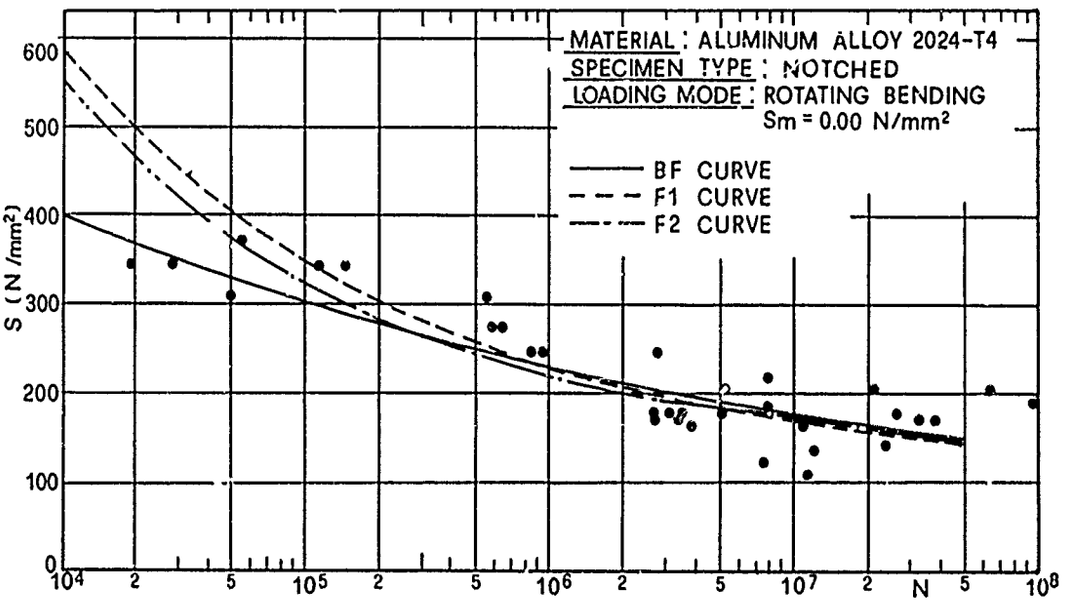


Fig.1b - Comparison between representations of fatigue strength.Material aluminum alloy 2024-T4. Alcoa.

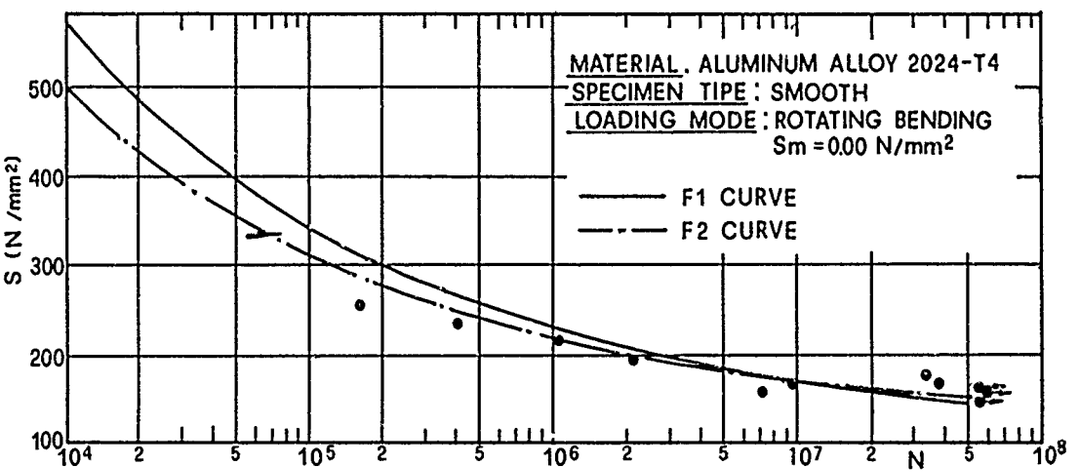


Fig.1c - Comparison between representations of fatigue strength.Material aluminum alloy 2024-T4.

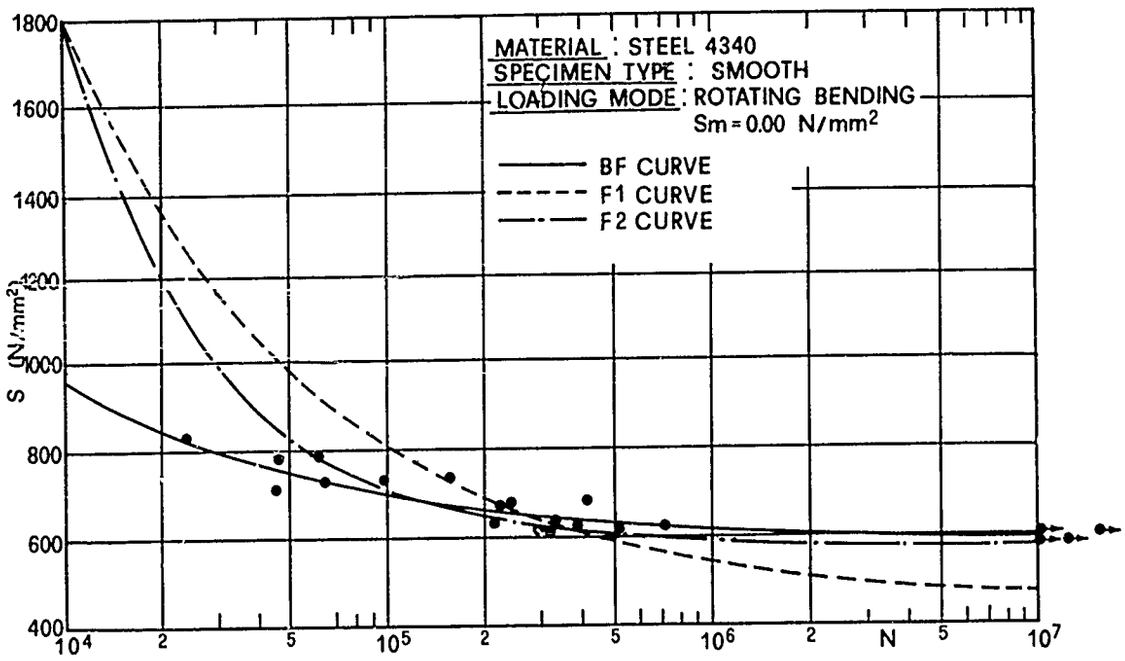


Fig.1d - Comparison between representations of fatigue strength.Material: steel 4340.

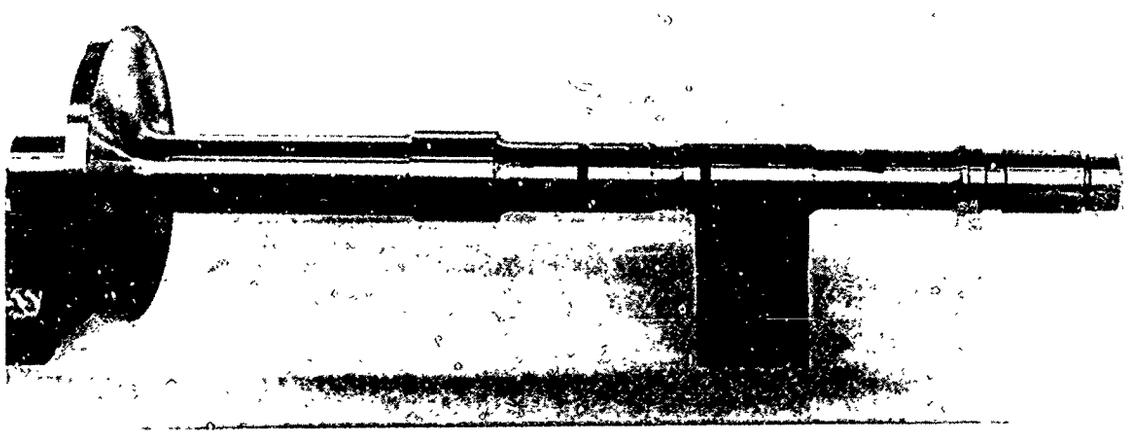


Fig. 2 - Photo of the component for fatigue tests. The tail rotor mast of the A 109A helicopter.

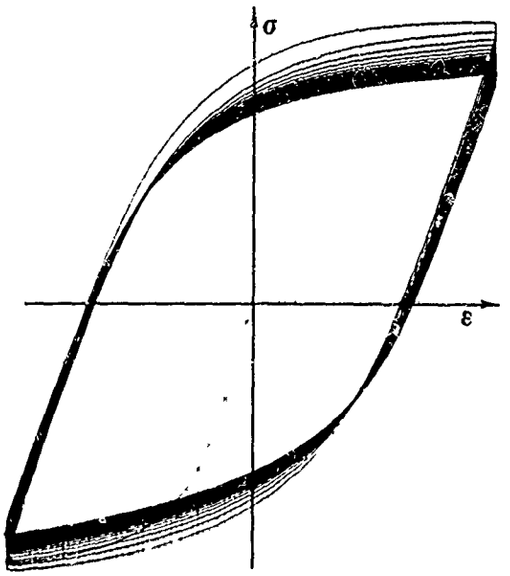


Fig. 3a - Hysteresis loops of 9310 steel.

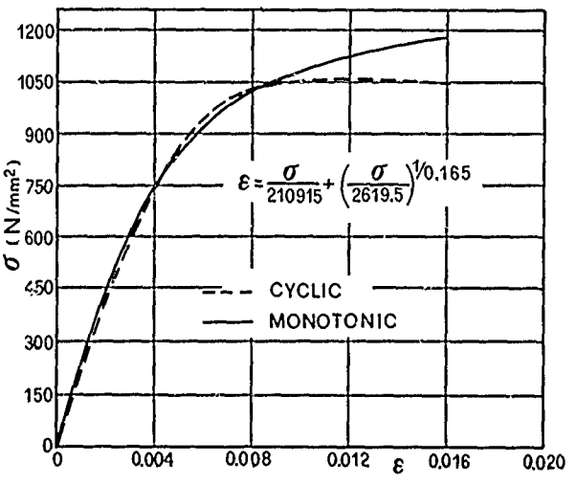


Fig. 3b - The cyclic and monotonic σ-ε curve for 9310 steel.

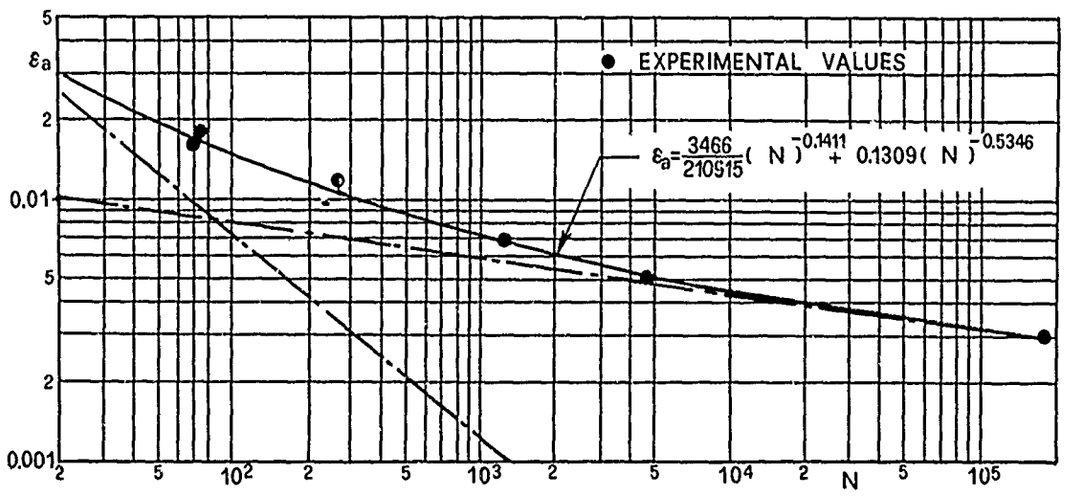


Fig. 4 - The strain amplitude fatigue life for 9310 steel.

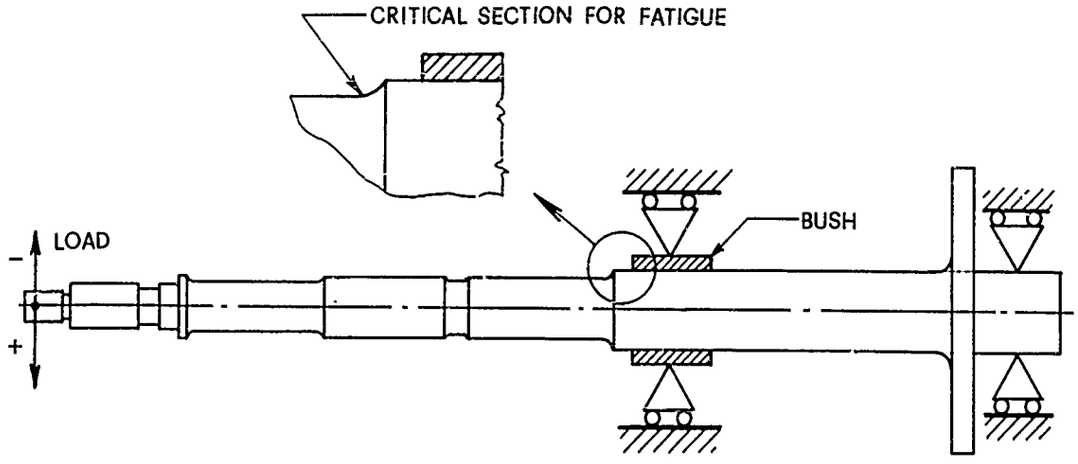


Fig. 5 - Sketch of loading and restraint conditions of the component.

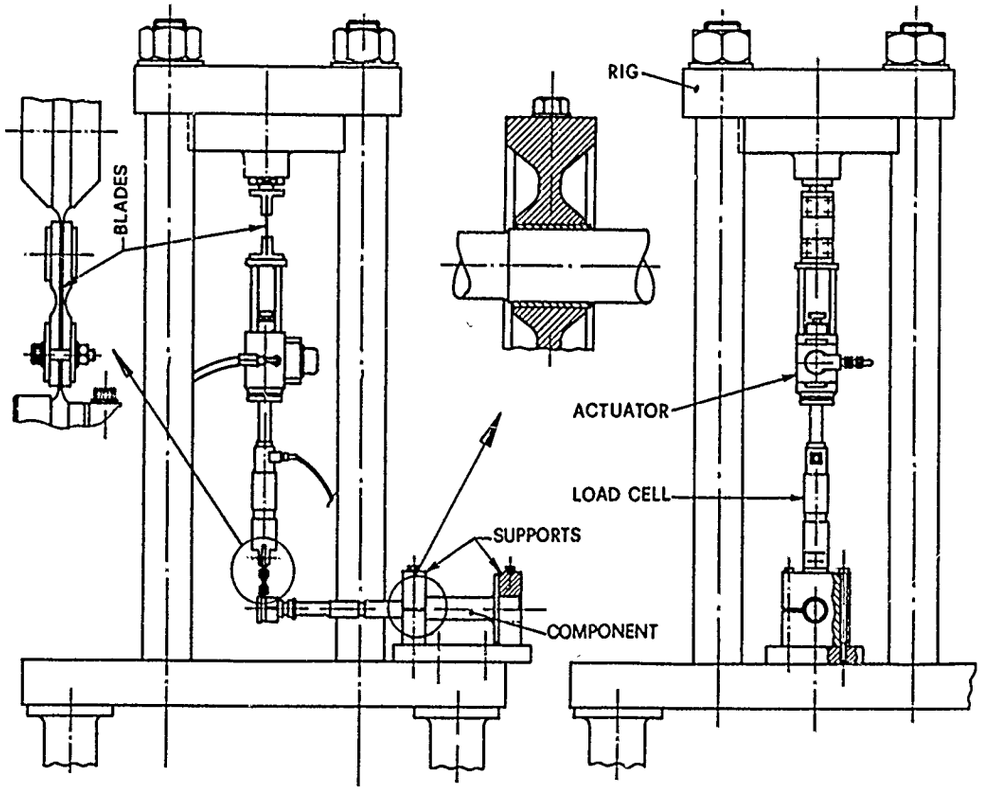


Fig. 6 - Loading apparatus for fatigue tests of the component.

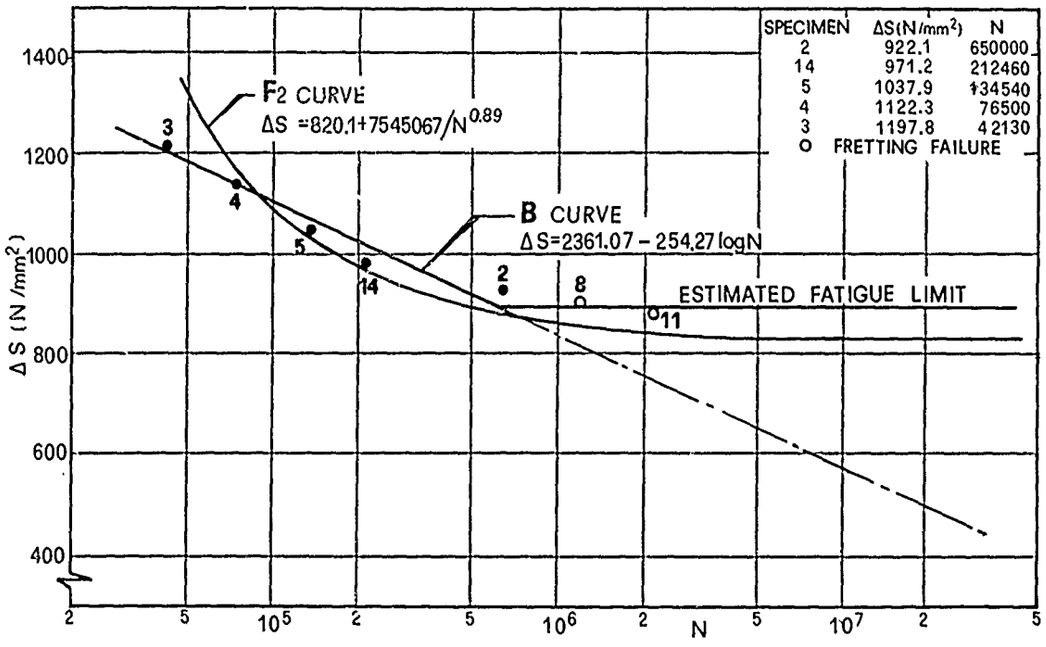


Fig. 7 - Constant amplitude fatigue test results for the component.

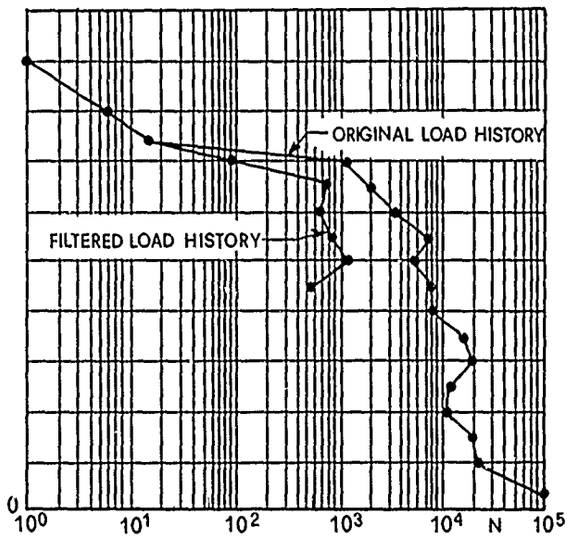


Fig. 8 - Load cycle amplitude distribution of the original and filtered time hystory. Rain-flow counting method.

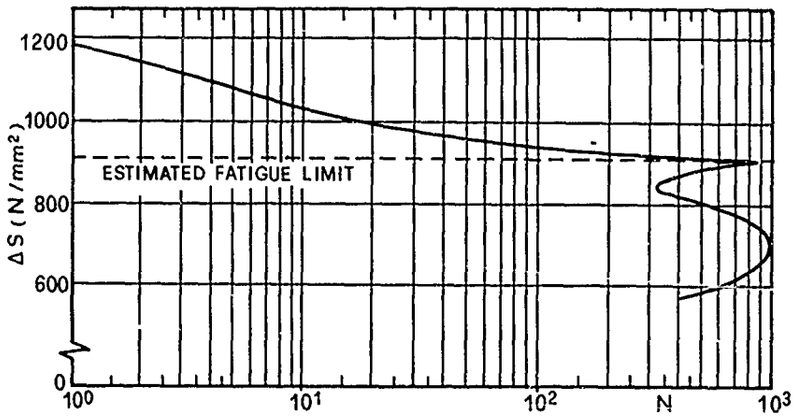


Fig. 9 - Nominal stress cycle amplitude distribution. Rain-flow counting method.

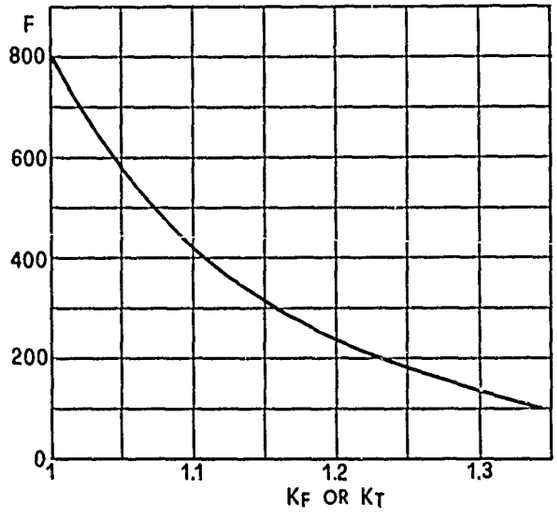


Fig. 10 - Fatigue life versus K_t value as calculated by the local stress-strain method.

Report on Session V

CONSTANT AMPLITUDE VERSUS SPECTRUM FATIGUE LOADING

by

Pietro Alli
C.A.G. Agusta SpA.
Cascina Costa
21017 Samarate (Varese), Italy

The fifth session concerned the. Constant amplitude versus spectrum fatigue loading and the main purpose was an evaluation of the potential role of variable amplitude fatigue test in the design against helicopter fatigue.

Three papers were presented. The first by Mr J.Dart: *Development of Standardised Test Load Histories for Helicopter Rotors. Basic Considerations and Definition of H. & F.* deals with the problem of defining a meaningful standardized load sequency suitable for testing rotor blades.

Two standardized load sequences have been developed. one, Helix, useful for hinged rotors and the other, Felix, to be used for semirigid rotors.

These load sequencies have been implemented to drive servohydraulic fatigue machines and were derived by an intensive flight load survey on existing helicopters.

The standardized load sequencies are, as the author of the paper points out, a tool suitable for comparison purposes and not for certifying specific helicopter items.

The second paper was presented by Mr Schütz on the *Development of a Standardized Fatigue Test Loading History for Helicopter Rotors.* It deals with the same subject as the previous one and would have presented a test data set to demonstrate the inherent capability of standardized load sequences in helicopter fatigue design. Test results will be available next year.

The third paper presented by myself on *Fatigue Behaviour of Helicopter Dynamic Components under Constant Amplitude and Spectrum Loading* deals with the problem of helicopter dynamic component fatigue analysis methodologies:

- Fatigue strength representation
- Counting methods
- Fatigue life estimation methods

were theoretically analysed and evaluated against the results of an appropriate test program both in constant amplitude and spectrum loading.

From the first results, it seems possible to conclude that a well selected counting method together with a suitable S-N curve can lead to satisfactory life prediction, utilizing moreover the Miner's rule.

Besides, the Haibach method, which undoubtedly has a more rational background, works at least in the same way once the fatigue limit idea is forgotten.

Anyway the substantiation of all the new ideas need more experimental results and the problem of the reduction coefficients still remain open.

In conclusion, due to the fact that new approaches proposed in the three papers are powerful of future great developments, it seems worthwhile to prepare a chapter of the planned handbook with the aim of having a detail description of variable amplitude test techniques, a collection of the existing test results and, at last, a deeper evaluation of all the fatigue analysis methods on the grounds of such results.

SESSION VI

ROUND TABLE DISCUSSION

Chairman: J.M.Fehrenbach

Rapporteur: G.Stiévenard
Aerospatiale, Division Hélicoptères
B.P.13, 13722 Marignane
France

Plusieurs thèmes ont été sélectionnés par les participants afin d'orienter la discussion.

Les thèmes retenus sont les suivants :

1) PROCEDURES COURANTES

2) CRITERE DE TOLERANCE AUX DOMMAGES

3) VARIABILITE DES CHARGES DE VOL

4) SIMULATION AU LABORATOIRE

5) EXPERTISE

6) SURVEILLANCE DES ENDOMMAGEMENTS (fatigue monitoring)

7) MOTIVATION DES ESSAIS DE CELLULE

8) NOUVELLES CONCEPTIONS DE ROTOR

---

1) PROCEDURES COURANTES :

Ce premier sujet de discussion visait à faire le point des méthodes de justification utilisées dans le monde afin de dégager une analyse critique susceptible de garantir une meilleure sécurité des vols.

Une première question est posée : quelle est la valeur du risque d'accident considéré comme admissible par les organismes de certification ?

Pour la CAA la probabilité d'accident ne doit pas dépasser 10^{-7} par heure de vol, ce pour des missions à caractère civil.

Cette probabilité peut être portée à 10^{-6} pour des utilisations plus spécifiques et présentant de par leur nature des risques d'accident plus importants (lutte contre l'incendie, Mission OFF SHORE, opération de sauvetage, etc...)

Ce risque correspond au risque global d'accident toutes causes confondues et non uniquement au risque de rupture en fatigue. Ceci implique donc que tous les risques élémentaires soient bien inférieurs à 10-7 .

Sikorsky fait remarquer qu'il est très difficile d'identifier toutes les causes susceptibles de provoquer un accident et encore plus difficile de chiffrer les valeurs des risques leur correspondant.

La SNIAS est d'accord avec la remarque de Sikorsky tout en faisant observer que le risque revendiqué par la CAA est un risque par heure de vol à ne pas confondre avec celui qui est associé aux durées de vie des pièces travaillant en fatigue.

La SNIAS pense qu'en fatigue les coefficients de sécurité doivent être importants afin que la probabilité de rupture demeure extrêmement faible.

Une exploitation statistique effectuée par la SNIAS d'essais de lot de pales montre que pour garantir une probabilité de rupture inférieure à 10^{-4} il convient d'utiliser un coefficient de sécurité d'environ 1,7 sur les contraintes.

Ce risque de 10^{-4} s'il correspond à une durée de vie de 1000 heures se traduit donc par un risque de 10^{-7} par heure de vol.

Ce coefficient de sécurité peut conduire à des écarts très significatifs sur les durées de vie calculées Le meilleur exemple en est l'exercice proposé par l'American Helicopter Society et qui conduit à des durées allant de 10 h à 20 000 h selon le coefficient de sécurité utilisé.

Cet exercice présente cependant par sa nature de nombreuses causes susceptibles de créer des écarts. En particulier la pièce analysée est en acier 4340 travaillant sans fretting. La forme de courbe S/N de ce matériau est très plate et engendre de ce fait des écarts en nombre de cycles très importants (1 à 100) pour de faibles écarts de contraintes.

Les ruptures rencontrées en utilisation ont généralement pour origine des dégradations qui n'avaient pas été prises en compte lors de l'homologation initiale (corrosion, usures, etc....)

Le seul remède selon M. De Jong serait de justifier toutes les pièces suivant le concept "tolérance aux hommages" concept qui n'est pas à ce jour considéré comme obligatoire.

Les raisons sont les suivantes : tout d'abord il n'est pas toujours possible d'obtenir ce concept certaines pièces ne s'y prêtant pas, ensuite le prix élevé des essais nécessaires à sa démonstration. Les programmes de justification classique qui portent déjà sur 6 essais par pièces vitales sont déjà aux limites du supportable par les constructeurs.

L'important selon Sikorsky est d'effectuer un minimum de 6 essais de fatigue et de tout mettre en oeuvre pour garantir une constance de la qualité de fabrication. Sikorsky recommande aussi une surveillance sérieuse du matériel en utilisation, surveillance pouvant conduire à une reprise des essais de fatigue sur des pièces présentant des dégradations survenues en service.

2) CRITERE DE TOLERANCE AU DOMMAGE :

L'Aérospatiale soulèvent les questions suivantes :

Quels sont les coefficients de sécurité utilisés par les constructeurs américains sur les temps de propagation des détériorations ?

En cas de découverte en utilisation d'un problème non prévu initialement quel est le coefficient de réduction de vie appliqué à l'ensemble de la flotte par rapport au temps de vol effectué par l'élément ayant fait l'objet de l'incident ?

Les constructeurs présents ne répondent pas aux deux questions posées par l'Aérospatiale.

3) VARIABILITE DES CHARGES DE VOL :

Quelles sont les précautions à prendre pour s'assurer que les mesures d'efforts en vol couvrent bien du point de vue sécurité tout le domaine d'utilisation revendiqué pour les machines ?

En particulier comment tient-on compte de la dispersion qui affecte les efforts des maneouvres effectuées au ras du sol ?

Une façon de se prémunir contre ce genre de problème consiste à multiplier le nombre d'enregistrement et à les exploiter statistiquement. Ceci implique évidemment un surcroît d'activité pour les pilotes mais présente l'avantage d'augmenter l a probabilité d'appréhender des manoeuvres mal coordonnées susceptibles de majorer les endommagements en fatigue.

Ces phénomènes sont à l'étude aux Etats Unis basés sur l'acquisition de données avec traitement statistique des charges statiques et dynamiques.

Cette analyse est compliquée par le fait que les charges peuvent évoluer en fonction du vieillissement des machines. Quelques exemples classiques sont rappelés tel l'influence de l'érosion des pales faisant varier les limites de décrochage et de ce fait le spectre des charges.

4) SIMULATION AU LABORATOIRE :

Au cours de la discussion il est rappelé tous les risques de résultats d'essai faussés en raison des difficultés de simulation des charges de vol.

Par exemple une pale comporte de multiples types de mise en charge qu'il est difficile de reproduire de façon rigoureuse (Force centrifuge, Moment de Battement, Moment de Trainée, Moment de torsion,etc...)

Si la simulation n'est pas correcte le mode de rupture peut être changé ainsi que les zones critiques le spectre de charge a aussi dans ce domaine une importance non négligeable.

Il est souligné l'intérêt de faire les essais de structure en atmosphère ouverte, ce qui présente l'avantage de simuler au moins partiellement les effets de condensation fretting et corrosion.

5) EXPERTISE :

Les inspections des pièces en essais devront être si possible réalisées avec les mêmes moyens et dans les mêmes conditions que ceux dont disposera l'utilisateur afin de guider la rédaction du manuel de maintenance.

Les pièces essayées devront être expertisées avec le plus grand soin car elles sont riches en enseignement sur l'avenir des pièces en utilisation. Par la suite l'expertise des pièces en service lors des révisions devraient permettre de vérifier si les dégradations constatées sont garanties par les essais de fatigue effectués.

6) FATIGUE MONITORING :

La surveillance de l'endommagement en fatigue est difficile en raison de la diversité des paramètres

Certains procédés sont à l'étude notamment par comptabilisation des endommagements à l'aide de capteurs optiques. Ces méthodes présentent certaines limites dont la principale dépend de la structure elle-même, en raison de l'inaccessibilité des zones critiques.

Ces capteurs modernes présentent cependant un intérêt certain ne serait-ce que pour surveiller des variations anormales du comportement de la structure.

La deuxième approche consiste à relever directement et en continu les efforts de vol. Cette méthode est très difficile à réaliser en service (diversité des efforts, difficulté d'enregistrer ceux-ci sur éléments rotatifs,etc....)

L'application de cette méthode est donc difficile en série. Il est fait état de quelques exemples : Indicateur de guide de croisière sur CH 47 (Bétamètre du Super Frelon permettant la surveillance des efforts de commande).

Finalement la méthode la plus rationnelle consiste a calculer l'endommagement de manière indirecte à partir du spectre d'utilisation des appareils, ce spectre étant déterminé à l'aide d'enregistrement en continu portant sur certains paramètres de vol en utilisation (vitesse, facteur de charge, positions des commandes, etc....)

7) ETUDES DES CAUSES D'ACCIDENT :

Depuis 10 ans 6000 accidents d'hélicoptère ont été constatés dont un quart pour des causes inconnues.

Afin de diminuer ce pourcentage d'accidents inexpliqués, un enregistreur de crash est à l'étude aux US. Cet enregistreur sera capable de relever durant au moins 30 minutes de vol certains paramètres de vol essentiels pour expliquer l'accident et par la suite éviter qu'il puisse se reproduire.

8) MOTIVATION DES ESSAIS DE CELLULE :

Ces essais permettent en avance de phase de détecter les points critiques de la cellule, de valider des périodicités d'inspection en fonction des vitesses de propagation constatées en essai et par la suite de justifier des solutions de réparation.

L'inconvénient majeur de cet essai est son prix de revient.

En France, la première tentative a été réalisée au titre d'un programme de Recherche afin de vérifier la validité d'une telle expérimentation. Ce genre d'essai sera vraisemblablement développé à la demande des Services Officiels dans la mesure où le coût demeurera raisonnable. Un moyen de rendre cet essai moins onéreux peut consister à le morceler afin de sélectionner les zones prioritaires à tester.

9) ROTORS DESIGN :

L'utilisation des matériaux composites dans la fabrication des rotors présente de nombreux centres d'intérêt qui portent entre autres sur :

- Meilleurs ajustement des fréquences propres des pièces permettant de minimiser les phénomènes de fatigue, afin d'éviter d'avoir à les combattre
- Comportement fail safe évident (délaminage généralement facile à détecter et vitesse de propagation des délaminages lente.
- Technologie permettant une réduction du nombre de pièce (suppression des pièces servant à la lubrification) d'où gain sur la masse.
- Fiabilité améliorée et maintenance simplifiée
- Coût de fabrication diminué.

SESSION VI

ROUND TABLE DISCUSSION
Chairman: J.M.Fehrenbach

Rapporteur: G.Stiévenard
Aerospatiale, Division Hélicoptères
B.P.13, 13722 Marignane
France

Several themes were selected by the participants in order to guide the discussion. The following themes were retained:

1. CURRENT PROCEDURES
2. DAMAGE TOLERANCE CRITERIA
3. VARIABILITY OF FLIGHT LOADS
4. LABORATORY SIMULATION
5. EXAMINATION
6. FATIGUE MONITORING
7. MOTIVATION FOR STRUCTURAL TESTS
8. NEW ROTOR CONCEPTS

---

1. CURRENT PROCEDURES

The aim of the first subject of discussion was to survey the substantiation methods in world-wide use in order to define a critical analysis method likely to guarantee maximum flight safety.

The first question which arose was: what is the level of accident risk considered acceptable by certification authorities? For the CAA, the probability of accident should not exceed 10^{-7} per flight hour, that is for missions of a civil character. This probability can be increased to 10^{-6} for more specific utilizations which, by their nature, incur a greater risk of accident (fire-fighting, off-shore missions, rescue operations, etc.). This level of risk corresponds to the overall risk of accident from all causes and not solely to the risk of fatigue failure. This implies, therefore, that all the basic risks should be well below 10^{-7}. Sikorsky remarked that it is very difficult to identify all the sources likely to induce an accident and more difficult still to quantify the corresponding risk.

SNIAS agreed with Sikorsky's comment while pointing out that the risk specified by the CAA is a risk per flight hour, not to be confused with that which is associated with the service life of parts subjected to fatigue. SNIAS thought that under fatigue conditions, safety factors should be high so that the probability of failure remains extremely low.

A statistical investigation carried out by SNIAS on blade tests showed that, in order to guarantee a failure probability of less than 10^{-4}, it is advisable to use a safety factor of about 1.7 on the stresses. If this 10^{-4} risk corresponds to a life of 1000 hours, it becomes equivalent to a risk of 10^{-7} per flight hour. This safety factor can lead to some very significant variations in predicted service life. The best example is in the exercise presented by the American Helicopter Society which resulted in lives varying from 10 h. to 20 000 h. according to the safety factor used. However, by its very nature, this exercise presented numerous sources liable to create discrépancies. In particular, the part analyzed was of 4340 steel, not subjected to fretting. The shape of the S/N curve for this material is very flat and, consequently, results in very large variations in the number of cycles (1:100) for small differences in stress.

Failures met with in service generally originate from forms of degradation which had not been taken into account at the time of initial certification (corrosion, wear, etc.). The only remedy, according to Ir de Jonge, would be to substantiate all parts in accordance with the "damage tolerance" concept, which is not at the moment considered to be mandatory. The reasons are the following: firstly, it is not always possible to apply this concept, as certain parts do not lend themselves to it, and because of the high cost of the tests necessary for its demonstration. The conventional substantiation programmes, which already require six tests on each vital part, are already at the limit acceptable to the manufacturers. The important point, according to Sikorsky, is to carry out a minimum of six fatigue tests and to use every possible means to ensure consistent manufacturing quality. Sikorsky also recommended close monitoring of the material in service, such monitoring making possible a repeat of the fatigue tests on parts which show degradation occurring in service.

2. DAMAGE TOLERANCE CRITERIA

Aérospatiale raised the following questions:

What are the safety factors on damage propagation rates used by American manufacturers? In the event of the discovery in service of an initially unforeseen problem, what is the safety factor on life reduction applied to the whole fleet as a function of the flight time achieved by the component responsible for the incident?

The manufacturers present did not reply to the two questions raised by Aerospatiale.

3. VARIABILITY OF FLIGHT LOADS

What precautions should be taken in order to ensure that the measurements of flight loads fully cover, from the safety aspect, the whole service envelope specified for the aircraft? In particular, how is the spread in manoeuvre loads close to the ground taken into account?

One way of providing against this type of problem is to multiply the number of recordings taken and to use them statistically. This obviously implies additional activity for the pilots but offers the advantage of raising the probability of detecting badly coordinated manoeuvres likely to increase fatigue damage. These phenomena are being investigated in the United States, based on data acquisition with statistical treatment of the static and dynamic loads. This analysis is complicated by the fact that the loads can evolve as a function of the life of the aircraft. Some classical examples were mentioned, such as the effect of blade erosion on the stall limits and, consequently, on the load spectrum.

4. LABORATORY SIMULATION

During the discussion, the risks of obtaining distorted test results, due to difficulties in the simulation of flight loads, were reviewed. For example, a blade sustains multiple types of loading which it is difficult to reproduce accurately (Centrifugal force, flapping moment, drag moment, torsional moment, etc.). If the simulation is not correct, the failure mode can be modified as well as the critical areas. The load spectrum is also not unimportant in this context. The value of making structural tests in the open air, which offers the advantage of, at least partially, simulating the effects of condensation, fretting and corrosion, was emphasized.

5. EXAMINATION

Inspection of parts under test must, if possible, be made by the same means and under the same conditions as those which the user will have available, so as to guide the preparation of the maintenance manual. The parts tested must be examined with the greatest care since they will provide considerable information on the future service life of the parts. Subsequently, examination of parts in service at the time of inspection should enable it to be determined whether the observed degradation is covered by the fatigue tests made.

6. FATIGUE MONITORING

Monitoring of fatigue damage is difficult owing to the diversity of parameters. Certain procedures are being investigated, in particular by keeping account of damage by means of optical sensors. Such methods have their limitations, the main one depending on the structure itself due to the inaccessibility of critical areas. However, these modern sensors are of unquestionable value, be it only to monitor abnormal variations in structural behaviour.

The second approach consists of recording flight stresses directly and continuously. This method is very difficult to apply in service (variety of stresses, difficulties in recording these stresses on rotating components, etc.) It is therefore difficult to apply this method in production. A few examples were mentioned: cruise guide indicator on the CH-47 (Bétamètre of the Super Frelon, which makes it possible to monitor control forces).

7. ACCIDENT INVESTIGATION

In the last ten years there have been 6000 helicopter accidents of which a quarter were due to unknown causes. In order to reduce this fraction of unaccountable accidents, a crash recorder is being developed in the United States. This recorder will be capable of recording, for at least 30 minutes of flight, certain flight parameters which are necessary to account for the accident and, subsequently, to avoid its re-occurrence.

8. MOTIVATIONS FOR STRUCTURAL TESTS

These tests provide the means of detecting critical points in the structure, of validating inspection periods as a function of propagation rates observed in tests and, eventually, of substantiating repair schemes. The main drawback of this test is its cost.

In France, the first attempt was made within the framework of a research programme in order to check the validity of such experiments. This type of test will probably be developed at the request of the official authorities as long as the cost remains reasonable. A means of making this test less costly may consist of dividing it up in order to select priority areas to be tested.

9. ROTOR DESIGN

The use of composite materials in rotor manufacture offers a great deal of interest, especially with regard to the following points:

- Better adjustment of the natural frequencies of components in order to minimize fatigue phenomena and to avoid having to combat them.
- Obvious fail-safe behaviour (delamination usually easily detectible and low delamination propagation rate).
- Technology allowing a reduction in the number of parts (elimination of parts used for lubrication), hence reduction in mass.
- Improved reliability and simplified maintenance.
- Reduced manufacturing cost.

REPORT DOCUMENTATION PAGE			
1. Recipient's Reference	2. Originator's Reference AGARD-CP-297	3. Further Reference ISBN 92-835-0289-2	4. Security Classification of Document UNCLASSIFIED

5. Originator: Advisory Group for Aerospace Research and Development
North Atlantic Treaty Organization
7 rue Ancelle, 92200 Neuilly sur Seine, France

6. Title

HELICOPTER FATIGUE LIFE ASSESSMENT

7. Presented at the 51st Meeting of the AGARD Structures and Materials Panel held in Aix-en-Provence, France on 14–19 September 1980.

8. Author(s)/Editor(s): Various

9. Date: March 1981

10. Author's/Editor's Address: Various

11. Pages: 268

12. Distribution Statement: This document is distributed in accordance with AGARD policies and regulations, which are outlined on the Outside Back Covers of all AGARD publications.

13. Keywords/Descriptors

Helicopters
Airframes
Rotary wings
Fatigue life
Fatigue tests

14. Abstract

The major objective of this Meeting was to take a further step towards the collection of experience on the fatigue evaluation and substantiation of new helicopters. The Meeting included surveys of current procedures and service experience, consideration of new concepts associated with the introduction of new technologies such as composite materials, new philosophies relevant to service damage and combat damage, and a review of testing techniques and methodologies for airframes and dynamic components. Finally, presentations were made on a European exercise aimed at the development of standardized fatigue load histories for helicopter rotors.

AGARD Conference Proceedings No.297 Advisory Group for Aerospace Research and Development, NATO HELICOPTER FATIGUE LIFE ASSESSMENT Published March 1981 268 pages The major objective of this Meeting was to take a further step towards the collection of experience on the fatigue evaluation and substantiation of new helicopters. The Meeting included surveys of current procedures and service experience, consideration of new concepts associated with the introduction of new technologies such as composite materials, new philosophies relevant to service damage and combat damage, and a review of testing techniques and methodologies for airframes and P.T.O.	AGARD-CP-297 Helicopters Airframes Rotary wings Fatigue life Fatigue tests	AGARD Conference Proceedings No.297 Advisory Group for Aerospace Research and Development, NATO HELICOPTER FATIGUE LIFE ASSESSMENT Published March 1981 268 pages The major objective of this Meeting was to take a further step towards the collection of experience on the fatigue evaluation and substantiation of new helicopters. The Meeting included surveys of current procedures and service experience, consideration of new concepts associated with the introduction of new technologies such as composite materials, new philosophies relevant to service damage and combat damage, and a review of testing techniques and methodologies for airframes and P.T.O.	AGARD-CP-297 Helicopters Airframes Rotary wings Fatigue life Fatigue tests
AGARD Conference Proceedings No.297 Advisory Group for Aerospace Research and Development, NATO HELICOPTER FATIGUE LIFE ASSESSMENT Published March 1981 268 pages The major objective of this Meeting was to take a further step towards the collection of experience on the fatigue evaluation and substantiation of new helicopters. The Meeting included surveys of current procedures and service experience, consideration of new concepts associated with the introduction of new technologies such as composite materials, new philosophies relevant to service damage and combat damage, and a review of testing techniques and methodologies for airframes and P.T.O.	AGARD-CP-297 Helicopters Airframes Rotary wings Fatigue life Fatigue tests	AGARD Conference Proceedings No.297 Advisory Group for Aerospace Research and Development, NATO HELICOPTER FATIGUE LIFE ASSESSMENT Published March 1981 268 pages The major objective of this Meeting was to take a further step towards the collection of experience on the fatigue evaluation and substantiation of new helicopters. The Meeting included surveys of current procedures and service experience, consideration of new concepts associated with the introduction of new technologies such as composite materials, new philosophies relevant to service damage and combat damage, and a review of testing techniques and methodologies for airframes and P.T.O.	AGARD-CP-297 Helicopters Airframes Rotary wings Fatigue life Fatigue tests

dynamic components. Finally, presentations were made on a European exercise aimed at the development of standardized fatigue load histories for helicopter rotors.

Papers presented at the 51st Meeting of the AGARD Structures and Materials Panel held in Aix-en-Provence, France on 14–19 September 1980.

ISBN 92-835-0289-2

dynamic components. Finally, presentations were made on a European exercise aimed at the development of standardized fatigue load histories for helicopter rotors.

Papers presented at the 51st Meeting of the AGARD Structures and Materials Panel held in Aix-en-Provence, France on 14–19 September 1980.

ISBN 92-835-0289-2

dynamic components. Finally, presentations were made on a European exercise aimed at the development of standardized fatigue load histories for helicopter rotors.

Papers presented at the 51st Meeting of the AGARD Structures and Materials Panel held in Aix-en-Provence, France on 14–19 September 1980.

ISBN 92-835-0289-2

dynamic components. Finally, presentations were made on a European exercise aimed at the development of standardized fatigue load histories for helicopter rotors.

Papers presented at the 51st Meeting of the AGARD Structures and Materials Panel held in Aix-en-Provence, France on 14–19 September 1980.

ISBN 92-835-0289-2

B192
4

AGARD
NATO OTAN
7 RUE ANCELLE · 92200 NEUILLY-SUR-SEINE
FRANCE
Telephone 745.08.10 · Telex 610176

DISTRIBUTION OF UNCLASSIFIED AGARD PUBLICATIONS

AGARD does NOT hold stocks of AGARD publications at the above address for general distribution. Initial distribution of AGARD publications is made to AGARD Member Nations through the following National Distribution Centres. Further copies are sometimes available from these Centres, but if not may be purchased in Microfiche or Photocopy form from the Purchase Agencies listed below.

NATIONAL DISTRIBUTION CENTRES

BELGIUM
Coordonnateur AGARD – VSL
Etat-Major de la Force Aérienne
Quartier Reine Elisabeth
Rue d'Evere, 1140 Bruxelles

CANADA
Defence Science Information Services
Department of National Defence
Ottawa, Ontario K1A 0K2

DENMARK
Danish Defence Research Board
Østerbrogades Kaserne
Copenhagen Ø

FRANCE
O.N.E.R.A. (Direction)
29 Avenue de la Division Leclerc
92320 Châtillon sous Bagneux

GERMANY
Fachinformationszentrum Energie,
Physik, Mathematik GmbH
Kernforschungszentrum
D-7514 Eggenstein-Leopoldshafen 2

GREECE
Hellenic Air Force General Staff
Research and Development Directorate
Holargos, Athens

ICELAND
Director of Aviation
c/o Flugrad
Reykjavik

ITALY
Aeronautica Militare
Ufficio del Delegato Nazionale all'AGARD
3, Piazzale Adenauer
Roma/EUR

LUXEMBOURG
See Belgium

NETHERLANDS
Netherlands Delegation to AGARD
National Aerospace Laboratory, NLR
P.O. Box 126
2600 A.C. Delft

NORWAY
Norwegian Defence Research Establishment
Main Library
P.O. Box 25
N-2007 Kjeller

PORTUGAL
Direcção do Serviço de Material
da Força Aerea
Rua da Escola Politécnica 42
Lisboa
Attn: AGARD National Delegate

TURKEY
Department of Research and Development (ARGE)
Ministry of National Defence, Ankara

UNITED KINGDOM
Defence Research Information Centre
Station Square House
St. Mary Cray
Orpington, Kent BR5 3RE

UNITED STATES
National Aeronautics and Space Administration (NASA)
Langley Field, Virginia 23365
Attn: Report Distribution and Storage Unit

THE UNITED STATES NATIONAL DISTRIBUTION CENTRE (NASA) DOES NOT HOLD STOCKS OF AGARD PUBLICATIONS, AND APPLICATIONS FOR COPIES SHOULD BE MADE DIRECT TO THE NATIONAL TECHNICAL INFORMATION SERVICE (NTIS) AT THE ADDRESS BELOW.

PURCHASE AGENCIES

Microfiche or Photocopy
National Technical
Information Service (NTIS)
5285 Port Royal Road
Springfield
Virginia 22161, USA

Microfiche
Space Documentation Service
European Space Agency
10, rue Mario Nikis
75015 Paris, France

Microfiche
Technology Reports
Centre (DTI)
Station Square House
St. Mary Cray
Orpington, Kent BR5 3RF
England

Requests for microfiche or photocopies of AGARD documents should include the AGARD serial number, title, author or editor, and publication date. Requests to NTIS should include the NASA accession report number. Full bibliographical references and abstracts of AGARD publications are given in the following journals:

Scientific and Technical Aerospace Reports (STAR)
published by NASA Scientific and Technical
Information Facility
Post Office Box 8757
Baltimore/Washington International Airport
Maryland 21240, USA

Government Reports Announcements (GRA)
published by the National Technical
Information Services, Springfield
Virginia 22161, USA

Printed by Technical Editing and Reproduction Ltd
Harford House, 7–9 Charlotte St, London W1P 1HD

ISBN 92-835-0289-2